@RevFCAUNCuyo

REV FCA UNCuyo

Tomo 57 N° 2 | Año 2025
ISSN on line 1853 8665
Mendoza | Argentina

Evaluadores 2025 (2)

Macarena Acasuso
INTA

Marta Alonso
Universidad de León-España

Marcelo Amado
UBA

Nora Andrada
UNSan Luis

Nancy Apóstolo
UNLuján

Carlos Tubay Bermudez
Instituto Politécnico de Leiria-España

Roberto Bisang
CONICET

Aníbal Catania
INTA

Gabriel Céccoli
CONICET

Lucrecia Couretot
INTA

Liliana Di Feo
INTA

Deolindo Dominguez
UNCuyo

Georgina Escoriaza
INTA

Rodrigo Espíndola
INTA

Hebe Fernandez
CONICET

Gabriela Fernández Pepi
UBA

Fernando Flores
INTA

Franca Giannini-Kurina
Aarhus University-Dinamarca

Javier Gyenge
INTA

Alberto Gochez
INTA

Yanina Guzmán
INTA

Carla Guzzo
INTA

Claudia F. Martinez
CONICET

Yuridia B. Martínez
UAutónoma de Tamaulipas-México

Evangelina Natale
UNRío Cuarto

Claudio Oddino
UNRío Cuarto

Carlos Osella
UNLitoral

Andrea Peña-Malavera
EEAOC-CONICET

Diego Pipino
UNRío Cuarto

Mariana Puente
INTA

Rosana Rotondo
UNRosario

Diakaridia Sangaré
CIRAD-Francia

Gabriel Valentini
INTA

Federico Vera
INTA

Gabriel Vinderola
CONICET

Alejandra Yommi
INTA

Eduardo Wright
UBA

Pablo Arenas Báez
Unidad Regional Universitaria de Zonas Áridas-Chapingo-México

Revista de la Facultad de Ciencias Agrarias
Universidad Nacional de Cuyo

Tomo 57 (2) - Diciembre | December 2025

Índice | Index

Ecofisiología y manejo de cultivo | Ecophysiology and crop management

Recursos naturales y ambiente | Natural resources and environment

Economía y Política Agraria | Economy and agricultural politics

Protección vegetal | Plant protection

Producción y sanidad animal | Production and animal health

Tecnologías agroindustriales | Agroindustrial technologies

Revisión | Review

Effects of Gibberellic Acid on Flowering Reduction, Fruit Quality and Yield of 'd'Agen' Plum (*Prunus domestica* L.) in Mendoza, Argentina

Efecto del ácido giberélico sobre la reducción de la floración, calidad de fruta y rendimiento del ciruelo 'd'Agen' (*Prunus domestica* L.) en Mendoza, Argentina

Georgina Leoncelli [1], Norma G. Micheloud [2], Hilario Lázaro [3], Norberto F. Gariglio [2*]

Originales: *Recepción:* 08/05/2025- *Aceptación:* 23/08/2025

Abstract

In Mendoza, the primary industrial plum-producing region in Argentina, the 'd'Agen' cultivar represents approximately 90% of the cultivated area. The limited implementation of fruit thinning has a detrimental effect on final fruit size. The objective of this study was to determine the timing of flower induction in 'd'Agen' plum and to evaluate the response to gibberellic acid (GA) application to reduce flower density and improve fruit size. Over three growing seasons in San Rafael (Mendoza), experiments were conducted on plants grafted onto 'Marianna 2624', spaced at 5x3 m and drip irrigated. GA (100 ppm) was applied at four distinct phenological stages: fruit set, young fruit, fruit near final size, postharvest, and a control with no GA application. In the first two seasons, the H phenological stage (fruit set, Baggiolini scale) was identified as the optimum time for reducing flowering via GA application. In the third season, increasing GA concentrations (0, 25, 50, 75 and 100 ppm) were evaluated. All concentrations reduced floral density compared to the control. However, fruit set was negatively affected by the 75 and 100 ppm treatments. The decline in flowering (between 60% and 90%) was incompatible with commercial yields. It was concluded that the optimal time for GA application to reduce floral density in 'd'Agen' plum was during phenological stage H. Further research is required to determine the most effective dose below 25 ppm.

Keywords
chemical thinning • flower induction • fruit load • fruit size • *Prunus domestica*

1 Universidad Nacional del Litoral. Facultad de Ciencias Agrarias. Kreder 2805. (3080). Esperanza. Santa Fe. Argentina.
2 ICiAgro Litoral-UNL-CONICET-FCA. Kreder 2805. Esperanza. Santa Fe. Argentina. * ngarigli@fca.unl.edu.ar
3 Estación Experimental Agropecuaria del INTA Rama Caída. El Vivero s/n. (5600) Rama Caída. Mendoza. Argentina.

Resumen

En Mendoza, la principal provincia argentina productora de ciruelas para industria, el cv. 'd'Agen' representa aproximadamente el 90% de la superficie cultivada. La limitada aplicación de prácticas de aclareo impacta negativamente en el tamaño de frutos. El objetivo de este trabajo fue determinar el momento de inducción floral y evaluar la aplicación de ácido giberélico (GA) para reducir la densidad floral y mejorar el tamaño de los frutos. Durante tres temporadas, en San Rafael (Mendoza), se realizaron ensayos con plantas injertadas sobre 'Marianna 2624', con espaciamiento de 5x3 m y riego por goteo. GA (100 ppm) se aplicó en cuatro estadios fenológicos: cuajado de frutos; frutos jóvenes; frutos próximos al tamaño final; postcosecha; y un control, sin tratamiento de GA. En las dos primeras temporadas, el estado fenológico H (cuajado de frutos, Baggiolini) resultó ser el momento óptimo para reducir la floración mediante aplicaciones de GA. En la siguiente temporada, se evaluaron diferentes concentraciones de GA (0, 25, 50, 75 y 100 ppm) aplicadas en dicha etapa. Todas las dosis redujeron la floración en comparación con el control. No obstante, las dosis de 75 y 100 ppm afectaron negativamente el cuajado de frutos. La reducción de la floración (entre 60 y 90%) resultó incompatible con rendimientos comerciales. La etapa fenológica H resultó el momento óptimo de aplicación de GA con el fin de reducir la densidad floral del ciruelo 'd'Agen'. Se requieren investigaciones para evaluar la dosis más efectiva por debajo de 25 ppm.

Palabras clave
carga frutal • inducción floral • raleo químico • tamaño de fruto • *Prunus domestica*

Introduction

World production of dried plums is estimated at 270,000 metric tons, with the United States, Chile, France and Argentina as the primary producers and exporters (9). However, the United States and Chile together account for over 70% of global production. The predominant cultivar used for dehydration is 'd'Agen', which accounts for over 98% of worldwide production (16). The increasing global demand for dried plums can be attributed to the well-documented health benefits of this fruit (13).

In Argentina, annual dried plum consumption is estimated at 3,500 metric tons (7). The province of Mendoza is the main contributor to the industry's plum production, with 10,000 hectares cultivated and 51,317 metric tons of fresh fruit harvested during the 2020/21 season (9). The cultivated area underwent expansion between 1992 and 2010 (7), with the 'd'Agen' group occupying over 90% of the area (9). In the southern region of the province (departments of San Rafael and General Alvear), approximately 70% of "d'Agen" plums are cultivated and dehydrated (9), with 95% destined for export. However, the 'Oasis Sur' region is subject to high climatic risk, characterized by hailstorms and late frosts, resulting in substantial fluctuations in its annual production (8).

Under typical conditions, fruit trees often set more fruit than they can support to reach satisfactory commercial quality (12). In order to mitigate these effects, fruit thinning is implemented and is considered one of the most critical cultural practices in fruit tree management (12, 14, 15).

Floral induction marks the onset of the reproductive phase and, consequently, the initiation of competition among developing floral organs. Gibberellins have been identified as inhibitors of floral induction in several fruit tree species (1). A high fruit load, particularly in plants bearing fruits with numerous seeds capable of synthesising gibberellin, has been shown to induce alternate bearing patterns (10).

Aiming at efficacious agronomic intervention and regulation of floral density, knowing the precise temporal dynamics of floral induction across different crop and cultivar types turns imperative. The application of gibberellins during floral induction has been used to modulate flowering density in various crops, including citrus (1), apple (14) and stone fruit (2, 5, 6, 15). The reduction in floral bud number resulting from the application of GA decreases the time required for manual fruit thinning in peach trees (6). This finding was

corroborated in other stone fruit species (5, 10). In the 'Opal' plum cultivar, gibberellin application during stage I of fruit development effectively reduced floral induction and the next year's crop load (11).

In European plum (*Prunus domestica* L.), fruit load can be managed through manual, mechanical or chemical thinning techniques. These practices are used to achieve marketable fruit size and to mitigate alternate bearing (11). However, manual thinning is applied in only approximately 10% of plum orchards in Mendoza, as it is not considered cost-effective (9). The price received by farmers is strongly dependent on fruit size, with annual decrease in the international prices of smaller fruits (49-62 fresh units per kg) (7).

Particularly considering 'd'Agen' plums, there is scarce experimental data on the use of chemical thinning to reduce crop load and improve fruit quality and profitability (11). Moreover, knowledge is limited regarding the timing of floral induction and the effect of GA on flowering reduction and fruit size improvement in this cultivar. The use of gibberellins has been identified as a potentially cost-effective strategy for crop load regulation and supporting agronomic decision-making under the environmental and production conditions of the Oasis Sur region in Mendoza.

The objective of this study was to determine the timing of floral induction and to evaluate the optimal concentration of gibberellic acid for reducing flower density and crop load, thereby improving the commercial fruit size in 'd'Agen' plums.

Materials and methods

The trial was conducted in a commercial plum orchard in the San Rafael department, Mendoza province (34°06'S, 68°33'W, 750 m above sea level). It spanned three consecutive growing seasons, from November 2018 to February 2021. On 5 October 2020, the occurrence of frost led to partial damage as the crop was at the flowering to fruit set phenological stages. These stages are particularly susceptible to frost injury in temperate fruit orchards (4).

European plum trees (*Prunus domestica* L.) of the 'd'Agen' cultivar, 12 years old, grafted onto 'Mariana 2624' (*Prunus cerasifera* x *Prunus munsoniana*) were used. The trees were cultivated in loamy soil, with drip irrigation and protected from hail damage by nets. They were selected based on their uniformity in canopy size and trunk diameter, and were trained in a narrow vase system, with a spacing of 5x3 m. Trunk cross-sectional area (TCSA) was measured at the beginning of each growing season.

Determination of Floral Induction Timing (2018/2019 season)

Gibberellic acid (GA) treatments (Gibberellin KA; S. Ando y Cía. S.A.) were applied at a concentration of 100 mg l^{-1} (ppm), with the solution pH adjusted to 5.5 using 1 M acetic acid. Manual spraying was performed until runoff, with an average application volume of 2.3 liters per plant. Applications were conducted in mid-morning at four phenological stages according to the Baggiolini scale (8), resulting in five treatment groups: T1, H stage (fruit set, 02/11/2018); T2, I stage (young fruits, 20/11/18); T3, J stage (fruit near final size, 02/01/19); T4, postharvest (one week after harvest, 15/02/19). A control group (T0) received no GA treatment.

Determination of the Gibberellin doses (2019/2020 season)

In this study, GA applications were performed on 1 November 2019 at stage H (fruit set). Five treatments were established based on GA concentration: Control (C, 0 ppm); T1 (25 ppm); T2 (50 ppm); T3 (75 ppm); T4 (100 ppm). Manual fruit thinning was not applied in any of the treatments.

To monitor the evolution of plant parameters in both trials, four branches of similar size were selected per tree during the winter period. These were distributed in the four quadrants of the canopy at a uniform height of approximately 1.5 m above ground level. The diameter of each branch at the point of insertion and its total length were measured. Reproductive structures (flowers and fruits) on the selected branches were counted weekly throughout the spring. Data were expressed as the number of flowers and fruits per unit of branch cross-sectional area (cm^2). The relative fruit drop rate (RFDR) was calculated for each interval between observation dates (13).

Harvesting began once the fruits reached a minimum soluble solids content of 22°Brix, as measured using an Arcano DBR0045nD digital refractometer, and a pulp firmness of 3-4 lb in^{-2}, as determined using a Turoni FT327 penetrometer equipped with an 8 mm diameter tip. The total weight and number of fruits per plant were recorded for subsequent analysis. Results were also expressed as the number of fruits per unit of trunk cross-sectional area (TCSA). A sub-sample of 50 fruits per plant was used to measure individual fruit diameter using a SCHWYZ digital caliper. Commercial fruit size was determined by randomly selecting three 1 kg samples per tree and counting the number of fruits in each. Fruit size classification followed the fresh weight standard of the Plum Exporters Committee of Mendoza (CECIM, unpublished data), which defined three categories: large fruits (< 34 fruits kg^{-1}), medium fruits (35-48 fruits kg^{-1}), and small fruits (49-62 fruits kg^{-1}).

In both experiments, a completely randomized block experimental design was used, with five replications per treatment, totaling 25 plants per trial. Irrigation (tree row) was used as a blocking factor. The experimental unit was the individual tree, while the observation unit comprised the selected branches. Data were then analyzed using analysis of variance (ANOVA) and means were compared using the DGC test at a 5% significance level. Statistical analyses were performed using the INFOSTAT software (3). A general linear and mixed model was used to analyze variables such as flowering density, fruit set, and fruit yield. Conversely, variables related to the dynamics of flower and fruit abscission, including the relative fruit abscission rate, were treated as repeated measures over time and analyzed with a general mixed model. Additionally, regression analysis was conducted to evaluate the relationships between crop load and individual fruit weight, as well as between floral density, fruit set, and fruit yield.

Results and discussion

Determination of Floral Induction Timing

In the control treatment, flowering density of 'd'Agen' plum reached approximately 180 flowers per cm^2 of branch cross-section area. The application of GA at 100 ppm during the phenological stage H, which corresponds with the fruit-setting period, five weeks after full bloom, resulted in a 90% reduction in the flowering density. In contrast, no effect on flower density was observed when GA was applied in the phenological stages I, J, and post-harvest (figure 1A, page 5).

The results indicate that the phenological stage H corresponds to the period of floral induction for the 'd'Agen' plums. This finding is consistent with previous observations in the European plum, cv. 'Opal', where the application of GA five weeks after full bloom was identified as the most efficacious timing for the reduction of flowering (11). Later applications of GA were ineffective, suggesting that floral induction had already occurred and that the buds were at a more advanced stage of floral differentiation. This finding is consistent with the established understanding that gibberellins are only effective when applied before or during the floral induction period (6).

In the second-year trial, 'd'Agen' plum exhibited high sensitivity to all GA concentrations applied at phenological stage H. Even the lowest dose (25 ppm GA) resulted in a significant reduction in flowering density, with a decrease of approximately 60% (figure 1B, page 5). Floral density declined exponentially with increasing GA doses, from 140 flowers cm^{-2} of branch cross-sectional area in the control to less than 10 flowers cm^{-2} in the 75 and 100 ppm GA treatments. Significant differences in flowering density were observed among the different GA concentrations, except between the 75 and 100 ppm treatments (figure 1B, page 5). The flowering response to the 100 ppm GA application at stage H was comparable in both years of the study (figure 1A, page 5).

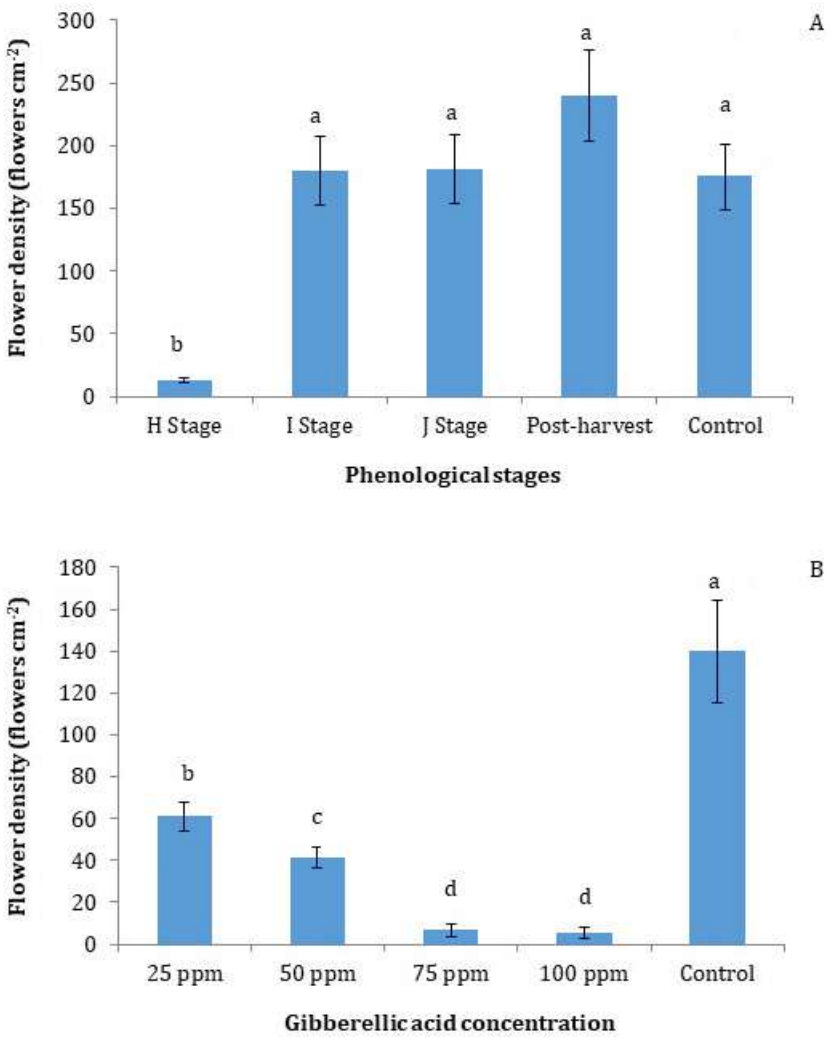

Different letters on bars indicate significant differences, DGC test ($P < 0.05$). Vertical bars indicate standard error. Data correspond to the first year of the trial. H Stage: fruit set; I Stage: young fruits; J Stage: fruit near final size; Postharvest: one week after harvest; Control: without treatment.

Letras diferentes sobre las barras indican diferencias significativas, test DGC ($P < 0,05$). Barras verticales indican el error estándar. Los datos corresponden al primer año del experimento. Estado H: cuajado de frutos; Estado I: frutos jóvenes; Estado J: frutos próximos al tamaño final; Poscosecha: una semana posterior a la cosecha; Control: sin tratamiento.

Figure 1. Floral density per unit of branch cross-sectional area (flowers cm^{-2}) of 'd'Agen' plums in response to: (A) application of gibberellic acid (GA; 100 ppm) at different phenological stages of the previous growing season, and (B) different GA concentrations applied during stage H of the previous growing season.

Figura 1. Densidad floral por unidad de área de sección transversal de rama (flores cm^{-2}) del ciruelo 'd'Agen' en respuesta a: (A) aplicación de ácido giberélico (AG; 100 ppm) en diferentes estados fenológicos de la estación de crecimiento previa, y (B) diferentes concentraciones de AG aplicado en el estado H de la estación de crecimiento previa.

The response of 'd'Agen' plum to increasing GA concentration is consistent with findings reported in other fruit-tree crops. In Japanese plums, the application of 75 and 100 ppm GA, 106 days after full bloom, resulted in a 75-90% reduction in floral density (1). Similarly, GA application 60 days after full bloom in peach trees reduced flower number and minimized the time required for manual fruit thinning in peach trees (6). Furthermore, the time required for final thinning was inversely correlated with GA concentration. In nectarines, cultivars 'May Fire' and 'May Glo' exhibited a 25-40% reduction in flowering following the application of 118 ppm GA, while the cultivar 'Zincal' showed a reduction of up to 65% (2). Comparable results have been reported in apricot and cherry trees, where 100 ppm GA effectively reduced flower density in the following season (10).

Abscission of Reproductive Structures

In the control group, the rate of flower and fruit drop increased markedly after 10 October and remained high until the end of the month. A similar trend was observed in the GA treatments at stages I, J, and post-harvest. However, GA application at stage H showed a one-week advance in flower and fruit drop compared to the other treatments (figure 2A).

In the second year of the study, the effect of different GA concentrations at stage H was assessed (figure 2B). The persistence of reproductive structures and their abscission rate in the 25 and 50 ppm GA treatments exhibited a similar trend to that of the control, while the 75 ppm GA dose resembled that of the 100 ppm GA treatment. The highest abscission rate was observed on 17 October, while in the 75 and 100 ppm GA treatments, the highest abscission rate was recorded one week earlier (7 to 9 October) (figure 2B), as was previously described for the application of 100 ppm GA at stage H during the first year of the study (figure 2A).

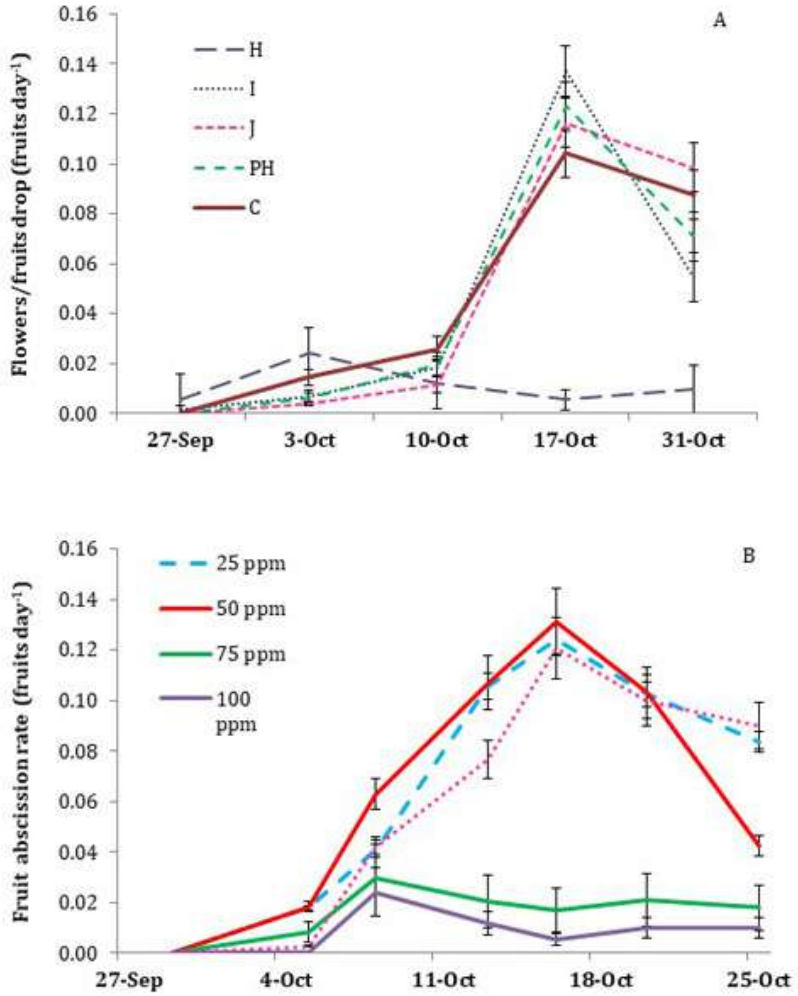

Vertical bars correspond to standard error. Data correspond to the first year of the experiment. H stage: fruit set; I stage: young fruit; J stage: fruit near final size; PH: post-harvest, one week after harvest; C: control plants without gibberellic acid treatment.

Barras verticales indican error estándar. Los datos corresponden al primer año del experimento. Estado H: cuajado de frutos; Estado I: frutos jóvenes; Estado J: frutos próximos al tamaño final; poscosecha: una semana posterior a cosecha; Control: sin tratamiento.

Figure 2. Evolution of flower/fruit abscission rate (flower/fruits day^{-1}) of 'd'Agen' plum in response to: (A) 100 ppm gibberellic acid (GA) application at different phenological stages of the previous growing season, and (B) different concentrations of GA applied during the pit-hardening stage of the previous growing season.

Figura 2. Evolución de la tasa de abscisión de flores/frutos (flores/frutos día^{-1}) del ciruelo 'd'Agen' en respuesta a: (A) aplicación de ácido giberélico (AG) en diferentes estados fenológicos, de la estación de crecimiento previa; (B) diferentes concentraciones de AG aplicadas durante el endurecimiento del carozo del fruto, de la estación de crecimiento previa.

The observations made in mid-October correspond to the first phase of fruit development, known as stage I, characterized by cell division (2). Additionally, in the second year, the occurrence of high temperatures and "Zonda" winds during the flowering period, followed by a late frost, affected the persistence of flowers and fruits. Despite these differing environmental conditions, the period of maximum fruit drop for the 'd'Agen' cultivar occurred in mid-October in both years. Furthermore, the H phase is also characterized by the sprouting and vegetative growth of the plant. These results are of great agronomic importance, as they indicate that the H phase is a sensitive period for the 'd'Agen' plum plant due to the competition between flower induction and developing fruits, as well as the increases in vegetative growth (12).

Gibberellins affect flower differentiation and sexual determination, resulting in abnormalities and masculinizing effects (16). This could explain the increase in flower/fruit drop in treatments with higher GA concentrations (75 and 100 ppm). However, this effect was only observed in treatments applied at the time of maximum sensitivity to flowering inhibition (H stage).

Fruit Set

Application of GA at the phenological stage H not only reduced flower density but also led to a marked decrease in final relative fruit set, which was less than 1% of the initial number of flowers. GA applications at the later phenological stage (stage I) also reduced fruit set by about 30% compared to later treatments, which achieved a fruit set percentage of around 12% (figure 3A, page 8).

In the second year, at different doses of GA during the H stage, the 75-ppm GA treatment exhibited the same negative effect on fruit set as the 100-ppm treatment during the two-year observation period. Conversely, lower concentrations of GA (25 and 50 ppm) did not affect fruit set (figure 3B, page 8). This reduction in fruit set can be attributed to the masculinizing effects of gibberellins, as previously discussed (16). In 'Patterson' apricot (15), fruit set was not affected by GA applications; however, in 'Opal' plum, fruit set for the following year was significantly reduced for all GA treatments compared to the control (11).

Fruit Size and Yield

In the first year of the trial, the application of 100 ppm GA during fruit set (stage H) improved fruit size at harvest in the following growing season by approximately 3 mm compared to later applications, which did not differ from each other or from the control (figure 4A, page 9). Furthermore, according to the regulations of the Plum Exporters Committee of Mendoza (CECIM), the application of gibberellins at stage H resulted in an improved fruit size category from 'small' (39-62 fruits per kg) to 'medium' (35-48 fruits per kg).

In the second year, the range of fruit sizes in the treatments was similar to that observed in the first year (figure 4A and 4B, page 9), despite the large difference in crop load between the two growing seasons. Fruit size differed significantly among GA concentrations, except between the 50 and 75 ppm treatments (figure 4B, page 9). According to the Plum Exporters Committee of Mendoza (CECIM), GA concentrations of 50, 75, and 100 ppm resulted in 'medium-sized' plums, whereas the 0 and 25 ppm treatments produced 'small-sized' fruits.

Fruit size is influenced by multiple factors, but it is well established that there is an inverse relationship between the number of fruits per tree and their final size (5). Fruit thinning reduces carbohydrate competition among the remaining fruits, promotes cell division and elongation, and thus ensures a commercially appropriate fruit size (2). By reducing flower density through gibberellic acid applications, competition between reproductive structures is decreased from the outset. As a result, this technique has the potential to produce larger fruit compared to traditional fruit thinning methods.

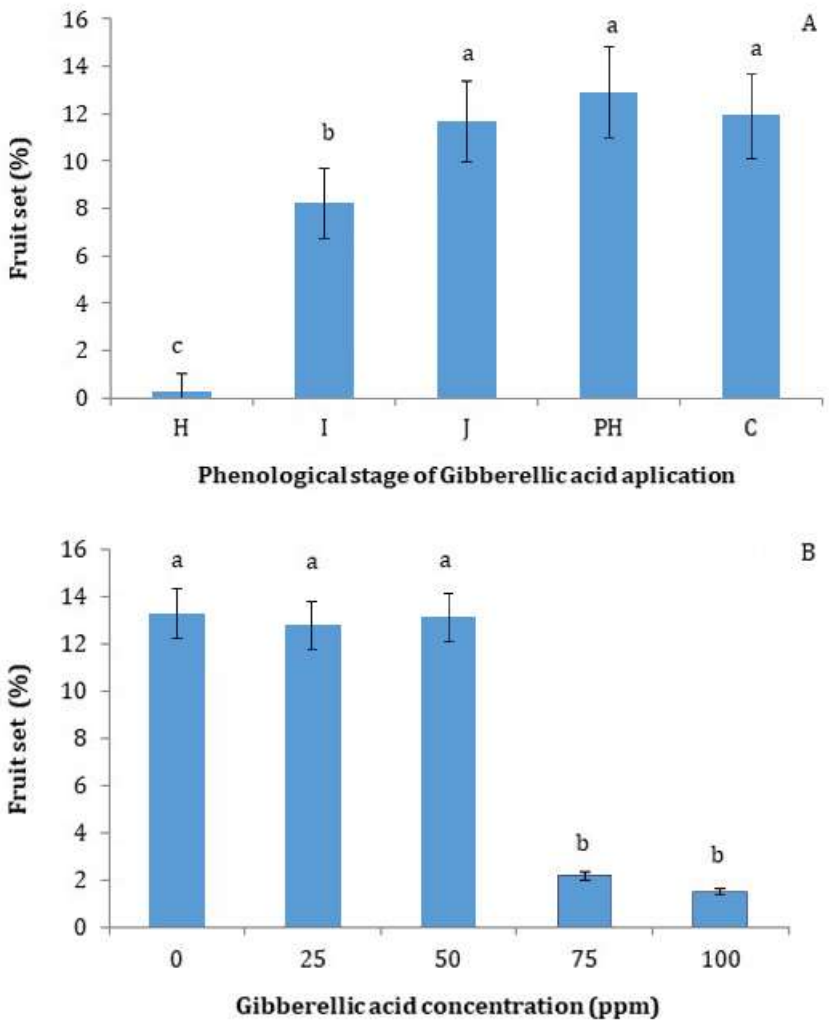

Means with different letters within columns indicate significant differences according to the DGC test ($P < 0.05$). Vertical bars represent standard error. H stage: fruit set; I stage: young fruit; J stage: fruit near final size; PH: post-harvest, one week after harvest; C: control, plants not treated.

Medias con diferentes letras en las columnas indican diferencias significativas según test DGC ($P < 0,05$). Barras verticales corresponden al error estándar. Estado H: cuajado de frutos; Estado I: frutos jóvenes; Estado J: fruto alcanzando el tamaño final; Estado PH: poscosecha, una semana posterior a la cosecha; C: Control, plantas sin tratamiento con AG.

Figure 3. Fruit set (%) of 'd'Agen' plum plants: (A) treated with 100 ppm gibberellic acid (GA) at different phenological stages during the previous growing season, and (B) in response to different concentrations of gibberellic acid (GA) treatments applied at the phenological stage H of the previous season.

Figura 3. Cuajado de frutos (%) de plantas de ciruelo 'd'Agen': (A) tratadas con 100 ppm de ácido giberélico (AG) en diferentes estados fenológicos en la estación de crecimiento previa, y (B) en respuesta a tratamientos con diferentes concentraciones de AG aplicadas en el estado fenológico H (cuajado de frutos) durante la estación de crecimiento previa.

The reduction in flower density and fruit set percentage induced by 100 ppm GA applied at the phenological stage H in the previous growing season resulted in a decrease in the number of fruits per tree and total fruit yield, which decreased from over 30 kg per tree in the control to just over 8 kg per tree in the GA-treated trees (table 1, page 10). In contrast, the reduction in fruit set induced by GA at stage I had a significant effect on the number of fruits per plant and per unit of TCSA, but no effect on fruit weight or total fruit yield (table 1, page 10).

In the second year, significant differences were observed among GA treatments for all yield components. Treatments with higher GA concentrations resulted in greater reductions in crop load, both expressed as fruits per tree and per unit TCSA, as well as in total fruit yield (table 1, page 10). The 75 and 100 ppm GA treatments showed no significant differences in yield components, except for fruit weight. In contrast, the 25 and 50 ppm GA treatments and the control trees differed from each other and from the higher GA treatments in most of the parameters evaluated.

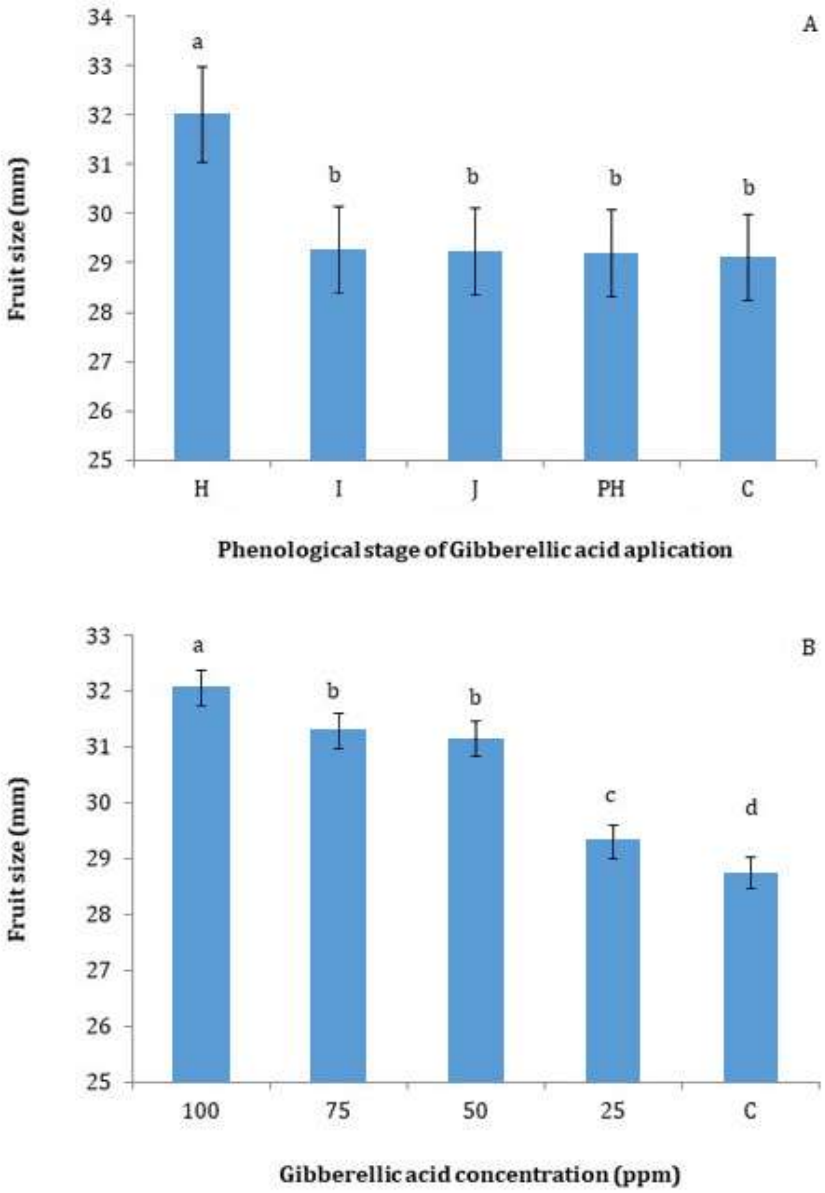

Columns with different letters indicate significant differences according to DGC test ($P < 0.05$). Vertical bars represent standard error. H stage: fruit set; I stage: young fruit; J stage: fruit near final size; Post-harvest: one week after harvest; Control: untreated plants.

Medias con diferentes letras en las columnas indican diferencias significativas según test DGC ($P < 0,05$). Barras verticales corresponden al error estándar. Estado H: cuajado de frutos; Estado I: frutos jóvenes; Estado J: fruto alcanzando el tamaño final; Estado PH: poscosecha, una semana posterior a la cosecha; C: Control, plantas sin tratamiento con AG.

Figure 4. Fruit size (mm) at harvest of 'd'Agen' plums, (A) treated with 100 ppm gibberellic acid (GA) at different phenological stages during the previous growing season, and (B) as a function of different GA concentrations (ppm) applied at the pit-hardening stage of the previous season.

Figura 4. Tamaño de frutos (mm) a cosecha del ciruelo 'd'Agen', (A) tratados con 100 ppm de ácido giberélico (AG) en diferentes estados fenológicos durante la estación de crecimiento previa, y (B) en función de diferentes concentraciones (ppm) de AG aplicadas en el estado de endurecimiento de carozo durante la estación de crecimiento previa.

Notably, crop load in the second year was about a quarter of that observed in the first year. This reduction was attributed to high temperatures and "Zonda" winds during full flowering, followed by spring frosts at the fruit set stage, which is the most sensitive period to frost (4). These events hindered the establishment of optimal gibberellin concentration for 'd'Agen' plums in our trials. In a year marked by extreme weather conditions, the reduction in flower density resulting from the application of GA at flower induction had a detrimental effect on the fruit yield per tree.

Table 1. Yield components of 'd'Agen' plums, (A) treated with 100 ppm gibberellic acid (GA) at different phenological stages during the previous growing season and (B) treated with different concentrations of GA in the previous growing season at fruit set (phenological stage H).

Tabla 1. Componentes del rendimiento del ciruelo 'd'Agen', (A) tratamientos con 100 ppm de ácido giberélico (AG) en diferentes estados fenológicos durante la estación de crecimiento previa, y (B) tratamientos con diferente concentración de AG en la estación de crecimiento previa en el estado fenológico de cuajado de frutos (estado H).

(A) Phenological stage	Crop load		Fruit weight (g fruit^{-1})	Fruit yield (Kg pl^{-1})	(B) GA (ppm)	Crop load		Fruit weight (g fruit^{-1})	Fruit yield (Kg pl^{-1})
	Fruits pl^{-1}	Fruits cm^{-2} TCSA				Fruits pl^{-1}	Fruits cm^{-2} TCSA		
Control	2178.7 ^{a}	38.7 ^{a}	15.7 ^{b}	34.6 ^{a}	0	542.4 ^{a}	10.1^{a}	17.9 ^{d}	10.6 ^{a}
Stage H	377.8 ^{c}	6.8 ^{c}	21.5 ^{a}	8.1 ^{b}	25	393.7 ^{b}	7.5 ^{b}	18.5 ^{c}	7.1 ^{b}
Stage I	2111.4 ^{b}	38.4 ^{b}	15.6 ^{b}	30.9 ^{a}	50	281.1^{c}	5.3 ^{c}	20.1 ^{b}	5.3 ^{c}
Stage J	2180.7 ^{a}	39.5 ^{a}	15.9 ^{b}	32.4 ^{a}	75	219.9 ^{d}	4.2 ^{d}	20.4 ^{b}	4.0 ^{d}
PH	2182.6 ^{a}	39.5 ^{a}	16.8 ^{b}	35.7 ^{a}	100	199.8 ^{d}	3.8 ^{d}	21.1 ^{a}	3.9 ^{d}

Different letters in the rows indicate significant differences between treatments according to DGC test (P<0.05).

References: H stage: fruit set; I stage: young fruit; J stage: fruit near final size; PH: post-harvest, one week after harvest; Control: plants not treated; GA: gibberellic acid.

Letras distintas en las celdas de cada columna indican diferencias significativas entre tratamientos según el test DGC (P<0,05).

Referencias: Estado H: cuajado de frutos; Estado I: frutos jóvenes; Estado J: fruto alcanzando el tamaño final; PH: poscosecha, una semana posterior a la cosecha; C: Control, sin tratamiento; GA: ácido giberélico.

When data on fruit number and size from both years are plotted on a single graph, it is observed that the initial phase of the experiment was characterized by a high crop load (2,178 fruits per tree in the control), with a negative linear correlation between fruit size and crop load (figure 5). This behavior has been observed in plums (5), and peaches (6, 12). Data from the second year showed a tendency on the left side of the graph, with fruit weight values slightly below the trend observed in the first year, but with increased variation in fruit size relative to crop load (figure 5). This response can be explained by the greater sensitivity of fruit size to change in the low crop load range of the response curve compared to the high crop load range, where fruit size tends to stabilize at lower values (11).

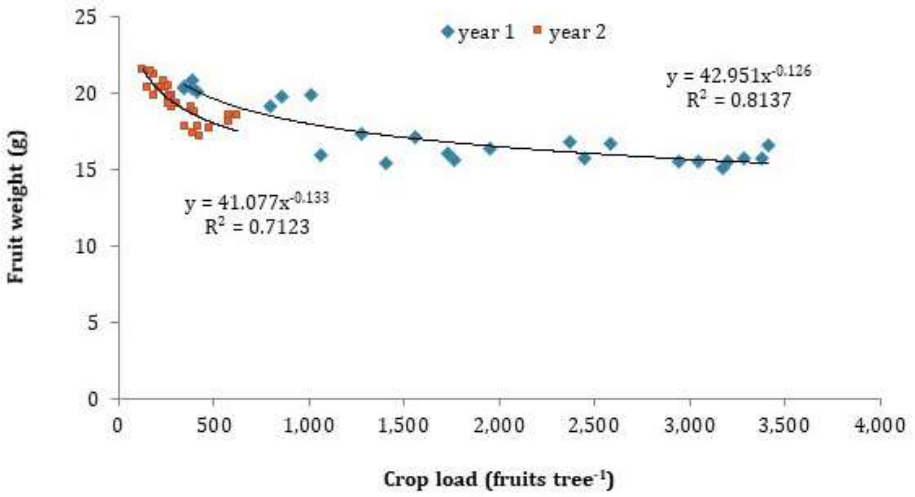

Figure 5. Relationship between crop load (fruits per plant) and fruit weight (g) over two growing seasons in 'd'Agen' plum. Data were collected during the 2019/2020 and 2020/2021.

Figura 5. Relación entre carga (frutos por planta) y peso de fruto (g) de dos estaciones de crecimiento de ciruelo 'd'Agen'. Datos correspondientes a 2019/2020 y 2020/2021.

Fruit load in the second year was nearly one-quarter of that measured in the first year, while fruit size in the control treatment increased by only 2.2 g (14%) compared to the first year. In general, a reduction in flowering density in stone fruit trees allows for an increase in fruit size, although this typically results in a decrease in yield. This phenomenon has been observed in peach (6), nectarine, and cherry (2), as well as in European and Japanese plums (11).

Growth of individual plant organs can be constrained by assimilation capacity (source limitation) or the ability to utilize assimilates (sink limitation) (2). Fruit capacity to absorb assimilates is considered the primary factor influencing competition for these resources. This capacity is initially determined by flower quality, which is influenced by the nature of the inflorescence and the number of flowers produced per tree (5). Furthermore, the sink capacity may be affected by late frosts or other unfavorable environmental conditions that influence embryo growth. Such damage may result in premature fruit drop or become apparent during the ripening process. These factors can influence the shape, appearance, or size of the fruits (4). This may explain the limited response in fruit size during the second year of the study. Despite a reduction in crop loads compared to the previous year, no discernible difference in fruit size was observed between the two years. In situations where crop loads are low and the growing environment is conducive, source limitations are considered negligible, and sink strength becomes the main determinant of growth. This is representative of the second year of the study, during which each fruit tends to achieve its potential size or weight. Consequently, it is reasonable to hypothesize that the climatic adversities experienced during the second year affected sink strength and constrained fruit size, despite the low competition among developing fruits.

A positive correlation (r^2= 0.84) was observed between floral density and fruit set for the two growing seasons. However, when the 75 and 100 ppm gibberellin treatments, which directly affected fruit set, were excluded from the analysis, fruit set percentage was not influenced by floral density. This pattern was consistent across a wide range of flowering densities, from 40 to 250 flowers per square centimeter of branch. This finding is consistent with those reported for peach (15). Consequently, a positive linear relationship was evident between floral density and fruit yield in the 'd'Agen' plum trees ($y = 0.1496x + 1.65$; $r^2 = 0.86$).

To achieve a yield of between 20,000 and 25,000 kg ha^{-1} (30–35 kg per tree) for 'd'Agen' plums, it is necessary to have a crop load of between 2,000 and 2,500 fruits per plant. This corresponds to an average fruit size of approximately 29 mm or between 16.0 and 16.5 g per fruit, as evidenced by the data obtained in this experiment. These values align with the typical dimensions of a small plum, and achieving at least 20 grams per fruit is necessary to reach the medium size category.

To reach the target yield components mentioned above, a floral density of over 150 flowers per cm^2 of branch is required. The lowest gibberellin dose used in the present study (25 ppm) resulted in a reduction in floral density of approximately 60%, with values falling below 100 flowers per cm^2. This is insufficient to achieve the anticipated yield components. Therefore, reducing floral density to improve fruit size of 'd'Agen' plum without a significant reduction in yield would require the use of a gibberellin concentration lower than 25 ppm, not evaluated in this study.

On the other hand, the most consistent response in increased fruit size was observed with a crop load under 1,000 fruits per tree (figure 5, page 10), insufficient for an acceptable fruit yield. Therefore, the reduction in floral density should be less drastic than that achieved in this study. Moreover, agronomic management should be complemented with practices that promote the final fruit size. These included adjustments to pruning techniques, fertilization, irrigation during critical periods of the crop, and direct techniques aimed at improving fruit size (12).

Conclusions

The reduction of flowering density with gibberellic acid application during the previous growing season allowed the determination that the phenological stage of fruit set (stage H, occurring five weeks after full bloom) corresponds to the moment of floral induction for 'd'Agen' plums. Gibberellic acid application effectively reduced floral density and modified

fruit size at harvest. However, all tested concentrations excessively reduce the floral density needed to achieve an acceptable fruit yield. Therefore, future research should focus on evaluating gibberellic acid concentrations below 25 ppm, and refining this technique in response to interannual variability.

References

1. Agustí, M.; Reig, C.; Martínez-Fuentes, A.; Mesejo, C. 2022. Advances in Citrus flowering: A review. Frontiers in plant science. 13:868831. DOI: 10.3389/fpls.2022.868831
2. Cerri, M.; Rosati, A.; Famiani, F.; Reale, L. 2019. Fruit size in different plum species (genus *Prunus* L.) is determined by postbloom developmental processes and not by ovary characteristics at anthesis. Scientia Horticulturae. 255: 1-7. DOI:10.1016/j.scienta.2019.04.064
3. Di Rienzo, J. A.; Casanoves, F.; Balzarini, M. G.; González, L.; Tablada, M.; Robledo, C. W. 2020. InfoStat 2020. Centro de Transferencia InfoStat. FCA. Universidad Nacional de Córdoba. Argentina. http://www.infostat.com.ar
4. Drepper, B.; Bamps, B.; Gobin, A.; Van Orshoven, J. 2021. Strategies for managing spring frost risks in orchards: effectiveness and conditionality-A systematic review protocol. Environmental Evidence. 10: 32. DOI:10.1186/s13750-021-00247-7
5. Erogul, D.; Sen, F. 2015. Effects of gibberellic acid treatments on fruit thinning and fruit quality in Japanese plum (*Prunus salicina* Lindl.). Scientia Horticulturae. 186: 137-142. DOI:10.1016/j.scienta.2015.02.019
6. Giovanaz, M. A.; Fachinello, J. C.; Spagnol, D.; Weber, D.; Carra, B. 2016. Gibberellic acid reduces flowering and time of manual thinning in "Maciel" peach trees. Revista Brasileira de Fruticultura. 38(2): e-692. DOI:10.1590/0100-29452016692
7. IDR (Instituto de Desarrollo Rural). 2015. Informe por producto: Panorama del Sector Ciruela Deshidratada de Mendoza. Argentina http://www.idr.org.ar/wp-content/uploads/2016/04/Panorama-Ciruela-deshidratada-2015-.pdf/ (Access: 29 April 2025).
8. IDR (Instituto de Desarrollo Rural). 2020. Informe anual: Fenología de frutales 2020. Mendoza. Argentina. https://www.idr.org.ar/fenologia-de-frutales/ (Access: 29 April 2025).
9. IDR (Instituto de Desarrollo Rural). 2021. Censo de ciruela para industria. Producción primaria. Recolección geoespacial de producción primaria e industrial. Mendoza. Argentina https://www.idr.org.ar/wp-content/uploads/2022/10/censo_produccion_ primaria.pdf (Access: 29 April 2025).
10. Kaur, A.; Maness, N.; Ferguson, L.; Deng, W.; Zhang, L. 2021. Role of plant hormones in flowering and exogenous hormone application in fruit/nut trees: a review of pecans. Fruit Research. 1: 15. DOI:10.48130/FruRes-2021-0015
11. Lammerich, S.; Kunz, A.; Damerow, L.; Blanke, M. 2020. Mechanical crop load management (CLM) improves fruit quality and reduces fruit drop and alternate bearing in European plum (*Prunus domestica* L.). Horticulturae. 6: 52. DOI:10.3390/horticulturae6030052
12. Reginato, G.; Sotomayor, J. P. 2020. Cómo cosechar para obtener fruta de calidad en ciruelo europeo. Extension UC Davis Chile. https://www.plataformaextension.cl/ciclos/ciruelo-europeo/ (Access: 29 April 2025).
13. Sidhu, R. S.; Bound, S. A.; Hunt, I. 2022. Crop load and thinning methods impact yield, nutrient content, fruit quality, and physiological disorders in 'Scilate' apples. Agronomy. 12: 1989. DOI:10.3390/agronomy12091989
14. Wang, S.; Wang, Q.; Jiang, W.; Wang, Y.; Yan, J.; Li, X.; Wang, J.; Guan, Q.; Ma, F.; Zhang, J.; Zheng, Q.; Zou, Y.; Xu, J. 2024. Evaluating the sustainable cultivation of 'Fuji' apples: suitable crop load and the impact of chemical thinning agents on fruit quality and transcription. Fruit Research. 4: e009. DOI: 10.48130/frures-0024-0002
15. Yañez Toro, R. M. 2019. Regulación de la carga frutal en duraznero y nectarino (*Prunus pérsica*) cvs. Elegant Lady y Ruby Diamond mediante el uso de giberelinas y su efecto sobre el retorno floral bajo las condiciones de Chile central. Master's thesis, Agronomy and Forest Engineering Course. Pontificia Católica de Chile University.
16. Zhebentyayeva, T.; Shankar, V.; Scorza, R.; Callahan, A.; Ravelonandro, M.; Castro, S.; DeJong, T.; Saski, C. A.; Dardick, C. 2019. Genetic characterization of worldwide *Prunus domestica* (plum) germplasm using sequence-based genotyping. Horticulture Research. 6: 12. DOI:10.1038/s41438-018-0090-6

Acknowledgements

This study was funded by INTA in collaboration with Universidad Nacional del Litoral (CAI+D 2024, 85420240100028LI; and PEICID-2023-045).

The Native Dryland PGPR '*Pseudomonas* 42P4' Promotes Adventitious Rooting in Woody Cuttings of *Vitis* spp.

La PGPR nativa de zonas áridas '*Pseudomonas* 42P4' promueve la fomación de raíces adventicias en estacas leñosas de *Vitis* spp.

Maria Gabriela Gordillo [1], Ana Carmen Cohen [1, 2], Fanny Colombo [3], Carina Verónica González [1, 2*]

Originales: *Recepción:* 16/04/2025 - *Aceptación:* 06/07/2025

Abstract

This study evaluated the effect of two native PGPR strains from an arid region (Mendoza, Argentina) on the rooting of woody cuttings of *Vitis* spp. These strains are known for their growth-promoting capacity, including auxin production. Dormant *V. vinifera* cv. Malbec cuttings were grafted onto four rootstocks - 1103 Paulsen, 110 Richter, 101-14 MGt and SO4. Then, basal ends of these grafted cuttings and own rooted controls were incubated for 12 h in solutions of (1) *Pseudomonas* 42P4 at 10^7 CFU mL^{-1}, (2) *Enterobacter* 64S1 at 10^7 CFU mL^{-1}, (3) autoclaved LB medium, (4) water, and (5) a quick-dip immersion of Indole-3-butyric acid (IBA). After treatment, the cuttings were placed in a forcing chamber at 28°C and relative humidity ~100% for 21 days. Rooting parameters and scion-rootstock union percentages were recorded. *Pseudomonas* 42P4 significantly promoted rooting in Malbec own-rooted cuttings. However, *Enterobacter* 64S1 had negative or null effects. Furthermore, *Pseudomonas* 42P4 enhanced rooting in Malbec grafted onto 1103 Paulsen, but not on 101-14 MGt, 110 Richter or SO4. This strain also improved graft union success on SO4, but did not affect the other rootstocks. These results suggest that a dryland native strain such as Pseudomonas 42P4 could sustainably enhance the quality of both own-rooted and grafted grapevine plants in commercial nurseries.

Keywords
PGPR • grapevine rootstock • Malbec • rooting • graft union • nursery

1 Universidad Nacional de Cuyo. Facultad de Ciencias Agrarias. Instituto de Biología Agrícola de Mendoza (IBAM-CONICET). Almirante Brown 500. Chacras de Coria. M5528AHB. Mendoza. Argentina. * cgonzalez@fca.uncu.edu.ar
2 Universidad Nacional de Cuyo. Facultad de Ciencias Agrarias. Almirante Brown 500. Chacras de Coria. M5528AHB. Mendoza. Argentina.
3 Trapiche Winery. Calle Nueva Mayorga s/n. Maipú. Mendoza. Argentina. CPA: M5513.

Resumen

El objetivo de este estudio fue evaluar el efecto de dos cepas PGPR nativas de zonas áridas (Mendoza, Argentina) con capacidad promotora del crecimiento (que producen auxinas) sobre el enraizamiento de estacas leñosas de *Vitis* spp. La base de las estacas de *Vitis vinifera* cv. Malbec, tanto francas como injertadas sobre cuatro portainjertos:1103 Paulsen, 110 Richter, 101-14 MGt y SO4, se incubaron durante 12 h en soluciones de 1) *Pseudomonas* 42P4 y 2) *Enterobacter* 64S1 10^7 UFC mL^{-1}, 3) medio LB autoclavado, 4) agua y 5) una inmersión rápida de ácido indol-3-butírico (IBA). Posteriormente, las estacas se colocaron en una cámara de forzadura a 28°C y humedad relativa ~100% durante 21 d. Se midieron diferentes parámetros de enraizamiento y el porcentaje de unión del injerto. Los resultados mostraron que *Pseudomonas* 42P4, pero no *Enterobacter* 64S1 promovió el enraizamiento, de forma similar a IBA en estacas de Malbec. La cepa *Pseudomonas* 42P4 también promovió el enraizamiento de estacas injertadas sobre 1103 Paulsen, pero no sobre 101-14, 110 Richter y SO4. Además, *Pseudomonas* promovió la unión del injerto en SO4, pero no en 110 Richter, 1103 Paulsen y 101-14. Estos resultados sugieren que una cepa nativa de zonas áridas podría utilizarse como una herramienta sustentable para mejorar la calidad de plantas francas e injertadas de vid.

Palabras clave
PGPR • portainjertos de vid • Malbec • enraizamiento • unión del injerto • vivero

Introduction

A significant portion of worldwide agricultural land (45%) is dryland. Climate change (CC) threatens agroecosystems, causing detrimental effects on crop productivity (Berdugo *et al.*, 2020; Burrel *et al.*, 2020). Viticulture covers 7.3 million hectares of the world, with over 60% of grapes produced in drylands (OIV 2023; Flexas *et al.*, 2010). Argentina ranks seventh, with the largest cultivated vineyard area globally. This country mainly develops irrigated viticulture in drylands (OIV 2023, INV 2023).

Grapevines are clonally propagated through one-year woody cuttings. Grafted or ungrafted woody cuttings are forced under high relative humidity (RH) and ± 27°C to stimulate adventitious root formation and scion-rootstock healing (in grafted plants). External factors (temperature, humidity, substrate aeration) and internal factors (carbohydrate reserves, hormones, and genotype) influence these processes (Hartmann *et al.*, 2014).

Rootstocks exhibit resistance to pathogens and diseases, and confer tolerance to abiotic stresses (Hartmann *et al.*, 2014; Ollat *et al.*, 2016, Keller, 2020, D'Innocenzo *et al.*, 2024). *V. vinifera* cultivars are generally grafted onto American *Vitis* spp. hybrid rootstocks due to their resistance to phylloxera (Mudge *et al.*, 2009). Grafting is essential in most European wine-growing regions. However, outside Europe, vineyards can be planted with own-rooted *V. vinifera* plants.

One main problem in grapevine propagation is the differential rooting capacity of rootstocks. Rootstocks 110 Richter (110 R) and Selection Oppenheim 4 (SO4) are recalcitrant to form adventitious roots. This differs from other widely used grapevine rootstocks like 1103 Paulsen (1103 P) and 101-14 Millardet et de Grasset (101-14 MGt), which induce more root development (Keller, 2020). Low rooting capacity causes significant economic losses to nurseries. Additionally, scion-rootstock interaction plays a crucial role in rooting. The scion may affect root dry weight per woody cutting (Tandonnet *et al.*, 2009), as the scion-rootstock union simultaneously occurs with rooting, depending on cutting reserves.

Auxins are the main phytohormones in adventitious root production of woody cuttings (Burnoni *et al.*, 2022), though their effect varies among genotypes. For example, indole-3-butyric acid (IBA), a primary synthetic auxin used for grapevine rooting (Machado *et al.*, 2005), promotes rooting in woody cutting of 110 R, SO4 and 101-14 MGt (Gordillo *et al.*, 2022; Satisha *et al.*, 2008). In contrast, IBA may promote (Satisha *et al.*, 2008; Daskalakis *et al.*, 2018) or not (Boeno *et al.*, 2023; Gordillo *et al.*, 2022) rooting of 1103 P woody cuttings. However, synthetic agrochemicals are progressively being excluded as organic and agroecological agriculture gains attention (Centeno *et al.*, 2008).

Plant Growth-Promoting Rhizobacteria (PGPR) are plant symbiotic bacteria that colonize the rhizosphere and produce indole acetic acid (IAA)-type auxins (Glick *et al.*, 2012; Pantoja Guerra *et al*., 2023). Some PGPR strains promote rooting of difficult-to-root rootstocks, while others have no effect (Isçi *et al*., 2019; Toffanin *et al.*, 2016). Our group isolated and characterized two PGPR strains from Mendoza´s arid soils of Argentina. *Pseudomonas* 42P4 (42P4) and *Enterobacter* 64S1 (64S1) produce IAA (Pérez-Rodríguez *et al.*, 2020a) and promote seedling growth of *Solanum lycopersicum* (Pérez-Rodríguez *et al.*, 2022) and *Capsicum annuum* seedlings (Lobato Ureche *et al.*, 2021), alleviate saline stress in tomato (Pérez-Rodríguez *et al.*, 2022), and increase drought tolerance in *Arabidopsis thaliana* plants (Jofré *et al.*, 2024). Furthermore, *Pseudomonas* 42P4 enhances tomato growth, yield and fruit quality under field conditions (Pérez-Rodríguez *et al.*, 2020b). Both strains also exhibit biocontrol activity, inhibiting tomato and pepper crop diseases (unpublished data). Native strains easily adapt to edaphic conditions, resist local environmental stresses, and are more successful when inoculated into the plant rhizosphere.

PGPR improve rooting and survival of young plants of various species. However, few studies report PGPR´s effect on woody plant production or grapevine woody cuttings, specifically (Bartolini *et al.*, 2017; Köse *et al.*, 2003, 2005; Tofanin *et al.*, 2016). Currently, exploring sustainable tools is imperative, especially given global warming threats, particularly challenging in drylands.

Therefore, this work evaluated the effect of two native PGPR strains from Mendoza's arid soils, *Pseudomonas* 42P4 and *Enterobacter* 64S1, on adventitious root production of the Argentinean emblematic cultivar: Malbec, and the four most widespread rootstocks in global viticulture and Argentine arid areas: SO4, 110 R, 1103 P, and 101-14 MGt (Riaz *et al.*, 2019). These strains, adapted to arid soils, could constitute a sustainable alternative for synthetic agrochemicals in grapevine propagation.

Materials and Methods

Bacterial Culture

Pseudomonas 42P4 (42P4) and *Enterobacter* 64S1 (64S1) were collected, isolated and characterized by the Plant Physiology and Microbiology Group (IBAM- FCA, CONICET-UNCuyo, Mendoza, Argentina). The partial 16S rRNA sequence of both strains was deposited in GenBank under accession numbers MT045993.1 and MT047267, respectively (Pérez-Rodríguez *et al.*, 2020a). Inocula were prepared in 1 L Erlenmeyer Flask with 400 mL of Luria Broth (LB) culture medium (10 g Peptone, 5 g Yeast Extract, 5 g NaCl in 1 L of bidistilled H_2O). Bacteria were cultured in an orbital shaker at 120 rpm and 32°C for 24 h. Strain concentration was estimated by optical density at 540 nm in a spectrophotometer according to Pérez-Rodriguez *et al*. (2020a). From these cultures, a dilution to 10^7 colony-forming units (CFU) mL^{-1} was prepared for each strain in PBS (phosphate buffer saline).

Plant Material, Inoculation and Rooting Conditions

Two experiments were conducted in the grapevine nursery of Grupo Peñaflor S.A. (Trapiche Winery), located in Santa Rosa, Mendoza, Argentina (33°15'39.4" S 68°07'48.9" W). The first experiment was conducted during the 2020 season (September-October) and the second, in 2021. Cuttings (length: 40 cm and diameter: 9 mm) were collected in winter and stored at 4°C until experiment initiation.

In the first experiment, we tested different doses of *Pseudomonas* 42P4 and *Enterobacter* 64S1 on the rooting capacity of *V. vinifera* cv. Malbec woody cuttings. Before forcing, we applied five treatments: (1) 30-second quick immersion in 1000 ppm IBA solution (Gordillo *et al*. 2022); or 12-hour incubation in solutions of: (2) *Pseudomonas* 42P4 at 10^7 CFU mL^{-1}, (3) *Enterobacter* 64S1 at 10^7 CFU mL^{-1}, (4) autoclaved LB, and (5) tap water (control treatment) on the base (1.5 cm) of 50 woody cuttings per treatment.

In a second experiment, we evaluated *Pseudomonas* 42P4 on the rooting of Malbec cuttings (with 2 buds and approximately 5 cm long) grafted onto cuttings of 101-14 MGt (*V. riparia* × *V. rupestris*), SO4 (*V. berlandieri* × *V. riparia*), 1103 Paulsen, and 110 Richter

(*V. berlandieri* × *V. rupestris*), with 5 buds (approximately 35 cm long and 9 mm in diameter). We used an Omega grafting machine (Fornasier Cesare & C., Italy). Each grafted cutting was 40 cm long. The grafting zone was covered with a commercial initiation wax (Guerowax Crecimiento 78, Guerola Industries, Spain) to prevent dehydration and diseases during forcing. Before forcing we applied the following treatments: (1) a 30-second quick immersion at 750 ppm IBA (Gordillo *et al*. 2022), and 12-hour incubations with: (2) *Pseudomonas* 42P4 at 10^7 CFU mL^{-1}, (3) autoclaved LB, and (4) tap water (control) on the base (1.5 cm) of 50 grafted cuttings per treatment.

Subsequently, in both experiments, cuttings were horizontally placed in plastic boxes with peat (KEKKILÄ professional, https://www.kekkilaprofessional.com/). Then, cuttings were forced and maintained for 21 days at 28°C and 100% RH.

The experimental design was a completely randomized design, considering each cutting as an experimental unit.

Morphological Parameters

Treatment effect was evaluated by callus and rooting percentages, followed by root number and biomass (g) per cutting. Rooting percentage is the percentage of cuttings that produced at least one root. Callus percentage was visually determined as the proportion of the cutting base occupied by callus (0-25, 25-50, 50-75, and 75-100%). Root biomass was determined as dry weight (DW) of all adventitious roots from a cutting, oven-dried at 60°C to constant weight. In grafted cuttings, the percentage of scion-rootstock union was visually determined as well (0-25, 25-50, 50-75, and 75-100%).

Statistical Analysis

Statistical analyses were performed using the InfoStat P 2020v software (Di Rienzo *et al.*, 2020). Rooting, callus and graft union percentages, along with root number and biomass, were analysed with Generalized Linear Models. A binomial distribution was used for the first three parameters and the Poisson distribution for the fourth. Root biomass was first tested for ANOVA assumptions (using Shapiro-Wilks test for normality and Levene test for homoscedasticity). Different letters indicate significant differences among treatments according to the post-hoc test DGC ($\alpha = 0.05$). Data visualization was conducted in R (R Core Team, 2024) and the ggplot2 package (Wickham, 2016).

Results

Own-rooted Malbec cuttings

Basal callus percentage on Malbec was similar among treatments (>75%, $p > 0.05$) (figure 1A, page 17). *Pseudomonas* 42P4 and IBA 1000 ppm increased rooting percentage (>80%), compared to autoclaved LB and water treatments (70%). However, *Enterobacter* 64S1 decreased rooting percentage (25%) compared to water (figure 1B, page 17). The number of roots per cutting was similar in cuttings incubated with 42P4 and IBA (~ 6 roots per cutting), and higher than in the remaining treatments (~ 4 roots per cutting) (figure 1C, page 17). Root biomass per cutting was 30% higher in cuttings incubated in IBA than in 42P4. The remaining treatments yielded lower biomass (figure 1D, page 17). *Pseudomonas* 42P4 promoted three of the four rooting parameters compared to the water control: rooting percentage, number of roots per cutting, and root biomass. In contrast, the native *Enterobacter* 64S1 strain did not promote any evaluated parameter.

Based on these results, we assessed the ability of the native *Pseudomonas* 42P4 strain (but not *Enterobacter*) to promote rooting and graft union of Malbec cuttings grafted onto four grapevine rootstocks.

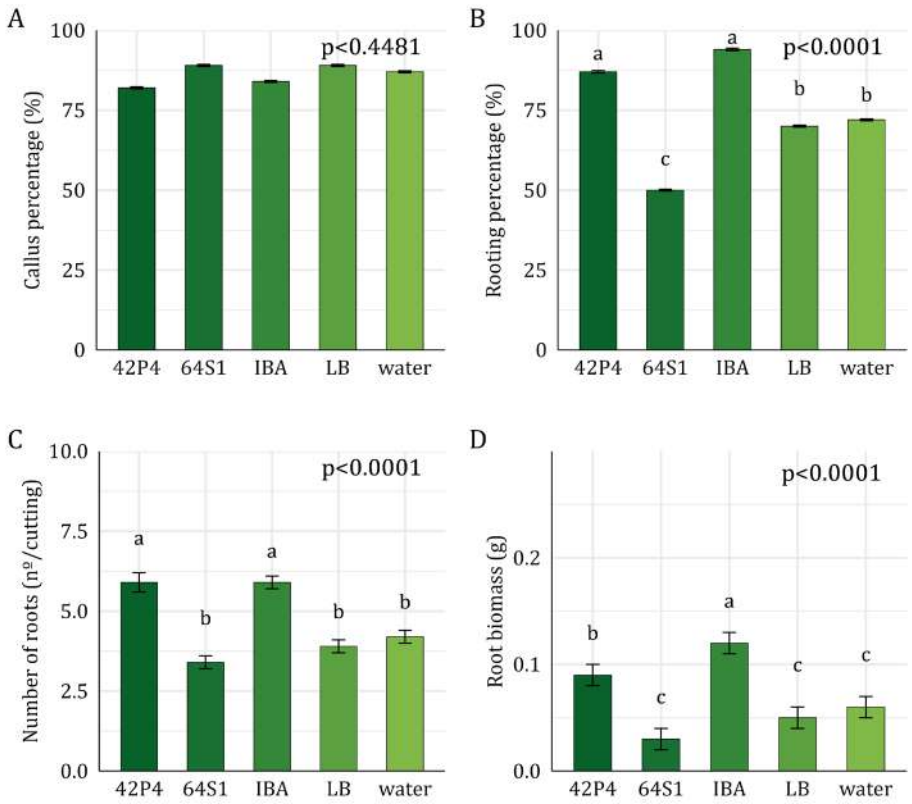

A) Callus percentage, B) Rooting percentage, C) Number of roots per cutting, and D) Root biomass per cutting.

Values correspond to adjusted means ± SEM (n=50). Data were analysed with General or Generalized Mixed Linear Models. Different letters indicate significant differences among treatments according to the post-hoc test DGC (α = 0.05).

42P4: *Pseudomonas* 42P4, 64S1: *Enterobacter* 64S1, IBA: Indole-3-butyric acid, LB: Luria Broth culture medium, water: tap water.

A) Porcentaje de callo, B) Porcentaje de enraizamiento, C) Número de raíces por estaca y D) Biomasa de raíces por estaca.

Los valores corresponden a las medias ajustadas ± EE (n=50). Los datos fueron analizados mediante Modelos Lineales Mixtos Generales o Generalizados. Letras diferentes indican diferencias significativas entre tratamientos según el test post-hoc DGC (α = 0,05).

42P4: *Pseudomonas* 42P4, 64S1: *Enterobacter* 64S1, IBA: ácido indol-3-butírico, LB: medio de cultivo Luria Broth, water: agua de red.

Figure 1. Own-rooted Malbec cuttings.

Figura 1. Estacas de Malbec a pie franco.

Grafted Cuttings

1103 Paulsen

The graft union percentage (~75%) between Malbec and 1103 P rootstock, and callus percentage (~100%, p > 0.05, data not shown) were unaffected by treatments (figure 2A, page 18). Rooting percentage was higher (~90%) in cuttings incubated with *Pseudomonas* 42P4 (figure 2B, page 18) than in other treatments (~75%). The number of roots per cutting was duplicated in 42P4 and IBA treatments than in the controls (water and LB) (figure 2C, page 18). However, root biomass was 10% higher in cuttings incubated with 42P4 and IBA compared to the other treatments (figure 2D, page 18). *Pseudomonas* 42P4 promoted a 15% increase in rooting percentage compared to IBA, while matching root number and biomass results to this hormone treatment.

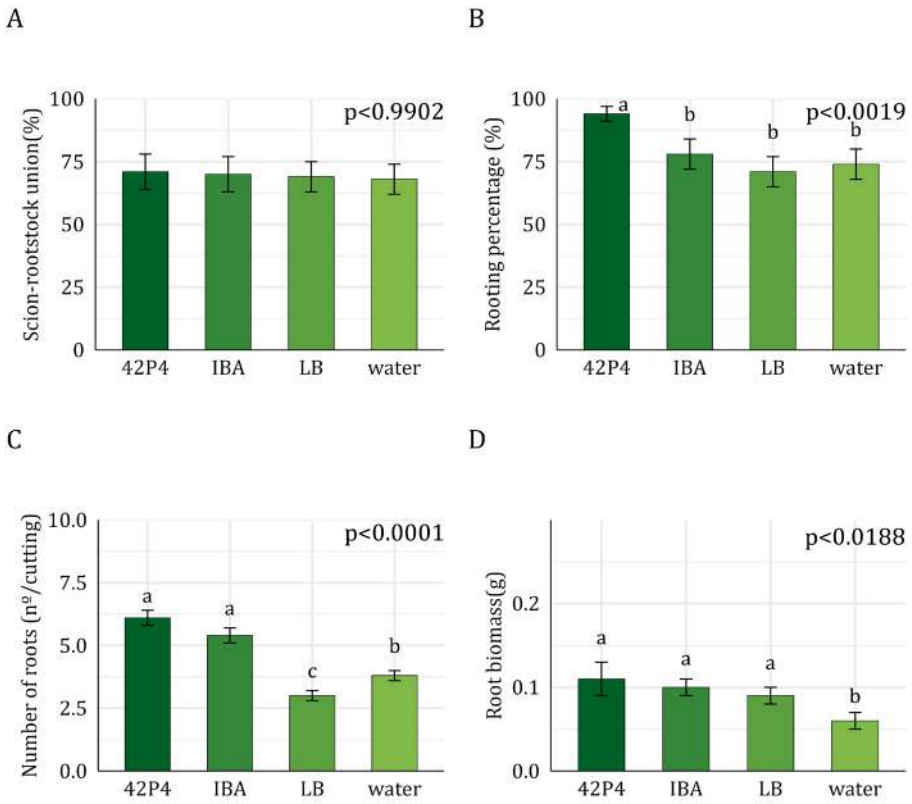

A) Scion-rootstock union percentage, B) Rooting percentage, C) Number of roots per cutting, and D) Root biomass per cutting. Values correspond to adjusted means ± SEM (n=50). Data were analysed with General or Generalized Linear Models. Different letters indicate significant differences between treatments according to the post-hoc test DGC (α = 0.05). 42P4: *Pseudomonas* 42P4, 64S1: *Enterobacter* 64S1, IBA: Indole-3-butyric acid, LB: Luria Broth culture medium, water: tap water.

A) Porcentaje de unión entre la púa y el portainjerto, B) Porcentaje de enraizamiento, C) Número de raíces por estaca y D) Biomasa de raíces por estaca. Los valores corresponden a las medias ajustadas ± EE (n=50). Los datos fueron analizados mediante Modelos Lineales Mixtos Generales o Generalizados. Letras diferentes indican diferencias significativas entre tratamientos según el test post-hoc DGC (α = 0,05). 42P4: *Pseudomonas* 42P4, 64S1: *Enterobacter* 64S1, IBA: ácido indol-3-butírico, LB: medio de cultivo Luria Broth, water: agua de red.

Figure 2. Rootstock 1103 Paulsen.

Figura 2. Portainjerto 1103 Paulsen.

101-14 MGt

The scion-rootstock union percentage between Malbec and 101-14 MGt rootstock decreased by 25% when cuttings were incubated with IBA compared to the other treatments (figure 3A, page 19). Callus percentage (~100%, p>0.05) (data not shown), rooting percentage (~100%), and root biomass of 101-14 MGt were not affected by the treatments (figure 3B and 3D, page 19). The IBA treatment increased the number of roots per cutting (20 roots per cutting) compared to the water control (10 roots per cutting) (figure 3C, page 19), while 42P4 and LB treatments decreased this variable to 7 roots per cutting compared to the water control. Inoculation of 101-14 rootstock cuttings with the 42P4 native strain did not promote rooting or graft union.

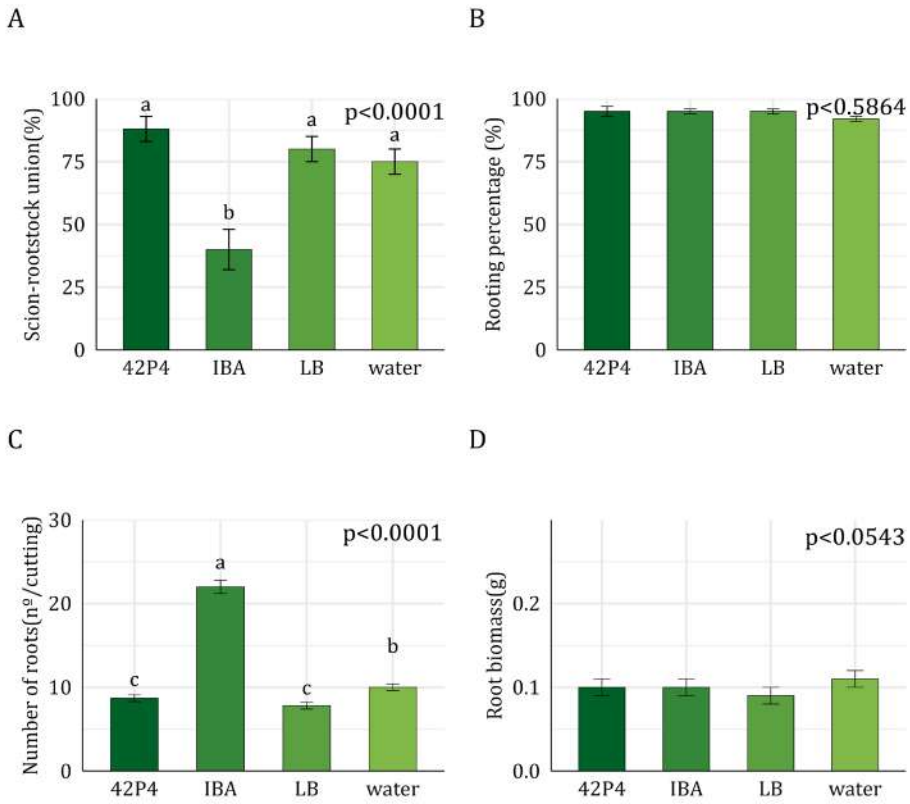

A) Scion-rootstock union percentage, B) Rooting percentage, C) Number of roots per cutting, and D) Root biomass per cutting. Values correspond to adjusted means ± SEM (n=50). Data were analyzed with General or Generalized Linear Models. Different letters indicate significant differences between treatments according to the post-hoc test DGC (α = 0.05). 42P4: *Pseudomonas* 42P4, 64S1: *Enterobacter* 64S1, IBA: Indole-3-butyric acid, LB: Luria Broth culture medium, water: tap water.

A) Porcentaje de unión entre la púa y el portainjerto, B) Porcentaje de enraizamiento, C) Número de raíces por estaca y D) Biomasa de raíces por estaca. Los valores corresponden a las medias ajustadas ± EE (n=50). Los datos fueron analizados mediante Modelos Lineales Mixtos Generales o Generalizados. Letras diferentes indican diferencias significativas entre tratamientos según el test post-hoc DGC (α = 0,05). 42P4: *Pseudomonas* 42P4, 64S1: *Enterobacter* 64S1, IBA: ácido indol-3-butírico, LB: medio de cultivo Luria Broth, water: agua de red.

Figure 3. Rootstock 101-14 MGt.
Figura 3. Portainjerto 101-14 MGt.

110 Richter

Graft union percentage between Malbec and 110 R rootstock was higher in autoclaved LB compared to the other treatments (figure 4A, page 20). However, callus percentage (~100%, p > 0.05, data not shown), rooting percentage (~75%), and root biomass per cutting were similar among treatments (figure 4B and 4D, page 20). Root number per cutting was higher in cuttings incubated with IBA (4 roots per cutting) than in other treatments (2.5 roots per cutting) (figure 4C, page 20). *Pseudomonas* 42P4 did not promote rooting or graft union of 110 R.

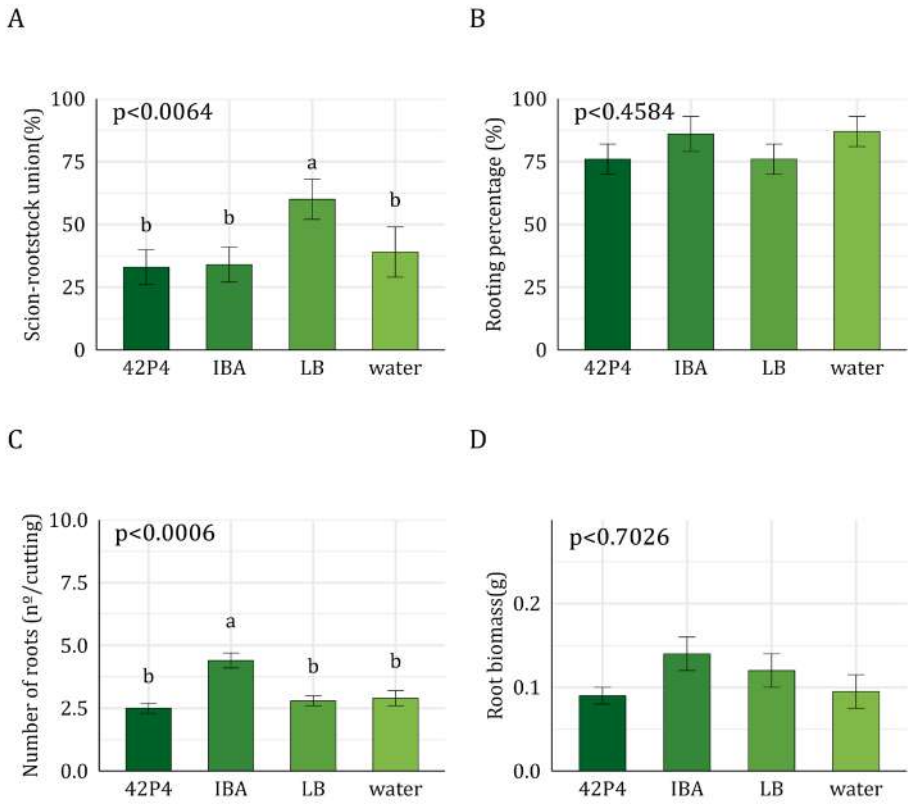

A) Scion-rootstock union percentage, B) Rooting percentage, C) Number of roots per cutting, and D) Root biomass per cutting. Values correspond to adjusted means ± SEM, n=50. Data were analysed with General or Generalized Linear Models. Different letters indicate significant differences between treatments according to the post-hoc test DGC (α = 0.05). 42P4: *Pseudomonas* 42P4, 64S1: *Enterobacter* 64S1, IBA: Indole-3-butyric acid, LB: Luria Broth culture medium, water: tap water.

A) Porcentaje de unión entre la púa y el portainjerto, B) Porcentaje de enraizamiento, C) Número de raíces por estaca y D) Biomasa de raíces por estaca. Los valores corresponden a las medias ajustadas ± EE (n=50). Los datos fueron analizados mediante Modelos Lineales Mixtos Generales o Generalizados. Letras diferentes indican diferencias significativas entre tratamientos según el test post-hoc DGC (α = 0,05). 42P4: *Pseudomonas* 42P4, 64S1: *Enterobacter* 64S1, IBA: ácido indol-3-butírico, LB: medio de cultivo Luria Broth, water: agua de red.

Figure 4. Rootstock 110 Richter.
Figura 4. Portainjerto 110 Richter.

SO4

Union percentage between Malbec and SO4 was higher in cuttings incubated with 42P4 compared to the other treatments (50% higher than IBA and water, and 25% higher than the LB treatment) (figure 5A, page 21). Callus percentage (~80%, p>0.05) and rooting percentage (40%) of the SO4 rootstock were similar among treatments (figure 5B, page 21). Root number and biomass per cutting were higher in cuttings incubated with IBA than in other treatments (figure 5C and 5D, page 21). *Pseudomonas* 42P4 did not promote rooting but increased scion-rootstock union percentages.

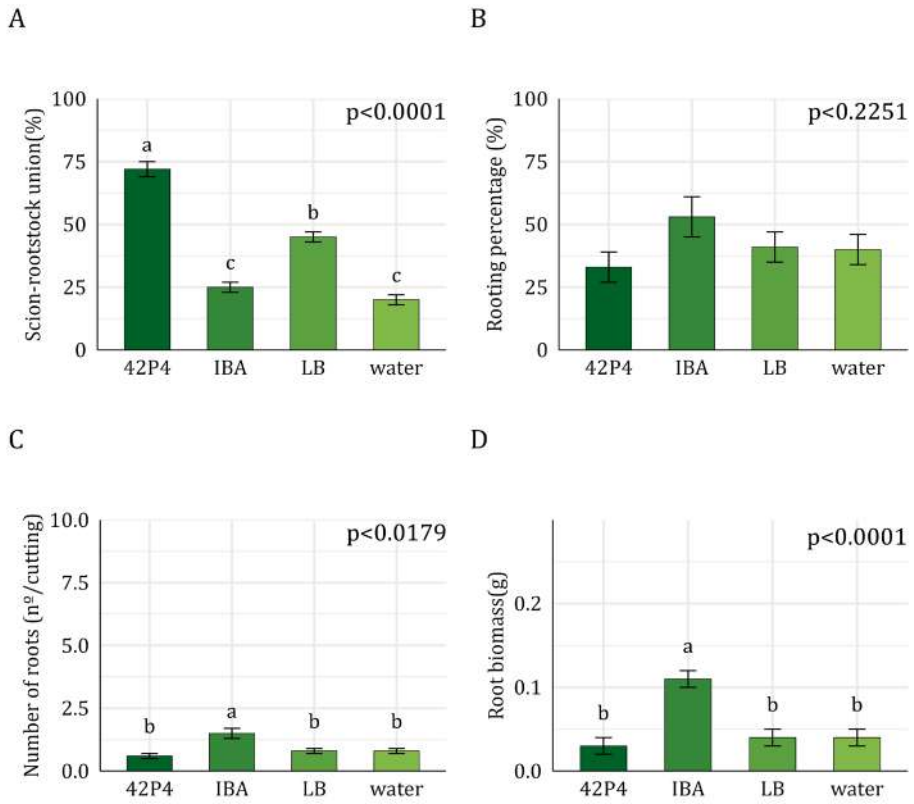

A) Scion-rootstock union percentage, B) Rooting percentage, C) Number of roots per cutting, and D) Root biomass per cutting. Values correspond to adjusted means ± SEM (n=50). Data were analysed with General or Generalized Linear Models. Different letters indicate significant differences between treatments according to the post-hoc test DGC (α = 0.05). 42P4: *Pseudomonas* 42P4, 64S1: *Enterobacter* 64S1, IBA: Indole-3-butyric acid, LB: Luria Broth culture medium, water: tap water.

A) Porcentaje de unión entre la púa y el portainjerto, B) Porcentaje de enraizamiento, C) Número de raíces por estaca y D) Biomasa de raíces por estaca. Los valores corresponden a las medias ajustadas ± EE (n=50). Los datos fueron analizados mediante Modelos Lineales Mixtos Generales o Generalizados. Letras diferentes indican diferencias significativas entre tratamientos según el test post-hoc DGC (α = 0,05). 42P4: *Pseudomonas* 42P4, 64S1: *Enterobacter* 64S1, IBA: ácido indol-3-butírico, LB: medio de cultivo Luria Broth, water: agua de red.

Figure 5. Rootstock SO4.

Figura 5. Portainjerto SO4.

Discussion

This study is the first to report applications of native PGPR strains from drylands in grapevine propagation. We found that a *Pseudomonas* PGPR can improve rooting in vine woody cuttings. We evaluated the ability of two native PGPR from arid zones, *Pseudomonas* 42P4 and *Enterobacter* 64S1, to stimulate rooting of ungrafted and grafted *Vitis* woody cuttings. Concerning Malbec's rooting, *Pseudomonas* 42P4 improved rooting compared to the control, matching IBA results (figure 1, page 17 and figure 6, page 22). Conversely, *Enterobacter* 64S1 failed to promote rooting of Malbec cuttings. Concerning grafted material, *Pseudomonas* 42P4's promoted rooting and graft union in a rootstock-dependent fashion, enhancing rooting in 1103 Paulsen, but not affecting the other rootstocks (figure 2, page 18; figure 3, page 19; figure 4, page 20; figure 5 and figure 7, page 22).

Optimal auxin concentrations stimulate adventitious rooting, while higher concentrations are inhibitory (Garay-Arroyo *et al.*, 2014). The root-promoting effect of *Pseudomonas* 42P4 on Malbec own-rooted woody cuttings could be attributed to IAA production by this bacterium (Perez-Rodriguez *et al.*, 2020a).

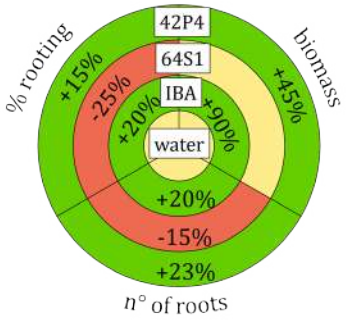

Chart sectors show the evaluated variables: rooting percentage, number of roots, and root biomass per cutting. Green indicates significant promotion of the parameter compared to the water control. Red indicates lower values, and yellow indicates no significant differences among means. 42P4: *Pseudomonas* 42P4, 64S1: *Enterobacter* 64S1, IBA: indole-3-butiric acid, water: tap water.

Los sectores del gráfico muestran las variables evaluadas: porcentaje de enraizamiento, número de raíces y biomasa de raíces por estaca. El color verde indica que el tratamiento promovió significativamente el parámetro en comparación con el control con agua; el color rojo indica una disminución en los valores observados, y el color amarillo indica que no hubo diferencias significativas entre las medias. 42P4: *Pseudomonas* 42P4, 64S1: *Enterobacter* 64S1, IBA: ácido indol-3-butírico, wáter: agua de red.

Figure 6. Malbec. Coloured rings represent the treatments (water, IBA, 42P4, and 64S1).

Figura 6. Malbec. El gráfico representa a los tratamientos (agua, IBA, 42P4 y 64S1) como anillos.

Each chart represents a treatment (water, IBA, 42P4) as rings. Chart sectors show the evaluated variables rooting percentage, number of roots, and root biomass per cutting. Green indicates significant promotion of the parameter compared to the water treatment; red indicates lower values, and yellow indicates no significant differences among means. 42P4: *Pseudomonas* 42P4, IBA: indole-3-butiric acid, water: tap water.

Cada gráfico representa los tratamientos (agua, IBA, 42P4) como anillos. Los sectores del gráfico muestran las variables evaluadas: porcentaje de enraizamiento, número de raíces y biomasa de raíces por estaca. El color verde indica que el tratamiento promovió significativamente el parámetro en comparación con el tratamiento con agua; el color rojo indica una disminución en los valores observados, y el color amarillo indica que no hubo diferencias significativas entre las medias. 42P4: *Pseudomonas* 42P4, IBA: ácido indol-3-butírico, wáter: agua de red.

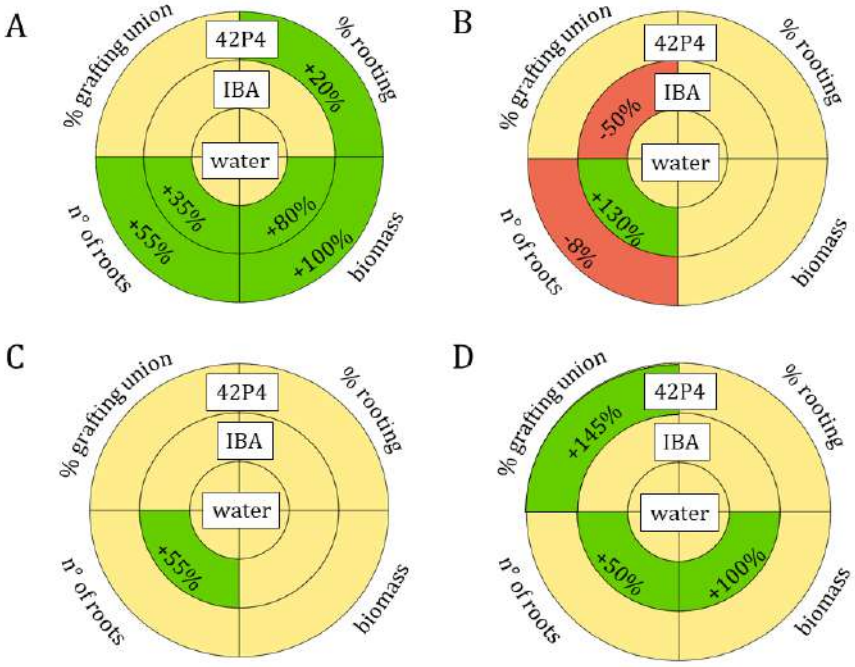

Figure 7. Rootstocks A) 1103 Paulsen, B) 101-14 MGt, C) 110 Richter and D) SO4.

Figura 7. Portainjertos A) 1103 Paulsen, B) 101-14 MGt, C) 110 Richter y D) SO4.

However, as *Enterobacter* produces an *in vitro* higher concentration of auxins than *Pseudomonas* 42P4 (six times more) (Perez-Rodriguez *et al.*, 2020a), an excessive concentration of IAA may have led to an inhibitory effect. Considering this, we had previously tested lower *Enterobacter* dilutions (10^4, 10^5 and 10^6 CFU mL^{-1}) and observed no rooting promotion. Another plausible explanation is the plant recognizing *Enterobacter* as a pathogen. However, this would indicate a species-specific response. In this regard, we previously reported *Enterobacter* promoted growth in pepper and tomato (Perez-Rodriguez *et al.*, 2020a; Lobato Ureche *et al.*, 2021).

Rooting capacity varied with rootstock (Keller 2020; Ollat *et al.*, 2016). We found that 101-14 MGt showed the highest rooting compared with the control treatment, followed by 1103 P and 110R, while SO4 had the lowest rooting (figure 2, page 18; figure 3, page 19; figure 4, page 20 and figure 5, page 21). SO4 (*Berlandieri-Riparia* family), 1103 P (*Berlandieri-Rupestris* family), and 110R (*Berlandieri-Rupestris* family) were expected to have lower rooting capacity than 101-14 MGt (*Riparia-Rupestris* family), because they are hybrids of *V. berlandieri*, an American difficult-to-root *Vitis* species (Keller *et al.*, 2020; Riaz *et al.*, 2019). Cuttings of 1103 P incubated with *Pseudomonas* 42P4 showed increased rooting compared to the control. Additionally, rooting percentage was 15% higher than with the synthetic rooting agent IBA, which only promoted two of the four assessed parameters. However, contrasting reports exist regarding IBA's effectiveness in 1103 P (Boeno *et al.*, 2023; Daskalakis *et al.*, 2018; Gordillo *et al.*, 2022; Satisha *et al.*, 2008). Rooting of 110 R, 101-14, and SO4 cuttings inoculated with *Pseudomonas* showed no significant improvements compared to the control. Isçi *et al.* (2019) evaluated a commercial bacteria consortium on Ramsey rootstock after nursery forcing, successfully increasing rooting percentage and root DW compared to IBA. Rootstock response to *Pseudomonas* 42P4 and IBA treatments may depend on genetic diversity and the presence of inhibitors (Wilson and Van Staden, 1990).

Scion-rootstock union percentage in SO4 cuttings inoculated with *Pseudomonas* 42P4 was threefold higher than in water or with IBA (75% vs. 25%). This result aligns with Köse *et al.* (2005), who reported that *Pseudomonas* BA8 promoted graft union of the Italia and Beyaz Çavuş scions onto 41B and 5BB rootstocks. Similarly, Toffanin *et al.* (2016) evaluated the effect of inoculating nine rootstock cuttings with *Azospirillum brasilense* Sp245 and found improved union only in 1103 P grafted onto Sangiovese. Likewise, *A. brasilense* Sp245 only improved the union of Colorino grafted onto 420A (Bartolini *et al.*, 2017). Our native *Pseudomonas'* failure to improve graft union in three out of the four evaluated rootstocks could be explained by impaired polar auxin transport. Auxins may not have moved towards the rootstock-scion union, but rather accumulate at the cutting's basal end, probably given its genetic origin. *V. riparia* and *V. berlandieri* develop callus on both extremities, while *V. rupestris* predominantly forms it on the upper extremity (Galet, 1993).

Considering the *Vitis* genus cuttings lack preformed root primordia, adventitious root formation is a prerequisite for successful cutting propagation (Hartmann *et al.*, 2014). Once cuttings are removed from the plant (wounding), a series of wound responses occur, and *de novo* adventitious root generation proceeds. *De novo* adventitious rooting involves four stages: cell dedifferentiation (possibly medullary rays in grapevine), cell proliferation, development and organization of root primordia, and growth of root primordia (Hartmann *et al.*, 2014). In early rooting stages, high auxin concentrations either from buds or exogenous sources like IAA are necessary for dedifferentiation and cell proliferation (Hartmann *et al.*, 2014; Jarvis, 1986). Under our conditions, the native *Pseudomonas* synthetised and exuded IAA into the medium where bacteria had grown and cuttings were incubated. Although we do not know whether the strains can colonise cuttings endophytically or epiphytically, we believe bacteria may have produced IAA in the medium, promoting rooting. Currently, IBA and NAA are the most commonly used auxins in nurseries (Waite *et al.*, 2014). Synthetic growth regulators often excessively used, can be sufficiently replaced by organic products for plant rooting, at least for some species and varieties (Atak *et al.*, 2024). However, further investigation should consider the mechanisms underlying bacterium-plant interaction between *Pseudomonas* 42P4 and *Vitis* spp. and long-term effects.

Conclusions

Pseudomonas 42P4, but not *Enterobacter* 64S1 promoted rooting (rooting percentage, root number and biomass per cutting) of Malbec cuttings reaching similar values as IBA 1000 ppm. Furthermore, this strain increased 1103 P rooting (rooting percentage, root number and biomass per cutting), compared to the water treatment, but. This was not observed in 101-14 MGt, 110 R or SO4. In 1103 P, this strain increased rooting percentage, exceeding IBA treatment. *Pseudomonas* 42P4 also increased SO4 graft union threefold compared to IBA and water. The use of this bacterium, native to arid soils, enhances rooting parameters of ungrafted and grafted *V. vinifera* cv. Malbec cuttings. This capacity of *Pseudomonas* 42P4 presents a promising sustainable alternative for improving grapevine production in commercial nurseries.

References

Atak, A. (2024). Climate change and adaptive strategies on viticulture (*Vitis* spp.). *Open Agriculture, 9*, 1-16. https://doi.org/10.1515/opag-2022-0258

Bartolini, S., Carrozza, G., Scalabrelli, G., & Toffanin, A. (2017). Effectiveness of *Azospirillum brasilense* Sp245 on young plants of *Vitis vinifera* L. *Open Life Sciences*, *12*, 365-372. https://doi.org/10.1515/biol-2017-0042

Berdugo, M., Delgado-Baquerizo, M., Soliveres, S., Hernandez-Clemente, R., Zhao, Y., Gaitan, JJ, Gross, N., Saiz, H., Maire, V., & Lehmann, A. (2020). Global ecosystem thresholds driven by aridity. *Science*, *367*, 787-790. https://doi.org/10.1126/science.aay5958

Boeno, D., & Zuffellato-Ribas, KC. (2023). A quantitative assessment of factors affecting the rooting of grapevine rootstocks (*Vitis vinifera* L.). *Acta Scientiarum Agronomy*, *45*. https://doi.org/10.4025/actasciagron.v45i1.57987

Brunoni, F., Vielba, JN, & Sanchez, C. (2022). Plant growth regulators in tree rooting. *Plants*, *11*(6), 805. https://doi.org/10.3390/plants11060805

Burrel, AL, Evans, JP, & De Kauwe, MG. (2020). Anthropogenic climate change has driven over 5 million km^2 of drylands towards desertification. *Nature Communications*, *11*, 3853. https://doi.org/10.1038/s41467-020-17710-7

Centeno, A., & Gómez del Campo, M. (2008). Effect of root-promoting products in the propagation of organic olive (*Olea europaea* L. cv. Cornicabra). *HortScience*, *43*(7), 2066-2069. https://doi.org/10.21273/HORTSCI.43.7.2066

Daskalakis, I., Biniari, K., Bouza, D., & Stavrakaki, M. (2018). The effect that indolebutyric acid (IBA) and position of cane segment have on the rooting of cuttings from grapevine rootstocks and from Cabernet Franc (*Vitis vinifera* L.) under conditions of a hydroponic culture system. *Scientia Horticulturae*, *227*, 79-84. https://doi.org/10.1016/j.scienta.2017.09.024

D'Innocenzo, SH, Escoriaza, G, Diaz, ME. (2024). First report of the causal agent of vine crown gall in Mendoza, Argentina. *Revista de la Facultad de Ciencias Agrarias. Universidad Nacional de Cuyo. Mendoza. Argentina. 56*(2): 87-96. DOI: https://doi.org/10.48162/rev.39.139

Di Rienzo, JA, Casanoves, F., Balzarini, MG, Gonzalez, L., Tablada, M., & Robledo, CW. (2020). *InfoStat 2020/P*. https://www.infostat.com.ar/

Flexas, J., Galmés, J., Gallé, A., Gulías, J., Pou, A., Ribas-Carbó, M., Tomas, M., & Medrano, H. (2010). Improving water use efficiency in grapevines: Potential physiological targets for biotechnological improvement. *Australian Journal of Grape and Wine Research*, *16*, 106 121. https://doi.org/10.1111/j.1755-0238.2009.00057.x

Galet, P. (1993). *Précis de viticulture*. Dehan Ed.

Garay-Arroyo, A., de La Paz Sánchez, M., García-Ponce, B., Álvarez-Buylla, ER & Gutiérrez, C. (2014). La homeostasis de las auxinas y su importancia. *Revista de Educación Bioquímica*, *33*(1), 13-22.

Glick, BR. (2012). Plant growth-promoting bacteria: Mechanisms and applications. *Scientifica*, *2012*, 963401. https://doi.org/10.6064/2012/963401

Gordillo, MG, Cohen, AC, Roge, M., Belmonte, M., & González, CV. (2022). Effect of quick-dip with increasing doses of IBA on rooting of five grapevine rootstocks grafted with 'Cabernet Sauvignon'. *Vitis*, *61*(3), 147-152. http://dx.doi.org/10.5073/vitis.2022.61.147-152

Hartmann, HT, Kester, DE, Davies, FT, Jr., & Geneve, RL. (2014). *Plant propagation: Principles and practices* (8th ed.). Pearson.

Instituto Nacional de Vitivinicultura. (2023). *Superficie cultivada con viñedos en Argentina*. https://www.argentina.gob.ar/inv/vinos/estadisticas

Isçi, B., Kacar, E., & Altindisli, A. (2019). Effects of IBA and plant growth-promoting rhizobacteria (PGPR) on rooting of ramsey american grapevine rootstock. *Applied Ecology and Environmental Research*, *17*(2), 4693-4705. http://dx.doi.org/10.15666/aeer/1702_46934705

Jarvis, BC. (1986). Endogenous control of adventitious rooting in non-woody species. En M. B. Jackson (Ed.), *New root formation in plants and cuttings* (p. 137-162). Martinus Nijhoff Publishers. https://doi.org/10.1007/978-94-009-4358-2_6

Jofré, MF, Mammana, S., Pérez-Rodríguez, MM, Silva, MF, Gómez, F., & Cohen, AC. (2024). Native rhizobacteria improve drought tolerance in tomato plants by increasing endogenous melatonin levels and photosynthetic efficiency. *Scientia Horticulturae*, *329*, 112984. http://dx.doi.org/10.1016/j.scienta.2024.112984

Keller, M. (2020). *The science of grapevines* (3rd ed.). Elsevier. https://doi.org/10.1016/B978-0-12-816365-8.00001-4

Köse, C., Güleryüz, M., Şahin, F., & Demirtaş, İ. (2003). Effects of some plant growth promoting rhizobacteria (PGPR) on rooting of grapevine rootstocks. *Acta Agrobotanica*, *56*(1), 47-52. https://doi.org/10.5586/aa.2003.005

Köse, C., Güleryüz, M., Şahin, F., & Demirtaş, İ. (2005). Effects of some plant growth promoting rhizobacteria (PGPR) on graft union of grapevine. *Journal of Sustainable Agriculture*, *26*(2), 139-147. https://doi.org/10.1300/J064v26n02_10

Lobato Ureche, MA, Perez-Rodriguez, MM, Ortiz, R., Monasterio, RP, & Cohen, AC. (2021). Rhizobacteria improve the germination and modify the phenolic compound profile of pepper (*Capsicum annuum* L.). *Rhizosphere*, *18*, 100334. https://doi.org/10.1016/j.rhisph.2021.100334

Machado, MP, Mayer, JLS, Ritter, M., & Biasi, LA. (2005). Indole butyric acid on rooting ability of semihardwood cutting of grapevine rootstock 'VR 043-43' (*Vitis vinifera* x *Vitis rotundifolia*). *Revista Brasileira de Fruticultura*, *27*(3), 476-479. https://doi.org/10.1590/S0100-29452005000300032

Mudge, K., Janick, J., Scofield, S., & Goldschmidt, EE. (2009). A history of grafting. *Horticultural Reviews*, *35*, 437-483. https://doi.org/10.1002/9780470593776.CH9

OIV (International Organization of Vine and Wine). (2023). *State of the world vine and wine sector*. https://www.oiv.int/node

Ollat, N., Bordenave, L., Tandonnet, JP, Boursiquot, JM, & Marguerit, E. (2016). Grapevine rootstocks: Origins and perspectives. *Acta Horticulturae*, *1136*, 11-22. https://doi.org/10.17660/ActaHortic.2016.1136.2

Pantoja Guerra, M., Valero Valero, N., & Ramírez, CA. (2023). Total auxin level in the soil-plant system as a modulating factor for the effectiveness of PGPR inocula: A review. *Chemical and Biological Technologies in Agriculture*, *10*, 6. https://doi.org/10.1186/s40538-022-00370-8

Pérez-Rodríguez, MM, Piccoli, P., Anzuay, MS., Baraldi, R., Neri, L., Taurian, T., Lobato Ureche, MA, Segura, DM, & Cohen, AC. (2020a). Native bacteria isolated from roots and rhizosphere of *Solanum lycopersicum* L. increase tomato seedling growth under a reduced fertilization regime. *Scientific Reports*, *10*, 1-14. https://doi.org/10.1038/s41598-020-72507-4

Pérez-Rodríguez, MM, Pontin, M., Lipinski, V., Botini, R., Piccoli, P., & Cohen, AC. (2020b). *Pseudomonas fluorescens* and *Azospirillum brasilense* increase yield and fruit quality of tomato under field conditions. *Journal of Soil Science and Plant Nutrition*, *20*(3), 1614-1624. https://doi.org/10.1007/s42729-020-00233-x

Pérez-Rodríguez, MM, Pontin, M., Piccoli, P., Lobato Ureche, MA, Gordillo, MG, Funes Pinter, I., & Cohen, AC. (2022). Halotolerant native bacteria *Enterobacter* 64S1 and *Pseudomonas* 42P4 alleviate saline stress in tomato plants. *Physiologia Plantarum*, *174*(1), 13472. https://doi.org/10.1111/ppl.13742

R Core Team. (2024). *R: A language and environment for statistical computing*. R Foundation for Statistical Computing. https://www.R-project.org/

Riaz, S., Pap, D., Uretsky, J., Laucou, V., Boursiquot, JM, & Kocsis, L. (2019). Genetic diversity and parentage analysis of grape rootstocks. *Theoretical and Applied Genetics*, *132*(6), 1847-1860. https://doi.org/10.1007/s00122-019-03320-5

Satisha, J., & Asdule, PG. (2008). Rooting behaviour of grape rootstocks in relation to IBA concentration and biochemical constituents of mother vines. *Acta Horticulturae*, *785*, 121-125. https://doi.org/10.17660/ActaHortic.2008.785.14

Tandonnet, JP, Cookson, SJ, Vivin, P., & Ollat, N. (2009). Scion genotype controls biomass allocation and root development in grafted grapevine: Scion/rootstock interactions in grapevine. *Australian Journal of Grape and Wine Research*, *16*(1), 290-300. https://doi.org/10.1111/j.1755-0238.2009.00090.x

Toffanin, A., D'Onofrio, C., Carroza, GP, & Scalabrelli, G. (2016). Use of beneficial bacteria *Azospirillum brasilense* Sp245 on grapevine rootstocks grafted with 'Sangiovese'. *Acta Horticulturae*, *1136*, 24. https://doi.org/10.17660/ActaHortic.2016.1136.24

Waite, H., Whitelaw-Weckert, M., & Torley, P. (2014). Grapevine propagation: Principles and methods for the production of high-quality grapevine planting material. *New Zealand Journal of Crop and Horticultural Science*, *43*(2), 144-161. https://doi.org/10.1080/01140671.2014.978340

Wickham, H. (2016). *ggplot2: Elegant graphics for data analysis*. Springer-Verlag. https://ggplot2.tidyverse.org

Wilson, PJ, & Van Staden, J. (1990). Rhizocaline, rooting co-factors, and the concept of promoters and inhibitors of adventitious rooting - A review. *Annals of Botany*, *66*(4), 479-490. https://doi.org/10.1093/oxfordjournals.aob.a088051

Acknowledgements

The authors would like to thank Diana Segura, Micaela Perez-Rodriguez, Martín López, Walter Tulle and Carlos Blanquer for their assistance with morphological measurements.
This study was supported through funding from Fondo para la Investigación Científica y Tecnológica de Argentina (FONCYT, PICT 2020-3618 to ACC); Universidad Nacional de Cuyo (SIIP-UNCUYO M021-T1 to CVG and ACC), Fundación Williams (to ACC) and CONICET (PIP-KA1 11220210100195CO to ACC and CVG).
ACC and CVG are CONICET researchers and UNCUYO Professors, MGG is a PhD fellow from CONICET and FC is a member of Trapiche winery staff.

Foxtail Millet (*Setaria italica* L.) Performance under Irrigation. Sowing Dates and Cultivars in the Northern Oasis of Mendoza

Producción de moha (*Setaria italica* L.) bajo riego: evaluación de fechas de siembra y cultivares en el oasis norte de Mendoza

Cecilia Rébora *, Leandra Ibarguren, Alejandra Bertona, Álvaro López, Diego Guerrero, Alejo Argumedo, José Martín, Mariana Savietto

Originales: *Recepción:* 05/08/2024 - *Aceptación:* 14/10/2025

Abstract

Foxtail millet is a short-season, summer annual forage crop primarily used for haymaking in Argentina. Valued for its efficient water use, it provides effective fiber for various milk and meat production systems. This trial evaluated two sowing dates (mid-November and mid-December) for the three commercially available foxtail millet cultivars in Argentina (Yaguané Plus INTA, Carapé Plus INTA, and Nará INTA) across two production cycles (2022/2023 and 2023/2024). The experiment was conducted at the Facultad de Ciencias Agrarias, Universidad Nacional de Cuyo, in Mendoza (33°00'38" S and 68°52'28" W). Yields of up to 14,000 kg DM/ha were obtained in the northern oasis of Mendoza. Significant differences in yield were observed between sowing dates, with December sowing yielding more than November. Additionally, Nará INTA was the highest-yielding cultivar.

Keywords
Setaria italica • forage • yield • arid zone

Universidad Nacional de Cuyo. Facultad de Ciencias Agrarias. Almirante Brown 500. Chacras de Coria. M5528AHB. Mendoza. Argentina. * crebora@fca.uncu.edu.ar

Resumen

La moha es un forraje estival anual, cuyo principal destino en Argentina es la henificación. Este cultivo es valorado por su eficiente uso del recurso hídrico; es muy utilizado como heno en todos los sistemas productivos de leche y carne. En este ensayo se contrastan dos fechas de siembra (mediados de noviembre y mediados de diciembre) de los tres cultivares de moha disponibles en Argentina (Yaguané Plus INTA, Carapé Plus INTA y Nará INTA), en dos ciclos (2022/2023 y 2023/2024). El ensayo se realizó en la Facultad de Ciencias Agrarias de la Universidad Nacional de Cuyo, Mendoza (33°00'38" S y 68°52'28" O). Se obtuvieron rendimientos superiores a los 14.000 kg MS/ha de moha en el oasis norte de Mendoza, observándose diferencias significativas de rendimiento entre fechas de siembra (la siembra de diciembre rindió más que la de noviembre) y entre cultivares (Nará INTA rindió más que los otros cultivares).

Palabras clave
Setaria italica • forraje • rendimiento • zona árida

Introduction

Foxtail millet *Setaria italica* (L.) *P. Beauvois* is an annual summer forage crop primarily grown for haymaking in Argentina. Renewed interest in this crop is linked to climate change and the need for drought-tolerant varieties. Foxtail millet is known for its efficient use of resources, particularly water (Srikanya *et al.*, 2020). It also helps suppress weeds within agroecosystems. Furthermore, its short growing season (2-3 months), high photosynthetic efficiency as a C4 plant, and resistance to pests and diseases make it a suitable forage crop (Shanthi *et al.*, 2017; Yang *et al.*, 2016).

According to the Censo Nacional Agropecuario 2018 (INDEC, 2021), Argentina cultivates approximately 1.6 million hectares of annual summer forage grasses. Of this total, 60,000 hectares are dedicated to foxtail millet, primarily in the provinces of Córdoba, Buenos Aires, and Santa Fe, mostly under rainfed conditions. It ranks third among cultivated summer green crops after corn and sorghum. Previous trials in the northern Mendoza oasis have shown high yields of corn and sorghum silage. However, both species require over three months from sowing to harvest, while consuming over 550 mm of water per cycle (Ibarguren *et al.*, 2020; Rebora *et al.*, 2018). In contrast, foxtail millet requires less water and has a shorter cycle, making it potentially suitable as a preceding crop for alfalfa and winter greens (Sardiña and Diez, 2016). Additionally, foxtail millet is an energy-rich forage mainly providing effective fiber in milk and meat production systems. Additionally, given its short growing cycle and the consequent flexible sowing period, this crop also fits rotation plans. As a megathermic grass, soil temperatures should be approximately 18-20°C for rapid emergence, subjecting sowing times to regional climatic conditions (Curia, 2018). In Bordenave, southern Buenos Aires, the recommended sowing period is November to December (Bolletta *et al.*, 2009). INTA Pergamino suggest the second half of November as optimal, while Rafaela, in Santa Fe, might benefit from sowing in the first half of November (Mattera *et al.*, 2016). Therefore, thermal requirements dictate an environment-dependent sowing period to ensure optimal forage quality for haymaking.

INTA has developed three improved foxtail millet cultivars of national origin: a) Yaguané Plus INTA, well-suited for haymaking with high dry matter production and a plant structure with few tillers and wide blades. It performs best in high-productivity environments. b) Carapé Plus INTA offers greater potential and performance stability in less productive environments while maintaining high forage quality. Its good regrowth capacity makes it ideal for direct grazing. It is also well-suited for hay production due to its rapid dry matter accumulation, fine stems, and high leaf proportion. C) Nará INTA yields 20-30% more than the other Argentine cultivars, primarily due to its slightly longer growing cycle (10-15 days). This cultivar is tolerant to lodging and disease. Visually, Nará INTA is distinguished by reddish color in various plant parts and orange seeds (Carta *et al.*, 2017; Mich, 2020).

Considering absent scientific references regarding foxtail millet cultivation in irrigated oases in Mendoza, this study aims to generate information on suitable sowing dates for the northern oasis, performance of available cultivars, water requirements, and potential yields.

We hypothesized that yield and cycle duration would vary depending on cultivar and sowing dates under irrigated conditions. Our objectives were to evaluate dry matter (DM) yield per hectare for three foxtail millet cultivars across different sowing dates and under irrigated conditions, determine cycle duration for each cultivar and sowing date combination, quantify water needs, and determine forage quality during the cycle 2022/2023.

Materials and Methods

The experiment was conducted at the Facultad de Ciencias Agrarias, Universidad Nacional de Cuyo, in Luján de Cuyo, Mendoza, Argentina (33°00'38" S and 68°52'28" W). The site has alluvial soil with a silty loam texture and limited vertical development. Average annual temperature is 16.5°C, relative humidity is 50%, and precipitation averages 225 mm per year.

During the spring seasons of 2022 and 2023, three foxtail millet cultivars (Yaguané Plus INTA, Carapé Plus INTA, and Nará INTA) were sown on two dates: mid-November and mid-December. Each experimental plot was 5 m^2 and consisted of five 5-meter rows spaced 0.20 m. Sowing density was 700 viable seeds per m^2 (equivalent to 20 kg/ha). Urea was applied at a rate of 150 kg/ha at sowing time. The experiment used a completely randomized design (CRD), resulting in 18 experimental plots (3 cultivars x 2 sowing dates x 3 replicates).

The trial was irrigated using a center pivot sprinkler system, with an average daily sheet of approximately 5 mm.

Weeds were controlled manually. Harvest occurred at panicle stage, with a cutting height of 10 cm above the ground. The three central rows of each experimental plot were harvested, discarding 0.5 m from each end. Fresh weight of the harvested material was measured. Then, 200 g samples from each plot were oven-dried at 65°C until constant weight. Forage quality was evaluated in the first year of sowing (2022) for each treatment combination (cultivar * sowing date) by spectrophotometry at the FEEDLAB laboratory of Biofarma S.A. Total digestible nutrients, metabolizable energy, dry matter, crude protein, neutral detergent fiber, acid detergent fiber, and DM digestibility were determined. The analysis was performed on combined samples from the three replicates of each cultivar-sowing date combination in the 2022/2023 cycle.

Forage yield and kgDM/mm (rain + irrigation) data were subjected to ANOVA using Infostat software. The model included cultivars, sowing date, and crop cycle as fixed effects. Tukey's test was used for means comparison.

Results

An initial General Linear Model (GLM) was fitted, including second and third-order interactions. In this full model, only the cultivar × crop cycle interaction was significant ($p < 0.05$). A second model adjustment was performed, iteratively removing non-significant interactions. The cultivar × crop cycle interaction remained in the simplified model, showing a marginal significance level ($p=0.05$). Although this borderline value suggests a possible genotype × environment interaction over the cycles, its effect was weaker than the main effects. Significant differences ($p=0.0001$) were found among cultivars, with Nará INTA yielding more than Carapé Plus INTA and Yagané Plus INTA (figure 1, page 30). Likewise, significant differences ($p=0.0112$) were observed between sowing dates, with

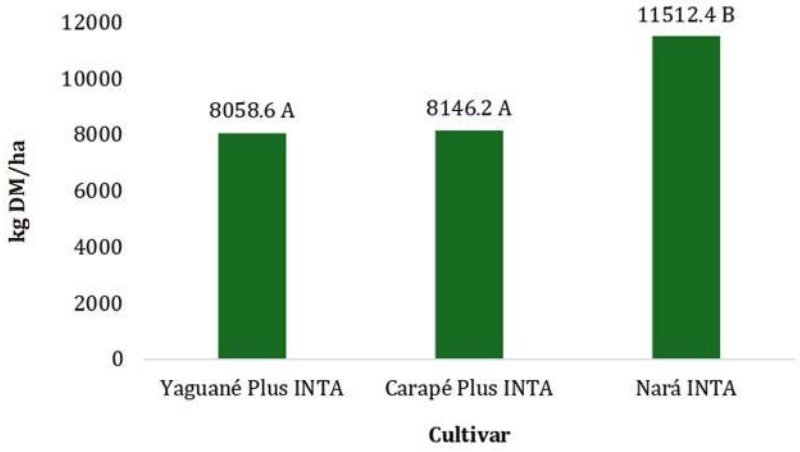

Figure 1. Average dry matter of foxtail millet cultivars across two growing cycles and two sowing dates.

Figura 1. Rendimiento de materia seca de cultivares de moha, promedio de dos ciclos de cultivo y dos fechas de siembra.

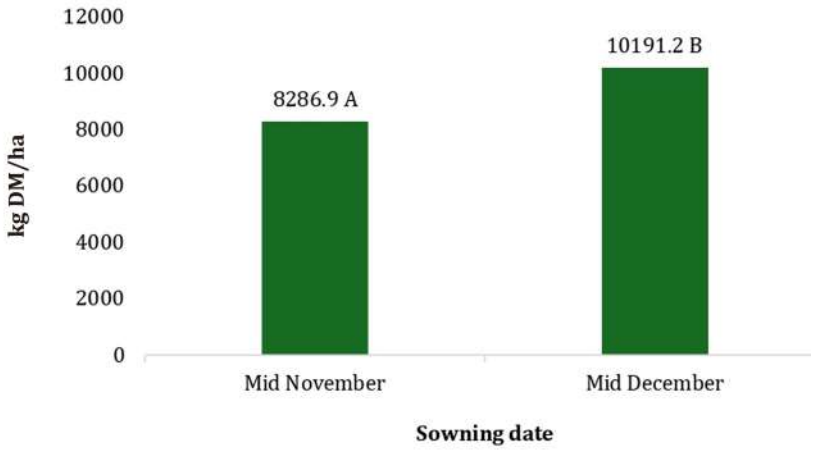

Figure 2. Average dry matter of foxtail millet considering two productive cycles and three cultivars at different sowing dates.

Figura 2. Rendimiento de materia seca de moha, en distintas fechas de siembra, promedio de dos ciclos productivos y tres cultivares.

mid-December showing a higher yield than mid-November (figure 2, page 30).

Tables 1 and 2 (page 31), show yield information for the two crop cycles (2022/2023 and 2023/2024).

Yields in our oasis exceeded those obtained in some dryland environments in Argentina. Narà standed as the most productive cultivar across these contrasting environments. Trials in various sites of the Argentine Pampas region (Bolivar, Pergamino, Concepción del Uruguay, Rafaela, Manfredi) indicated Narà INTA yields the highest values, from 7.92 to 10.97 T DM/ha. Yaguané Plus INTA yielded between 6.05 and 8.25 T DM/ha, ranking second in Bolivar, Pergamino, and Rafaela. Carapé Plus INTA yielded between 6.38 and 8.10 T DM/ha in the mentioned places, but exceeded Yaguané Plus INTA in Concepción del Uruguay and Manfredi

Table 1. Sowing date, harvest date, days from sowing to harvest, forage production (kg DM/ha), rainwater and irrigation during the cycle, DM production per mm of water (rain plus irrigation) for each cultivar and sowing date combination in the 2022/2023 crop cycle, Luján de Cuyo, Mendoza, Argentina.

Tabla 1. Fecha de siembra, fecha de cosecha, días desde siembra hasta cosecha, producción de forraje (kg MS/ha), mm de agua de lluvia y mm de agua aplicada por riego durante el ciclo, producción de MS por mm de agua (lluvia más riego), para cada combinación de cultivar de moha y fecha de siembra, ciclo productivo 2022/2023, Luján de Cuyo, Mendoza, Argentina.

Cultivar	Sowing date	Harvest date	Days from sowing to harvest	kg DM/ha	Rain (mm)	Irrigation (mm)	*Kg DM/ mm
Yaguané Plus INTA	15/11/22	26/01/23	72	7983	30	398.2	18.64
Carapé Plus INTA	15/11/22	26/01/23	72	7605	30	398.2	17.76
Nará INTA	15/11/22	13/02/23	90	12123	40.75	451.8	24.61
Yaguané Plus INTA	15/12/22	22/02/23	69	9297	38.5	334.2	24.94
Carapé Plus INTA	15/12/22	22/02/23	69	8991	38.5	334.2	24.12
Nará INTA	15/12/22	09/03/23	84	14098	40.5	385.2	33.11

* kg DM/mm (rain + irrigation).
* kg MS/mm (lluvia + riego).

Table 2. Sowing date, harvest date, days from sowing to harvest, forage production (kg DM/ha), rainwater and irrigation during the cycle, DM production per mm of water (rain plus irrigation) for each cultivar and sowing date combination in 2023/2024, Luján de Cuyo, Mendoza, Argentina.

Tabla 2. Fecha de siembra, fecha de cosecha, días desde siembra hasta cosecha, producción de forraje (kg MS/ha), mm de agua de lluvia y mm de agua aplicada por riego durante el ciclo, producción de MS por mm de agua (lluvia más riego) para cada combinación de cultivar de moha y fecha de siembra, ciclo productivo 2023/2024, Luján de Cuyo, Mendoza, Argentina.

Cultivar	Sowing date	Harvest date	Days from sowing to harvest	kg DM/ha	Rain (mm)	Irrigation (mm)	*Kg DM/ mm
Yaguané Plus INTA	16/11/23	29/01/24	74	6631	39.25	369	16.24
Carapé Plus INTA	16/11/23	29/01/24	74	7173	39.25	369	17.57
Nará INTA	16/11/23	08/02/24	84	8256	51	396	18.47
Yaguané Plus INTA	13/12/23	20/02/24	69	8305	31.5	356	21.43
Carapé Plus INTA	13/12/23	20/02/24	69	8815	31.5	356	22.75
Nará INTA	13/12/23	04/03/24	82	11608	35.5	388	27.44

* kg DM/mm (rain + irrigation).
* kg MS/mm (lluvia + riego).

(Velazco, 2020).

Table 3 (page 32), shows quality data for each cultivar by sowing date combination, during the 2022-2023 cycle.

Foxtail millet is a highly palatable crop with good nutritional value. The literature reports crude protein (CP) values of 10-12% and digestibility exceeding 60% for cuts made

Table 3. Forage quality variables for each cultivar combination by sowing date (1=mid-November and 2=mid-December) in the 2022/2023 cycle.

Tabla 3. Variables de calidad de forraje para cada combinación de cultivar y fecha de siembra (1=mediados de noviembre y 2=mediados de diciembre) en el ciclo 2022/2023.

Cultivar / Sowing date	TDN (%)	Energy (Mcal/kg)	DM (%)	Crude protein (%)	NDF (%)	ADF (%)	Dig. (%)
Yaguané Plus INTA 1	50.4	1.82	22.4	8.24	62.7	45.94	53.11
Carapé Plus INTA 1	42.89	1.54	20.93	7.16	73.17	53.18	47.47
Nará INTA 1	56.17	2.02	22	6.21	S/D	40.28	57.52
Yaguané Plus INTA 2	57.17	2.06	25.51	8.95	66.3	39.56	58.08
Carapé Plus INTA 2	56.22	2.03	23.76	10.03	69.59	40.46	57.38
Nará INTA 2	53.66	1.93	25.7	5.15	68.33	42.91	55.47

Total digestible nutrients (TDN), metabolizable energy (Energy), dry matter (DM), crude protein, neutral detergent fiber (NDF), acid detergent fiber (ADF), and DM digestibility (%)= 88.9 - (%FDA * 0.779).

Nutrientes digestibles totales (NDT), energía metabolizable (Energía), materia seca (MS), proteína cruda, fibra detergente neutro (FDN), fibra detergente ácido (FDA) y digestibilidad de MS (digestibilidad (%) = 88,9 - (%FDA * 0,779).

between flowering and milky/pasty grain stages (Fernández Mayer *et al.,* 2009).

Field trials across several locations and cycles found average digestibility of 65.2% for Carapé Plus INTA, 64.8% for Nará INTA, and 63.5% for Yaguané Plus INTA (Velazco, 2020). In our study, however, CP values ranged from 5.15 to 10.03% and digestibility fell between 47% and 58%. These lower values could be explained by the phenological state at the time of cutting, which in our case occurred at panicle stage. Anticipating harvest could improve forage quality.

Conclusions

High yields of foxtail millet were obtained in the northern oasis of Mendoza. Sowing in December produced more forage than in November for three cultivars tested. Nará INTA was the most productive cultivar on both sowing dates. Additionally, December sowing resulted in the highest water use efficiency (yield *vs.* water). Therefore, sowing foxtail millet in mid-December is recommended for the study area.

References

Bolletta, A., Venanzi, S., Kruger, H., Lagrande, S., & Larrea, D. (2009). Mijo y Moha: Generalidades, Producción y Calidad. Producción Animal. https://www.produccion-animal.com.ar/produccion_y_manejo_pasturas/pasturas%20artificiales/182-Mijo_y_ Moha.pdf

Carta, H., Richmond, P., Perez, G., Torrens Baudrix, L., & Camarasa, J. (2017). Moha, una forrajera versátil. Experiencias en el centro oeste de Buenos Aires. *Revista Técnica Agropecuaria, 10*(35), 36-38.

Curia, J. (2018). Moha, una muy buena opción. Producción Animal. https://www.produccion-animal.com.ar/produccion_y_manejo_pasturas/pasturas%20 artificiales/229-Moha.pdf

Fernández Mayer, A., Lagrange, S., Bolletta, A., Tulesi, M. (2009). Calidad nutricional en diferentes estados de madurez de moha y mijo para heno o silaje de planta entera. https://www.produccion-animal.com.ar/produccion_y_manejo_reservas/reservas_ henos/37-calidad_nutricional_moha_mijo.pdf

Ibarguren, L., Rebora, C., Bertona, A., & Antonini, C. (2020). Sorghum silage production in the northern oasis of Mendoza, Argentina. *Revista de la Facultad de Ciencias Agrarias. Universidad Nacional de Cuyo, 52*(1), 121–127. https://revistas.uncu.edu.ar/ojs3/index.php/RFCA/article/view/2983/2614

INDEC. (2021). *Censo Nacional Agropecuario 2018. Resultados definitivos.* Ministerio de Economía Argentina. 747 p. https://www. indec.gob.ar/ftp/cuadros/economia/cna2018_resultados_definitivos.pdf

Mattera, J., Martinez, E., Romero, L., & Velazco, J. (2016). Evaluación productiva de moha bajo diferentes manejos agronómicos en dos ambientes de la región pampeana. *Revista Técnica Agropecuaria, 10*(32), 44-46.

Mich, L. (2020). Moha forrajera, un cultivo de verano estratégico ante la incertidumbre climática. *Repositorio INTA.* https://repositorio.inta.gob.ar/bitstream/ handle/20.500.12123/8127/ INTA_CRBsAsNorte_EEAPergamino_Velazco_Julio_ Moha_forrajera_un_cultivo_de_verano_ estrategico_ante_incertidumbre_climatica. pdf?sequence=1&isAllowed=y

Rebora, C., Ibarguren, L., Barros, A., Bertona, A., Antonini, C., Arenas, F., Calderón, M., & Guerrero, D. (2018). Producción de maíces sileros en el oasis norte de Mendoza, Argentina. *Revista de la Facultad de Ciencias Agrarias. Universidad Nacional de Cuyo, 50*(2), 369–375. https:// revistas.uncu.edu.ar/ ojs3/index.php/RFCA/article/view/2969/2121

Sardiña, C., & Diez, M. (2016). Evaluación de moha (*Setaria italica*) con y sin fertilización nitrogenada en siembra tardía. En *Memoria Técnica 2015-2016,* (p. 72-73). INTA.

Shanthi, P., Radha Kumari, C., Niveditha, M., Pavan Kumar Reddy, P., & Sahadeva Reddy, B. (2017). Genetic Variability Studies in Italian Millet (*Setaria italica* (L.) Beauv) cultivars under Rainfed conditions in Scarce Rainfall Zone of Andhra Pradesh. *The Andhra Agricultural Journal, 64*(2), 330-334.

Srikanya, B., Revathi, P., Malla Reddy, M., & Chandrashaker, K. (2020). Effect of Sowing Dates on Growth and Yield of Foxtail Millet (*Setaria italica* L.) cultivars. *International Journal of Current Microbiology and Applied Sciences, 9*(4).

Velazco, J. (2020). El tiempo de la moha. En *ON24 | Información Precisa. Periodismo en serio*. Agroempresario. Recuperado de https://agroempresario.com/publicacion/25833/el-tiempo-de-la-moha/

Yang, Q., Yu, Z., Guimei, C., Panpan, Z., Hui, S., & Baili, F. (2016). Water use efficiency of foxtail millet (*Panicum italicum* L.) under climate change conditions in northwest regions of China. *Agrociencia, 50*, 665-676.

Acknowledgments

To the company CEREAGRO for providing the seed of the cultivars used in the Project, to the FCA field staff, and to the Agr. Engineer. Juan Manuel Moreno (Salto de las Rosas S.A.) for his support in forage quality determinations.

Compensatory Growth in *Pinus ponderosa* (Dougl Ex Laws) Plantations Under Early Silvicultural Treatments

Crecimiento compensatorio en plantaciones de *Pinus ponderosa* (Dougl Ex Laws) bajo tratamientos silviculturales tempranos

Federico Jorge Letourneau [1*], Andrea Alejandra Medina [2], Marcos Ancalao [1], Matías Horacio Saihueque [1]

Originales: *Recepción:* 20/11/2023 - *Aceptación:* 24/10/2025

Abstract

Early pruning and thinning in *Pinus ponderosa*, plantations in Andean Patagonia triggered compensatory growth, characterized by greater trunk growth and structural adjustments. We used a factorial design and mixed-effects models to evaluate stem growth, crown light dynamics, tracheid length (TL), foliar biomass (FB), wood density (WD), and Huber values (Hv) five years after treatment. Trees under combined pruning and thinning (PT) showed the greatest basal area increment, indicating resource reallocation to supportive structures despite early foliage loss. Pruned trees maintained higher Hv and achieved partial recovery of FB. Tracheid elongation was greatest in treated trees, suggesting accelerated xylem maturation, while WD remained unchanged. These results demonstrate the structural plasticity of *P. ponderosa*, which maintains hydraulic function and growth after canopy disturbance. Our findings provide useful guidance for silvicultural planning in temperate plantations.

Keywords
compensatory growth • hydraulic architecture • adaptive response

1 Campo Anexo San Martín - IFAB (INTA - CONICET)- Instituto de Investigaciones Forestales y Agropecuarias de Bariloche. Ruta Nacional N° 40 Km 1911. C. P. 8430. Paraje Las Golondrinas. Lago Puelo. Chubut. Argentina. * letourneau.federico@inta.gob.ar

2 Universidad Nacional del Comahue. Centro Regional Universitario San Martín de los Andes (CRUSMA). Pasaje de la Paz 235. San Martín de los Andes. C. P. 8370. Neuquén. Argentina.

Resumen

Los tratamientos tempranos de poda y raleo en plantaciones de *Pinus ponderosa* en la Patagonia Andina provocaron respuestas de crecimiento compensatorio, evidenciadas por un mayor desarrollo del fuste y ajustes estructurales. Mediante un diseño factorial y modelos de efectos mixtos, se evaluaron el crecimiento del tallo, la dinámica de luz en la copa, la longitud de traqueidas (TL), la biomasa foliar, la densidad de la madera y la razón de Huber (Hv) cinco años después del tratamiento. Los árboles sometidos al tratamiento combinado de poda y raleo (PT) mostraron el mayor incremento en el área basal, indicando una reasignación de recursos hacia estructuras de sostén a pesar de la pérdida foliar inicial. Los árboles podados mantuvieron valores elevados de Hv y lograron una recuperación intermedia de biomasa foliar, mientras que la elongación de traqueidas fue mayor en los árboles tratados, lo que sugiere una maduración acelerada del xilema. La densidad de la madera no se vio afectada. Estos resultados demuestran la plasticidad estructural de *P. ponderosa*, evidenciando su capacidad para mantener la funcionalidad hidráulica y sostener el crecimiento ante modificaciones en la copa. Los hallazgos aportan herramientas útiles para la planificación silvícola en plantaciones templadas.

Palabras clave
crecimiento compensatorio • arquitectura hidráulica • respuesta adaptativa

Introduction

Pinus ponderosa is the most widespread conifer species in forest plantations in Andean Patagonia, Argentina (24). Its cultivation in ecotone zones has government support for its establishment and silvicultural management. This species shows intermediate growth and numerous basal branches requiring pruning to reduce fire risk or improve wood quality. Forest managers must apply these cultural practices at an early, pre-commercial thinning stage for these cultural practices to be effective. However, researchers have not fully clarified how pruning and thinning affect early tree growth and development.

Previous studies have explored the influence of pruning and planting density on *Pinus ponderosa's* growth and physiological performance. For Gyenge *et al.* (2009, 2010) demonstrated that pruning temporarily reduces diameter growth, while planting density significantly affects resource availability and individual tree growth. Additionally, Gyenge *et al.* (2012) analyzed responses to water stress under different competition levels, showing short- and long-term physiological adjustments. Similarly, Martínez-Meier *et al.* (2015), highlighted that intraspecific competition alters the wood structure in high-density stands, increasing earlywood density and reducing the hydraulic efficiency of trees, affecting their ability to respond to water stress conditions.

Cambial maturation is a key process in woody plants. It produces secondary xylem composed of tracheids and other cellular elements. Tracheid size is a key indicator of this maturation, influencing both hydraulic and mechanical function (13). In *P. ponderosa* from this region, tracheid length (TL) increases during the transition from juvenile to mature wood (17, 34).

TL in conifers also correlates with tracheid diameter (30). Together, these traits determine water transport efficiency through the xylem. Therefore, TL provides valuable information on cambial maturation and its impact on wood function and quality.

Pine productivity depends strongly on canopy structure, including crown shape, leaf area index, leaf distribution, and shoot architecture. Tree growth is directly related to the ability to intercept solar radiation (31, 32, 33). As trees grow, vertical foliage distribution generates self-shading and reduces light to lower branches. This loss of light often triggers crown recession, the shedding of shaded leaves, which strongly influences growth dynamics (7, 15).

These conditions alter biomass partitioning among foliage, branches, and trunk. After pruning, they also modify the relationship between conductive tissue and leaf biomass (14). The Huber value (Hv), defined as the ratio of xylem cross-sectional area (G) to total leaf biomass (FB), is a key indicator of hydraulic function (23). Because gas exchange occurs through the leaf surface, predicting biomass partitioning requires considering both G and FB.

Silvicultural practices modify this functional relationship. Pruning reduces active leaf area, temporarily increasing Hv. This may enhance the ability of conductive tissue to supply water to residual foliage but can cause short-term hydraulic imbalance during drought (9, 21). In contrast, thinning reduces competition and promotes both greater leaf area and conductive tissue, thereby enhancing growth efficiency (11).

These responses depend on treatment intensity, initial stand conditions, and resource availability. To analyze them, we used linear mixed-effects models (MEMs). MEMs decompose variability into components associated with treatments and site or individual differences (4, 19, 35). They also handle covariates effectively by adjusting for interactions and accounting for dependencies such as repeated or nested data. This approach provides more precise comparisons between treatments and controls, even in heterogeneous or unbalanced datasets.

This study evaluates the effects of pruning and thinning on aboveground biomass allocation in *Pinus ponderosa*. We focus on the relationship between foliar biomass and trunk growth, and how this relationship changes after treatment. By analyzing biomass partitioning, we aim to determine whether silvicultural practices alter the balance between foliage and conductive tissue, thereby influencing growth dynamics and hydraulic function.

We hypothesize that pruning reduces photosynthetic capacity by removing basal branches. This reduction may decrease trunk growth and alter basal taper due to changes in branch structure and radial growth. In contrast, thinning increases light availability for remaining trees and reduces intraspecific competition. This effect may compensate for foliage loss caused by pruning, favoring resource allocation to trunk growth and potentially modifying xylem structure.

Given tracheid size is a key determinant of hydraulic efficiency, we further hypothesize that pruning and thinning induce adjustments in TL. These changes may represent compensatory responses to altered canopy structure and resource availability.

If Hv values in pruned and thinned trees converge toward those of controls, this would indicate xylem adjustment to balance water transport and mechanical support. However, if Hv differences persist, this would suggest long-term changes in biomass allocation and a departure from the expected proportionality between conductive tissue and foliage biomass.

These hypotheses guide the assessment of whether pruned trees adjust hydraulic and mechanical structures to maintain functional integrity under different management regimes. Additionally, analyzing TL as an indicator of xylem plasticity, together with wood density (WD), offers insight into how structural adjustments help trees cope with changes in resource availability and canopy modification.

Materials and Methods

We conducted a completely randomized factorial design in a 12-year-old *P. ponderosa* plantation in northwestern Chubut Province, Argentina (latitude -42.300059°, longitude -71.296954°). The stand had a mean diameter at breast height (dbh) of 8.5 cm and a mean top height of 4.43 m, with 3 × 3 m spacing. The site quality index ranged from 13 to 15 m (1).

Four silvicultural treatments were applied: pruning (P), thinning (T), pruning plus thinning (PT), and a control (C). Each treatment was assigned to five experimental units (EUs), for 20 units.

Each EU was a 144 m^2 plot with 16 trees, separated by a buffer row. Before applying treatments, and again five years later, we measured all trees (n = 215). Measurements included dbh with dendrometric tape, crown base height (CrwH) with metric tape, and total height (TH) with a Haglöf Vertex III hypsometer. The dbh point was permanently marked for consistent re-measurement. The crown base was defined as the lowest whorl with at least three live branches, provided that all branches below were dead or pruned.

Pruning removed 50% of the basal crown. Thinning eliminated 50% of the trees, primarily smaller and less vigorous individuals.

At the end of the experiment, we randomly selected 32 trees for destructive sampling. Each treatment contributed eight trees, with at least two per EU.

Vertical light profiles were measured immediately after treatment and again five years later. Eight HOBO sensors were mounted horizontally on a rod at 1 m intervals, from 0.3 m above ground to the apex. The top sensor served as the reference. The rod was positioned at the crown periphery in four cardinal directions per tree for at least one minute each time. Mean light intensity was then calculated per tree, and integrated light intensity (ILI) along the crown was obtained using Simpson's rule (3).

Five years after treatment, we felled the sampled trees and collected stem disks at stump height (0.1 m) and at breast height (1.3 m). Polished and digitized discs were analyzed with Map Maker v3.5 to measure total cross-sectional area (including bark) and under-bark area. The latter represented woody tissues without separating xylem and phloem. Bark proportion was also compared among treatments and excluded from further analyses. Annual ring areas corresponding to the experimental period were extracted to calculate cross-sectional area increment at both heights, incGdbh and incGstump, respectively.

Tracheid length (TL) was assessed in two annual rings per tree-one formed before and four years after treatment. Wood samples corresponding to each ring were macerated following the Franklin (1937) technique. Tracheids were measured under an optical microscope at 40× magnification equipped with an ocular micrometer, following the anatomical measurement standards of the IAWA (2004) and the recommendations of Muñiz and Coradin (1991). A total of 1,920 tracheids were measured (30 tracheids × 2 rings × 32 trees).

In addition, oven-dried wood samples were used to determine anhydrous density at breast height (2 annual rings × 32 trees; n = 64 samples). For this purpose, samples were first saturated in water to determine their saturated weight, then air-dried for 24 h, and subsequently oven-dried at 103°C to obtain anhydrous weight. Between drying and weighing, samples were kept in a desiccator with silica gel to prevent moisture absorption. Basic density was then calculated using saturated and anhydrous weights, applying the maximum moisture content formula described by Smith (1954).

We estimated total tree foliar biomass (FBtree) in two steps. First, we developed an allometric model predicting needle biomass from branch diameter (FBbranch), using 59 trees from 15 regional plots.

These trees represented a wide range of sizes (dbh: 5-38 cm; height: 3-21 m; crown length: 1.5-15.5 m; age: 9-34 years). One branch per tree was sampled. Twigs and needles were separated, oven-dried at 60 °C, and weighed. The branch diameter was measured 5 cm from the insertion using a digital caliper. In a second step branch model was then applied to all branches of the sample trees to estimate FBtree. Then we fitted a mixed-effects model (MEM) to predict FBtree using "crown length × dbh^2" as the main predictor. The model was validated with a jackknife resampling procedure (5, 8).

We also tested whether site quality (intercept growth, 1) was a significant covariate. The allometric equation for branch biomass was: FBbranch [g] = 0.299 × dbh [mm]^2.186. Following Nakagawa and Schielzeth (2013), this model explained 84% of the variance (marginal R^2 = 0.84). For FBtree, the marginal R^2 was 0.859, with no significant effect of site quality. We therefore applied the following equation to the factorial experiment: FBtree [kg] = 91.20 × crown length [m] × dbh^2 [m^2].

Statistical analyses addressed the following variables: 1) incGdbh, 2) the relationship of incGdbh vs Hv and FBtree, 3) the relationship of incGdbh vs incGstump, 4) TL, 5) WD, and 6) Hv.

We fitted MEMs for variables 1), 2), 3), and 4) (table 1, page 38), and assessed fixed effects with likelihood ratio tests (LRT).

For all variables, treatment differences were tested with Tukey-adjusted pairwise comparisons using estimated marginal means (EMMs) (16). MEMs were adjusted according to Bates *et al.* (2015). All analyses were performed in R (2021).

The general model structure was:

$$y \sim \text{Fixed factors} + \text{Covariates} + (1 \mid \text{Grouping factor}).$$

Specific cases for variables 1)- 3) are detailed in table 1 (page 38).

Table 1. Full MEMs formulations to perform tests. incGdbh: the dependent cross-sectional area increments under bark at breast height.

Tabla 1. Descripción del modelo lineal completo de efectos mixtos utilizados para los análisis. incGdbh: variable dependiente, incremento del área transversal del tronco bajo la corteza a la altura del pecho.

Test	Full model formulation
1)	incGdbh ~ intercept + Treatment + FBtree-f + (1|plot:tree)
2)	incGdbh ~ intercept + Hv-f + FBtree-f + (1|plot:tree)
3)	incGdbh ~ intercept + Treatment + incGstump + (1|plot:tree)
4)	TL ~ intercept + Treatment + age + (1|plot:tree)

The fixed effects factor was silvicultural treatment with levels C, P, PT, and T as Treatment. Covariates FBtree-f: Tree foliar biomass at the end of the experiment, Hv-f: Huber value at the end of the experiment, incGstump: cross–sectional area increments under bark at stump height. Random effects: grouping the individual tree nested in the EU, experimental unit, or plot.

El factor de efectos fijos fue el tratamiento silvícola con niveles C, P, PT y T. Covariables: FBtree-f: biomasa foliar del árbol al final del experimento; Hv-f: valor de Huber al final del experimento; incGstump: incremento del área transversal del tronco bajo la corteza a la altura del tocón. Efectos aleatorios: agrupamiento del árbol individual anidado en la unidad experimental (EU), o parcela.

Results

Bark proportion at breast height did not differ among treatments (LRT; F = 0.582, df = 3, p = 0.633). Bark represented 19.7 ± 3.1% of trunk cross-sectional area. It was excluded from all subsequent analyses.

At the beginning of the experiment, integrated light intensity (ILI-i) (table 2) was higher in pruned treatments P (90.4 ± 2%) and PT (90.1 ± 1%) than in control C (70.8 ± 2%) and thinning T (84.2 ± 1%). The similarity between P and PT indicates that pruning was the main factor increasing crown light exposure, primarily by raising crown base height (CrwH) (table 2).

By the end of the experiment, integrated light intensity (ILI-f) decreased in all treatments: - 9.9% C,

-18.6% P, - 20.9% PT , - 7.5% T. Despite this reduction, pruned treatments retained the highest final values-P (73.6%) and PT (71.3%)-showing a lasting structural effect on canopy light penetration.

Table 2. Tree biometric values in the factorial experiment.

Tabla 2. Valores biométricos observados de los árboles en el experimento factorial.

Treatment	Dbh_i [mm]	Dbh_f [mm]	$CrwH_i$ [m]	$CrwH_f$ [m]	TH_i [m]	TH_f [m]	ILI_i [%]	ILI_f[%]	$incG_{dbh}$[mm^2]
C	88 ± 16 a	151 ± 20	0.10 ± 0.1	1.1 ± 0.4	3.8 ± 0.4 a	6.1 ± 0.6 a	71 ± 2 c	64 ± 2 a	9,659.0 ± 2.263
P	86 ± 22 a	142 ± 21	2.08 ± 0.4	2.03 ± 0.3	3.7 ± 0.6 a	5.7 ± 0.5 a	90 ± 2 a	74 ± 4 d	8,123.0 ± 2.089
PT	88 ± 19 a	150 ± 22	2.28 ± 0.2	2.16 ± 0.3	3.8 ± 0.5 a	5.8 ± 0.6 a	90 ± 1 a	72 ± 2 b	9,445.0 ± 2.592
T	88 ± 20 a	160 ± 27	0.11 ± 0.1	0.92 ± 0.4	3.8 ± 0.5 a	6.1 ± 0.6 a	84 ± 1 b	78 ± 3 c	11,406.0 ± 3.543

Mean ± standard deviation for each treatment. Dbh: diameter at 1.3 m height, CrwH: live crown base height, TH: total height, ILI: integrated light intensity, incGdbh: increment in cross-sectional area of woody tissues at breast height. Suffixes "-i" and "-f" denote the initial and final moments of the experiment. Different letters show significant statistical differences.

Media ± desviación estándar para cada tratamiento. Dbh: diámetro a 1,3 m de altura, CrwH: altura de la base de la copa viva, TH: altura total, ILI: intensidad lumínica integrada, incGdbh: incremento del área seccional de tejidos leñosos a la altura del pecho. Los sufijos "i" y "f" indican los momentos inicial y final del experimento. Letras distintas indican diferencias estadísticas significativas.

Leaf biomass (FBtree) increased in all treatments during the experiment (table 3). The magnitude of change, however, differed among treatments. Control (C) and thinning (T) reached the highest final values, 10.8 ± 3.8 kg and 12.6 ± 5.2 kg, respectively. Both started from similar baselines, 2.8 ± 1.3 kg and 2.9 ± 1.7 kg, corresponding to increases of 287% and 331%.

Table 3. Functional and structural values of tree traits in the factorial experiment.

Tabla 3. Valores funcionales y estructurales observados de los atributos del árbol en el experimento factorial.

Treatment	FBtree -i [kg]	FBtree -f [kg]	Hv-i [mm² / kg]	Hv-f [mm² / kg]	TL-i [µm]	TL-f [µm]
C	2.79 ± 1.3 a	10.81± 3.8 a	1,901.0 ± 243 a	1,412.0 ± 197 a	1,690.0 ± 212 ac	1,752.0 ± 145 ad
P	1.23 ± 0.8 b	7.03 ± 2.7b	4,709.0 ± 1,715 b	1,920.0 ± 203 b	1,614.0 ± 145 ac	1,763.0 ± 129 ad
PT	1.27 ± 0.8 b	7.97 ± 3.3 b	4,803.0 ± 1,424 b	1,940.0 ± 341 b	1,403.0 ± 292 ac	1,546.0 ± 263 ad
T	2.93 ±1.7 a	12.64 ± 5.2 a	1,896.0 ± 331 a	1,359.0 ± 165 a	1,680.0 ± 267 ac	1,893.0 ± 277 ad

Treatment	WD-i [g/cm³]	WD-f [g/cm³]
C	0.384 ± 0.01 a	0.373 ± 0.02 a
P	0.385 ± 0.03 a	0.373 ± 0.02 a
PT	0.375 ± 0.05 a	0.379 ± 0.04 a
T	0.393 ± 0.05 a	0.381 ± 0.04 a

FBtree: tree foliar biomass, Hv: Huber value, TL: tracheid length, and WD: wood density. Mean ± standard deviation. Different letters show significant statistical differences. For TL-i and TL-f, the first letter compares treatment, and the second letter compares experimental moment - initial *vs* final- for the same treatment. Suffixes "i" and "f" denote the initial and final moments of the experiment.

FBtree: biomasa foliar del árbol, Hv: valor de Huber, TL: longitud de traqueidas y WD: densidad de la madera. Media ± desviación estándar. Letras distintas indican diferencias estadísticas significativas. Para TL-i y TL-f, la primera letra corresponde a la comparación entre tratamientos y la segunda al momento del experimento -inicial *vs* final- para el mismo tratamiento. Los sufijos "i" y "f" indican los momentos inicial y final del experimento.

In contrast, pruning treatments began with significantly lower FBtree due to foliage removal. Initial values were 1.2 ± 0.8 kg in P and 1.3 ± 0.8 kg in PT. By the end, both reached intermediate levels: 7.0 ± 2.8 kg in P and 8.0 ± 3.3 kg in PT. These increases of 472% and 528% indicate compensatory foliage regrowth in pruned trees, while unpruned treatments followed steady canopy expansion.

Initial Hv-i (figure 1, page 40; table 3) was substantially higher in P (4,709 ± 1,715 mm^2/kg) and PT (4,803 ± 1,424 mm^2/kg) than in C (1,901 ± 243 mm^2/kg) and T (1,896 ± 331 mm^2/kg). This pattern reflected the immediate pruning-induced reduction in leaf biomass. Over time, Hv declined in all treatments, showing a rebalancing between conductive tissue and foliage. The greatest declines occurred in P (-59.2%) and PT (-59.6%). Yet, both treatments retained higher final Hv values than controls, indicating a persistent structural effect of pruning.

Tracheid length varied widely but increased in all treatments (figure 2, page 40), consistent with age-related xylem maturation (Test 4 in table 1, page 38; AIC = 864.9, model p = 0.0001, Age coefficient = 28.35, p = 0.003). Increases were largest in T (+12.7%) and PT (+10.2%), followed by P (+9.2%) and C (+3.7%). These results suggest that silvicultural treatments may accelerate tracheid elongation. Although differences were not statistically significant, treatment effects revealed biologically relevant trends.

Wood density remained stable across treatments during the five years (table 3). Initial values ranged from 0.375 to 0.393 g/cm^3. Final values showed only slight variation (0.373-0.381 g/cm^3). No significant differences were detected, indicating that treatments did not markedly affect wood density.

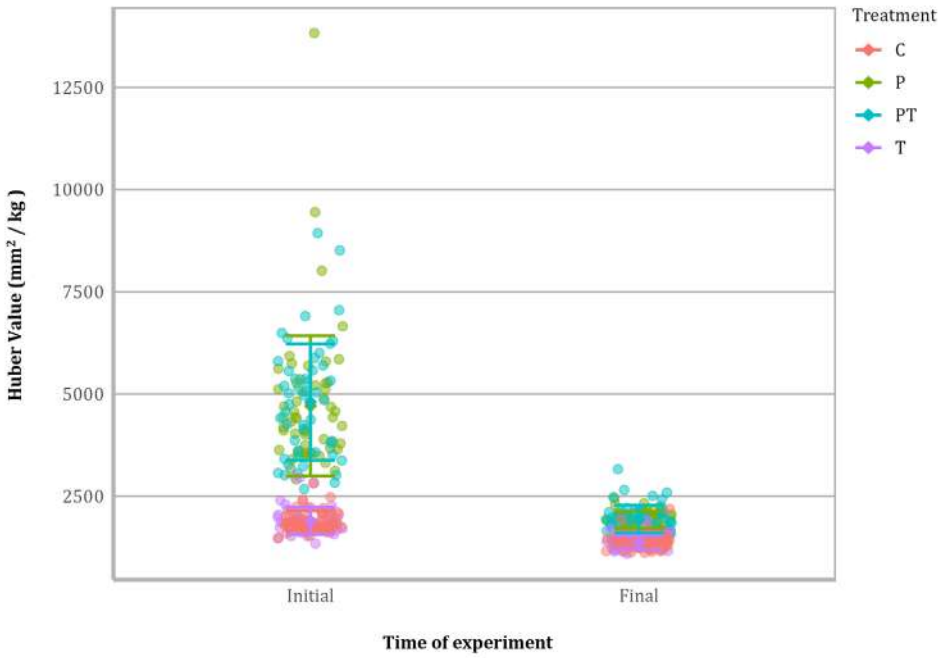

Dots jittered to provide a more comprehensive understanding.

Los puntos están desplazados (jitter) para facilitar su visualización.

Figure 1. Huber values (Hv) for initial and final treatment moments.

Figura 1. Valores observados de la razón de Huber (Hv) al inicio y al final de los tratamientos.

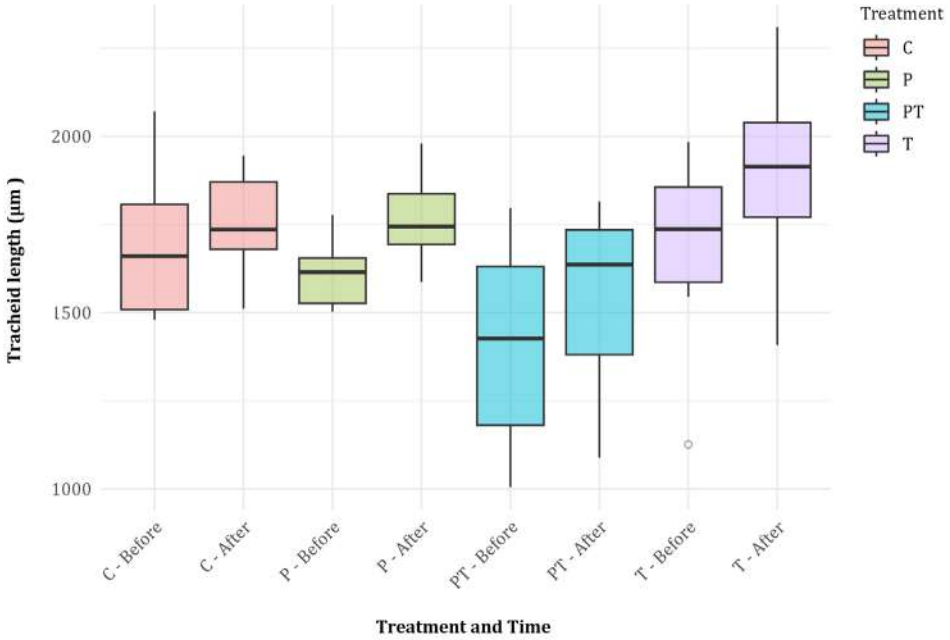

Figure 2. Tracheid length distribution, before and after treatment (C control, P Pruning, PT Pruning plus thinning, T thinning).

Figura 2. Distribución de la longitud de traqueida, antes y después del tratamiento (C testigo, P poda, PT poda y raleo, T raleo).

In Test 1 (table 1, page 38; figure 3), the full model with treatments and FBtree-f explained trunk growth variation (LRT: χ^2 = 422, df = 7, p < 2.2e-16). Predicted intercepts were highest for PT (5,341.0 mm^2), followed by P (4,492.0 mm^2), T (4,013.0 mm^2), and C (3,315.0 mm^2). PT differed significantly from C (Δ = 1,626.0 ± 454 mm^2, p = 0.007). The PT-T contrast approached significance (p = 0.076), suggesting a trend. A complementary model using Hv-f and FBtree-f (Test 2) had similar explanatory power (AIC = 3,556.5 *vs.* 3,547.8). This supports the hypothesis that hydraulic adjustments mediate post-treatment growth.

Predictions according to the full model of test 1.

Predicciones según el modelo completo del test 1.

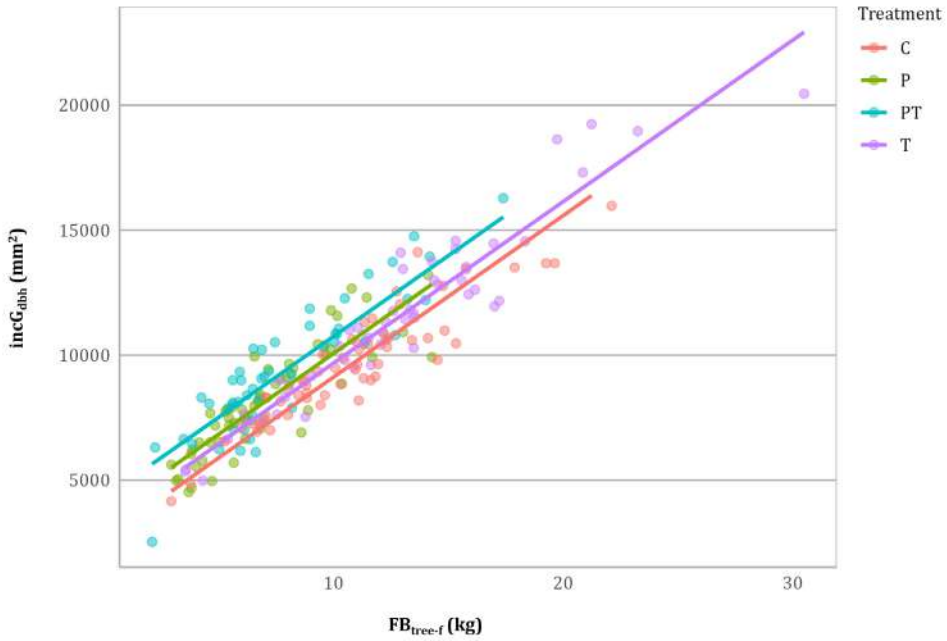

Figure 3. Observed (dots) and predicted (lines) values of increment of cross-sectional trunk area (incGdbh) for treatments along tree foliar biomass at the end of the experiment (FBtree-f).

Figura 3. Valores observados (puntos) y predichos (líneas) del crecimiento del área transversal del tronco (incGdbh) para los tratamientos, en función de la biomasa foliar final del árbol (FBtree-f).

Finally, the proportionality incGdbh *vs* incGstump, was not significantly affected by treatments (Test 3, χ^2 = 1.6198, df = 3, p-value = 0.6549). Stem allocation patterns, therefore, remained consistent despite pruning.

Discussion

Early silvicultural treatments in *Pinus ponderosa* plantations produced clear changes in growth and crown structure. Pruning and thinning, especially when combined, enhanced trunk growth rates despite the initial reduction in foliar biomass. Pruning increased crown light penetration, stabilized crown architecture, and promoted compensatory foliage development.

These treatments also triggered structural and functional adjustments. Pruned trees maintained higher Huber values (Hv) than controls during the study period. Tracheid length increased across all treatments, with greater elongation in treated trees. These anatomical shifts, although not always linked to higher trunk growth, indicate xylem maturation adjustments that may improve hydraulic efficiency.

The increased trunk growth in the pruning plus thinning treatment (PT) supports the hypothesis that *P. ponderosa* shows compensatory responses to early canopy interventions. Despite foliage loss from pruning, treated trees -particularly under PT- displayed greater xylem area increments, likely reallocating resources to supportive structures. These dynamics align with compensatory growth theory, which describes adaptive responses to sudden reductions in foliage (21, 22).

Our findings also indicate that *P. ponderosa* adjusts hydraulic architecture without compromising wood density. The separation between enhanced structural growth and stable density suggests anatomical plasticity via tracheid elongation and crown reconfiguration, not faster or lower-quality wood formation.. This result agrees with previous studies (9, 10, 11), which reported morphological and physiological adjustments under pruning, thinning, and drought, including crown restructuring and improved water-use efficiency, without changes in wood density. Likewise, Martínez-Meier *et al.* (2015) detected fine-scale density variations with microdensitometry, while our ring-level estimates revealed no significant effects, reinforcing the idea of macro-anatomical rather than biochemical adaptation.

Although this study focused on structural traits, the compensatory responses in trunk growth, foliage regrowth, and xylem anatomy likely reflect ecophysiological adjustments. Canopy opening in pruned treatments increased light exposure, possibly enhancing stomatal conductance and photosynthetic rates. These changes likely promoted carbon assimilation and foliage regeneration (20, 31).

Tracheid elongation and shifts in Huber values further suggest adjustments in stem hydraulic architecture. Such changes may improve specific hydraulic conductivity and support water transport to the regenerating canopy (10, 13, 30). Reduced competition in thinned plots likely improved water availability, favoring higher leaf water potential and maintaining stomatal function (9, 11). Although not directly measured, these responses match known mechanisms of resource reallocation and water–carbon coupling in conifers under stress (15, 18).

These findings refine the broader hypothesis by Fernández *et al.* (2011), who proposed that Pinus species show lower physiological plasticity than Eucalyptus. While this may hold at the biochemical level, our results highlight structural adaptability in *P. ponderosa*. This species compensates for canopy changes by adjusting conduit dimensions and crown structure to maintain hydraulic function while keeping wood density stable. Such capacity has important implications for resilience and productivity under silvicultural management and environmental variability.

This study has several limitations: a small sample size, a five-year monitoring period, and the absence of direct physiological measurements. Another limitation is that our design does not explicitly account for soil or landform heterogeneity, which can modulate radial growth patterns in arid environments (27). Future work should extend monitoring, include direct evaluations of stomatal conductance, photosynthesis, and hydraulic conductivity, assess vascular reuse after pruning, and incorporate spatial variation in site conditions. These efforts will help clarify the functional mechanisms driving compensatory responses in *P. ponderosa*.

Conclusions

This study confirms that early pruning and thinning in *Pinus ponderosa* plantations trigger compensatory growth, especially when both treatments are combined. The main effects included greater conductive tissue area, partial recovery of foliar biomass, and tracheid elongation, while wood density remained unchanged.

These structural adjustments support the hypothesis that hydraulic and anatomical plasticity drive the observed responses. The findings highlight the value of early silvicultural interventions to enhance growth and maintain hydraulic function, providing guidance for management in temperate conifer plantations. A deeper understanding of physiological and structural adjustments will further inform strategies to optimize productivity and resilience in *P. ponderosa*, especially in the early stages.

References

1. Andenmatten, E.; Letourneau, F. J. 1997. Funciones de intercepción de crecimiento para predicción de índice de sitio en pino ponderosa, de aplicación en la Región Andino Patagónica de Río Negro y Chubut. Revista Quebracho. 5: 5-9.
2. Bates, D.; Mächler, M.; Bolker, B.; Walker, S. 2015. Fitting Linear Mixed-Effects Models Using lme4. Journal of Statistical Software. 67(1): 1-48. https://doi.org/10.18637/jss.v067.i01
3. Chapra, S. C.; Canale, R. P. 2015. Numerical Methods for Engineers, 7th ed. McGraw- Hill Education. https://archive.org/details/numerical-methods-for-engineers-7th-edit/mode/2up
4. Demidenko, E. 2013. Mixed models: Theory and applications with R (2nd ed.). John Wiley & Sons. (Wiley Series in Probability and Statistics). p 717.
5. Fernández, M. E.; Fernández Tschieder, E.; Letourneau, F. J.; Gyenge, J. E. 2011. Why do Pinus species have different growth dominance patterns than Eucalyptus species? A hypothesis based on differential physiological plasticity. Forest Ecology and Management. 261(6): 1061-1068. https://doi.org/10.1016/j.foreco.2010.12.028
6. Franklin, G. L. 1937. Permanent preparations of macerated wood fibres. Tropical Woods. 49: 21-22.
7. Garber, S. M.; Monserud, R. A.; Maguire, D. A. 2008. Crown recession patterns in three conifer species of the Northern Rocky Mountains. Forest Science. 54(6): 633-646. https://doi.org/10.1093/forestscience/54.6.633
8. Gregoire, T. G. 1984. The jackknife: A resampling technique with application to linear models. Canadian Journal of Forest Research. 14(3): 483-487. https://doi.org/10.1139/x84-092
9. Gyenge, J.; Fernández, M. E.; Schlichter, T. 2009. Effect of pruning on branch production and water relations in widely spaced ponderosa pines. Agroforest Syst. 77: 223-235. https://doi.org/10.1007/s10457-008-9183-9
10. Gyenge, J. E.; Fernández, M. E.; Schlichter, T. M. 2010. Effect of stand density and pruning on growth of ponderosa pines in NW Patagonia, Argentina. Agroforestry Systems. 78(3): 233-241. https://doi.org/10.1007/s10457-009-9240-z
11. Gyenge, J.; Fernández, M. E.; Varela, S. A. 2012. Short-and long-term responses to seasonal drought in ponderosa pines growing at different plantation densities in Patagonia, South America. Trees. 26(6): 1905-1917. https://doi.org/10.1007/s00468-012-0759-7
12. IAWA Committee. 2004. IAWA list of microscopic features for softwood identification. IAWA Journal. 25(1): 1-70. https://doi.org/10.1163/22941932-90000349
13. Lachenbruch, B.; McCulloh, K. A. 2014. Traits, properties, and performance: how woody plants combine hydraulic and mechanical functions in a cell, tissue, or whole plant. New Phytologist. 204(4): 747-764. https://doi.org/10.1111/nph.13035
14. Långström, B.; Hellqvist, C. 1991. Effects of different pruning regimes on growth and sapwood area of Scots pine. Forest Ecology and Management. 44: 239-254. https://doi.org/10.1016/0378-1127(91)90011-J
15. Ledermann, T. 2011. A non-linear model to predict crown recession of Norway spruce (*Picea abies* [L.] Karst.) in Austria. Eur J Forest Res. 130: 521-531.
16. Lenth, R. V. 2024. Emmeans: Estimated Marginal Means, aka Least-Squares Means. R package version.
17. Letourneau, F. J.; Medina, A. A.; Pampiglioni, A.; Ancalao, M.; Saihueque, M.; González, A. 2016. Efecto de tratamientos silvícolas sobre la maduración de la madera de una plantación de Pino ponderosa. V Jornadas Forestales Patagónicas.
18. Li, C.; Barclay, H.; Roitberg, B.; Lalonde, R. 2021. Ecology and Prediction of Compensatory Growth: From Theory to Application in Forestry. Frontiers in Plant Science. 12. https://doi.org/10.3389/fpls.2021.655417
19. Macêdo Araújo da Silva, D.; Pereira da Silva Santos, N.; de Sousa Araújo Santos, E. E.; Alves Pereira, G.; Barbosa da Silva Júnior, G.; Gomes da Cunha, J. 2022. Effects of formative and production pruning on fig growth, phenology, and production. Revista de la Facultad de Ciencias Agrarias. Universidad Nacional de Cuyo. Mendoza. Argentia. 54(1): 13-24. DOI: https://doi.org/10.48162/rev.39.061
20. Martínez-Meier, A.; Fernández, M. E.; Dalla-Salda, G.; Gyenge, J.; Licata, J.; Rozenberg, P. 2015. Ecophysiological basis of wood formation in ponderosa pine: Linking water flux patterns with wood microdensity variables. Forest Ecology and Management. 346: 31-40. https://doi.org/10.1016/j.foreco.2015.02.021
21. Maschinski, J.; Whitham, T. G. 1989. The continuum of plant responses to herbivory: The influence of plant association, nutrient availability, and timing. The American Naturalist. 134(1): 1-19. https://doi.org/10.1086/284962
22. McNaughton, S. J. 1983. Compensatory plant growth as a response to herbivory. Oikos. 40(3): 329-336. https://doi.org/10.2307/3544305
23. Mencuccini, M.; Rosas, T.; Rowland, L.; Choat, B.; Cornelissen, H.; Jansen, S.; Kramer, K.; Lapenis, A.; Manzoni, S.; Niinemets, Ü.; Reich, P. B.; Schrodt, F.; Soudzilovskaia, N.; Wright, I. J.; Martínez-Vilalta, J. 2019. Leaf economics and plant hydraulics drive leaf: wood area ratios. New Phytologist. 224(4): 1544-1556. https://doi.org/10.1111/nph.15998
24. Ministerio de Agroindustria. Unidad Para El Cambio Rural-CIEFAP. 2017. Inventario de Plantaciones Forestales en Secano. Región Patagonia. p. 136.

25. Muñiz, G.; Coradin, V. 1991. Norma de procedimientos em estudios de anatomía de madeira. II Gimnospermae. Brasília: Laboratorio de Produtos Florestais. Serie Técnica. 117 p.
26. Nakagawa, S.; Schielzeth, H. 2013. A general and simple method for obtaining R^2 from generalized linear mixed-effects models. Methods in Ecology and Evolution. 4(2): 133-142. https://doi.org/10.1111/j.2041-210X.2012.00261.x
27. Piraino, S.; Roig, F. A. 2024. Landform heterogeneity drives multi-stemmed *Neltuma flexuosa* growth dynamics. Implication for the Central Monte Desert forest management. Revista de la Facultad de Ciencias Agrarias. Universidad Nacional de Cuyo. Mendoza. Argentina. 56(1): 26-34. DOI: https://doi.org/10.48162/rev.39.120
28. R Core Team. 2021. R: A language and environment for statistical computing. R Foundation for Statistical Computing.
29. Smith, D. M. 1954. Maximum moisture content method for determining specific gravity of small wood samples. Report N° 2014. USDA Forest Service. Forest Products Laboratory.
30. Sperry, J. S.; Hacke, U. G.; Pittermann, J. 2006. Size and function in conifer tracheids and angiosperm vessels. American Journal of Botany. 93(10): 1490-1500. https://doi.org/10.3732/ajb.93.10.1490
31. Wang, Y.; Liu, Z.; Li, J.; Cao, X.; Lv, Y. 2024. Assessing the Relationship between Tree Growth, Crown Size, and Neighboring Tree Species Diversity in Mixed Coniferous and Broad Forests Using Crown Size Competition Indices. Forests. 15(633): 1-17. https://doi.org/10.3390/f15040633
32. Zeng B. 2003. Aboveground biomass partitioning and leaf development of Chinese subtropical trees following pruning. Forest Ecology and Management 173: 135-144. https://doi.org/10.1016/S0378-1127(01)00821-0
33. Zhu, Z.; Kleinn, C.; Nölke, N. 2021. Assessing tree crown volume-a review. Forestry: An International Journal of Forest Research. 94(1): 18-35. https://doi.org/10.1093/forestry/cpaa037
34. Zingoni, M. I.; Andia, I.; Mele, U. 2007. Longitud de traqueidas y madera juvenil en el fuste de un árbol de pino ponderosa de 50 años-SO Neuquén. III Congreso Iberoamericano de Productos Forestales IBEROMADERA 2007.
35. Zuur, A. F.; Ieno, E. N.; Walker, N. J.; Saveliev, A. A.; Smith, G. M. 2009. Mixed effects models and extensions in ecology with R. Springer Science & Business Media. https://doi.org/10.1007/978-0-387-87458-6

Acknowledgments

We thank the support staff of Campo Anexo San Martín - INTA for assistance during sampling and Ea. El Maitén for providing the experimental site. We are also grateful to the anonymous reviewers for their constructive feedback, which improved the quality and rigor of the manuscript.

Isolation of Polyhydroxyalkanoate (PHA)-Producing *Azotobacter* spp. from Crop Rhizospheres Located in Lima, Peru

Selección de *Azotobacter* spp. productores de polihidroxialcanoatos (PHA) aislados de rizósfera de cultivos ubicados en la región de Lima - Perú

Lisset Tupa-Andrade, Junior Caro-Castro, Jorge León-Quispe *

Originales: *Recepción:* 07/09/2023 - *Aceptación:* 02/07/2025

Abstract

PHAs are polyesters found as internal granules in several microorganisms. *Azotobacter* is known for its ability to produce PHA. This study aimed to isolate *Azotobacter* from the rhizosphere of selected crops located in Lima and evaluate their PHA-producing potential. Nile Red medium was used for PHA detection, and Sudan Black B staining allowed microscopic observation. Biopolymer production and quantification were carried out in Burk's medium, PHA minimal medium (PHAMM), and modified PHAMM. In Nile Red medium, 68.2% of strains produced PHA, with *Azotobacter* AzoLur20 exhibiting the highest production, 2.1 g/L of PHA at 96 hours in PHAMM. However, strain AzoLur19 showed higher productivity and stability, achieving 0.06 g/L*h of PHA. Additionally, Sudan Black B staining in Burk's medium revealed larger *Azotobacter* cells with more defined granules. AzoLur19 was classified as *Azotobacter chroococcum*. In conclusion, *Azotobacter* species isolated from crops located in Lima can produce PHA with high yields, with *A. chroococcum* as the predominant species.

Keywords
Azotobacter • polyhydroxyalkanoate • PHA production • bioplastics

Universidad Nacional Mayor de San Marcos. Facultad de Ciencias Biológicas. Laboratorio de Ecología Microbiana. Lima-Perú. * jleonq@unmsm.edu.pe

Resumen

Los PHA son poliésteres que se encuentran como gránulos internos en varios microorganismos. *Azotobacter* se caracteriza por producir PHA. El objetivo de este estudio fue aislar *Azotobacter* de la rizósfera de cultivos ubicados en la región de Lima y evaluar su potencial productor de PHA. Se utilizó el medio Rojo de Nilo para la detección de PHA y la tinción con Sudan Black B para la observación microscópica. La producción y cuantificación del biopolímero se realizó en medio Burk, medio mínimo PHA (PHAMM) y PHAMM modificado. El 68,2% de las cepas produjeron PHA en el medio Rojo de Nilo, siendo la cepa de *Azotobacter* AzoLur20 la más importante produciendo 2,1 g/L de PHA a las 96 horas en el PHAMM; sin embargo, la cepa AzoLur19 fue la más productiva y estable con 0,06 g/L*h de PHA. En cuanto a la tinción con Sudan Black B en medio Burk, se observaron células de *Azotobacter* de mayor tamaño y con gránulos más definidos. Además, el análisis molecular de la cepa AzoLur19 la identificó como *Azotobacter chroococcum*. En conclusión, *Azotobacter* sp. es capaz de producir PHA con un alto rendimiento, destacándose la especie predominante *A. chroococcum* en la rizósfera de varios cultivos.

Palabras clave
Azotobacter • polihidroxialcanoato • producción de PHA • bioplásticos

Introduction

Petroleum-derived plastics significantly contribute to global pollution. Their slow degradation process can take several decades. As a result, the quest for eco-friendly alternatives has become urgent, and polyhydroxyalkanoates (PHAs) are one majorly investigated bioplastics. PHAs share similar properties with petrochemical plastics and have various applications, including the production of disposable everyday items, biomedical devices, pharmaceutical products, agricultural materials, textiles, and nanotechnology products (11, 19, 25, 27).

PHAs are polyesters produced and stored by various microorganisms as internal granules, which serve as carbon and energy sources (26). Although PHA-producing bacteria typically synthesize this compound under stress conditions like an excess of carbon sources or a nutrient limitation, certain exceptions, such as *Azotobacter,* can produce PHA without a stress inducer (23).

Azotobacter species, primarily isolated from the rhizosphere, synthesize PHA continuously during growth. They produce higher quantities when ammonium salts, like ammonium acetate, are supplied to the culture medium (16). Studies achieving high PHA production using *Azotobacter* mutant strains include Burk medium with 0.12% NH_4Cl (7) and PHA minimal medium (PHAMM) with urea (20). Both studies achieved high PHA production using *Azotobacter* mutant strains.

Although further research is still needed, *Azotobacter* is recognized as a good PHA producer (8), easy-to-handle, non-pathogenic, and versatile microorganism. Among *Azotobacter* species, *A. chroococcum* has recently received significant attention (1). Currently, efforts enhancing PHA production and recovery, particularly the most predominant type of PHA, polyhydroxybutyrate (PHB), focus on optimizing media formulation for production, extraction methods, and quantification techniques (17, 22).

This study evaluated the PHA-producing potential of *Azotobacter* isolated from crop rhizospheres in Lima, Peru, determining physicochemical parameters for optimizing PHA production.

Materials and Methods

Collection of Rhizosphere Samples

Rhizosphere samples were collected from the districts of Lurin (latitude: -12.261063, longitude: -76.888297) and Pachacamac (latitude: -12.166853, longitude: -76.857761) in

Lima, Peru. Three crops from Lurin (onion, corn, and sweet potato) and five from Pachacamac (corn, strawberry, cucumber, chilli pepper, and sweet potato) were selected. The samples were transported to the Laboratorio de Ecología Microbiana at the Universidad Nacional Mayor de San Marcos.

***Azotobacter* Isolation and Selection**

Microbial isolation was performed according to Escobar *et al.* (2011). Initially, 10 g of each sample were diluted in 90 mL of saline (10^{-1}). Then, a subsequent dilution (1:10) in saline obtained a second dilution (10^{-2}). The resulting dilution was seeded on Ashby Mannitol Agar and Burk Agar solid media. Simultaneously, a selective enrichment was performed in Ashby Sucrose Broth, later seeded in the mentioned solid media. Isolated bacterial colonies were subcultured until pure strains were obtained and preserved at -20°C in glycerol-containing media.

Biochemical Characterization of *Azotobacter* Strains

Strains exhibiting presumptive morphological features of *Azotobacter* were evaluated through biochemical tests, including sugar fermentation, denitrification, urease testing, and cyst formation.

PHA Detection in Nile Red Medium

Azotobacter strains were inoculated into Nile Red medium. PHA detection was conducted using a 365 nm UV transilluminator (JUNYI brand, model JY02S), reading every 24 hours for 4 days. Presence or absence of intense pink to fuchsia fluorescence classified strains as PHA positive or negative, respectively (5).

PHA Production in Liquid Culture Media

The top five PHA-positive strains from Nile Red medium were subjected to quantitative tests for PHA production in the following liquid media: A) Burk medium with 2% glucose and 0.12% ammonium chloride (7); B) PHA minimal medium (PHAMM), with 0.54 g/L urea and 2% sucrose (20); and C) a modified PHAMM containing 2% glucose and 0.12% ammonium acetate. Aliquots were taken at 24-hour intervals, up to 96 hours, determining dry cell weight, Sudan Black B cell staining, and medium absorbance. Retains were also processed for polymer extraction using sodium hypochlorite and chloroform. The polymer was quantified using sulfuric acid.

Analytical Methods for the Evaluation of PHA Production

Biopolymer accumulation and productivity were evaluated according to Becerra (2013):

A- Percentage of PHA accumulation: $\%PHA = \frac{g_{PHA}}{g_X} \times 100$

B- PHA Productivity: $P_{PHA} = \frac{g_{PHA}}{L \times h}$

where:
gPHA = grams of PHA
gX = grams of biomass
L = liters
h = hours.

In addition, ANOVA, Tukey's test and correlation analysis ($p < 0.05$) were performed using InfoStat v. 2020.

Molecular Characterization of *Azotobacter*

Bacterial DNA extraction was performed using the GeneJET Genomic DNA Purification Kit (Thermo Fisher, USA). Subsequently, the 16S rRNA gene was amplified by PCR with the primers 27F (5'-AGAGTTTGATCCTGGCTCAG-3') and 1492R (5'-GGTTACCTTGTTACGACTT-3'). The PCR products were shipped to Macrogen Inc. (Seoul, Korea) for Sanger sequencing.

The obtained sequences were assembled and aligned with other 16S rRNA gene sequences from different *Azotobacter* species recovered from the GenBank database (2). Phylogenetic inference was conducted using MEGA11 (2021), employing the Neighbor-Joining method with 1000 bootstrap replications.

Results and discussion

Isolation and Characterization of *Azotobacter* sp.

Twenty-two *Azotobacter* strains were isolated. Eighteen (82%) strains were recovered from Lurin (table 1). Although there are no previous studies from this area, Lurin offers more suitable edaphic conditions for *Azotobacter* than Pachacamac. Additionally, most isolates were obtained from corn crops, as typically seen (3). Malynovska *et al*. (2021) emphasized that the highest prevalence of *Azotobacter* occurs in extensive crops, particularly in soils with fewer contaminants.

Table 1. Source and Origin of *Azotobacter* Strains.
Tabla 1. Fuentes y origen de las cepas de *Azotobacter*.

Geographic location	Crop	Total number of isolated strains	Strains confirmed as *Azotobacter*
Pachacamac	Cucumber (*Cucumis sativus*)	AzoMan1, AzoMan2, AzoMan25, AzoMan26, AzoMan27, AzoMan28	
	Corn (*Zea mays*)	AzoMan3, AzoMan4, AzoMan5, AzoMan24	
	Sweet potato (*Ipomoea batatas*)	AzoMan6, AzoMan7, AzoMan8, AzoMan9, AzoMan19, AzoMan20, AzoMan21, AzoMan22, AzoMan23	
	Strawberry (*Fragaria × ananassa*)	AzoMan10, AzoMan11, AzoMan12, AzoMan13	AzoMan12
	Yellow chili (*Capsicum baccatum*)	AzoMan14, AzoMan15, AzoMan16, AzoMan17, AzoMan18	AzoMan14, AzoMan16, AzoMan18
Lurin	Onion (*Allium cepa*)	AzoLur1, AzoLur2, AzoLur11, AzoLur12, AzoLur13, AzoLur14	AzoLur11, AzoLur12, AzoLur13, AzoLur14
	Corn (*Zea mays*)	AzoLur4, AzoLur5, AzoLur6, AzoLur7, AzoLur8, AzoLur9, AzoLur10, AzoLur15, AzoLur16, AzoLur17, AzoLur18, AzoLur19, AzoLur20, AzoLur21	AzoLur4, AzoLur5, AzoLur6, AzoLur7, AzoLur8, AzoLur10, AzoLur15, AzoLur17, AzoLur18, AzoLur19, AzoLur20, AzoLur21
	Sweet potato (*Ipomoea batatas*)	AzoLur3, AzoLur22, AzoLur23	AzoLur22, AzoLur23

Qualitative Selection of PHA in Nile Red Medium

Fifteen of the 22 strains (68%) tested positive for PHA detection using Nile Red medium. The highest fluorescence was observed between 72 and 96 hours of analysis (figure 1, page 49). The best results were obtained when acetone was used as a solvent for the lipophilic dye Nile Red, as suggested by Giraldo *et al*. (2020). When using agar medium as suggested by Carballo (2003), strong fluorescence was observed in the positive strains.

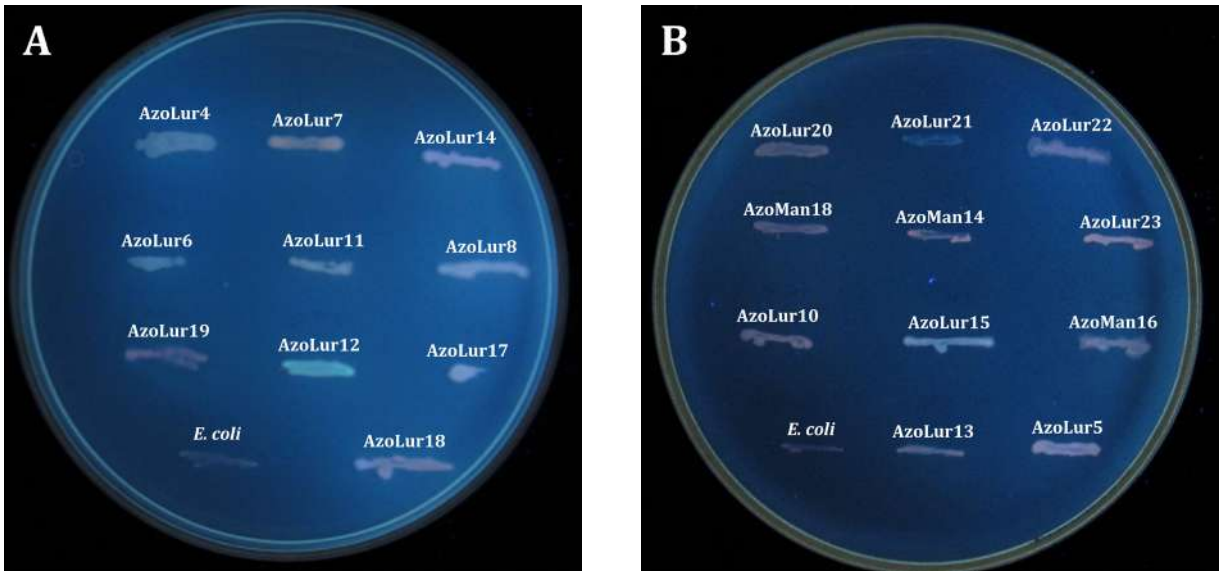

Figure 1. PHA production by *Azotobacter* strains in Nile Red medium observed under a 365 nm transilluminator at A) 72 hours, and B) 96 hours.

Figura 1. Producción de PHA por cepas de *Azotobacter* en medio Rojo de Nilo visto a través de un transiluminador (365nm) a A) 72 horas y B) 96 horas.

Quantitative Evaluation of PHA in Different Media

The highest PHA producer strain in Burk medium was AzoLur23, generating 1.25 g PHA/L at 48 hours from a biomass of 1.58 g/L (figure 2, page 50). In contrast, Cerrone (2011) reported 2.3 g PHA/L at 72 hours for a hyperproducing mutant strain using the same medium. Our result is notably high.

The highest PHA producer in PHAMM was AzoLur20, generating 2.1 g PHA/L at 96 hours from a biomass of 2.99 g/L (figure 2, page 50). Pei *et al*. (2017) obtained 1.5 g PHA/L from one of their evaluated mutant strains. Our higher result indicates that the AzoLur20 strain has potential for future biopolymer biosynthesis.

Considering the modified PHAMM, AzoLur7 was the highest PHA producer, generating 1.66 g PHA/L at 96 hours from a biomass of 2.5 g/L (figure 2, page 50). Although the result was lower than that obtained with the unmodified PHAMM, it is still higher than the values reported by Pei *et al*. (2017).

Biomass production and PHA concentration followed a normal distribution across all media ($p > 0.05$). Significant differences ($p < 0.05$) were observed when comparing the biomass obtained in the Burk and PHAMM media with the biomass in the modified PHAMM medium (figure 3A, page 51). In contrast, no significant differences in PHA concentration were found among the three media evaluated (figure 3B, page 51).

Staining with Sudan Black B

Cell staining with Sudan Black B dye was observed under a light microscope, allowing the dark internal granules to be differentiated from the pink-colored cytosol by the counterstain safranin, as described by Mohammed *et al*. (2019). Cells from Burk medium were larger, and the granules were more prominent compared to the cells recovered from PHAMM and modified PHAMM media (figure 4, page 51). Metals present in the composition of the latter two media may have affected cell growth and development, as previously noted by Lara *et al*. (2010).

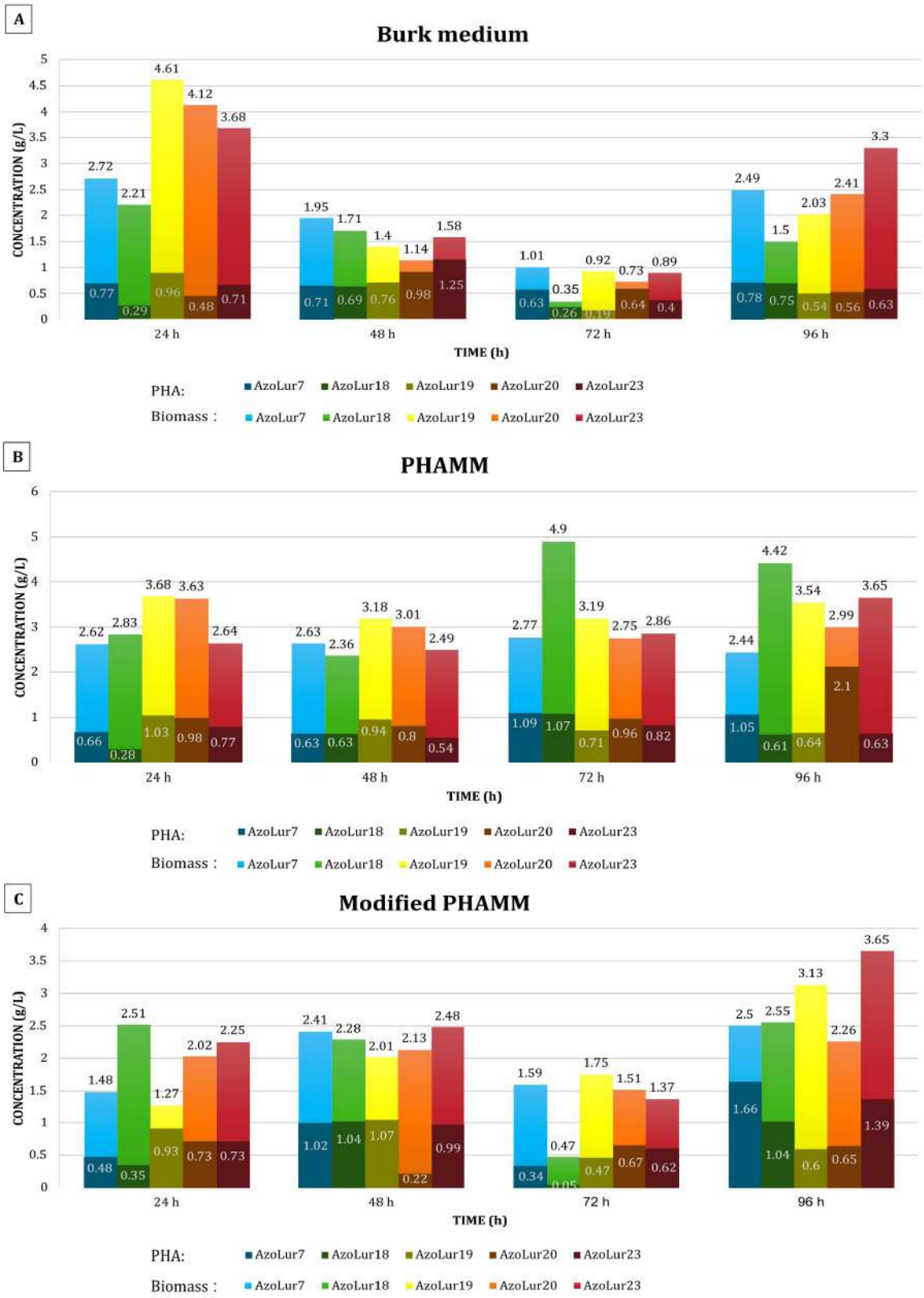

A) Burk medium, B) PHAMM, and C) Modified PHAMM. / A) Medio Burk, B) MMPHA y C) MMPHA modificado.

Figure 2. Determination of biomass and PHA production at 24, 48, 72, and 96 hours.
Figura 2. Evaluación de la biomasa y producción de PHA a las 24, 48, 72 y 96 horas de evaluación.

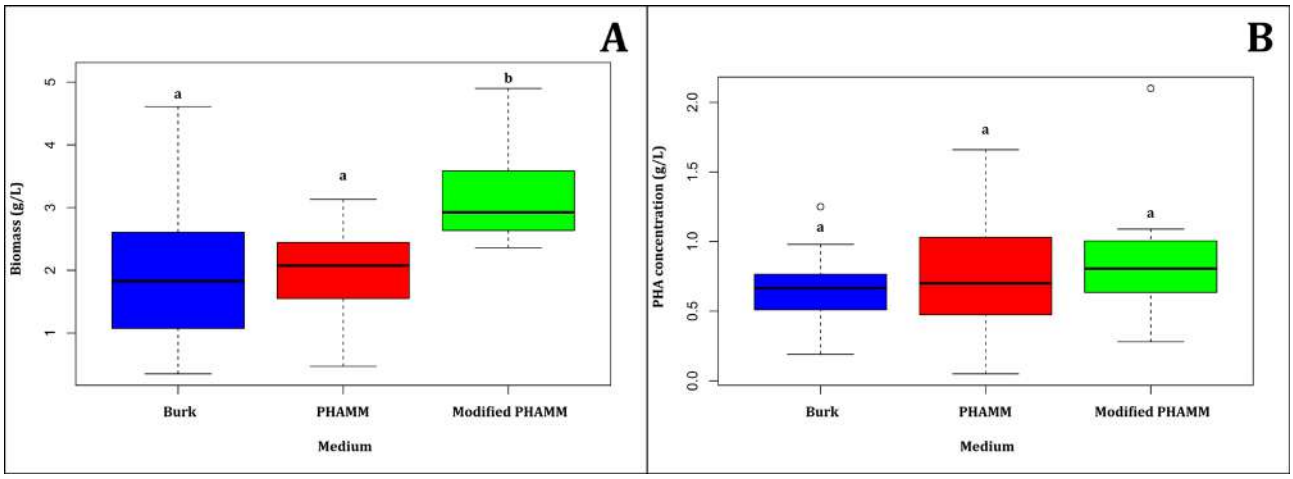

A) biomass and B) PHA concentration across different production media. Lowercase letters indicate significant differences ($p < 0.05$) among the production media.

A) biomasa y B) concentración de PHA en diferentes medios de producción. Las letras minúsculas indican diferencias significativas ($p < 0,05$) entre los medios de producción.

Figure 3. Statistical analysis of biomass and PHA concentration across different production media.

Figura 3. Análisis estadístico de la biomasa y concentración de PHA en diferentes medios de producción.

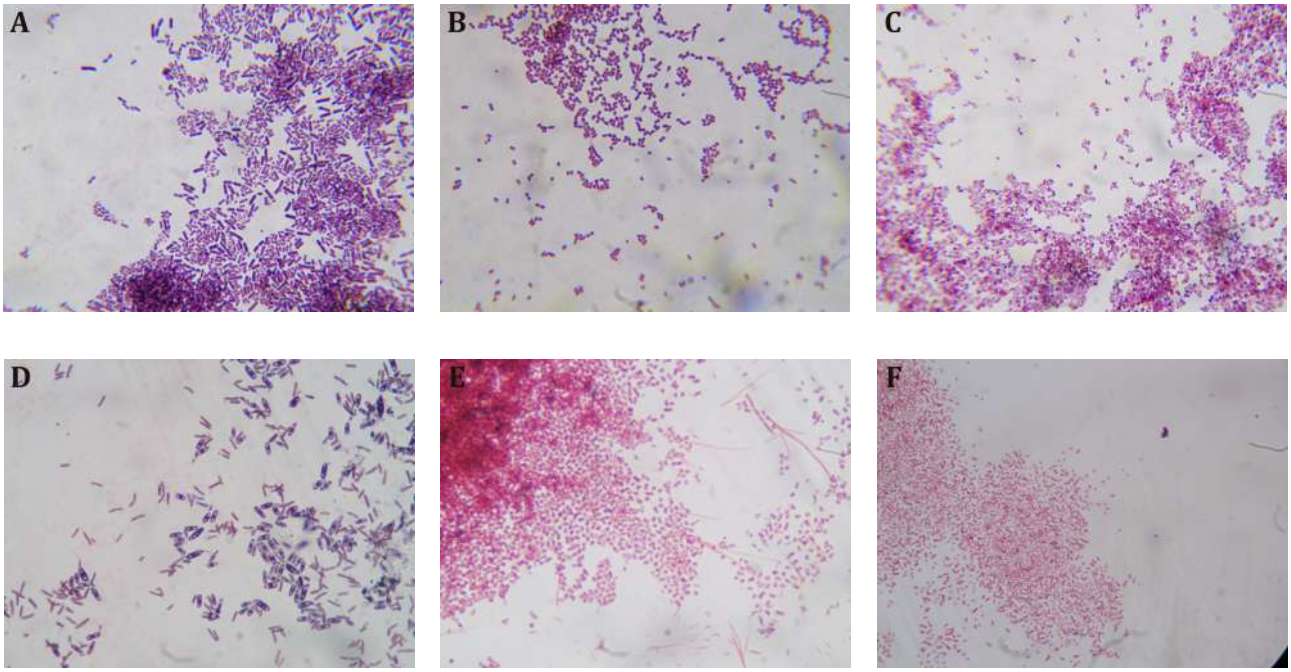

A) AzoLur19 in Burk medium, B) AzoLur23 in PHAMM, C) AzoLur19 in modified PHAMM, D) AzoLur19 in Burk medium, E) AzoLur19 in PHAMM, F) AzoLur23 in modified PHAMM.

A) AzoLur19 en medio Burk, B) AzoLur23 en MMPHA, C) AzoLur19 en MMPHA modificado, D) AzoLur19 en medio Burk, E) AzoLur19 en MMPHA, F) AzoLur23 en MMPHA modificado.

Figure 4. Cell staining with Sudan Black B dye, observed under an optical microscope at 24 hours (A, B, and C) and 96 hours (D, E, and F).

Figura 4. Tinción de células con Negro de Sudán B vistas al microscopio óptico a las 24 horas (A, B y C) y a las 96 horas (D, E y F).

PHA Organic Extraction

As previously mentioned (9), sodium hypochlorite and chloroform effectively extracted the PHA biopolymer.

PHA Accumulation and Productivity

According to strain evaluation, the highest biopolymer accumulation in PHAMM was 70.23% at 96 hours for the AzoLur20 strain (table 2). In contrast, the highest accumulation in the modified PHAMM medium was 74.33% at 96 hours for the AzoLur23 strain (table 3). Additionally, the highest PHA accumulation across all strains was observed in Burk medium with the AzoLur20 strain, reaching 87.67% at 72 hours (table 4). El-Nahrawy *et al.* (2018) reported similar results, using ammonium sulfate $(NH_4)_2SO_4$ with a final concentration of 0.2%. In contrast, Castillo *et al*. (2017) utilized the same culture medium but achieved 80% PHA accumulation, lower than that observed in our study.

Table 2. Percentage of PHA accumulation in selected strains in Burk medium.
Tabla 2. Porcentaje de acumulación de PHA de las cepas seleccionadas en medio Burk.

	24 h	48 h	72 h	96 h
AzoLur7	28.31%	36.41%	62.38%	31.33%
AzoLur18	13.12%	40.35%	74.29%	50.00%
AzoLur19	20.82%	54.29%	20.65%	26.60%
AzoLur20	11.65%	85.96%	87.67%	23.24%
AzoLur23	19.29%	79.11%	44.94%	19.09%

Table 3. Percentage of PHA accumulation in selected strains in PHAMM.
Tabla 3. Porcentaje de acumulación de PHA de las cepas seleccionadas en MMPHA.

	24 h	48 h	72 h	96 h
AzoLur7	25.19%	23.95%	39.35%	43.03%
AzoLur18	9.89%	26.69%	21.84%	13.80%
AzoLur19	27.99%	29.56%	22.26%	18.08%
AzoLur20	27.00%	26.58%	34.91%	70.23%
AzoLur23	29.17%	21.69%	28.67%	22.19%

Table 4. Percentage of PHA accumulation in selected strains in the modified PHAMM.
Tabla 4. Porcentaje de acumulación de PHA de las cepas seleccionadas en PHAMM modificado.

	24 h	48 h	72 h	96 h
AzoLur7	32.43%	42.32%	21.38%	66.40%
AzoLur18	13.94%	45.61%	10.64%	40.78%
AzoLur19	73.23%	53.23%	26.86%	19.17%
AzoLur20	36.14%	10.33%	44.37%	28.76%
AzoLur23	32.44%	39.92%	45.26%	74.33%

Considering productivity, AzoLur19 strain achieved the highest value of 0.04 g/L*h across all three tested media. Upon repeating the evaluation in triplicate, productivity values reached up to 0.06 g/L·h in both PHAMM and modified PHAMM. These results were comparable to those reported by Ramirez *et al*. (2011), who reported a productivity of 0.04 g/L·h in *Azotobacter* OPN mutant strain using Burk medium with ammonium acetate.

No significant differences were observed in AzoLur19 productivity between 24 and 48 hours. However, at 96 hours, significant differences in productivity were noticed in Burk medium compared to PHAMM and modified PHAMM. This disparity arose because, at 96 h, the culture in Burk medium was in exponential phase, whereas cultures growing in both PHAMM and modified PHAMM were in stationary phase (figure 5). Although values obtained by AzoLur19 strain did not exceed the ones reported by Cerrone (2011) and Pei *et al*. (2017), the analysis provided insight about strain behavior in different culture media and PHA production over time. Additionally, it supports the proposal of modified PHAMM for potential PHA production.

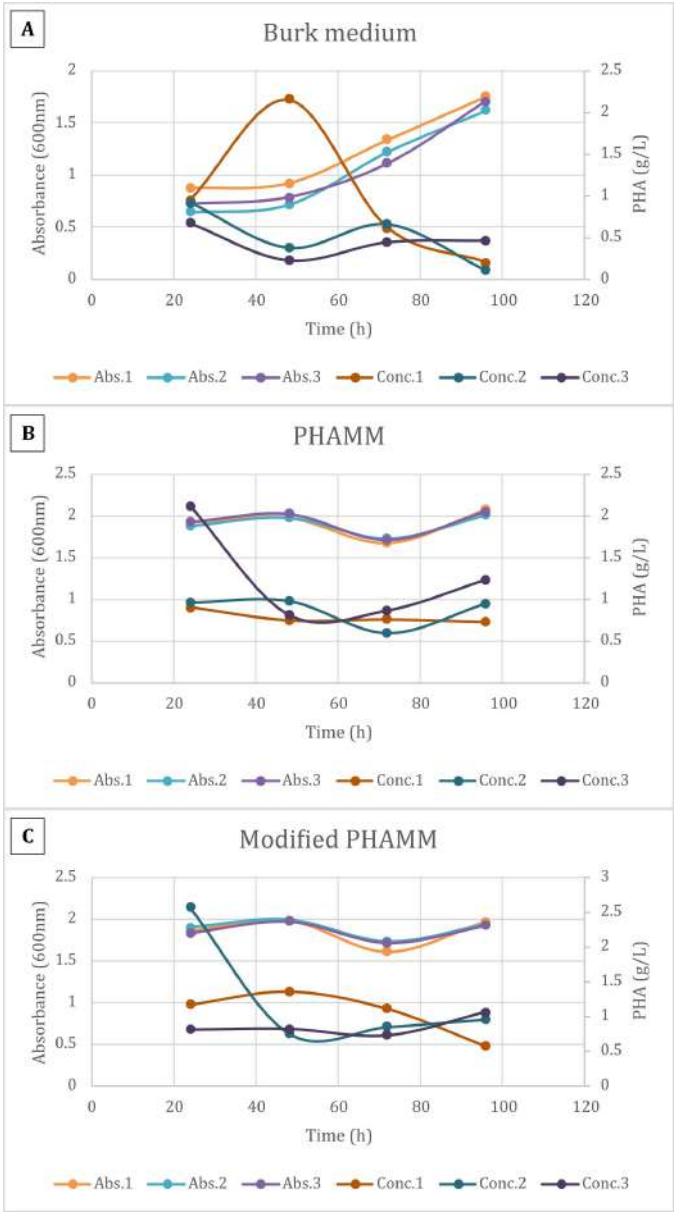

A) Burk medium, B) PHAMM and C) modified PHAMM. Abs. 1: Absorbance 1. Abs. 2: Absorbance 2. Abs. 3: Absorbance 3. Conc. 1: Concentration 1. Conc. 2: Concentration 2. Conc. 3: Concentration 3.

A) medio Burk, B) MMPHA y C) MMPHA modificado. Abs. 1: Absorbancia 1. Abs. 2: Absorbancia 2. Abs. 3: Absorbancia 3. Conc. 1: Concentración 1. Conc. 2: Concentración 2. Conc. 3: Concentración 3.

Figure 5. Comparison between cell growth and PHA production of AzoLur19 strain.

Figura 5. Comparación entre el crecimiento celular y la producción de PHA de la cepa AzoLur19.

Molecular Analysis

Based on BLASTN and phylogenetic analysis, the AzoLur19 strain was identified as *Azotobacter chroococcum* (GenBank accession number: MZ570428.1) (figure 6). Previous biochemical tests are consistent with this analysis. Aasfar *et al*. (2021) noted that *A. chroococcum* is predominant in the rhizosphere of several crops. Before this, Kim and Chan (1998) had demonstrated its high capacity to produce PHA.

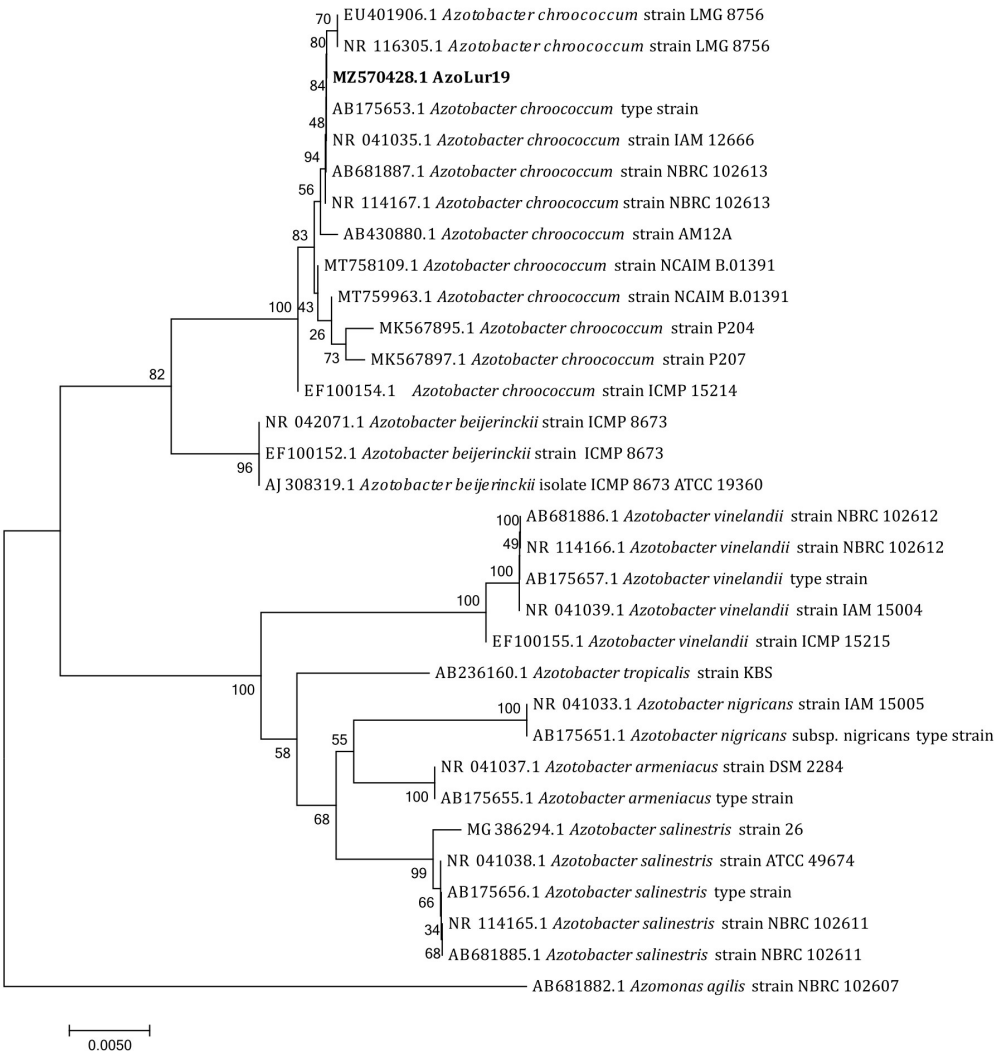

The 16S rRNA sequence from *Azomonas agilis* was selected as outgroup.

La secuencia de ARNr 16S de *Azomonas agilis* se eligió como grupo externo.

Figure 6. Phylogenetic tree of the 16S rRNA gene of the AzoLur19 strain and other sequences of *Azotobacter* sp., inferred using the Neighbor-Joining method with 1000 bootstrap replicates.

Figura 6. Árbol filogenético del gen 16S rRNA de la cepa AzoLur19 y otras secuencias de *Azotobacter* sp. inferido utilizando el método de unión de vecinos y 1000 de *bootstrap*.

Conclusions

Azotobacter strains are predominant in the rhizospheres of several crops. *A. chroococcum* is easily isolated and characterized, while being an effective PHA producer, especially after 24 and 48 hours of incubation. In this study, PHA detection was effectively achieved using the Nile Red medium, facilitating the selection of top-producing strains and allowing for production and quantitative evaluation. Additionally, staining with Sudan Black B enabled the observation of PHA intracellular granules. Finally, the AzoLur19 strain exhibited high productivity in both PHAMM and modified PHAMM, highlighting its potential for PHA synthesis.

References

1. Aasfar, A.; Bargaz, A.; Yaakoubi, K.; Hilali, A.; Bennis, I.; Zeroual, Y.; Kadmiri, I. 2021. Nitrogen Fixing *Azotobacter* Species as Potential Soil Biological Enhancers for Crop Nutrition and Yield Stability. Frontiers in Microbiology. 12: 1-19.
2. Altschul, S.; Madden, T.; Schaffer, A.; Zhang, J.; Zhang, Z.; Miller, W.; Lipman, D. 1997. Gapped BLAST and PSI- BLAST: a new generation of protein database search programs. Nucleic Acids Research. 2(17): 3389-3402.
3. Arsita, R.; Karim, H.; Hala, Y.; Iriany, N.; Jumadi, O. 2020. Isolation and identification of nitrogen-fixing bacteria in the corn rhizosphere (*Zea mays* L.) originating from Jeneponto Regency, South Sulawesi. IOP Conf. Series: Earth and Environmental Science. 484: 012051.
4. Becerra, M. 2013. Producción de un polímero tipo polihidroxialcanoato (PHA) empleando residuos de la producción de biodiesel. Tesis de Magister en Ciencias, Microbiología. Facultad de Ciencias. Universidad Nacional de Colombia. Bogotá. Colombia. 129 p.
5. Carballo, M.; Iglesias, Y.; Martínez, J.; Solano, R.; Fernández, A.; Villaverde, M. 2003. Evaluación de la producción de polihidroxialcanoatos por cepas bacterianas marinas. Revista Biología. 17(1): 52-57.
6. Castillo, C.; Flores, C.; Segura, D.; Espín, G.; Sanguino, J.; Cabrera, E.; Barreto, J.; Díaz, A.; Peña, C. 2017. Production of polyhydroxybutyrate (PHB) of high and ultra-high molecular weight by *Azotobacter vinelandii* in batch and fed-batch cultures. Journal of Chemical Technology & Biotechnology. 92: 1809-1816.
7. Cerrone, F. 2011. Producción de poliésteres biopoliméricos (PHAs) desde alpeorujo por medio de bacterias fijadoras de nitrógeno. Tesis doctoral, Doctorado europeo. Instituto del agua. Universidad de Granada. Granada. España. 152 p.
8. Chávez, M. 2021. Metabolitos de *Azotobacter* spp. con posible aplicación biotecnológica. Tesis de grado en Biología. Facultad de Ciencias Biológicas. Benemérita Universidad Autónoma de Puebla. Puebla. México. 108 p.
9. El-Nahrawy, S.; El-Kodoos, R.; El-Sayed, B.; El-Shouny, W. 2018. Production of Poly-β-hydroxybutyrate (PHB) by *Azotobacter* sp. Isolated from Different Sources. Environmental Biodiversity and Soil Security. 2: 183-192.
10. Escobar, C.; Horna, Y.; Carreño, C.; Mendoza, G. 2011. Caracterización de cepas nativas de *Azotobacter* spp. y su efecto en el desarrollo de *Lycopersicon esculentum* Mill. "tomate" en Lambayeque. Scientia Agropecuaria. 2(1): 39-49.
11. Gatea, I.; Sabr, A.; Abdul, E.; Abbas, A.; Halob, A.; Mahmood, M. 2019. Isolation and characterization of local *Azotobacter* isolate producing bio-plastics and consuming waste vegetable oils. IOP Conf. Series: Earth and Environmental Science. 388: 012082.
12. Giraldo, J.; Castaño, G.; Rivera, F. 2020. Bacteria from industrial waste: potencial producers of polyhydroxyalkanoates (PHA's) in Manizales, Colombia. Environmental Monitoring and Assessment. 192(7): 480.
13. Kim, B.; Chang, H. 1998. Production of poly(3-hydroxybutyrate) from starch by *Azotobacter chroococcum*. Biotechnology Letters. 20(2): 109-112.
14. Lara, C.; García, L.; Oviedo, L. 2010. Medio de cultivo utilizando residuos-sólidos para el crecimiento de una bacteria nativa con potencial biofertilizante. Revista Colombiana de Biotecnología, 12(1): 103-112.
15. Malynovska, I.; Yula, V.; Asanishvili, N.; Ptashnik, M.; Lyubchich, A. 2021. Influence of crop species on quantity and physiological activity of rhizosphere microorganisms. Ukrainian Journal of Ecology, 11(1): 286-290.
16. Martinez, M.; Gonzalez, J.; Rodelas, B.; Pozo, C.; Salmeron, V. 1995. Production of poly-β-hydroxybutyrate by *Azotobacter chroococcum* H23 in chemically defined medium and alpechin médium. Journal of Applied Bacteriology. 78: 413-418.
17. McAdam, B.; Brennan, M.; Mcdonal, P.; Mojicevic, M. 2020. Producción de polihidroxibutirato (PHB) y factores que afectan sus características químicas y mecánicas. Polímeros. 12(12): 2908.
18. Mohammed, S.; Panda, A.; Ray, L. 2019. An investigation for recovery of polyhydroxyalkanoates (PHA) from *Bacillus* sp. BPPI-14 and *Bacillus* sp. BPPI-19 isolated from plastic waste landfill. International Journal of Biological Macromolecules. 134: 1085-1096.

19. Navia Porras, D. P.; Poveda Perdomo, L. G.; Cuervo Mulet, R. A.; Esparza Estrada, J.; Hernández Umaña, J. 2024. Antibacterial activity and physicochemical characterization of bioplastic films based on cassava (*Manihot esculenta* Crantz) starch and rosemary (*Salvia rosmarinus*) essential oil. Revista de la Facultad de Ciencias Agrarias. Universidad Nacional de Cuyo. Mendoza. Argentina. 56(2): 126-136. DOI: https://doi.org/10.48162/rev.39.136
20. Pei, M.; Kumar, S.; Woan, L.; Bor, J.; Najimudin, N. 2017. Characterization of polyhydroxyalkanoate production by mutant *Azotobacter vinelandii*. Malaysian Applied Biology. 46(1): 1-8.
21. Ramírez, M. E.; Herrera, S. L.; Domínguez, M.; Romo, Á.; Segura, D.; Peña, C. 2011. Evaluación de la producción y peso molecular del polihidroxibutirato (PHB) sintetizado por diversas cepas mutantes de *A. vinelandii*. Sociedad Mexicana de Bioquímica, Congreso Nacional 2011. Querétaro. Cartel CV-68.
22. Ramos, A. 2019. Extracción, purificación y modificación de un biopolímero del tipo poli (3-hidroxibutirato) obtenido de la fermentación de ácidos grasos con *B. cepacia*. Tesis de Maestría en Ingeniería Química. Facultad de Ingeniería. Universidad Nacional de Colombia. Bogotá. Colombia. 192 p.
23. Sharma, V.; Sehgal, R.; Gupta, R. 2021. Polyhydroxyalkanoate (PHA): Properties and Modifications. Polymer, 212: 123161.
24. Tamura, K.; Stecher, G.; Kumar, S. 2021. MEGA11: Molecular Evolutionary Genetics Analysis Version 11, Molecular Biology and Evolution. 38(7): 3022-3027.
25. Vega, O. 2016. Extracción y caracterización estructural de un PHA, obtenido de residuos de cáscaras de yuca y piña mediante procesos de fermentación; y su aplicación en la fabricación de fibras por electrospinning. Tesis de doctor en Ingeniería. Facultad de Ingeniería. Universidad de Antioquia. Medellín. Colombia. 163 p.
26. Villota-Calvachi, G.; González, K.; Marulanda, S.; Galeano, N.; Velasco, D.; Ocampo, L.; Castañeda, L.; Giraldo, C.; Rodríguez, N. 2022. Aislamiento y caracterización de bacterias productoras de biopolímeros a partir de efluentes industriales. Revista Colombiana de Biotecnología. 24(1): 27-45.
27. Zambrano, H.; Riera, M. 2021. Desafío de los polihidroxialcanoatos como solución al problema de los plásticos de un solo uso. Publicaciones en Ciencia y Tecnología. 15(1): 15-26.

Acknowledgment

This research was funded by the Universidad Nacional Mayor de San Marcos - RR N° 05969-R-18 (code B18100214) of the Vicerrectorado de Investigación y Posgrado - VRIP- Undergraduate Thesis Promotion Program -2018. Our special thanks to Juan José Aponte and Liliana Salazar for their support during the manuscript review.

Data-driven Method for the Delimitation of Viticultural Zones: Application in the Mendoza River Oasis, Argentina

Método basado en datos para la delimitación de zonas vitivinícolas: Aplicación en el oasis río Mendoza, Argentina

Mariano Córdoba [1, 2*], Rosana Vallone [3], Pablo Paccioretti [1], Francisco Corvalán [3], Mónica Balzarini [1, 2]

Originales: *Recepción:* 17/06/2025- *Aceptación:* 16/10/2025

Abstract

In viticulture, understanding the spatial variability of natural factors influencing vineyard potential is essential for terroir characterization. In the present study, we present a data-driven protocol that integrates climate, geomorphology, and soil data to delineate viticultural zones. The method combines spatial layers with statistical tools to partition a region into areas with similar characteristics. The protocol comprises: 1) rescaling multiple spatial data layers, 2) applying spatial multivariate analysis to group spatial units, and 3) using machine-learning algorithms to identify key zoning drivers. The approach was applied to the Mendoza River oasis in Argentina. Climate and geomorphology layers were used first, as they varied at a broader spatial scale than soil data. Two climatic zones were identified, mainly differentiated by elevation and thermal indices. Subsequent soil-based zoning within each climatic zone revealed five distinct edaphoclimatic zones. These zones showed statistically significant differences in environmental variables and exhibited spatial coherence aligned with landscape features. Results showed that this protocol facilitates the integration of diverse data sources and supports a deeper understanding of the uniqueness of vineyard zones in wine-producing regions.

Keywords
spatial clustering • edaphoclimatic zoning • zoning drivers

1 Universidad Nacional de Córdoba. Facultad de Ciencias Agropecuarias. Ing Agr. Félix Aldo Marrone 746. Ciudad Universitaria. X5000HUA. Córdoba. Argentina.
* mariano.cordoba@unc.edu.ar
2 Unidad de Fitopatología y Modelización Agrícola (UFyMA), Instituto Nacional de Tecnología Agropecuaria. Consejo Nacional de Investigaciones Científicas y Técnicas. Av. 11 de Septiembre 4755, X5020ICA. Córdoba. Argentina.
3 Universidad Nacional de Cuyo. Facultad de Ciencias Agrarias. Almirante Brown 500. Chacras de Coria. M5528AHB. Mendoza. Argentina.

Resumen

En viticultura, comprender la variabilidad espacial de los factores naturales que influyen en el potencial vitivinícola es esencial para caracterizar el terroir. En este estudio presentamos un protocolo basado en datos de clima, geomorfología y suelo para delimitar zonas vitivinícolas. El método integra capas de datos espaciales con herramientas estadísticas para subdividir una región en áreas con características similares. La metodología comprende: 1) el reescalado de múltiples capas de datos espaciales, 2) el análisis multivariado espacial para agrupar unidades espaciales, y 3) la aplicación de algoritmos de aprendizaje automático para identificar las principales variables determinantes de la zonificación. El protocolo se aplicó al oasis del río Mendoza, en Argentina. Primero se utilizaron los datos climáticos y geomorfológicos, que mostraban variabilidad a una escala espacial mayor, identificándose dos zonas climáticas diferenciadas principalmente por la altitud y los índices térmicos. Posteriormente, dentro de cada zona climática, se realizó una zonificación adicional basada en propiedades de suelo, lo que permitió identificar cinco zonas edafoclimáticas. Estas zonas presentaron diferencias estadísticamente significativas en variables ambientales y una alta coherencia espacial en correspondencia con las características del paisaje. Este enfoque permite integrar datos diversos y contribuye a lograr una comprensión más profunda de los ambientes vitícolas en regiones productoras de vino.

Palabras clave

agrupamiento espacial • zonificación edafoclimática • importancia de variables en zonificación

Introduction

Viticulture is one of the most widespread horticultural activities worldwide, with wine grapes cultivated across diverse climates and landscapes. Sustainable viticulture requires integrating large volumes of soil and climate data to support vineyard management and long-term planning (Visconti *et al.*, 2024). In Argentina, vineyards extend across multiple mesoclimates, landscapes, and soils. National grape and wine production is led by Mendoza province, in the central west of the country, accounting for nearly 70% of the total (INV, 2024). Viticulture in Mendoza province is concentrated in four main oases located between 33° and 36° S. This arid to semi-arid region depends on irrigation from Andean meltwater and shows high variability in climate and soils (Puscama *et al.*, 2025; Straffelini *et al.*, 2023). Recently, the Argentine Viticultural Corporation (COVIAR) conducted a comprehensive soil and climate survey of wine-producing regions, fostering a deeper understanding of natural variability and its influence on productivity and regional differences in grape production. The concept of terroir -used to explain differences in wine style and quality- is fundamentally geographical and supports spatial analysis of edaphoclimatic influences (Van Leeuwen *et al.*, 2010). This concept is also recognized as a socio-ecological construct, shaped not only by natural conditions but also by cultural, technical, and economic factors (Vaudour *et al.*, 2010). Terroir is multifactorial, with climate, topography, and soil as its main environmental pillars (Van Leeuwen *et al.*, 2010; Vaudour *et al.*, 2010). Climatic factors like temperature, radiation, precipitation, and thermal amplitude influence grape phenology and sugar accumulation (Jones *et al.*, 2005). Topographic or geomorphometric factors -particularly elevation, slope, and aspect- influence climate, water dynamics, and solar exposure (Hall & Jones, 2010; Irimia *et al.*, 2014). Soils regulate water and nutrient supply, shaping vegetative growth, yield, and grape composition (Morlat & Bodin, 2006). The interaction among these factors drives spatial heterogeneity in vineyard performance and wine typicity, underscoring the need to integrate them into zoning studies. When referring specifically to areas sharing similar biophysical features that influence vine development and grape composition, the term “edaphoclimatic zones” is commonly used. Advances in proximal and remote sensing technologies now allow the acquisition of large volumes of georeferenced data, which in turn permits delimiting these edaphoclimatic zones. Combined with geostatistical and machine-learning methods, these data are used to develop digital maps

of biophysical variables relevant to viticulture (Ferro & Catania, 2023). Nevertheless, many terroir studies still rely on expert-based assessments rather than systematic, data-driven approaches (Bramley *et al.*, 2020). In recent years, data-driven methods have emerged as powerful tools to analyze terroir, enabling subregional classifications and explaining within-region variations in grape quality and vineyard performance (Bramley *et al.*, 2023; Bramley & Gardiner, 2021).

Data-driven delineation of edaphoclimatic zones requires: 1) statistical methods that integrate the spatial distribution of multiple variables, and 2) clustering algorithms that group sites with similar attributes and identify the key drivers defining each zone. The success of such zoning depends on the spatial resolution, type, and quality of input data (Van Leeuwen *et al.*, 2010). Although several zoning approaches exist (Ghilardi *et al.*, 2023), few address the dual challenge of handling high-dimensional environmental datasets while accounting for the spatial autocorrelation typical of edaphoclimatic variables. Many studies have classified viticultural areas by using soil, climate, and topographic variables (Ferretti, 2020; Ghilardi *et al.*, 2023), yet most rely on conventional multivariate techniques that do not explicitly incorporate spatial structure. Ignoring spatial dependence can result in fragmented zones or biased interpretations of terroir. Integrating spatially explicit methods -such as spatial principal components or geostatistical models- remains limited but offers a promising path toward more robust and geographically coherent zoning. Thus, this study describes a data-driven approach to delineate edaphoclimatic zones in a viticultural region by integrating multiple environmental variables across spatial scales. In this approach, spatial principal components are first computed and used in a hierarchical clustering process to delineate zones. Because soil variables typically exhibit greater spatial heterogeneity than climatic and geomorphometric variables, we adopted a nested clustering strategy: initial zoning was based on climate and geomorphology -variables occurring at a broader spatial scale- followed by refinement with soil data to capture finer-scale variability.

Spatial principal components were applied to ensure that spatial autocorrelation was explicitly considered in the clustering process (Córdoba *et al.*, 2012). Although the loadings of input variables on each component provide insights into spatial correlations, they do not always identify the main drivers of zoning- particularly when multiple correlated factors shape the results (Jolliffe & Cadima, 2016). For this reason, we complemented the spatial principal component analysis with machine-learning-based feature selection. This approach allowed us to quantify the relative importance of each predictor while handling high-dimensional, multicollinear datasets. The full analytical workflow was applied to climatic, geomorphometric, and soil data from the Mendoza River oasis in Argentina. The resulting maps and descriptions of the edaphoclimatic zones identified are publicly available through an open-access website (https://caracterizacion-fisico-ambiental-coviar.hub.arcgis.com/), which provides interactive visualizations and detailed zone characterizations.

Materials and Methods

Study area

The study area (figure 1, page 60) is located in the Mendoza River Oasis, Argentina, and includes the departments of Lavalle, Capital, Las Heras, Guaymallén, Maipú, and Luján de Cuyo. Elevations range from 600 to 1,200 meters above sea level (m a. s. l.). The region has a warm-temperate arid climate with low annual precipitation (228.8 mm, minimum 148.8 mm in Lavalle), low humidity, and moderate winds. The annual mean temperature is 15.8°C, with higher values in the north and urban areas. The mean diurnal temperature variation is 14.3°C. Extreme heat (>35°C) occurs on 15.4 days per year on average, reaching 36 in Lavalle, with 3.9 heatwave events. The area records 1,536.6 annual cold hours, being the highest in Luján de Cuyo. Frost and hailstorms are major meteorological risks. Frost occurs on 43.4 days on average, peaking in Perdriel-Agrelo (87 days) and northern Lavalle (57 days). Rainfall is highest in February (42.1 mm), which increases the risk of cryptogamic disease before grape maturation.

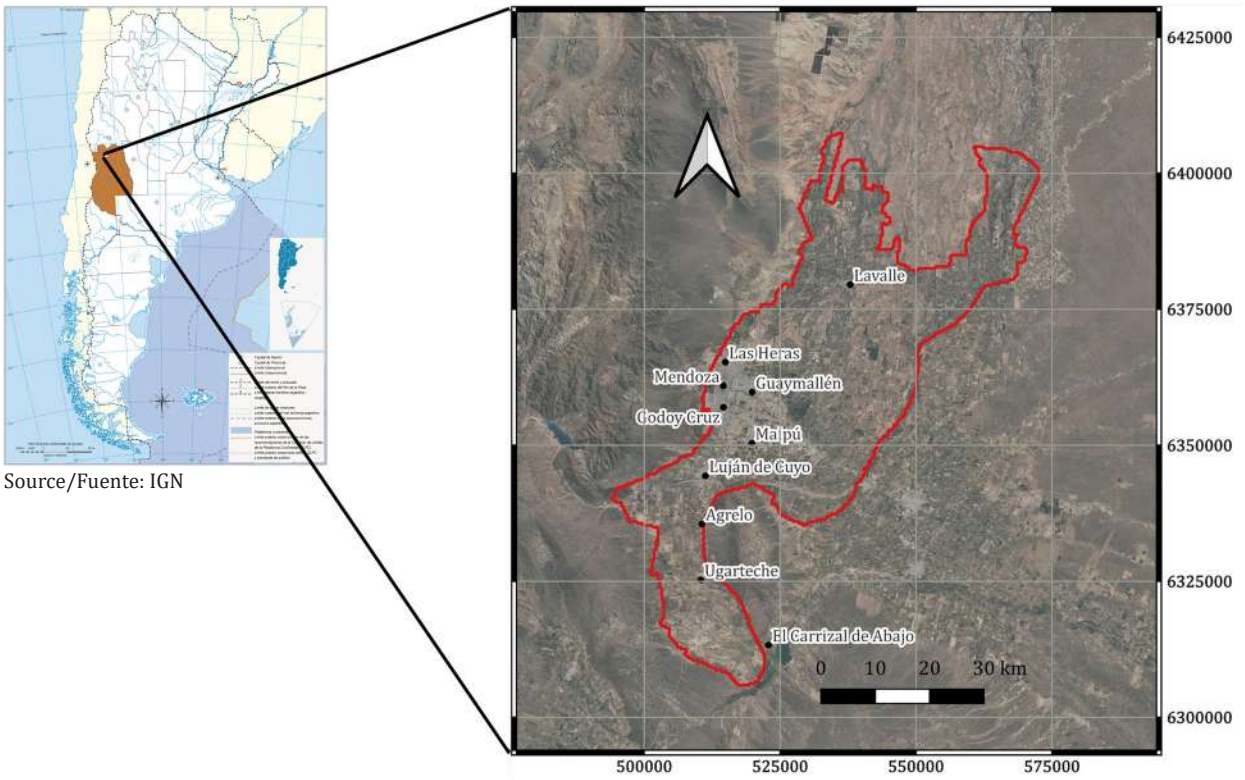

Source/Fuente: IGN

Figure 1. Study area: Mendoza River oasis, Mendoza province, Argentina.
Figura 1. Área de estudio, oasis río Mendoza, provincia de Mendoza, Argentina.

Spatial Data Layers

The study area boundaries were defined using digital maps of geomorphometric and soil variables from vineyard test pits (Vallone *et al.*, 2023), combined with bioclimatic indices. Bioclimatic maps were derived from a national survey of Argentina's wine regions (Cavagnaro *et al.*, 2023). Weather records were obtained from nine World Meteorological Organization (WMO)-certified stations with 41 years of data (1980-2020), supplemented by public and private networks. Climatic maps were generated using kriging interpolation for variables such as cumulative seasonal precipitation (CSP) (September-April). Standard viticultural indices included: a) Growing Degree Days (GDD) (Mullins *et al.*, 1992), b) Winkler Index (WI) (Amerine & Winkler, 1944), c) Huglin Heliothermal Index (HI) (Huglin, 1983), d) Cool Night Index (CNI) (Tonietto & Carbonneau, 2004), and e) Thermal Integral above 13°C (TIB13). Shuttle Radar Topography Mission (SRTM) elevation data were processed with SAGA GIS to derive geomorphometric variables: slope, aspect, curvature, convergence, slope length factor (L-S), topographic wetness index, multiresolution valley bottom flatness, and vertical distance to drainage. Additional land suitability maps and geomorphometric studies from COVIAR were incorporated (Vallone *et al.*, 2007). A total of 153 soil samples were analyzed for physicochemical properties. Digital soil maps were generated (McBratney *et al.*, 2003) and harmonized into 0-50 cm and 50-100 cm horizons (Malone *et al.*, 2009). Plant available water (PAW), field capacity (FC), permanent wilting point (PWP), and saturated hydraulic conductivity (Ksat) were estimated from field data (bulk density, particle size) and pedotransfer functions. A soil water storage capacity map was produced using geostatistical interpolation. All spatial layers were resampled to a 4-ha grid (200 × 200 m).

Analytical Method

Step 1. Delimitation of Climatic Zones

Climatic zones were delimited using the KM-sPC algorithm (Córdoba *et al.*, 2012), which combines fuzzy k-means clustering with spatial principal components (sPCs) to account for spatial autocorrelation. Input variables included climatic and bioclimatic indices and elevation, which strongly influence viticultural potential. The first two sPCs were retained because they explained at least 80% of the total climatic variance; that is, they captured the main patterns in the data. Clustering was performed for 2 to 6 classes (*i.e.*, five clustering runs), with the optimal number determined using the partition coefficient, classification entropy, and a combined summary index (Albornoz *et al.*, 2018). The clustering was conducted on a 4-ha grid, resolution value to which all spatial layers were previously resampled. The analysis was implemented in R (R Core Team, 2024) using the "paar" package (Paccioretti *et al.*, 2024).

Step 2. Soil Zoning within each Climatic Zone

Within each climatic zone, a finer edaphic partition was performed using KM-sPC with soil and geomorphometric variables. This nested clustering approach reflects the natural hierarchy between broader climatic-geomorphological controls and finer edaphic variability.

Step 3. Characterization of Delimited Edaphoclimatic Zones

Radar Plots

Radar plots were used to visualize the multidimensional attributes of each zone. Each axis represents a variable, with spoke lengths scaled to relative magnitudes. These plots enabled comparison between individual zones and the overall mean profile. Radar plots were generated using the "fmsb" package (Nakazawa, 2023).

Random Forest (RF)

RF is an ensemble method that builds multiple decision trees from bootstrap samples and aggregates their predictions to improve accuracy and reduce overfitting (Breiman, 2001). In this study, RF classification was applied to evaluate the relative importance of each variable in distinguishing individual zones by contrasting one zone against all others. Variable importance was quantified as the mean decrease in accuracy after permuting the values of each predictor in the out-of-bag samples. This analysis identified the predictors that most contributed to zone distinctiveness. Model tuning involved optimizing the number of variables randomly selected at each split (mtry) through grid search. The number of trees and the minimum terminal node size were fixed at 500 and 5, respectively. Model performance was evaluated using 10-fold cross-validation. The RF model was implemented in R using the "caret" (Kuhn & Max, 2008) package.

Identification of Key values for each Zone

Key characteristics of each zone were summarized into "zone notes", describing typical climatic, geomorphological, and soil attributes. These summaries were developed in collaboration with domain experts to emphasize the distinctive features of each viticultural zone.

Step 4. Zone Validation

The appropriateness of the delineated zones was evaluated by comparing the means of the most important variables identified by the RF analysis. A permutation-based statistical test accounting for spatial correlation was applied to evaluate whether these variables differed significantly among zones. The analysis was performed using the "ofemeantest" package (Córdoba *et al.*, 2024) in R.

Results and Discussion

Delimitation of Climatic Zones

Figure 2 shows the first two components of the sPC analysis (sPCA), which explained 96.5% of the total climatic variability. The most influential variables for differentiating climatic zones were WI, TIB13, and HI. These indices were positively correlated, as indicated by the small angles between their vectors. In contrast, these variables were negatively correlated with Digital Elevation Model (DEM), as shown by the angle close to 180°. GDD and CSP contributed to spatial variability but were less important, being primarily associated with the second axis.

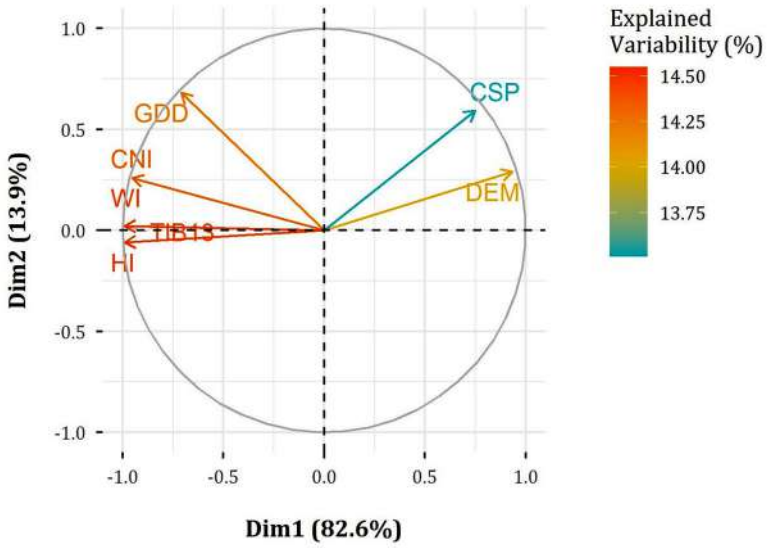

CNI: Cool Night Index, HI: Huglin Index, (°GDD), TIB13: Thermal Integral with Base 13°C (°GDD), WI: Winkler Index (°GDD), CSP: Cumulative Seasonal Precipitation (mm), GDD: Growing Degree Days (days), DEM: Digital Elevation Model (m a. s. l.).

CNI: Índice de Frescor Nocturno, HI: Índice Huglin (°GDD), TIB13: Integral Térmica con Base 13°C (°GDD), WI: Índice Winkler (°GDD), CSP: Precipitación Estacional Acumulada (mm), GDD: Duración del periodo activo (días), DEM: Modelo Digital de Elevación (m s. n. m.).

Figure 2. Graphical representation of the first two axes of the spatial principal components analysis, which together explained 96.5% of the total variance. The percentage contribution of each variable to the variance explained by these components is shown.

Figura 2. Representación gráfica de los dos primeros ejes del análisis de componentes principales espaciales, los cuales explican el 96,5% de la varianza total. Se muestra el porcentaje de contribución de cada variable a la varianza explicada por estas componentes.

Based on the three indices, the climate zoning identifies two zones (figure 3, left, page 63). Zone 1, located on the left bank of the Mendoza River, between 600 and 900 m a. s. l., encompasses the transition and low areas of the river basin, including peri-urban areas of the Capital, Godoy Cruz, and the departments of Guaymallén, Maipú, Las Heras, and Lavalle (zone 1). This zone exhibits the highest temperatures and the lowest precipitation levels within the oasis. Zone 2, covering the river basin and right bank between 900 and 1,100 m a. s. l., is characterized by cooler temperatures and higher rainfall.

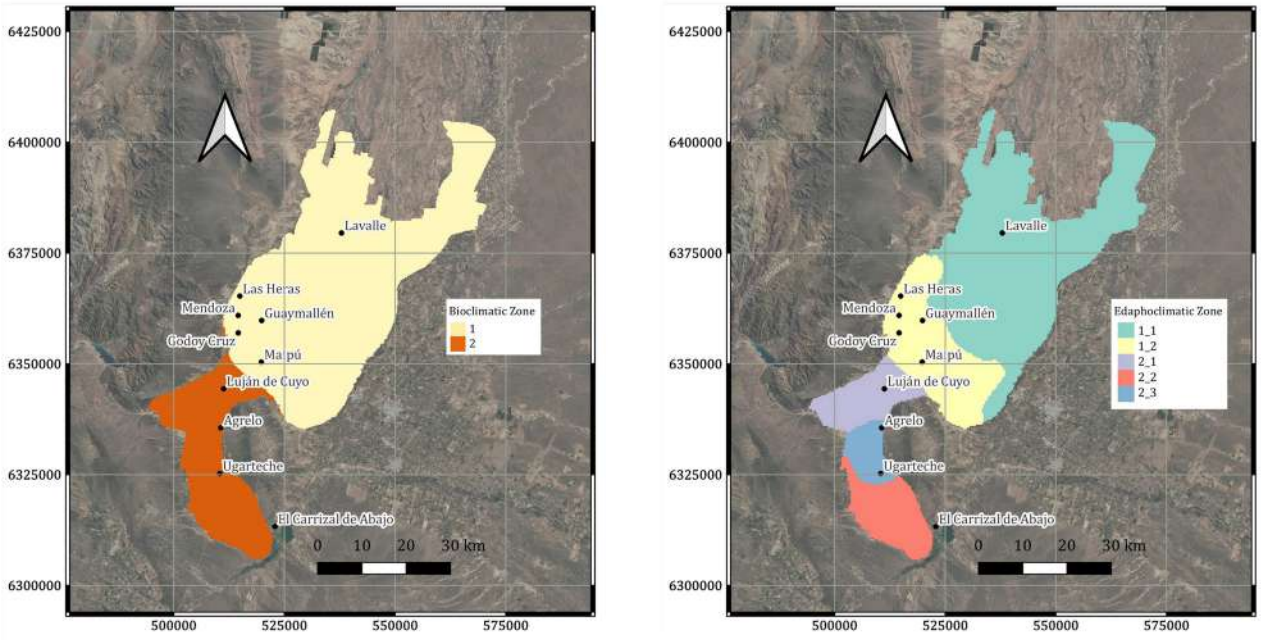

Figure 3. Bioclimatic zoning (left) and edaphoclimatic zoning (right) of the Mendoza River oasis, Argentina.
Figura 3. Zonificación bioclimática (izquierda) y edafoclimática (derecha) del oasis río Mendoza, Argentina.

Soil Zoning within each Climatic Zone

Clustering based on geomorphometric and edaphic properties showed that topography strongly influences soil variation in the oasis. The relative importance of variables for differentiating the finer partitions indicated that DEM was one of the most important predictors, especially for differentiating areas within climatic zone 1. In zone 2_1, DEM was again influential, together with the CNI. In contrast, in zones 2_2 and 2_3, the most discriminative variables were CSP and Sedimentation Volume at 50-100 cm depth (SV_100), respectively. The eigenvector loadings from the sPCA described the contribution of each variable to overall variance (Córdoba *et al.*, 2013). We complemented this with RF classification to evaluate variable importance in terms of their discriminatory power for clustering. RF is advantageous for handling complex, non-linear relationships and interactions among variables, which are common in environmental datasets (Fox *et al.*, 2020). Combining sPCA and RF enabled a nuanced understanding of variable influence, both from a structural and predictive perspective.

Characterization and Validation of Edaphoclimatic Zones

Figure 3 (right) shows the multivariate zoning of the Mendoza River oasis. The edaphoclimatic zoning delineated five zones. Figure 4 (page 64) presents star plots summarizing the main characteristics of each zone. The five delimited zones showed statistically significant differences for most key soil and climatic variables ($p<0.05$).

Zone 1_1 is characterized by bioclimatic indices placing it in a very warm viticultural climate with mild nights. Annual precipitation in this zone is the lowest in the oasis (140 mm), while the active period lasts more than 260 days. Morphometric indicators revealed gentle slopes throughout most of the zone, with terrain aspects oriented mainly northeast and north in the final stretch of the river in the Lavalle sector. Topography-related factors (convergence, surface flow accumulation, and slope length) suggest a lower risk of water erosion in this alluvial plain compared with the lower Mendoza River basin, where defined channels are absent. Evidence of gully erosion is observed along the Mendoza River, Leyes Stream, and Tulumaya Stream. Soils in zone 1_1 show high effective rooting depth, with loamy to sandy loam texture. In addition, they show lower permeability and

more restricted natural drainage than soils of the other zones. Soil salinity reaches the highest levels in the oasis. Accumulations of limestone and gypsum can be observed at both surface and subsurface horizons. Mean comparison of key variables indicated statistically significant differences between zone 1_1 and the other zones ($p<0.05$).

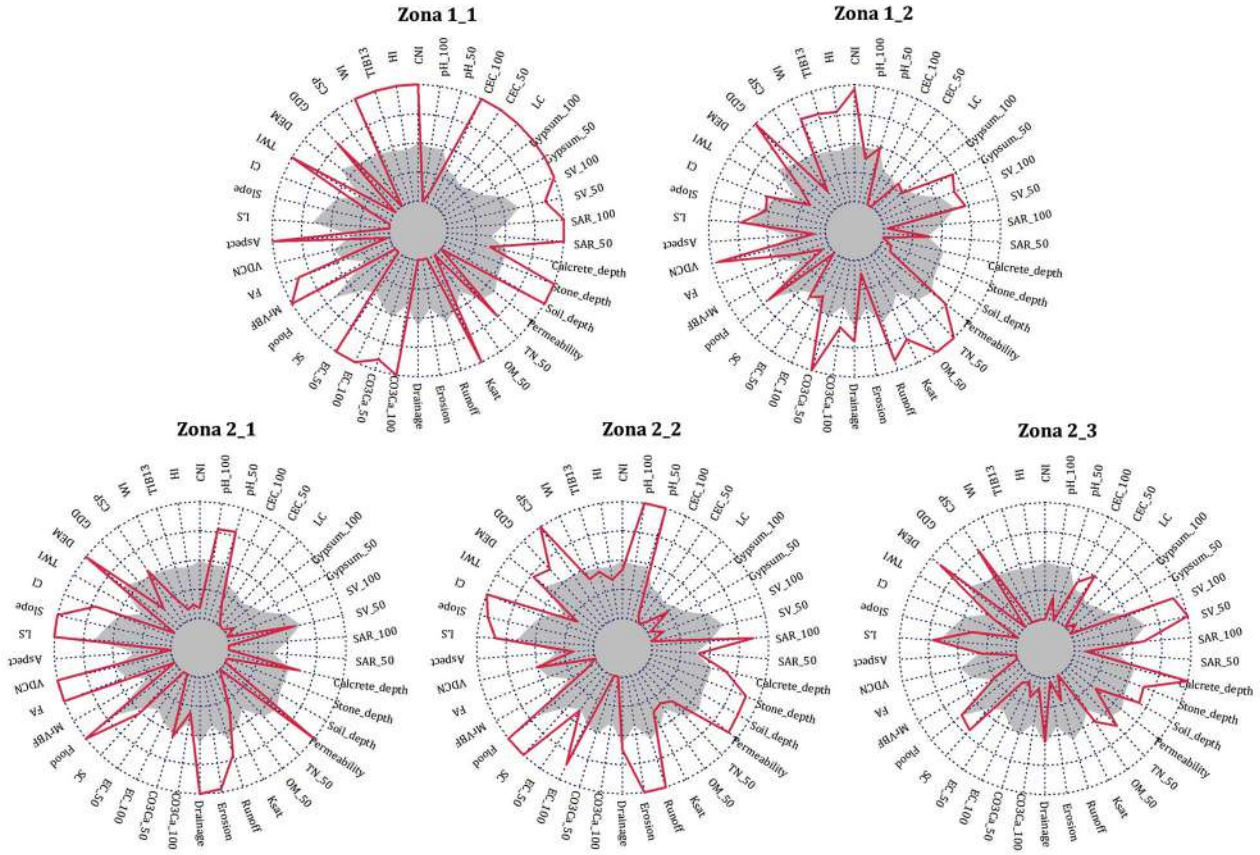

Variables are listed clockwise from 12 o'clock. Suffixes _50 and _100 indicate values for the 0-50 cm and 50-100 cm soil layers, respectively. Variables include: Cool Night Index (CNI), pH_50, pH_100, Cation Exchange Capacity (CEC_50), Gypsum_50, Gypsum_100, Sedimentation Volume (SV_50, SV_100), Sodium Adsorption Ratio (SAR_50, SAR_100), Calcrete depth, Stone depth, Soil depth, Permeability, Total Nitrogen (TN_50), Organic Matter (OM_50), Saturated Hydraulic Conductivity (Ksat), Runoff, Erosion, Drainage, Calcium Carbonate ($CaCO_3$_50, $CaCO_3$_100), Electrical Conductivity (EC_50, EC_100), Storage Capacity (SC), Flooding, Multi-resolution Valley Bottom Flatness (MrVBF), Flow Accumulation (FA), Vertical Distance to Drainage Network (VDCN), Aspect, Longitudinal Slope (LS), Slope, Convergence Index (CI), Topographic Wetness Index (TWI), Digital Elevation Model (DEM), Growing Degree Days (GDD), Cumulative Seasonal Precipitation (CSP), Winkler Index (WI), Thermal Integral with Base 13°C (TIB13), Huglin Index (HI).

Las variables se enumeran en el sentido horario desde las 12 en punto. Los sufijos _50 y _100 indican valores correspondientes a las profundidades de 0-50 cm y 50-100 cm, respectivamente. Las variables incluyen: Índice de Frescor Nocturno (CNI), pH_50, pH_100, Capacidad de Intercambio Catiónico (CIC_50), Yeso_50, Yeso_100, Volumen de Sedimentación (VS_50, VS_100), Relación de Adsorción de Sodio (RAS_50, RAS_100), Profundidad de tosca, Profundidad de piedra, Profundidad del suelo, Permeabilidad, Nitrógeno Total (NT_50), Materia Orgánica (MO_50), Conductividad Hidráulica Saturada (Ksat), Escorrentía, Erosión, Drenaje, Carbonato de Calcio (CO_3Ca_50, CO_3Ca_100), Conductividad Eléctrica (CE_50, CE_100), Capacidad de Almacenamiento (CA), Anegamiento, Índice de Multiresolución del Fondo de Valle (MrVBF), Acumulación de Flujo (AF), Distancia Vertical a la Red de Drenaje (VDCN), Orientación, Pendiente Longitudinal (PL), Pendiente, Índice de Convergencia (IC), Índice Topográfico de Humedad (TWI), Modelo Digital de Elevación (DEM), Grados-Día Acumulados (GDD), Precipitación Estacional Acumulada (CSP), Índice de Winkler (WI), Integral Térmica con Base 13°C (TIB13), Índice de Huglin (HI).

Figure 4. Star plots illustrating the average profile of each edaphoclimatic zone in the Mendoza River oasis.

Figura 4. Gráficos de estrellas que ilustran el perfil promedio de cada zona edafoclimática en el oasis del río Mendoza.

Zone 1_2 is characterized by a very warm climate with mild nights and low precipitation (170 mm annually). It shows the highest GDD in the oasis. Morphometric indices suggest a generally lower risk of water erosion than in zone 1_1, except for the cone area in the Barrancas sector. This zone comprises higher lands transitioning towards zone 1_1. It includes the areas of Maipú and Guaymallén. Soils are constrained by shallow groundwater and surface accumulations of calcium carbonate (locally known as "tosca" in Mendoza). At depth, soils transition to clayey loam with higher organic matter and total nitrogen, especially in the green belt area at district of Km 8 and Corralitos. These soils derive from former lagoons and are classified as intrazonal. Salinity levels are moderate, lower than in zone 1_1.

Zone 2_1 includes the highlands of the Mendoza River basin and the right bank of the river (Chacras de Coria, Las Compuertas, Vistalba, Perdriel, and Lunlunta). The climate is warm with cold nights. Annual precipitation averages 230 mm. This is the highest zone and, according to geomorphometric indicators, is at risk of water erosion. Soils are loamy and sandy loam at depth. They show the lowest values of Electrical Conductivity (EC) and Sodium Adsorption Ratio (SAR), both superficially and at depth, with slight salinity. Soil permeability is high, and drainage is somewhat excessive. Soils are the shallowest in the oasis, averaging 115 cm, due to rocky subsoil.

Zone 2_2 includes the southern part of Ugarteche and the area of El Carrizal. Bioclimatic indices classify it as a warm zone with cold nights. Average minimum night air temperature in March ranges between 12 and 14°C. Seasonal precipitation is the highest in the oasis, with an annual average of 295 mm.

Finally, zone 2_3 is the coolest zone, with cold nights. The WI classifies it as temperate-warm. Minimum night air temperatures in March are below 12°C. Average annual seasonal precipitation is 260 mm. The active period is the shortest in the oasis. Morphometric indicators revealed a higher risk of water erosion in the proximal sector of Agrelo, with signs of gully erosion. Soil water storage capacity is the highest (160 mm on average). Soils are sandy loam with rocky subsoil limiting effective depth. The predominant slope orientation is southeast. The edaphoclimatic zone map (figure 3, page 63) closely matches field observations (Vallone *et al.*, 2023).

The methodological approach used here integrates bioclimatic, soil, and geomorphometric variables while accounting for their spatial correlation. By combining the original variables into sPCs and clustering them, the method reduces the effects of spatial autocorrelation on total variability. As a result, the delineated zones are more contiguous and geographically coherent, minimizing fragmentation and better reflecting landscape continuity (Córdoba *et al.*, 2013). This approach addresses a common limitation of traditional terroir studies that rely on non-spatial multivariate methods (Ghilardi *et al.*, 2023). The primary link between wine and soil lies soil regulating water and nutrient availability for vines. Soil heterogeneity over space and time, and complex soil-climate interactions are widely recognized as major drivers of terroir differentiation, especially at regional to sub-regional scales (Lanyon *et al.*, 2004; Piraino & Roig, 2024). In this study, soil properties emerged as a fundamental component of zoning, reinforcing their central role in the terroir concept. Our findings confirm the importance of soils in defining viticultural zones. However, the direct relationships between soil characteristics, vine performance, and wine sensory attributes remain a key area for future validation.

Beyond the overarching effect of altitude, other key variables identified during the zoning process included soil depth, depth to stone or hardpan layers, soil permeability, and thermal indicators. Soil depth influences root development, water retention, and nutrient uptake, ultimately shaping vine vigor and overall water status (Morlat & Bodin, 2006). The presence of stones or calcareous hardpans ("tosca") can constrain root penetration, modify drainage, and influence nutrient availability, often creating moderate water stress conditions that are beneficial for grape quality (Pracilio *et al.*, 2006). Soil permeability controls water movement and aeration within the root zone, with direct consequences for vine vigor and fruit composition (Lanyon *et al.*, 2004). Elevation, in turn, regulates microclimatic conditions like temperature regimes and rainfall distribution, both critical for grape development and ripening (Ferretti, 2020).

Temperature accumulation, expressed through indices such as the WI and HI, also emerged as an important climatic factor. These indices are widely used to characterize

grapevine phenology, berry composition, and ripening dynamics, all of which have direct implications for sugar accumulation, acidity, and aromatic potential (Jarvis *et al.*, 2017). Topography -including elevation, slope, and aspect-, although not explicitly detailed among the most influential variables here, is well established as a determinant of local microclimatic conditions and wine characteristics (Biss, 2020). Other soil properties, although not primary drivers of clustering in this study, remain essential to vine growth and contribute to intra-zone variability. These include soil pH and nutrient availability, both influenced by the underlying geological substrate (Retallack & Burns, 2016). While grapevines tolerate a relatively wide pH range, deviations from the optimal levels can hinder nutrient uptake, reduce growth, and affect yield. Soil organic matter and localized precipitation play pivotal roles in soil fertility and water availability. Vineyards exposed to high runoff and erosion risk may experience reduced grape and wine quality due to the loss of topsoil and organic matter (de Sosa *et al.*, 2023). Furthermore, gypsum-rich soils influence soil structure and nutrient balance, thereby affecting vine performance and grape composition (Lanyon *et al.*, 2004).

From a practical perspective, the successful implementation of this zoning approach depends on the availability and quality of spatial input data. While some viticultural regions benefit from long-term climate records and detailed soil surveys, others lack the resolution or coverage required. Defining a minimum dataset -including soil depth, topographic indices, and key climate metrics- has been suggested as a way to enhance the transferability and operational use of zoning protocols (Bramley *et al.*, 2023). Moreover, the reproducible workflows applied in this study facilitate wider adoption and ensure transparency. Importantly, the method provides more than just classification: by identifying and characterizing zones based on influential biophysical drivers, it offers a framework for site-specific vineyard management, land-use planning, and even the development of appellation criteria. Future work should integrate vine performance metrics -such as yield, grape composition, and sensory attributes- to validate and refine the delineated zones in relation to the terroir concept.

Conclusion

This study presents a data-driven approach for delineating edaphoclimatic zones that ensures spatial coherence and identifies areas according to the most influential climatic, geomorphometric, and soil variables driving regional variability. By integrating spatially explicit clustering with visual and statistical tools -such as star plots and the random forest algorithm- the method enables the simultaneous assessment of variable importance and the detailed characterization of each zone. This framework provides a robust basis for terroir identification and supports a deeper understanding of the uniqueness of vineyard environments, offering practical guidance for viticultural zoning, vineyard management, and regional planning in wine-producing regions.

References

Albornoz, E. M., Kemerer, A. C., Galarza, R., Mastaglia, N., Melchiori, R., & Martínez, C. E. (2018). Development and evaluation of an automatic software for management zone delineation. *Precision Agriculture*, *19*(3), 463-476. https://doi.org/10.1007/s11119-017-9530-9

Amerine, M. A., & Winkler, A. J. (1944). Composition and Quality of Musts and Wines of California Grapes. *Hilgardia*, *15*(6), 493-675. https://doi.org/10.3733/hilg.v15n06p493

Biss, A. J. (2020). Impact of vineyard topography on the quality of Chablis wine. *Australian Journal of Grape and Wine Research*, *26*(3), 247-258. https://doi.org/10.1111/ajgw.12433

Bramley, R., Ouzman, J., & Trought, M. C. T. (2020). Making sense of a sense of place: precision viticulture approaches to the analysis of terroir at different scales. *OENO One*, *54*(4), 903-917. https://doi.org/10.20870/oeno-one.2020.54.4.3858

Bramley, R., & Gardiner, P. S. (2021). Underpinning terroir with data: a quantitative analysis of biophysical variation in the Margaret River region of Western Australia. *Australian Journal of Grape and Wine Research*, *27*(4), 420-430. https://doi.org/10.1111/ajgw.12491

Bramley, R., Ouzman, J., Sturman, A. P., Grealish, G. J., Ratcliff, C. E. M., & Trought, M. C. T. (2023). Underpinning Terroir with Data: Integrating Vineyard Performance Metrics with Soil and Climate Data to Better Understand Within-Region Variation in Marlborough, New Zealand. *Australian Journal of Grape and Wine Research*, 1-23. https://doi.org/10.1155/2023/8811402

Breiman, L. (2001). Random Forests. *Machine Learning*, *45*(1), 5-32. https://doi.org/10.1023/A:1010933404324

Cavagnaro, M., Pappalardo, C., & Dalmasso, J. (2023). *Caracterización climática de regiones vitivinícolas de Argentina. Provincia Mendoza*. https://caracterizacion-fisico-ambiental-coviar.hub.arcgis.com/

Córdoba, M., Balzarini, M., Bruno, C., & Costa, J. L. (2012). Análisis de componentes principales con datos georreferenciados. Una aplicación en agricultura de precisión. *Revista de la Facultad de Ciencias Agrarias. Universidad Nacional de Cuyo, 44*(1), 27-39.

Córdoba, M., Bruno, C., Costa, J., & Balzarini, M. (2013). Subfield management class delineation using cluster analysis from spatial principal components of soil variables. *Computers and Electronics in Agriculture*, *97*, 6-14. https://doi.org/10.1016/j.compag.2013.05.009

Córdoba, M., Paccioretti, P., & Balzarini, M. (2024). *Ofemeantest: On Farm Experimentation Mean Test. R package version 0.0.900*. https://github.com/PPaccioretti/ofemeantest

de Sosa, L. L., Navarro-Fernández, C. M., Panettieri, M., Madejón, P., Pérez-de-Mora, A., & Madejón, E. (2023). Application of seaweed and pruning residue as organic fertilizer to increase soil fertility and vine productivity. *Soil Use and Management*, *39*(2), 794-804. https://doi.org/10.1111/sum.12882

Ferretti, C. G. (2020). A new geographical classification for vineyards tested in the South Tyrol wine region, northern Italy, on Pinot Noir and Sauvignon Blanc wines. *Ecological Indicators*, *108*, 105737. https://doi.org/10.1016/j.ecolind.2019.105737

Ferro, M. V., & Catania, P. (2023). Technologies and Innovative Methods for Precision Viticulture: A Comprehensive Review. *Horticulturae*, *9*(3), 399. https://doi.org/10.3390/horticulturae9030399

Fox, E. W., Ver Hoef, J. M., & Olsen, A. R. (2020). Comparing spatial regression to random forests for large environmental data sets. *PLOS ONE*, *15*(3), e0229509. https://doi.org/10.1371/journal.pone.0229509

Ghilardi, F., Virano, A., Prandi, M., & Borgogno-Mondino, E. (2023). Zonation of a Viticultural Territorial Context in Piemonte (NW Italy) to Support Terroir Identification: The Role of Pedological, Topographical and Climatic Factors. *Land*, *12*(3), 647. https://doi.org/10.3390/land12030647

Hall, A., & Jones, G. V. (2010). Spatial analysis of climate in winegrape-growing regions in Australia. *Australian Journal of Grape and Wine Research*, *16*(3), 389-404. https://doi.org/10.1111/j.1755-0238.2010.00100.x

Huglin, P. (1983). Possibilites d' appreciation objective du milieu viticole. *Bulletin de l'OIV*, *56*, 823-833.

INV. (2024). *Informe anual de cosecha y elaboración 2024.*

Irimia, L. M., Patriche, C. V., & Quénol, H. (2014). Analysis of viticultural potential and delineation of homogeneous viticultural zones in a temperate climate region of Romania. *OENO One*, *48*(3), 145. https://doi.org/10.20870/oeno-one.2014.48.3.1576

Jarvis, C., Barlow, E., Darbyshire, R., Eckard, R., & Goodwin, I. (2017). Relationship between viticultural climatic indices and grape maturity in Australia. *International Journal of Biometeorology*, *61*(10), 1849-1862. https://doi.org/10.1007/s00484-017-1370-9

Jolliffe, I. T., & Cadima, J. (2016). Principal component analysis: a review and recent developments. *Philosophical Transactions of the Royal Society A: Mathematical, Physical and Engineering Sciences*, *374*(2065), 20150202. https://doi.org/10.1098/rsta.2015.0202

Jones, G. V., White, M. A., Cooper, O. R., & Storchmann, K. (2005). Climate Change and Global Wine Quality. *Climatic Change*, *73*(3), 319-343. https://doi.org/10.1007/s10584-005-4704-2

Kuhn, & Max. (2008). Building Predictive Models in R Using the caret Package. *Journal of Statistical Software*, *28*(5), 1-26. https://doi.org/10.18637/jss.v028.i05

Lanyon, D. M., Hansen, D., & Cass, A. (2004). *The effect of soil properties on vine performance*. CSIRO Land and Water Technical Report N°. 34/04.

Malone, B. P., McBratney, A. B., Minasny, B., & Laslett, G. M. (2009). Mapping continuous depth functions of soil carbon storage and available water capacity. *Geoderma*, *154*(1-2), 138-152. https://doi.org/10.1016/j.geoderma.2009.10.007

McBratney, A. B., Mendonça Santos, M. L., & Minasny, B. (2003). On digital soil mapping. *Geoderma*, *117*(1-2), 3–52. https://doi.org/10.1016/S0016-7061(03)00223-4

Morlat, R., & Bodin, F. (2006). Characterization of Viticultural Terroirs using a Simple Field Model Based on Soil Depth – II. Validation of the Grape Yield and Berry Quality in the Anjou Vineyard (France). *Plant and Soil*, *281*(1-2), 55-69. https://doi.org/10.1007/s11104-005-3769-z

Mullins, M. G., Bouquet, A., & Willians, L. E. (1992). *Biology of the Grapevine*. Cambridge University Press.

Nakazawa, M. (2023). *fmsb: Functions for Medical Statistics Book with some Demographic Data*. https://minato.sip21c.org/msb/

Paccioretti, P., Córdoba, M., Giannini-Kurina, F., & Balzarini, M. (2024). *paar: Precision Agriculture Data Analysis. R package version 1.0.1, https://CRAN.R-project.org/package=paar*

Piraino, S.; Roig, F. A. 2024. Landform heterogeneity drives multi-stemmed *Neltuma flexuosa* growth dynamics. Implication for the Central Monte Desert forest managemen. Revista de la Facultad de Ciencias Agrarias. Universidad Nacional de Cuyo. Mendoza. Argentina. 56(1): 26-34. DOI: https://doi.org/10.48162/rev.39.120

Pracilio, G., Smettem, K. R. J., Bennett, D., Harper, R. J., & Adams, M. L. (2006). Site assessment of a woody crop where a shallow hardpan soil layer constrained plant growth. *Plant and Soil*, *288*(1-2), 113-125. https://doi.org/10.1007/s11104-006-9098-z

Puscama, F., Gil, R., & Berli, F. (2025). Impact of intra-vineyard soil heterogeneity on Malbec. Vine growth, yield and wine elemental composition and sensory profile. *Revista de la Facultad de Ciencias Agrarias. Universidad Nacional de Cuyo, 57*(1), 1-18. https://doi.org/10.4816210.48162/rev.39.147

R Core Team. (2024). *R: A Language and Environment for Statistical Computing. R Foundation for Statistical Computing, Vienna, Austria.* R Foundation for Statistical Computing. https://www.R-project.org/

Retallack, G. J., & Burns, S. F. (2016). The effects of soil on the taste of wine. *GSA Today*, *26*(5), 4-9. https://doi.org/10.1130/GSATG260A.1

Straffelini, E., Carrillo, N., Schilardi, C., Aguilera, R., Estrella Orrego, M. J., & Tarolli, P. (2023). Viticulture in Argentina under extreme weather scenarios: Actual challenges, future perspectives. *Geography and Sustainability*, *4*(2), 161-169. https://doi.org/10.1016/j.geosus.2023.03.003

Tonietto, J., & Carbonneau, A. (2004). A multicriteria climatic classification system for grape-growing regions worldwide. *Agricultural and Forest Meteorology*, *124*(1-2), 81-97. https://doi.org/10.1016/j.agrformet.2003.06.001

Vallone, R., Olmedo, G., Maffei, J., Morábito, J., Mastrantonio, l., Lipinski, V., & Filippini, M. (2007). *Mapa de Aptitud de suelos con fines de Riego y de riesgo de contaminación edáfica de los Oasis Irrigados de la Provincia de Mendoza*. FCA-DGI-OEI.

Vallone, R., Moreiras, S., Cáceres, M., Arzalluz, I., Zuin, J., Martín, T., & Corvalán, F. (2023). *Caracterización geológica, geomorfológica y edafológica de zonas vitícolas argentinas. Provincia Mendoza. Oasis Norte*. https://caracterizacion-fisico-ambiental-coviar.hub.arcgis.com/

Van Leeuwen, C., Roby, J. P., Pernet, D., & Bois, B. (2010). Methodology of soil-based zoning for viticultural terroirs. *Bulletin de l'OIV*, *83*(947), 0-13.

Vaudour, E., Carey, V. A., & Gilliot, J. M. (2010). Digital zoning of South African viticultural terroirs using bootstrapped decision trees on morphometric data and multitemporal SPOT images. *Remote Sensing of Environment*, *114*(12), 2940-2950. https://doi.org/10.1016/j.rse.2010.08.001

Visconti, F., López, R., & Olego, M. Á. (2024). The Health of Vineyard Soils: Towards a Sustainable Viticulture. Horticulturae, 10(2), 154. https://doi.org/10.3390/horticulturae10020154

Variations of Atmospheric Emissions in the Biomass Burning of Tree Species as an Environmental Indicator

Variaciones de emisiones atmosféricas en la quema de biomasa de especies arbóreas como indicador ambiental

Jorge Alonso Alcalá Jáuregui [1*], María Fernanda Ramírez Cubos [1], Ángel Natanael Rojas Velázquez [1], Idrissa Diedhiou [2], María Flavia Filippini [3], Daniela Cónsoli [3], Eduardo Martínez Carretero [4], Juan Carlos Rodríguez Ortiz [1] Oscar Iván Guillén Castillo [1], Marcela Ontivero [4]

Originales: *Recepción:* 18/04/2025 - *Aceptación:* 17/11/2025

Abstract

Biomass burning (BB) serves as both an energy source and an environmental indicator. This study examined how CO_2 and fine particle emissions vary during the combustion of biomass from three tree species to determine their contribution to environmental pollution. Leave and stem samples were taken from *A. farnesiana* (huizache) tree, *S. molle* (pirul), and *P. laevigata* (mesquite). The dry biomass was thermally processed in a muffle furnace at temperatures ranging from 50°C to 450°C. Emissions of CO_2, particles smaller than 2.5 microns ($PM_{2.5}$), particles smaller than 10 microns (PM_{10}), and total volatile organic compounds (TVOC) were measured. The highest emission levels occurred during the pyrolysis process between 250°C and 450°C in both leaves and stems. Among the leaves, the highest emissions of $PM_{2.5}$ and PM_{10} were found in huizache, while the highest values were found in mesquite stems. In terms of leaves, mesquite had the highest CO_2 emissions, followed by huizache and pirul. Regarding the stems, pirul had the highest atmospheric emissions of CO_2, followed by huizache and mesquite. In all cases, emission levels exceeded the limits established by Mexican and international environmental regulations, indicating a significant risk to the environment and public health.

Keywords
Carbon dioxide • fine particles • incineration temperature • permissible limits

1 Universidad Autónoma de San Luis Potosí. Facultad de Agronomía y Veterinaria. Km. 14.5 Carretera San Luis-Matehuala Apdo. Postal 32 CP 78321 Soledad de Graciano Sánchez. San Luis Potosí. México. * jorge.alcala@uaslp.mx
2 Universidad EARTH. Las Mercedes de Guácimo. Guácimo 70602. Costa Rica.
3 Universidad Nacional de Cuyo. Facultad de Ciencias Agrarias. Catedra Química Agrícola. Almirante Brown 500. M5528AHB. Chacras de Coria. Mendoza. Argentina.
4 IADIZA (CONICET). Geobotánica y Fitogeografía. Mendoza. Argentina.

Resumen

La quema de biomasa (BB) sirve tanto como fuente de energía como indicador medioambiental. Este estudio examinó las variaciones de las emisiones de CO_2 y partículas finas durante la combustión de biomasa de tres especies de árboles para determinar su contribución a la contaminación medioambiental. Se tomaron muestras de hojas y tallos de *A. farnesiana* (huizache), *S. molle* (pirul) y *P. laevigata* (mezquite). La biomasa seca se procesó térmicamente en un horno de mufla a temperaturas que oscilaron entre 50°C y 450°C. Se midieron las emisiones de CO_2, partículas menores de 2,5 micras ($PM_{2.5}$), partículas menores de 10 micras (PM_{10}) y compuestos orgánicos volátiles totales (TVOC). Los niveles más altos de emisión se produjeron durante el proceso de pirólisis entre 250°C y 450°C, tanto en las hojas como en los tallos. Entre las hojas, las emisiones más altas de $PM_{2.5}$ y PM_{10} se encontraron en el huizache, mientras que los valores más altos se encontraron en los tallos del mezquite. En cuanto a las hojas, el mezquite tuvo las emisiones más altas de CO_2, seguido del huizache y el pirul. En cuanto a los tallos, el pirul tuvo las emisiones atmosféricas más altas de CO_2, seguido del huizache y el mezquite. En todos los casos, los niveles de emisión superaron los límites establecidos por las regulaciones ambientales mexicanas e internacionales, lo que indica un riesgo significativo para el medio ambiente y la salud pública.

Palabras clave

Dióxido de carbono • partículas finas • temperatura de incineración • límites permisibles

Introduction

Biomass burning (BB) is the combustion of plant materials, which are widely used for energy production. It is increasingly recognized as an environmental indicator, particularly of air quality. Energy sources can be broadly classified as solid or non-solid fuels. The former includes coal, biomass, unprocessed wood, charcoal, manure, and crop residues. The latter includes kerosene, liquefied petroleum gas, natural gas, electricity, and others (8, 45, 51). Furthermore, BB is a significant contributor to air pollution with global, regional, and local implications for air quality, public health, and climate (21, 45). It emits trace gases and particulate matter into the atmosphere (19). It emits trace gases and particulate matter into the atmosphere. Therefore, the quantification of emissions and their impact assessment have been studied in various regions of the world (21, 45). In urban areas, around 50% of households use solid fuels, primarily coal and biomass, for energy, exposing themselves to the harmful effects of combustion residues. This affects nearly 50% of the global population, *i.e.*, over 3 billion people (51). Biomass originates from trees, agricultural crops, and other living plant materials. Furthermore, burning is a common, cost-effective, and time-efficient method of disposing of biomass residues from agricultural processes and other sectors. This practice has become increasingly widespread during the pre- and post-harvest seasons (41). From a health perspective, CO_2 is produced when biomass burns efficiently. Oxygen from the atmosphere combines with carbon from plants to produce CO_2 at a technological level. In the field of biomass-to-energy conversion, several technologies are in use, including combustion, anaerobic digestion (biogas plants), and thermochemical pretreatment. Promising emerging technologies include thermal gasification, torrefaction, and pyrolysis (33). The main technologies used in experimentation to exploit organic waste or biomass focus on chemical-biological processes, bioenergy, environmental treatment, pyrolysis, gasification, combustion, synthesis, hydrolysis, fermentation, and product separation (1). Other sources indicate that biomass conversion technologies fall into three categories: combustion, thermal gasification, and pretreatment. In pyrolysis, a thermochemical route, biomass is heated between 400°C and 600°C in the absence of oxygen. The process produces three products: solid charcoal, liquid pyrolysis oil (bio-oil), and a gaseous product (33). Pyrolysis is characterized by high heating rates, with temperature control close to 500°C (1, 12, 14). In contrast, torrefaction is considered a mild form of pyrolysis ($200°C<T<300°C$) and is carried out in an inert atmosphere or with steam. This brings the biomass into contact with a heating medium that gradually raises its temperature by less than 50°C per

minute until it reaches 200-300°C (13). In practice, these burning processes release various pollutants, mainly gases and particulate matter, into the atmosphere. These pollutants include formaldehyde (HCHO), methane (CH_4), sulfur oxides (SOx), nitrogen oxides (NOx), carbon monoxide (CO), carbon dioxide (CO_2), and different sizes of respirable particulate matter ($PM_{3.5}$), such as PM_1, $PM_{2.5}$, and PM_{10} (9, 43, 51, 53, 55). The process is cyclical because CO_2 and water are produced, which are then used in the photosynthetic process to produce carbohydrates that form the basic components of biomass (9). In contrast, particulate matter emissions have been linked to severe damage, including alterations in photosynthesis, changes in plant growth, and alterations in plant reproduction (36). In line with global monitoring efforts, the United Nations Agenda 2030 for Sustainable Cities and Communities evaluates air quality by considering fine suspended particles $PM_{2.5}$ and PM_{10}, as indicators (38). $PM_{2.5}$ is the environmental factor posing the greatest health risk, contributing to over 4.1 million deaths worldwide in 2016 (31). For instance, a study of 708 European urban areas found that 22% of PM emissions came from urban cores and commuting areas. The average contributions of industrial activity, agriculture, and road transport were 18%, 17%, and 14%, respectively. Furthermore, 27% of the emissions came from a group of cities in northern Italy, while eastern Europe contributed more than 50% (58). The World Health Organization (WHO) recommends annual mean exposures of 10 $\mu g/m^3$ of $PM_{2.5}$ and 20 $\mu g/m^3$ of PM_{10} to minimize health impacts (34, 40, 56). In Mexico, NOM-021-SSA1-2021 establishes permissible values for suspended particulate matter PM_{10} and $PM_{2.5}$ in ambient air, including evaluation criteria (25). Furthermore, studies of air pollution by BB combine a series of variables and perspectives. These variables and perspectives consider the spatial and temporal scales, as well as the associated implications and impacts on human health, regional air quality, ecosystem health, climate change, and intercontinental pollution (52). Along these lines, studies of biomass derived from organic sources, such as agricultural and forest residues and dedicated energy crops, aim to identify sustainable energy options while evaluating their environmental impact, such as greenhouse gas emissions (8, 26). The species *Prosopis laevigata* (mesquite), *Schinus molle* (pirul), and *Acacia farnesiana* (huizache) have been associated with studies on environmental pollution in the state of San Luis Potosi (3, 4, 5, 6, 23). In some regions of Mexico, species such as mesquite (*Prosopis sp*.) are used as a source of charcoal due to their calorific potential (23). This indicates the need to explore alternatives to assess the impact of biochar (BB) on tree species. In some cases, dry leaves, bark, and pruning residues are used as fuel (45). Thus, this study aimed to evaluate variations in atmospheric emissions from burning biomass (stems and leaves) of these tree species to expand pollution research in San Luis Potosi, Mexico. The hypothesis is that emissions differ among species and between biomass types (leaves *vs.* stems), influencing compliance with environmental regulations in a laboratory-scale pilot test under a controlled pyrolysis/combustion process.

Materials and Methods

The study was conducted at Ejido Palma de la Cruz, Soledad de Graciano Sanchez, San Luis Potosi, Mexico (24°14’58’’N and 100°51’53’’W; 1,836 m a. s. l.) (figure 1, page 72).

Sample Collection

Nine sampling points were randomly selected within stands dominated by *Prosopis laevigata*, *Acacia farnesiana*, and *Schinus molle*, focusing on individuals taller than two meters. For each species, leaf and stem material was collected 1.6-1.8 meters above the ground after flowering. The samples were transported to the laboratory. The leaves and stems were separated, rinsed to remove dust and debris, and air-dried at room temperature. Fresh and dry biomass weights (g) were recorded to estimate total fresh weight per species and per plant organ (leaves and stems) (table 1, page 72). In total, nine composite samples per species were obtained (n=9 per organ per species). To determine the total dry weight per species, biomass was placed in a drying oven at 60°C for 48 hours in a RIOSSA H-48-48 stove.

Figure 1. Study area and sampling points for biomass collection.
Figura 1. Área de estudio y puntos de muestreo de la colecta de biomasa.

Table 1. Estimated total fresh and dry biomass weight of the tree species (g).
Tabla 1. Estimación del peso fresco y seco total de la biomasa de las especies arbóreas (g).

Tree species	Biomass	Fresh weight (g)	Mean	Dry weight (g)	Mean	Difference in %
A. farnesiana	Leaf	18.38	2.04	9.09	1.01	49.49
	Stem	23.4	2.60	15.35	1.71	65.63
S. molle	Leaf	98.24	10.92	30.95	3.44	31.5
	Stem	19.35	2.15	6.13	0.68	31.66
P. laevigata	Leaf	50.88	5.65	22.64	2.52	44.5
	Stem	31.57	3.51	17.3	1.92	54.78

Measurement of Incineration Gases and Atmospheric Particles

Ambient concentrations of carbon dioxide (CO_2), particulate matter (particles smaller than 2.5 and 10 microns), $PM_{2.5}$, PM_{10}, total volatile organic compounds, relative humidity, and temperature were recorded before measurement. The dry weight generated by each species (leaf and stem) was divided into six crucibles, each containing an average sample of 1.5 g, for the dry weight samples of leaves of each species. For the stems, four crucibles were used with an average dry weight range of 1.5 g. This was done because the total biomass of the leaves and stems of each species lost between 31.5% and 54.78% of their weight. To homogenize the distribution of biomass, an average of 1.5 g per sample was used (table 1). This could be a limitation to consider when increasing the amount of experimental dry biomass in future studies. According to certain criteria of some authors, the biomass was subjected to the pyrolysis process at temperatures ranging from 50°C to 450°C (1, 12, 14).

The prepared samples were incinerated in an electric muffle furnace (LabTech® Daiha Lantech Co. LTD) at 50, 100, 150, 200, 250, 300, 350, 400, and 450°C. Measurements of CO_2 (ppm), $PM_{2.5}$ (μ/m³), PM_{10} (μ/m³), TVOC (total volatile organic compounds, g/m³), % relative humidity, and temperature (°C) were performed using HT-9600 (Dust Particle Counter®) and BLATN Smart (Portable Air Quality Monitor®) equipment. These devices were stabilized for an average of two hours for the environmental measurement. Some methodological criteria regarding sample handling and particle measurement were considered in previous studies (7). Results were interpreted using guideline values from the United States Environmental Protection Agency and the World Health Organization (34, 35, 40), as well as those referred to in the manuals of the measuring equipment.

Additionally, the Mexican Official Standard NOM-025-SSA1-2021 (25) was considered by comparing the average emission values with the 24-h permissible limits established by the standard of the real emission (maximum and minimum values).

Statistical Analysis

The variables included total and specific biomass (leaves and stems) by species, ambient temperature, percent relative humidity, incineration temperatures, gas, atmospheric particulate emissions, dry weight, and residual ash. The data were analyzed using Minitab® software, version 16. Analysis of variance was used with Tukey's test at a significance level of $p \leq 0.05$. Correlation analysis (Pearson correlation coefficient) and principal component analysis (PCA) were also performed on all variables studied in this experiment.

Results and Discussion

A significant Pearson correlation ($p \leq 0.05$) was detected between gaseous emissions (CO_2, TVOC) and fine particles ($PM_{2.5}$, PM_{10}) and ambient conditions (relative humidity and air temperature). Additionally, the Tukey test distinguished between total biomass emissions and emissions generated by the pyrolysis of leaves and stems from the three species, revealing pronounced differences at 200-400°C. On the other hand, principal component analysis revealed the set of data (gases and particles) that explains variation in incineration temperatures and species with higher or lower biomass emissions. Regarding the Pearson correlation (table 2), the strongest significant associations among the total emission variables were between $PM_{2.5}$ and TVOC ($r^2=0.76$) and between $PM_{2.5}$ and PM_{10} ($r^2=0.62$). Higher values were observed for leaf biomass with $PM_{2.5}$-TVOC ($r^2=0.75$) and TVOC-PM_{10} ($r^2=0.73$). Higher correlations were also observed for leaf biomass with $PM_{2.5}$-TVOC and TVOC-PM_{10}. Ten significant correlations were identified in stem biomass; the strongest was between $PM_{2.5}$ and TVOC ($r^2=0.79$).

Table 2. Results of Pearson's Correlation Coefficient on atmospheric variables in biomass incineration (pyrolysis process) of three tree species ($p \leq 0.05$).

Tabla 2. Resultados del coeficiente de correlación de Pearson en las variables atmosféricas de la incineración (proceso de pirólisis) de biomasa de tres especies arbóreas ($p \leq 0,05$).

Criteria	Variables	Pearson's Correlation Coefficient	Value of p
Total emissions (n=135)	$PM_{2.5}$-CO_2	0.180	0.036
	$PM_{2.5}$-TVOC	0.769	0.000
	$PM_{2.5}$-PM_{10}	0.624	0.000
	CO_2-Temperature	0.151	0.081
	TVOC-PM_{10}	0.674	0.000
	$PM_{2.5}$-$C0_2$	0.210	0.060
Leaf biomass (n=81)	$PM_{2.5}$-TVOC	0.753	0.000
	$PM_{2.5}$-PM_{10}	0.542	0.000
	TVOC-PM_{10}	0.734	0.000
	$PM_{2.5}$-CO_2	0.482	0.000

Criteria	Variables	Pearson's Correlation Coefficient	Value of p
Stem biomass (n=54)	$PM_{2.5}$-TVOC	0.796	0.000
	$PM_{2.5}$-PM_{10}	0.735	0.000
	$PM_{2.5}$-Temperature	0.288	0.034
	CO_2-TVOC	0.507	0.000
	CO_2-PM_{10}	0.542	0.000
	CO_2-Temperature	0.409	0.002
	CO_2-% HR	-0.272	0.047
	TVOC-PM_{10}	0.631	0.000
	TVOC-% HR	0.283	0.038

Total Biomass Burning Emissions

An analysis of 181 samples revealed that incineration temperature, biomass origin (tree species), and biomass type (leaf or stem) significantly affected total CO_2, $PM_{2.5}$, PM_{10}, and TVOC emissions (Tukey, $p \leq 0.05$). Considering the effect of incineration temperature (50°C-450°C), physically bound moisture is removed at 20-120°C. Above 160°C, chemically bound water is released through thermal condensation.

Between 120 and 150°C, the -H- and -C- bonds break, producing short-chain polymers that condense within the pores. As the temperature increases to between 150 and 270°C, carbon dioxide (CO_2), carboxylic acids, phenol, furfural, methanol, and other organic molecules are generated. This is primarily due to hemicellulose depolymerization and the release of carbonyl and carboxyl groups from cellulose. Lignin also overgoes reactions of aromatic rings in lignin (5, 13, 15, 16, 22, 23, 39). As the process progresses, the biomass darkens and begins to resemble coal in terms of its properties. The most intense heat consumption and mass loss occur in the early stages (13). According to another technical source, volatile gases are released when the temperature of dry biomass reaches 200°C-350°C during pyrolysis. These include carbon monoxide (CO), carbon dioxide (CO_2), methane (CH_4), and high-molecular-weight compounds (tar), which condense into a liquid when cooled. These gases mix with oxygen in the air and burn to produce a yellow flame. This self-sustaining process involves heat from gas combustion, drying fresh fuel, and releasing additional volatiles. Once all the volatiles have burned, the remaining solid is coal (44). Other contributing factors include species-specific chemical compositions and structural differences. For instance, a study of *Schinus molle* L. essential oil identified nineteen compounds, with the major ones being bicyclogermacrene, beta-caryophyllene, and spathulenol (37). As for *P. leavigata*, different compounds have been found in its various organs, including the fruit, leaves, and flowers. These compounds include phenolic compounds and alkaloids, as well as the concentrations of 4-hydroxybenzoic acid, p-coumaric acid, gallic acid, chlorogenic acid, cinnamic acid, and p-coumaric acid (29). Studies on the composition of *A. farnesiana* demonstrate that it essentially contains terpenes, phenolic acids, flavonoids, tannins, alkaloids, fatty acids from seed oils, polysaccharides, non-protein amino acids, and other phytochemicals (20).

CO_2 emissions from the total biomass of the three species were prioritized among the results because of their relevance as a greenhouse gas. The CO_2 emissions data revealed that the highest mean value was reached at 300°C, with a difference of 3,014.7 ppm. The lowest emissions occurred at 50°C (table 3, page 75). Due to its biogenic origin, the CO_2 released during biomass combustion is generally equivalent to the CO_2 absorbed during growth of trees, crops, and other plant-based residues (8). CO_2 is a greenhouse gas present in the global atmosphere at approximately 412 ppm, and it is projected to increase (17). Using this reference level, the emission measured in this study at 300°C (3,639.9 ppm) exceeded the atmospheric reference by 8.83 times and the maximum average reported for the study area by 8.39 times. Additionally, outdoor air typically contains 300-400 ppm of CO_2 and can reach up to 550 ppm in urban areas (49).

Table 3. Ratio of total gas emissions and total atmospheric particulate matter from biomass burning of three tree species (Tukey, p≤0.05, n=135).

Tabla 3. Relación de emisiones totales de gases y partículas atmosféricas totales de la quema de biomasa de tres especies arbóreas (Tukey, p≤0,05, n=135).

	Incineration temperature (pyrolysis process)								
Temperature	**50°C**	**100°C**	**150°C**	**200°C**	**250°C**	**300°C**	**350°C**	**400°C**	**450°C**
Variable	Mean								
CO_2 ppm	625.2a	867.8a	821.7a	810.8a	863.3a	**3639.9a**	1333.4a	1703.5a	2239.2a
$PM_{2.5}$ µ/m³	14.2c	13.5c	13.7c	91.7c	384.1b	700.3a	**905.2a**	843.2a	787.2a
PM_{10} µ/m³	290.4d	364.5d	164.7d	342.2d	2,893cd	13,519.2ab	11,087.4bc	20,434.6ab	**21,416.5a**
TVOC mg/m³	0.7c	0.8c	0.9c	0.8c	1.7c	4.6b	6.5ab	**8.1a**	7.9a
Temperature	26.6a	26.8a	27.6a	27.1a	27.8a	27.1a	27.3a	28.3a	28.4a
Relative Humidity (%)	56.8a	56.4a	56.6a	55.9a	56.5a	56.3a	56.2a	55.9a	55.7a

	Gases and atmospheric particles			
	Mean			
Species	CO_2 ppm	$PM_{2.5}$ µ/m³	PM_{10} µ/m³	TVOC g/m³
Huizache	1106.27a	**459.22**a	7166.60a	3.85a
Mesquite	**2140.07a**	407.49a	**8925.40a**	3.85a
Pirul	1055.29a	384.33a	7412.18a	2.99a

	Gases and atmospheric particles			
	Mean			
Biomass	CO_2	$PM_{2.5}$	PM_{10}	TVOC
	ppm	µ/m³	µ/m³	g/m³
Leaf	**1756.48a**	**424.26a**	6913.65a	**3.75a**
Stem	949.96a	406.15a	**9216.33a**	3.28a

Note: Maximum and minimum reference levels for $PM_{2.5}$ (41-25 µg/m³ as a 24-hour average and 10 µg/m³ as an annual average). PM_{10} would range as a 24-hour average from 70-50 µg/m³ to 36-20 µg/m³, as an annual average NOM-025-SSA1-2021 (25) and International Levels References (34, 35, 40). Daily ambient average during the study days: $PM_{2.5}$ (23.03 µg/m³), PM_{10} (88.70 µg/m³), CO_2 (400-433.62 ppm), and TVOC (0.664 g/m³). Columns with different letters indicate significant differences.

Nota: Niveles máximos y mínimos de referencia para $PM_{2.5}$ (41-25 µg/m³ como promedio de 24 horas y 10 µg/m³ promedio anual). PM_{10} oscilarían como promedio de 24 horas en 70-50 µg/m³ y 36-20 µg/m³, como promedio anual NOM-025-SSA1-2021 (25) y Niveles internacionales de referencia (34, 35, 40). Promedio diario en el ambiente durante los días del estudio: $PM_{2.5}$ (23.03 µg/m³), PM_{10} (88.70 µg/m³), CO_2 (400-433.62 ppm) y TVOC (0.664 g/m³). Columnas con letras diferentes indican diferencia significativa.

Other studies indicate that CO and CO_2 are primarily released at temperatures below 450°C and exhibit similar patterns. Increasing the heating rate positively influences the yield of combustible gases (46). At 450°C, PM_{10} emissions were higher, with an average of 21,416.5 µ/m³, compared to an average of 21,251.8 µ/m³ from the incinerated biomass at 150°C. Mexico's NOM-025-SSA1-2021 establishes permissible PM_{10} concentration limits maximum at 70 µg/m³, minimum at 50 µg/m³ (24-hour average) and 36 µg/m³ (annual average) (25). Using the 24-hour criterion (70 µg/m³), the highest emission average over 24 hours was 892.25 µ/m³, and the lowest was 6.86 µ/m³. At 450°C, PM_{10} exceeded the 24-hour permissible limit by a factor of 12.74, highlighting a significant environmental hazard. The value of 892.25 µ/m³ was 10.05 times higher than the average recorded in the study area during the experimental phase. Using the 24-hour criterion (50 µg/m³), the highest emission average over 24 hour at 450°C, PM_{10} exceeded the permissible limit by a factor of 17.84 times. Elevated PM_{10} levels have been linked to adverse effects on plant physiological functions, including photosynthesis and growth inhibition (36).

A study that burned olive tree pruning waste and performed a chemical characterization estimated average PM_{10} concentrations at 2,165 µg/m³, about fifty times higher than the PM_{10} concentrations estimated at reference sites under normal conditions. These emissions were associated with carbonaceous fractions, such as potassium (K), lead (Pb), and

polycyclic aromatic hydrocarbons (PAHs), as well as benzo(a)anthracene, benzo(a)pyrene, and benzo(K)fluoranthene, for the biomass combustion source (10).

The highest $PM_{2.5}$ emission, 905.2 μ/m^3, was observed at 350°C, which is 891.7 μ/m^3 higher than the average emission at 100°C. In accordance with NOM-025-SSA1-2021 (25), the maximum and minimum permissible limits for $PM_{2.5}$ are 41 μg/m^3 and 25 μg/m^3 (24-hour average) and 10 μg/m^3 (annual average). In this context, the highest recorded emission was 37.71 μg/m^3 over a 24-hour period, not exceeding the permissible limit of 41 μg/m^3. This value was 39.30 times higher than those recorded during the experimental days in the study area atmosphere. However, with the minimum reference level (25μg/m^3), this limit is 1.50 times higher. $PM_{2.5}$ can originate from various sources and therefore exhibits differences in chemical composition and physical characteristics. Common components of $PM_{2.5}$ include sulfates, black carbon, nitrates, and ammonium. Sources of anthropogenic $PM_{2.5}$ are mainly related to combustion engines, industrial processes, power generation, burning coal and wood, agricultural activities, and construction. Natural sources include dust storms, forest fires, and sandstorms (35). On the other hand, $PM_{2.5}$ has been linked to toxic levels of nickel (Ni), chromium (Cr), lead (Pb), arsenic (As), and black carbon (BC). Its main sources of emission include coal combustion, industrial activity, resuspended dust, and biomass burning. This indicates the urgent need for control measures (32, 35). $PM_{2.5}$ commonly contains sulfates, black carbon, nitrates, and ammonium (35). According to the U.S. Air Quality Index, $PM_{2.5}$ concentrations over 250.5 μg/m^3 pose a high risk to public health and the environment (34). In agricultural areas, high levels of PM_{10} and $PM_{2.5}$ have been reported, reaching 800 μg/m^3 and 485 μg/m^3, respectively (57). Populations in low- and middle-income countries are exposed to environmental $PM_{2.5}$ levels between 1.3 and 4 times higher (31). While the interspecific ratio of mean total emissions was not statistically significant, *P. laevigata* emitted 1,084.78 ppm of CO_2, surpassing *S. molle*. Among the evaluated species, *A. farnesian*a exhibited the highest $PM_{2.5}$ emissions, surpassing *S. molle* by 74.89 μg/m^3. *P. laevigata* showed the highest levels of PM_{10}, surpassing *A. farnesiana* by 1,758.8 μg/m^3 (table 3, page 75). This highlights notable interspecific variation in particulate emissions. The chemical analysis of *P. laevigata* wood revealed that it contains 7.36% hemicellulose, 48.28% cellulose, 30.57% lignin, and 13.53% extractives (42).

Other studies on the energy characterization of charcoal from species such as Prosopis have found elements like magnesium (Mg), calcium (Ca), copper (Cu), zinc (Zn), and iron (Fe) in charcoal and ash. These studies reported a higher calorific value of 27,669 kJ/kg for this species. These findings have been linked to particle size distribution, moisture content, volatile material content, ash content, fixed carbon content, and calorific value (23). Another key finding was that total leaf biomass emitted higher levels of CO_2, $PM_{2.5}$, and TVOC than total stem biomass. Leaf emissions of CO_2 exceeded stem emissions by 806.52 ppm across the three species. For $PM_{2.5}$, a difference of 18.11 μg/m^3 was observed between leaf and stem emissions. However, stem biomass emitted 2,302.68 μg/m^3 more PM_{10} than leaf biomass across the three evaluated species (table 3, page 75). In both cases, the emission levels exceeded the limits set by NOM-025-SSA1-2021 for PM_{10}, even when averaged over 24 hours (25).

The values obtained were higher than those measured in the environment during the study (table 3, page 75). This result should consider that the area is influenced by stone extraction, agricultural activities, and climatic factors that can cause environmental variability, even though the experiment was conducted under controlled conditions. The biomass's biomolecular components are lignocellulosic, comprising cellulose, hemicellulose, and lignin, which have recognized potential for bioenergy systems (4, 22, 50). Some authors have studied biomass' potential as a fuel source, emphasizing the importance of the chemical composition of different plant types. Processes such as torrefaction, in which biomass is heated to temperatures between 200 and 300°C, can enhance its energy properties (18). $PM_{2.5}$ emissions in Thailand have been reported to range from 0 to over 4,001 milligrams per year, considering contributions from agricultural residue burning, forest fires, and open biomass burning (50). Factors influencing particle numbers include tree species and combustion rate, which reflect the materials' slow-to-fast burning capacity, such as wood, leaves, and branches (21, 54). The most prominent emission produced during biomass combustion is CO_2, which serves as a proxy for the biomass carbon content and as a principal greenhouse gas. Combustion efficiency is often assessed based on the amount of carbon oxidized to CO_2. While biomass generally contains about 45% carbon weight, coal typically contains over 60% (24, 26).

Leaf Emissions of Three Tree Species

There was significant variation in gas and particle emissions during the leaf BB for the three species (Tukey, p≤0.05). Table 3 (page 75), shows that CO_2 emissions were higher at an incineration temperature of 300°C, with a difference of 4916.8 ppm compared to the emissions reported at 50°C (5541.2 ppm). The maximum emission detected exceeds the atmospheric concentration of 512 ppm reported in technical documents by 13.44 times (17). The highest PM_{10} emission occurred at 450°C, at 22,910.8 µ/m^3, showing a significant difference of 22,683.4 µ/m^3 relative to values at 150°C (figure 2B). In this case, the estimated 24-hour average concentration was 954.61 µg/m^3, which is 13.78 times higher than the 70 µg/m^3 and 19.09 times higher than the 50 µg/m^3 permissible limit established by the Mexican Official Standard NOM-025-SSA1-2021 for this type of particulate matter (25). The highest concentration of $PM_{2.5}$ emissions was recorded at 350°C, reaching 869.1 µg/m^3. This represents an 852.5 µg/m^3 difference compared to the 16.6 µg/m^3 emission recorded at 150°C (figure 2A). Based on this peak value, the estimated 24-hour average concentration is 36.21 µg/m^3, not exceeding the maximum limit of 41 µg/m^3, but if the minimum limit of 25 µg/m^3 (1.39 times) established by NOM-025-SSA1-2021 (25). Table 4 (page 78), shows atmospheric gas and particle emissions from tree species of leafy biomass origin. *P. laevigata* had higher CO_2 emissions, with a significant difference of 1,980.5 ppm compared to *S. molle* leaves. This difference is 4.8 times higher than the reported average atmospheric concentration (412 ppm) (17). The leaves of *A. farnesiana* emitted higher levels of $PM_{2.5}$ and PM_{10} than those of the other species. *A. farnesiana* had the highest PM_{10} emissions at 8,167.6 µ/m^3, which is 4.86 times higher than the maximum limit (41 µ/m^3) and 6.80 times minimum limit (50 µ/m^3) established by NOM-025-SSA1-2021. The corresponding 24-hour average would be 340.31 µ/m^3. A pairwise comparison between *A. farnesiana* and *S. molle* revealed that $PM_{2.5}$ was 136.4 µ/m^3 higher and PM_{10} was 2,971.5 µ/m^3 higher in *A. farnesiana* (table 4, page 78). The highest $PM_{2.5}$ value in *A. farnesiana* (514.4 µ/m^3) had a 24-hour average of 21.43 µ/m^3, wich is well below the limit specified in NOM-025-SSA1-2021 (25). Regarding the ash generated from the total incinerated leaf biomass (g), *S. molle* was significantly higher (0.444a) than *A. farnesiana* (0.349b) and *P. laevigata* (0.294) (Tukey, p≤0.05).

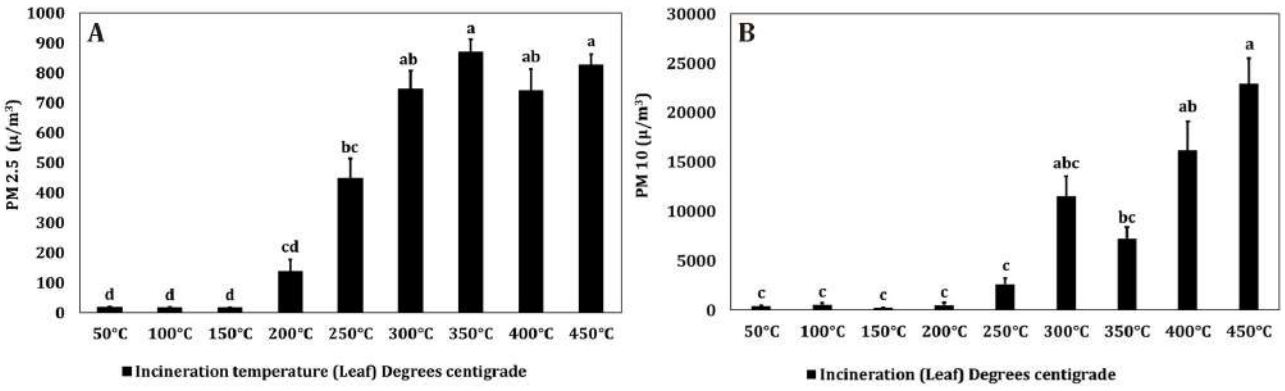

The data shown refers to the mean ± standard error (different letters indicate significant differences).
Los datos representados refieren la media ± error estándar (letras diferentes indican diferencia significativa).

Figure 2. Ratio of $PM_{2.5}$ (A) and PM_{10} (B) emissions in leaves of three tree species according to different incineration temperatures (Tukey, p≤0.05, n=81).

Figura 2. Relación emisiones de $PM_{2.5}$ (A) y PM_{10} (B) en hojas de tres especies arbóreas de acuerdo con las diferentes temperaturas de incineración (Tukey, p≤0,05, n=81).

Table 4. Ratio of gas emissions and total atmospheric particulate matter from burning leaves of three tree species (Tukey, p≤0.05, n=81).

Tabla 4. Relación de emisiones de gases y partículas atmosféricas totales de la quema de hojas de tres especies arbóreas (Tukey, p≤0,05, n=81).

	Incineration temperature (pyrolysis process)								
Temperature	**50°C**	**100°C**	**150°C**	**200°C**	**250°C**	**300°C**	**350°C**	**400°C**	**450°C**
Variable	**Mean**								
CO_2 ppm	624.4a	887.1a	829.8a	834.6 a	843a	**5541.2a**	1505.6a	1923.7a	2819.0a
TVOC g/m³	0.7c	1.0c	1.1c	0.8c	1.9bc	5.1ab	7.0a	8.5a	7.7a
Temperature °C	27.5a	27.7a	28.9a	28.0a	28.1a	27.9a	28.0a	28.5a	29.2a
Relative Humidity (%)	55.2a	54.4a	55.7a	53.8a	54.8a	54.0a	54.1a	53.8a	53.0a

Gases and atmospheric particles				
Mean				
Species	CO_2	$PM_{2.5}$	PM_{10}	TVOC
	Ppm	µ/m³	µ/m³	mg/m³
Huizache	1268a	**514.5a**	**8167.6a**	4.1a
Mesquite	**2991.0a**	380.1a	7377.2a	4.1a
Pirul	1010.5a	378.1a	5196.1a	3.1a

Note: Maximum and minimum reference levels for $PM_{2.5}$ (41-25 µg/m³ as a 24-hour average and 10 µg/m³ as an annual average). PM_{10} would range as a 24-hour average from 70-50 µg/m³ to 36-20 µg/m³, as an annual average NOM-025-SSA1-2021 (25) and International Levels References (34, 35, 40). Daily ambient average during the study days: $PM_{2.5}$ (23.03 µg/m³), PM_{10} (88.70 µg/m³), CO_2 (400-433.62 ppm), and TVOC (0.664 g/m³). Columns with different letters indicate significant differences.

Nota: Niveles de referencia máximo y mínimo para $PM_{2.5}$ (41-25 µg/m³ como promedio de 24 horas y 10 µg/m³ promedio anual). PM_{10} oscilarían como promedio de 24 horas en 70-50 µg/m³ y 36-20 µg/m³, como promedio anual NOM-025-SSA1-2021 y niveles internacionales de referencia (34, 35, 40). Promedio diario en el ambiente durante los días del estudio: $PM_{2.5}$ (23.03 µg/m³), PM_{10} (88.70 µg/m³), CO_2 (400-433.62 ppm) y TVOC (0.664 g/m³). Columnas con letras diferentes indican diferencia significativa.

Stem Emissions of the Three Tree Species

Table 5 (page 79) (Tukey, p≤0.05) shows significant differences in gas particle emissions from stem biomass. The highest mean total volatile organic compound (TVOC) emission occurred between 300°C and 450°C, reaching 8.2 g/m³. The highest CO_2 emission was observed at 450°C, with a concentration of 1,284.3 ppm. This represents a difference of 632.3 ppm compared to the emission at 50°C. *S. molle* had the highest mean CO_2 emissions (1,122.4 ppm), which was 338.06 ppm higher than the remaining species, such as mesquite (figure 3, page 79). Based on *S. molle's* emissions at 450°C, atmospheric CO_2 concentrations would be between 2.5 and 2.7 times the normal level (17). The highest PM_{10} emissions occurred at 400°C (26,787.8 µ/m³), differing in 26,710.4 µ/m³ relative to emissions at 150°C (figure 4, page 80). Averaging this peak over 24 hours (1,116.15 µ/m³) shows that the NOM-025-SSA1-2021 (25) standard is exceeded by 15.94 times (maximum level 70 µ/m³) and 22.32 times (minimum level 50 µ/m³). As for $PM_{2.5}$, the highest emissions occurred between 300 and 400°C. The peak value was 997.5 µg/m³, representing a significant mean difference of 989.4 µg/m³ relative to emissions at 50°C. This elevated emission would result in a 24-hour average concentration of 41.56 µg/m³, which exceeds the NOM-025-SSA1-2021 limit by a factor of 0.56 µg/m³, the maximum level of 41 µ/m³ and 1.66 times the minimum level of 25 µ/m³ (25). The ratio of residual ash to total biomass differed significantly among species in stem samples. *A. farnesiana* had the highest ratio (0.427 g), followed by *P. laevigata* (0.325 g) and *S. molle* (0.265 g), according to Tukey's test at p ≤ 0.05. Biomass burning causes a loss of organic matter and nutrients from the soil through particle dispersion or volatilization. BB leads to the loss of nutrients, soil biota, and total nitrogen (N) and carbon (C) in the topsoil, and it promotes soil erosion. Although nutrients are retained in ash, ash deposition increases the pH of the surface layer. The presence of ash increases surface concentrations of Ca, Mg, K, Na, and P; however, the high solubility of basic cations enhances leaching and promotes soil crusting (30).

Table 5. Ratio of gas emissions and total atmospheric particulate matter from the burning of stems of three tree species (Tukey, p≤0.05, n=54).

Tabla 5. Relación de emisiones de gases y partículas atmosféricas totales de la quema de tallos de tres especies arbóreas (Tukey, p≤0,05, n=54).

	Incineration temperature (pyrolysis process)							
Temperature	**50°C**	**100°C**	**150°C**	**250°C**	**300°C**	**350°C**	**400°C**	**450°C**
Variable	**Mean**							
TVOC g/m^3	0.6c	0.6c	0.7c	1.4bc	4.0abc	5.6ab	7.6a	8.2a
Temperature °C	25.3a	25.5a	25.7a	27.3a	26.0a	26.2a	28.1a	27.3a
Relative Humidity (%)	59.2a	59.3a	59.4a	59.1a	59.7a	59.2a	58.9a	59.6a

Gases and atmospheric particles			
Mean			
Species	$PM_{2.5}$	PM_{10}	TVOC
Huizache	376.3a	5665.1a	3.5a
Mesquite	**448.5a**	**11247.7a**	3.5a
Pirul	393.7a	10736.2a	2.8a

Note: Maximum and minimum reference levels for $PM_{2.5}$ (41-25 µg/m^3 as a 24-hour average and 10 µg/m^3 as an annual average). PM_{10} would range as a 24-hour average from 70-50 µg/m^3 to 36-20 µg/m^3, as an annual average NOM-025-SSA1-2021 (25) and International Levels References (34, 35, 40). Daily ambient average during the study days: $PM_{2.5}$ (23.03 µg/m^3), PM_{10} (88.70 µg/m^3), CO_2 (400-433.62 ppm), and TVOC (0.664 g/m^3). Columns with different letters indicate significant differences.

Nota: Niveles de referencia máximo y mínimo para $PM_{2.5}$ (41-25 µg/m^3, como promedio de 24 horas y 10 µg/m^3 promedio anual). PM_{10} oscilarían como promedio de 24 horas entre 70-50 µg/m^3 y 36-20 µg/m^3, como promedio anual NOM-025-SSA1-2021 (25) y Niveles internacionales de referencia (34, 35, 40) Promedio diario en el ambiente durante los días del estudio: $PM_{2.5}$ (23,03 µg/m^3), PM_{10} (88,70 µg/m^3), CO_2 (400-433,62 ppm) y TVOC (0,664 g/m^3). Columnas con letras diferentes indican diferencia significativa.

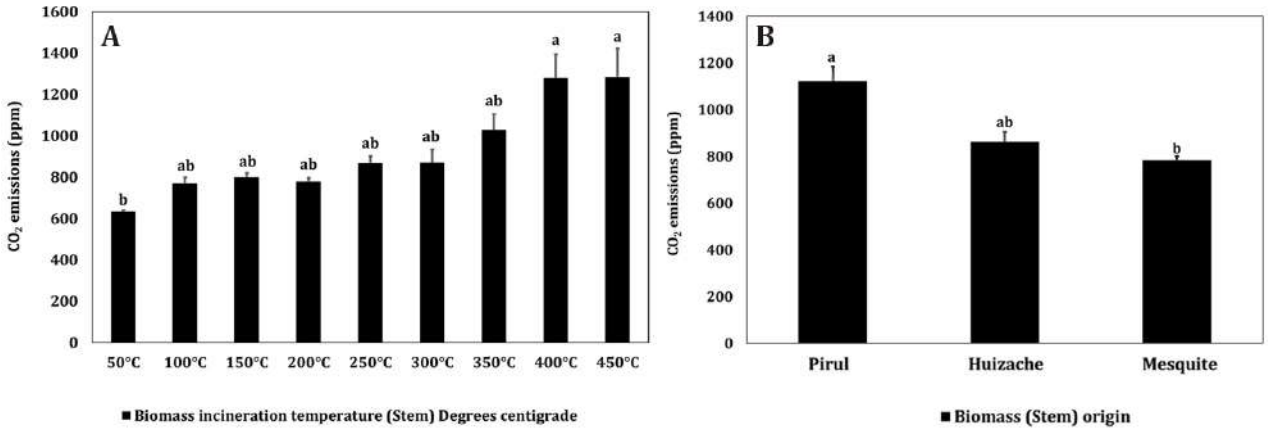

The data shown refers to the mean ± standard error (different letters indicate significant differences).

Los datos representados refieren a la media ± error estándar (letras diferentes indican diferencia significativa).

Figure 3. Ratio of CO_2 emissions (A) according to different incineration temperatures and CO_2 (B) in related stems and the three species of stem origin (Tukey, p≤0.05, n=81).

Figura 3. Relación emisiones de CO_2 (A) de acuerdo con las diferentes temperaturas de incineración y CO_2 (B) en tallos en relación con las tres especies de origen del tallo (Tukey, p≤0,05, n=81).

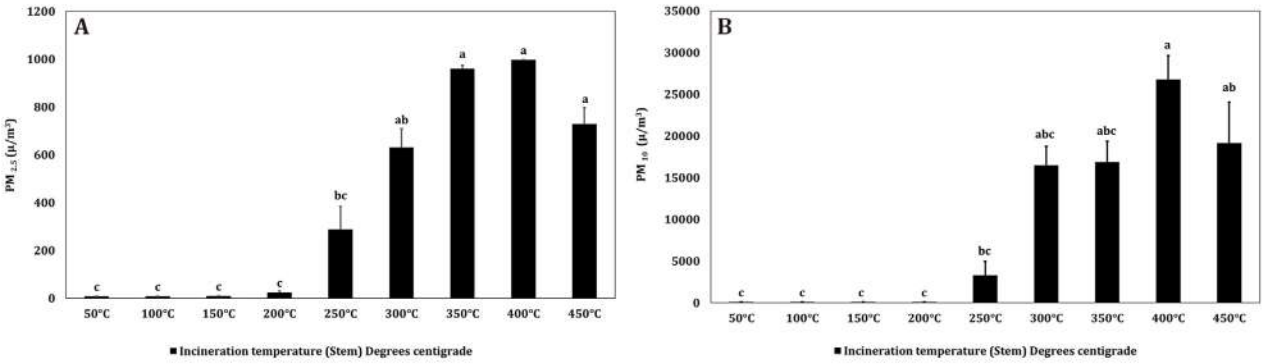

The data shown refers to the mean ± standard error (different letters indicate significant differences).
Los datos representados refieren a la media ± error estándar (letras diferentes indican diferencia significativa).

Figure 4. Ratio of $PM_{2.5}$ (A) and PM_{10} (B) emissions in the stems of three tree species according to different incineration temperatures (Tukey, p≤0.05, n=81).

Figura 4. Relación de emisiones de $PM_{2.5}$ (A) y PM_{10} (B) en tallos de tres especies arbóreas de acuerdo con las diferentes temperaturas de incineración (Tukey, p≤0,05, n=81).

Principal Component Analysis

In the leaf-biomass dataset for the three tree species, the first three components explained 74% of the variance (figure 5A, 5B; 6A, and 6B, page 81). PC1 explained 31% of the variance, PC2 explained 29.7%, and PC3 explained 14%. PC1 was driven by % relative humidity (0.528), TVOC (0.316), $PM_{2.5}$ (0.284), and dry weight (-0.440). PC2 was mainly associated with TVOC (0.509), $PM_{2.5}$ (0.478), PM_{10} (0.478), and ambient temperature (0.326). PC3 was primarily defined by CO_2 (0.758), ash weight (-0.540), and dry weight (-0.250). In the stem biomass analysis, the first three PCs explained 80% of the variance. PC1 was mainly driven by $PM_{2.5}$ (0.505), PM_{10} (0.488), CO_2 (0.442), and TVOC (0.467). PC2 accounted for 27% of the variance and had positive loadings on dry weight (0.535) and temperature (0.454), as well as negative loadings on % relative humidity (-0.619) and TVOC (-0.296).

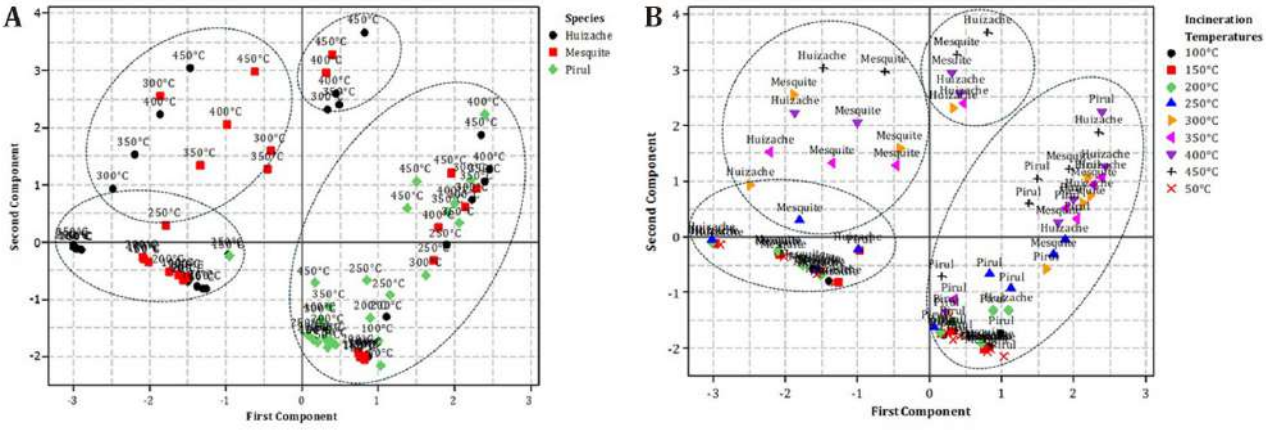

Figure 5. Eigenvalues resulting from principal component analysis of the emission of gases and atmospheric particles from burning leaves of three tree species according to species (A) and incineration temperature (B).

Figura 5. Distribución de eigenvalores resultante del análisis de componentes principales de la emisión de gases y partículas atmosféricas de la quema de hojas de tres especies arbóreas de acuerdo con la especie (A) y la temperatura de incineración (B).

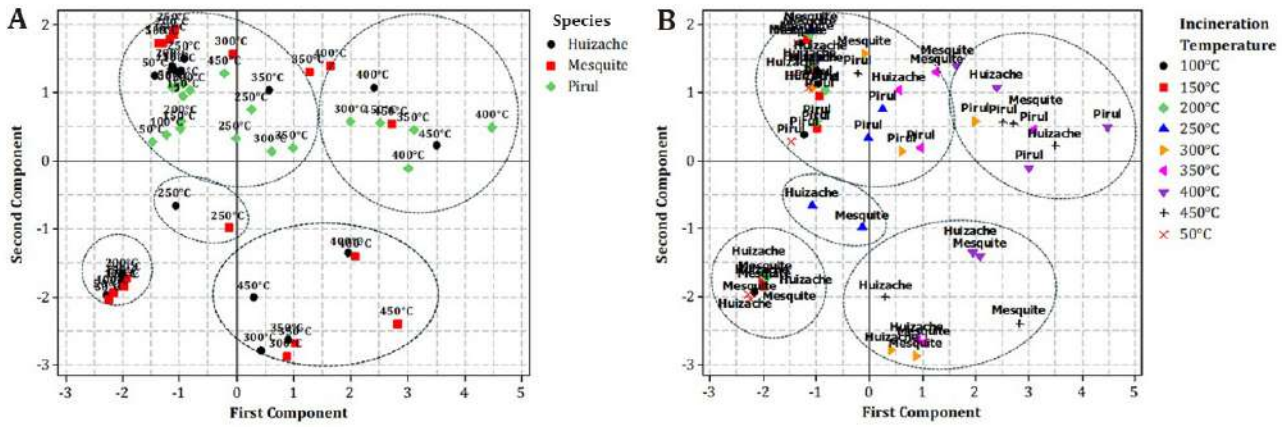

Figure 6. Eigenvalues resulting from the principal component analysis of the emission of gases and atmospheric particles from the burning of stems of three tree species according to species (A) and incineration temperature (B).

Figura 6. Distribución de eigenvalores resultante del análisis de componentes principales de la emisión de gases y partículas atmosféricas de la quema de tallos de tres especies arbóreas de acuerdo con la especie (A) y la temperatura de incineración (B).

These findings revealed significant variation in emission behavior among biomass components, likely driven by differences in the physicochemical structure of leaf and stem tissues across the three evaluated tree species. This variability was also evident across incineration temperatures from 50°C to 450°C, both in the analysis of total biomass and within the leaf and stem fractions. This criterion is important because most emissions are concentrated in the respirable fraction of PM. Emission size distribution and chemical characteristics vary with appliance type, combustion rate, fuel moisture, and biomass type; therefore, measurement is required to comply with air quality standards (2). Particulate matter (PM) is a key indicator of air pollution levels. The type of PM and the ratio between size particles (fine and coarse) determine its effects on human health and atmospheric processes. PM is commonly classified as dust, mixed aerosols, and anthropogenic aerosols (28). Another relevant observation is that leaf biomass from *S. molle* had the highest ash content (0.44 ± 0.03 g), and stem biomass from *A. farnesiana* produced the most ash among stems (0.42±0.06 g). Residual ash can have further environmental impacts. Its accumulation and the combustion of organic matter can significantly alter soil properties. For example, burned soils have a darker color, which results in lower albedo, increased environmental heat absorption, and higher soil temperature (30).

Complete combustion and open-air burning of residues require sufficient heat flux, an adequate oxygen supply, and sufficient combustion time. The magnitude and composition of emissions from this type of combustion depend on factors such as fuel density, moisture content, topography (*e.g.*, slope and terrain profile), and meteorological conditions (*e.g.*, wind and precipitation) (48). Emissions from major contributors to atmospheric particulate matter (PM), especially the $PM_{2.5}$ and PM_{10} fractions, have been linked to biomass burning (BB), forest fires, agricultural residue burning, and motor vehicles. These associations highlight challenges and inform policy recommendations for improving air quality (50).

Burning biomass fuels, especially wood-based ones, releases less CO_2 into the atmosphere than burning coal (26). However, BB is a major source of particulate matter and trace gases. Incomplete combustion likely contributes to global warming, and its overall contribution to climate change remains debated (9). Given the global concern about air pollution, studies like this one can contribute not only to our understanding of the impact of these reported levels on complex environmental processes but also provide opportunities for integral environmental improvements (35). Other studies have linked PM_{10} emissions to phytotoxic effects and elevated heavy metal concentrations (36). Additionally, BB is a

significant source of greenhouse gases (GHGs) and air pollutants (35). Another study found that air pollutants generally impact plant species, causing morphological, physiological, and biochemical damage (11).

In Mexico, anthropogenic emissions from stationary sources account for 22.5% of PM_{10}, 20.9% of $PM_{2.5}$, and 4.7% of VOCs. Area sources (pollutant sources that are too numerous and dispersed to be classified as fixed sources) account for 73.0%, 73.3%, and 89%, respectively. Mobile sources account for 4.5%, 5.8%, and 6.3%, respectively (47). The National Air Strategy, under Axis 5 (Responsible and Participatory Society), seeks to establish mechanisms for the community to understand air pollution impact and actively participate in improving air quality. It is recognized that the most commonly used solid fuels in Mexico are biomass, agricultural waste, and primarily firewood, accounting for 80% of the energy consumed in rural households (47). Therefore, it is crucial to acknowledge the risks and impacts that the emissions and residues of these gases and particles pose to public health and ecosystems. Evidence from PM_{10} studies includes data on indoor smoke dispersion among household members engaged in activities such as cooking, doing chores, warming up by the stove, playing, resting, eating, and sleeping. These studies demonstrated an exposure-response relationship, with a higher rate of increase for daily exposures below 1,000–2,000 $\mu g/m^3$ (27). Figure 7 shows how this pilot experiment clarifies the interplay between environmental factors and biomass intrinsic physicochemical characteristics (as in the three evaluated species) and the behavior of biomass components (leaves and stems) during pyrolysis across the laboratory-scale temperature range. The experiment also evaluates atmospheric gases and particles for regulatory compliance and highlights opportunities to extend the study to open field conditions and incorporate additional variables of interest.

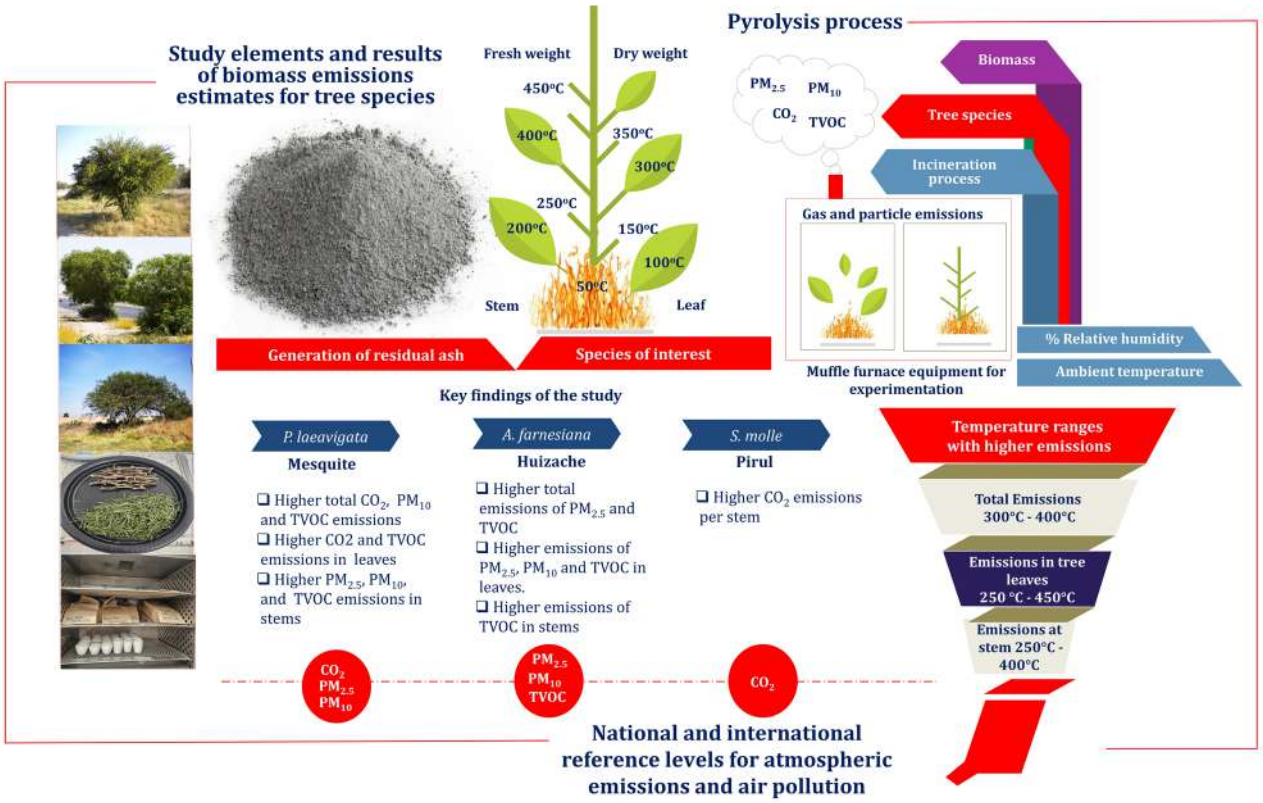

Figure 7. Summary of the main results of the study on atmospheric emissions from tree species (own elaboration).

Figura 7. Resumen de los principales resultados del estudio sobre las emisiones atmosféricas de las especies arbóreas (elaboración propia).

Conclusions

This study experimentally verified the environmental impacts of biomass burning for three tree species under a laboratory pyrolysis process. The emissions of $PM_{2.5}$, PM_{10}, CO_2, and total and specific VOCs varied between leaves and stems. This likely reflects the anatomical and physicochemical differences in the biomass that affect combustion at different incineration temperatures (50°C to 450°C). The highest $PM_{2.5}$ and PM_{10} emissions occurred in *A. farnesiana* leaves and in *P. laevigata* stems. The order of highest CO_2 emissions in leaves was *P. laevigata* > *A. farnesiana* > *S. molle*; in stems, it was *S. molle* > *A. farnesiana* > *P. laevigata*. The $PM_{2.5}$, PM_{10}, and CO_2 levels observed in this study exceeded the limits established by Mexican and international air quality regulations. CO_2 levels exceeded the technical reference for atmospheric averages (412 ppm) by 8.83 times and the average level in the study area by 8.39 times. PM_{10} exceeded the limit allowed by Mexican environmental regulations and international references (*e.g.*, the World Health Organization) by 12.74 times (maximum level) and 17.84 times the minimum level, as well as the level in the environment adjacent to the study area by 10.05 times. Similarly, the level of $PM_{2.5}$ does not exceed the permitted 24-hour maximum limit. However, with the minimum reference level, this limit is 1.50 times higher. The biomass emissions were 39.30 times higher than those measured in the area surrounding the study site. These elevated concentrations pose significant environmental risks and potential public health impacts. They can also harm ecosystems, including phytotoxic effects on plants and broader environmental degradation. Future studies should evaluate differences in residual ash quantities and compare biomass burning technologies and processes, as these differences may introduce additional environmental impacts. Experimental limitations include the need to standardize the mass of biomass and the size of samples when comparing materials such as leaves and stems. This is where variables such as fresh weight, dry weight, and moisture content are critical. To obtain more reliable results across samples, especially when comparing laboratory and field emissions, environmental conditions (temperature, humidity, wind speed, and solar radiation) and proper instrument calibration must also be considered. These results can inform assessments of the environmental impacts of using plants as an energy source and support the integration of additional environmental variables into future research and air pollution monitoring programs. Further comparisons across biomass burning sources and processes should strengthen evaluations of environmental impact considering air pollution.

References

1. Aguiar, S.; Enríquez Estrella, M.; Uvidia Cabadiana H. 2022. Residuos agroindustriales: su impacto, manejo y aprovechamiento. AXIOMA. 1(27): 5-11. https://doi.org/10.26621/ra.v1i27.803
2. Air Quality Expert Group. 2017. The Potential Air Quality Impacts from Biomass Combustion. https://uk-air.defra.gov.uk/assets/documents/reports/cat11/1708081027_170807_AQEG_Biomass_report.pdf%20
3. Alcalá Jáuregui, J.; García Arreola, M. E.; Rodríguez Ortiz, J. C.; Beltrán Morales, F. A.; Villaseñor Zuñiga, M. E.; Rodríguez Fuentes, H.; Hernández Montoya, A. 2013. Vegetación bioindicadora de metales pesados en un sistema semiárido. Revista de la Facultad de Ciencias Agrarias. Universidad Nacional de Cuyo. Mendoza. Argentina. 45(1): 27-42.
4. Alcalá Jáuregui, J.; Rodríguez Ortíz, J. C.; Hernández Montoya, A.; Filippini, M. F.; Martínez Carretero, E.; Diaz Flores, P. E. 2018a. Capacity of two vegetative species of heavy metal accumulation. Revista de la Facultad de Ciencias Agrarias. Universidad Nacional de Cuyo. Mendoza. Argentina. 50(1): 123-139.
5. Alcalá Jáuregui, J.; Rodríguez Ortiz, J. C.; Hernández Montoya, A.; Filippini, M. F.; Martínez Carretero, E.; Díaz Flores, P. E.; Rojas Velázquez, A. N.; Rodríguez-Fuentes, H.; Beltrán Morales, F. A. 2018b. Heavy metals in atmospheric dust deposited in leaves of *Acacia farnesiana* (Fabaceae) and *Prosopis laevigata* (Fabaceae). Revista de la Facultad de Ciencias Agrarias. Universidad Nacional de Cuyo. Mendoza. Argentina. 50(2): 173-185.
6. Alcalá Jáuregui, J.; Rodríguez Ortiz, J. C.; Filippini, M. F.; Martínez Carretero, E.; Hernández Montoya, A.; Rojas Velázquez, Á. N.; Méndez Cortés, H.; Beltrán Morales, Felix A. 2022. Metallic elements in foliar material and fruits of three tree species as bioindicators. Revista de la Facultad de Ciencias Agrarias. Universidad Nacional de Cuyo. Mendoza. Argentina. 54(2): 61-72. https://doi.org/10.48162/rev.39.083

7. Alcalá Jáuregui, J. A.; Ochoa Arriaga, A.; Martínez Carretero, E.; Navas Romero, A.; Ontivero, M.; Filippini, M. F.; Rojas Velázquez, A. N.; Guillén Castillo, O. I.; Lara Izaguirre, A. Y.; Duplancic, A.; Villegas Rodríguez, F. 2024. Evaluación de emisiones de CO_2 y partículas finas en la incineración de biomasa de calabacita (*Cucurbita pepo* L.-Cucurbitaceae). Multequina 33: 105-120. http://id.caicyt.gov.ar/ark:/s18527329/wviayjl94
8. Ali, F., Dawood, A.; Hussain, A.; Alnasir, M. H.; Khan, M. A.; Butt, T. M.; Janjua, N. K.; Hamid, A. 2024. Fueling the future: biomass applications for green and sustainable energy. Discover Sustainability. https://doi.org/10.1007/s43621-024-00309-z
9. Almsatar, T. 2020. Environmental Issues of Biomass-Burning in Sub-Saharan African Countries. In: Mammino, L. (eds). Biomass Burning in Sub-Saharan Africa. Springer. https:// doi. org/10.1007/978-94-007-0808-2_1
10. Amodio, M.; Andriani, E.; Dambruoso, P.; Daresta, B.; de Gennaro, G.; Gilio, A.; 2012. Impact of biomass burning on PM10 concentrations. Fresenius Environ. Bull. 21: 3296-3300.
11. Anand, P.; Mina, U.; Khare, M.; Kumar, P.; Kota, S. H. 2022. Air pollution and plant health response-current status and future directions. Atmospheric Pollution Research. 13(6): 101508. DOI: 10.1016/j.apr.2022.101508
12. Arteaga, J.; Arenas, E.; López, D.; Sanchéz, C.; Zapata, Z. 2012. De la pirólisis rápida de residuos de palma africana (*Elaeis guineensis* Jacq). Biotecnología en el Sector Agropecuario y Agroindustrial. 10(2): 144-151. http://www.scielo.org.co/pdf/bsaa/v10n2/ v10n2a17.pdf
13. Arteaga-Pérez, L. E.; Segura, C.; Santana, K. D. 2016. Procesos de torrefacción para valorización de residuos lignocelulósicos. Análisis de posibles tecnologías de aplicación en Sudamérica. Afinidad. 73(573).
14. Baray, M. del R. 2016. Pirólisis a abaja temperatura en materiales avanzados de la pomasa de manzana para la producción de biocombustibles. Centro de Investigación en Materiales Avanzados. https://cimav.repositorioinstitucional.mx/jspui/handle/1004/363
15. Basu, P.; Sadhukhan, A. K.; Gupta, P.; Rao, S.; Dhungana, A.; Acharya, B. 2014. An experimental and theoretical investigation on torrefaction of a large wet wood particle. Bioresource technology. 159: 215-222.
16. Bergman, P. C. 2005. Combined torrefaction and pelletisation. The TOP process. ECN-C-05-073.
17. Buis, A. 2019. The Atmosphere: Getting a Handle on Carbon Dioxide-Climate Change: Vital Signs of the Planet. Retrieved December 6, 2020. https:// climate.nasa.gov/news/2915/ the-atmospheregetting-a-handle-on-carbon-dioxide/
18. Bustamante García, V.; Carrillo Parra, A.; Prieto Ruíz, J. A.; Corral-Rivas, J. J.; Hernández Díaz, J. C. 2016. Química de la biomasa vegetal y su efecto en el rendimiento durante la torrefacción: Revisión. Revista mexicana de Ciencias Forestales. 7(38): 5-23. http://www.scielo.org.mx/ scielo.php?script=sci_arttext&pid=S2007-11322016000600005&lng=es&tlng=es.
19. Chang, D.; Li, Q.; Wang, Z.; Dai, J.; Fu, X.; Guo, J.; Zhu, L.; Pu, D.; Cuevas, C. A.; Fernandez, R. P.; Wang, W.; Ge, M.; Fung, J. C. H.; Lau, A. K. H.; Granier, C.; Brasseur, G.; Pozzer, A.; Saiz-Lopez, A.; Song, Y.; Wang, T. 2024. Significant chlorine emissions from biomass burning affect the long-term atmospheric chemistry in Asia. National Science Review. 11(9): nwae285. https://doi. org/10.1093/nsr/nwae28520
20. Chekchaki, S.; Zaafour, M. D.; Chekchaki, N. 2025. *Acacia farnesiana* (L.) Willd: Ecology, uses and phytochemical composition. African Journal of Biological Sciences. 7(4): 547-566. https://doi.org/10.48047/AFJBS.7.4.2025.547-566
21. Chen, J.; Li, C.; Ristovski, Z.; Milic, A.; Gu, Y.; Islam, M. S.; Wang, S.; Hao, J.; Zhang, H.; He, C.; Guo, H.; Fu, H.; Miljevic, B.; Morawska, L.; Thai, P.; LAM, Y. F.; Pereira, G.; Ding, A.; Huang, X.; Dumka, U. C. 2017. A review of biomass burning: Emissions and impacts on air quality, health and climate in China. Science of the Total Environment. 579: 1000-1034. https://doi. org/10.1016/j.scitotenv.2016.11.025
22. Chuetor, S.; Panakkal, E. J.; Ruensodsai, T.; Cheenkachorn, K.; Kirdponpattara, S.; Cheng, Y. S.; Sriariyanun, M. 2022. Improvement of Enzymatic Saccharification and Ethanol Production from Rice Straw Using Recycled Ionic Liquid: The Effect of Anti-Solvent Mixture. Bioengineering. 9(3): 115. https://doi.org/10.3390/bioengineering9030115
23. Cruz Montelongo, C.; Herrera Gamboa, J.; Ortiz Sánchez, I.; Ríos Saucedo, J. C.; Rosales Serna, R.; Carrillo-Parra, A. 2020. Caracterización energética del carbón vegetal producido en el Norte-Centro de México. Madera y bosques. 26(2): e2621971. https://doi.org/10.21829/myb.2020.2621971
24. Demirbas, A. 2004. Combustion characteristics of different biomass fuels. Progress in energyand combustion science. 30(2): 219-230.
25. Diario Oficial de la Federación. 2021. NORMA Oficial Mexicana NOM-021-SSA1-2021. Salud ambiental. Valores límite permisibles para la concentración de partículas suspendidas PM_{10} y $PM_{2.5}$ en el aire, ambiente y criterios para su evaluación. https://rama.edomex. gob.mx/sites/rama.edomex.gob.mx/files/files/NOM-025-SSA1-2021.pdf%20
26. Dula, M.; Kraszkiewicz, A. 2025. Theory and Practice of Burning Solid Biofuels in Low-Power Heating Devices. Energies. 18(1): 182. https://doi.org/10.3390/en18010182
27. Ezzati, M.; Kammen, D. M. 2002. The health impacts of exposure to indoor air pollution from solid fuels in developing countries: Comprehension, gaps, and data needs. Environ Health Perspect. 110(11): 1057-68. https://doi.org/10.1289/ehp.021101057

28. Fan, H.; Zhao, C.; Yang, Y.; Yang, X. 2021. Spatio-Temporal Variations of the $PM_{2.5}/PM_{10}$ Ratios and Its Application to Air Pollution Type Classification in China. Front. Environ. Sci. 9: 692440. DOI: 10.3389/fenvs.2021.692440
29. García-Azpeitia, L.; Montalvo-González, E.; Loza-Cornejo, S. 2022. Caracterización nutricional y fitoquímica de hojas, flor y fruto de *Prosopis laevigata*. Botanical Sciences. 100(4): 1014-1024.
30. Grillo, G.; Tabasso, S.; Cravotto, G.; van Ree, T. 2020. Burning Biomass: Environmental Impact on the Soil. In: Mammino, L. (eds) Biomass Burning in Sub-Saharan Africa. Springer. https://doi.org/10.1007/978-94-007-0808-2_2
31. Health Efects Institute. 2024. State of Global Air 2024. Special Report.
32. Hua, C.; Ma, W.; Zheng, F.; Zhang, Y.; Xie, J.; Ma, L.; Song, B.; Yan, C.; Li, H.; Liu, Z.; Liu, Q.; Kulmala, M.; Liu, Y. 2024. Health risks and sources of trace elements and black carbon in $PM_{2.5}$ from 2019 to 2021 in Beijing. Journal of Environmental Sciences. 142: 69-82. https://doi.org/10.1016/j.jes.2023.05.023
33. IFC. International Finance Corporation. 2017. Converting Biomass to Energy: A Guide for Developers and Investors.
34. IQAir. Air Visual. 2018. 2018 World Air Quality Report. Region & City $PM_{2.5}$ Ranking. Region & City $PM_{2.5}$ Ranking. https://www.iqair.com/ dl/2018_world-air-quality-report-2018-en.pdf
35. IQAir. Air Visual. 2023. 2023 World Air Quality. Region and City $PM_{2.5}$ Ranking. https://www.iqair.com/ dl/2023_World_Air_Quality_Report.pdf%20
36. Moscoso-Vanegas, D.; Monroy-Morocho, L.; Narváez-Vera, M.; Espinoza-Molina, C.; Astudillo-Alemán, A. 2019. Efecto fitotóxico del metraila particulado PM_{10} recolectado en el área urbana de la Ciudad de Cuenca, Ecuador. Iteckne. 16(1): 12-20. https://doi.org/10.15332/iteckne.v16i1.2157
37. Muhd, P. S. D.; Cuelho, C. H. F.; Brondani, J. C.; Manfron, M. P. 2015. Chemical composition of the *Schinus molle* L. essential oil and their biological activities. Revista Cubana de Farmacia. 49(1): 132-143.
38. Naciones Unidas. 2018. La Agenda 2030 y los Objetivos de Desarrollo Sostenible: una oportunidad para América Latina y el Caribe. LC/G.2681-P/Rev.3.
39. Nhuchhen, D. R.; Basu, P.; Acharya, B. 2014. A comprehensive review on biomass torrefaction. Int. J. Renew. Energy Biofuels. 1-56.
40. Organización Mundial de la Salud. 2021. Directrices mundiales de la OMS sobre la calidad del aire: materia particulada ($MP_{2.5}$ y MP_{10}), ozono, dióxido de nitrógeno, dióxido de azufre y monóxido de carbono: resumen ejecutivo. Organización Mundial de la Salud. https://iris.who.int/handle/10665/346062.
41. Pinakana, S. D.; Raysoni, A. U.; Sayeed, A.; Gonzalez, J. L.; Temby, O.; Wladyka, D.; Sepielak, K.; Gupta, P. 2024. Review of Agricultural Biomass Burning and its Impact on Air Quality in the Continental United States of America. Environmental Advances. Vol.: 16. https://doi.org/10.1016/j.envadv.2024.100546
42. Pintor-Ibarra, L. F.; Alvarado-Flores, J. J.; Rutiaga-Quiñones, J. G.; Alcaraz-Vera, J. V.; Ávalos-Rodríguez, M. L.; Moreno-Anguiano, O. 2024. Chemical and Energetic Characterization of the Wood of *Prosopis laevigata*: Chemical and Thermogravimetric Methods. Molecules. 29(11): 2587. https://doi.org/10.3390/molecules29112587
43. Reinhardt, T. E.; Ottmar, R. D.; Castilla, C. 2001. Smoke impacts from agricultural burning in a rural Brazilian town. Journal of the Air & Waste Management Association (1995). 51(3): 443-450. https://doi.org/10.1080/10473289.2001.10464280
44. Sadaka, S.; Johnson, D. M. 2011. Biomass Combustion. Cooperative Extension Service. University of Arkansas. US Department of Agriculture and county governments cooperating. FSA1056.
45. Saleem M. 2022. Possibility of utilizing agriculture biomass as a renewable and sustainable future energy source. Heliyon. 8(2): e08905. https://doi.org/10.1016/j.heliyon.2022.e08905
46. Sangaré, D.; Belandria, V.; Bostyn, S.; Moscosa-Santillan, M.; Gökalp, I. 2024. Pyro-gasification of lignocellulosic biomass: online quantification of gas evolution with temperature, effects of heating rate, and stoichiometric ratio. Biomass Conversion and Biorefinery. 14(8): 9763-9775.
47. Secretaría de Medio Ambiente y Recursos Naturales. 2016. Estrategia Nacional de Calidad del Aire. ENCA. https://www.gob.mx/cms/uploads/attachment/file/195809/Estrategia_Nacional_Calidad_del_Aire.pdf%20
48. Sivertsen, B. 2006. Air pollution impacts from open air burning. WIT Transactions on Ecology and the Environment. 92.
49. Subils, M. J. B.; Domínguez, F. B. 2000. NTP 549: El dióxido de carbono en la evaluación de la calidad del aire interior. España: Centro Nacional de Condiciones de Trabajo. 124p.
50. Suriyawong, P.; Chuetor, S.; Samae, H.; Piriyakarnsakul, S.; Amin, M.; Furuuchi, M.; Hata, M.; Inerb, M.; Phairuang, W. 2023. Airborne particulate matter from biomass burning in Thailand: Recent issues, challenges, and options. Heliyon. 9(3): e14261. https://doi.org/10.1016/j.heliyon.2023.e14261

51. Torres-Duque, C.; Maldonado, D.; Pérez-Padilla, R.; Ezzati, M.; Viegi, G. 2008. Forum of International Respiratory Studies (FIRS) Task Force on Health Effects of Biomass Exposure. Biomass fuels and respiratory diseases: A review of the evidence. Proceedings of the American Thoracic Society. 5(5): 577-590. https://doi.org/10.1513/pats.200707-100RP
52. Tripathi, S.; Yadav, S.; Sharma, K. 2024. Air pollution from biomass burning in India. Environ Res Lett. 19:073007. https://doi.org/10.1088/1748-9326/ad4a90
53. Valencia, G. M.; Anaya, J. A.; Caro-Lopera, F. J. 2022. Bottom-up estimates of atmospheric emissions of CO_2, NO_2, CO, NH_3, and Black Carbon, generated by biomass burning in the north of South America. Revista de Teledetección. 59: 23-47. https://doi.org/10.4995/raet.2021.15594
54. Wardoyo, A. Y.; Morawska, L.; Ristovski, Z. D.; Marsh, J. 2006. Quantifcation of particle number and mass emission factors from combustion of Queensland trees. Environ. Sci. Technol. 40(18): 5696-5703.
55. WHO. 2023. Who Ambient Air Quality Database, 2022 update: status report. https://www.who.int/publications/i/item/9789240047693
56. WHO. 2024. Ambient (outdoor) air pollution. https://www.who.int/ news-room/fact-sheets/detail/ambient-(outdoor)-air-quality-and-health%20//%20
57. Wu, Y.; Han, Y.; Voulgarakis, A.; Wang, T.; Li, M.; Wang, Y.; Xie, M.; Zhuang, B.; Li, S. 2017. An agricultural biomass burning episode in eastern China: Transport, optical properties, and impacts on regional air quality, J. Geophys. Res. Atmos. 122: 2304-2324. DOI: 10.1002/2016JD025319
58. Zauli-Sajani, S.; Thunis, P.; Pisoni, E.; Bessagnet, B.; Monforti-Ferrario, F.; De Meij, A.; Pekar, F.; Vignati, E. 2024. Reducing biomass burning is key to decrease $PM_{2.5}$ exposure in European cities. Scientific reports. 14(1): 10210. https://doi.org/10.1038/s41598-024-60946-2

Strategic Pathways for the Olive Oil Chain in Argentina: Profitability, Sustainability and Oleo tourism

Rutas estratégicas para la cadena de aceite de oliva en Argentina: rentabilidad, sostenibilidad y oleoturismo

Patricia Lilian Winter *, Alejandro Juan Gennari, Vanina Fabiana Ciardullo, Leonardo Javier Santoni

Originales: *Recepción:* 28/07/2025 - *Aceptación:* 08/10/2025

Abstract

The olive oil agri-food chain in Argentina is strategically relevant for rural development, employment, exports and tourism. Despite quality production and industrial capacity, the sector faces structural problems: high labour and energy costs, limited domestic consumption, and dependence on subsidized international competitors. This study analyses the chain using multicriteria programming across five dimensions: productive, economic-financial, commercial, environmental and tourism-territorial. The baseline was built from data collected between 2018 and 2024 (Agricultural Census 2018, official reports and international benchmarks), covering the country's most representative producing regions (Catamarca, La Rioja, San Juan and Mendoza), which together account for over 90% of national output. Results from scenario simulations reveal trade-offs: export-oriented strategies maximize profit but increase vulnerability to global prices; internal consumption growth strengthens resilience yet moderates revenues; environmental sustainability improves efficiency through lower water use; and balanced development with olive oil tourism achieves robust outcomes across all dimensions. A novel contribution is the quantitative inclusion of tourism, showing its potential to generate rural employment and enhance brand value. The findings support forward-looking strategies that combine technological reconversion, market diversification, efficient resource use and tourism integration, offering policy guidelines for sustainable territorial development.

Keywords

olive oil supply chain • costs • competitiveness • sustainability • bioeconomy • tourism • Argentina

Universidad Nacional de Cuyo. Facultad de Ciencias Agrarias. Cátedra de Economía y Política Agraria. Almirante Brown 500. M5528AHB. Chacras de Coria. Mendoza. Argentina. * pwinter@fca.uncu.edu.ar

Resumen

La cadena agroalimentaria del aceite de oliva en Argentina es estratégica para el desarrollo rural, el empleo, las exportaciones y el turismo. A pesar de su calidad productiva y capacidad industrial, el sector enfrenta problemas estructurales: altos costos laborales y energéticos, bajo consumo interno y dependencia de competidores internacionales subsidiados. Este estudio analiza la cadena mediante programación multicriterio en cinco dimensiones: productiva, económico-financiera, comercial, ambiental y turística-territorial. El escenario base se construyó con datos relevados entre 2018 y 2024 (Censo Agropecuario 2018, informes oficiales y referencias internacionales), abarcando las provincias más representativas (Catamarca, La Rioja, San Juan y Mendoza), que concentran más del 90% de la producción nacional. Los resultados de las simulaciones por escenarios evidencian compensaciones: las estrategias orientadas a la exportación maximizan beneficios pero aumentan la vulnerabilidad a precios globales; el desarrollo del consumo interno fortalece la resiliencia aunque reduce ingresos; la sostenibilidad ambiental mejora la eficiencia al reducir uso de agua; y un desarrollo equilibrado con oleoturismo logra resultados robustos en todas las dimensiones. El aporte novedoso es la incorporación cuantitativa del turismo, que muestra su potencial para generar empleo rural y valor de marca. Los hallazgos sustentan estrategias prospectivas que combinan reconversión tecnológica, diversificación de mercados, uso eficiente de recursos e integración turística, ofreciendo lineamientos para políticas públicas y desarrollo sustentable.

Palabras clave

cadena de valor del aceite de oliva • costos • competitividad • sustentabilidad • bioeconomía • turismo • Argentina

Introduction

Argentina's olive oil sector holds strategic relevance not only for its product but also for its role in rural development, employment, and the diversification of semi-arid territories. Extra virgin olive oil (EVOO) from Argentina has achieved international recognition for quality (Benencia *et al.*, 2014), supported by industrial capacity and technological advancement. However, the sector faces persistent structural problems: high labour and energy costs compared to competitors (Ministerio de Economía, 2024), strong dependence on subsidized producers such as Spain and Italy, and limited domestic demand (CREA, 2021). These factors have hindered competitiveness and limited the capacity to capture value at national level. Argentina ranks 10th worldwide in olive oil production, with annual outputs fluctuating between 28,000 and 36,000 tons in peak years (IOC, n. d.; Ministerio de Economía, 2024). The sector employs around 30,000 temporary rural workers, equivalent to nearly three million daily wages per year (CREA, 2021), representing 8.1% of the national agricultural labour requirement. Despite this production capacity, domestic consumption remains extremely low (180-250 cc per capita annually), far below Mediterranean standards (Spain: ~15 litters per capita). This imbalance highlights a major challenge: while Argentina has structural potential, it captures limited value internally, depending heavily on exports and leaving domestic demand underdeveloped. These structural conditions justify the need for a comprehensive approach that analyses the chain not only in economic terms but also through its productive, commercial, environmental and territorial dimensions. Beyond its productive dimension, the olive oil chain must be understood as a networked agri-food system, where interdependencies extend to logistics, marketing, tourism and environmental management (García-Cascales *et al.*, 2021). This broader view enables policies to shift from a narrow "sectoral plan" to a flexible "roadmap" capable of adapting to disruptive changes in technology, trade and regulations (Romero, 1993). Moreover, the concept of bioeconomy reinforces this approach: olive cultivation generates biomass, by-products and ecosystem services whose valorisation expands the economic and territorial impacts (Stark *et al.*, 2021). The present study therefore adopts an integrated five-dimension perspective: (i) productive efficiency, (ii) economic-financial

profitability, (iii) logistics and commercialization, (iv) environmental sustainability, and (v) tourism and territorial valorisation. This framework moves beyond isolated analysis of costs or yields, proposing instead a systemic evaluation of Argentina's olive oil chain as both a production network and a driver of local development. The research is guided by the following objectives:

(a) analyse the chain's structure and bottlenecks.
(b) simulate scenarios of value creation through multicriteria programming; and
(c) evaluate trade-offs between profitability, sustainability, domestic demand and oleo tourism.

The central hypothesis is that multicriteria programming can identify optimal strategic pathways for the olive oil chain in western Argentina, showing that a balanced approach integrating technological reconversion, sustainability and tourism improve resilience and competitiveness compared to purely export-oriented strategies. The analysis focuses on Argentina's main producing provinces (Catamarca, La Rioja, San Juan and Mendoza), which together account for over 90% of national olive oil output. While the baseline data correspond to 2018-2024, the scenarios are prospective, designed to explore strategic pathways for the future of the sector.

Materials and Methods

Methodological Approach: Multicriteria Linear Programming (MCP)

The methodological framework chosen was Multicriteria Linear Programming (MCP), as it enables the simultaneous evaluation of multiple, and often conflicting, objectives relevant to the olive oil value chain. This approach goes beyond single-objective optimization by capturing trade-offs between profitability, production, market allocation, environmental impacts and tourism valorisation. The focus of this study is not on statistical sampling, but on the integration of aggregated data from national censuses, official sectoral reports and international benchmarks. In this sense, concepts such as "sample" or "survey" are not applicable, since the analysis is systemic and chain oriented. The model is structured across five dimensions -productive, economic-financial, commercial, environmental, and tourism-territorial- which together reflect the sustainability and strategic development goals of the sector. Within this framework, MCP was applied to determine the optimal allocation of land, production, investments and market shares under real-world constraints. The method allows the generation of Pareto-efficient solutions, making visible the compromises between objectives and enabling the design of alternative strategic scenarios. This orientation provides a rigorous yet flexible analytical tool, adaptable not only to olive oil but also to other perennial crop systems embedded in similar ecological and territorial contexts (García-Cascales *et al,* 2021; Romero, 1993).

Justification of Multicriteria Programming (MCP *vs.* MCDM)

The choice of Multicriteria Linear Programming (MCP) is justified by the complexity of the olive oil value chain, where multiple and often conflicting objectives must be considered simultaneously. Traditional single-objective models fail to capture trade-offs between profitability, domestic consumption, exports, environmental impact and tourism valorisation. MCP provides a quantitative framework that integrates these dimensions and generates optimal solutions under real-world constraints. It is important to distinguish MCP from Multicriteria Decision Making (MCDM) approaches: while MCDM is designed to select among a finite set of alternatives (qualitative decision-making), MCP allows continuous optimization of resource allocation across multiple objectives. This distinction is relevant because the study does not evaluate pre-defined options but rather allocates hectares, production volumes and investments dynamically, reflecting real strategic planning needs.

The capacity of MCP to explore Pareto-efficient solutions and identify trade-offs among objectives strengthens its applicability to agri-food systems embedded in uncertain international markets and resource constraints (García-Cascales *et al,* 2021; Romero, 1993).

Data Collection and Update

Data consolidation was carried out by integrating official and sectoral sources rather than through statistical sampling. The structural base was provided by the 2018 National Agricultural Census (INDEC, 2019), complemented with annual sectoral reports from the Ministerio de Economía (2024), CREA (2021), and international benchmarks (IOC, 2015). Production volumes, costs and yields were compiled from these sources, covering the four main olive-producing provinces (Catamarca, La Rioja, San Juan, Mendoza). Given Argentina's inflationary context, all values were expressed in constant U.S. dollars, updated through official price indices. This procedure ensured comparability with international cost studies and positioned Argentina in a medium-to-high cost range relative to major competitors such as Spain and Portugal. As a result, the estimated average cost of a 500 ml bottle of olive oil was US$3.26, distributed as 50% primary production, 19% industrial processing and 31% packaging and fractionation. This calculation does not stem from a statistical survey but from sector-wide structural data, reflecting the systemic focus of chain analysis. Therefore, terms like "sample" or "survey" are not applicable: the analysis is based on censual and aggregated information integrated into the programming model income. From a bioeconomy perspective, olive cultivation also generates by-products such as pomace, pits, leaves, and pruning residues. These can be valorised through energy (biofuels, pellets), compost and soil amendments, animal feed, as well as tourism and ecosystem services. Although not explicitly included as decision variables in the model, these alternatives were acknowledged as part of the conceptual framework.

Continuous Decision Variables

The following decision variables capture the strategic choices available to the olive oil chain. They are associated mainly with the productive, commercial and tourism dimensions, representing cultivated hectares, production volumes, market allocation, and visitor flows. These variables are optimized by the model to explore alternative scenarios and resource allocation strategies.

- H_{trad}: Hectares in production of traditional olive groves (ha).
- H_{int}: Hectares in production of intensive olive groves (ha).
- Q_{trad}: Olive oil production obtained from traditional systems (ton).
- Q_{int}: Olive oil production obtained from intensive systems (ton).
- E: Volume of olive oil destined for export (ton).
- D: Volume of olive oil destined for the domestic market (ton).
- M: Investment in marketing and promotion for the domestic market (millions of USD).
- T_i: Number of tourists visiting province i (persons), quantifying olive oil tourism activity in each region.
- I_i: Investment in tourism infrastructure and promotion in province i (millions of USD), reflecting strategic capital allocation for tourism development.
- (H_{org}): Hectares under organic certification (optional, if a specific organic production objective is modelled).

Parameters (Fixed by Scenario or Context):

The parameters correspond to fixed or contextual values that condition the system. They include aspects of the productive dimension (yields, water and energy use), the economic-financial dimension (costs, prices, taxes), the environmental dimension (emission coefficients, water limits), and the tourism-territorial dimension (capacity, income per visitor). By defining these constants, the model ensures comparability across scenarios and consistency with official and international data sources.

r_{trad}, r_{int}: Oil yield per hectare (ton/ha) for traditional and intensive systems, respectively (e.g., $r_{trad}=0.5, r_{int}=1.5$ ton/ha).

$\alpha_{trad}, \alpha_{int}$: Water requirement per hectare (m^3/ha) for traditional and intensive systems (e.g., $\alpha_{trad}=3000$, $\alpha_{int}=5000$).

$\beta_{trad}, \beta_{int}$: Energy consumption per hectare (kWh/ha) for traditional and intensive systems (e.g., $\beta_{trad}=50, \beta_{int}=200$).

P_{exp}, P_{dom}: Price per ton of oil in the export and domestic market (e.g., $P_{exp}=4000, P_{dom}=3500$ USD/ton).

t_{exp}: E_{xport} tax rate (decimal, e.g., $t_{exp}=0.05$).

c_{trad}, c_{int}: Total cost per ton of oil produced in each system (e.g., $c_{trad}=3800, c_{int}=2300$ USD/ton).

C_{mkt}: Marketing cost per ton for the domestic market (e.g., $C_{mkt}=500$ USD/ton).

W_{max}: Total water availability for irrigation (m^3) (e.g., $W_{max}=300\times106$ m^3).

H_{max}: Maximum usable area for cultivation (ha) (e.g., $H_{max}=90{,}000$ ha).

p_i: Average income per tourist in province i (USD/tourist).

e_i^T: Associated jobs per tourist in province i (jobs/tourist).

e_i^A: Associated jobs per ton of oil produced in province i (jobs/ton).

c_i^T: CO_2 emission coefficient per tourist in province i (kg CO_2/tourist).

c_i^A: CO_2 emission coefficient per ton of oil in province i (kg CO_2/ton).

$capacitat_e$: Installed tourist capacity limit in province i (persons/day).

σ: Tourist seasonality coefficient (decimal).

C_{max}: Maximum allowed CO_2 emissions limit (kg CO_2).

personal disponible: Total available rural labour (jobs).

Objective Functions of the Integrated Model

The model incorporates multiple objective functions, each reflecting a strategic goal of the olive oil chain. Together, they cover the five sustainability dimensions:

- Economic-financial: profitability maximization.
- Productive: total oil production.
- Commercial: exports and domestic demand.

• Environmental: efficient use of resources and reduced footprint.

• Tourism-territorial: revenues, employment and territorial valorisation.

This configuration allows the model to simulate different policy or market priorities and to quantify their trade-offs.

Economic (Z_{econ}): Maximization of Net Profit

This function maximizes the net margin, considering sales revenues (export and domestic) and total costs (agricultural, industrial, commercial, taxes, marketing).

$$Z_{econ}=(1-t_{exp})P_{exp}E+P_{dom}D-c_{trad}Q_{trad}-c_{int}Q_{int}-C_{mkt}D$$

Technical (Z_{tec}): Maximization of Total Oil Production

This objective reflects the pursuit of productive efficiency and optimal input use, boosting agricultural and industrial yields.

$$Z_{tec}=Q_{trad}+Q_{int}$$

Commercial-External ($Z_{com-ext}$): Maximization of Exported Volume

This objective incentivizes allocating the largest possible production to external markets, capitalizing on the quality advantage of Argentine oil and consolidating international presence.

$$Z_{com-ext}=E$$

Commercial-Internal ($Z_{com-int}$)

Maximization of Volume Destined for the Domestic Market

This objective seeks to increase internal olive oil consumption in Argentina, contributing to food security and cultural product development.

$$Z_{com-int}=D$$

Environmental (Z_{amb})

Minimization of Environmental Impact (Water and Carbon Footprint)

This objective focuses on reducing the value chain's environmental impact, promoting long-term sustainability. It is formulated as the minimization of water and energy use, and total CO_2 emissions from both oil production and tourist activities.

$$Z_{amb}=-(\alpha_{trad}H_{trad}+\alpha_{int}H_{int})-\gamma(\beta_{trad}H_{trad}+\beta_{int}H_{int})-\sum i(c_{iT}Ti+c_{iA}A_i)$$

where

γ = a weighting factor for energy.

Productive (Z_{sup})

Maximization of Olive Grove Area in Production

This objective seeks to expand the olive agricultural frontier and rehabilitate underutilized plantations, increasing sectoral productive potential.

$$Z_{sup}=H_{trad}+H_{int}$$

Tourism-Revenue ($Z_{tur-ing}$)

Maximization of Olive Oil Tourism Revenue

This function maximizes income generated by visits to oil mills, tastings, tourist product sales, and accommodation services.

$$Z_{tur-ing}=\sum_i p_i T_i$$

Tourism-Employment ($Z_{tur\text{-}emp}$)
Maximization of Rural Employment Associated with Tourism
This objective focuses on maximizing job creation in rural areas, including guides, accommodation, and catering staff, contributing to curbing depopulation.

$$Z_{tur-emp}=\sum_i(e_{iT}T_i+e_{iA}A_i)$$

Tourism-Territorial Valorisation ($Z_{tur\text{-}val}$)
Maximization of Territorial Valorization
This objective, partly qualitative, seeks to intensify the social and economic recognition of the olive growing landscape as a heritage resource. It can be modelled as a tourist satisfaction index, a brand score, or a weighted sum of income per tourist and quality certifications (DOP/IG), reflecting public appreciation for authenticity, quality, and local culture.

Restrictions of the Integrated Model
The restrictions define the operational, resource and environmental boundaries within which the system must operate. They ensure feasibility of the solutions by linking production with demand, limiting land and water use, respecting labor and capacity constraints, and capping environmental impacts. In this way, restrictions reflect the real conditions faced by the olive oil chain and guarantee that the scenarios generated are both consistent and applicable:

Production-Market Balance
All oil production must be assigned to a market (internal or external), assuming no significant stock variations.

$$Q_{trad}+Q_{int}=D+E$$

Production Limits per System
The oil production of each system cannot exceed its potential yield per hectare.
$Q_{trad}\leq r_{tradHtrad}$
$Q_{int}\leq r_{int}H_{int}$

Water Availability
Total water consumption for irrigation cannot exceed the maximum available annual allocation.

$$\alpha_{trad}H_{trad}+\alpha_{int}H_{int}\leq W_{max}$$

Land Availability
The total cultivated area cannot exceed the maximum usable area.

$$H_{trad}+H_{int}\leq H_{max}$$

Maximum Internal Demand
The demand of the internal market can be limited by its maximum consumption potential.

$$D\leq D_{max}$$

Installed Tourist Capacity
The number of tourists in each province cannot exceed the physical capacity of local tourist infrastructures.

$T_i\leq Capacity$ (*e.g.*, Mendoza's olive oil tourism providers can serve about 2,533 people per day).

Tourist Seasonality
The annual tourist offer may be limited by seasonal factors, reflected by a coefficient.

$$T_i\leq Capacity\times Operative\ days$$

CO_2 Emissions Limit

Total emissions generated by production and tourism must not exceed a maximum threshold, reflecting a commitment to environmental sustainability.

$$\sum_i (c_{iT} T_i + c_{iA} A_i) \leq C_{max}$$

Labour Balance

The total rural labour required for agricultural and tourist activities cannot exceed the availability of personnel.

$\sum_i (w_{iT} T_i + w_{iA} A_i) \leq$ *personal disponible* (where w_{iT} and w_{iA} are labour coefficients per tourist and per ton of oil, respectively).

Budgetary Restrictions for Tourist Investment

Investment in tourism in each province may be limited by available financing.

$I_i \leq$ Tourism Investment Budget

Non-Negativity

All decision variables must be greater than or equal to zero.

$$H_{trad}, H_{int}, Q_{trad}, Q_{int}, D, E, M, T_i, I_i \geq 0$$

Transformation to Goal or Weighted Model

To solve this multi-objective programming problem, the approach of weighted goal programming or the weighted sum of objective functions can be adopted. Goal programming allows for the establishment of a desired level for each objective, subsequently minimizing deviations from these targets using deviation variables (d_i-,d_i+) to represent non-compliance or excess.

Alternatively, and often more intuitively for scenario exploration, a single scalar function can be defined as the weighted sum of all individual objective functions:

$$\max Z_{total} = \omega econ Z_{econ} + \omega tec Z_{tec} + \omega_{com}\text{-}extE + \omega com\text{-}intD + \omega amb Zamb + \omega supH + \omega_{tur}\text{-}ingZ_{tur}\text{-}ing + \omega_{tur}\text{-}e_{mp}Z_{tur}\text{-}e_{mp} + \omega tur\text{-}valZtur\text{-}val$$

Here, ωk represents the weights assigned to each objective, reflecting its strategic priority in a given scenario. It is crucial to normalize or scale the objective functions prior to assigning weights, as their units and magnitudes vary significantly (e.g., Z_{econ} in millions of USD, Z_{tec} in thousands of tons, Z_{amb} in millions of m^3 or kg CO_2). This normalization ensures that the weights accurately reflect the relative importance of each objective. By adjusting these weights, this method enables the emulation of various strategic scenarios and the identification of efficient Pareto solutions, which represent the best possible compromises among conflicting objectives.

Results

Descriptive Overview of the Argentine Olive Oil Sector

As described in the Introduction, Argentina is a mid-scale producer with low domestic consumption. Building on this context, the following overview summarizes sectoral features relevant for scenario modelling. The low domestic consumption, despite Argentina being a producing nation, suggests either a market failure or a lack of strategic focus on developing internal demand. This presents one of the most significant opportunities for the Argentine olive oil business strategy: internal consumption could potentially increase by 500% to reach one litter per capita per year, though even this would remain minimal compared to European averages. Globally, olive oil consumption has seen an average annual growth of approximately 3.5% over the last five years, indicating a favourable international trend.

In 2021, the sector's total turnover, encompassing both internal consumption and exports, reached US$223 million, with olive oil accounting for 57% and table olives for 43%. The predominant primary production system in Argentina is traditional, although newer plantations have adopted more efficient crown systems (MAGyP, 2023). The country boasts excellent olive varieties and the potential for qualifying specific geographical indications. The industrial oil sector comprises approximately 120 processing establishments, which vary in size, personnel, and performance.

For the domestic market, which accounts for about 20% of total production, sales volume is distributed across major regions: AMBA (Área Metropolitana de Buenos Aires) (CABA Ciudad Autónoma de Buenos Aires and 40 municipalities of Provincia de Buenos Aires) (50-58%), Interior de Buenos Aires) (15%), Litoral and NEA (NEA: Northeast Area) (10-11%), Cuyo and NOA (Nordeste Argentino) (9-10%), Córdoba (6-7%), and the Patagonia (Patagonia: South Area) Area (3-4%). The 500cc container is the best-selling format, comprising 89% of the market, significantly outpacing the 1-liter container (7.4%). PET containers are the most widely used (35-45%), followed by cans (30-35%), while glass accounts for 12-17% of sales. Approximately four brands (SolFrut/Oliovita, Nucete, AGD/Zuelo, Laur/Fam. Millán) dominate the market as the dominant finge and the rest integrate the competitive fringe in the mixed oligopoly structure.

Quantitative Performance by Scenario

The multicriteria model quantifies the Argentine olive oil value chain's performance under various strategic priorities. Table 1 summarizes key outcomes: estimated annual net profit, total olive oil production, exports, internal consumption, annual irrigation water usage, and total cultivated area. For the balanced development and value added with olive oil tourism scenario, values are hypothetical, showing the potential of this integrated approach.

Table 1. Quantitative performance by scenario.
Tabla 1. Rendimiento cuantitativo por escenario.

Scenario	Net Profit (USD million/year)	EVOO Production (ton/year)	Exports (ton/year)
Base (Conservative)	~10 (low)	~35,000	24
Export-Oriented	140 (very high)	95	85
Internal Consumption	~50 (moderate)	~50,000	~35,000
Environmental Sustainability	~100 (high)	~80,000	~70,000
Balanced Development and Value Added with Olive Oil Tourism	~110 (high)	~70,000	~50,000
Scenario	**Internal Consumption (ton/year)**	**Water Used (Mm^3/year)**	**Area in Production (ha)**
Base (Conservative)	~8,000	210	~70,000
Export-Oriented	~10,000	300 (100% avail.)	~90.000
Internal Consumption	15	~250	~80,000
Environmental Sustainability	~10,000	250 (83% avail.)	~75,000
Balanced Development and Value Added with Olive Oil Tourism	~12,000	~270	~85,000

A novel contribution of this study is the quantitative inclusion of olive oil tourism as a modelled variable. This expands traditional economic-environmental analyses by incorporating territorial valorisation and rural employment, aspects rarely integrated in optimization models of agri-food chains. The Base (Conservative) scenario shows low profit (~US$10 million) from narrow margins and low production (~35,000 tons). Most production (24,000 tons) is exported, with minimal domestic consumption (8,000 tons). Despite not maxing out water use, it's inefficient, with high water consumption per ton and underutilized capacity.

The Export-Oriented scenario achieves the highest profit (US$140 million) by nearly tripling production (95,000 tons) and massively increasing exports (85,000 tons). This model uses maximum land (90,000 ha) and all available water (300 Mm^3). While water efficiency improves, domestic consumption barely rises, showing a strong external market focus.

The Internal Consumption scenario significantly boosts domestic availability, with 15,000 tons for local use, nearly doubling current levels. Total production rises to 50,000 tons, reducing exports to 35,000 tons. Net profit is US$50 million, lower than the export scenario but much higher than the base. Water use (250 Mm^3) is below maximum, and cultivated area reaches 80,000 ha. This approach prioritizes the domestic market, accepting some trade-off in export revenue.

The Environmental Sustainability scenario balances high production (80,000 tons) and exports (70,000 tons) with substantial profit (US$100 million). Notably, it achieves this while using 50 Mm^3 less water than the export scenario, highlighting water-saving technologies. Its water efficiency is highest, and it uses less land (75,000 ha) for significant volume. Domestic consumption remains low. This shows that high volumes are possible with reduced water impact, even if profit is slightly lower due to initial costs or less aggressive resource use. It demonstrates that a balanced approach yields broader benefits than maximizing a single objective.

Finally, the Balanced Development and Value Added with Olive Oil Tourism scenario offers a well-rounded profile. With US$110 million profit, it produces 70,000 tons, exporting 50,000 and allocating 12,000 to domestic consumption. Water use (270 Mm^3) is efficient, and it uses 85,000 ha. While not maximizing any single objective, it shows the chain's ability to generate significant income and rural employment through tourism, while performing strongly across production, commerce, and environment (Guida-Johnson *et al.*, 2024) . The comparative visualizations reinforce the multidimensional nature of trade-offs, directly linking results to the five sustainability dimensions outlined in the Introduction

Figure 1 (page 97), visually compares these scenarios using a radar chart, showing their relative performance across five key areas: Economic Benefit, Total Production, Internal Consumption, Water Efficiency, and Area Used. Each axis is normalized from 0 (worst) to 100 (best).

(Elaboration based on the conceptual radar chart described in the source document)

The export-oriented scenario (orange line) excels in Economic Benefit, Total Production, Area Used, and Water Efficiency, but lags in Internal Consumption. The internal consumption scenario (red line) leads in Internal Consumption, but scores lower in Economic Benefit and Water Efficiency. The environmental sustainability scenario (magenta line) is balanced, with high Water Efficiency and strong performance in Production, Area Used, Economic Benefit, and Internal Consumption. The base scenario (yellow line) consistently underperforms. The Balanced Development and Value Added with Olive Oil Tourism scenario (blue line, hypothetical) shows solid, consistent performance across all dimensions, including additional benefits from tourism not directly shown here, like tourism revenues and rural employment. Figure 2 (page 97), presents radar charts comparing the performance of Argentina's four main olive-producing provinces (Catamarca, La Rioja, Mendoza, and San Juan) under different strategic scenarios. This visual analysis confirms that no single strategy is universally best; the optimal choice depends on specific priorities. The results also identify leverage points for improvement, particularly technological reconversion in primary production to reduce unit costs, diversification of products and markets to stabilize demand, and investment in tourism infrastructure to enhance value creation. These elements extend beyond descriptive analysis, offering actionable strategies for sectoral competitiveness.

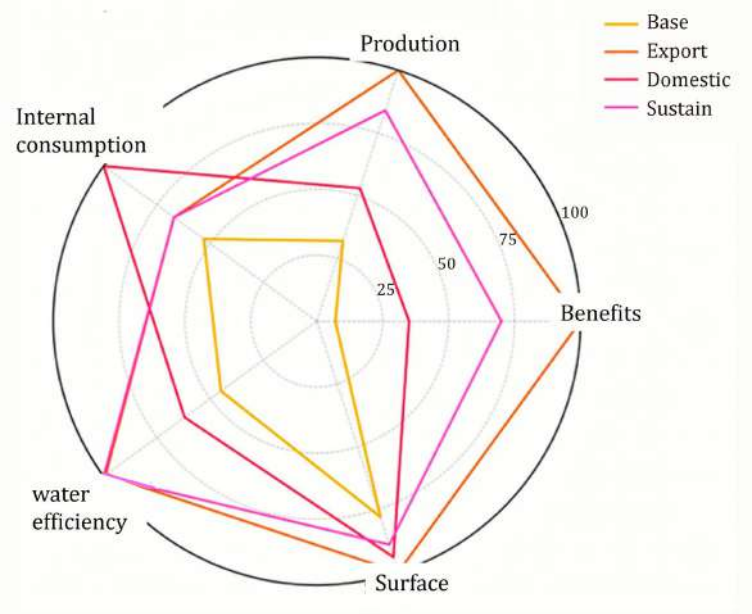

Figure 1. Comparison of relative performance of strategic scenarios on key criteria.

Figura 1. Comparación de desempeño relativo de los escenarios estratégicos en criterios clave en las principales provincias productoras.

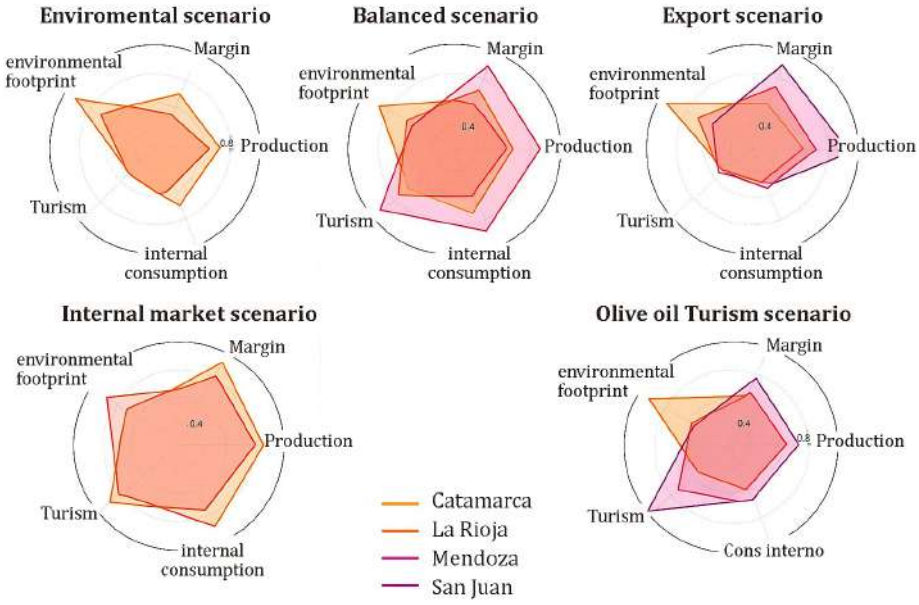

Figure 2. Impacts of each scenario in the main producing provinces.

Figura 2. Impactos de cada escenario en las principales provincias productoras.

Iterations and Sensitivity Analysis

While scenarios provide specific performance points, sensitivity analysis and gradual iterations are crucial to understand how optimal solutions shift with changing priorities or parameters, defining the Pareto frontier. This helps answer questions about trade-offs, such as how much economic gain must be sacrificed for water savings or increased domestic consumption.

Sensitivity to Domestic Objective Weight (ωD)

Increasing the importance of domestic consumption (ωD) in an export-focused model shows how production shifts from external to local markets. Initially, small increases in domestic consumption have minor profit impacts. However, pushing domestic consumption beyond 12,000-15,000 tons leads to significant economic losses, as the model must sacrifice profitable exports or expand production less efficiently. This indicates diminishing returns for boosting internal consumption; a compromise point around 12,000 tons allows maintaining about 75% of original exports. Beyond this, each extra domestic ton roughly replaces an export ton, further reducing profit. This analysis is vital for setting realistic domestic consumption targets.

Sensitivity to Water Limit (W_{max})

Reducing water availability in the export-oriented model by 10% (from 300 Mm^3 to 270 Mm^3) cut optimal production by about 15% and exports by 18%. This means a small water reduction leads to a proportionally larger drop in exportable output, as the model replaces water-intensive intensive hectares with less productive traditional ones or leaves land uncultivated. In contrast, the environmental sustainability scenario saw less than a 10% production drop with the same water restriction, as it already operates efficiently. This suggests that environmentally optimized olive growing is more resilient to water scarcity, highlighting sustainability practices as enhancing operational resilience.

Impact of International Price

A significant drop in international olive oil prices (*e.g.*, from US4,000 to US3,000 per ton) would drastically reduce the export-oriented model's profitability, potentially halving sectoral benefit. In such a case, the optimal strategy would shift towards the domestic market, as the price difference narrows. This suggests that promoting internal consumption can act as a counter-cyclical policy, providing a stable domestic market buffer against global price volatility (Pérez-Aleman, 2012).

Pareto Analysis (Benefit vs. Water Footprint)

A Pareto analysis showed that the first 50 Mm^3 of additional water (from 200 to 250 Mm^3) significantly boost production and profit. However, beyond 250-260 Mm^3, the marginal profit from additional water diminishes, following the law of diminishing returns. This indicates an optimal point where further water use yields minimal economic gain, making water conservation highly justifiable. Around 250-260 Mm^3, conserving 40-50 Mm^3 (about 15%) barely reduces maximum profit by 5-10%. This provides a quantitative basis for sustainable water management.

Land vs. Technology (Intensive vs. Traditional Hectares)

Optimized model runs consistently showed that intensive hectares (H_{int}) are maximized before expanding traditional ones (H_{trad}), as intensive systems are more resource efficient. Only when H_{int} was artificially limited did the model expand H_{trad} significantly, but this led to lower overall production and no notable water savings. This confirms the importance of technological reconversion: prioritizing modern, productive systems is more advantageous for maximizing yield and efficiency than simply increasing cultivated land.

Sensitivity to Olive Oil Tourism Integration

Integrating olive oil tourism allows evaluating how increased tourism investment (Ii) impacts visitors (Ti), tourism revenues, rural employment, and overall economic benefit. For example, analysing Mendoza's tourist capacity (approx. 2,500 people/day) reveals tourism growth potential with infrastructure expansion or diversified offerings to reduce seasonality. A Pareto analysis between tourism revenues and carbon footprint (including transport emissions) would show trade-offs between tourism growth and environmental goals. If olive oil tourism enhances brand image and quality perception (*e.g.*, through certifications), it could increase export prices (P_{exp}) for premium products, mitigating economic trade-offs and generating quantifiable intangible benefits. Beyond direct revenue, tourism acts as a marketing multiplier, boosting brand value and potentially increasing premium product export prices, creating a virtuous cycle between tourism and product sales.

Overall, these iterations demonstrate the multicriteria model's sensitivity to varying preferences and parameters, allowing a comprehensive exploration of how optimal solutions shift with altered assumptions or strategic emphases, providing valuable planning information. This sensitivity analysis not only validates the robustness of the model but also supports the central hypothesis: balanced strategies integrating economic, environmental and tourism variables yield more resilient outcomes than single-objective approaches.

Discussion

The multicriteria optimization results confirm the initial hypothesis: no single-objective strategy is sufficient to ensure competitiveness and sustainability in Argentina's olive oil chain. Balanced approaches that integrate economic, environmental and territorial objectives provide more resilient outcomes, particularly under resource and price volatility. The Export-Oriented scenario demonstrates the sector's potential to generate high revenues yet reinforces dependence on international markets and exposes vulnerability to price fluctuations. Similar dynamics have been observed in Spain, where strong export orientation has increased exposure to EU policy shifts and global price cycles (IOC, 2015). By contrast, the Internal Consumption scenario highlights opportunities for domestic market development. Previous studies confirm that per capita consumption below 0.3 litters is anomalously low for a producing country (Benencia *et al.*, 2014), suggesting that targeted campaigns and tax incentives could unlock latent demand. The Environmental Sustainability scenario reveals that water and energy-efficient technologies allow significant production while reducing resource pressure. Comparable findings have been reported in Portugal, where reconversion to super-intensive systems doubled yields while reducing unit costs (Branquinho *et al.*, 2021). The novelty of this study lies in the Balanced Development with Olive Oil Tourism scenario, which integrates agricultural and service-based activities. Olive oil tourism has been qualitatively addressed in prior works (Enolife, 2025), but this model quantitatively demonstrates its capacity to generate revenues, rural employment and territorial branding. From a broader perspective, the olive oil chain should be understood as an agri-food network or "entramado", not just a linear chain (Díaz-Chao *et al*., 2016). This resonates with bioeconomy approaches that emphasize valorisation of biomass and by-products, ranging from pomace energy use to ecosystem services. Incorporating this perspective enriches the interpretation of results: scenarios that prioritize diversification, circular use of resources and tourism services achieve more robust territorial impacts. Overall, the findings demonstrate that policy strategies for the olive oil sector must balance profitability, sustainability and territorial development. These results contribute to the literature on multicriteria programming applied to agri-food systems by explicitly incorporating tourism and territorial valorisation (Millán-Vázquez de la Torre *et al.*, 2017). They also provide actionable insights for public policy, suggesting that integrated sectoral planning should foster innovation, sustainability and experiential marketing as complementary drivers of competitiveness**.** The acknowledgment of these biomass valorisation pathways reinforces the interpretation of the olive oil chain as a bioeconomic network, extending its impact beyond oil production toward energy, environmental services, and territorial development.

Recommendations

Strengthen The Domestic Market

- Increase per capita consumption (≈0.3-0.5 kg) through fiscal incentives, educational campaigns and promotional programs.
- This provides a buffer against international price volatility.

Promote Technological Reconversion

- Modernize groves (super-intensive systems, mechanization, replanting).
- Reduces unit costs and improves competitiveness, following experiences in Chile and Portugal (Vargas & Garrido, 2019).

Diversify Products And Markets

- Expand exports beyond Brazil/USA toward emerging markets (China, India) and regional partners (Mexico, Colombia).
- Prioritize bottled EVOO under Argentine brands to capture more value.

Leverage Sustainability As Opportunity

- Implement certifications (organic, carbon-neutral, GAP).
- Access premium markets and align with global consumer trends.

Ensure Efficient Water Use

- Generalize technified irrigation, promote wastewater reuse and solar-powered pumping.
- Avoid exceeding thresholds where marginal returns diminish.

Integrate Olive Oil Tourism Strategically

- Develop routes, infrastructure and certified experiences.
- Generates rural employment, strengthens territorial identity and enhances brand value.
- Promote sustainable practices to minimize environmental trade-offs.

Conclusions

The results of the multicriteria programming model confirm that no single-objective strategy is sufficient to ensure competitiveness and sustainability in Argentina's olive oil chain. Instead, a balanced approach -integrating economic profitability, technological reconversion, environmental sustainability and tourism- yields the most resilient outcomes under volatile market and resource conditions. The analysis highlights three key findings: Technological reconversion in primary production is the most effective lever for reducing costs and improving international competitiveness. Domestic market development is feasible up to moderate levels, strengthening resilience without severely compromising export revenues. Olive oil tourism, when modelled quantitatively, emerges as a central driver of value creation, rural employment and territorial branding. These findings validate the initial hypothesis: balanced strategies outperform purely export-oriented or consumption-focused approaches. They also expand the literature by incorporating tourism and territorial valorisation into an optimization framework, offering a broader bioeconomic interpretation of value chains. Finally, the study provides actionable insights for public policy and sectoral planning: fostering innovation, sustainability and experiential marketing can consolidate Argentina's olive oil sector as a competitive and resilient player in global markets.

References

Benencia, R., Quaranta, G., & Pedreño Cánovas, A. (2014). *Mercados de trabajo, instituciones y trayectorias en distintos escenarios migratorios*. Ediciones CICCUS.

Branquinho, S., Rolim, J., & Teixeira, J. L. (2021). Climate Change Adaptation Measures in the Irrigation of a Super-Intensive Olive Orchard in the South of Portugal. *Agronomy, 11*(8), 1658. https://doi.org/10.3390/agronomy11081658

CREA. (2021). *Reporte de actualidad agro*. Movimiento CREA. https://proyectos.crea.org.ar/reporte-de-actualidad-agro/

Díaz-Chao, Á., Sainz-González, J., & Torrent-Sellens, J. (2016). The competitiveness of small network-firm: A practical tool. *Journal of Business Research, 69*(5), 1867-1872. https://doi. org/10.1016/j.jbusres.2015.10.053

Enolife. (21 de mayo de 2025). *Mendoza ya tiene 21 almazaras y olivares que ofrecen oleoturismo*. Enolife.com.ar. https://enolife.com.ar/es/mendoza-ya-tiene-21-almazaras-y-olivares-que-ofrecen-oleoturismo-con-120-000-visitantes-al-ano/

García-Cascales, M. S., Molina-García, A., Sánchez-Lozano, J. M., Mateo-Aroca, A., & Munier, N. (2021). Multi-criteria analysis techniques to enhance sustainability of water pumping irrigation. *Energy Reports, 7*, 4623-4632. https://doi.org/10.1016/j.egyr.2021.07.026

Guida-Johnson, B.; Vignoni, A. P.; Migale, G. M.; Aranda, M. A.; Magnano, A. 2024. Rural abandonment and its drivers in an irrigated area of Mendoza (Argentina). Revista de la Facultad de Ciencias Agrarias. Universidad Nacional de Cuyo. Mendoza. Argentina. 56(1): 35-47. DOI: https://doi.org/10.48162/rev.39.121

INDEC. (2019). *Censo Nacional Agropecuario 2018: Resultados finales*. https://www.indec.gob.ar/indec/web/Nivel4-Tema-3-8-71

International Olive Oil Council. (2015). *Estudio internacional sobre los costes de producción del aceite de oliva*. https://www.internationaloliveoil.org/wp-content/uploads/2019/11/ESTUDIO-INTERNACIONAL-SOBRE-COSTES-DE-PRODUCCI%C3%93N-DEL-ACEITE-DE-OLIVA.pdf

International Olive Oil Council. (n.d.). *International Olive Oil Council*. https://www.internationaloliveoil.org/

MAGyP (Ministerio de Agricultura, Ganadería y Pesca). (2023). *Informe síntesis. Economía regional Olivo*. 1-13. https://alimentosargentinos.magyp.gob.ar/HomeAlimentos/economias-regionales/producciones-regionales/informes/INFORME_ DE_Olivo2023.pdf

Millán-Vázquez de la Torre, M. G., Arjona-Fuentes, J. M., & Amador-Hidalgo, L. (2017). Olive oil tourism: Promoting rural development in Andalusia (Spain). *Tourism Management Perspectives, 21*, 100-108. https://doi.org/10.1016/j.tmp.2016.12.003

Ministerio de Economía de la República Argentina. (2024). *Informe sectorial: Olivícola* (Año 9 N° 80). https://www.argentina.gob.ar/sites/default/files/informe_sectorial_olivo.pdf

Pérez-Aleman, P. (2012). Global standards and local knowledge building: Upgrading small producers in global value chains. *Proceedings of the National Academy of Sciences, 109*(31), 12344-12349. https://doi.org/10.1073/pnas.1000968108

Romero, C. (1993). *Teoría de la decisión multicriterio: conceptos, técnicas y aplicaciones*. Alianza Editorial.

Stark, S., Biber-Freudenberger, L., Dietz, T., Escobar, N., Förster, J., Henderson, J., Laibach, N., Börner, J. (2022). Sustainability implications of transformation pathways for the bioeconomy. *Science Direct, 29,* 215-227. https://doi.org/10.1016/j.spc.2021.10.011

Vargas, R., & Garrido, A. (2019). Competitiveness of Mediterranean olive oil production: A comparative analysis of Spain and Portugal. *Spanish Journal of Agricultural Research*, *17*(4), e0112. https://doi.org/10.5424/sjar/2019174-14535

Essential Oils and Extracts from Argentinian Northwest Plants as Potential Biofungicides for Olive and Grapevine Pathogens: *in vitro* Studies

Aceites esenciales y extractos de plantas del noroeste argentino como potenciales biofungicidas de patógenos de olivo y vid: estudios *in vitro*

María Sayago [1, 2], Ivana Ormeño [2], María Teresa Ajmat [2], Natalia Barbieri [1, 2*]

Originales: *Recepción:* 07/05/2024 - *Aceptación:* 23/12/2024

Abstract

This work studies the effect of 12 botanical products from Argentinian northwest plants on spores and mycelium of *Verticillium dahliae* and *Phaeoacremonium parasiticum*, two pathogens of agronomic importance for the region. The fungi were exposed to essential oils (EOs) or ethanolic extracts (EEs), determining the percentage of germinated spores and mycelial growth. All tested EOs and EEs showed varying degrees of antifungal activity, dependent on plant species, extract type, pathogen, and targeted fungal structures. *V. dahliae* germination was completely inhibited by *Zuccagnia punctata* and *Clinopodium gilliesii* EOs. In experiments with EEs, *Z. punctata* EE was the most effective in suppressing spore germination of both fungi. The *C. gilliesii* EE also controlled *V. dahliae* germination. The EEs of *Z. punctata, C. gilliesii* and *Lippia turbinata* were the most active against mycelial growth. These three EEs had a fungistatic effect on *P. parasiticum* while *Z. punctata* and *L. turbinata* EEs showed a fungicidal effect on *V. dahliae*. The products obtained from *Z. punctata*, *C. gilliesii* and *L. turbinata* have potential as biocontrollers against *V. dahliae* and *P. parasiticum.* This is encouraging since no effective treatments are available for the diseases involving these pathogens.

Keywords

Verticillium dahliae Kleb • *Phaeoacremonium parasiticum* (Ajello, Georg & C. J. K. Wang) W. Gams, Crous & M. J. Wingf • botanical antifungals • mycelial inhibition • conidial susceptibility

1 Universidad Nacional de Chilecito. CONICET. Departamento de Ciencias Básicas y Tecnológicas. 9 de Julio 22, Chilecito F5360CKB. La Rioja. Argentina.
* nbarbieri@undec.edu.ar
2 Universidad Nacional de Chilecito. Instituto de Ambiente de Montaña y Regiones Áridas.

Resumen

Este trabajo estudia el efecto de 12 productos de plantas del noroeste argentino sobre las esporas y micelio de *Verticillium dahliae* y *Phaeoacremonium parasiticum*, dos patógenos de importancia agronómica. Los hongos fueron expuestos a los aceites esenciales (AE) o extractos etanólicos (EE), y se determinó el porcentaje de germinación y crecimiento micelial. Todos los AE y EE mostraron actividad antifúngica, la cual dependió de la especie vegetal, del extracto, del patógeno y de las estructuras fúngicas objetivo. La germinación de *V. dahliae* fue inhibida con los AE de *Zuccagnia punctata* y *Clinopodium gilliesii*. El EE de *Z. punctata* fue el más efectivo para suprimir la germinación de ambos hongos. El EE de *C. gilliesii* también fue capaz de controlar la germinación de *V. dahliae*. Mientras que los EE de *Z. punctata*, *C. gilliesii* y *Lippia turbinata* fueron los más activos sobre el micelio. Estos tres EE fueron fungistáticos sobre *P. parasiticum* mientras que los EE de *Z. punctata* y *L. turbinata* fueron fungicidas sobre *V. dahliae*. Los productos obtenidos de *Z. punctata, C. gilliesii* y *L. turbinata* son potenciales biocontroladores de *V. dahliae* y *P. parasiticum*. Esto es alentador ya que no se dispone de tratamientos eficaces para las enfermedades en las cuales participan estos patógenos.

Palabras clave

Verticillium dahliae Kleb • *Phaeoacremonium parasiticum* (Ajello, Georg & C. J. K. Wang) W. Gams, Crous & M. J. Wingf • antifúngicos botánicos • inhibición micelial • susceptibilidad conidial

Introduction

Olive and grapevine cultivation in La Rioja province (northwest Argentina) is economically significant. Fungal diseases affect productivity causing considerable losses (7, 12). Vascular wilt disease in olives caused by *Verticillium dahliae* Kleb has acquired great importance worldwide producing tree mortality, fruit yield reduction, and organoleptic defects in virgin olive oil extracted from infected plants (18, 19). Olive verticillium wilt is one major concern for olive growers in the semi-arid regions of Argentina. Rattalino (2023) has recently shown that *V. dahliae* is widely spread in La Rioja olive-growing regions, estimating 24% disease incidence.

Grapevine trunk diseases are the principal fungal diseases affecting viticulture worldwide (17). Among these pathologies, *hoja de malvón* (related to Esca) and young vine decline (Petri disease) are among the most devastating and challenging diseases in many wine regions of Argentina. They are caused by multiple wood fungal pathogens, with *Phaeoacremonium parasiticum* being mostly prevalent (9, 10).

Unfortunately, effective treatments against these mycoses are not available, and their management remains difficult. To date, recommendations focus on timely monitoring of these diseases and integrated management strategies including biological control as a potential tool (17, 19).

Plant essential oils (EOs), extracts and related molecules have demonstrated inhibitory efficacy against pathogenic fungi (3, 26). They represent eco-friendly control alternatives for integrated disease management, contributing to sustainable agricultural production. The antifungal activity (AA) of some EOs and a few plant extracts is reported against *V. dahliae* (6, 8, 11, 14, 24). However, insufficient studies focus on biological control of *P. parasiticum* using plant products. This study focused on plant species with previous AA against dermatophytes or molds: *Zuccagnia punctata, Clinopodium gilliesii, Lippia turbinata, Lippia integrifolia, Argemone subfusiformis, Erythrostemon gilliesii*, and *Senecio subulatus* var. *salsus* (1). We explore their AA against olive and grapevine pathogenic fungi, hypothesizing that plant products from these species could control plant pathogenic fungi in regional crops. We evaluated the effect of 12 botanical products (secondary metabolites) obtained from the mentioned plants on spore viability and mycelial growth of *V. dahliae* and *P. parasiticum*.

Material and methods

Plant Material

Z. punctata Cav., *C. gilliesii* Kuntze, *L. turbinata* Griseb., *L. integrifolia* Hieron., *A. subfusiformis* Ownbey., *E. gilliesii* (Hook.) Klotzsch and *S. subulatus var. salsus* (Griseb.) were collected in 2018. Georeferenced specimens were deposited in the herbarium of the Universidad Nacional de Chilecito (UNDEC). Supplementary Table 1 provides data on collection sites, yield and voucher specimens.

Obtaining Essential Oils (EOs) and Ethanolic Extracts (EEs)

Air-dried canopies were used. EOs were obtained by hydrodistillation in a Clevenger-type apparatus and stored at -20°C until further use. To obtain EEs, the plant material was macerated in ethanol 96° for 24 h, filtered and the solvent evaporated. Then, waxes were removed by precipitation from an ethanol-water solution. Later, EEs were dissolved in 50% ethanol, shaken using a 40 kHz ultrasonic cleaning bath (1 h) and centrifuged (5000 rpm, 10 min). Finally, the separated supernatants were evaporated and samples were stored until use (2).

Phytopathogenic Fungi

We used a native non-defoliating strain of *V. dahliae* Kleb. previously isolated from an infected olive plant in La Rioja (21). The *P. parasiticum* strain was obtained from the Phytopathology Laboratory of INTA Mendoza, Argentina. First, stock cultures (stored at -80°C) were activated in potato dextrose agar (PDA, Britania, Argentina) and grown in microcultures (PDA block on a microscopic slide) to check morphological traits (Supplementary Figure 1). Secondly, fungi were maintained in PDA for antifungal assays.

Inhibition of Spore Germination

The phytopathogens *V. dahliae* and *P. parasiticum* were cultured for 7 and 14 days, respectively, allowing spore development. To obtain spores, 2 mL sterile distilled water were added, and mycelia was gently scraped with a Drigalsky spatula. The suspension was recovered and adjusted to 1 x 10^3 spores/mL using a Neubauer counting chamber. For the assays, a 100 uL spore suspension was incubated with 100 uL of different concentrations of EO or EE (1-3 mg/mL) for 1h at 24°C. For plant products with 100% inhibitory activity at 1 mg/mL, lower concentrations (range of 0.2-1 mg/mL) were also evaluated. Following incubation, an aliquot was taken and seeded in PDA. After 48 h for *V. dahliae* and 72 h for *P. parasiticum* at 24°C incubation, spores were counted and the percentage of inhibited spores (number of non-germinated spores/total number of spores × 100) was determined (16). Growth control for each tested phytopathogen (distilled water), solvent control (DMSO or ethanol 96°) and EO and EE sterility controls were included. According to own experimental data, Benomyl (fungicide) constituted the positive control in concentrations ranging from 0.1 to 0.4 mg/mL for *V. dahliae* and 7 to 10 mg/mL for *P. parasiticum*. The minimum inhibitory concentration (MIC) was defined as the lowest EO or EE concentration producing 100% inhibition of spore germination.

Synergism (Checkerboard Test)

The MIC values obtained previously served as a reference and combinations ranging from 0.125xMIC to 1xMIC of EOs, EEs and Benomyl were formulated. Inhibition on spore germination was determined using the methodology described above. To evaluate combination effects, the fractional inhibitory concentration (FIC) index was calculated as FIC index = FICA + FICB, where FICA and FICB are the minimum concentrations inhibiting fungal growth (MIC) for samples A and B, respectively. FICA = (Combination MICA) / (MICA alone), FICB = (Combination MICB)/ (MICB alone). According to the FIC index, results indicated synergism (≤ 0.5), addition (> 0.5 and ≤ 1.0), indifference (> 1.0 and ≤ 2.0), or antagonism (> 2.0) (25).

Inhibition of Mycelial Growth

EEs were added at different concentrations (0.25-3 mg/mL) on molten PDA. Petri dishes with PDA plus EE were inoculated with a 5-mm diameter mycelial disc obtained from the edge of 7-and 14-day-old cultures of *V. dahliae* and *P. parasiticum*, respectively. Growth control for each tested phytopathogen (PDA plate with the mycelial disc), solvent control (PDA plate plus 96° ethanol with the mycelial disc), and positive control (PDA plate plus Benomyl with the mycelial disc) were included. Inoculated plates were incubated at 24°C and growth of *V. dahliae* and *P. parasiticum* was evaluated at 7 days by measuring mycelial diameter of each colony. Percentage of growth inhibition was calculated by equation 1:

$$\% \text{ inhibition} = ((D-d)/D) \times 100) \quad (1)$$

where
D = colony diameter of growth controls
d = diameter in EE or Benomyl treatments

The MIC was equal to the lowest EE concentration at which mycelial growth was completely inhibited (24). When EEs inhibitory effects were fungicidal or fungistatic, PDA plates with mycelium discs and different EE treatments would be incubated for 2-5 additional days (mycelial inhibition at 9 days for *V. dahliae* and 12 days for *P. parasiticum*). When no mycelium re-growth occurred during additional incubation, EE was considered fungicidal. Otherwise, it was considered fungistatic.

Total Phenolic and Flavonoid Content (PC and FC) in the EEs

Total PC was determined by the Folin-Ciocalteu spectrophotometric method. Different volumes of EE solutions were mixed with Folin-Ciocalteu reagent and sodium carbonate. After incubation, absorbance was measured at 765 nm. The PC was determined using a Gallic acid calibration curve and results were expressed as mg Gallic acid equivalents/g of dry extract (mg GAE/g) (2). FC was estimated by a spectrophotometric assay based on aluminum chloride complexes. Serial dilutions from EEs were mixed with aluminum chloride, and incubated for 1 h. Absorbance was measured at 420 nm. FC was calculated using a Quercetin calibration curve and expressed as mg quercetin equivalents/g of dry extract (mg QE/g) (2).

Statistical Analysis

Each treatment had two replicates, and experiments were conducted at least three times using a randomized design. Results are expressed as mean ± standard deviation/standard error. Statistical significance of the data was determined by ANOVA followed by Tukey's test (MINITAB software version 15 for Windows, SPSS Inc., Chicago, IL), $p \geq 0.05$. Pearson's correlation coefficient was calculated between AA and phenols or flavonoid content of EEs using InfoStat software (5).

Results

Effect of EOs and EEs on *V. dahliae* and *P. parasiticum* Spore Germination

The AA of five EOs and seven EEs obtained from plants in northwest Argentina was evaluated against spore germination of *V. dahliae* and *P. parasiticum*. Inhibition of conidia germination varied among treatments and increased with increasing EO or EE concentration.

Only the EOs from *Z. punctata* and *C. gilliesii* exhibited 100% inhibitory activity on *V. dahliae* spores, with MIC values of 3 mg/mL each (figures 1a and b, page 106). At the highest concentration tested, the EOs from *L. turbinata* and *L. integrifolia* showed remarkable activity against *V. dahliae* spores, with inhibition values of 96.4 and 96% respectively (figure 1c and d, page 106).

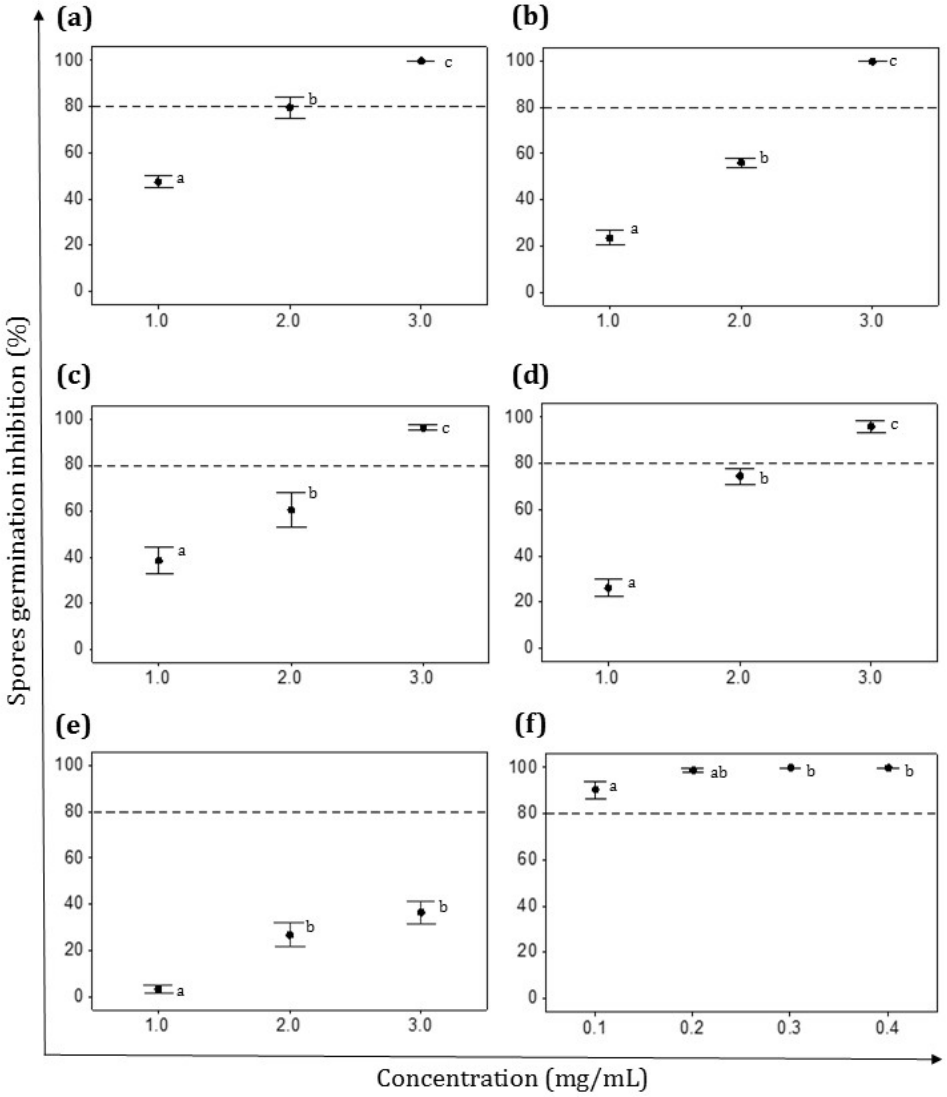

(a) *Z. punctata*, (b) *C. gilliesii*, (c) *L. turbinata*, (d) *L. integrifolia*, (e) *S. subulatus* var. *salsus*, (f) Benomyl (Fungicide).

Data are expressed as mean ± standard error, n=6-8. Different letters indicate significant differences among concentrations of the same EO. (p< 0.05).

(a) *Z. punctata*, (b) *C. gilliesii*, (c) *L. turbinata*, (d) *L. integrifolia*, (e) *S. subulatus* var. *salsus*, (f) Benomil (fungicida).

Los datos se expresan como la media ± error estándar, n=6-8. Letras distintas indican diferencias significativas entre concentraciones del mismo AE. (p< 0,05).

Figure 1. Effect of essential oils (EOs) on *V. dahliae* spore germination.

Figura 1. Efecto de los aceites esenciales (AE) sobre la germinación de las esporas de *V. dahliae*.

Concerning spore germination of *P. parasiticum*, no EO had a 100% inhibitory effect. *C. gilliesii* EO inhibited 85.8% of spores at 3 mg/mL, while the remaining oils showed low activity, with 30-54 % inhibition at the highest concentration evaluated (Supplementary Figure 2).

On the other hand, in assays with EEs, only *Z. punctata* EE effectively controlled spore germination of both pathogenic fungi (figure 2a and 3a, page 107). The effective concentration (MIC) of this extract on *V. dahliae* was 0.4 mg/mL, similar to the MIC obtained with the synthetic antifungal Benomyl (MIC=0.3 mg/mL) (figure 2a and h, page 107).

Spore germination of *V. dahliae* was also completely inhibited at 3 mg/ml of *C. gilliesii* EE (MIC), while other EEs showed inhibitions ranging between 54% and 89% (figure 2, page 107). *P. parasiticum* spore germination was controlled at 0.75 mg/mL of *Z. punctata* EE (MIC), a much lower value than the obtained with the antifungal Benomyl (MIC=10 mg/mL) (figure 3a and h, page 108). In addition, significant inhibition of *P. parasiticum* spore germination (94%) was obtained at 3 mg/mL of *E. gilliesii* EE (figure 3f, page 108).

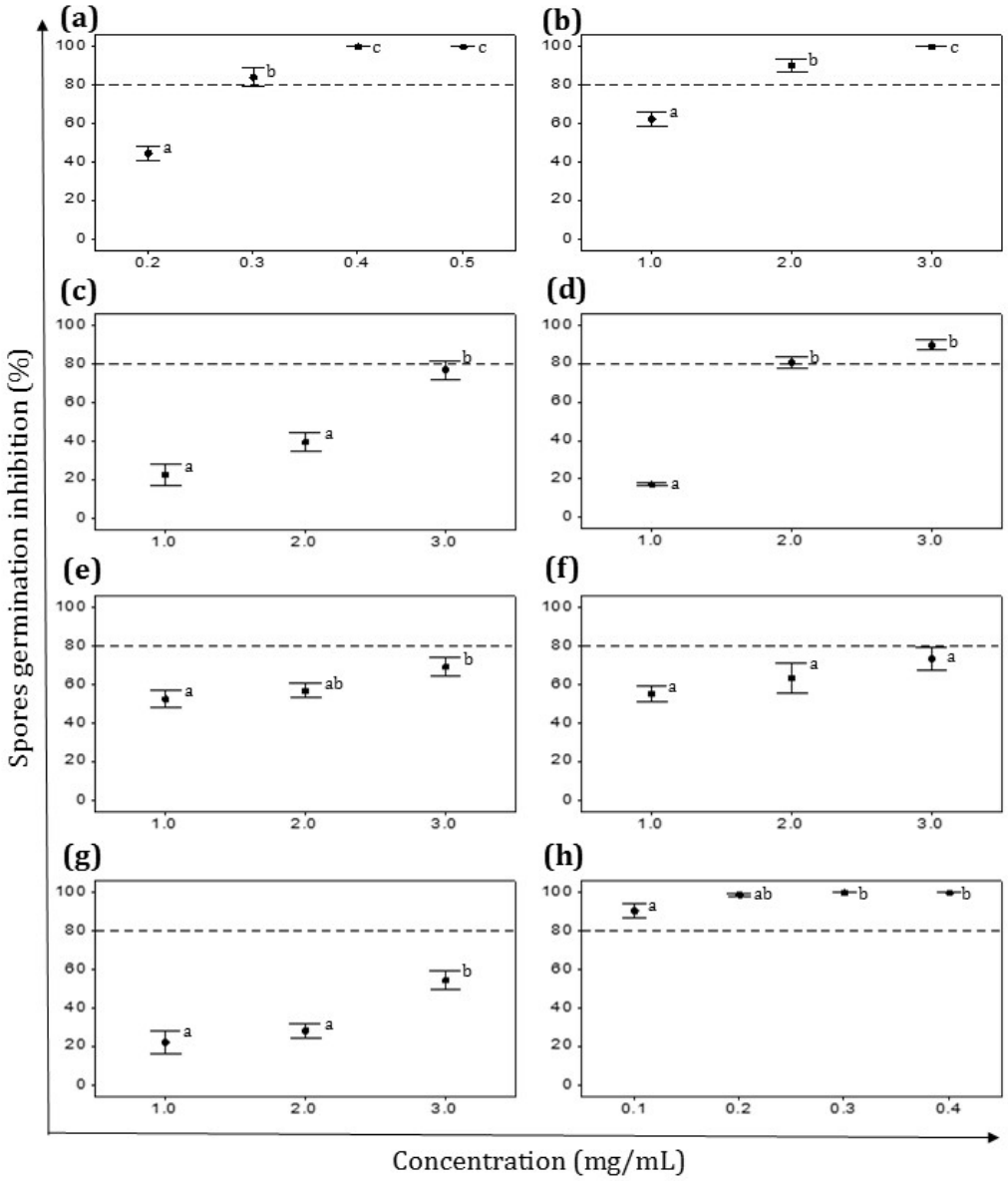

(a) *Z. punctata*, (b) *C. gilliesii*, (c) *L. turbinata*, (d) *L. integrifolia*, (e) *A. subfusiformis*, *(f) E. gilliesii*, (g) *S. subulatus* var. *salsus*, (h) Benomyl (Fungicide). Data are expressed as mean ± standard error, n=6-8. Different letters indicate significant differences among concentrations of the same EE. (p< 0.05).

(a) *Z. punctata*, (b) *C. gilliesii*, (c) *L. turbinata*, (d) *L. integrifolia*, (e) *A. subfusiformis*, (f) *E. gilliesii*, (g) *S. subulatus* var. *salsus*, (h) Benomyl (Fungicida). Los datos se expresan como la media ± error estándar, n=6-8. Letras distintas indican diferencias significativas entre concentraciones del mismo EE. (p< 0,05).

Figure 2. Effect of ethanolic extracts (EEs) on *V. dahliae* spore germination.

Figura 2. Efecto de los extractos etanólicos (EEs) sobre la germinación de esporas de *V. dahliae*.

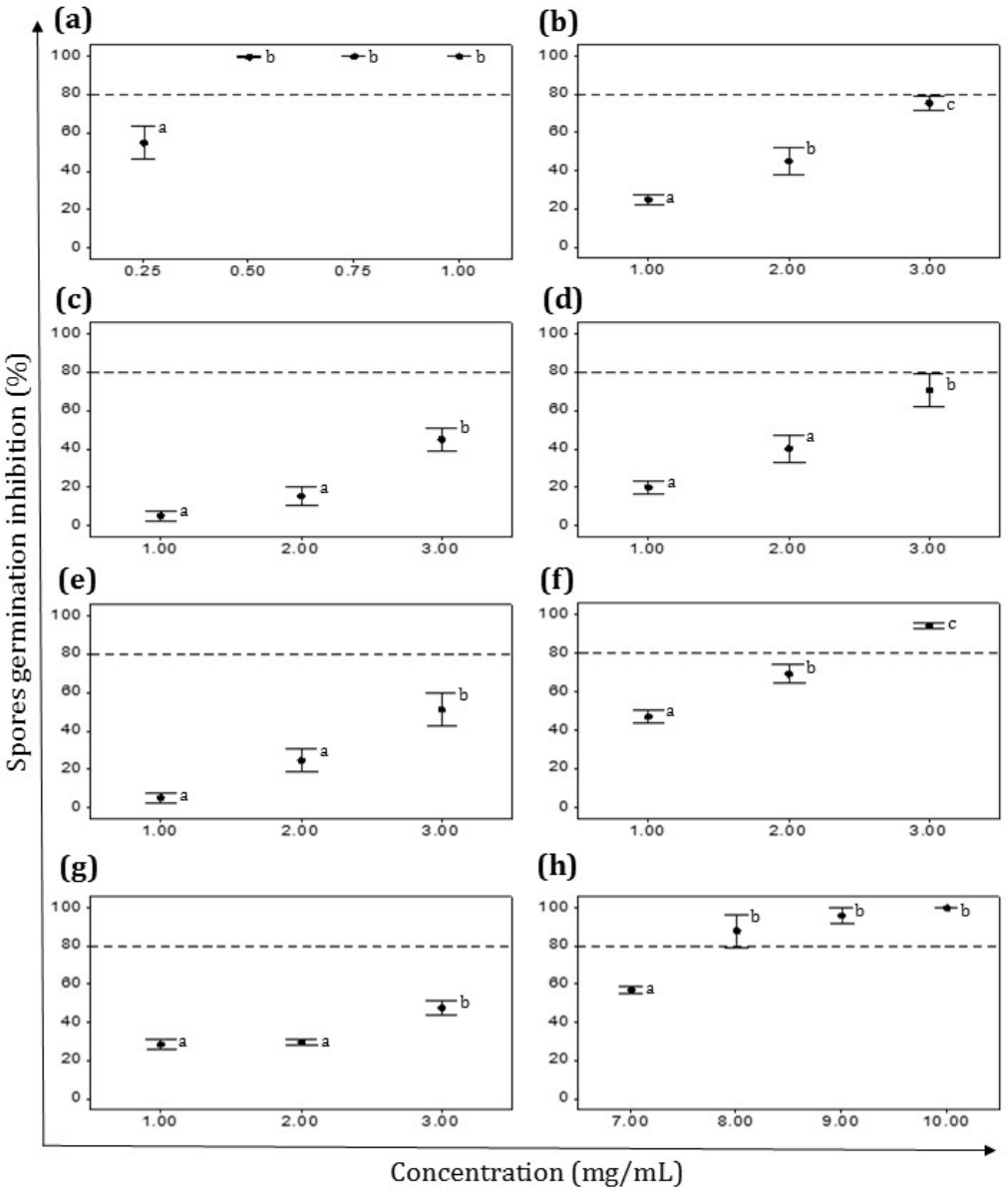

(a) *Z. punctata*, (b) *C. gilliesii*, (c) *L. turbinata*, (d) *L. integrifolia*, (e) *A. subfusiformis*, (f) *E. gilliesii*, (g) *S. subulatus* var. *salsus*, (h) Benomyl (Fungicide). Data are expressed as mean ± standard error, n=6-8. Different letters indicate significant differences among concentrations of the same EE. ($p < 0.05$).

(a) *Z. punctata*, (b) *C. gilliesii*, (c) *L. turbinata*, (d) *L. integrifolia*, (e) *A. subfusiformis*, (f) *E. gilliesii*, (g) *S. subulatus* var. *salsus*, (h) Benomyl (Fungicida). Los datos se expresan como la media ± error estándar, n=6-8. Letras distintas indican diferencias significativas entre concentraciones del mismo EE. ($p < 0,05$).

Figure 3. Effect of ethanolic extracts (EEs) on *P. parasiticum* spore germination.

Figura 3. Efecto de los extractos etanólicos (EEs) sobre la germinación de esporas de *P. parasiticum*.

Evaluation of Synergistic Antifungal Effect

The results demonstrated no synergistic effect against *V. dahliae* and *P. parasiticum* spores for any of the evaluated combinations. Antifungal interaction was additive or indifferent (Supplementary Table 2).

Effect of EEs on Mycelial Growth of *V. dahliae* and *P. parasiticum*

Since no EOs could completely inhibit *P. parasiticum* spore germination, and their activity on *V. dahliae* spore germination was weaker than the extracts, assays considering mycelial growth inhibition were performed with EEs only.

Mycelial growth inhibition increased with EEs concentration. All seven EEs tested showed growth inhibition of over 25% for both phytopathogens (figure 4, page 110 and figure 5, page 111).

Considering EEs inhibitory effect on *V. dahliae*, three treatments (EEs from *Z. punctata, C. gilliesii* and *L. turbinata*) completely inhibited mycelial growth (figure 4a-c, page 110). *Z. punctata* EE was the most effective, obtaining the lowest MIC value (MIC=1.5 mg/mL for *Z. punctata* EE, MIC=2.5 mg/mL for *C. gilliesii* EE and MIC=3 mg/mL for *L. turbinata* EE; (figure 4a-c, page 110). The EEs of *L. integrifolia* and *E. gilliesii* reached inhibition values of 93.7% and 89.5% against *V. dahliae* at 3 mg/mL (figure 4d and f, page 110). The two remaining EE treatments (*A. subfusiformis* and *S. subulatus*) achieved 60-70% inhibition (figure 4e and g, page 110). Given that no mycelium re-growth occurred during additional incubation time (day 9), *Z. punctata, L. turbinata, L. integrifolia, A. subfusiformis* and *S. subulatus* EEs resulted fungicidal against *V. dahliae* (figure 4, page 110). In the case of *C. gilliesii* and *E. gilliesii*, mycelial recovery was observed at 9 days. The *C. gilliesii* EE MIC value changed from 2.5 to 3 mg/mL while inhibition percentage of *E. gilliesii* EE at 3 mg/mL decreased significantly (figure 4b and f, page 110). Thus, AA of these EEs on *V. dahliae* was considered fungistatic.

P. parasiticum mycelial growth was completely inhibited by *Z. punctata* and *L. turbinata* EEs (MIC=1 mg/mL for *Z. punctata* EE and MIC=2 mg/mL for *L. turbinata* EE) (figure 5a and c, page 111). In addition, the EEs of *C. gilliesii, L. integrifolia,* and *E. gilliesii* showed strong inhibitory effects on *P. parasiticum* mycelial growth reaching 92.6, 81.4 and 84.9% at 3 mg/mL, respectively (figure 5b, d and f, page 111). The EE treatments *A. subfusiformis* and *S. subulatus* also inhibited 60-70% of mycelial growth (figure 5e and g, page 111). The EE treatments produced reversible inhibition of *P. parasiticum* mycelium growth. During additional incubation time, the MIC value of *Z. punctata* and *L. turbinata* EEs increased to 2 mg/mL and 3 mg/mL, respectively. A significant reduction in inhibition percentage of the other EEs was also observed on day 12 (figure 5, page 111). Therefore, these EEs were fungistatic against *P. parasiticum*.

Phenolic and Flavonoid Contents (PC and FC) in EEs

Both PC and FC of the studied EEs were significantly different (Supplementary Table 3). The EE of *Z. punctata* showed the highest PC, followed by *C. gilliesii* EE, *L. turbinata* EE, *L. integrifolia* EE = *A. subfusiformis* EE = *E. gilliesii* EE, and *S. subulatus* EE. Regarding FC, *Z. punctata* EE presented the highest value (327.6 mg QE/g) and the other EEs ranged between 13 and 73 mg QE/g.

Pearson's correlation coefficient between PC and spore germination inhibition was $r=0.63$ ($p < 0.0001$) for *V. dahliae* and $r=0.39$ ($p < 0.0001$) for *P. parasiticum.* Additionally, a significant correlation was observed between PC and mycelial growth inhibition, with values of $r=0.79$ ($p < 0.0001$) for *V. dahliae* and $r=0.78$ ($p < 0.0001$) for *P. parasiticum*. The FC and inhibition of spore germination showed correlation coefficients of $r=0.73$ ($p < 0.0001$) for *V. dahliae* and $r=0.72$ ($p < 0.0001$) for *P. parasiticum,* while for FC and mycelial growth inhibition, $r=0.60$ ($p < 0.0001$) was observed for *V. dahliae* and $r=0.67$ ($p < 0.0001$) for *P. parasiticum*.

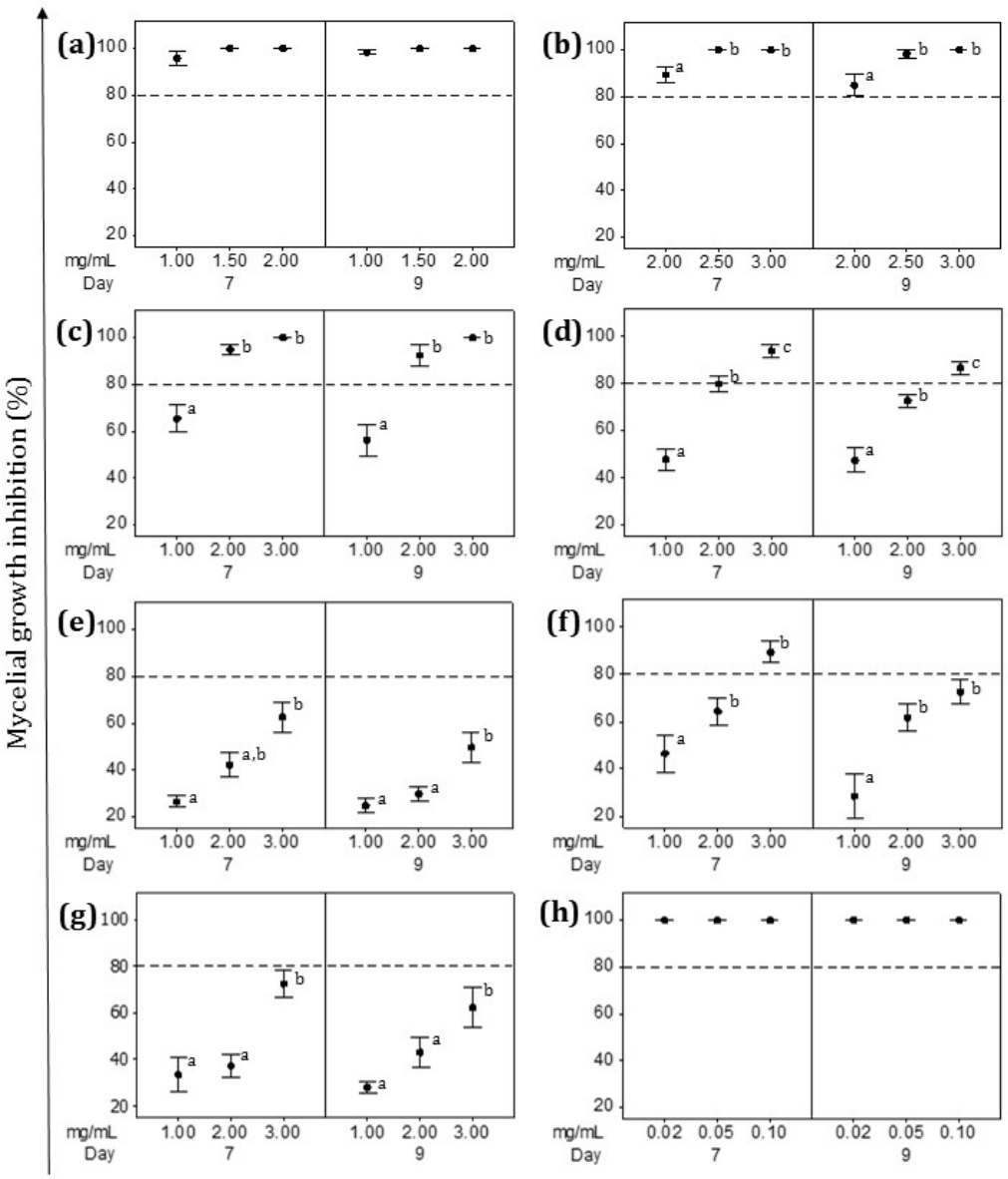

(a) *Z. punctata*, (b) *C. gilliesii*, (c) *L. turbinata*, (d) *L. integrifolia*, (e) *A. subfusiformis*, (f) *E. gilliesii*, (g) *S. subulatus* var. *salsus*, (h) Benomyl (Fungicide). The percentage of inhibition was determined at 7 and 9 days of incubation at 24°C. Data are expressed as mean ± standard error, n=6-8. Different letters indicate significant differences among the concentrations tested (p< 0.05).

(a) *Z. punctata*, (b) *C. gilliesii*, (c) *L. turbinata*, (d) *L. integrifolia*, (e) *A. subfusiformis*, (f) *E. gilliesii*, (g) *S. subulatus* var. *salsus*, (h) Benomyl (Fungicida). El porcentaje de inhibición se determinó a los 7 y 9 días de incubación a 24°C. Los datos se expresan como media ± error estándar, n=6-8. Letras diferentes indican diferencias significativas entre las concentraciones ensayadas. (p< 0,05).

Figure 4. Effect of ethanolic extracts (EEs) on *V. dahliae* mycelial growth.

Figura 4. Efecto de los extractos etanólicos (EE) sobre el crecimiento micelial de *V. dahliae*.

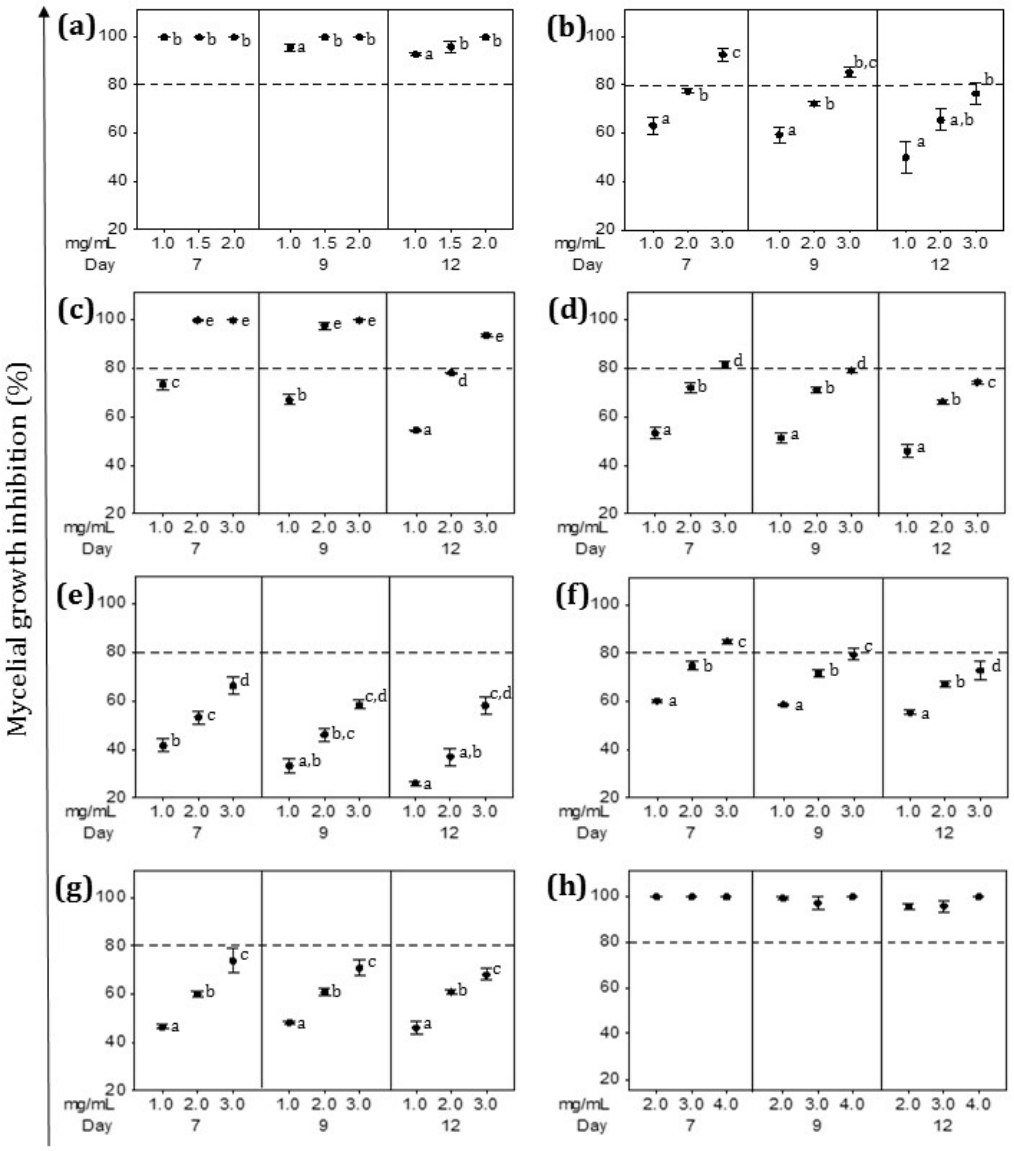

(a) *Z. punctata*, (b) *C. gilliesii*, (c) *L. turbinata*, (d) *L. integrifolia*, (e) *A. subfusiformis*, (f) *E. gilliesii*, (g) *S. subulatus* var. *salsus*, (h) Benomyl (Fungicide). The percentage of inhibition was determined at 7, 9 and 12 days of incubation at 24°C. Data are expressed as mean ± standard error, n=6-8. Different letters indicate significant differences among concentrations. (p< 0.05).

(a) *Z. punctata*, (b) *C. gilliesii*, (c) *L. turbinata*, (d) *L. integrifolia*, (e) *A. subfusiformis*, (f) *E. gilliesii*, (g) *S. subulatus* var. *salsus*, (h) Benomyl (Fungicida). El porcentaje de inhibición se determinó a los 7, 9 y 12 días de incubación a 24°C. Los datos se expresan como media ± error estándar, n=6-8. Letras diferentes indican diferencias significativas entre concentraciones. (p< 0,05).

Figure 5. Effect of ethanolic extracts (EEs) on *P. parasiticum* mycelial growth.

Figura 5. Efecto de los extractos etanólicos (EE) sobre el crecimiento micelial de *P. parasiticum*.

Discussion

V. dahliae and *P. parasiticum* are important phytopathogens in La Rioja province, involved in Verticillium wilt of olive and grapevine trunk diseases, respectively (10, 20). Given the lack of control treatments, searching for antifungal agents is strategic (17, 19). We tested EOs and EEs from seven Argentinian northwest plants as natural alternatives against *V. dahliae* and *P. parasiticum*.

Three mg/mL of our EOs had remarkable activity against *V. dahliae* spore germination (100% inhibitory activity for *Z. punctata* and *C. gilliesii* EOs, and 96% inhibitory activity for *L. turbinata* and *L. integrifolia* EOs). Similarly, other EOs (orégano, thyme, laurel, and lavender) block *V. dahliae* conidia germination at concentrations ranging from 0.2 to 3 mg/mL (11, 14).

On the other hand, only the *C. gilliesii* EO was able to significantly inhibit *P. parasiticum* conidia germination, suggesting *V. dahliae* spores are more susceptible to the tested EOs than *P. parasiticum*. In addition, although previous reports demonstrated the activity of *C. gilliesii* and *L. turbinata* EOs against other phytopathogenic fungi (15, 22, 27), this is the first report on AA of *Z. punctata* and *L. integrifolia* EOs against this type of pathogens.

Based on EEs activity on conidia germination, only *Z. punctata* EE was able to control both *V. dahliae* (MIC= 0.4 mg/mL) and *P. parasiticum* (MIC=0.75 mg/mL). These results coincide with previous research showing the *Z. punctata* EE effectiveness against soybean pathogenic and brown rot fungi spore development at concentrations between 0.25-0.5 mg/mL (4, 23). Our results also showed that *C. gilliesii* EE controlled germination of *V. dahliae* spores, apparently never studied before against phytopathogenic fungi.

Although no synergistic antifungal effect was found for the mixtures of EO and EE tested, antagonistic absence and additive effects of the combinations of *Z. punctata* EO/*Z. punctata* EE and *C. gilliesii* EO/*Z. punctata* EE, constitute encouraging outcomes. This suggests that the botanical effective antifungal concentration (MIC) could be halved when combined.

On the other hand, the most effective inhibitors of mycelial growth of both phytopathogens were *Z. punctata*, *C. gilliesii,* and *L. turbinata* EEs. All three extracts behaved as fungistatic on *P. parasiticum,* while *Z. punctata* and *L. turbinata* EEs killed *V. dahliae* mycelium (fungicidal effect), evidencing that *V. dahliae* vegetative growth was more susceptible to our EEs than *P. parasiticum.*

In vitro studies with *Z. punctata* EE at 1.6 mg/mL could not completely inhibit hyphal growth of *Fusarium* species associated with Ear Rot in cereals (13). In contrast, our findings showed that the AA of *Z. punctata* EE, ranging from 1-1.5 mg/mL could completely inhibit mycelial growth of *V. dahliae* and *P. parasiticum*. Results also showed that *Z. punctata* EE MIC values were 2-3 times lower on the spores than on the mycelium of both phytopathogens, consistent with previous findings (13). Considering *C. gilliesii* EE, MIC was similar for conidia germination and mycelial growth of *V. dahliae*. Surprisingly, a complete reduction of *V. dahliae* and *P. parasiticum* mycelial growth was observed with *L. turbinata* EE. However, it did not provide complete control over conidia germination, suggesting a differential effect of extract components on each fungal structure.

Considering all the evaluated EEs, *Z. punctata* EE was the most effective at suppressing spore germination and mycelial growth. Previous research has corroborated the AA of *Z. punctata* EE against other phytopathogenic fungi, attributing this property to polyphenolic compounds, especially chalcone type (4, 13, 23). Considering the difference in the AA observed among the different EEs evaluated, phenols and flavonoid content were quantified, showing that *Z. punctata* EE had the highest content of phenols and flavonoids likely responsible for its potent AA.

Finally, we found that total phenols had the best correlation with mycelial growth inhibition, while flavonoid levels best correlated with inhibition of spore germination. Thus, the AA of studied EEs on conidial germination could be mainly attributed to flavonoid content, while phenols would be responsible for inhibitory effects on mycelial growth.

Conclusions

This work searched for antifungals of plant origin against pathogenic fungi involved in grapevine trunk diseases and Verticillium wilt of olive. We explored the *in vitro* antifungal properties of five EOs and seven EEs obtained from Argentinian northwest plants. All tested EOs and EEs showed varying AA degrees against both phytopathogenic fungi. This activity depended on plant species, extract type (EO or EE), pathogen identity, and targeted fungal structures. According to our findings, the products obtained from *Z. punctata*, *C gilliesii* and *L. turbinata* were the most effective against *V. dahliae* and *P. parasiticum*, suggesting their potential as biofungicides for integrated disease control. This is particularly encouraging considering absent effective treatments against these two pathogens. Further research should determine antifungal effectiveness of these botanical products in plants and identify their specific antifungal compounds.

Supplemmentary material

https://drive.google.com/drive/folders/1O7n5y_WfEk5QOQJzHepnvtvOcieXZhuG?usp=sharing

References

1. Alonso, J.; Desmarchelier, C. 2015. Plantas medicinales autóctonas de la Argentina. Corpus Libros Médicos y Científicos. Buenos Aires. 748 p.
2. Barbieri, N.; Gilabert, M.; Benavente, A. 2023. Phytochemical analysis and biological potential of Argentinian plant essential oils and extracts. Braz J Med Plants 25: 17-28.
3. Boiteux, J.; Fernández, M. de los Á.; Espino, M.; Silva, M. F.; Pizzuolo, P. H.; Lucero, G. S. 2023. *In vitro* and *in vivo* efficacy of *Larrea divaricata* extract for the management of *Phytophthora palmivora* in olive trees. Revista de la Facultad de Ciencias Agrarias. Universidad Nacional de Cuyo. Mendoza. Argentina. 55(2): 97-107. DOI: https://doi.org/10.48162/rev.39.112.
4. Di Liberto, M. G.; Stegmayer, M. I.; Fernández, L. N.; Quiroga, A. D.; Svetaz, L. A.; Derita, M. G. 2023. Control of brown rot produced by *Monilinia fructicola* in peaches using a full-spectrum extract of *Zuccagnia punctata* Cav. Horticulturae. 9(10): 1141. DOI: 10.3390/horticulturae9101141
5. Di Rienzo, J. A.; Casanoves, F.; Balzarini, M. G.; Gonzalez, L.; Tablada, M.; Robledo, C. W. InfoStat versión 2020. Centro de Transferencia InfoStat, FCA. UNC. Córdoba. Argentina. http://www.infostat.com.ar
6. Đorđević, M.; Dolovac, N.; Ivanović, M.; Damnjanović, J.; Zečević, B. 2013. Effectiveness of essential oils in control of *Verticillium dahliae in vitro*. Zaštita bilja. 64(3): 162-168.
7. EPSA. 2023. Estrategia provincial para el sector agroalimentario. Provincia de La Rioja. Ministerio de Producción y Ambiente. www.argentina.gob.ar/sites/default/files/2023/05/la_rioja_2023.pdf
8. Erdogan, O.; Çelik, A.; Zeybek, A. 2016. *In vitro* antifungal activity of mint, thyme, lavender extracts and essential oils on *Verticillium dahliae* Kleb. Fresenius Environ Bull. 25: 4856-4862.
9. Escoriaza, G.; Sansberro, P.; Lampasona, S. G.; Gatica, M.; Piccoli, P. 2013. *In vitro* cultures of *Vitis vinifera L.* cv Chardonnay synthesize the phytoalexin nerolidol upon infection by *Phaeoacremonium parasiticum*. Phytopathol Mediterr. 52(2): 289-297.
10. Escoriaza, G.; García Lampasona, S.; Gomez Talquenca, S.; Piccoli, P. 2019. *In vitro* plants of *Vitis vinifera* respond to infection with the fungus *Phaeoacremonium parasiticum* by synthesizing the phytoalexin nerolidol. PCTOC. 138(3): 459-466. DOI: 10.1007/s11240-019-01641-3
11. Giamperi, L.; Fraternale, D.; Ricci, D. 2002. The *in vitro* action of essential oils on different organisms. J Essent Oil Res. 14(4): 312-318. DOI: 10.1080/10412905.2002.9699865
12. INV. 2023. Informe anual de superficie. 2022. Instituto Nacional de Vitivinicultura. www.argentina.gob.ar/inv/vinos/estadisticas/superficie/anuarios
13. Jimenez, C. M.; Sampietro, D. A.; Sgariglia, M. A.; Soberón, J. R.; Vattuone, M. A. 2014. Isolation, identification and usefulness of antifungal compounds from *Zuccagnia punctata* for control of toxigenic ear rot pathogens. Nat Prod Commun. 9(10): 1934578X1400901.
14. Kadoglidou, K.; Lagopodi, A.; Karamanoli, K.; Vokou, D.; Bardas, G.; Menexes, G.; Constantinidou, H. I.; Kadoglidou, K.; Karamanoli, K.; Lagopodi, A.; Bardas, G.; Vokou, D.; Menexes, G. 2011. Inhibitory and stimulatory effects of essential oils and individual monoterpenoids on growth and sporulation of four soil-borne fungal isolates of *Aspergillus terreus, Fusarium oxysporum, Penicillium expansum*, and *Verticillium dahliae*. Eur. J. Plant Pathol. 130. DOI: 10.1007/s10658-011-9754-x
15. Leal, L. E.; Alarcón, A. A.; Ortega-Baes, P.; Cayo, F.; Alarcón, R. 2018. Effects of essential oils from two Lippia species on growth of phytopathogenic fungi. BLACPMA. 17(1): 30-35.
16. Liu, J.; Hagberg, I.; Novitsky, L.; Hadj-Moussa, H.; Avis, T. J. 2014. Interaction of antimicrobial cyclic lipopeptides from *Bacillus subtilis* influences their effect on spore germination and membrane permeability in fungal plant pathogens. Fungal Biol. 118(11): 855-861. DOI: 10.1016/j.funbio.2014.07.004
17. Mondello, V.; Songy, A.; Battiston, E.; Pinto, C.; Coppin, C.; Trotel-Aziz, P.; Clément, C.; Mugnai, L.; Fontaine, F. 2018. Grapevine trunk diseases: A review of fifteen years of trials for their control with chemicals and biocontrol agents. Plant Dis. 102(7): 1189-1217.
18. Montes-Osuna, N.; Mercado-Blanco, J. 2020. Verticillium wilt of olive and its control: What did we learn during the last decade? Plants. 9(6): 735. DOI: 10.3390/plants9060735
19. Mulero-Aparicio, A.; Varo, A.; Agustí-Brisach, C.; López-Escudero, F. J.; Trapero, A. 2020. Biological control of *Verticillium wilt* of olive in the field. Crop Protection 128: 104993. DOI: 10.1016/j.cropro.2019.104993
20. Rattalino, D. 2023. Identificación molecular y variabilidad genética de *Verticillium dahliae* su relación con la incidencia y prevalencia de la verticilosis del olivo en la zona olivícola de la provincia de La Rioja. Tesis de Doctorado en ciencias agropecuarias. Universidad Nacional de Córdoba. Argentina. 146 p.

21. Rattalino, D.; Otero, M. L.; Moriconi, D. N.; Rivera, P. C. 2021. Mejora de la detección del patotipo no defoliante de *Verticillium dahliae* en olivo mediante PCR anidada. AgriScientia. 38(1): 79-91. DOI: 10.31047/1668.298x.v38.n1.28985
22. Stegmayer, M. I.; Fernández, N. L.; Álvarez, N. H.; Olivella, L.; Gutiérrez, H. F.; Favaro, M. A.; Derita, M. G. 2021. Aceites esenciales provenientes de plantas nativas para el control de hongos fitopatógenos que afectan a frutales. FAVE. 20(1): 317-329. DOI: 10.14409/fa.v20i1.10273
23. Svetaz, L.; Tapia, A.; López, S. N.; Furlán, R. L. E.; Petenatti, E.; Pioli, R.; Schmeda-Hirschmann, G.; Zacchino, S. A. 2004. Antifungal chalcones and new caffeic acid esters from *Zuccagnia punctata* acting against Soybean Infecting Fungi. J. Agric. Food Chem. 52(11): 3297-3300. DOI: 10.1021/jf035213x
24. Varo, A.; Mulero-Aparicio, A.; Adem, M.; Roca, L. F.; Raya-Ortega, M. C.; López-Escudero, F. J.; Trapero, A. 2017. Screening water extracts and essential oils from Mediterranean plants against *Verticillium dahliae* in olive. Crop Protection. 92: 168-175. DOI: 10.1016/j.cropro.2016.10.018
25. Yadav, M. K.; Chae, S. W.; Im, G. J.; Chung, J. W.; Song, J. J. 2015. Eugenol: A phyto-compound effective against methicillin-resistant and methicillin-sensitive *Staphylococcus aureus* clinical strain biofilms. Plos One. 10(3): e0119564. DOI: 10.1371/journal.pone.0119564
26. Zaker, M. 2016. Natural plant products as eco-friendly fungicides for plant diseases control- A Review. The Agriculturists. 14(1): 134-141. DOI: 10.3329/agric.v14i1.29111
27. Zygadlo, J. A.; Grosso, N. R. 1995. Comparative study of the antifungal activity of essential oils from aromatic plants growing wild in the central region of Argentina. Flavour Fragr J. 10(2): 113-118. DOI: 10.1002/ffj.2730100210

Acknowledgments

This research was funded by Secretaría de Políticas Universitarias and Universidad Nacional de Chilecito, Argentina (grants PAFCyT I+D 35/18 and FICyT-2022).

We thank Translator A. López López for improving English in the manuscript and M.J. Loyola from UNDEC Herbarium for assisting with plant taxonomic identification.

M.S is a fellow and N.B is a researcher, both at CONICET, Argentina.

Fungicide Management of Late Leaf Spot and Peanut Smut

Uso de fungicidas para el manejo de la viruela tardía y del carbón del maní

Damian Francisco Giordano [1, 2 *], Agostina Del Canto [1], Jessica Gabriela Erazo [1], Nicolas Alejandro Pastor [1], Ana Cecilia Crenna [1, 2], Melina Rosso [3], Adriana Mabel Torres [1], Claudio Marcelo Oddino [1, 2, 3]

Originales: *Recepción:* 11/02/2024 - *Aceptación:* 16/10/2024

Abstract

Late leaf spot (LLS), caused by *Nothopassalora personata*, is the most devastating peanut disease in the world. In Argentina, peanut smut (*Thecaphora frezii*) has increased significantly in recent decades. LLS is mainly managed through chemical fungicides, however, peanut smut is not effectively controlled, except for some resistant peanut genotypes. This study evaluated the effects of widely used fungicides for LLS control on both diseases and crop yield. Field trials were conducted over three consecutive years in two locations, with different fungicide doses and number of applications. Disease intensities were significantly higher in General Cabrera (GC) than in Vicuña Mackenna (VM) resulting in higher yields in VM. This could be due to the longer history of peanut cultivation in GC, where fungicide applications reduced LLS intensity. Among fungicides, chlorothalonil showed the best performance. However, these treatments were ineffective against peanut smut, likely due to difficulties reaching the infection site. Considering fungicides are one major management tool, further study of different active ingredients against both diseases should also consider sustainable integrated management.

Keywords

Arachis hypogaea • chemical control • fungal diseases • *Nothopassalora personata* • *Thecaphora frezii*

1 Universidad Nacional de Río Cuarto (UNRC). Instituto de Investigación en Micología y Micotoxicología (IMICO). Consejo Nacional de Investigaciones Científicas y Técnicas (CONICET). 5800. Ruta Nacional 36 km 601. Río Cuarto. Cordoba. Argentina.

2 Universidad Nacional de Río Cuarto (UNRC). Facultad de Agronomía y Veterinaria. Departamento de Biología Agrícola. * dgiordano@exa.unrc.edu.ar

3 Criadero El Carmen. 5809. Av. Italia 871. General Cabrera. Córdoba. Argentina.

Resumen

La viruela tardía (VT) ocasionada por *Nothopassalora personata* es la enfermedad del maní más desvastadora a nivel mundial, mientras que el carbón (*Thecaphora frezii*), es la enfermedad con mayor incremento en Argentina en las últimas décadas. VT es principalmente manejada a través de fungicidas químicos, mientras que, para el carbón del maní, no existen herramientas efectivas, salvo algunos genotipos resistentes. En este trabajo, se evaluó el efecto de fungicidas ampliamente utilizados para el control de VT, sobre ambas enfermedades y sobre el rendimiento del cultivo. Los ensayos de campo fueron realizados en dos localidades por tres años consecutivos, donde se probaron fungicidas en diferentes dosis y número de aplicaciones. La intensidad de ambas enfermedades fue más alta en General Cabrera (GC) que en Vicuña Mackenna (VM), resultando en mayores rendimientos en VM. Esto se debió posiblemente al mayor historial de producción de maní en GC, donde la aplicación de fungicidas redujo la intensidad de VT. Entre los fungicidas, clorotalonil demostró la mejor performance. Sin embargo, estos tratamientos no fueron efectivos frente al carbón del maní, posiblemente debido a no alcanzar el sitio de infección. Teniendo en cuenta que los fungicidas son una de las principales herramientas de manejo, se necesitan más estudios de diferentes ingredientes activos sobre ambas enfermedades, considerando un manejo integrado sustentable.

Palabras clave

Arachis hypogaea • control químico • enfermedades fúngicas • *Nothopassalora personata* • *Thecaphora frezii*

Introduction

Peanut (*Arachis hypogaea* L.) world production exceeds 49 million metric tons in pods. This oilseed is cultivated in over 100 countries, but approximately 80% of the production is concentrated in 10 countries, with China leading 18 million metric tons annually. Argentina is the tenth peanut producer with more than 950.000 metric tons, and the second exporter, with 16% of worldwide production. The province of Córdoba is the largest producer, accounting for 80% of the national output (32).

Several diseases affect peanut production in Argentina and other countries. Early leaf spot (ELS) caused by *Passalora arachidicola* (Hori) and late leaf spot (LLS) caused by *Nothopassalora personata* (Berk. & Curtis) are the most important foliar diseases worldwide, being LLS the most frequent in some main producing regions (14, 24). These diseases can generate important yield losses, and consequent economic imbalance (2). On the other hand, peanut smut by *Thecaphora frezii* (Carranza & Lindquist) has become the most important soil-borne disease in Argentina due to recent increasing prevalence and intensity (30), causing significant yield losses (25). LLS benefits from rainfall (16), while smut typically thrives under drought conditions, particularly during grain filling (28).

Even though different tools aim to control LLS, its management relies mainly on chemical fungicides (17) like systemic single-site mode carboxamides, strobilurins and triazoles. Many studies have shown beneficial effects of using fungicide mixtures from different chemical groups, mainly with carboxamides (10, 23). Among contact fungicides with multiple modes of action, the majorly used chlorothalonil presents consistent results (9). However, other options must be considered given that some active ingredients (a.i.) may soon be prohibited or useless against resistant strains.

Different management strategies have been tested against peanut smut, without successful effects on intensity. On the other hand, genetics have contributed resistant varieties (5): EC - 191 RC (AO), EC - 394 RC (AO) and EC - 420 RC (AO) (2), still grown only on a reduced area of the country. Meanwhile, biological control agents have proven useful regarding disease severity and grain weight at field scale (15), although still mostly preliminary. Regarding chemical control, many fungicide groups have shown variable results (8, 22). Such variability in disease control may be due to low fungicide efficacy or the impossibility of accessing gynophores, the infection site for *T. frezii* (20). Considering this, Paredes *et al.* (2021) tested 12 different a.i. *in vitro,* pots and field trials, using 1.5 times

the recommended dose for the LLS control. Fungicides were applied at night directly to the plant base and pegs in pot trials and targeting the soil in field trials. These authors observed high disease control with azoxystrobin (strobilurin) in pots and a 2016 field trial, and with cyproconazole (triazole) in a 2015 field trial, while chlorothalonil did not control peanut smut, probably given its limited mobility in the plant compared to the other a.i. (6). The one product registered against peanut smut, composed of two triazole fungicides (triadimenol and myclobutanil), is ineffective against LLS (19).

Currently, chemical control of fungal pathogens can be achieved by different target site fungicides, depending on their mode of action. Fungicides with varying modes of action can be used mixed or in alternating regimes on the same crop. Before testing new a.i. against a given disease we should evaluate efficacy of currently registered fungicides. Another key aspect is to evaluate dose and number of applications with the lowest environmental impact. If some a.i. registered for LLS could impact smut, a simultaneous control of both diseases would be highly beneficial. Thus, we evaluated the effect of widely used fungicides against LLS in peanut crops, simultaneously considering LLS and smut intensities, and crop production.

Materials and methods

Field trials were conducted during three consecutive seasons, 2017/18, 2018/19 and 2019/2020, in General Cabrera (GC) and Vicuña Mackenna (VM), Córdoba, Argentina (table 1). GC is representative of the historical peanut-producing area, while in VM, peanut has been recently introduced. They have loam and sandy loam soil texture, respectively.

Table 1. Coordinates, sowing and harvest dates and accumulated rainfalls at both locations for three agricultural seasons.

Tabla 1. Coordenadas, fechas de siembra y cosecha y precipitaciones acumuladas para ambas localidades durante las tres campañas agrícolas.

Location, season	Coordinates	Sowing date	Harvest date	Accumulated rainfalls (mm)
GC 2017/18	32°49'39.49''S 63°51'55.57''W	10/31/2017	03/22/2018	263
GC 2018/19	32°49'46.80''S 63°51'57.73''W	11/06/2018	04/12/2019	616
GC 2019/20	32°49'42.13''S 63°51'56.42''W	11/21/2019	04/13/2020	468
VM 2017/18	33°56'14.39''S 64°27'51.95''W	10/24/2017	04/03/2018	298
VM 2018/19	33°56'33.07''S 64°28'20.68''W	11/08/2018	04/05/2019	563
VM 2019/20	33°46'11.41''S 64°25'12.34''W	11/19/2019	04/04/2020	398

GC: General Cabrera.
VM: Vicuña Mackenna.

All trials followed a randomized complete block design with three replications, and four furrows 5 m long, spaced 0.70 m. Ten treatments were composed of different a.i. or mixtures, doses, and number of applications (table 2, page 118). All fungicides are registered in Argentina for LLS control (7). Applications were performed with a carbon dioxide pressurized backpack sprayer equipped with six hollow cone spray nozzles spaced 0.35 m apart, calibrated to 180 L/ha. Applications began upon the first symptoms of LLS. Seeds of cv. Granoleico (INASE Reg. N° 7907) were treated with 2.5 g (a.i.) of ipconazole + 2 g of metalaxyl and 30 g of carboxin + 30 g of thiram per 100 kg of seeds, preventing other soil pathogens and those carried by seeds.

Table 2. Treatments at both locations during three agricultural seasons.
Tabla 2. Tratamientos en ambas localidades durante tres campañas agrícolas.

Treat.	Active ingredients	Doses (g a.i./ha)	Number of applications
1	Control	-	-
2	Pyraclostrobin + epoxiconazole	99.75 + 37.5	4
3	Fluxapyroxad + epoxiconazole + pyraclostrobin	60 + 60 + 97.2	4
4	Chlorothalonil	1008	5
5	Pyraclostrobin + epoxiconazole	99.75 + 37.5	2
6	Fluxapyroxad + epoxiconazole + pyraclostrobin	60 + 60 + 97.2	2
7	Chlorothalonil	1008	3
8	Pyraclostrobin + epoxiconazole	59.85 + 22.5	4
9	Fluxapyroxad + epoxiconazole + pyraclostrobin	36 + 36 + 58.32	4
10	Chlorothalonil	604.8	5

g a.i/ha: grams of active ingredient per hectare.
Gramos de ingrediente activo por hectárea.

Treatments 2, 3 and 4 implied using fungicides in the registered doses and number of applications, considering residual periods. Treatments 5, 6 and 7 maintained doses but reduced applications. Finally, treatments 8, 9 and 10, reduced a.i. dose to 60% of the recommended. Treatments 5, 6, 7, 8, 9 and 10 tested whether a different dose and application number was as efficient as the registered, representing a more interesting option for peanut producers. However, risks of generating resistance must be considered at reduced doses that should not be massively adopted (as in treatments 8 to 10) (1). For all cases, the Environmental Impact Quotient (EIQ) was calculated according to Kovach *et al.* (1992), determining the environmental impact for each a.i. based on physicochemical and toxicological information. This widely used indicator evaluates pesticide risks and is useful for selecting less harmful molecules (13).

Before harvest, two cotyledonary branches per plot were collected (one branch per central furrow) and LLS intensity was calculated through incidence and severity. The first represents the percentage of diseased leaflets and the last considers the percentage of affected tissue. Incidence was calculated as the number of leaflets with LLS spots over the total number of leaflets. Severity (S) was calculated through the equation proposed by Plaut and Berger (1980): S = [(1-D) * Sx] + D, considering defoliation (D), and average severity (Sx) (calculated by a diagrammatic scale) (31).

At harvest maturity (150 days after planting), all plants in 1 m^2 per plot were collected. Pods were separated and allowed to dry until constant weight, in a dry and ventilated place. Once weighted and shelled, yield was estimated via total and confectionery quality weights, considering confectionary quality as those grains greater than 7,5 mm sieve size. Simultaneously, peanut smut incidence (percentage of affected pods) and severity (degree of symptoms in pods, through the disease severity index (DSI)) (27) were evaluated. The DSI involves a five levels scale: 0 = healthy pod, 1 = normal pod with a small sorus in a single seed, 2 = deformed or normal pod with one seed half affected, 3 = deformed pod and a completely smutted seed, 4 = deformed pod, both seeds completely smutted. The DSI was calculated using the following equation:

$$\mathbf{DSI = [(n \times 0) + (n \times 1) + (n \times 2) + (n \times 3) + (n \times 4)]\ N^{-1}}$$

where:
n = number of pods corresponding to each level (0-4)
N = total number.

For all parameters, ANOVA was performed, and means were compared using Tukey's test ($p \leq 0.05$) with InfoStat software (12).

Results and Discussion

According to a.i., concentration, dose and number of applications, EIQ values per treatment were: 1=0, 2=17.16, 3=21.80, 4=202.5, 5=8.58, 6=10.9, 7=121.23, 8=10.29, 9=13.08, and 10=121.5.

During the first year, LLS was not observed given environmental conditions, mainly precipitation (21). For the other campaigns, the disease appeared in both locations with higher intensity values in GC. In the GC 2018/19 trial (figure 1A, page 120), the lowest incidence levels were observed with chlorothalonil in five applications (treatments 4 and 10), while severity was higher only in the control (treatment 1). This agrees with Culbreath *et al.* (2018), who found chlorothalonil more efficient than almost all evaluated triazoles. Concerning the 2019/20 trial, treatment 4 had, once more, the best performance. However, other treatments, like treatment 4, achieved lower incidence (5: pyraclostrobin + epoxiconazole in 2 moments, and 7: chlorothalonil in 3 moments), and severity (3 and 9: fluxapyroxad + epoxiconazole + pyraclostrobin in 4 moments) levels. These last results show effective disease management with mixes including carboxamides, and better behavior with shorter periods between applications, as previously found (10, 23). Treatments 8 to 10, with a.i. in reduced doses, achieved effective LLS control. However, it should not constitute a strategy to be applied solely due to the possibility of creating fungal resistance (1). Nevertheless, treatments with fewer applications and thus, lower EIQ, represent a good option considering environmental risk (13). Another interesting fact is that treatments 4 and 10, with chlorothalonil, led to better control than other a.i., but with higher EIQ values. However, this a.i. has significantly low selection pressure (Fungicide Resistance Action Committee, Code M5). On the other hand, no differences were evidenced among VM treatments (figure 1B, page 120), probably because of the low disease intensity registered in that location. However, the highest LLS incidence and severity were observed without fungicides (treatment 1).

Thecaphora frezii field inoculum was quantified before planting according to Marinelli *et al.* (2008), estimating 10000 and less than 2000 teliospores per gram of soil in GC and VM, respectively. Given this disease is less dependent on weather conditions than LLS, we could evaluate smut intensity during three seasons in both locations (27). Intensity was high in GC and moderate in VM (figure 2A and 2B, page 121), incidence reached 72.08% and severity 2.34 in GC, while in VM, maximum values were 22.66% and 0.55, respectively. These results may depend on GC long history of peanut cultivation and processing, and thus, high inoculum (27). We did not observe fungicide effect on disease intensity when compared to the untreated control throughout all trials. Some authors (3, 4, 33) cite the action of chlorothalonil, triazoles, strubilurins and carboxamides for controlling soil pathogens. However, for peanut smut, effects are variable probably because of low efficacy or inability to reach gynophores through spraying (8, 20, 25). We evaluated fungicides with different mobility in plants: a non-penetrating a.i. (chlorothalonil) that cannot translocate through tissues and penetrant and mobile a.i. (epoxiconazole, pyraclostrobin and fluxapyroxad) transported through the xylem (6). These mobility differences could help these a.i reach gynophores and stop infections. Paredes *et al.* (2021) observed lower severity with azoxystrobin when compared to other fungicides and control pots. On the other hand, smut intensity in untreated control did not differ from treatments with chlorothalonil and pyraclostrobin. These outcomes align with our findings. Finally, in field trials, cyproconazole and azoxystrobin showed the best control efficiency among all treatments.

Since peanut smut intensity is directly related to crop production losses (25), and no significant effect of fungicides was observed on the former, we expected no differences in yield (table 3, page 122). In GC, differences in grain and confectionery quality grain yields were observed during the 2017-2018 season, where the untreated control presented higher production than other treatments. These results could be given by decreased yield when fungicides are applied to stressed plants (11). Treatments 1 (untreated control), 2, 3 and 5 had the highest total grain yield (864, 892, 917 and 914 kg/ha, respectively), and confectionery quality grain yield (757, 804, 791 and 792 kg/ha, respectively).

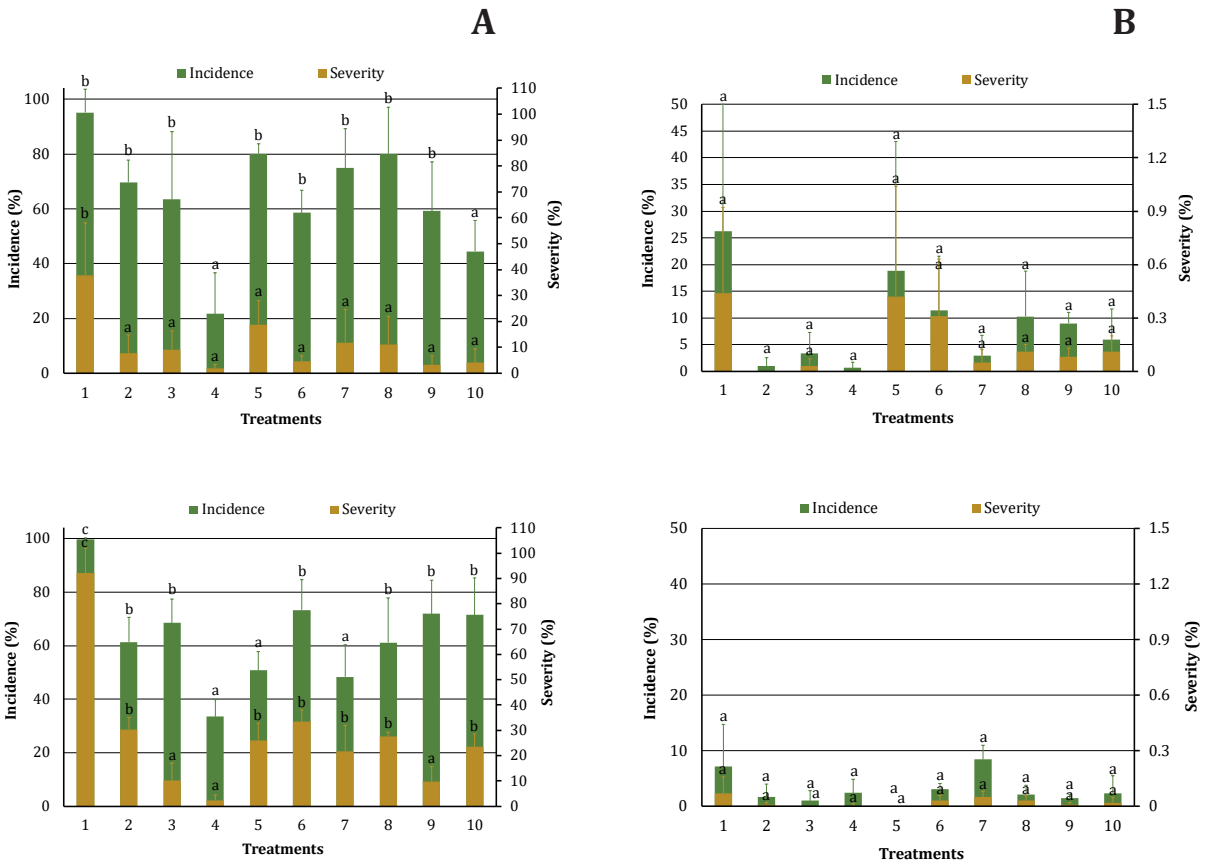

Treatments: 1) untreated control; 2) pyraclostrobin + epoxiconazole four times, 3) fluxapyroxad + epoxiconazole + pyraclostrobin four times; 4) chlorothalonil five times; 5) pyraclostrobin + epoxiconazole twice; 6) fluxapyroxad + epoxiconazole + pyraclostrobin twice; 7) chlorothalonil three times; 8) pyraclostrobin + epoxiconazole four times, reduced dose; 9) fluxapyroxad + epoxiconazole + pyraclostrobin four times, reduced dose; and 10) chlorothalonil five times, reduced dose. Different letters indicate significant differences (p<0.05).

Tratamientos: 1) control sin fungicida; 2) pyraclostrobin + epoxiconazole 4 aplicaciones; 3) fluxapyroxad + epoxiconazole + pyraclostrobin 4 aplicaciones; 4) clorotalonil 5 aplicaciones; 5) pyraclostrobin + epoxiconazole 2 aplicaciones; 6) fluxapyroxad + epoxiconazole + pyraclostrobin 2 aplicaciones; 7) clorotalonil 3 aplicaciones; 8) pyraclostrobin + epoxiconazole 4 aplicaciones, dosis reducida; 9) fluxapyroxad + epoxiconazole + pyraclostrobin 4 aplicaciones, dosis reducida; y 10) clorotalonil 5 aplicaciones, dosis reducida. Letras diferentes indican diferencias significativas (p<0,05).

Figure 1. Incidence and severity of late leaf spot in 2018/19 and 2019/20 on General Cabrera (A) and Vicuña Mackenna (B) field trials.

Figura 1. Incidencia y severidad de viruela tardía en 2018/19 y 2019/20 en los ensayos de campo de General Cabrera (A) y Vicuña Mackenna (B).

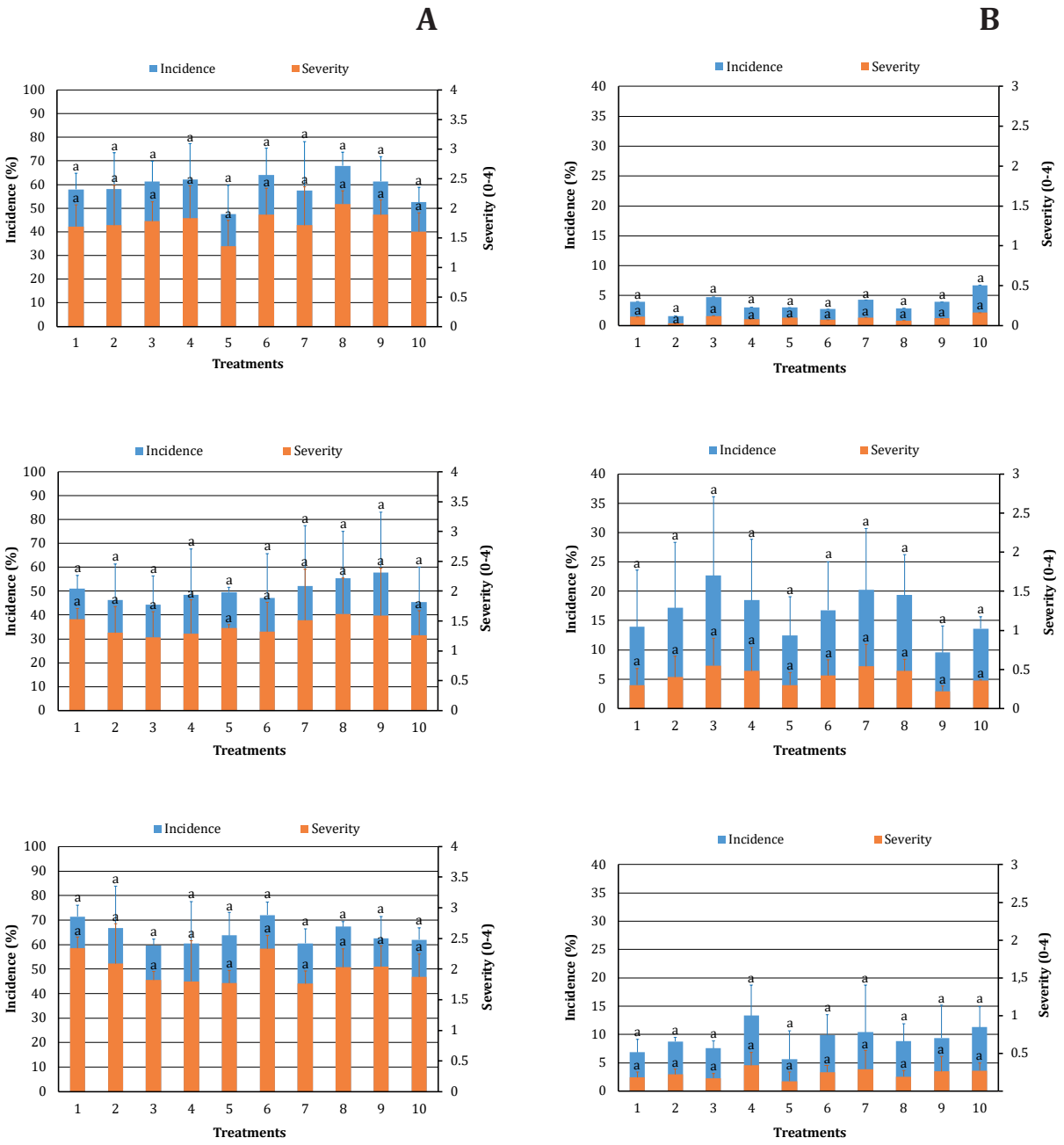

Treatments: 1) untreated control; 2) pyraclostrobin + epoxiconazole four times, 3) fluxapyroxad + epoxiconazole + pyraclostrobin four times; 4) chlorothalonil five times; 5) pyraclostrobin + epoxiconazole twice; 6) fluxapyroxad + epoxiconazole + pyraclostrobin twice; 7) chlorothalonil three times; 8) pyraclostrobin + epoxiconazole four times, reduced dose; 9) fluxapyroxad + epoxiconazole + pyraclostrobin four times, reduced dose; and 10) chlorothalonil five times, reduced dose. Different letters indicate significant differences (p<0.05).

Tratamientos: 1) control sin fungicida; 2) pyraclostrobin + epoxiconazole 4 aplicaciones; 3) fluxapyroxad + epoxiconazole + pyraclostrobin 4 aplicaciones; 4) clorotalonil 5 aplicaciones; 5) pyraclostrobin + epoxiconazole 2 aplicaciones; 6) fluxapyroxad + epoxiconazole + pyraclostrobin 2 aplicaciones; 7) clorotalonil 3 aplicaciones; 8) pyraclostrobin + epoxiconazole 4 aplicaciones, dosis reducida; 9) fluxapyroxad + epoxiconazole + pyraclostrobin 4 aplicaciones, dosis reducida; y 10) clorotalonil 5 aplicaciones, dosis reducida. Letras diferentes indican diferencias significativas (p<0,05).

Figure 2. Incidence and severity of peanut smut in 2017/18, 2018/19 and 2019/20 in General Cabrera (A) and Vicuña Mackenna (B) field trials.

Figura 2. Incidencia y severidad de carbón del maní en 2017/18, 2018/19 y 2019/20 en los ensayos de campo de General Cabrera (A) y Vicuña Mackenna (B).

Table 3. Peanut yield parameters (kg/ha) recorded in General Cabrera (GC) and Vicuña Mackenna (VM) for the three agricultural seasons.

Tabla 3. Parámetros de rendimiento de maní (kg/ha) medidos en General Cabera (GC) y Vicuña Mackenna (VM) para las tres campañas agrícolas.

Location	Treat.	2017-2018			2018-2019			2019-2020		
		P.	G.	C.Q.	P.	G.	C.Q.	P.	G.	C.Q.
GC	1	1977±550	864±145*	757±109*	4390±588	2451±314	2174±245	2867±1051	1138±481	856±326
	2	1907±245	892±180*	804±155*	4850±331	2832±316	2535±261	4491±946	1981±750	1682±688
	3	1940±207	917±174*	791±128*	5801±402	3354±424*	2860±262*	4179±1059	1978±683	1625±571
	4	1717±368	708±249	631±249	4997±662	2735±734	2405±775	3921±2063	1791±1023	1544±890
	5	1777±453	914±224*	792±148*	5045±1149	2812±624	2430±451	3327±1013	1508±277	1202±132
	6	1407±699	576±243	483±263	4395±637	2348±98	2078±98	4115±1536	1527±578	1231±498
	7	1063±131	471±157	433±152	4417±1478	2378±110	1888±718	3067±958	1401±519	1140±461
	8	1330±140	518±28	457±60	4443±584	2259±470	1995±453	3499±914	1553±733	1318±611
	9	1400±234	623±124	581±120	4711±709	2459±239	2142±313	4160±1269	1825±902	1551±840
	10	1423±193	695±133	606±135	5880±509	3362±461*	2996±632*	4597±1858	2273±1248	1907±1048
VM	1	6807±202	5038±314	4590±477	6009±751	4264±476	3799±427	2761±691*	1973±683*	1316±377*
	2	5200±223	3887±1825	3456±165	5076±293	3206±258	2587±177	3520±268	2645±198	2175±119
	3	6303±200	4655±1621	4262±160	5109±383	3279±401	2729±376	5404*±363	3959*±62	3130±180
	4	5030±215	3715±1679	3216±154	5452±438	3652±331	3140±504	4371±1246	3241±896	2656±933
	5	7610±275	5617±1860	5064±168	5586±413	3854±272	3167±133	3705±671	2808±445	2197±452
	6	5267±173	3946±1404	3496±140	5963±1689	3986±865	3370±747	4065±483	2935±428	2488±756
	7	5727±772	4158±745	3664±691	5134±268	3422±104	2846±109	4589±523	3326±499	2580±1152
	8	4277±190	3140±1485	2850±133	5065±1163	3369±947	2844±1025	4417±852	3297±649	2740±607
	9	5923±879	4405±668	3839±659	4931±1209	3332±106	2664±1141	4136±166	3089±249	2582±490
	10	5323±847	3876±517	3594±498	5922±557	4087±311	3451±230	4335±850	3164±686	2671±694

Pod (P.), grain (G.) and confectionery quality grain (C.Q.) yields (kg/ha). Means ± standard deviation. Treatments: 1) untreated control; 2) pyraclostrobin + epoxiconazole four times; 3) fluxapyroxad + epoxiconazole + pyraclostrobin four times; 4) chlorothalonil five times; 5) pyraclostrobin + epoxiconazole twice; 6) fluxapyroxad + epoxiconazole + pyraclostrobin twice; 7) chlorothalonil three times; 8) pyraclostrobin + epoxiconazole four times, reduced dose; 9) fluxapyroxad + epoxiconazole + pyraclostrobin four times, reduced dose; and 10) chlorothalonil five times, reduced dose. Significant differences (p<0.05) per column are represented by *.

Rendimientos (kg/ha) de vainas, granos y granos calidad confitería. Medias ± error estándar. Tratamientos: 1) control sin fungicida; 2) pyraclostrobin + epoxiconazole 4 aplicaciones; 3) fluxapyroxad + epoxiconazole + pyraclostrobin 4 aplicaciones; 4) clorotalonil 5 aplicaciones; 5) pyraclostrobin + epoxiconazole 2 aplicaciones; 6) fluxapyroxad + epoxiconazole + pyraclostrobin 2 aplicaciones; 7) clorotalonil 3 aplicaciones; 8) pyraclostrobin + epoxiconazole 4 aplicaciones, dosis reducida; 9) fluxapyroxad + epoxiconazole + pyraclostrobin 4 aplicaciones, dosis reducida; y 10) clorotalonil 5 aplicaciones, dosis reducida. Las diferencias significativas (p<0,05) dentro de la misma columna, están representados con *.

On the other hand, during the 2018-2019 season, treatments 3 and 10 showed the highest grain yield (3354 and 3362 kg/ha, respectively) and confectionery quality yield (2860 and 2996 kg/ha, respectively). Both treatments achieved lower LLS intensity than control, as previously found (9, 23). Finally, during the 2019-2020 season, no statistical differences were found for productivity parameters in GC. For VM trials, statistical differences for crop yield were only found in the 2019-2020 season. Treatment 1 had 22-49%, 25-50% and 40-58% lower values than the rest of the treatments for pod, grain and confectionery quality grain yields, respectively. In contrast, treatment 3 had 18-53% and 19-50% higher pod and grain yields than the other treatments. Finally, the difference between treatments 1 and 3 was approximately 100%, as found by Culbreath *et al.* (2018).

Considering each season, results were statistically different between locations. Table 4 shows markedly higher LLS and peanut smut incidence and severity in GC than in VM. Although Paredes *et al*. (2024) report that peanut smut benefits from drought, we did not observe any correlation between the highest intensities and lowest rainfall, except for GC when comparing the first and second seasons. However, this behavior is not linear and depends on whether soil moisture falls below 30% of soil water-holding capacity and on which growth stage (28). Regarding yield, all values were superior in VM for all years. Disease intensity and crop yield are possibly explained by cultivation history in each area.

Table 4. LLS intensity, peanut smut intensity and crop yield, across trials.
Tabla 4. Intensidad de VT, carbón del maní y rendimiento del cultivo a lo largo de los años.

	2017-2018		2018-2019		2019-2020	
	GC	VM	GC	VM	GC	VM
LLS[a] Incidence (%)	-	-	64.73 b	8.95 a	64.01 b	2.97 a
LLS Severity (%)	-	-	10.99 b	0.16 a	27.66 c	0.02 a
Smut Incidence (%)	58.98 b	3.70 a	49.76 b	16.41 a	64.63 b	9.19 a
Smut Severity	1.76 b	0.09 a	1.40 b	0.40 a	1.99 b	0.23 a
P[b] (kg/ha)	1594 b	5746 a	4892 b	5424 a	3822 a	4130 a
G[c] (kg/ha)	717 b	4243 a	2699 b	3645 a	1697 b	3043 a
CQ[d] (kg/ha)	633 b	383 a	2350 b	3059 a	1405 b	2453 a

[a] Late leaf spot. [b] Pod yield. [c] Grain yield. [d] Confectionery quality grains yield. Comparison between locations partitioned by year. Different letters represent significant differences (p<0.05).

[a] Viruela tardía. [b] Rendimiento en vainas. [c] Rendimiento en granos. [d] Rendimiento en granos calidad confitería. Comparación entre localidades, particionadas por año. Letras diferentes representan diferencias significativas (p<0,05).

Fungicide application leads peanut LLS management. Additionally, considering peanut smut is hard to control, having a fungicide against both diseases simultaneously would be significantly useful. Considering two different sites and three cropping seasons, this study showed how some majorly used fungicides for peanut crops in Argentina could control LLS even at lower doses and application frames than usual. However, these treatments proved no effects against peanut smut. Further testing should consider different a.i., their combinations, doses and application frames against LLS and peanut smut. Additionally, considering genetic resistance and biocontrol strategies with microorganisms is key for integrated management strategies.

Conclusions

Disease intensities of late leaf spot (LLS) and peanut smut are closely linked to the agricultural history of locations and weather conditions in a certain season. Chemical control of LLS has been effective, and certain options exhibit a lower environmental impact, particularly important for integrated management strategies. Conversely, fungicides demonstrated inefficacy against peanut smut in these field trials. We also demonstrated the importance of quantifying inoculum density given its direct relationship with disease levels to avoid certain locations or choose resistant varieties. Further studies on the biology of *T. frezii* and management of peanut smut should contribute to genetic resistance development.

References

1. Amaradasa, B. S.; Everhart, S. E. 2016. Effects of sublethal fungicides on mutation rates and genomic variation in fungal plant pathogen, *Sclerotinia sclerotiorum*. PLoS One. 11(12): e0168079. https://doi.org/10.1371/journal.pone.0168079
2. Anco, D. J.; Thomas, J. S.; Jordan, D. L.; Shew, B. B.; Monfort, W. S.; Mehl, H. L.; Small, I. M.; Wright, D. L.; Tillman, B. L.; Dufault, N. S.; Hagan, A. K.; Campbell, H. L. 2020. Peanut yield loss in the presence of defoliation caused by late or early leaf spot. Plant Disease. 104: 1390-1399. https://doi.org/10.1094/PDIS-11-19-2286-RE
3. Augusto, J.; Brenneman, T. B. 2011. Implications of fungicide application timing and post-spray irrigation on disease control and peanut yield. Peanut Science. 38(1): 48-56. https://doi.org/10.3146/PS10-11.1
4. Augusto, J.; Brenneman, T. B.; Culbreath, A. K.; Sumner, P. 2010. Night spraying peanut fungicides. I. Extended fungicide residual and integrated disease management. Plant Disease. 94(6): 676-682. https://doi.org/10.1094/PDIS-94-6-0676
5. Bressano, M.; Massa, A.; Arias, R.; De Blas, F.; Oddino, C.; Faustinelli, P.; Soave, J.; Soave, S.; Perez, A.; Sololev, V.; Marshall, C.; Balzarini, M.; Buteler, M.; Seijo, G. 2019. Introgression of peanut smut resistance from landraces to elite peanut cultivars (*Arachis hypogaea* L.). PLoS ONE. 14(2): e0211920. https://doi.org/10.1371/journal.pone.0211920
6. Carmona, M.; Sautua, F.; Pérez-Hérnandez, O.; Reis, E. M. 2020. Role of fungicide applications on the integrated management of wheat stripe rust. Frontiers in Plant Science. 11: 733. https://doi.org/10.3389/fpls.2020.00733
7. CASAFE. 2023. Cámara de Sanidad Agropecuaria y Fertilizantes. Guía online de productos fitosanitarios. https://guiaonline.casafe.org/ (Accessed on: Sep. 6 2023).
8. Cazón, I.; Bisonard, E. M.; Conforto, C.; March, G.; Rago, A. 2013. Estrategias para el manejo del carbón del maní. Actas de resúmenes XXVIII Jornada Nacional del Maní. General Cabrera, Córdoba. Argentina. p: 28-30.
9. Culbreath, A. K.; Gevens, A. J.; Stevenson, K. L. 2018. Relative effects of demethylation-inhibiting fungicides on late leaf spot of peanut. Plant Health Progress. 19(1): 23-26. https://doi.org/10.1094/PHP-09-17-0053-RS
10. Culbreath, A. K.; Brenneman, T. B.; Kemerait, R. C.; Stevenson, K. L.; Henn, A. 2020. Effect of DMI and QoI fungicides mixed with the SDHI fungicide penthiopyrad on late leaf spot of peanut. Crop Protection. 137: 105298. https://doi.org/10.1016/j.cropro.2020.105298
11. Dias, M. A. 2012. Phytotoxicity: An overview of the physiological responses of plants exposed to fungicides. Journal of Botany. Article ID 135479. https://doi.org/10.1155/2012/135479
12. Di Rienzo, J. A.; Casanoves, F.; Balzarini, M. G.; Gonzales, L.; Tablada, M.; Robledo, C. W. InfoStat versión 2020. Centro de Transferencia InfoStat, FCA, Universidad Nacional de Córdoba, Argentina. http://www.infostat.com.ar
13. Dugan, S. T.; Muhammetoglu, A.; Uslu, A. 2023. A combined approach for the estimation of groundwater leaching potential and environmental impacts of pesticides for agricultural lands. Science of The Total Environment. 901: 165892. https://doi.org/10.1016/j.scitotenv.2023.165892
14. Fulmer, A. M. 2017. Differentiation, prediction and management of early and late leaf spot of peanut in the southeastern United States and Haiti. Ph.D. thesis. University of Georgia, Athens, GA.
15. Ganuza, M.; Pastor, N.; Erazo, J.; Andrés, J.; Reynoso, M.; Rovera, M.; Torres, A. 2018. Efficacy of the biocontrol agent *Trichoderma harzianum* ITEM 3636 against peanut smut, an emergent disease caused by *Thecaphora frezii*. European Journal of Plant Pathology. 151(1): 257-262. https://doi.org/10.1007/s10658-017-1360-0
16. Giordano, D.F.; Pastor, N.; Palacios, S.; Oddino, C.; Torres, A. 2021. Peanut leaf spot caused by *Nothopassalora personata*. Tropical plant pathology. 46: 139-151. https://doi.org/10.1007/s40858-020-00411-3
17. Jordan, B. S.; Culbreath, A. K.; Brenneman, T. B.; Kemerait, R. C.; Branch, W. D. 2017. Late leaf spot severity and yield of new peanut breeding lines and cultivars grown without fungicides. Plant Disease. 101(11): 1843-1850. https://doi.org/10.1094/PDIS-02-17-0165-RE
18. Kovach, J.; Petzoldt, C.; Degni, J.; Tette, J. 1992. A method to measure the environmental impact of pesticides. New York's Food and Life Sciences Bulletin. 139: 1-8.
19. Laboratorios NOVA. 2023. IRIDIUM. https://laboratorios-nova.com/fungicidas-fungicidas-insecticidas/iridium/ (Accessed on Sep. 12 2024).
20. Marinelli, A.; March, G.; Oddino, C. 2008. Aspectos biológicos y epidemiológicos del carbón del maní (*Arachis hypogaea* L.) causado por *Thecaphora frezii* Carranza & Lindquist. AgriScientia. 25(1): 1-5.
21. Marinelli, A.; Oddino, C.; March, G. 2017. 2ª ed. Enfermedades fúngicas del maní. En: Fernández, E.; Giayetto, O. (Ed.). El cultivo de maní en Argentina. Río Cuarto, Córdoba. Ediciones UNRC. p: 285-311.
22. Oddino, C.; Mortigliengo, S.; Moresi, A.; Soave, J.; Giuggia, J.; Ferrari, S.; Cassano, C.; Martinez, F.; Molineri, A.; Moran, F.; Soave, S.; Torre, D.; Butteler, M.; Bianco, C.; Bressano, M.; De Blas, F. 2017. Efecto de fungicidas foliares sobre la intensidad de viruela y carbón en diferentes cultivares de maní. Ciencia y tecnología de Cultivos Industriales. 6(9): 99-105.

23. Oddino, C.; Giordano, F.; Paredes, J.; Cazón, L.; Giuggia, J.; Rago, A. 2018. Efecto de nuevos fungicidas en el control de viruela del maní y el rendimiento del cultivo. Ab Intus. 1(1): 9-17.
24. Oddino, C.; Rosso, M.; Soave, J.; Soave, S.; Mendoza, M.; Giordano, D. F.; Bressano, M.; De Blas, F.; Mortigliengo, S.; Butteler, M. 2023. Comportamiento de variedades de maní resistentes a carbón a través de los años. Actas de resúmenes XXXVIII Jornada Nacional del Maní. General Cabrera, Córdoba. Argentina.
25. Paredes, J. 2017. Importancia regional del carbón del maní (*Thecaphora frezii*) y efecto de ingredientes activos de fungicidas sobre la intensidad de la enfermedad. Master thesis. Universidad Nacional de Río Cuarto, Córdoba.
26. Paredes, J. A.; Cazón, L. I.; Oddino, C.; Monguillot, J. H.; Rago, A. M.; Edwards Molina, J. P. 2021. Efficacy of fungicidal management of peanut smut. Crop Protection. 140: 105403. https://doi.org/10.1016/j.cropro.2020.105403
27. Paredes, J. A.; Edwards Molina, J. P.; Cazón, L. I.; Asinari, F.; Monguillot, J. H.; Morichetti, S. A.; Rago, A. M.; Torres, A. M. 2022. Relationship between incidence and severity of peanut smut and its regional distribution in the main growing region of Argentina. Tropical Plant Pathology. 47: 233-244. https://doi.org/10.1007/s40858-021-00473-x
28. Paredes, J. A.; Guzzo, M. C.; Monguillot, J. H.; Asinari, F.; Posada, G. A.; Oddino, C. M.; Giordano, D. F.; Morichetti, S. A.; Torres, A. M.; Rago, A. M.; Monteoliva, M. I. 2024. Low water availability increases susceptibility to peanut smut (*Thecaphora frezzii*) in peanut crop. Plant Pathology. 73(2): 316-325. https://doi.org/10.1111/ppa.13810
29. Plaut, J. L.; Berger, R. D. 1980. Development of *Cercosporidium personatum* in three peanut canopy layers. Peanut Science. 7(1): 46-49. https://doi.org/10.3146/i0095-3679-7-1-11
30. Rago, A.; Cazón, I.; Paredes, J.; Edwards Molina, J.; Bisonard, M.; Oddino, C. 2017. Peanut Smut: From an emerging disease to an actual threat to Argentine peanut production. Plant Disease. 101(3): 400-408. http://dx.doi.org/10.1094/PDIS-09-16-1248-FE
31. Shokes, F. M.; Berger, R. D.; Smith, D. H.; Rasp, J. M. 1987. Reliabity of disease assessment procedures. A case study with late leafspot of peanut. Oléagineux. 42: 245-251.
32. USDA. 2023. United States Department of Agriculture. Peanut explorer. https:// ipad.fas.usda.gov/cropexplorer/cropview/commodityView.aspx?cropid=2221000&sel_year=2022&rankby=Production (Accessed on Sep. 12 2023).
33. Woodward, J. E.; Brenneman, T. B.; Kemerait, R. C.; Smith, N. B.; Culbreath, A. K.; Stevenson, K. L. 2008. Use of resistant cultivars and reduced fungicide programs to manage peanut diseases in irrigated and non-irrigated field. Plant Disease. 92(6): 896-902. http://dx.doi.org/10.1094/PDIS-92-6-0896

Temporal Analysis of Northern Corn Leaf Blight (*Exserohilum turcicum* Pass. Leonard & Suggs) Epidemics

Análisis temporal de epidemias del tizón foliar común del maíz causado por *Exserohilum turcicum* (Pass.) Leonard & Suggs

Roberto Luis De Rossi [1*], Fernando Andrés Guerra [1], María Cristina Plazas [1], Ezequiel Vuletic [1], Gustavo Darío Guerra [1], Erlei Melo Reis [2]

Originales: *Recepción:* 22/05/2023 - *Aceptación:* 24/06/2025

Abstract

Field trials were conducted in six locations in central-northern Córdoba, Argentina, using four maize hybrids with varying resistance to northern corn leaf blight (NCLB), caused by *Exserohilum turcicum*. Naturally occurring NCLB epidemics were evaluated. We analyzed disease severity (S%), disease progress curve (DPC), area under the disease progress curve, final severity (FS%) and apparent infection rate (r). Disease progress curves were simultaneously analyzed by fitting nonlinear epidemiological models (Gompertz and Logistic). Ballesteros and Villa María were the localities with the highest FS in susceptible hybrids (45% and 37.5%, respectively). Levels of FS were below 5% in Jesús María, Río Segundo and Freyre, and under 1% in El Tío. The highest AUDPC values were also observed in Ballesteros and Villa María (2150.1 and 1335.7, respectively). In the other locations, AUDPC values remained under 320, with statistically significant differences in all cases ($p< 0.05$). The resistant hybrid exhibited the lowest apparent infection rate compared to the other genotypes. Epidemic progress displayed, to varying degrees, sigmoid-shaped curves characteristic polycyclic diseases. On average, the Gompertz model best fitted disease progress data across all evaluated genotypes with an R^2 of 0.909 and an adjusted coefficient (R^{2*}) of 0.849. The temporal analysis provided key epidemiological insights into the maize-NCLB pathosystem, supporting the development of effective management strategies.

Keywords
Zea mays • *Helminthosporium* • epidemiology • AUDPC • Córdoba

1 Universidad Católica de Córdoba. Avda. Armada Argentina N° 3555. C P. X5016DHK. Córdoba. Argentina. * roberto.derossi@ucc.edu.ar
2 Instituto Agris. Passo Fundo. Río Grande do Sul. Brasil.

Resumen

Se realizaron ensayos de campo en seis localidades de la región centro-norte de Córdoba, utilizando cuatro híbridos de maíz con diferentes niveles de resistencia al tizón foliar común del maíz (TFC), causado por *Exserohilum turcicum*. Se evaluaron epidemias de la enfermedad generadas de forma natural. Se analizó la severidad (S%), la curva de progreso de enfermedad (CPE), el área bajo la curva de progreso de la enfermedad (ABCPE), la severidad final (SF%) y tasa infección aparente (r). Las curvas de progreso de la enfermedad se analizaron simultáneamente según el ajuste a los modelos epidemiológicos no lineales Logístico y de Gompertz. Ballesteros y Villa María fueron las localidades con mayor SF en materiales susceptibles, siendo de 45% y 37,5% respectivamente. Los niveles de SF fueron inferiores al 5% en Jesús María, Río Segundo y Freyre, y menores al 1% en El Tío. Así mismo, las mayores ABCPE se registraron en Ballesteros y Villa María (2150,1 y 1335,7, respectivamente). En las demás localidades los valores de ABCPE fueron menores a 320, presentando en todos los casos diferencias estadísticamente significativas ($p<0,05$). El híbrido resistente obtuvo la menor tasa de infección aparente en comparación con los otros genotipos. El progreso de las epidemias determinó, en mayor o menor magnitud, curvas de formato sigmoidal típicas de enfermedades policíclicas. En promedio, el modelo de Gompertz fue el que mejor se ajustó a los datos de progreso de la enfermedad en todos los genotipos evaluados, con un R^2 de 0,909 y un coeficiente ajustado (R^{2*}) de 0,849. El análisis temporal proporcionó información epidemiológica clave sobre el patosistema maíz - tizón foliar común, que ayuda a la implementación de técnicas efectivas para su manejo y control.

Palabras clave
Zea mays • *Helminthosporium* • epidemiología • ABCPE • Córdoba

Introduction

Corn (*Zea mays* L.) is a strategic crop in Argentina. According to the final report elaborated by the Bolsa de Cereales de Buenos Aires (2019) for 2020-21, more than 6.6 million hectares were sown, producing 57 million tons of grains. Average national production was 8280 kg. ha^{-1}, contributing over 14.8 billion USD to the country´s gross domestic product.

Among several diseases affecting corn, northern corn leaf blight (NCLB) is highly prevalent, with increasing incidence and severity in Argentina (8). NCLB is caused by the fungus *Exserohilum turcicum* (Pass.) K. J. Leonard & Suggs [synonym: *Helminthosporium turcicum* Pass.], anamorph of *Setosphaeria turcica* (Luttr.) K. J. Leonard & Suggs. This disease can cause severe yield losses under particular host-pathogen-environment interactions. Yield reductions typically range between 15 and 50% (7, 10, 28) but may even reach 98% (18).

In general, effective management strategies are based on epidemiological studies. Temporal analysis of disease progress is critical for many epidemiological investigations (23). Understanding temporal dynamics of NCLB is essential to describe disease progression, develop sampling plans, design controlled experiments, and asses yield losses. To date, Argentina has scarce information on NCLB development in different corn hybrids, and thus, we hypothesize that temporal epidemiological information can contribute to more effective management decisions.

Temporal analysis allows constructing disease progress curves (DPCs) representing the epidemic process (19) and pathogen, host, and environment interactions (31). Curve shapes and their components, initial disease level (y_0), apparent infection rate (r), final disease level (y_f), and area under the progress disease curve (AUDPC), allow epidemic characterization and management (3).

DPCs can be studied using mathematical models that quantitatively describe epidemic biological dynamics, considering parameter estimates, like Logistic, Gompertz, and monomolecular models (23).

NCLB severity and temporal progress significantly vary among maize hybrids with different resistance. These differences can be characterized using nonlinear epidemiological models, under the agro-climatic conditions of the central-northern region of Córdoba.

NCLB epidemiology provides the basis for developing management strategies within an agroecosystem. This study conducted a temporal analysis of NCLB epidemics by comparing hybrids with different disease responses across multiple localities.

Materials and Methods

Experimental Sites, Hybrids and Experimental Design

During the 2015/2016 growing season, six field experiments were conducted across six locations of central-northern Córdoba, Argentina (latitudes -32.519004 to -29.432741 and longitudes -62.185749 to -64.069798) (table 1). Four corn hybrids were evaluated at each site in a randomized complete block design with four replicates. Plots consisted of eight rows, 4 m wide and 10 m long, spaced 0.52 m. The four hybrids were KWS 4321 (susceptible, S), KWS 1516 (moderately susceptible, MS), KWS 1529 (moderately resistant, MR), and KWS Exp20 (resistant, R). All seeds were provided by KWS Argentina corn seed company.

Sowing was performed between December 2015 and February 2016, following soybean season. Crop rotation scheme was corn-soybean-corn under non-tillage conditions; thus, corn debris from the two preceding seasons remained in the fields. Seeding rates varied by location according to yield potential, with an average of 72.000 seeds. ha^{-1}. Each experiment followed standard commercial agronomic practices, including fertilization with 240 kg. ha^{-1} urea at sowing and 4 L. ha^{-1} of liquid nitrogen at the V4 stage. Insecticides were not required, and no fungicides were applied to allow natural development of foliar diseases.

Table 1. Site, sowing date, and georeferencing of trials conducted in central-northern Córdoba, Argentina, during the 2015-16 maize season.

Tabla 1. Lugar, fecha de siembra y georreferenciación de los ensayos establecidos en la región centro-norte de Córdoba durante la campaña agrícola 2015-16 para maíz.

Trial (n°)	Site	Sowing date	Latitude	Longitude
1	Ballesteros	02/02/2016	-32.538153	-62.963570
2	Villa María	14/12/2015	-32.478755	-63.236600
3	Jesús María	17/12/2015	-30.790571	-64.069798
4	Río Segundo	23/12/2015	-31.614026	-63.937066
5	Freyre	15/12/2015	-31.153642	-62.185749
6	El Tío	10/01/2016	-31.366282	-62.825914

Field Evaluations

Experimental plots were established in intensively cultivated areas. NCLB epidemics developed naturally. Initial inoculum originated from the experimental sites (infected seeds and saprophytically infected corn residues) and airborne spores from neighboring fields, generating primary and secondary infection cycles.

Disease severity was assessed at 30, 45, 60, 85, 100 and 120 days after sowing (DAS) in each locality. Six plants per block were randomly selected, totaling 24 plants per hybrid at each time point. Leaf blight severity was estimated as the ratio of affected to healthy leaf area, expressed as a percentage, using the diagrammatic scale by Fullerton (1982). Evaluations were performed on the four uppermost unfolded leaves during vegetative stages and on the ear leaf (el), plus leaves immediately above (el+1) and below (el-1) ear leaves, during reproductive stages.

Final severity (FS, %) was determined at 100 DAS, corresponding to the dough grain stage (R4) (29). Severity assessments over time were used to calculate AUDPC for each hybrid using the following equation:

$$AUDPC = \sum_{i=1}^{n-1} \left[\left(\frac{Yi+(Yi+1)}{2} \right) ((ti+1) - ti) \right]$$

where:
Y_i and $Y1 + 1$ = disease severity values recorded in two consecutive assessments
$[(ti + 1) - ti]$ = time interval between assessments
n = number of evaluations (23).

FS and AUDPC were subjected to ANOVA and Tukey test (p= 0.05), with InfoStat statistical package (11).

DPCs were constructed by plotting accumulated disease severity (dependent variable) against time (independent variable). Disease progress rate curves (*dy/dt*) were also plotted for each hybrid at each location.

Disease severity data were fitted with nonlinear Logistic and Gompertz models (20) for each hybrid x location x replicate combination:

$$y = (1 + Be^{-rLt})^{-1} \quad (i)$$

for the Logistic model, and

$$y = exp(-Be^{-rGt}) \quad (ii)$$

for the Gompertz model

where $B = (1 - y_0) / y_0$ in Equation *i* and $-\ln(y_0)$ in Equation *ii*
y = disease severity (as a proportion)
rL and rG = rate parameters for the Logistic and Gompertz models, respectively
t = time
y_0 = disease severity at epidemic start (at V4, t = 0). Model fit was evaluated using the coefficient of determination (R^2) of transformed disease proportion vs. time, and the adjusted coefficient of determination (R^{2*}) of predicted *vs.* observed values (nonlinearized, untransformed) (20).

Results and Discussion

The temporal analysis of NCLB epidemics revealed differences in DPCs, AUDPC, FS, and r among the four evaluated hybrids across six localities during the 2015-16 growing season (table 2, page 130 and table 3, page 131; figure 1, page 132 and figure 2, page 133).

All hybrids exhibited similar disease progress trends across the six localities. However, FS and AUDPC showed statistically significant differences among localities (p<0.05). The highest FS values in susceptible (S) hybrids were recorded in Ballesteros and Villa María (45 and 37.5 %, respectively) (figure 3, page 134). In contrast, FS values in Jesús María, Río Segundo and Freyre were under 5%, while in El Tío, under 1 %. Although disease pressure was low in the latter locations, differences in FS remained statistically significant (p<0.05). Similarly, the highest AUDPC values were observed in Ballesteros and Villa María (2150.1 and 1335.7, respectively), whereas in the remaining localities, AUDPC values were below 320, with statistically significant differences (p<0.05) (table 2, page 130). Notably, the February sowing date in Ballesteros was experimentally included to expose the hybrids to different environmental conditions.

Both FS and AUDPC effectively differentiated hybrid reactions across localities. FS is a practical and easy-to-measure parameter, whereas AUDPC requires greater sampling effort but discriminates between hybrids with similar disease behavior (table 2, page 130). The FS assessed on el, el+1 and el-1 at R4 stage has been frequently reported as strongly associated with yield losses, differentiating hybrids with responses to NCLB (12, 25, 26).

Table 2. Final severity (FS) and area under the disease progress curve (AUDPC) in maize hybrids with different reactions to northern corn leaf blight (*Exserohilum turcicum*) in central-northern Córdoba, Argentina, during 2015-16.

Tabla 2. Severidad final (FS) y área bajo la curva de progreso de la enfermedad (ABCPE) en híbridos de maíz con diferente respuesta al tizón foliar común del maíz (*Exserohilum turcicum*) en la región centro-norte de Córdoba, Argentina, durante la campaña agrícola 2015-16.

Site	Reaction	FS (%)		AUDPC	
Ballesteros	R	2.0	a*	147.4	a*
	MR	15.0	ab	640.1	b
	MS	18.0	b	911.1	b
	S	45.0	c	2150.1	c
Villa María	R	3.3	a	165.3	a
	MR	3.0	a	161.0	a
	MS	4.7	a	244.3	a
	S	37.5	b	1335.7	b
Jesús María	R	0.0	a	8.0	a
	MR	3.0	b	161.9	b
	MS	3.0	b	206.0	b
	S	5.0	b	270.3	b
Río Segundo	R	1.0	a	29.5	a
	MR	1.5	a	68.3	b
	MS	2.0	a	83.0	bc
	S	4.0	b	142.1	c
Freyre	R	1.0	a	90.0	a
	MR	1.0	a	92.8	a
	MS	1.5	a	151.6	a
	S	3.5	b	319.4	b
El Tío	R	0.0	a	7.5	a
	MR	0.0	a	3.6	a
	MS	0.0	a	7.5	a
	S	0.1	b	13.1	b

Reaction: R = resistant, MR = moderately resistant,MS=moderately susceptible, S = Susceptible; FS (%) = final severity; AUDPC = area under the disease progress curve; * Different letters indicate statistically significant differences, Tukey test (α = 0.05).

Reacción: R = resistente, MR = moderadamente resistente, MS = moderadamente susceptible, S = Susceptible; FS (%) = Severidad final; ABCPE = área bajo la curva de progreso de la enfermedad; * Letras diferentes indican diferencias estadísticamente significativas, test de Tukey (α = 0,05).

Table 3. Nonlinear regression for Logistic and Gompertz models fitted to disease severity data of northern corn leaf blight (*Exserohilum turcicum*) in the 2015/16 season, in Ballesteros, Villa María and Jesús María, central-northern Córdoba, Argentina, for four maize hybrids with different reaction to NCLB.

Tabla 3. Regresión no lineal para modelos Logísticos y Gompertz ajustados a los datos de la severidad del tizón foliar común del maíz (*Exserohilum turcicum*) en la campaña agrícola 2015/16, en las localidades de Ballesteros, Villa María y Jesús María, de la región centro-norte de Córdoba, Argentina para cuatro híbridos de maíz con diferente reacción a la enfermedad.

Site	Hybrid reaction	Models	R^2	R^{*2}	y_0	r
Ballesteros	R	Logistic	0.745	0.352	-9.205	0.060
		Gompertz	0.812	0.506	-2.200	0.009
	MR	Logistic	0.893	0.795	-9.545	0.082
		Gompertz	0.985	0.943	-2.340	0.017
	MS	Logistic	0.900	0.697	-7.972	0.067
		Gompertz	0.942	0.863	-2.165	0.016
	S	Logistic	0.890	0.867	-7.736	0.078
		Gompertz	0.957	0.971	-2.210	0.023
Villa María	R	Logistic	0.865	0.711	-8.648	0.053
		Gompertz	0.874	0.814	-2.194	0.009
	MR	Logistic	0.859	0.647	-8.625	0.052
		Gompertz	0.867	0.765	-2.187	0.009
	MS	Logistic	0.894	0.764	-8.371	0.055
		Gompertz	0.944	0.891	-2.165	0.010
	S	Logistic	0.979	0.842	-9.738	0.084
		Gompertz	0.894	0.939	-2.607	0.022
Jesús María	R	Logistic	-	-	-	-
		Gompertz	-	-	-	-
	MR	Logistic	0.821	0.861	-7.819	0.043
		Gompertz	0.914	0.936	-2.064	0.008
	MS	Logistic	0.779	0.654	-7.623	0.043
		Gompertz	0.879	0.775	-2.026	0.008
	S	Logistic	0.822	0.839	-7.685	0.048
		Gompertz	0.926	0.936	-0.009	0.009

Reaction: R = Resistant. MR = moderately resistant. MS = moderately susceptible. S = susceptible.

R^2 = coefficient of determination; R^{*2} = adjusted coefficient of determination between non-transformed observed and predicted values; y_0 = initial inoculum; r = apparent infection rate

Reacción: R = resistente. MR = moderadamente resistente. MS = moderadamente susceptible. S = susceptible.

R^2 = coeficiente de determinación; R^{*2} = coeficiente de determinación entre los valores predichos y observados no transformados; y_0 = inóculo inicial; r = tasa de infección aparente.

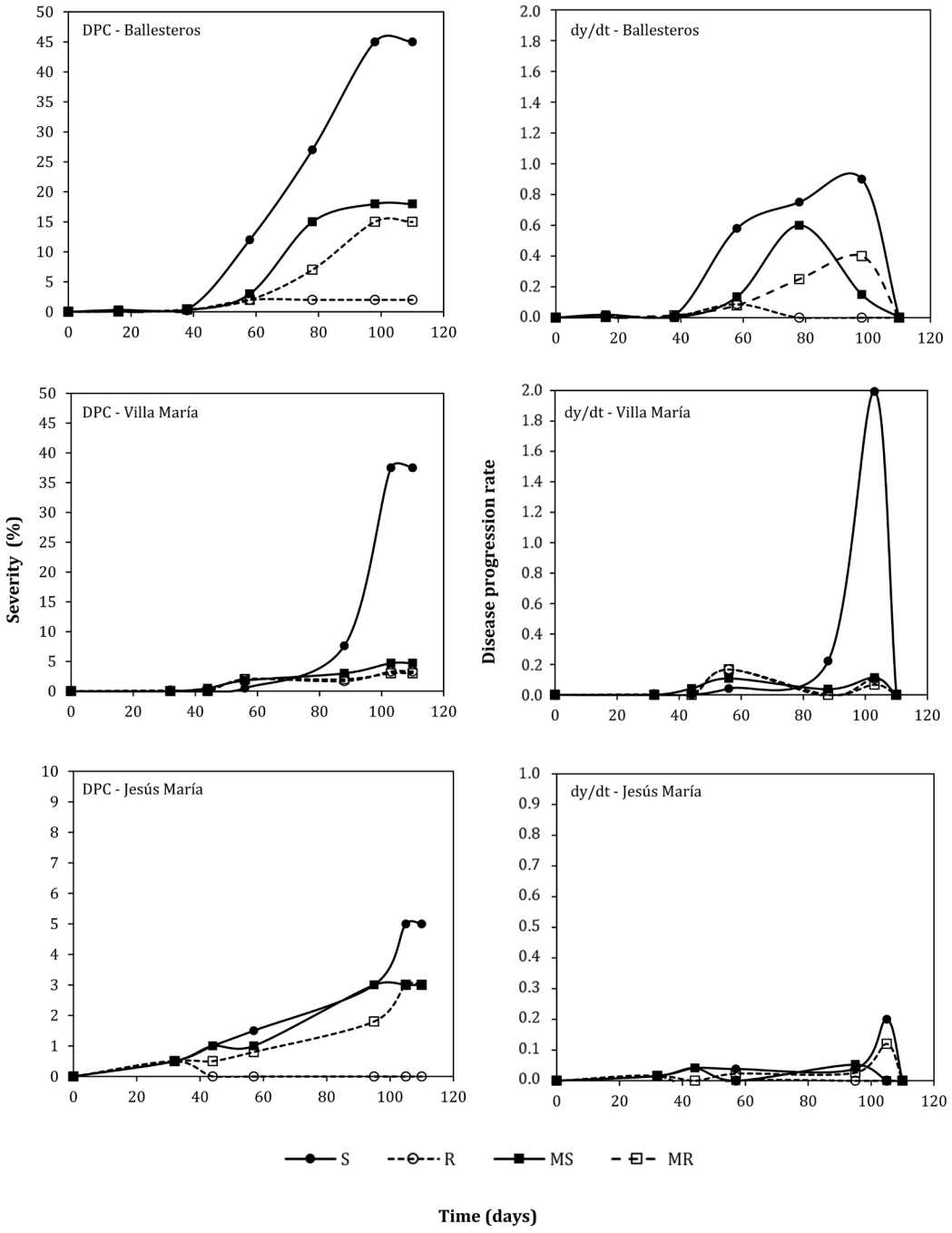

Reaction: R = Resistant. MR = moderately resistant. MS = moderately susceptible. S = susceptible.

Reacción: R = resistente. MR = moderadamente resistente. MS = moderadamente susceptible. S = susceptible.

Figure 1. Disease progress curves (DPCs) and disease progress rate curves (dy/dt) of northern corn leaf blight (NCLB) (*Exserohilum turcicum*) in Ballesteros, Villa María, and Jesús María, central-northern Córdoba, Argentina, during the 2015-16 season, for four maize hybrids with different reactions to NCLB.

Figura 1. Curvas de progreso de la enfermedad (DPC) y curvas de la tasa de progreso de la enfermedad en el tiempo (dy / dt) del tizón foliar común del maíz (*Exserohilum turcicum*) en las localidades de Ballesteros, Villa María y Jesús María, pertenecientes a la región centro-norte de Córdoba, Argentina, durante la campaña agrícola 2015-16, para cuatro híbridos de diferente reacción a la enfermedad.

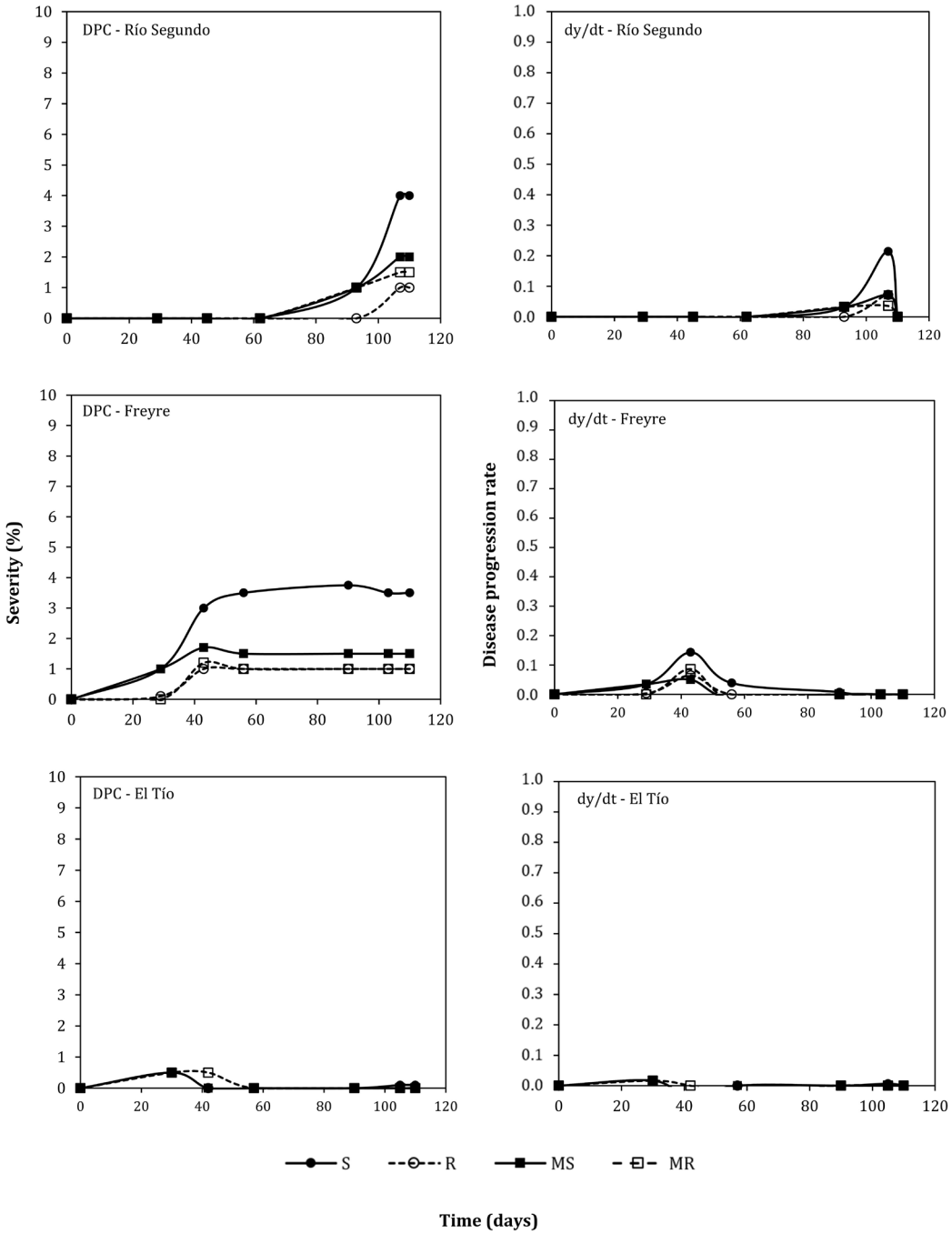

Reaction: R = Resistant. MR = moderately resistant. MS = moderately susceptible. S = susceptible.

Reacción: R = resistente. MR = moderadamente resistente. MS = moderadamente susceptible. S = susceptible.

Figure 2. Disease progress curves (DPCs) and disease progress rate curves (dy/dt) of northern corn leaf blight (NCLB) (*Exserohilum turcicum*) in Río Segundo, Freyre and El Tío, central-northern Córdoba, Argentina, during the 2015-16 season, for four maize hybrids with different reactions to NCLB.

Figura 2. Curvas de progreso de la enfermedad (DPC) y curvas de la tasa de progreso de la enfermedad en el tiempo (dy / dt) del tizón foliar común del maíz (*Exserohilum turcicum*) en las localidades de Río Segundo, Freyre and El Tío, pertenecientes a la región centro-norte de Córdoba, Argentina, durante la campaña agrícola 2015-16, para cuatro híbridos de maíz de diferente reacción a la enfermedad.

The picture shows, from left to right, the leaf immediately below the ear leaf, the ear leaf, and the leaf immediately above the ear leaf, at R4 phenological stage in four maize hybrids with different reaction to NCLB: a) resistant, b) moderately resistant, c) moderately susceptible and d) susceptible.

La imagen muestra, de izquierda a derecha, la hoja inmediatamente inferior a la hoja de la espiga, la hoja de la espiga y la hoja inmediatamente superior a la hoja de la espiga, en la etapa fenológica R4, en cuatro híbridos de maíz con diferente reacción al TFC: a) resistente, b) moderadamente resistente, c) moderadamente susceptible y d) susceptible.

Figure 3. Final severity of northern corn leaf blight (NCLB), caused by *Exserohilum turcicum*, in Ballesteros, central-northern Córdoba, Argentina, during the 2015-16 season.

Figura 3. Severidad final del tizón foliar común del maíz (TFC), causado por *Exserohilum turcicum*, en Ballesteros, Córdoba, Argentina, durante la campaña 2015-16.

The resistant (R) hybrid showed the lowest FS and AUDPC values across all localities, remaining symptomless in El Tío and Jesús María (table 2, page 130). Similarly, apparent infection rates (r), estimated by the b parameter, ranged from 0.008 to 0.084 (table 3, page 131) in Ballesteros, Villa María, and Jesús María. The R hybrid had the lowest r among all genotypes, emphasising the importance of genetic resistance in reducing disease prevalence in maize production systems. These findings align with numerous reports emphasising the use of resistant cultivars as the most cost-effective and sustainable approach for disease management (6, 27, 30).

Although nonlinear models provided a reliable description of the temporal dynamics of NCLB across different hybrids and locations, certain methodological limitations should be acknowledged. First, the negative y_0 values (initial inoculum) observed in both models should not be interpreted as actual inoculum levels but as model-derived parameters resulting from mathematical fitting, lacking direct biological meaning. Additionally, given extremely low or null infection levels, we could not fit a model for the R hybrid in Jesús María, confirming the high resistance level of this hybrid at this location.

Generally, the Gompertz model provided better fits, consistent with its suitability for polycyclic diseases. However, some exceptions were noted. The S hybrid in Villa María exhibited higher R2 with the Logistic model, likely due to environmental factors or differences in epidemic progression. This warrants further investigation.

Substantial NCLB development in Ballesteros, Villa María, and Jesús María provided suitable conditions for fitting and comparing temporal epidemiological models. This was not feasible in Río Segundo, Freyre and El Tío; thus, results from these localities are not presented. Epidemics exhibited sigmoidal curves (figure 1, page 132 and figure 2, page 133), characteristic of polycyclic diseases with multiple infection cycles during the cycle (2, 13). The widely used Logistic and Gompertz models well describe such development (1, 2, 5, 21, 33). Both models had highly significant fits, with R^2 exceeding 80%. On average, the Gompertz model provided the best fit across all genotypes, with R^2= 0.909 and R^{2*}= 0.849, outperforming the Logistic model in all cases* (table 3, page 131). These findings agree with Oddino *et al.* (2010), who reported significant fits with both models for NCLB epidemics in a susceptible corn genotype grown in Olaeta (southern Córdoba). The Gompertz model had R^2 over 80%, providing the best fit across DPCs obtained under various fungicide application timings.

Both Logistic and Gompertz curves are useful for modeling growth data. Despite certain limitations, they share similar features. Symmetry is a drawback of the Logistic model, whereas the asymmetrical Gompertz model has an earlier inflexion point, making it more suitable for representing rapid-growth biological phenomena (9).

The better fit of the Gompertz model to NCLB epidemics reflects that the maximum disease rate occurs earlier in this model than in the Logistic curve. Consequently, according to this model, management decisions should be implemented earlier. This observation aligns with Achicanoy López (2000) and March *et al.* (2012), who emphasize that epidemiological models should be employed to predict future disease levels and guide management action, avoiding crop damage. Understanding DPCs enables accurate predictions of disease progression and helps select optimal management strategies for specific pathosystems.

Several criteria may identify the best-fitting model. However, R^2 may not suit model evaluation (15, 17). Instead, the adjusted coefficient of determination (R^{2*}) derived from the regression between non-transformed observed and predicted values provides a more accurate representation of disease progress (5). We provide both coefficients, facilitating model comparison (table 3, page 131).

This study compared different maize genotypes across multiple locations. In polycyclic diseases such as NCLB, the initial inoculum has relatively little influence on FS, whereas the number of infection cycles is critical (2, 22). Management tools in polycyclic diseases, like quantitative resistance, environmental modification, and chemical control at sowing, are commonly employed to reduce apparent infection rates, limiting the number of infection cycles (32). Epidemiological models summarize the disease *vs.* time relationship into simple mathematical expressions, easing the analysis of disease progression and resistance levels (2). While these models simplify reality, they provide insights experimentally difficult or impossible to obtain.

However, considering no model has been specifically developed for plant pathology, biological interpretations concerning variables and parameters require caution. Proper analysis of these models helps elucidate field conditions and disease progression patterns, supporting effective prevention and control strategies (1).

Vanderplank (1963) emphasized that genetics and chemistry constitute excellent disease control tools, but epidemiology defines strategy. This link between epidemiology and disease management remains essential (16, 34). Temporal analysis provides quantitative insights for understanding epidemic drivers, pathosystem comparisons, prediction systems development, risk mapping, and strategy formulation (23). For the maize-NCLB pathosystem, temporal analysis provides fundamental epidemiological knowledge for mitigating disease impact in central-northern Córdoba.

Conclusions

The temporal analysis of northern corn leaf blight (NCLB) epidemics in central-northern Córdoba differentiated maize hybrids based on resistance levels and emphasized epidemiological importance of genetic background. The evaluated hybrids exhibited distinct disease progression dynamics, reflected in differences in disease progression curves, final severity, area under the disease progression curve, and apparent infection rates, validating their expected reactions to NCLB.

Among the nonlinear models tested, the Gompertz model consistently provided the best fit, suggesting an early exponential phase and gradual disease progression, typical of NCLB under field conditions. These findings help understand disease temporal dynamics and support the use of quantitative epidemiological tools to guide hybrid selection and optimize integrated disease management strategies against NCLB in maize production systems.

References

1. Achicanoy López, H. 2000. Descripción cuantitativa de las epidemias de las plantas. Revista Facultad Nacional de Agronomía. Medellín. 53(1): 941-968.
2. Bergamin Filho, A. 1995. Curvas de Progresso da doença. En: Bergamin Filho, A.; Kimati, H.; Amorim, L. Manual de Fitopatologia. Vol.1: Princípios e Conceito. São Paulo: Agronômica Ceres. p. 902-626.
3. Bergamin Filho, A.; Amorin, L. 1996. Doencas de plantas tropicais: Epidemiologia e controle económico. Sao Paulo: Ceres. p. 289.
4. Bolsa de Cereales de Buenos Aires (BCBA), 2019. Panorama agrícola semanal (PAS). Departamento de estimaciones agrícolas. Septiembre de 2019. Histórico.
5. Campbell, C. L.; Madden, L. V. 1990. Introduction to plant disease epidemiology. New York. John Wiley. p. 532.
6. Cia, E.; Fuzatto, M. G. 1999. Manejo de doenças na cultura do algodão. En: Cia, E.; Freire, E. C. & Santos, W. J. (Eds.) Cultura do algodoeiro. Piracicaba: Potafós. p. 121-131.
7. CIMMYT. Centro Internacional de Mejoramiento de Maíz y Trigo. 1985. Managing trails and reporting data for CIMMYT's International Maize Testing Programme. CIMMYT. El Batan. Mexico.
8. De Rossi, R. L.; Giménez Pecci, M. P.; Guerra, F. A.; Plaza, M. C.; Brücher, E.; Guerra, G. D.; Torrico, A. K.; Camiletti, B. X.; Maurino, M. F.; Barontini, J.; Ferrer, M.; Lucini, E.; Laguna, I. G. 2017. Enfermedades del maíz de siembra tardía causadas por hongos. Libro resúmenes del I° Congreso de Maíz Tardío. Buenos Aires, 20 de septiembre de 2016.
9. De Rossi, R. L.; Guerra, F. A.; Plazas, M. C.; Vuletic, E. E.; Brücher, E.; Guerra, G. D.; Reis, E. M. 2022. Crop damage, economic losses, and the economic damage threshold for northern corn leaf blight. Crop Protection. Elsevier SCI LTD. vol. 154.
10. Dhar, M.; Bhattacharya, P. 2018. Comparison of the Logistic and the Gompertz curve under different constraints. Journal of Statistics and Management Systems. 21(7): 1189-1210. DOI:10.1080/09720510.2018.1488414
11. Di Rienzo, J. A.; Balzarini, M.; Casanoves, F.; Gonzalez, L.; Tablada, M.; Robledo, C. W. 2010. InfoStat, software estadístico. Universidad Nacional de Córdoba, Argentina.
12. Fischer, K. S.; Palmer, F. E. 1984. Tropical maize. En: Goldsworthy, P. R.; Fisher, N. M. (Eds.). The physiology of tropical field crops. Wiley. p. 231-248.
13. Fry, W. E. 1982. Principles of plant disease management. Academic Press, Inc. p. 378.
14. Fullerton, R. A. 1982. Assessment of leaf damage caused by northern leaf blight in maize. New Zealand Journal of Experimental Agriculture. 10(3): 313-316. DOI:10.1080/03015521.1982.10427890.
15. Jeger, M. J. 1986. The potencial of analytic compared with simulation approaches to modeling in plant disease epidemiology. In Leonard, K. J. & Fry, W. E. (ed). Plant Disease Epidemiology. Population, Dynamics and Management. MacMillan, p. 255-281.
16. Jeger, M. J. 2000. Theory and plant epidemiology. Plant Pathology. 49: 651-658.
17. Jeger, M. J. 2004. Analysis of disease progress as a basis for evaluating disease management practices. Annu. Rev. Phytopathology. 42: 61-82.
18. Kachapur, M. R.; Hegde, R. K. 1988. Studies on *Turcicum blight* of maize (*Zea mays* L.) caused by *Exserohilum turcicum* (Pass) Leonard & Suggs with special reference to crop loss assessment. Plant pathology newsletter. 6: 33-35.
19. Kranz, J. 1974. Comparison of epidemics. Ann. Rev. of Phytopathology. 12: 355-374.
20. Madden L. V.; Hughes G.; Van Den Bosch, F. 2007. The study of plant disease epidemics. APS Press. St. Paul, MN. p. 432.
21. March, G. J.; Marinelli, A.; Oddino, C. M. 2004. Epidemiología aplicada al manejo de las enfermedades de los cultivos. Manual Curso de Especialización en Protección Vegetal. Universidad Católica de Córdoba. p. 110.
22. March, G. J.; Marinelli, A.; Oddino, C. M. 2010. Manejo de enfermedades de los cultivos según parámetros epidemiológicos. Córdoba: INTA-UNRC. p. 193.
23. March, G. J.; Marinelli, A.; Oddino, C. M. 2012. Análisis del progreso de epidemias y pérdidas que causan. Manual Curso de Especialización en Protección Vegetal. Universidad Católica de Córdoba. p. 86.
24. Oddino, C.; Marinelli, A.; García, J.; Garcia, M.; Tarditi, L.; Ferrari, S.; D´Eramo, L.; March, G. J. 2010. Comparación del efecto de momentos de tratamientos fungicidas sobre enfermedades foliares del maíz a través de modelos epidemiológicos no flexibles. Libro de Actas IX° Congreso Nacional de Maíz, Rosario, Argentina, p. 235-237.
25. Pataky, J. K. 1992. Relationships between yield of sweet corn and northern leaf blight caused by *Exserohilum turcicum*. Phytopathology. 82: 370-375.
26. Paul, P. A.; Munkvold, G. P. 2004. A model-based approach to preplanting risk assessment for gray leaf spot of maize. Phytopathology. 94: 1350-1357.
27. Pereira, A. A.; Zambolim, L.; Chaves, G. M. 1985. Melhoramento visando a resistência a doenças. Informe Agropecuário, Belo Horizonte. 11(122): 82-92.
28. Perkins, J. M.; Hooker, A. L. 1981. Reactions of eighty-four sources of chlorotic lesion resistance in corn to three biotypes of *Helminthosporium turcicum*. Plant Dis. 65: 502-504.

29. Ritchie, S. W.; Hanway, J. J.; Benson, G. O. 1986. How a corn plant develops? Iowa State. Univ. Coop. Ext. Serv. Spec. Rep. N° 48. p. 1-21.
30. Sharma, R. C.; Rai, S. N.; Batsa, B. K. 2005. Identifying resistance to banded leaf and sheath blight of maize. Indian Phytopathology. 58: 121-122.
31. Teng, P. S.; Zadoks, J. C. 1980. Computer simulation of plant disease epidemics. In: McGraw-Hill Yearbook of Science and technology. p. 23-31.
32. Vanderplank, J. E. 1963. Plant diseases: Epidemics and control. Academic Press, New York. p 349.
33. Waggoner, P. E. 1986. Progress curves of foliar disease: their interpretation and use. In: Leonard, K. J.; Fry, N. E. eds. Plant Disease Epidemiology: Population dynamics and management. New York. MacMillan. p. 3-54.
34. Zadoks, J. C.; Schein, R. D. 1979. Epidemiology and plant disease management. New York. Oxford University Press. p. 427.

Acknowledgements

We thank KWS Argentina S.A., for seed material, sowing support and plot maintenance across the six locations.

First Report of the Black Soybean Weevil *Rhyssomatus subtilis* Fiedler (Coleoptera: Curculionidae) in Córdoba, Argentina. Crop Damage Estimation

Primer registro del picudo negro de la soja *Rhyssomatus subtilis* Fiedler (Coleoptera: Curculionidae) en la provincia de Córdoba, Argentina, y estimación de daño en el cultivo

Celso Roberto Peralta [1, 2, 3*], Matías Rinero [3], Daniel Antonio Igarzábal [3], Roberto Luis De Rossi [1]

Originales: *Recepción:* 20/05/2025 - *Aceptación:* 01/09/2025

Abstract

The black soybean weevil is an endemic pest in northwestern and northeastern Argentina, causing significant damage. The objective of this study was to confirm the presence of this species in Córdoba, describe symptomatology and evaluate the potential impact on the crop. Surveys were conducted in plots located in the north-central part of the province. Individuals were collected and a quantitative assessment of symptoms and damage was conducted. Twenty compound samples were taken from sectors showing different physiological appearances (green *vs.* yellowish). In each group, total pod number and damaged pod number allowed calculating damage percentage. Data were analyzed by ANOVA and Fisher's test ($\alpha = 0.05$). All collected individuals matched the morphological descriptions reported in the literature for the species *Rhyssomatus subtilis* Fiedler. Green plants had a higher proportion of damaged pods (0.89) and fewer pods (31.85) compared to yellowish plants (0.53 and 46.65, respectively). This relationship suggests a direct effect on biomass partitioning. Our finding remaps the pest's distribution range, warning areas of high agricultural production in Córdoba and raising the need to link public-private actions to minimize its spread.

Keywords
damaged pods • yield losses • distribution • *Glycine max*

1 Universidad Católica de Córdoba. Avda. Armada Argentina N° 3555. C. P. X5016DHK. Córdoba. Argentina. * 0424746@ucc.edu.ar
2 Universidad Nacional de Córdoba. Ing. Agr. Félix Aldo Marrone 746. C. P. 5000. Córdoba. Argentina.
3 Moha S. A. Calle Tucumán 255 Of 14. X5220BBE. Jesús María. Córdoba. Argentina.

Resumen

El picudo negro de la soja es una plaga endémica en el norte de Argentina, donde genera daños significativos. El objetivo del trabajo fue confirmar la presencia de esta especie en Córdoba, describir los síntomas observados y evaluar el impacto potencial sobre el cultivo. Se realizaron relevamientos en lotes del centro-norte de la provincia, se recolectaron individuos y se realizó una evaluación cuantitativa de los síntomas y daños. Se realizaron veinte muestreos compuestos de cinco plantas cada una en sectores que presentaban plantas con distinto aspecto fisiológico (verdes *vs.* amarillentas). En cada grupo se evaluó el número total de vainas, el número de vainas dañadas, y se calculó el porcentaje de daño, las diferencias registradas fueron analizadas mediante ANOVA y sus medias diferenciadas por test de Fisher (α 0,05). Todos los individuos recolectados coincidieron con las medidas morfológicas y descripciones registradas en la literatura para la especie *Rhyssomatus subtilis* Fiedler. Las plantas verdes presentaron mayor proporción de vainas dañadas (0,89) y menor número total de vainas (31,85) en comparación con las amarillentas (0,53 y 46,65 respectivamente), con diferencias significativas (p< 0,05). Esta relación sugiere un efecto directo del insecto sobre la fisiología del cultivo, asociado con alteraciones en la relación fuente-destino. Este hallazgo amplía el rango de distribución conocida de esta plaga, alertando sobre su posible establecimiento en zonas de alta producción agrícola de Córdoba y planteando la necesidad de vincular acciones público y privadas para minimizar o contener la expansión de la plaga.

Palabras claves
vainas dañadas • pérdidas de rendimiento • distribución • *Glycine max*

Introduction

Soybean (*Glycine max* L.) is a major pillar of agricultural production in Argentina. In Córdoba Province, soybean occupies approximately 4,758,800 hectares, which represents 62% of the total summer crop area estimated at 7,668,200 hectares (Bolsa de Cereales de Córdoba, 2024). In this context, phytosanitary monitoring has gained importance due to the emergence and spread of pests holding significant agronomic impact.

Until recently, the phytosanitary status of soybean in Córdoba remained relatively stable, with a pest complex dominated by well-known, routinely monitored species. However, in recent seasons, isolated insects, rarely found in the region, have been recorded. Some lack clear antecedents as pests in the local production system (Peralta, 2022).

The genus *Rhyssomatus* Schönherr (Coleoptera: Curculionidae) comprises South American native species, several of which are associated with legume crops (Wibmer & O'Brien, 1986; Lanteri *et al*., 2002). In north-western Argentina (NOA), the weevil complex associated with soybean constitutes an important phytosanitary problem, given direct damage and rapid dispersal capacity. Within this group, *Rhyssomatus subtilis* Fiedler, known as the soybean black weevil, has become a major pest in the region due to its high biotic potential, its impact on reproductive structures and its adaptation to different environments (Socías *et al*., 2009; Cazado *et al.*, 2014).

In recent years, its presence has been documented in new expansion zones in north-west Argentina (NOA) like eastern Santiago del Estero, on soybean and cotton crops (Casuso *et al*., 2022). *R. subtilis* shows a strong association with cultivated and volunteer legumes and is characterized by ovipositing in soybean pods, where larvae feed on the seeds, hindering early detection, and causing direct yield losses (Cazado *et al*., 2014).

Confirmation of the presence of *R. subtilis* in soybean fields of north-central Córdoba would not only imply an expansion of its geographic range but also serve as a warning for phytosanitary surveillance systems in the Pampas region.

This work aimed to document the presence of *R. subtilis* in soybean crops in Córdoba Province, describe field symptomatology, assess damage level and discuss potential agronomic, ecological, and productive implications.

Materials and Methods

Sampling Sites

During the 2024/25 growing season, seven sites located in north-center Córdoba, within Colón and Santa María Departments, were visited following grower reports of pod damage. All sites were at advanced reproductive stages (R6-R7), (Fehr & Caviness, 1977) when sampled (table 1).

Table 1. Sampling sites for detection of the soybean black weevil (*Rhyssomatus subtilis*) located in the north-center of Córdoba Province, 2024/25 growing season.

Tabla 1. Sitios de muestreo en el centro-norte de la provincia de Córdoba, campaña agrícola 2024-25, para la determinación de la presencia del picudo negro de la soja (*Rhyssomatus subtilis*).

Site	Farm	Locality	Department	Coordinates
1	Agnolon	Malvinas Argentinas	Colón	31°21'58.37" S / 63°59'33.73" O
2	Dr. Lucero	Malvinas Argentinas	Colón	31°22'36.80" S / 63°59'23.19" O
3	Salazar	Monte Cristo	Colón	31°21'45.87" S / 63°58'1.42" O
4	Caburé	Monte Cristo	Colón	31°22'13.37" S / 64°0'32.79" O
5	Capelino	Villa Posse	Santa María	31°26'41.72" S / 64°2'16.93" O
6	La Curva	Monte Cristo	Colón	31°21'32.00"S / 63°59'23.10"O
7	Santa Julia (UCC)	Malvinas Argentinas	Colón	31°20'47.60"S / 64° 0'45.30"O

Field Characteristics and Management

All seven sites were commercial soybean fields under no-tillage. Only one site had received a specific insecticide spray targeting curculionids. Previous summer-crop rotations differed among fields (table 2). Additionally, a comparative map showed historical phytosanitary monitoring sites in north-central Córdoba and the sites where *R. subtilis* was detected in 2024/25. The historical database (15 seasons, 2009/10-2024/25) was generated by Moha S. A. (firm to which the authors belong). These data were overlaid with the 2024/25 detection sites.

Table 2. Crop management indicators of seven soybean fields showing pod damage caused by the black weevil (*Rhyssomatus subtilis*), Córdoba, 2024/25.

Tabla 2. Detalle de manejo de cultivo de siete lotes de producción de soja con presencia de daño de picudo negro (*Rhyssomatus subtilis*) en vainas. Córdoba, campaña agrícola 2024-25.

Site	Cultivar	Sowing date	Summer crops in the last 7 year's*	Insecticides for weevils
1	DM 46i20 IPRO	12/12/2024	Sy-Sy-Sy-Sy-Mz-Sy-Sy	No
2	DM 46i20 IPRO	14/11/2024	Sy-Mz-Sy-Mz-Sy-Mz-Sy	No
3	DM 50i17 IPRO STS	18/11/2024	Mz-Sy-Sy-Mz-Sy-Sy-Sy	No
4	LDC 5.3	17/11/2024	Sy-Mz-Sy-Mz-Sy-Mz-Sy	No
5	DM 50i17 IPRO STS	16/11/2024	Sy-Mz-Sy-Mz-Sy-Mz-Sy	No
6	NS 5021 STS	20/11/2024	Sy-Sy-Sy-Mz-Sy-Sy-Sy	Yes
7	NS 5021 STS	20/11/2024	Mz-Sy-Mz-Sy-Sy-Mz-Sy	No

* Sy.: Soybean; Mz.: Maize.

Date, Plot Segmentation and Sampling Procedure

Damage assessment was carried out on April 2, 2025 at Site 1 (Agnolon Farm), with the crop at advanced R6 (Fehr & Caviness, 1971). At the remaining sites (2-7), samples of adult weevils, damaged pods and other affected plant structures were collected for morphological identification.

At Site 1, structured damage evaluation was performed by random sampling within two contrasting areas of the field: (i) zones with naturally yellowing plants (considered slightly damaged) and (ii) zones with completely green plants (considered severely damaged). At each zone, 20 composite samples were taken, each composed of five consecutive plants manually removed along the sowing row. Plants were transported to the laboratory, where all pods per sample were removed and counted. Total pod number and damaged pod number (attributable to *R. subtilis*) were recorded, allowing estimation of relative incidence. Pod set differences among areas and percentage of damaged pods were calculated in each site. ANOVA and Fisher's LSD test ($\alpha < 0.05$) were performed using InfoStat statistical software (Di Rienzo *et al*., 2010).

At Sites 2-7, only adult curculionids, damaged pods and other affected tissues were collected. Samples were kept in ventilated glass containers and taken to the laboratory for taxonomic confirmation. Photographic records of damage were obtained with a compact digital camera (Olympus Tough TG-4 iHS, Sony ZV-1) and a DJI Mavic Pro drone. Drone images were acquired with stacked exposures to enhance contrast. Chromatic classification of RGB channels was performed using color-histogram thresholds and digital-image analysis tools in Python. Classified zones were delineated by contour detection for visual and quantitative comparison. Color interpretation was based on field observations of symptoms like foliage persistence, green pods, and adult presence.

Insect Identification

The collected specimens were morphologically identified in the laboratory with binocular magnifying glass and using taxonomic keys Fiedler (1937-1938).

Results

Insect Identification

All collected individuals matched the descriptions recorded for *Rhyssomatus subtilis* Fiedler (Coleoptera: Curculionidae) (Fiedler, 1937-1938; Socías *et al*., 2009; Cazado *et al*., 2014). The finding was reported to Servicio Nacional de Sanidad y Calidad Agroalimentaria (SENASA) through the Sistema Nacional de Vigilancia y Monitoreo de plagas (SINAVIMO) (communication No. 1368) on April 12, 2025.

Córdoba specimens were identified based on the original characters of Fiedler (1939) and the morphological syntheses of Socías *et al*. (2009) and Cazado *et al*. (2014): (I) length 4.8-5.2 mm, width 2.5-3 mm, body oval-elongate, somewhat sub-rhombic; (II) integument dark brown-black, lacking scales or bands; (III) head very finely and densely punctate, strongly arched, the eyes separated dorsally by more than the width of the rostrum; (IV) rostrum very slender, moderately curved, considerably longer than the head and pronotum, recessed at the base so that the head and the base of the rostrum are not aligned in profile; (V) elytra with longitudinal striae and well-marked rows of punctures; (VI) female fore leg with a weak, angulate femur and the presence of an uncus (u) and mucro (m) on the tibia; (VII) apodous larvae 5-6 mm long, body curved in a "C" shape, milky white, with a light-brown to caramel head (figure 1, page 142).

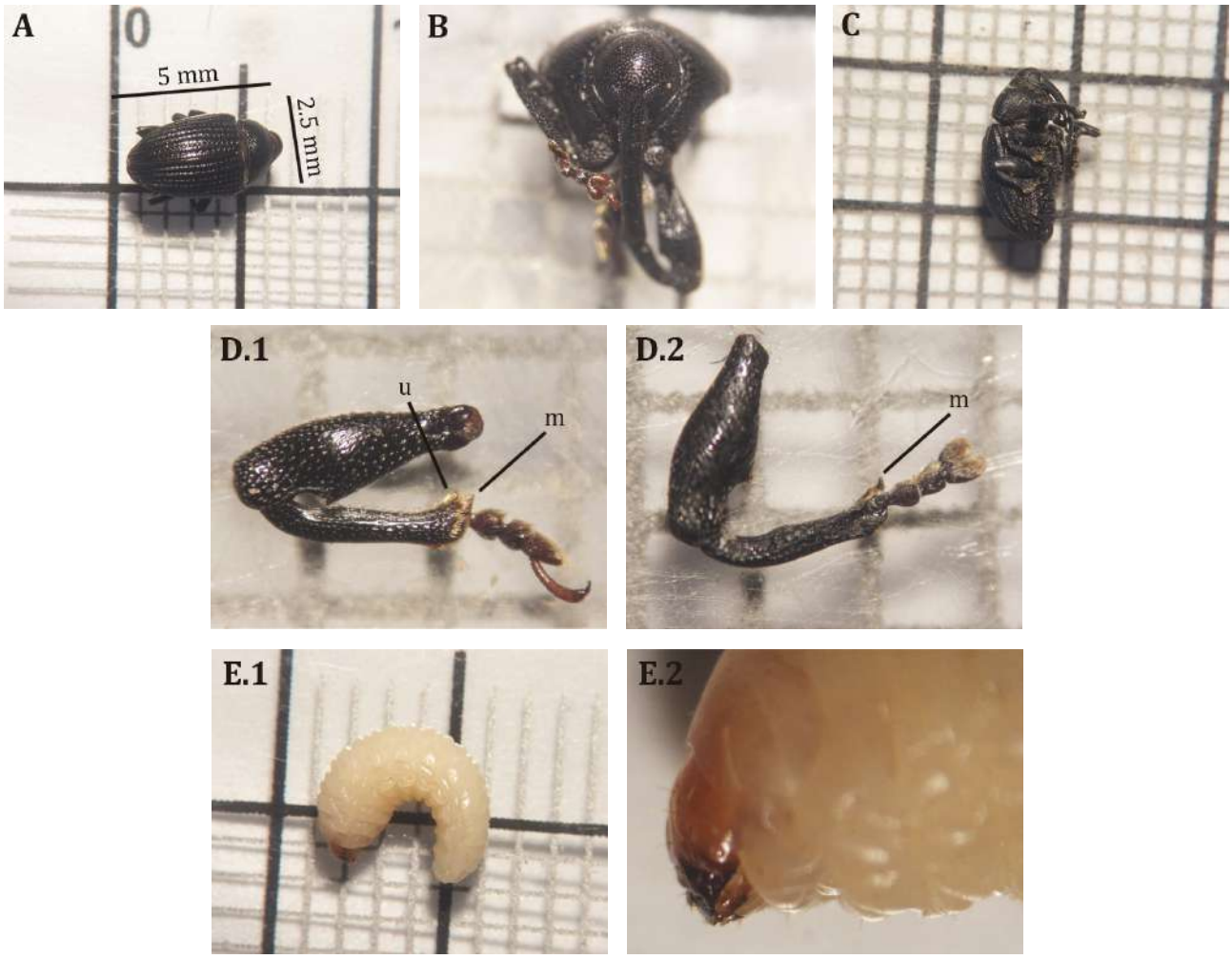

A) adult dimensions and color details; B) frontal view of the head, its punctures and eyes separated above the rostrum; C) adult lateral view; D.1) detail of female fore legs with presence of uncus (u) and mucro; D.2) detail of male fore legs only with presence of mucro; E.1) lateral view of apodous larva with curved body; E.2) lateral view of head in apodous larva.

A) dimensiones y detalles de color de adulto; B) vista frontal de cabeza, sus puntuaciones y ojos separados por encima de la probóscide; C) adulto vista lateral; D.1) detalle de patas delanteras de hembra con presencia de uncus (u) y mucro; D.2) detalle de patas delanteras de macho solo con presencia de mucro; E.1) vista lateral de larva ápoda con cuerpo curvado; E.2) vista lateral de la cabeza en larva ápoda.

Figure 1. *Rhyssomatus subtilis* adults and larvae.

Figura 1. Adultos y larvas de *Rhyssomatus subtilis.*

Sampling

Adults, larvae, eggs, and soybean crop damage matched the literature describing *R. subtilis* at the seven evaluated sites (figure 2, page 143).

Considering historical phytosanitary monitoring points previously surveyed by Moha S.A. over 15 growing seasons, and the seven sites where we detected *R. subtilis* during the 2024/25 season, the geographical distribution of the new detections is shown in relation to previously pest-free areas (figure 3, page 143).

A) Adult, B) Larva, C) Egg.
A) Adulto, B) Larva, C) Huevo.

Figure 2. Details of *Rhyssomatus subtilis* specimens found in north-central Córdoba during the 2024-25 growing season.

Figura 2. Detalle de especímenes de *Rhyssomatus subtilis* encontrados en el centro-norte de Córdoba durante la campaña agrícola 2024-25.

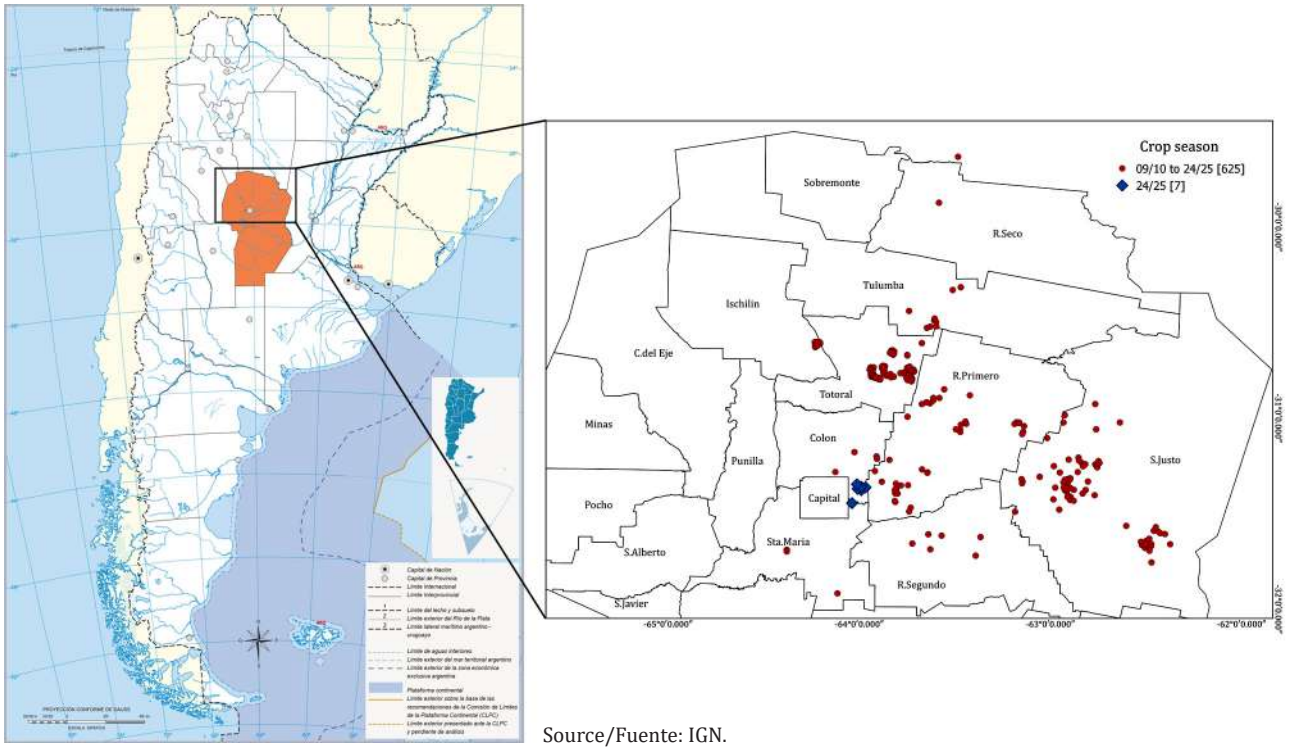

Source/Fuente: IGN.

Figure 3. Comparative map between historical phytosanitary monitoring sites (2009-10 to 2024-25) surveyed by Moha S.A. (red circles) and sites with detection of *Rhyssomatus subtilis* during the 2024/25 season (blue diamonds), showing the location of the new detections in relation to previously monitored areas with no pest records.

Figura 3. Mapa comparativo entre sitios históricos de monitoreo fitosanitario (2009-10 a 2024-25) realizados por la consultora Moha S.A. (círculos rojos) y los sitios con detección de *Rhyssomatus subtilis* durante la campaña 2024/25 (rombos azules), donde se denota la localización de las nuevas detecciones en relación con las áreas previamente monitoreadas sin registro de la plaga.

Damage Assessment

At Site 1, plants with contrasting physiological appearances revealed significant differences regarding proportion of damaged pods and total number of pods per plant (figure 4). Damage percentage was significantly higher ($p < 0.0001$) in green plants (0.89 ± 0.01) than in yellowing plants (0.53 ± 0.01). The CV was 9.04 %, and the adjusted R^2 was 0.89, indicating modeling high explanatory power. Likewise, total number of pods differed significantly ($p = 0.0015$), averaging 46.65 ± 3.05 pods in yellowing plants *versus* 31.85 ± 3.05 in green plants. These results indicate a strong association between damage intensity and plant physiological status, suggesting that *R. subtilis* may be affecting both pod number and pod integrity at crop advanced reproductive stages.

At the remaining sites (2-7), although quantitative assessments were not conducted, damage was observed at varying degrees of severity. In all cases, adults were found on plants and damaged pods, together with signs of integument perforation, injured seeds, and *R. subtilis* larvae feeding (figure 4).

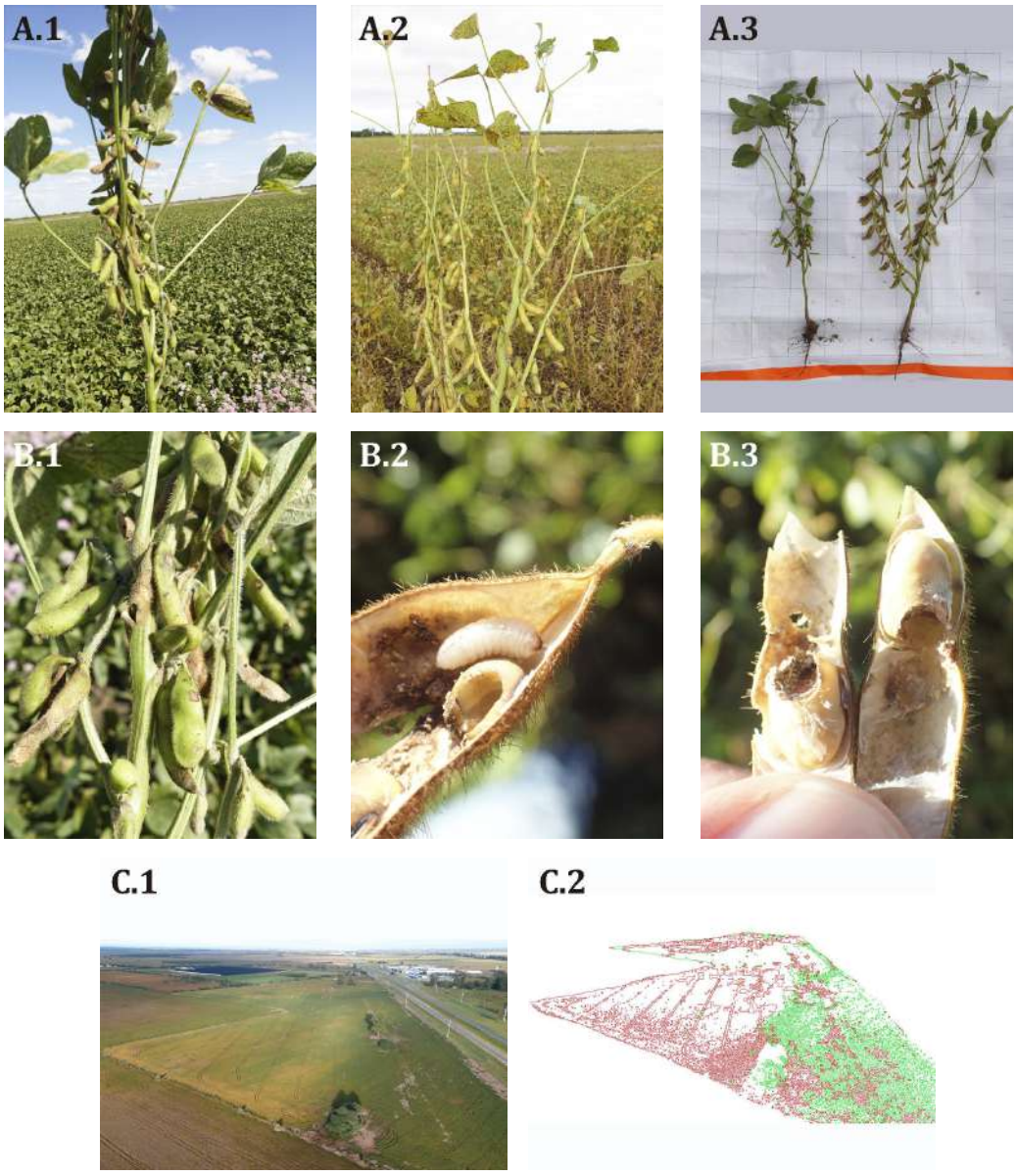

A.1, A.2, A.3) Plants with different behavior (green *vs.* yellowing); B.1, B.2, B.3) detail of affected pods; C.1) drone image of the field with high infestation in Malvinas Argentinas, Córdoba, showing sectors with yellowing and green plants; C.2) image of the same field produced through chromatic classification based on the assessments performed, In red, sectors with lower infestation (yellowing plants due to natural senescence) and in green, sectors with higher infestation (green plants with foliage retention).

A.1, A.2, A.3) Plantas con distintos comportamientos (verdes vs. amarillentas); B.1, B.2) detalle de vainas afectadas; C.1) Imagen aérea (drone) del lote con alta afección en la localidad de Malvinas Argentinas, Córdoba, donde se visualizan sectores con plantas amarillentas y plantas verdes; C.2) Imagen de ese lote realizada con clasificación cromática con base en las evaluaciones realizadas, siendo el color rojo la representación de sectores con menor afección (plantas amarillentas por senescencia natural) y en verde los sectores con mayor afección (plantas verdes con retención foliar).

Figure 4. Damage recorded by *Rhyssomatus subtilis* in north-central Córdoba during the 2024-2025 growing season.

Figura 4. Detalle de los daños registrados por *Rhyssomatus subtilis* en el centro-norte de Córdoba durante la campaña agrícola 2024-2025.

Discussion

Confirmation of *R. subtilis* Fiedler in the Colón and Santa María Departments of Córdoba extends its geographic distribution towards center Argentina by approximately 450 km with respect to historical reports from NOA (Salta, Tucumán and Santiago del Estero). The species has been verified in more than 53 localities in that region (Cazado *et al*., 2014), with these new determinations confirming a significant latitudinal dispersal capacity, colonizing new soybean areas of the Chaco ecoregion.

The adults sampled from north-central Córdoba exhibited cited characters (Socías *et al*., 2009; Cazado *et al*., 2014), ruling out possible confusion with other local curculionid species of wider regional distribution like *Pantomorus leucoloma* (Aragón, 2007) (table 3).

Table 3. Comparative table of morphological traits of soybean black weevil (*Rhyssomatus subtilis*) and alfalfa weevil (*Pantomorus leucoloma*).

Tabla 3. Tabla comparativa de características morfológicas para la diferenciación entre el Picudo negro de la soja (*Rhyssomatus subtilis*) y el Gorgojo de la alfalfa (*Pantomorus leucoloma*).

Trait	***Rhyssomatus subtilis*** **(Soybean black weevil)**	***Pantomorus leucoloma*** **(alfalfa weevil)**
Adult length	4.8-5.2 mm	8-12 mm (≈ 10 mm average)
Color	Slightly shiny black, no scales, no bands	Brownish-gray with a continuous white stripe along the elytral margins; brown scales
Rostrum	Long, slender, curved (≈ head + pronotum)	Relatively short and robust
Pronotum	Two converging oblique ridges	Convex, no ridges; often with light scale lines
Elytra	Deep longitudinal striae with well-marked rows of punctures	Striae covered by scales; powdery appearance
Type of damage in soybean	Damage to terminal shoots by adults and pod perforations (R5-R7) with grain feeding by larvae (occasionally other legumes)	Seedling defoliation and root damage by larvae (mainly in alfalfa; occasional in soybean)

In the NOA region, yield losses of up to 100% have been documented under high, uncontrolled populations of *R. subtilis*. In the grain-filling reproductive phase (R5 to R6)- a critical stage-losses can reach 60% (Cazado *et al*., 2014). In eastern Santiago del Estero Province, pod damage ranges between 21% and 42% (Casuso *et al*., 2023).

Site 1 showed that plants with the highest proportion of damaged pods, approximately 90% attributable to *R. subtilis*, displayed an active vegetative state (green). In contrast, less damaged plants, 53% damaged pods, exhibited a normal progression of crop senescence (yellowing), coinciding with previous studies (Cazado *et al*., 2014; Casuso *et al*., 2023).

Different physiological maturity among plants with greater damage suggests that affected reproductive structures may have altered biomass partitioning, generating stem greening and vegetative-tissue retention as a compensatory response to physiological imbalance.

This behavior partly resembles the green stem syndrome (GSS) in soybeans, characterized by persistent green tissues at harvest, linked to physiological imbalances in assimilate redistribution, abiotic stress, insect or disease damage, and even management practices (Rotundo *et al*., 2012; Salvagiotti *et al*., 2020). Particularly, the loss of sink structures like pods or seeds can result in sugar accumulation in vegetative tissues, delaying maturity and provoking symptoms like GSS (Egli & Bruening, 2006).

A similar situation occurs in the so-called "soja loca" ("crazy soybean") syndrome, reported mainly in Brazil and northern Argentina, where prolonged leaf retention, green stems and pod abortion have also been associated with infections by the nematode *Aphelenchoides besseyi* and hormonal alterations (Ferreira *et al*., 2010). Although nematodes were not detected in our study, symptoms shared some eco-physiological patterns like the loss of reproductive structures and the persistence of active vegetative tissues. This reinforces the need to broaden entomological and eco-physiological monitoring.

Larval activity caused direct seed loss and partitioning alterations, leading to physiological imbalances like those described in the green stem and/or crazy soybean syndromes. These effects compromise yield and hinder visual assessment of phenological progress, generating risks in harvest scheduling.

To date, no documented records of *R. subtilis* existed for Córdoba Province. This finding becomes invaluable from agronomic, sanitary, and ecological perspectives, marking a significant expansion in the known geographic distribution of this pest in Argentina.

We highlight the need to adapt monitoring schemes within regional phytosanitary surveillance systems to facilitate timely detection of *R. subtilis*, and advance local studies assessing population behavior, crop-pest interactions and possible integrated management strategies.

Conclusions

For the first time, the presence of the soybean black weevil *R. subtilis* was confirmed in fields of Córdoba Province.

Physiological differences were observed among plants with different levels of damage, linked to the intensity of the infestation.

The productive sector of Córdoba is on alert due to the presence of a new pest with high damage potential. Public-private actions should minimize pest spread.

References

Aragón, J. & Imwinkelried, JM. (2007). Manejo integrado de plagas de la alfalfa. En DH Basigalup (Ed.), *El cultivo de la alfalfa en la Argentina*, (p. 165-197). Ediciones INTA - EEA Manfredi.

Bolsa de Cereales de Córdoba. (2024). *Informe de campaña agrícola 2023/2024*. https://www.bccba. org.ar

Casuso, M., Tarragó, J., Cazado, L., Casmuz, A., Cancino, C., Soneira, D., & Gullini, L. (2022). Registro de *Rhyssomatus subtilis* Fiedler (Coleoptera: Curculionidae) en la zona de El Caburé (Santiago del Estero) sobre los cultivos de soja *Glycine max* (L.) Merr. y algodón (*Gossypium hirsutum*). INTA Las Breñas.

Casuso, VM, Cancino, CA, Tarragó, JR, & Pérez, GA (2023). Primeras evaluaciones para conocer el comportamiento del picudo negro de la soja *Rhyssomatus subtilis* Fiedler (Coleoptera: Curculionidae) en el este de Santiago del Estero. En XXVIII Reunión de Comunicaciones Científicas, Técnicas y de Extensión. Universidad Nacional del Nordeste, Facultad de Ciencias Agrarias. p. 38. https://repositorio.unne.edu.ar/handle/123456789/55928

Cazado, LE, Casmuz, AS, Scalora, F., Murúa, MG, Socías, MG, Gastaminza, GA, & Willink, E. (2014). El picudo negro de la soja, *Rhyssomatus subtilis* Fiedler (Coleoptera: Curculionidae). *Avance Agroindustrial*, *35*(4), 55-60.

Di Rienzo, JA, Balzarini, M., Casanoves, F., Gonzalez, L., Tablada, M., Robledo, CW. (2010). InfoStat, Software Estadístico. Universidad Nacional de Córdoba, Argentina.

Egli, DB, & Bruening, WP. (2006). Depodding causes green-stem syndrome in soybean. *Crop Management, 5*(1), 1-5. https://doi.org/10.1094/CM-2006-0104-01-RS

Fehr, WR, & Caviness, CE. (1977). Stages of soybean development (Special Report N° 80). Iowa State University Cooperative Extension Service.

Ferreira, AB, de Almeida, MR, & Dias, WP. (2010). Incidência de *Aphelenchoides besseyi* em cultivares de soja com sintomas de "soja louca". *Nematologia Brasileira, 34*(1), 39-45.

Fiedler, C. (1937-1938). Neue südamerikanische Arten der Gattung *Rhyssomatus* Schönh. (Col. Curc. Chryptorhynch.). *Entomologisches Nachrichtenblatt (Troppau), 12*: 81-96.

Lanteri, AA, del Río, MG, & Marvaldi, AE. (2002). Curculionoidea (Coleoptera). In LE Claps, J. Morrone & MC Roig-Juñent (Eds.), *Biodiversidad de artrópodos argentinos, 1:* 327-349. Ediciones Sur.

Peralta, CR. (2022). Congreso N°30 AAPRESID: Un congreso a suelo abierto. Tecnologías para el manejo integrado de insectos.

Rotundo, JL, Salvagiotti, F., & Andrade, FH. (2012). Physiological and management causes of the green stem disorder in soybean. *Field Crops Research*, *134*: 186-195.

Salvagiotti, F., Rotundo, JL, & Pereyra, VR. (2020). Advances in understanding the green stem disorder in soybean. *Revista de la Facultad de Agronomía*, *119*(1), 1-9.

Socías, MG, Rosado-Neto, GH, Casmuz, AS, Zaia, DG, & Willink, E. (2009). *Rhyssomatus subtilis* Fiedler (Coleoptera: Curculionidae), primer registro para la Argentina y primera cita de planta hospedera, *Glycine max* (L) Merr. *Revista Industrial y Agrícola de Tucumán, 86*(1): 43-46.

Wibmer, GJ, & O'Brien, CW. (1986). Annotated checklist of the weevils (*Curculionidae sensu lato*) of South America. *Memoirs of the American Entomological Institute, 39*: 1-563.

Acknowledgments

Special thanks to the Agricultural Engineers Hugo Digón, Eduardo Vasallo and Daniela Vecchio for their contributions on sites where the pest is present and their very useful comments.
Thanks also to the producers Fabián Daga and Rolando Carando for facilitating access and collaborating in the survey.

Milk Production, Age at First Calving, and Calving-to-Conception Interval in Holstein, Brown Swiss, and Holstein x Brown Swiss Cows

Producción de leche, edad al primer parto e intervalo parto-concepción en vacas Holstein, Pardo Suizo y Holstein x Pardo Suizo

Victoria Cañete [1*], Belén Lazzarini [3], Agustín Alesso [4], Javier Baudracco [4], Pablo Roberto Marini [1, 2]

Originales: *Recepción:* 30/10/2024 - *Aceptación:* 17/03/2025

Abstract

The objective of this study was to evaluate milk production, age at first calving, and calving to conception interval in Holstein, Brown Swiss, and Holstein x Brown Swiss crossbred cows within a pasture-based dairy system in Argentina. The increasing global demand for more resilient and locally adapted dairy systems has led to a renewed interest in crossbreeding to enhance both reproductive and productive efficiency through heterosis. We analyzed data collected over 10 years (2014-2023) from 647 first-lactation cows, including Holstein, Brown Swiss, and Holstein x Brown Swiss crossbred cows. Data were examined using a mixed-effects linear model with breed, season, and their interactions as fixed effect and year as random effect. The results showed no significant differences in milk production between breeds or seasons. However, a significant interaction between breed and season was observed for the calving-to-conception interval, with a shorter interval for crossbred cows during spring-summer (102 days), compared to Holstein cows (156 days). This finding highlights a potential advantage of crossbreeding in reducing open days during the warmest months, thereby enhancing reproductive efficiency in pasture-based systems. This study suggests that crossbreeding can be a viable strategy for improving reproductive performance of dairy systems while maintaining similar milk yield compared to the other breeds, particularly in grazing systems.

Keywords
dairy cows • crossbreeding • Argentina • fertility • pasture-based systems • Holstein • Brown Swiss

1 Universidad Nacional de Rosario. Facultad de Ciencias Veterinarias. Ovidio Lagos y Ruta 33 (2170). Argentina. * victoria.canete.c06815@fcv.unr.edu.ar
2 Universidad Nacional de Rosario. Carrera del Investigador Científico (CIC). Maipú 1065 (2000). Argentina.
3 Universidad Nacional de Litoral. Facultad de Ciencias Agrarias. Kreder 2805 (3080) Esperanza. Santa Fe. Argentina.
4 Universidad Nacional del Litoral-CONICET. FCA. IciAgro Litoral. R. P. Kreder 2805. Esperanza 3080. Argentina.

Resumen

El objetivo de este estudio fue evaluar la producción de leche, la edad al primer parto y el intervalo parto-concepción en vacas Holstein, Pardo Suizo y cruzas Holstein x Pardo Suizo en un sistema lechero pastoril en Argentina. La creciente demanda mundial de sistemas lecheros más resilientes y adaptados a las condiciones locales ha generado un renovado interés por los cruzamientos para mejorar la eficiencia reproductiva y productiva mediante la heterosis. Se utilizaron datos recopilados durante 10 años (2014-2023) de 647 vacas de primera lactancia, incluyendo vacas Holstein, Pardo Suizo y cruzas de Holstein x Pardo Suizo. Los datos se analizaron utilizando un modelo lineal de efectos mixtos con la raza, la estación y sus interacciones como efecto fijo y el año como efecto aleatorio. Los resultados no mostraron diferencias significativas en la producción de leche entre razas o estaciones. Sin embargo, se encontró una interacción significativa entre raza y estación para el intervalo parto-concepción, teniendo las vacas cruza un intervalo parto-concepción más corto durante la primavera-verano (102 días) en comparación con las vacas Holstein (156 días), destacando una ventaja potencial del cruzamiento en la reducción de los días abiertos durante los meses más cálidos, mejorando así la eficiencia reproductiva en los sistemas pastoriles. Este estudio sugiere que el cruzamiento puede ser una estrategia viable para mejorar el rendimiento reproductivo de los sistemas lecheros, manteniendo al mismo tiempo una producción de leche similar a la de las demás razas, sobre todo en los sistemas pastoriles.

Palabras clave
vacas lecheras • cruzamientos • Argentina • fertilidad • sistemas pastoriles • Holstein • Pardo Suizo

Introduction

Holstein cows are the predominant dairy cattle breed around the world (6) and also in Argentina, where they account for 91.6% of the dairy cow population, followed by Jersey (4.7%) and other breeds, including Brown Swiss (9, 10, 15, 20). Despite the predominance of Holstein, Brown Swiss cows offer comparative advantages in milk composition, reproduction, and longevity, which are beneficial in challenging environments for dairy production (2, 8). These characteristics could potentially improve efficiency in dairy systems in regions with variable climatic conditions and variable forage availability, such as in pasture-based systems.

As global demand shifts toward more resilient and locally adapted dairy systems (18), farmers in Argentina have shown renewed interest in crossbreeding. This practice aims to improve the productive, reproductive, and economic efficiency of herds in pasture-based systems (18, 23). Heterosis in crossbred cattle can increase milk production up to 6.5% and enhance fertility and disease resistance by 10% (5, 12, 13).

Crossbreeding strategies worldwide integrate diverse production environments with different genetic groups, leading to greater diversification and optimization of productive systems (3, 21). Crossbreeding Holstein and Brown Swiss cows can combine desirable traits from both breeds. This study aimed to compare milk yield (MY305), calving-to-conception interval (CCI), and age at first calving (AFC) in Holstein (H), Brown Swiss (BS), and their crossbreed (H x BS) in a pasture-based dairy farm in Entre Ríos, Argentina.

Materials and methods

This study analyzed 10 years of records from a dairy farm at the "Las Delicias" Agricultural School, located in western Entre Ríos province (31°54’569’’ S, 60°25’253’’ W).

Database

The database included records from herd tests conducted over a 10-year period from January 2014 to December 2023. The records covered 647 first-lactation cows, including 565 H, 53 BS, and 29 H x BS. Monthly herd tests were conducted each year. Individual milk yield was recorded for each cow.

Dairy Herd and Analized Variables

In 2014, the farm had 165 milking cows and 23 dry cows. By 2023, the herd consisted of 153 milking cows and 38 dry cows, all managed on the same milking platform within a 190-hectare area. The average annual milk production per cow in 2023 was 17 liters/cow/day (3.9 fat% and 3.7% crude protein). The average diet consisted of approximately 50% grazed pasture, primarily alfalfa and seasonal grasses, while the remaining portion was supplemented with maize silage and concentrate (13% or 16% CP, depending on nutritional requirements) during milking.

Variables Analyzed

Year of calving: Year of first calving.
Season of calving: Season in which the first calving occurred.
Age at first calving (AFC): Cow's age at first calving, expressed in days.
Milk yield adjusted to 305 days (MY305): Milk produced in a 305-day period.
Calving-to-conception interval (CCI): Days between calving and conception.

Statistical analysis

Data were analyzed using a mixed-effects linear model, with breed and season as fixed and year as random effect. The model assumptions were verified by analyzing the residuals and adjusting the variance structures by season, breed, or interaction when necessary. The significance of the fixed effects was assessed using Type III ANOVA tables with a significance level of 5%. Significant effects were further analyzed using Tukey's post-hoc test for pairwise comparisons. All statistical analyses were conducted in the R statistical package (27) using the "nlme" (25) and "emmeans" (16) packages for modeling and post-hoc comparisons, respectively.

Results

Table 1 presents the p-values obtained from the Type III ANOVA for the variables analyzed. No significant effects for breed, season, or their interaction were detected on AFC and MY305, indicating that these factors do not influence these variables. However, for CCI a significant interaction between breed and season was found, suggesting that the effect of breed on this variable depends on the time of year.

Table 1. P-values for the fixed effects in the models adjusted for the studied variables, obtained from the marginal ANOVA (Type III) tables.
Tabla 1. Resumen de los valores-p de los efectos fijos en los modelos ajustados por las variables estudiadas, obtenidos a partir de las tablas de ANOVA marginal (Tipo III).

	AFC[1]	CCI[2]	MY305[3]
Breed	0.0699	0.8131	0.9331
Season	0.2497	0.1919	0.3843
Breed x Season	0.2143	0.0053	0.3735

[1] Age at first calving. [2] Calving-to-conception interval. [3] Milk yield adjusted to 305 days.
[1] Edad al primer parto. [2] Intervalo parto-concepción. [3] Producción de leche ajustada a 305 días.

Table 2 (page 151) shows the estimated means for each variable by breed and season, along with their standard errors and 95% confidence intervals. For CCI, the results show that H x BS cows have an average of 161 days in Autumn-Winter and 102 days in Spring-Summer. In contrast, H cows had fewer days of CCI in Autumn-Winter (131 days) than in Spring-Summer (156 days). Regarding MY305, higher values were observed across all

breeds for lactations from cows that calved in Autumn-Winter compared to Spring-Summer, although the differences were not statistically significant. For CCI no significant effect of season or breed was found.

Table 2. Estimated means, standard errors, and 95% confidence intervals for Age at first calving (AFC), calving-to-conception interval (CCI), and milk yield adjusted at 305 days in milk (MY305) for different breeds across Autumn-Winter and Spring-Summer.

Tabla 2. Medias estimadas, errores estándar e intervalos de confianza del 95% para la edad al primer parto (AFC), el intervalo parto-concepción (CCI) y la producción de leche ajustada a 305 días (MY305) para diferentes razas en otoño-invierno y primavera-verano.

Variable	Breed[1]	Autumn-Winter	Spring-Summer	Autumn-Winter Confidence Interval	Spring-Summer Confidence Interval
AFC (days)	H x BS	941 (37)	896 (68)	(858, 1024)	(742, 1050)
	H	928 (23)	957 (26)	(877, 979)	(897, 1016)
	BS	957 (35)	1053 (42)	(878, 1035)	(958, 1148)
CCI (days)	H x BS	161 (26)	102 (28)	(102, 220)	(37, 166)
	H	131 (11)	156 (13)	(107, 155)	(127, 185)
	BS	179 (25)	131 (17)	(123, 235)	(92, 170)
MY305 (lt/cow/year)	H x BS	6484 (275)	5703 (543)	(5862, 7106)	(4474, 6933)
	H	6308 (145)	6226 (174)	(5980, 6637)	(5833, 6619)
	BS	6490 (246)	6078 (303)	(5935, 7046)	(5394, 6763)

[1] HxBS: Holstein x Brown Swiss; H: Holstein; BS: Brown Swiss.

[1] HxBS: Holstein x Pardo Suizo; H: Holstein; BS: Pardo Suizo.

Discussion

This study evaluated the effect of dairy breed on AFC, MY305 and CCI in primiparous cows within a pasture-based system, emphasizing the need to select genotypes adapted to local agroecological conditions for improved efficiency (1).

Milk yield. Our results contrast with studies conducted in intensive systems where H, BS y H x BS produced higher milk yield. Dechow *et al.* (2007) reported that H x BS cows performed similarly to pure H cows in confined systems, exceeding 11,000 liters per lactation. However, in pasture-based systems, forage availability and seasonal variations limit potential milk production (17, 24). In our study, despite the higher productive potential, H cows did not outperform crossbred, likely due to these constraints. A previous study (31) conducted in the same production system (Agricultural School "Las Delicias") but during an earlier period (2007-2013), reported adjusted 305-day milk yield of 7162±856 liters (23.5 liters per cow per day) for H cows, 6168±1046 liters (20.2 liters per cow per day) for BS cows, and 6743±1048 liters (22.1 liters per cow per day) for H x BS cows, with significant differences among breeds. The findings of the previous study suggest that environmental conditions, particularly management and feeding practices, may have contributed to higher milk yields, especially among Holstein cows, which produced significantly more milk.

Age at first calving (AFC). Previous research highlights the benefits of hybrid vigor in improving the reproductive efficiency of crossbred dairy cows. García-Peniche *et al.* (2006) found that crossbred cows (H, BS and Jersey) tend to reach reproductive maturity earlier, offering farmers a significant economic advantage by reducing rearing costs and accelerating the return on investment. However, our study found no significant effect of breed on AFC.

Management and agroecological impacts become evident when comparing our results with previous studies (19). Hutchison *et al.* (2017), found that H cows in intensive systems reach first calving at an average of 24-25 months. In contrast, in our study, H and BS cows took longer to reach reproductive maturity, suggesting that pasture-based conditions impose additional constraints on the growth and development of heifers. This difference highlights the importance of adapting both nutritional and genetic management to local conditions to optimize reproductive efficiency (22).

Calving-to-conception interval (CCI) H x BS crossbred cows in our study had shorter CCI during the Spring-Summer than pure H cows, consistent with previous finding on their superior reproductive performance in warm months (7, 28, 29). In Argentina´s main dairy region cows are exposed to heat stress for at least 100 days per year, primarily in spring and summer (15). Thus, a shorter CCI is advantageous in grazing systems, enhancing reproductive efficiency and reducing unproductive periods. Similar trends have been reported by Blöttner *et al.* (2011a) and Prendiville *et al.* (2010), confirming higher pregnancy rates in crossbred cows.

The improvement in reproductive efficiency observed in H x BS crossbred cows could be attributed not only to hybrid vigor but also to the reduction of negative effects associated with inbreeding depression, which commonly affects pure H cows in intensive systems (5). This enhanced reproductive efficiency may be explained by the greater adaptability of crossbred cows to environmental fluctuations, such as forage quality and seasonal variations in temperature (30).

Conclusions

While no significant differences were observed in age at first calving (AFC) and 305-day milk yield (MY305) among breeds, the significant interaction between breed and season in calving-to-conception interval (CCI) suggests that both environmental conditions and genetic factors influence reproductive efficiency, particularly in H x BS cows during the warmest period of the year. Future studies could focus on further exploring the environmental and genetic factors that drive the observed interactions between breed and season, particularly in relation to optimizing reproductive efficiency in pasture-based systems.

References

1. Adriaens, I.; Bonekamp, G.; Ten Napel, J.; Kamphuis, C.; De Haas, Y. 2023. Differences across herds with different dairy breeds in daily milk yield-based proxies for resilience. Frontiers in Genetics. 14. Article 1120073. https://doi.org/10.3389/fgene.2023.1120073
2.Andersen, H. 2008. Alternativas genéticas para la ganadería lechera intensiva. En Manual de ganadería lechera (Capítulo 1.3). http://handresen.perulactea.com/manual-de-ganaderia-lechera/
3. Biga, P.; Barbona, I.; Lammoglia-Villagómez, M. Á.; Marini, P. R.; Hernández-Carbajal, G. R. 2022. Indicadores productivos y reproductivos de vacas Holstein y Holstein x Jersey durante la primera lactancia en sistemas a pastoreo. Revista Científica Biológico Agropecuaria Tuxpan. 10(2). http://www.revistabiologicoagropecuario.mx
4. Blöttner, S.; Heins, B. J.; Wensch-Dorendorf, M.; Hansen, L. B.; Swalve, H. H. 2011a. Brown Swiss × Holstein crossbreds compared with pure Holsteins for calving traits, body weight, backfat thickness, fertility, and body measurements. Journal of Dairy Science. 94(3): 1058-1068. https://doi.org/10.3168/jds.2010-3305
5. Buckley, F.; Lopez-Villalobos, N.; Heins, B. J. 2014. Crossbreeding: Implications for dairy cow fertility and survival. *Animal. 8*(1): 122-133. https://doi.org/10.1017/S1751731114000901
6. Cassell, B. G. 2001. Optimal genetic improvement for high producing cows. Journal of Dairy Science. 84: 144-150. https://doi.org/10.3168/jds.S0022-0302(01)70208-1
7. Dechow, C. D.; Rogers, G. W.; Cooper, J. B.; Phelps, M. I.; Mosholder, A. L. 2007. Milk, fat, protein, somatic cell score, and days open among Holstein, Brown Swiss, and their crosses. Journal of Dairy Science. 90(8): 3542-3549. https://doi.org/10.3168/jds.2006-889
8. El-Tarabany, M. S.; Nasr, M. A. 2015. Reproductive performance of Brown Swiss, Holstein, and their crosses under subtropical environmental conditions. Theriogenology. 84(4): 559-565. https://doi.org/10.1016/j.theriogenology.2015.04.012
9. Engler, P.; Cuatrin, A.; Apez, M.; Maekawa, M.; Litwin, G.; Centeno, A.; Moretto, M. 2022. Encuesta sectorial lechera del INTA: Resultados del ejercicio productivo 2020-2021. Paraná: INTA. Recuperado de https://www.ocla.org.ar/noticias/25641619-encuestalechera-inta-2020-2021-documento-completo

10. Fischman, M. L.; Torres, P. 2023. Estadísticas del mercado de semen bovino de la Argentina 2022. Cámara Argentina de Biotecnología de la Reproducción e Inseminación Artificial (CABIA). https://www.revistataurus.com.ar/entrada/estadisticas-del-mercado-de-semen-bovinode-la-argentina-2019-52212
11. Garcia-Peniche, T. B.; Cassell, B. G.; Misztal, I. 2006. Effects of breed and region on longevity traits through five years of age in Brown Swiss, Holstein, and Jersey cows in the United States. Journal of Dairy Science. 89(11): 3672-3680. https://doi.org/10.3168/jds.S0022-0302(06)72407-9
12. Heins, B. J.; Hansen, L. B.; Seykora, A. J. 2006a. Production of pure Holsteins versus crossbreds of Holstein with Normande, Montbéliarde, and Scandinavian Red. Journal of Dairy Science. 89: 2799-2804. https://doi.org/10.3168/jds.S0022-0302(06)72356-6
13. Heins, B. J.; Hansen, L. B.; Seykora, A. J. 2006b. Fertility and survival of pure Holstein versus crossbreds of Holstein with Normande, Montbéliarde, and Scandinavian Red. Journal of Dairy Science. 89: 4944-4951.
14. Hutchison, J. L.; VanRaden, P. M.; Null, D. J.; Cole, J. B.; Bickhart, D. M. 2017. Genomic evaluation of age at first calving. Journal of Dairy Science. 100(8): 6853-6861. https://doi.org/10.3168/jds.2016-12060
15. Lazzarini, B.; Llonch, P.; Baudracco, J. 2024. Animal welfare on Argentinean dairy farms based on the Welfare Quality® protocol framework. Journal of Animal Behaviour and Biometeorology. 12(2). Article 2024010. https://doi.org/10.31893/jabb.2024010
16. Lenth, R. 2024. EMMEANS: Estimated Marginal Means, aka Least-Squares Means. R package version 1.10.4, & lt; https://CRAN.Rproject.org/package=emmeans
17. Macdonald, K. A.; Verkerk, G. A.; Thorrold, B. S.; Pryce, J. E.; Penno, J. W.; McNaughton, L. R.; Burton, L. J.; Lancaster, J. A. S.; Williamson, J. H.; Holmes, C. W. 2008. Comparison of three strains of Holstein-Friesian grazed on pasture and managed under different feed allowances. Journal of Dairy Science. 91(4): 1693-1707. https://doi.org/10.3168/jds.2007-0441
18. Magne, M. A; Quénon, J. 2021. Dairy crossbreeding challenges the French dairy cattle sociotechnical regime. Agronomy for Sustainable Development. 41(2): 1-15. https://doi.org/10.1007/s13593-021-00683-2
19. Maldonado-Jáquez, J. A.; Torres-Hernández, G.; Hernández-Mendo, O.; Gallegos-Sánchez, J.; Mora-Flores, J. S.; Granados-Rivera, L. D. 2025. Long-term supplementation affects the production, composition and lactation curve of local grazing goats. Revista de la Facultad de Ciencias Agrarias. Universidad Nacional de Cuyo. 57(2): 155-164. DOI: https://doi.org/10.48162/rev.39.179
20. Mancuso, W. A. 2017. Evaluación y comparación de grupos genéticos lecheros en un sistema a pastoreo de la comarca lechera de Entre Ríos, Argentina. Recuperado de https://goo.gl/qbXa6Z
21. Marini, P. R.; García López, R.; Di Masso, R. J. 2015. Short communication: U.S. dairy selection programs impact in Argentina. Cuban Journal of Agricultural Science. 49(3): 299-305.
22. Melendez Retamal, P. 2011. Nutritional management of dairy heifers. En Risco, C. M., & Retamal, P. M. (Eds.), Dairy production medicine. 195-198.
23. Petraškienė, R.; Pečiulaitienė, N.; Jukna, V. 2013. Crossbreeding influence of dairy breeds cattle on average of lactation length and on average of productivity. Veterinarija ir Zootechnika (Vet Med Zoot). 64(86): 65-69.
24. Piccand, V.; Cutullic, E.; Meier, S.; Schori, F.; Kunz, P. L.; Roche, J. R.; Thomet, P. 2013. Production and reproduction of Fleckvieh, Brown Swiss, and 2 strains of Holstein-Friesian cows in a pasture-based, seasonal-calving dairy system. Journal of Dairy Science. 96(7): 5352-5363. https://doi.org/10.3168/jds.2012-6444
25. Pinheiro, J.; Bates, D.; R Core Team. 2024. Nlme: Linear and Nonlinear Mixed Effects Models. R package version 3.1-166. https://CRAN.R-project.org/package=nlme
26. Prendiville, R.; Lewis, E.; Pierce, K. M.; Buckley, F. 2010. Comparative grazing behavior of lactating Holstein-Friesian, Jersey, and Jersey × Holstein-Friesian dairy cows and its association with intake capacity and production efficiency. Journal of Dairy Science. 93(2): 764-774. https://doi.org/10.3168/jds.2009-2659
27. R Core Team. 2024. R: A language and environment for statistical computing. R Foundation for Statistical Computing. https://www.R-project.org/
28. Schaeffer, L. R.; Burnside, E. B.; Glover, P.; Fatehi, J. 2011. Crossbreeding results in Canadian dairy cattle for production, reproduction, and conformation. The Open Agriculture Journal. 5: 63-72.
29. Swalve, H. H.; Bergk, N.; Solms-Lich, P. H. 2008. Kreuzungszucht beim Milchrind - Ergebnisse aus einem Prazisbetrieb. Züchtungskunde. 80(6): 429-442.
30. Tao, S.; Dahl, G. E. 2013. Invited review: Heat stress effects during late gestation on dry cows and their calves. Journal of Dairy Science. 96(7): 4079-4093. https://doi.org/10.3168/jds.2012-6270
31. Vallone, R.; Camiletti, E.; Exner, M.; Mancuso, W.; Marini, P. 2014. Análisis productivo y reproductivo de vacas lecheras Holstein, Pardo Suizo y sus cruzas en un sistema a pastoreo. Revista Veterinaria. 25: 40-44.

Author contributions

JB: Conceptualization, Writing - review & editing; PRM: Supervision, Methodology, Writing -; VC: Data curation, Writing, review & editing; BL: Review & editing; AA: Statistical analysis.

Conflicts of interest

The authors declare no conflicts of interest.

Declaration of Funding and acknowledgments

Al Técnico Agropecuario Marcelo Exner y a la Escuela Agrotécnica "Las Delicias", por su colaboración en la recopilación de información y apoyo incondicional para la realización de este trabajo.

A data availability statement

The data that supports this study will be shared upon reasonable request to the corresponding author.

Long-term Supplementation Affects the Production, Composition and Lactation Curve of Local Grazing Goats

La suplementación a largo plazo afecta a la producción, la composición y la curva de lactación de cabras de pastoreo locales

Jorge Alonso Maldonado-Jáquez [1], Glafiro Torres-Hernández [2], Omar Hernández-Mendo [2], Jaime Gallegos-Sánchez [2], José Saturnino Mora-Flores [3], Lorenzo Danilo Granados-Rivera [4*]

Originales: *Recepción:* 05/08/2024 - *Aceptación:* 30/10/2024

Abstract

Twenty-four local goats were divided into two treatments: 1) control group fed only on grazing, and 2) supplemented group, which received supplemental feeding before parturition and during lactation. The highest values of milk production per goat, total milk production, days in milk production fat, protein and lactose yield per day were observed in goats of the supplemented treatment. No treatment effect was found for peak lactation production, persistence of peak production, duration of peak lactation production phase, total yield and fat, protein and lactose concentration, nor for milk production per goat, total milk production and days in milk production by type of calving (single or double). Wood's curve parameters had the lowest standard error of the estimator in control group, but the highest values of the estimator in supplemented group. We concluded that long-term dietary supplementation of local goats in northern Mexico increases milk production and milk protein, fat and lactose. In addition, it positively influences the estimation of lactation curve parameters.

Keywords
nutrition • small farmers • goats • milk quality

1 Instituto Nacional de Investigaciones Forestales, Agrícolas y Pecuarias. Campo Experimental La Laguna. 27440. Matamoros. Coahuila. México.
2 Colegio de Postgraduados. Campus Montecillo. Programa de Ganadería. 56230. Montecillo. Estado de México. México.
3 Colegio de Postgraduados. Campus Montecillo. Programa de Economía.
4 Instituto Nacional de Investigaciones Forestales, Agrícolas y Pecuarias. Campo Experimental General Terán. 67400. General Terán. Nuevo León. México.
* dgr_8422@hotmail.com

Resumen

Veinticuatro cabras locales se dividieron en dos tratamientos: 1) grupo control alimentadas solo a través del pastoreo, y 2) grupo suplementado que recibió alimentación suplementaria antes del parto y durante la lactación. Los valores más altos de producción de leche por cabra, producción total de leche, días en producción de leche, rendimiento de grasa, proteína y lactosa por día se observaron en las cabras del tratamiento control. No se observó ningún efecto del tratamiento sobre el pico de producción en lactación, la persistencia del pico de producción, la duración de la fase de pico de producción en lactación, el rendimiento total y la concentración de grasa, proteína y lactosa, ni sobre la producción de leche por cabra, producción total de leche y días en producción de leche según el tipo de parto (simple o doble). Los parámetros de la curva de Wood presentaron el error estándar más bajo del estimador en grupo control, pero los valores más altos del estimador en el grupo suplementado. Concluimos que la suplementación dietética a largo plazo de cabras locales en el norte de México incrementa la producción de leche, la proteína, grasa y lactosa en leche. Además, la suplementación influye positivamente en la estimación de los parámetros de la curva de lactación.

Palabras clave
nutrición • pequeños productores • cabras • calidad de la leche

Introduction

Breeding of local, native or indigenous goats offers nutritional and economic benefits, constituting a constant source of raw milk and dairy products, particularly for rural families (2, 17). Nevertheless, the scarce knowledge on production potential and milk composition of indigenous breeds has contributed to their replacement by specialized breeds.

In the arid and semi-arid marginalised regions of Mexico, to engage in goat production is common practice for smallholders (24). In these regions, goat herds are predominantly composed of animals referred to as criollos (15). This term is now widely accepted as a designation for 'locals', a category of goats that lack a clearly defined phenotype due to the introduction of diverse breeds, including Alpina, Saanen, Nubia and Toggenburg, through crossbreeding. This production system generates supplementary income in marginal regions in the north of the country, enhancing quality of life of families in these populations (25).

In this regard, several public genetic improvement programs have tried to introduce purebred (exotic) animals into local populations. However, most producers, particularly in northern Mexico, use animals *phenotypically* like purebreds, without genetic records or certainty regarding the expected improvement in production, leading to an erosion process in these populations, already well adapted to particular management conditions (24). This turns critical since genetic variability ensures animals cope with adverse environmental conditions (16).

Moreover, given overgrazed lands, poor soils, and periods of low rainfall, local breeds in extensive grazing systems show productive rates below the global average. Despite this, goats respond positively to supplementary feeding, and where strategies including both grazing and supplementation are incorporated, they improve profitability, milk production and its components than with solely grazing (3). However, supplementary feeding schemes for livestock are only offered during critical seasons, helping animals through drought events (10). Thus, establishing these feeding programs to exploit the production potential of local breeds constitutes an important issue (4), especially in northern Mexico. Although no studies in this region approach long-term supplementation of local goats, other studies have compared productivity under stabled conditions compared to grazing goats. These studies indicate that stabled goats produce 78% (14) and 71% (9) more milk than grazing goats, allowing us to infer that a long-term supplementation program can significantly increase milk production.

Our hypothesis stated that a long-term feed supplementation program increases overall productivity of goats. The objective was to evaluate goat response to a long-term feed supplementation program considering milk production, protein, lactose and milk fat composition and yield, and obtain a lactation curve.

Material and methods

This study strictly follows animal welfare and ethical guidelines according to the American Dairy Science Association, National Academy of Medicine (1, 6) and Mexican Institutionally with the approval of the project "Technological options to improve the productivity of extensive goat system in northern Mexico".

Twenty-four local goats with similar live weight (LW), body condition score (BCS; on a scale of 1 to 4), kidding number, and gestational age were taken from a commercial herd (n=125) located in Viesca, Coahuila, México, situated among 24° N and 102° W, at 1100 m a. s. l. Goats were assigned into two homogeneous groups under a repeated measures design. Treatments were randomly assigned to experimental units. Treatments were: 1) Control group (CG; n=12), LW of 38.5±4.8 kg, 1.9±0.2 BCS, 2.1±0.9 kidding's per goat, and 104±6 gestation days, fed with plant species normally obtained during grazing; 2) Supplemented group (SG; n=12), LW of 38.3±6.6 kg, 1.8±0.3 BCS, 2.2±1.2 kidding's per goat, and 104± 5 gestation days, received supplementary feeding (table 1) at a rate of 1.5% of animal LW, 45 days before kidding and throughout lactation (210 days in production).

Regular animal management is characterized by a prophylactic health management calendar, where the herd is vaccinated and dewormed twice a year. Animals grazed for approximately 9 h d^{-1} and returned to resting pens at 18:00 h, with access to fresh water.

The supplemented group was sheltered in individual pens of 2 x 3 m each. After grazing, animals were fed for approximately 10 minutes per goat, till full consumption.

Table 1. Ingredients and chemical composition of the total mixed diet as a supplement for local lactating goats under the extensive grazing system in northern Mexico.

Tabla 1. Ingredientes y composición química del suplemento para cabras lactantes locales bajo el sistema de pastoreo extensivo en el norte de México.

Ingredient	Quantity (g kg DM)	Nutritional content	
Rolled corn	18.0	CP	18.7
Rolled sorghum	18.0	ADF	21.6
Wheat bran	9.0	NDF	32.7
Soybean paste	9.0	NEm	1.8
Alfalfa hay	35.0	NEl	1.5
Molasses	8.0		
Urea	1.0		
Vitamin and Mineral premix*	2.0		

DM= dry matter; CP= crude protein; ADF= acid detergent fiber; NDF= neutral detergent fiber; NEm= net energy for maintenance (MCal/g kg EM); NEl= net energy for lactation (Mcal/g kg EM); *=mineral premix Ovi3ways® BIOTECAP Group.

MS= materia seca; PC= proteína bruta; FAD= fibra detergente ácido; FDN= fibra detergente neutro; NEm= energía neta de mantenimiento (MCal/g kg EM); NEl= energía neta de lactación (Mcal/g kg EM); *=premezcla mineral Grupo BIOTECAP Ovi3ways®.

Forage samples were collected during grazing (26), by observing chosen species. Forage samples were oven-dried at 65°C until constant weight, crushed in a hammer mill and sent to AGROLAB laboratory (Gómez Palacio, Durango, México) where a basic analysis was carried out with NIR (Foss NIRSystems 5000 M-Analyzer, Denmark). At the beginning of the study, (end of rainfall season) 14 plant species consumed were identified. Later, at the start of the dry season (middle of the experimental period) only 7 plant species and some crop-residues were identified.

The supplemented group was fed after grazing, individually, at 20:00 h, minimizing substitution effect on forage consumption while grazing (15), and until full consumption.

At parturition, kidding type, *i.e.* single or twins, and milk production were weekly assessed by the weighing-suckling-weighing technique (7), between 6:00 and 8:00h

and until weaning (30 days of age), starting the 5th day after kidding to ensure adequate colostrum consumption. The technique consisted of offspring weighing before and after suckling, after which MP was measured by weight difference. Once kids were weaned, MP was daily measured through individual production obtained from hand-milking until ceased milk production. Milk production expressed in grams (g) was measured using a standard electronic hook-type scale with a capacity of 45 kg±5 g (Metrology, Nuevo León, México). Milk quality (fat, protein, and lactose contents) was evaluated every 15 days with a 50ml sample, using the Milkoscope Expert Automatic® equipment (Razgrad, Bulgaria). Milk production per goat (MPG) and fat, protein, and lactose yields per day were measured according to the equation:

$$y= [(Pn+P(n-1)/2]* d$$

where
y = MPG and fat, protein, and lactose yields
Pn = Milk production on control day n
P(n-1) = milk production on previous control day
d = days between two controls

For lactation curve analysis, 1334 productive records of milk production (MP; n=574), and milk quality (MQ; n=760) were analysed. Total milk production per lactation (TMPL) and total fat, protein, and lactose yields per lactation (kg) were calculated using the Fleischamn method (2009), based on the following equation:

$$yi = (P1*D1+ \sum Pi+Pj+1/2* Di+Pk+1*DBR)$$

where
yi = trait
P1 = Milk production on the first record
D1 = interval between kidding and the first record
Pi, j, k = Milk production on the i,j,k-th record
Di = interval between the i-th record and the i+1(i=1,…,k) record
DBR = assumed as the number of days between recordings (7 in MP and 15 in MQ)

Variables determining the lactation curve were days in milk production (DMP; time between kidding and drying), production at lactation peak (PLP, kg; highest production), peak time production (PTP, d; time in which the doe reaches the highest yield); and duration of the lactation peak production phase (DLPPP, d; period of greatest production maintenance) (14).

Wood's incomplete gamma function, in its non-linear form (26), determined the parameters characterizing the lactation curve under the model:

$$yn=an^{b}e^{-cn}$$

where
yn = milk and/or fat, protein, and lactose production on the n-th day of lactation
e = base of the natural logarithm "a", "b" and "c" : constants
"a" = a scale factor, milk production or milk component at the beginning of lactation
"b" = rate of rise in milk production to peak
"c" = rate of decline in milk production to drying up

Statistical analysis was performed with SAS v9.4 statistical package. MPG, TMPL, PLP, PTP, DMP, DLPPP, content, and total fat, protein, and lactose yields were analyzed under a repeated measure mixed-effects model in a complete randomized design using the MIXED procedure. The model included the main effects of treatments, periods, and the interaction of treatment by period. The appropriate covariance structure for the analysis was determined by testing different structures, and the covariance structure with negative or near-zero values was chosen according to the Akaike and Schwartz criteria. MPG, TMP, and DMP were analysed by type of birth.

Results

Table 2 shows lactation results. The SG presented the higher values ($p<0.05$) for MPG, TMPL, and DMP variables. No effect was found for type of birth between treatments ($p>0.05$) for fat, protein, and lactose contents, nor for MPG, TMPL and DMP. The MPG increased 31% (0.140 kg) in SG goats with respect to CG. No differences were found for PLP, PTP, and DLPPP between treatments ($p>0.05$). Production peaks occurred on the third week at day 19 of lactation in both groups, with an average of 1.141 kg for SG and 0.820 kg for CG.

Table 2. Production performance by treatment and type of birth in local goats from northern Mexico.

Tabla 2. Desempeño productivo por tratamiento y tipo de parto en cabras locales del norte de México.

By Treatment			
	SG	**CG**	**P-Value**
Milk production per goat (kg d^{-1})	0.580±0.02	0.440±0.02	<0.0001
Total milk production per lactation (kg)	107.48±6.92	67.20±7.21	0.0008
Days in milk production (d)	184.49±9.62	151.98±10.02	0.0344
Peak lactation production (kg)	1.140±0.03	0.820±0.03	0.0756
Persistence of peak production (d)	19.0±2.00	19.0±2.00	0.9873
Duration of peak lactation production phase (d)	21.0±3.98	21.0±2.10	0.9602
Fat (%)	6.17±0.53	5.35±0.53	0.3093
Protein (%)	3.90±0.31	3.35±0.31	0.2490
Lactose (%)	5.83±0.47	5.01±0.47	0.2504
By kidding type			
	Single	**Double**	**P-Value**
Milk production per goat (kg d^{-1})	0.500±0.002	0.540±0.02	0.0584
Total milk production per lactation (kg)	89.50±8.70	94.12±5.88	0.5067
Days in milk production (d)	175.49±12.09	168.98±8.18	0.6480

SG= Supplemented group; CG= Control group; C.V. = Coefficient of variation.

SG= Grupo suplementado; CG= Grupo de testigo; C.V.= Coeficiente de variación.

No differences were found in milk fat, protein, and lactose percentages among treatments ($p>0.05$; table 3, page 160). Yet, differences were found between groups ($p<0.05$) in fat, protein, and lactose yields measured as kg d^{-1}. Furthermore, patterns of these components through lactation (figure 1, page 160) were similar, with different magnitude trends between treatments. In both groups, fat peaked at 47 days, and then decreased steadily until day 120. After day 120, fat content increased again and remained constant until the end of lactation. Meanwhile, protein and lactose showed average ranges throughout lactation between 2.9 and 3.1% and 4.2 and 4.6%, respectively. Also, a slight decrease was noted between 75 and 90 days for fat, protein and lactose contents (figure 1, page 160).

Table 3. Content (%) and yield (kg^{-1}) per day of fat, protein, and lactose between treatments in local goats from northern Mexico.

Table 3. Contenido (%) y rendimiento (kg^{-1}/día) de grasa, proteína y lactosa entre tratamientos en cabras locales del norte de México.

	SG	CG	P-Value	
			Treatment	Treat*Time
Fat (%)	5.26±0.19	5.30±0.20	0.6654	0.5417
Protein (%)	3.09±0.02	3.10±0.03	0.5651	0.5049
Lactose (%)	4.63±0.03	4.64±0.04	0.7162	0.6961
Fat (kg d^{-1})	0.032±0.0021	0.027±0.0023	0.0121	0.5192
Protein (kg d^{-1})	0.021±0.0013	0.017±0.0015	0.0026	0.4578
Lactose (kg d^{-1})	0.030±0.0022	0.025±0.0020	0.0024	0.4591

SG= Supplemented group; CG= Control group; Treat*Time= Interaction treatment* time effect. C.V= Coefficient of variation.

SG= Grupo suplementado; CG= Grupo testigo; Treat*Time= Efecto de interacción tratamiento*tiempo. C.V= Coeficiente de variación.

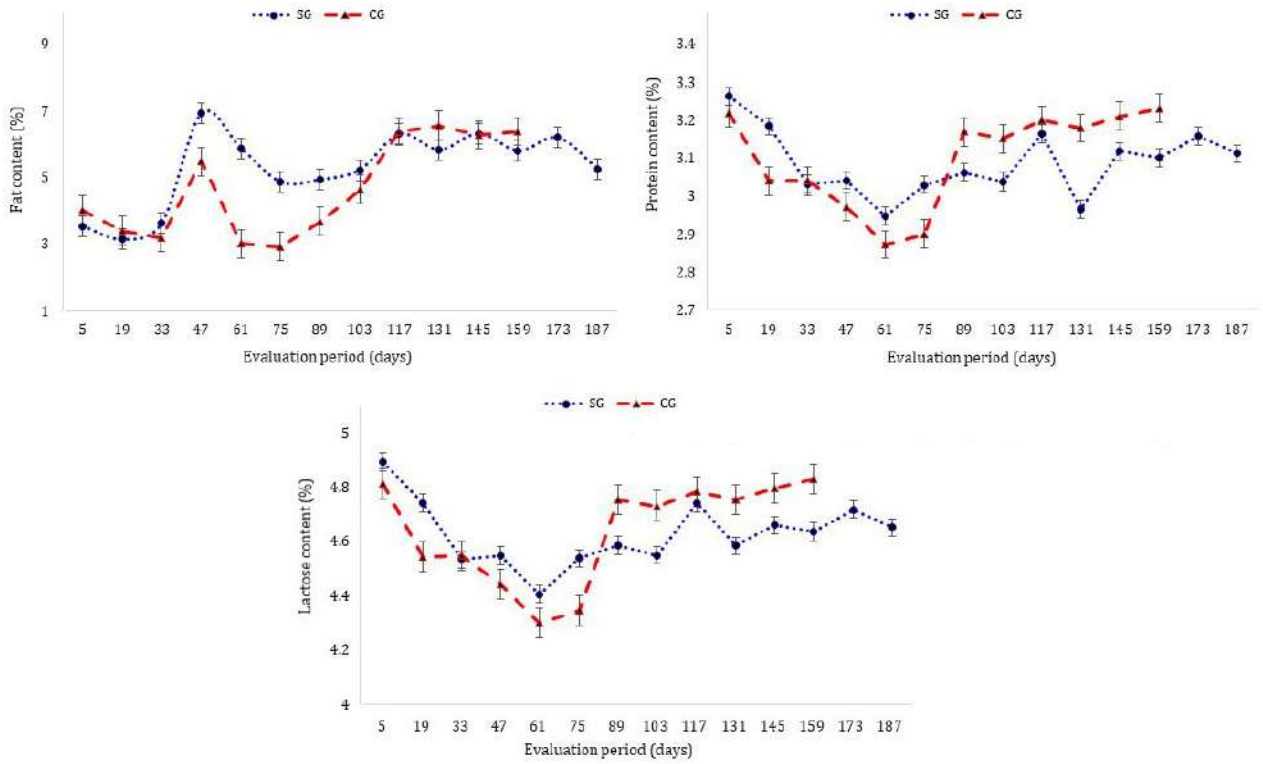

SG= Supplemented group; CG= Control group. / SG= Grupo suplementado; CG= Grupo de testigo.

Figure 1. Content (%) of fat, protein, and lactose in milk through lactation in local goats of northern Mexico.

Figura 1. Contenido (%) de grasa, proteína y lactosa en leche a lo largo de la lactancia en cabras locales del norte de México.

Table 4 (page 161), shows parameters a, b, and c characterizing milk production curve and fat, protein, and lactose yields. Likewise, figure 2 (page 161), shows milk production and milk components (fat, protein and lactose). Model best fit resulted for CG data in all variables, given a lower standard error. However, the higher estimator values ($p<0.05$) for parameter "a" and lower values for parameters "b" and "c" ($p>0.05$) were found in all variables for SG, indicating better productive performance throughout lactation for SG goats.

Table 4. Estimation of lactation curve parameters obtained through Wood's incomplete gamma function ([a, b, c]) according to treatments for local goats in northern Mexico.

Tabla 4. Estimación de los parámetros de la curva de lactancia obtenidos mediante la función gamma incompleta de Wood ([a, b, c]) según tratamientos para cabras locales del norte de México.

Trait	Parameter	SG ± S.E.	CG ± S.E.	P-Value
Milk yield	a	0.7848±0.1648	0.4303±0.0485	0.0256
	b	0.1390±0.0780	0.2841±0.0437	0.0482
	c	0.0103±0.0016	0.0155±0.0010	0.4821
Fat	a	0.0107±0.0068	0.0064±0.0022	0.0396
	b	0.5558±0.2157	0.7143±0.1235	0.0252
	c	0.0142±0.0039	0.0187±0.0024	0.1325
Protein	a	0.0264±0.0043	0.0059±0.0009	0.0534
	b	0.1628±0.1598	0.6258±0.0554	0.0039
	c	0.0115±0.0114	0.0196±0.0012	0.0638
Lactose	a	0.0397±0.0063	0.0088±0.0013	0.0335
	b	0.1598±0.0629	0.6260±0.0562	0.0069
	c	0.0114±0.0015	0.0195±0.0012	0.3211

SG= Supplemented group; CG= Control group; S.E.= Standard error; "a"= milk production or milk component at the beginning of lactation; "b"= rate of rise in milk production to peak; "c"= rate of decline in milk production to drying up.

SG= Grupo suplementado; GC= Grupo testigo; E.S.= Error estándar; "a"= producción de leche o componente lácteo al inicio de la lactación; "b"= tasa de aumento de la producción de leche hasta el pico de producción; "c" = tasa de disminución de la producción de leche hasta el secado.

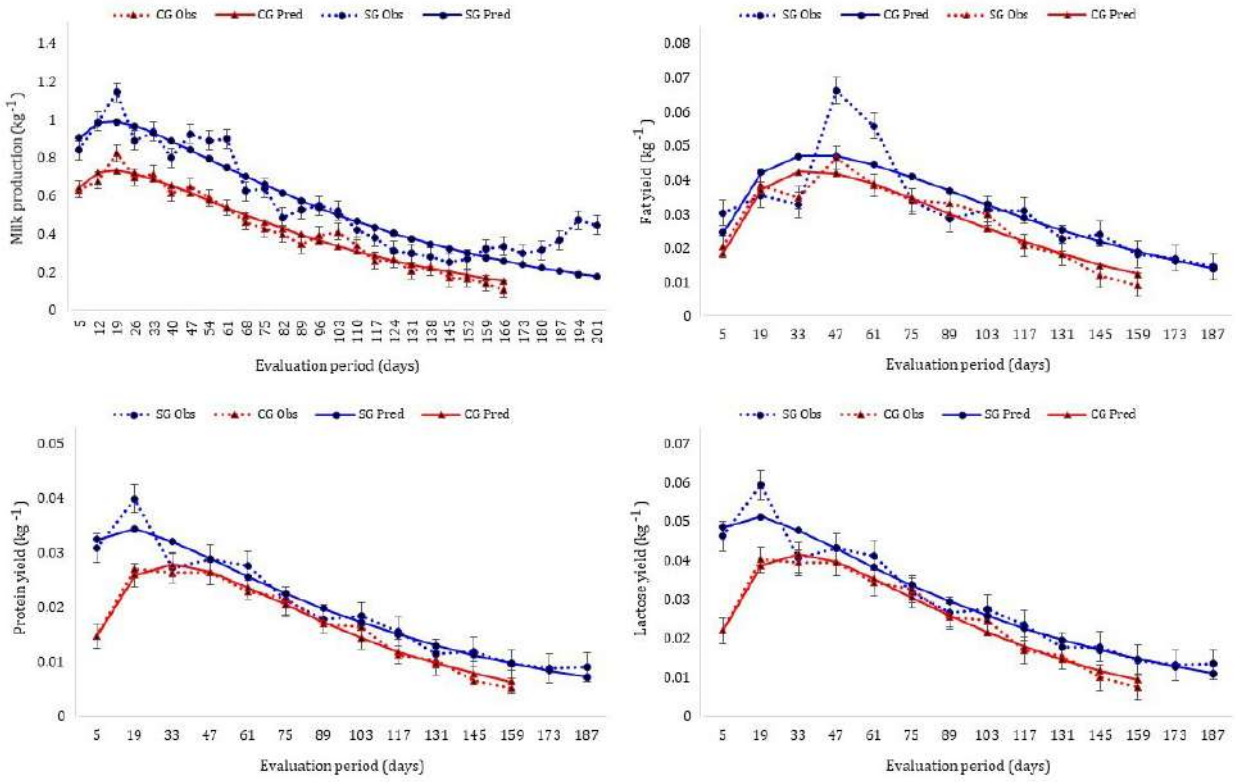

SG= Supplemented group; CG= Control group; Obs= Observed; Pred= Predicted; Prod= Production.
SG= Grupo suplementado; CG= Grupo testigo; Obs= Observado; Pred= Predicho; Prod= Producción.

Figure 2. Milk production and yield curves of fat, protein, and lactose in milk in local goats of northern Mexico.

Figura 2. Curvas de producción de leche y rendimiento de grasa, proteína y lactosa en leche en cabras locales del norte de México.

Discussion

After supplementation, positive effects were observed in milk production per goat, total production per lactation, days in milk production, and yield components, as noted by Bushara and Godah (2018) for desert goats in Sudan and by Otaru *et al.* (2020) in Red Sokoto goats in Nigeria.

Production levels of goats in SG were superior to other local genotypes (West African dwarf goats and Red Sokoto) receiving supplementary feeding (19), with lower values for CG, demonstrating the productive potential of this Mexican genotype. These animals significantly enriched production under improved environmental conditions like nutrient supply (20). Similarly, production levels differed from the reported by Oliveira *et al.* (2012) for Nubian goats (1.08 kg) whith a supplementation of 1.5% of the LW. Nevertheless, considering this particular case, exotic dairy breeds show a higher, though lower quality, milk production level than local goats (4). In our study, goats increased milk production, without affecting milk quality.

Results regarding PLP, PTP, and DLPPP were consistent with Salinas-González *et al.* (2015) and creole goats in Coahuila, México, where maximum milk production (0.848 kg) was found on day 16 of lactation. DLPPP was recorded on early lactation from days 12 to 33 in both groups, differing from Waheed and Khan (2013) for Beetal goats. These authors found a production peak of 1.340 kg, higher than in our study, with a maximum production phase in mid lactation (weeks 7-9) and a shorter duration. In addition, Henao *et al.* (2017) mentioned a lower PTP (10.02 d) for mestizo goats of Colombia and a higher PLP (1.710 kg d^{-1}) than the stated for our local goats. Local goats in northern Mexico are used for milk production, but the duration of lactation is mostly unknown (25).

Regarding TMPL, Arabia goats in Algeria and Carpathian goats in Rumania produce 168 kg and 160 kg, respectively (13) higher than our local goats. On the other hand, the control group had TMPL values above the reported for indigenous and mestizo goats from southern and northern Mexico (24, 25) with an average lactation length of 105 days. However, this control TMPL was lower than the 82.9 kg of indigenous goats in Morocco with lactations of 117 days (12). This valuable information prevents underutilization, erosion or elimination of superior productive animals (25).

On the other hand, SG showed a DMP of 32.5 days higher than CG, coinciding with the range reported for Bornova and Saanen goats in Turkey (180-200 d) (23), but under the 210 days reported for Alpine goats in Colombia (11). Likewise, CG coincided with lactation ranges (141-160 d) found in Sirohi goats in India under feeding supplementation (3). This information reveals that local goats in northern Mexico considerably improve DMP and TMPL when supplemented, evidencing feasibility of establishing genetic improvement schemes to increase milk production (8).

Regarding milk composition, the lowest values considering all components were found between the 5th and 7th week of lactation, just after production peaks, in accordance with Currò *et al.* (2019) for Italian indigenous goats. Component behaviour along lactation in local goats of northern Mexico has a constant trend. Fat varies less than 2%, while protein and lactose vary less than 0.3%, agreeing with Salinas-González *et al.* (2015) for local goats of northern Mexico, although total values were slightly lower for fat and superior in protein and lactose contents. Additionally, in Nguni, Boer, and Indigenous genotypes from South Africa, milk fat varies 3.5% throughout lactation while protein and lactose vary 0.5 and 0.7% respectively (13) coinciding with our patterns and maximum initial, lower middle and medium late values in lactation.

When supplementary feeding was offered, our contents of fat, protein, and lactose were superior to those reported by de Oliveira *et al.* (2020) for Nubian goats, even considering those goats produced more milk of poorer quality with more fat and lactose than other genotypes (3). Local or indigenous goats show better quality than specialized breed goats for milk production (5).

Regarding curve parameters, Takma *et al.* (2009) found superior “a” and “c” values for Bornova goats. Rojo-Rubio *et al.* (2015) found superior “a” and “b” parameters, but lower “c” values in Alpine, Saanen, and Anglo-Nubian goats. Torres-Hernández *et al.* (2022b), reported superior values in “a”, and lower “b” and “c” in local goats from northern Mexico

without supplementation, while Zambom *et al.* (2017) showed superior results in "a", but lower in "b" and "c" in supplemented Saanen goats from Brasil.

Our results highlight the productive potential of local goats from northern Mexico, since despite lactation curve parameters are lower than others, long-term feed supplementation promotes an increase in parameter "a" and lower declination values before and after production peaks (parameters "b" and "c") for MP and milk fat, protein, and lactose.

Conclusions

We conclude that under our experimental conditions, continuous supplementation from 1.5% of live weight in local goats of northern Mexico increases milk production and quality. Supplementation helps this local genotype express whole genetic potential.

In addition, continuous supplementary feeding from the last third of gestation increases milk production throughout lactation. Yet, this increase in production influences the standard error for the curve parameters, under or overestimating the predicted values.

It is essential to validate the findings of this study with the supplement used and with other supplements available in arid and semi-arid regions with goat attitude. This will facilitate the generation of additional feed options for use by small goat producers.

References

1. ADSA (American Diary Science Association). 2020. Guide for the care and use of agricultural animals in research and teaching, 4th ed. Champaing. IL. https://www.asas.org/docs/default-source/default-document-library/agguide_4th.pdf?sfvrsn=56b44ed1_
2. Bautista-Martínez, Y.; Granados-Rivera, L. D.; Jimenez-Ocampo, R.; Maldonado-Jáquez, A. 2024. Morphostructural composition and meat quality in local goat kids from the northeastern region of Mexico. Revista de la Facultad de Ciencias Agrarias. Universidad Nacional de Cuyo. Mendoza. Argentina. 56(1): 127-137. DOI: https://doi.org/10.48162/rev.39.129
3. Bhateshwar, V.; Datt, M.; Jat, G. R.; Pankaj-Rathaur, A.; Muwal, H. 2018. Effect of feeding different levels of concentrate mixture on yield and composition of milk and lactation length in Sirohi goats, International Journal of Livestock Research. 8: 113-119. http://dx.doi.org/10.5455/ijlr.20180416095835
4. Bushara, I.; Godah, F. G. I. 2018. Effect of supplementary feeding with residual of sesame capsule to lactating desert goat during dry period in north Kordofan state, Sudan. Advances in Biology & Earth Sciences. 3: 47-59.
5. Currò, S.; Manuelian, C. L.; De Marchi, M.; Claps, S.; Rufrano, D.; Neglia, G. 2019. Effects of breed and stage of lactation on milk fatty acid composition of Italian goat breeds. Animals. 9: 764. https://doi.org/10.3390/ani9100764
6. FASS (Federation of Animal Science Societies). Guide for the care and use of agricultural animal an agricultural research and teaching. 2010. In: Federation of Animal Science Societies [database online], 3rd. ed. Champaign. IL. http://www.fass.org/docs/agguide3rd/Ag_Guide_3rd_ed.pdf
7. Fernández, N.; Balasch, S.; Pérez, I.; Rodríguez, M.; Peris, C. 2013. Milk yield estimation during suckling using the double oxytocin injection-milking and the double weighing–suckling methods in dairy goats. Small Ruminant Research. 112: 181-185. https://doi.org/10.1016/j.smallrumres.2012.12.023
8. González-Peña, D.; Acosta, J.; Guerra, D.; González, N.; Acosta, M.; Sosa, D.; Torres-Hernández, G. 2012. Modeling of individual lactation curves for milk production in a population of Alpine goats in Cuba. Livestock Science. 150: 42-50. https://doi.org/10.1016/j.livsci.2012.07.026
9. Granados-Rivera, L. D.; Hernández-Mendo, O.; Maldonado-Jáquez, J. A. 2020. Energy balance in lactating goats: Response to mixture of conjugated linoleic acid. Animal Science Journal. e13347. https://doi.org/10.1111/asj.13347
10. Granados-Rivera, L. D.; Maldonado-Jáquez, J. A.; Bautista-Martínez, Y.; Garay-Martínez, J. R.; Álvarez-Ojeda, M. G. 2022. The feeding supplementation schedule modifies productive response of grazing dairy goats. Revista MVZ Córdoba. 27: e2340. https://doi.org/10.21897/rmvz.2340
11. Henao, K. T.; Blandón, Y. A.; González-Herrera, L. G.; Cardona-Cadavid, H.; Corrales, J. D.; Calvo, S. J. 2017. Efectos genéticos y ambientales sobre la curva de lactancia en cabras lecheras del trópico. Livestock Research for Rural Development. 29: 97.
12. Ibnelbachyr, M.; Boujenane, I.; Chikhi, A.; Noutfia, Y. 2015. Effect of some non-genetic factors on milk yield and composition of Draa indigenous goats under an intensive system of three kidding in 2 years. Tropical Animal Health and Production. 47: 727-733. https://doi.org/10.1007/s11250-015-0785-8

13. Idamokoro, E. M.; Muchenje, V.; Masika, P. J. 2018. Yield and milk composition at different stages of lactation from a small herd of Nguni, Boer, and Non-descript goats raised in an extensive production system. Sustainability. 9: 1000. https://doi.org/10.3390/su9061000
14. Macciotta, N. P. P.; Dimauro, C.; Steri, R.; Cappio-Borlino, A. 2008. Mathematical modelling of goat lactation curves. In: A. Cannas; G. Pulina (Eds.). Dairy goats feeding and nutrition. CAB International. p. 31-46. DOI: 10.1079/9781845933487.0031
15. Maldonado-Jáquez, J. A.; Granados-Rivera, L. D.; Hernández-Mendo, O.; Pastor-López, F. J.; Isidro-Requejo, L. M.; Salinas-González, H.; Torres-Hernández, G. 2017. Use of total mixed ration as supplement in grazing local goats: Milk production response and chemical composition. Nova Scientia. 9: 55-75. https://doi.org/10.21640/ns.v9i18.728
16. Moyao-Ariza, F.; Maldonado-Jáquez, J. A.; Granados-Rivera, L. D.; Martínez-Rojero, R. D.; Torres-Hernández, G.; Domínguez-Martínez, P. A.; Bautista-Martínez, Y.; Sánchez-Gutiérrez, R. A. 2022. Variabilidad morfoestructural, zoométrica y faneróptica de machos cabríos locales del norte de México. ITEA (Información Técnica Económica Agraria). 118: 361-376. https://doi. org/10.12706/itea.2021.030
17. Oliveira, J. G.; Dardengo Sant´Anna, D. F.; Lourenco, M. C.; Tavares, D. S.; Rodrigues, M. T.; Tedeschi, L. O.; Mendonça Vieira, R. A. 2020. The geometry of the lactation curve on Wood's equation: a two-step prediction. Revista Brasileira de Zootecnia. 49: e20200023. https://doi.org/10.37496/rbz4920200023
18. Oliveira, M.; Azevedo Alves, A.; Martins Rodriguez, M.; Lustosa de Moura, R.; Rodrigues Cavalcante, A. C.; Pinheiro Rogério, M. C. 2012. Goat milk production and quality on Tanzania-grass pastures, with supplementation. Acta Scientiarum. Animal Sciences. 34: 417-423. https://doi. org/10.4025/actascianimsci.v34i4.14339
19. Otaru, S. M.; Adamu, A. M.; Ehoche, O. W. 2020. Influence of levels of supplementary concentrate mixture on lactation performance of Red Sokoto does and the pre-weaning growth rate of their kids. Veterinary and Animal Science. 10: 100137. https://doi.org/10.1016/j.vas.2020.100137
20. Parra Ferrín, D.; Cusme Lucas, G.; Talledo Solórzano, V.; Loor Gorozabel, B.; Pazmiño Castro, A.; Cuenca-Nevárez, G. J. 2023. Efficacy of zinc lactate and *Lactobacillus bulgaricus* on nutrition and health of broiler chickens. Revista de la Facultad de Ciencias Agrarias. Universidad Nacional de Cuyo. Mendoza. Argentina. 55(2): 120-128. DOI: https://doi.org/10.48162/rev.39.114
21. Rojo-Rubio, R.; Kholif, A. E.; Salem, A. Z. M.; Mendoza, G. D.; Elghandour, M. M. M. Y.; Vázquez-Armijo, J. F.; Lee-Rangel, H. 2015. Lactation curves and body weight changes of Alpine, Saanen and Anglo-Nubian goats as well as pre-weaning growth of their kids. Journal of Applied Animal Research. 44: 331-337. http://dx.doi.org/10.1080/09712119.2015.1031790
22. Salinas-González, H.; Maldonado-Jáquez, J. A.; Torres-Hernández, G.; Triana-Gutiérrez, M.; Isidro-Requejo, L. M.; Meda-Alducin, P. 2015. Compositional quality of local goat milk in the Comarca Lagunera of Mexico. Revista Chapingo-Serie Zonas Áridas. 14(2): 175-184. https://doi.org/10.5154/r.rchsza.2015.08.008
23. Takma, C.; Akbaş, Y.; Taskin, T. 2009. Modeling lactation curves of Turkish Saanen and Bornova goats. Asian Journal of Animal and Veterinary Advances. 4: 122-129. https://dx.doi.org/10.3923/ajava.2009.122.129
24. Torres-Hernández, G.; Maldonado-Jáquez, J. A.; Granados-Rivera, L. D.; Salinas-González, H.; Castillo-Hernández, G. 2022a. *Status quo* of genetic improvement in local goats: a review. Archives Animal Breeding. 65: 207-221. https://doi.org/10.5194/aab-65-207-2022
25. Torres-Hernández, G.; Maldonado-Jáquez, J. A.; Granados-Rivera, L. D.; Wurzinger, M.; Cruz-Tamayo, A. A. 2022b. Creole goats in Latin America and the Caribbean: A priceless resource to ensure the well-being of rural communities. International Journal of Agricultural Sustainability. 20: 368-380. https://doi.org/10.1080/14735903.2021.1933361
26. Toyes-Vargas, E. A.; Murillo-Amador, B.; Espinoza-Villavicencio, J. L.; Carreón-Palau, L.; Palacios-Espinoza, A. 2013. Composición química y precursores de ácidos vaccénico y ruménico en especies forrajeras en Baja California Sur, México. Revista Mexicana de Ciencias Pecuarias. 4: 373-386.
27. Waheed, A.; Khan, M. S. 2013. Lactation curve of Beetal goats in Pakistan. Archives Animal Breeding. 56: 892-898. https://doi.org/10.7482/0003-9438-56-089
28. Wood, P. D. P. 1967. Algebraic model of the lactation curve in cattle. Nature. 216: 164-165. https://doi.org/10.1038/216164a0
29. Zambom, M. A.; Alcalde, C. R.; Gomes, L. C.; de Oliveira Ramos, C. E. C.; Rossi, R. M.; da Silva Kazama, D. C. 2017. Effect of soybean hulls on lactation curves and the composition of goat milk. Revista Brasileira de Zootecnia. 46: 167-173. http://dx.doi.org/10.1590/S1806-92902017000200012

Guava Leaf Meal (*Psidium guajava* L.) in Broiler Diets: Effects on Performance, Nutrient digestibilty, and Intestinal Morphology

Harina de hojas de guayaba (*Psidium guajava* L.) en dietas para pollos de engorde: efectos sobre el rendimiento, la digestibilidad de los nutrientes y la morfología intestinal

Juan Carlos Blandon Martínez *, Luz Estella Vásquez David, Hader Iván Castaño Peláez, Luis Fernando Londoño Franco, Camilo Soto Londoño

Originales: *Recepción:* 24/03/2025 - *Aceptación:* 11/08/2025

Abstract

This study investigated the effect of guava leaf meal (GLM) as a phytobiotic in broilers, focusing on its chemical properties and potential physiological benefits. 135 one-day-old male Cobb broilers were randomly allocated to five treatments (nine replicates per treatment and three birds per replicate): a basal diet with regulated commercial antibiotic (T1), without regulated commercial antibiotic or growth promoters (T2), 1% GLM (T3), 1.5% GLM (T4), and 2% GLM (T5) for 38 d. T2, T3, T4, and T5 reduced feed intake (FI) during the finishing phase (days 20–38, $P < 0.0001$), but there were no statistical differences in accumulated feed intake (AFI) between treatments. GLM groups had lower ADG during the starter phase (days 3-20, $P < 0.05$), but there were no statistical differences in accumulated gain. Accumulated feed conversión rate (FCR) was better in T2 to T5 compared to T1 ($P < 0.05$). GLM groups (T3, T4 and T5) showed significantly higher values of nutrient digestibility ($P < 0.05$). Duodenum morphology showed that number of villi ($P=0.02$) and the villus height ($P= 0.03$) increased with GLM supplementation with respect to control groups (T1 and T2). In conclusion, GLM-based diets enhanced nutrient digestibility and improved intestinal architecture, thereby supporting their inclusion in broiler chicken diets to optimize production efficiency.

Keywords
Intestinal architecture • phytobiotics • poultry • plant extracts • additives

Politécnico Colombiano JIC. Facultad de Ciencias Agrarias. Cra 48 No. 7-151 of P19-111A. C. P. 050022. Medellín. Colombia. * jcblandon@elpoli.edu.co

Resumen

Se estudió el efecto de la harina de hojas de guayaba como fitobiótico en pollos de engorde, centrándose en sus propiedades químicas y sus posibles beneficios fisiológicos. 135 pollos Cobb machos de un día de edad se aleatorizaron en 5 tratamientos (9 réplicas por tratamiento y 3 aves por réplica): una dieta basal con antibiótico comercial (T1), sin antibiótico comercial ni promotores de crecimiento (T2), 1% GLM (T3), 1,5% GLM (T4) y 2% GLM (T5) durante 38 días. T2, T3, T4 y T5 redujeron el consumo de alimento (CA) en fase de finalización (día 20-38, $P < 0,0001$), pero en consumo de alimento acumulado (CAA), no hubo diferencias estadísticas entre tratamientos. Los grupos GLM tuvieron menor ganancia media diaria (GMD) en fase de inicio (día 3-20, $P < 0,05$), pero en ganancia acumulada no hubo diferencias estadísticas. La tasa de conversión alimenticia acumulada (TCA) fue mejor en los grupos T2 a T5 en comparación con T1 ($P < 0,05$). Los grupos GLM (T3, T4 y T5) mostraron valores significativamente mayores de digestibilidad de nutrientes ($P < 0,05$). La morfología del duodeno mostró que el número de vellosidades ($P = 0,02$) y altura de vellosidades ($P = 0,03$) aumentaron con la adición de GLM en comparación con los grupos control (T1 y T2). En conclusión, las dietas adicionadas con GLM mejoraron la digestibilidad de los nutrientes y la arquitectura intestinal, lo que justifica su inclusión en las dietas de pollos de engorde, para optimizar la eficiencia productiva.

Palabras clave
Arquitectura intestinal • fitobióticos • aves de corral • extractos vegetales • aditivos

Introduction

Using technological or food additives is an effective strategy to enhance animal productivity while providing a natural approach to reducing production costs. Plant extracts, also known as phytobiotics or phytogenics, have been used for medicinal purposes since ancient times and are widely employed in traditional and alternative veterinary medicine (6). In recent years, the use of herbal medicines and plant-based extracts in livestock production has gained popularity, driven by concerns over the side effects of conventional drugs, high input costs, toxic residues in feed, microbial resistance, and the growing demand for organic and sustainable livestock production systems (16, 20). For this reason, plant-based additives have been widely investigated as alternatives to antibiotics and growth promoters for use in animal health and production, since they perform multiple beneficial functions in the gastrointestinal tract and are less likely to induce the development of microbial resistance (34).

Guava leaf, characterized by its unique chemical composition (28), has been demonstrated to exert various physiological effects in humans and animals. It serves as an antimicrobial agent (8, 10), provides health-promoting bioactive compounds (15, 19), offers protective effects on the gastrointestinal tract (33), and exhibits potential nutraceutical benefits (13), among other advantages.

Adding guava leaf extracts has been shown to enhance productive performance and reduce the incidence of diarrhea in weaned piglets (33). In broiler chickens, incorporating guava fruit by-products during the starter phase (7-21 days) improved productive performance and meat quality, with a linear increase in daily weight gain (DWG) as the by-product inclusion increased. Although no changes were observed in villus height or crypt depth, the villus height-to-crypt depth ratio increased with higher levels of the by-product (23). Similarly, diets containing guava leaf meal combined with olive oil in chickens led to improved weight gain, better feed conversion rates, reduced fat content in breast and thigh muscles, and lower total blood lipid levels (22).

The gastrointestinal tract plays a critical role in digestion and nutrient absorption, essential for proper animal growth and development, ultimately enhancing productive performance. Specifically, the morphology and histological structure of the small intestine, particularly the duodenum, are vital. The duodenal mucosa with its villi and microvilli, facilitates efficient nutrient assimilation. These structures significantly amplify nutrient

absorption, increasing it by approximately 10 and 20 times, respectively. Moreover, the quantity and length of villi and microvilli can further expand the intestinal mucosa's surface area, enhancing absorption capacity (11, 14, 31).

Research indicates that guava leaf meal and its extracts, when included in animal diets, positively influence intestinal morphology, immune response, and productive parameters. Specifically, these supplements enhance intestinal morphology, improving nutrient absorption (12, 16, 31). They also strengthen immune response, reducing microbial load and supporting better physiological outcomes (8, 10, 13, 18). Additionally, they contribute to improved productive parameters, such as growth and feed efficiency (1, 2). However, no prior studies have specifically investigated these effects in chickens, particularly regarding nutrient digestibility. Therefore, this study aims to evaluate the impact of adding guava leaf meal to chicken diets on intestinal morphology, nutrient digestibility, and productive parameters.

Materials and methods

The trial was conducted at the Experimental Farm of the Facultad de Ciencias Agrarias de la Universidad Politécnico Colombiano JIC (Jaime Isaza Cadavid). The experimental procedures in this trial were approved by the Ethical Committee Animal Care and Use of the University under filed protocol number 20610801-202301004049.

Experimental Design and Diets

A total of 135 male day-old broiler chickens (Avian Male Cobb) were purchased from a local authorized distribution company. The broiler chickens were randomly assigned to five groups in a completely randomized design. Each group consisted of nine replicate cages, with three birds housed per cage in an appropriate housing facility. The five dietary treatments consisted of a basal diet with a regulated commercial antibiotic (Zinc bacitracin 15%, 500 g/t and Halquinol 60, 100g/t) (T1), a basal diet without antibiotics or growth promoters (T2), and diets added with1% (T3), 1.5% (T4), or 2% (T5) guava leaf meal (GLM) in both starter (days 3-20) and finisher (days 21-38) phases. The basal diet, a corn-soybean meal-based commercial crumble feed, was formulated to meet broiler nutritional requirements per NRC (1994) and purchased from a recognized local feed company. Diets were isoproteic and isoenergetic, with their chemical composition analyzed following AOAC (2005) methods, as presented in table 1 (page 168). Broiler chickens were fed a basal diet during the first 2 days of acclimatization. The groups were provided a basal diet, either added with guava leaf meal (GLM) or unadded based on the treatment. The birds had ad libitum access to feed and water throughout the experimental period. Lighting was 24 hours per day during the first week and 16 hours of light and 8 hours of darkness in subsequent weeks. All birds were subjected to consistent environmental and management conditions.

GLM Collection

To prepare guava leaf meal (GLM), leaves were collected from the northern region of Antioquia in the Colombian tropics, located at 1,100 meters above sea level with an average temperature of 26°C. The leaves were cleaned, dried in a forced-air oven, and ground into a fine powder using a laboratory mill for incorporation into experimental diets. The composition of GLM is presented in table 2 (page 168).

Growth Performance

Initial body weight (BWi) was determined at the beginning of the experiment. Body weight was recorded weekly for each cage and subsequently analyzed by period (starter: days 3-20; finisher: days 21-38). In addition, the feed offered and the feed refused were weighed daily. The recorded data was used to calculate average daily gain (ADG, $g.chick^{-1}$), feed intake (FI, $g.chick^{-1}$), feed conversion ratio (FCR, $FI.WG^{-1}$) and weight gain (WG, $g.chick^{-1}$) for the starter, finisher and total periods.

Table 1. Composition and nutritional value of basal diets for starter and finisher periods (g.kg^{-1}).

Tabla 1. Composición y valor nutritivo de las dietas basales para periodo iniciador y terminador (g.kg^{-1}).

Diet (g.kg^{-1})		
	starter	**Finisher**
Ingredients		
Corn meal (*Zea mays*)	522	540
Soybean meal (46% CP)	218	193
Extruded soybean meal	200	200
Soy oil	21.5	31.8
Salt	3.3	4.0
$CaCO_3$	9.0	8.2
PO_4H_2Ca	19.8	17.5
DL-Methionine	2.4	1.4
Vitamin and mineral mixture [1]	4.0	4.0
Calculated Analysis [2]		
AME_n (kcal.kg^{-1})	3,100	3.200
Total lysine (g.kg^{-1})	12.1	11.5
Sulfur amino acids (g.kg^{-1})	9.0	7.7
Determined Analysis		
Dry matter (DM, g.kg^{-1})	880	885
Gross energy (GE, kcal.kg^{-1})	4,680	4.710
Crude protein (CP, g.kg^{-1})	215	191
Crude ash (g.kg^{-1})	70	65
Ca (Ca, g.kg^{-1})	10.5	8.9
P (total P, g.kg^{-1})	7.4	6.9

[1]Provided the following per kilogram of complete diet: vitamin A, 12,000 IU; vitamin D_3, 2,400 IU; vitamin E, 30 mg; vitamin K_3, 3 mg; vitamin B_1, 2.2 mg; vitamin B_2, 8 mg; vitamin B_6, 5 mg; vitamin B_{12}, 11 mg; folic acid, 1.5 mg; biotin, 150 mg; calcium pantothenate, 25 mg; nicotinic acid, 65 mg; Mn, 60 mg; Zn, 40 mg; I, 0.33 mg; Fe, 80 mg; Cu, 8 mg; Se, 0.15 mg; ethoxyquin, 150 mg. [2]FEDNA (2003).

[1]Se proporcionó lo siguiente por kilogramo de dieta completa: vitamina A, 12.000 UI; vitamina D3, 2.400 UI; vitamina E, 30 mg; vitamina K3, 3 mg; vitamina B1, 2,2 mg; vitamina B2, 8 mg; vitamina B6, 5 mg; vitamina B12, 11 mg; ácido fólico, 1,5 mg; biotina, 150 mg; pantotenato de calcio, 25 mg; ácido nicotínico, 65 mg; Mn, 60 mg; Zn, 40 mg; I, 0,33 mg; Fe, 80 mg; Cu, 8 mg; Se, 0,15 mg; etoxiquina, 150 mg. [2]FEDNA (2003).

Table 2. Chemical Composition of Guava Leaf Meal (GLM) (g.100^{-1}) on a Dry Matter Basis.

Tabla 2. Composición química (g.100^{-1}) de la harina de hoja de guayaba en base a materia seca.

Component	**Result**	**Analysis Method**
Calcium	1.17	Atomic Abs Spectrometry
Crude Protein	11.2	Volumetric (Kjeldahl)
Ash	5.58	Gravimetric
Fat content	2.73	Gravimetric
Phosphorus	0.15	UV-VIS Spectrophotometry
Moisture and Volatile matter	9.0	Gravimetric
Gross calorific value	4817 cal.g^{-1}	Calorimetry

Results are expressed on a dry matter basis. Crude protein content was calculated using a conversión factor of 6.25. Results apply only to the analyzed simple (Sample Code: 78376, Request: 12247).

Los resultados se expresan en materia seca. El contenido de proteína cruda se calculó utilizando un factor de conversión de 6,25. Los resultados corresponden únicamente a la muestra analizada (Código de muestra: 78376, Solicitud: 12247).

Digestibility

To assess nutrient digestibility, feed intake was recorded, and total excreta were collected on days 34 and 35. Excreta from each experimental diet were quantitatively collected daily from five cages per treatment. Excreta samples were homogenized, and subsamples were taken per cage. Both feed and excreta samples were dried in a forced-air oven at 103°C to constant weight to determine dry matter (DM) content, following AOAC method 925.09 (4). Ash content was determined by incinerating the samples in a muffle furnace at 525°C for 7 hours, according to AOAC method 923.03 (4). Organic matter (OM) was calculated as:

$$OM\ (\%) = 100 - \%\ Ash$$

Crude protein (CP) was determined using the Kjeldahl method, multiplying nitrogen content by 6.25, as per AOAC method 984.13 (4). Calcium (Ca) and phosphorus (P) were analyzed by atomic absorption spectrophotometry for Ca (AOAC method 927.02) and colorimetry for P (AOAC method 965.17) (4). Apparent digestibility for each nutrient (dry matter, organic matter, crude protein, calcium, and phosphorus) was calculated using the formula:

$$\text{Apparent Digestibility (\%)} = ((\text{Nutrient intake} - \text{Nutrient excreted}) / \text{Nutrient intake}) \times 100.$$

Experimental Sampling and Intestinal Morphology

On day 38, six birds per treatment were randomly selected from two replicate cages (three birds per cage) to ensure representative sampling. The birds were transported to the slaughterhouse and euthanized by cervical dislocation. Slaughter weight was recorded for each bird. A 1 cm segment of the medial duodenum was collected from each bird and immediately fixed in 10% neutral buffered formalin for preservation. Tissue samples were processed using a rotary microtome to obtain 5 µm sections, stained with hematoxylin and eosin (H&E) following standard histological procedures.

The intestinal mucosa was examined under a light microscope with a Moticam® digital camera at 4× and 10× magnifications. Morphometric analysis focused on the duodenal villi and crypts. Villus height was measured in microns from the basal edge (at the junction with the crypt) to the apical edge. Crypt depth was determined by measuring the distance from the base of the crypt to the villus-crypt junction. The number of villi per visual field (villi/visual field ratio) was quantified by counting the total number of intact villi within a standardized field of view at 4× magnification, ensuring consistent measurements across samples. All measurements were performed using calibrated image analysis software coupled with the Moticam® system.

Model and Statistical Analysis

The experiment was conducted using a completely randomized design with nine replicates per treatment. For performance parameters, the experimental unit was defined as a cage containing three birds, while for intestinal morphology measurements, six birds per treatment were sampled from two replicate cages (three birds per cage). The statistical model used for analysis was:

$$Yij = \mu + Ti + eij$$

where
Yij = the observed dependent variable
µ = the overall mean
Ti i = the fixed effect of the ith treatment
eij = the random error term.

Data were analyzed using the General Linear Model (GLM) procedure (PROC GLM) in SAS (version 9.4) (2017). Differences among treatment means were evaluated using analysis of variance (ANOVA), followed by Tukey test for comparisons when significant effects were detected ($P < 0.05$).

Results

Growth Performance

All broiler chickens fed with the experimental diets remained healthy throughout the study, with no observed adverse symptoms or signs of disease. Table 3 summarizes the growth performance parameters across starter (days 3-20), finisher (days 20-38), and accumulated phases for broiler chickens fed diets supplemented with guava leaf meal (GLM). Feed intake (FI) in the finisher phase was significantly reduced in treatments T2 (negative control), T3 (1% GLM), T4 (1.5% GLM), and T5 (2% GLM) compared to T1 (positive control with commercial antibiotic) ($P < 0.0001$). However, accumulated feed intake (AFI) showed no significant differences across treatments ($P = 0.29$). Average daily gain (ADG) in the starter phase was lower in T3 and T4 than T2 ($P = 0.009$), with T1 and T5 showing intermediate values. In contrast, no significant differences were observed in ADG during the finisher phase ($P = 0.26$) or accumulated ADG ($P = 0.26$). The accumulated feed conversion ratio (FCR) was significantly improved in T2, T3, T4, and T5 compared to T1 ($P = 0.007$), with T2 and T5 exhibiting the lowest FCR values (1.55 and 1.62, respectively).

Table 3. Effect of additing guava leaf meal (GLM) in the diet of broiler chickens on the growth performance during starter, finisher and accumulated phases.

Tabla 3. Efecto de la adición de harina de hoja de guayaba (GLM) en la dieta de pollos de engorde sobre parámetros productivos en las fases de crecimiento, finalización y acumulado.

Parameter	Treatment						
	T1 contr +	T2 contr -	T3 1% GLM	T4 1.5% GLM	T5 2% GLM	SEM	p-value
Starter Phase (days 3-20)							
FIi ($g\,d^{-1}$)	92.6	94.7	97.6	100.6	97.7	32.7	0.51
BWi (g)	909.6^{ab}	925.3^{a}	851.7^{ab}	841.7^{b}	876.6^{ab}	902	0.03
ADG i ($g\,d^{-1}$)	65.8^{ab}	67.5^{a}	59.15^{b}	58.6^{b}	61,5^{ab}	7.8	0.009
FCR i (FI.BW^{-1})	1.43^{a}	1.42^{a}	1.72^{bc}	1.77^{bc}	1.62^{ac}	0.008	0.002
Finisher Phase (days 20-38)							
FIf ($g\,d^{-1}$)	156,6^{a}	139^{b}	140^{b}	141,3^{b}	141,6^{b}	7.24	<.0001
BWf (g)	2197.8	2330.1	2212.6	2204.6	2254.1	63,8	0.29
ADG f ($g\,d^{-1}$)	92	100.3	97.2	97.3	98.4	18.2	0.26
FCR f (FI.BW^{-1})	1.95^{a}	1.52^{bce}	1.48^{cd}	1.52^{bd}	1.48^{cde}	0.018	0.008
Accumulated period							
AFI ($g\,d^{-1}$)	138.3	131.8	133.8	135.9	134.8	12.28	0.29
ADG ac ($g\,d^{-1}$)	81.8	87.5	82.3	82.2	83.9	10.8	0.26
FCR ac (FI.BW^{-1})	1.76^{a}	1.55^{b}	1.65^{ab}	1.69^{ac}	1.62^{bc}	0.002	0.007

Nutrient Digestibility

Table 4 shows apparent whole-tract digestibility of nutrients. Supplementation with GLM, particularly at 1.5% (T4) and 2% (T5), significantly enhanced crude protein (CP) digestibility compared to T1, T2, and T3 (P = 0.0002). Specifically, T4 and T5 achieved CP digestibility values of 0.52 and 0.45, respectively, compared to 0.32 (T1), 0.30 (T2), and 0.35 (T3), indicating that 1% GLM (T3) did not improve CP digestibility relative to the control groups. Organic matter (OM) digestibility was significantly higher in T4 (0.64) compared to T2 (0.52) (P = 0.045), with T1, T3, and T5 showing intermediate values. Dry matter (DM) digestibility was also improved in T4 (0.58) compared to T1, T2, and T3 (P = 0.003), and was statistically similar to T5 (0.52). Calcium (Ca) digestibility was highest in T3 (0.68) (P < 0.0001), followed by T2 and T4, with T1 and T5 exhibiting the lowest values. Phosphorus (P) digestibility was significantly enhanced with increasing GLM supplementation, peaking in T5 (0.56), followed by T4 (0.40) and T3 (0.37) (P < 0.0001), compared to T1 (0.19) and T2 (0.23).

Table 4. Effect of adding guava leaf meal (GLM) in the diet of broiler chickens on nutrient digestibility.

Tabla 4. Efecto de la adición de harina de hoja de guayaba (GLM) en la dieta de pollos de engorde sobre la digestibilidad de los nutrientes.

Parameter	Treatment					SEM	P-value
	T1 (Control+)	T2 (Control-)	T3 (1%GLM)	T4 (1.5%GM)	T5 (2%GLM)		
DMDig (%)	0.47 [a]	0.46 [a]	0.47 [a]	0.58 [b]	0.52 [ab]	0.0009	0.003
OMDig (%)	0.55 [ab]	0.52 [a]	0.54 [ab]	0.64 [b]	0.58 [ab]	0.0018	0.045
CPDig (%)	0.32 [a]	0 .3 [a]	0.35 [a]	0.52 [b]	0.45 [b]	0.0016	0.0002
Ca Dig (%)	0.35 [a]	0.50 [a]	0.68 [c]	0.45 [b]	0.35 [a]	0.0004	<.0001
P Dig (%)	0.19 [a]	0.23 [a]	0.37 [b]	0.40 [c]	0.56 [d]	0.0008	<.0001

Digestibility results are presented as means of five replicates per treatment. In the same row, values with no superscript or the same superscript indicate no significant difference (P > 0.05), while different superscripts indicate significant differences (P < 0.05). DM Dig: Dry Matter Digestibility; OM Dig: Organic Matter Digestibility; CP Dig: Crude Protein Digestibility; Ca Dig: Calcium Digestibility; P Dig: Phosphorus Digestibility. T1: Positive control with commercial antibiotic; T2: Negative control without antibiotic or growth promoters; T3: 1% GLM; T4: 1.5% GLM; T5: 2% GLM.

Los resultados de digestibilidad se presentan como medias de cinco réplicas por tratamiento. En la misma fila, los valores sin superíndice o con el mismo superíndice indican que no hay diferencia significativa (P > 0,05), mientras que diferentes superíndices indican diferencias significativas (P < 0,05). Dig. MS: Digestibilidad de la materia seca; Dig. MO: Digestibilidad de la materia orgánica; Dig. PC: Digestibilidad de la proteína cruda; Dig. Ca: Digestibilidad del calcio; Dig. P: Digestibilidad del fósforo. T1: Control positivo con antibiótico comercial; T2: Control negativo sin antibiótico ni promotores de crecimiento; T3: 1 % GLM; T4: 1,5 % GLM; T5: 2% GLM.

Duodenum Morphology

The effects of GLM inclusion on the duodenum morphology are detailed in table 5 and illustrated in figure 1, page 173. The number of villi per visual field (Villi/Vis field) was significantly higher in T5 (27 villi) compared to T2 (16.3 villi) (P = 0.02), with T1, T3, and T4 showing intermediate values. Villus height was significantly increased in T3, T4, and T5 (115.1 - 120.7 ţm) compared to T2 (80 ţm) (P = 0.031), and was comparable to T1 (116.8 ţm). Crypt depth did not differ significantly among treatments (P = 0.22). Figure 1 (page 173) illustrates the morphological differences in the small intestine, with T2 (negative control, figure 1A, page 173) exhibiting the shortest villi and T4 and T5 (figures 1C and 1D, page 173) showing enhanced villus height, supporting improved nutrient absorption capacity. These findings suggest that GLM supplementation, particularly at 1.5% and 2%, enhances intestinal morphology, potentially contributing to improved nutrient digestibility.

Table 5. Effect of adding guava leaf meal (GLM) in the diet of broiler chickens on duodenum morphology.

Tabla 5. Efecto de la adición de harina de hoja de guayaba (GLM) en la dieta de pollos de engorde sobre la morfología del duodeno.

Parameter	Treatment						
	T1 (Control+)	T2 (Control-)	T3 (1%GLM)	T4 (1.5%GM)	T5 (2%GLM)	SEM	P-value
Villi per visual field (n)	20.3 ^{ab}	16.3 ^{a}	22.6 ^{ab}	25.3 ^{ab}	27 ^{b}	0.11	0.02
Villus Height (ţm)	116.8 ^{b}	80 ^{a}	115.1 ^{b}	117.1 ^{b}	120.7 ^{b}	7.2	0.031
Crypt Depth (ţm)	30	21	33.7	26.2	22	1.3	0.22

Duodenum morphology results are presented as means of two replicates (six birds per treatment). In the same row, values with no superscript or the same superscript indicate no significant difference (P > 0.05), while different superscripts indicate significant differences (P < 0.05). T1: Positive control with commercial antibiotic; T2: Negative control without antibiotic or growth promoters; T3: 1% GLM; T4: 1.5% GLM; T5: 2% GLM.

Los resultados de la morfología del duodeno se presentan como medias de dos réplicas (seis aves por tratamiento). En la misma fila, los valores sin superíndice o con el mismo superíndice indican que no hay diferencia significativa (P > 0,05), mientras que los superíndices diferentes indican diferencias significativas (P < 0,05). T1: Control positivo con antibiótico comercial; T2: Control negativo sin antibiótico ni promotores de crecimiento; T3: 1% GLM; T4: 1,5% GLM; T5: 2% GLM.

Images were obtained by hematoxylin and eosin staining and observed under 40x magnification. A: Negative control (basal diet without GLM or commercial antibiotic). B: T3 (diet with 1% GLM). C: T4 (diet with 1.5% GLM). D: T5 (diet with 2% GLM). The scale represents 200 µm. Long lines indicate villi height, while short lines indicate crypt depth. Average villi height and crypt depth values are shown in table 5, page 172.

Las imágenes se obtuvieron mediante tinción con hematoxilina y eosina y se observaron con un aumento de 40x. A: Control negativo (dieta basal sin GLM ni antibiótico comercial). B: T3 (dieta con 1% de GLM). C: T4 (dieta con 1,5% de GLM). D: T5 (dieta con 2% de GLM). La escala representa 200 µm. Las líneas largas indican la altura de las vellosidades, mientras que las cortas indican la profundidad de las criptas. Los valores promedio de la altura de las vellosidades y la profundidad de las criptas se muestran en la tabla 5, pág. 172.

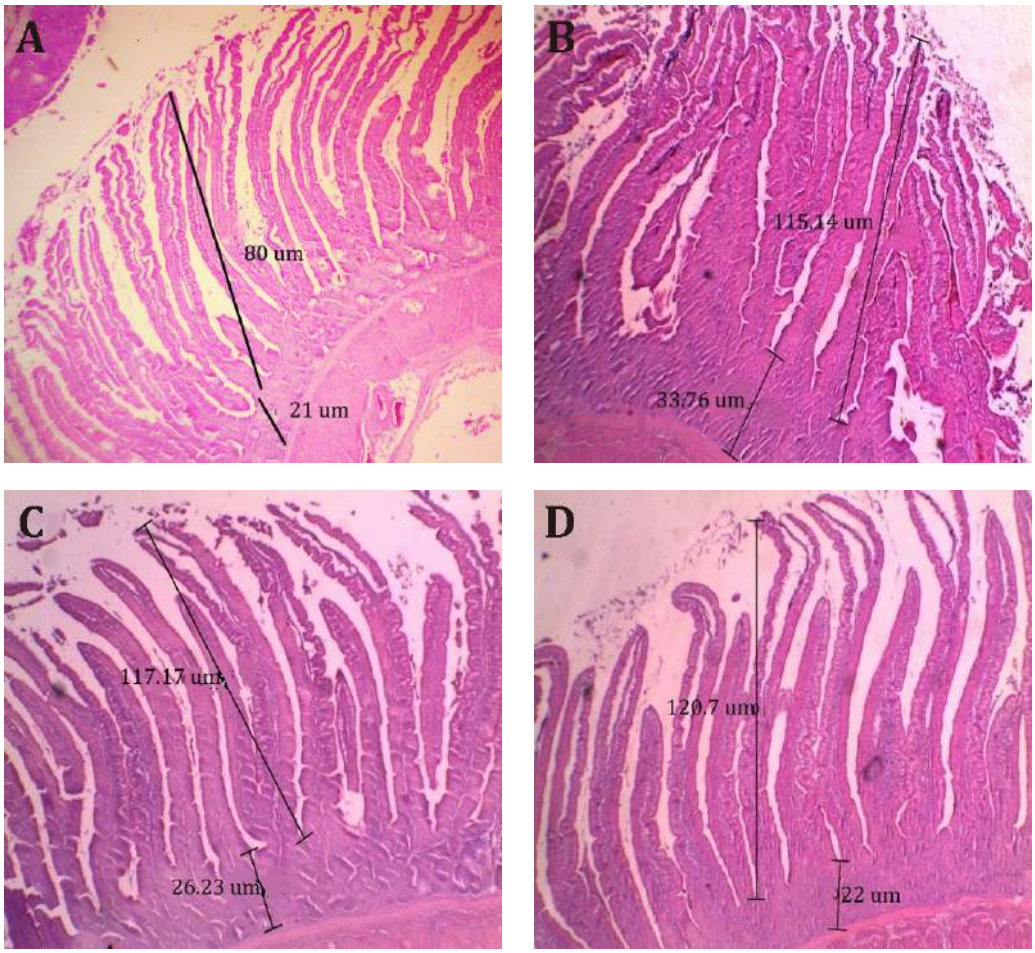

Figure 1. Small intestine (medial duodenum) morphology in broiler supplemented with guava leaf meal (GLM).

Figura 1. Morfología del intestino delgado (duodeno medial) en pollos de engorde suplementados con harina de hoja de guayaba (GLM).

Discussion

In the starter phase, feed intake (FIi) showed no significant differences across treatments (P=0.51), indicating that guava leaf meal (GLM) inclusion at 1% (T3), 1.5% (T4), and 2% (T5) did not affect early feed consumption compared to the positive (T1) and negative (T2) controls. However, body weight (BWi) and average daily gain (ADGi) varied significantly (P=0.03 and P=0.009, respectively). The negative control (T2) exhibited the highest ADGi (67.5 g), followed by T1 (65.8 g), while T3 and T4 showed lower values (59.15 g and 58.6 g, respectively), suggesting that GLM at 1% and 1.5% may not enhance early growth compared to T2. In contrast, T5 (2% GLM) displayed an intermediate ADGi (61.5 g), indicating a potential dose-dependent effect (2, 3, 26). Feed conversion ratio (FCRi) was significantly less efficient in T3 and T4 (1.72 and 1.77, respectively) compared to T1 and T2 (1.43 and 1.42, P=0.002). This suggests that lower GLM doses may reduce feed efficiency in the starter phase, possibly due to palatability issues or mild antinutritional effects (26).

In the finisher phase, feed intake (FIf) was significantly higher in T1 (156.6 g/d) compared to T2, T3, T4, and T5 (139-141.6 g/d, P<0.0001), indicating that GLM inclusion reduced feed consumption. Despite this, final body weight (BWf) and average daily gain (ADGf) showed no significant differences across treatments (P=0.29 and P=0.26, respectively), suggesting that GLM maintained overall growth despite lower feed intake. Notably, FCR in

the finisher phase (FCRf) improved significantly in T3, T4, and T5 (1.48-1.52) compared to T1 (1.95, P=0.008), with T2 showing an intermediate value (1.52). These results align with Langerudi *et al.* (2022), who reported improved FCR with guava leaf essential oil (5 mg/kg), and suggest that GLM enhances feed efficiency in later growth stages, likely due to improved nutrient utilization (1, 30).

Over the entire growth cycle, accumulated feed intake (AFI) and accumulated average daily gain (ADGac) showed no significant differences (P=0.29 and P=0.26, respectively), indicating that GLM did not affect overall feed consumption or weight gain. However, accumulated FCR (FCRac) was significantly better in T2, T3, T4, and T5 (1.55-1.69) compared to T1 (1.76, P=0.007), reinforcing the role of GLM in improving feed efficiency without compromising final body weight. These findings differ from Mahmoud *et al.* (2013), who reported significant improvements in body weight, daily gain, and FCR with 1% dried guava leaves, and Adeyemi *et al.* (2022), who noted differences in cumulative feed intake with 0.25-0.5% GLM. These discrepancies may arise from variations in GLM dosage, bird genetics, or environmental conditions (8, 27).

The GLM doses (1-2%) used in this study, compared to lower doses (0.25-0.5%) in Adeyemi *et al.* (2022), may explain the lack of consistent growth performance improvements. High GLM doses may introduce antinutritional factors, such as tannins or phenolic compounds, which can bind proteins and minerals, reducing bioavailability and negatively impacting early growth (5, 20). For example, tannins form complexes with dietary proteins, impairing digestion and absorption (20). The numerically higher FIi in T3 and T4 (97.6 and 100.6 g/d, respectively) compared to T1 (92.6 g/d) and T2 (94.7 g/d) may reflect reduced palatability or mild antinutritional effects. However, T5 (2% GLM) showed comparable FIi (97.7 g/d), suggesting that higher doses may not exacerbate these effects, possibly due to adaptive responses in gut microbiota or enzyme activity (24, 25). Excessive phenolic compounds at higher doses could also inhibit digestive enzymes or disrupt gut microbiota balance, as noted in studies on phytogenic additives (26).

Nutrient digestibility was significantly enhanced by GLM inclusion. Dry matter digestibility (DM Dig) was highest in T4 (0.58) compared to T1, T2, and T3 (0.46-0.47, P=0.003), with T5 (0.52) showing an intermediate value. Organic matter digestibility (OM Dig) followed a similar trend, with T4 (0.64) outperforming T2 (0.52, P=0.045). Crude protein digestibility (CP Dig) was markedly improved in T4 and T5 (0.52 and 0.45, respectively) compared to T1, T2, and T3 (0.30-0.35, P=0.0002). Calcium digestibility (Ca Dig) was highest in T3 (0.68) and significantly lower in T1 and T5 (0.35, P<0.0001), while phosphorus digestibility (P Dig) showed a dose-dependent increase, with T5 (0.56) outperforming all other treatments (0.19-0.40, P<0.0001). These improvements likely stem from the bioactive compounds of GLM, such as polyphenols, flavonoids, and essential oils, which stimulate digestive enzyme secretion, enhance bile acid synthesis, and modulate gut microbiota (25, 32, 35, 36). For instance, flavonoids promote villus development, increasing absorptive surface area, as evidenced by increased villi height in T3, T4, and T5 (115.1-120.7 µm) compared to T2 (80 µm, P=0.031). The dose-dependent increase in P Dig suggests that higher GLM levels (2%) enhance phosphorus absorption, possibly through improved phytase activity or reduced antinutritional interference (3). The variability in Ca Dig, with T3 showing the highest value, may reflect complex interactions between GLM bioactives and mineral metabolism, warranting further investigation (35).

Improved nutrient digestibility in GLM-supplemented groups contributed to enhanced FCR in the finisher and accumulated phases (P=0.008 and P=0.007, respectively), despite no significant differences in final body weight. This suggests that GLM enables broilers to achieve comparable growth with reduced feed intake, potentially lowering production costs (1, 30). GLM supplementation also improved intestinal morphology, with T5 showing higher villi counts (27 villi/visual field) and villi heights (115.1-120.7 µm) compared to T2 (16.3 villi/visual field and 80 µm, P=0.02 and P=0.031, respectively). Notably, T5 (2% GLM) achieved villi height and count comparable to or numerically surpassing T1 (positive control with antibiotics), suggesting that GLM can replicate the beneficial effects of antibiotics on gut health (1, 7, 18). Similar crypt depth in T5 (22 µm) and T2 (21 µm) indicates that GLM maintains mucosal integrity. These findings are consistent with what was reported by Wang *et al.* (2024), on the effect of GLM on intestinal structure.

Conclusions

GLM inclusion at 1-2% did not significantly enhance growth performance but significantly improved nutrient digestibility and feed efficiency, particularly in the finisher and accumulated phases. The dose-dependent effects on digestibility and gut morphology suggest that GLM's bioactive compounds enhance nutrient absorption and maintain intestinal integrity. These findings support further research to identify key bioactive compounds, evaluate interactions with dietary components, and determine optimal inclusion levels. Additionally, GLM's ability to replicate antibiotic effects on gut health positions it as a promising alternative to synthetic growth promoters, reducing reliance on antibiotics.

References

1. Abang, F. B.; Echeonwu, I. E.; Amu, M. U. 2023. Effect of graded levels of guava (*Psidium guajava* L.) leaf meal on productive performance and meat organoleptic properties of chicken. Online Journal of Animal and Feed Research. 13(1): 73-78.
2. Adeyemi, K. D., Agboola, K.; Quadri R. O.; Kelani, A. M.; Ahmed El-Imam, A. M.; Ishola, H. 2022. Influence of Dietary Supplementation of Guava Leaf, Oxytetracycline, and Tert-Butylhydroxytoluene on Growth Performance, Gut Microbial Population, Immune Status, Carcass, and Meat Quality in Broiler Chickens. Iranian Journal of Applied Animal Science. 12(2): 329-339.
3. Amad, A. A.; Männer, K.; Wendler, K. R.; Neumann, K.; Zentek, J. 2011. Effects of a phytogenic feed additive on growth performance and ileal nutrient digestibility in broiler chickens. Poult Sci. 90(12): 2811-6. doi: 10.3382/ps.2011-01515
4. Association of Official Analytical Chemists (AOAC). 2005. Official Methods of Analysis of AOAC International.
5. Buyse, K.; Delezie, E.; Goethals, L.; Van Noten, N.; Ducatelle, R.; Janssens, G. P. J.; Lourenço, M. 2021. Chestnut tannins in broiler diets: performance, nutrient digestibility, and meat quality. Poult Sci. 100(12):101479. doi: 10.1016/j.psj.2021.101479
6. Chechani, B.; Roat, P.; Hada, S.; Yadav, D. K.; Kumari, N. 2024. *Psidium guajava*: An Insight into Ethnomedicinal Uses, Phytochemistry, and Pharmacology. Comb Chem High Throughput Screen. 27(1):2-39. doi: 10.2174/1386207326666230426093315
7. Diaz-Sanchez, S.; D'Souza, D.; Biswas, D.; Hanning, I. 2015. Botanical alternatives to antibiotics for use in organic poultry production. Poult Sci. 94(6): 1419-30. doi: 10.3382/ps/pev014.
8. Dos Santos, A.; Da Silva, A. S.; Galli, G. M.; Paglia, E. B.; Dacoreggio, M. V.; Kempka, A. P.; Souza, C. F.; Baldissera, M. D.; Rosa, G.; Boiago, M. M.; Paiano, D. 2020. Addition of yellow strawberry guava leaf extract in the diet of laying hens had antimicrobial and antioxidant effect capable of improving egg quality. Biocatalysis and Agricultural Biotechnology. 29: 101788. https://doi.org/10.1016/j.bcab.2020.101788
9. FEDNA. 2003. Tablas FEDNA de composición y valor nutritivo de alimentos para la fabricación de piensos compuestos. 2° ed. Fundación Española para el Desarrollo de la Nutrición Animal. Madrid. España.
10. Geidam, Y. A.; Ambali, A. G.; Onyeyili, P. A.; Tijjani, M. B.; Gambo, H. I.; Gulani, I. A. 2015. Antibacterial efficacy of ethyl acetate fraction of *Psidium guajava* leaf aqueous extract on experimental *Escherichia coli* (O78) infection in chickens. Veterinary World. 8(3): 358-362. doi: 10.14202/vetworld.2015.358-362
11. Geneser, F. 1997. Histología. 2° Ed. Editorial Médica Panamericana S. A. 768 p.
12. Gheisar, M. M.; Kim, I. H. 2018. Phytobiotics in poultry and swine nutrition - a review. Italian Journal of Animal Science. 17(1): 92-99. DOI: 10.1080/1828051X.2017.1350120
13. Gupta, M.; Wali, A.; Anjali, Gupta, S.; Annepu, S. K. 2018. Nutraceutical Potential of Guava. In: Mérillon, J. M.; Ramawat, K. (eds) Bioactive Molecules in Food. Reference Series in Phytochemistry. Springer. Cham. https://doi.org/10.1007/978-3-319-54528-8_85-1
14. Jiang, S.; Mohammed, A. A.; Jacobs, J. A.; Cramer, T. A.; Cheng, H. W. 2020. Effect of synbiotics on thyroid hormones, intestinal histomorphology, and heat shock protein 70 expression in broiler chickens reared under cyclic heat stress. Poultry Science. 99(1): 142-150. https://doi.org/10.3382/ps/pez571
15. Kumar, M.; Tomar, M.; Amarowicz, R.; Saurabh, V.; Nair, M. S.; Maheshwari, C.; Sasi, M.; Prajapati, U.; Hasan, M.; Singh, S.; Changan, S.; Prajapat, R. K.; Berwal, M. K.; Satankar, V. 2021. Guava (*Psidium guajava* L.) Leaves: Nutritional Composition, Phytochemical Profile, and Health- Promoting Bioactivities. Foods. 10(4): 752. doi: 10.3390/foods10040752
16. Kuralkar, P.; Kuralkar, S. V. 2021. Role of herbal products in animal production - An updated review. Journal of Ethnopharmacology. 278:114246. doi: 10.1016/j.jep.2021.114246
17. Langerudi, M. T.; Youssefi, M. R.; Tabari, M. A. 2022. Ameliorative effect of *Psidium guajava* essential oil supplemented feed on chicken experimental coccidiosis. Tropical Animal Health and Production. 54(2): 120. doi: 10.1007/s11250-022-03117-7

18. Liu, M.; Zhou, J.; Li, Y.; Ding, Y.; Lian, J.; Dong, Q.; Qu, Q.; Lv, W.; Guo, S. 2023. Effects of dietary polyherbal mixtures on growth performance, antioxidant capacity, immune function and jejunal health of yellow-feathered broilers. Poultry Science. 102: 102714.
19. Luo, Y.; Peng, B.; Wei, W.; Tian, X.; Wu, Z. 2019. Antioxidant and Anti-Diabetic Activities of Polysaccharides from Guava Leaves. Molecules. 24(7): 1343. doi: 10.3390/molecules24071343
20. Mahfuz, S.; Shang, Q.; Piao, X. 2021. Phenolic compounds as natural feed additives in poultry and swine diets: a review. J Animal Sci Biotechnol. 12: 48. https://doi.org/10.1186/s40104-021-00565-3
21. Mahmoud, R. El-Sayed, Ibrahim, Doaa, Badawi, M. El-Sayed. 2013. Effect of supplementation of broiler diets with Guava Leaves and/or Olive Oil on growth, meat composition, blood metabolites and immune response. Benha Vet. Med. J. 25(2): 23-32.
22. National Research Council. 1994. Nutrient Requirements of Poultry. The National Academies Press. https://doi.org/10.17226/2114
23. Oliveira, M.; Mello, H.; Mascarenhas, A.; Arnhold, E.; Conceição, E.; Martins, J.; Junior, A. 2018. Antioxidant effect of the guava by product in the diet of broilers in the starter phase. Revista Brasileira de Zootecnia. 47. 10.1590/rbz4720160290
24. Parra Ferrín, D.; Cusme Lucas, G.; Talledo Solórzano, V.; Loor Gorozabel, B.; Pazmiño Castro, A.; Cuenca-Nevárez, G. J. 2023. Efficacy of zinc lactate and *Lactobacillus bulgaricus* on nutrition and health of broiler chickens. Revista de la Facultad de Ciencias Agrarias. Universidad Nacional de Cuyo. Mendoza. Argentina. 55(2): 120-128. DOI: https://doi.org/10.48162/rev.39.114
25. Pliego, A. B.; Tavakoli, M.; Khusro, A.; Seidavi, A.; Elghandour, M. M.; Salem, A. Z.; Márquez-Molina, O.; Rene Rivas Caceres, R. 2020. Beneficial and adverse effects of medicinal plants as feed supplements in poultry nutrition: A review. Animal Biotechnology. 33(2): 369-391.
26. Rafeeq, M.; Bilal, R. M.; Alagawany, M.; Batool, F.; Yameen, K.; Farag, M. R., Ali, S.; Elnesr, S. & El-Shall, N. A. 2022. The use of some herbal plants as effective alternatives to antibiotic growth enhancers in poultry nutrition, World's Poultry Science Journal. 78(4): 1067-1085. DOI: 10.1080/00439339.2022.2108362
27. Rahman, Z.; Siddique, M. N.; Khatun, M. A.; Kamruzzamen, M. 2013. Effect of guava (*Psidium guajava*) leaf meal on production performance and antimicrobial sensitivity in commercial broiler. Journal of Natural Products. 6: 177-187.
28. Ryu, B.; Cho, H. M.; Zhang, M.; Lee, B. W.; Doan, T. P.; Park, E. J.; Lee, H. J.; Oh, W. K. 2021. Meroterpenoids from the leaves of *Psidium guajava* (guava) cultivated in Korea using MS/MS-based molecular networking. Phytochemistry. 186:112723. doi: 10.1016/j.phytochem.2021.112723
29. SAS® Institute Inc. 2017. Statistical Analysis Systems Institute. SAS/STAT User's Guide. Version 14. 3rd ed. Cary, NC: Autor.
30. Singh, J.; Gaikwad, D. S. 2020. Phytogenic Feed Additives in Animal Nutrition. In: Singh, J., Yadav, A. (eds) Natural Bioactive Products in Sustainable Agriculture. Springer. Singapore. https://doi.org/10.1007/978-981-15-3024-113
31. Song, J.; Xiao, K.; Ke, Y. L.; Jiao, L. F.; Hu, C. H.; Diao, Q. Y.; Shi, B.; Zou, X. T. 2014. Effect of a probiotic mixture on intestinal microflora, morphology, and barrier integrity of broilers subjected to heat stress. Poultry Science. 93: 581-588.
32. Sugiharto, S.; Ranjitkar, S. 2019. Recent advances in fermented feeds towards improved broiler chicken performance, gastrointestinal tract microecology and immune responses: A review. Animal Nutrition. 5(1): 1-10. https://doi.org/10.1016/j.aninu.2018.11.001
33. Wang, D.; Zhou, L.; Zhou, H.; Hu, H.; Hou, G. 2021. Chemical composition and protective effect of guava (*Psidium guajava* L.) leaf extract on piglet intestines. Journal of the Science of Food and Agriculture. 101(7): 2767-2778. doi: 10.1002/jsfa.10904
34. Wang, J.; Deng, L.; Chen, M.; Che, Y.; Li, L.; Zhu, L.; Chen, G.; Feng, T. 2024. Phytogenic feed additives as natural antibiotic alternatives in animal health and production: A review of the literature of the last decade. Animal Nutrition. 17: 244-264. doi: 10.1016/j.aninu.2024.01.012
35. Windisch, W.; Schedle, K.; Plitzner, C.; Kroismayr, A. 2008. Use of phytogenic products as feed additives for swine and poultry. J Anim Sci. 86(14 Suppl): E140-8. doi: 10.2527/jas.2007-0459
36. Yitbarek, M. B. 2015. Phytogenics as feed additives in poultry: A review on their effects on gut health. International Journal of extensive research. 3: 49-60.

Comparison of Fatty Acid Profiles of Sacha Inchi Oil (*Plukenetia huayllabambana*), Sesame Oil (*Sesamum indicum*), and Peanut oil (*Arachis hypogaea*) Using Two Extraction Methods for Food Purposes

Comparación de los perfiles de ácidos grasos del aceite de sacha inchi (*Plukenetia huayllabambana*) aceite de sésamo (*Sesamum indicum*) y aceite de cacahuete (*Arachis hypogaea*) utilizando dos métodos de extracción con fines alimentarios

Jhoan Plua Montiel [1], Juan Alejandro Neira Mosquera [1, 2, 3],
Sungey Naynee Sanchez Llaguno [1], Jhonnatan Placido Aldas Morejon [4],
Karol Yannela Revilla Escobar [4, 5*], Edgar Caicedo-Álvarez [6]

Originales: *Recepción:* 03/09/2024 - *Aceptación:* 06/02/2024

Abstract

Vegetable oil consumption has increased in recent decades due to the high content of monounsaturated (Omega 9) and polyunsaturated (Omega 3 and 6) fatty acids. For this reason, this research compared the fatty acid profile of sacha inchi, sesame and peanut oils under two extraction methods for food purposes. A completely randomized experimental design considered an A*B factorial arrangement with 3 repetitions. Factor A corresponds to oilseed type and Factor B is extraction method. The results showed that both factors significantly influenced ($p<0.05$) bromatological characteristics (pH, acidity, peroxide value, relative density and ash). The lowest concentration of saturated fatty acids was obtained in sacha inchi oil + cold pressing (6.80 g/100 g), while monounsaturated fatty acids increased in peanut oil + hot pressing (51.51 g/100 g). Sacha inchi oil + cold pressing had the highest content of polyunsaturated fatty acids (84.36 g/100 g).

Keywords
fatty acids • agri-food • monounsaturated • polyunsaturated • saturated • oilseeds

1 Universidad de las Fuerzas Armadas-ESPE, Sede Santo Domingo de los Tsáchilas. Departamento de Ciencias de la Vida y la Agricultura, Luz de América Vía Quevedo km 24. Ecuador.
2 Universidad Pública de Santo Domingo de los Tsáchilas. UPSDT. km 28. vía Quevedo. Santo Domingo. Ecuador.
3 Universidad Técnica Estatal de Quevedo. Facultad de Ciencias de la Industria y Producción. Quevedo. Ecuador.
4 Universidad Nacional de Cuyo. Facultad de Ciencias Aplicadas a la Industria. San Rafael. M5600APG. Argentina.
5 Pontificia Universidad Católica del Ecuador. Carrera de Agroindustrias. SEDE Esmeraldas. Esmeraldas. Ecuador. *kyrevilla@pucese.edu.ec
6 Universidad Estatal del Sur de Manabí. Facultad de Ciencias Naturales y de la Agricultura. Jipijapa. Ecuador.

Resumen

El consumo de aceites vegetales ha aumentado en las últimas décadas debido a su alta composición de ácidos grasos monoinsaturados (Omega 9) y poliinsaturados (Omega 3 y 6). Por esta razón, la presente investigación comparó el perfil de ácidos grasos del aceite de sacha inchi, ajonjolí *y* maní a partir de dos métodos de extracción con fines alimentarios. Se utilizó un diseño experimental completamente aleatorizado, con arreglo factorial A*B con 3 repeticiones, donde el Factor A correspondió al tipo de oleaginosa y el Factor B es igual a los métodos de extracción. Los resultados mostraron que los factores de estudio influyeron significativamente ($p<0,05$) en los valores de las características bromatológicas (pH, acidez, índice de peróxidos, densidad relativa y cenizas). Por otro lado, la menor presencia de ácidos grasos saturados se obtuvo en el aceite de sacha inchi + prensado en frío (6,80 g/100g), mientras que, los ácidos grasos monoinsaturados incrementaron en el aceite de de maní + prensado en caliente (51,51 g/100g) y el aceite de sacha inchi + prensado en frío, presentó el mayor contenido de ácidos grasos poliinsaturados (84,36 g/100g).

Palabras clave

ácidos grasos • agroalimentario • monoinsaturados • poliinsaturados • saturados • oleaginosas

Introduction

In the constant search for food sources promoting health and well-being, vegetable oils provide unique fatty acid compositions and potential health benefits (36). Additionally, the Amazon region is home to various plant species with crucial roles in global agriculture (36). However, among lesser-known oilseed species with potential economic value due to their chemical properties, sacha inchi oil *(P. huayllabambana)*, sesame oil *(S. indicum),* and peanut oil *(A. hypogaea)* provide diverse nutritional profiles and versatile culinary applications (3).

P. huayllabambana belongs to the *Euphorbiaceae* family, native to the Amazon, known as "wild peanut", "Inca peanut", "Inca inchi" or "mountain peanut" (24). It is widely distributed in South America, particularly in the Amazon River basin. Currently, Peru leads the production and industrialization of this plant material, with annual seed production of approximately 1200 tons (14). However, countries such as Colombia, Ecuador and Bolivia have also begun to venture into agriculture and economy (10).

On the other hand, *S. indicum* is an oilseed plant cultivated in China, India, Sudan, Japan, Mexico, countries in West and Central Africa, and Central America (30). The growing interest in the nutritional value of sesame has led to a significant increase in its consumption and use in baking (9). This shift in consumption habits is reflected in the increasing use of seeds in food products at both domestic and industrial levels (9). Furthermore, *S. indicum* is the sixth most economically important oilseed crop globally, with nutritional value (fats, proteins, minerals, and vitamins) in food security (24).

Recent research stresses the importance of differentiating the fatty acid profiles of these oils to optimize their use in nutrition. Notably, sacha inchi oil is characterized by high alpha-linolenic acid (ALA), an essential omega-3 fatty acid with cardiovascular protective effects and contribution to cognitive development (37). Sesame oil is rich in polyunsaturated fatty acids, particularly linoleic and oleic acids with antioxidant and anti-inflammatory properties, positively influencing cardiovascular and metabolic health (25). In comparison, peanut oil has oleic and linoleic acids associated with reduced cardiovascular risk and improved lipid profiles (2). However, the instability of polyunsaturated fatty acids, especially in oils such as sacha inchi, can lead to oxidation and harmful compounds when exposed to high temperatures or improper storage. This instability can negatively affect nutritional quality and safety (37).

Oil extraction methods, such as cold and hot extraction, are crucial in determining oil nutritional quality and sensory properties while influencing the stability of fatty acids, antioxidants, and other bioactive compounds (31). Cold extraction is a mechanical process

that better preserves heat-sensitive compounds and maintains oil nutritional and sensory quality (22). In contrast, hot extraction uses high temperatures, accelerating extraction rates and increasing oil yield but degrading heat-sensitive compounds and affecting quality (32).

This study aimed to compare fatty acid profiles of sacha inchi oil (*P. huayllabambana*), sesame oil (*S. indicum*), and peanut oil (*A. hypogaea*) using two extraction methods for food purposes.

Materials and methods

Plant Material

For this study, sacha inchi was obtained from the Lago Agrio canton, Sucumbíos province, Ecuador, located 600 m a. s. l. with coordinates 0°05'05" N 76°52'58" W. Annual temperature ranges between 20 and 35°C, ideal for its cultivation. Sesame was acquired from the Quevedo canton, Los Ríos province, at 150 m a. s. l. with coordinates 1°02'00" S 79°27'00" W, featuring a monsoonal tropical climate and temperatures between 23°C and 32°C, enhancing its quality. *Peanut* seeds were obtained from the Pichincha canton, Manabí province, with an average altitude of 350 m a. s. l. and coordinates 1°02'50" S 79°49'07" W, dry tropical climate and temperatures between 24°C and 30°C, suitable for peanut cultivation.

Oil Extraction Methods

Cold Press Extraction

The seeds were dried at room temperature until 7% humidity. Once dried, 20 kg of each plant material were equally distributed for the different extraction methodologies. The oils were obtained by subjecting the nuts to a hydraulic pressing process between 246 and 250 Bar, with a piston-cylinder mechanism controlled by an electric panel. The nuts were introduced into a perforated basket and pressed. The expelled oil falls onto a stainless steel tray, where it is collected and filtered through a cloth before storage.

Hot Press Extraction

Similarly to cold pressing, seeds were subjected to indirect heating at 90°C for 20 minutes before pressing.

Bromatological Analysis

Oil physicochemical analysis included emulsifying the oils with water to determine pH, and acidity according to NTE INEN 0038:1973 standard (16). Oleic acid was considered the predominant acid. Peroxide evaluation followed the NTE INEN 277:1978 standard (17), and relative density followed the NTE INEN 0035:2012 standard (19). Humidity was analyzed by the Colombian Technical Standard NTC 287:2018 (15). Animal and vegetable fats and oils along with moisture and volatile matter content. Finally, ashes were quantified by the AOAC standard method (920,153).

Fatty Acid Analysis

Before HPLC according to Oubannin *et al.* (2024), all samples were esterified with 2 mL methanol and 0.5% KOH at 60 °C for 10 minutes. Then, fatty acid methyl esters were extracted with 2 mL hexane. This mixture was centrifuged at 3000 rpm for 5 minutes. The upper phase obtained after centrifugation was filtered with a 0.45 µm filter for later analysis. A C18 column (250 mm × 4.6 mm, 5 µm) was mounted in the HPLC system isocratically at 35°C column temperature and operating pressure of 2000 to 2500 psi. Acetonitrile and methanol (70:30 v/v) were passed through the mobile phase at a flow rate of 1 mL/min and detection was performed with a UV-Vis detector at 220 nm. Volumes of 10-20 µL were injected automatically with 30 minutes of analysis time.

Statistical Analysis

An ANOVA was conducted using a completely randomized block design with an A*B factorial arrangement in triplicate. Factors were oilseed (a0: sacha inchi, a1: sesame, and a2: peanut), and extraction method (b0: cold pressing and b1: hot pressing, table 1). The data obtained were analyzed with Statistica (39) including Tukey test at $p<0.05$ and Statgraphics (40).

Table 1. Factors involved in vegetable oil extraction.
Tabla 1. Factores que intervienen en la extracción de aceite vegetal.

Treatments	Factor A	Factor B	Code
1	Sacha inchi	Cold-pressed	S.I + C.P
2	Sacha inchi	Hot-pressed	S.I + H.P
3	Sesame	Cold-pressed	S.M + C.P
4	Sesame	Hot-pressed	S.M + H.P
5	Peanut	Cold-pressed	P.N + C.P
6	Peanut	Hot-pressed	P.N + H.P

Results and discussion

Bromatological Analysis of Oils from Three Oilseeds (sacha inchi, sesame, and peanut) Extracted by Cold and Hot Pressing

Figure 1A (page 181), shows pH variability of oils obtained by cold and hot extraction methods. We demonstrated that both extraction methods significantly ($p<0.05$) affect pH values. The highest and lowest pH values were 6.10 and 5.07, observed in sacha inchi oil extracted by cold pressing (S.I + C.P) and hot pressing (S.I + H.P), respectively. These results are consistent with previous studies reporting 6.11 for sacha inchi oil, 5.86 for peanut oil and 5.64 for sesame oil (29).

Figure 1B (page 181), shows that oilseed type significantly ($p<0.05$) affects acidity. Sacha inchi oil extracted by hot-pressing showed higher acidity (0.85%). In contrast, peanut oil showed lower acidity, with values of 0.11% and 0.17% for both extraction methods. These results indicate that oilseed type and extraction process determine free fatty acid content in vegetable oils. A higher free fatty acid content, indicated by higher acidity, can affect oil stability, shelf life and nutritional and sensory quality (12). Additionally Peroné *et al.* (1999) mention that cold extraction methods generally produce oils with lower acidity than methods involving high temperatures and solvents (28).

Figure 1C (page 181), shows how cold extraction significantly increased ($p < 0.05$) the peroxide content. Sesame oil extracted by cold pressing presented the highest value, with 6.60, while peanut oil extracted by hot pressing (P.N + H.P) showed the lowest value, 2.20. This agrees with previous studies suggesting that increasing temperature and heating time favors hydroperoxide formation. Varying conditions from 80°C for 10 minutes to 200°C for 20 minutes, peroxide content increased from 1.91 to 3.25 mEqO2/kg (6). This increase reflects a greater production of primary oxidation products, attributed to the action of free radicals on unsaturated fatty acids, such as linolenic acid, predominant in sacha inchi oils (37, 38). Our results are within the limit established by the Ecuadorian Technical Standard NTE INEN 34:2012 (20), which stipulates that peroxide index of oils for human consumption must not exceed 10 mEqO/kg.

In the relative density analysis (figure 1D, page 181), a significant influence of the type of oilseed on the variability of this property was observed ($p<0.05$), highlighting the sacha inchi oil obtained by the cold and hot extraction methods (S.I + C.P and S.I + H.P), with the

highest densities of 0.923 g/ml and 0.922 g/ml, respectively. On the other hand, peanut oil presented lower densities, with values of 0.905 g/ml and 0.907 g/ml for the mentioned methods. These results are consistent with previous research indicating that the density of Moringa stenopetala seed oil is 0.9 g/ml and values ranging from 0.99 to 0.97 g/ml for sacha inchi oil when different temperatures (90 to 110°C) are applied (18, 34). In addition, the oil extracted from pumpkin seeds (*Cucurbita pepo*) presented a density of 0.09 g/ml (1).

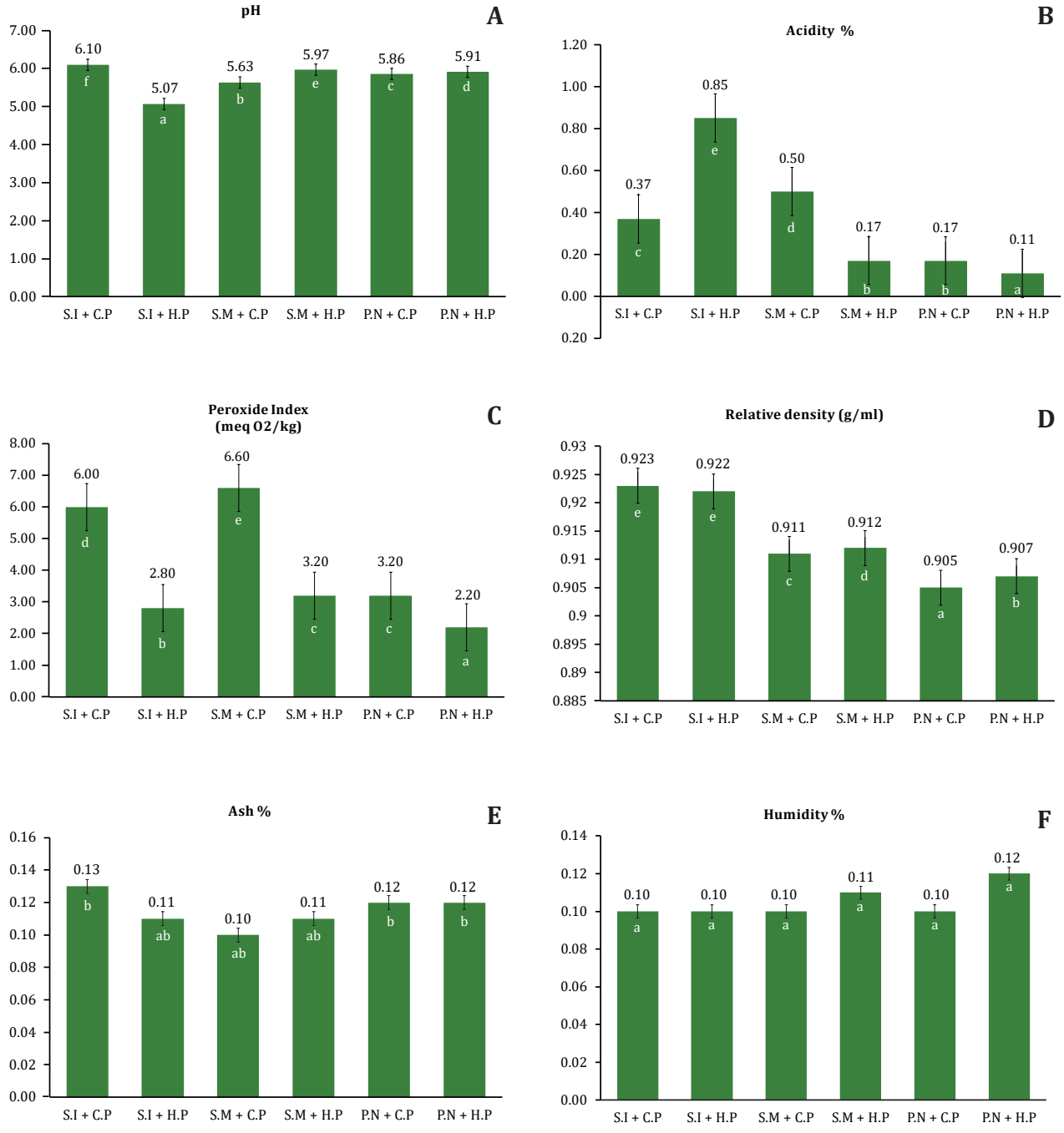

Sacha inchi + Cold -pressed (S.I + CP), Sacha inchi + Hot -pressed (S.I + HP), Sesame + Cold-pressed (S.M + CP), Sesame + Hot- pressed (S.M + H.P), Peanut + Cold-pressed (P.N +C.P), Peanut + Hot - pressed (P.N + H.P).

Sacha inchi + prensado en frío (S.I + CP), Sacha inchi + prensado en caliente (S.I + HP), Sésamo + prensado en frío (S.M + CP), Sésamo + prensado en caliente (S.M + H.P), Maní + prensado en frío (P.N + C.P), Maní + prensado en caliente (P.N + H.P).

Figure 1. Oil bromatological analyses obtained by two extraction methods.

Figura 1. Análisis bromatológicos de aceites obtenidos por dos métodos de extracción.

Figure 1E details ash contents ranging between 0.11% and 0.13%. No variability was found among oilseeds and extraction methods (p>0.05). These values are lower than the reported by Bonku *et al.* (2020), who determined ranges from 1.2% and 2.3% in peanut oil (*A. hypogaea*). Similarly, a study on sesame oil reported ash values from 1.44% to 5.93%, considering Mida and Woremog, two different study regions (5). Discrepancies in our crude ash content and literature values could be attributed to topographic and climatic differences, and variations in extraction methods.

No significant differences were found for moisture content between groups (p > 0.05), with average values ranging from 0.10% to 0.12% (figure 1E, page 181). These findings are consistent with previous studies reporting similar levels for oils from the same species (13). Other studies showed non-significant differences across production areas of sesame oil, (5.43% - 5.81%) (38), and peanut (4.2 ± 0.5% and 3.8 ± 0.37%) for Huaquechula and Tlapanalá varieties (8). However, other studies reported moisture variability in microencapsulated sacha inchi oil (*P. huayllabambana* and *P. volubilis*), ranging from 3.20% to 5.87% (3).

Profile of Fatty Acids

Saturated Fatty Acids

Most important saturated fatty acids in vegetable oils include C11:0 (undecanoic acid), C16:0 (palmitic acid), C17:0 (margaric acid), C18:0 (stearic acid), C20:0 (arachidic acid), C22:0 (behenic acid) and C24:0 (lignoceric acid). We showed that cold-pressed and hot-pressed peanut oils had the highest values of these acids, with 17.54 g/100 g and 18.05 g/100 g, respectively. In contrast, cold-pressed sacha inchi oil showed a lower value of 6.79 g/100 g, while hot-pressed sacha inchi oil had a similar value, of 7.57 g/100 g (table 2). These values for sacha inchi oils, obtained by both methods, are relatively low compared to those reported by Seid and Mehari (2022), who found a saturated fatty acid composition of 9.38 g/100 g (38), warned that excessive consumption of saturated fatty acids can increase cardiovascular risk. Therefore, the aforementioned oils are interesting alternatives for human diet, keeping cholesterol levels under control (35).

Table 2. Saturated fatty acids in oils (sacha inchi, sesame, and peanut) obtained by cold and hot extraction.

Tabla 2. Ácidos grasos saturados presentes en aceites (sacha inchi, ajonjolí y maní) obtenidos por extracción en frío y caliente.

Saturated Fatty Acids		Oilseed type + Extraction Method					
		S.I + C.P	S.I + H.P	S.M + C.P	S.M + H.P	P.N + C.P	P.N + H.P
Undecanoic acid	C11:0	0.00^{A}	0.00^{A}	0.00^{A}	0.05^{B}	0.13^{C}	0.16^{D}
Palmitic acid	C16:0	4.96^{A}	5.47^{B}	9.24^{C}	11.49^{D}	12.12^{E}	12.09^{E}
Margaric acid	C17:0	0.08^{A}	0.09^{A}	0.05^{A}	0.05^{A}	0.11^{A}	0.54^{A}
Stearic acid	C18:0	1.61^{A}	1.73^{B}	4.83^{F}	4.10^{E}	2.44^{D}	1.99^{C}
Arachidic acid	C20:0	0.10^{A}	0.13^{B}	0.61^{D}	0.57^{C}	0.98^{E}	1.00^{E}
Behenic acid	C22:0	0.04^{B}	0.08^{C}	0.00^{A}	0.22^{D}	1.32^{E}	$1.^{5}9F$
Lignoceric acid	C24:0	0.00^{A}	0.07^{B}	0.08^{C}	0.14^{D}	0.44^{E}	0.68^{F}
Total Saturated Fatty Acids		6.79^{A}	7.57^{B}	14.81^{C}	16.62^{D}	17.54^{E}	18.05^{E}

Different letters represent statistically significant differences (Tukey p < 0.05).

Diferentes letras representan diferencias estadísticamente significativas (Tukey p < 0,05).

Monounsaturated Fatty Acids

Table 3 (page 183), shows monounsaturated fatty acids in the analysed oils, highlighting the main ones: C16:1 (palmitoleic acid), C18:1 (oleic acid Omega 9), C20:1 (eicosenoic acid) and C24:1 (nervonic acid). The highest values of these fatty acids were observed in hot-pressed peanut oil (51.52 g/100 g) and cold-pressed peanut oil (50.25 g/100 g), close to the

monounsaturated fatty acid content of virgin olive oil (73.90 g/100 g), as reported in Spanish diets (37). Hot-pressed sesame oil (35.37 g/100 g) and cold-pressed sesame oil (32.89 g/100 g) present intermediate values, comparable to the 39 g/100 obtained after roasting temperature (4). In this study, the predominant monounsaturated fatty acid is omega-9, known for its ability to improve resistance to LDL oxidation (a crucial factor in atherosclerosis), given its phenolic compounds (23). According to the White Paper on Nutrition in Spain, consuming more than 51 g/100 g of monounsaturated fatty acids per day is inadvisable. In this context, oils obtained from different extraction methods comply with said report (11, 21).

Table 3. Monounsaturated fatty acids in oils (sacha inchi, sesame, and peanut) obtained by cold and hot pressing.

Tabla 3. Ácidos grasos monoinsaturados presentes en aceites (sacha inchi, ajonjolí y maní) obtenidos por diferentes métodos de extracción (prensado en frío y en caliente).

		Oilseeds + Extraction Method					
		S.I + C.P	**S.I + H.P**	**S.M + C.P**	**S.M + H.P**	**P.N + C.P**	**P.N + H.P**
Palmitoleic acid	C16:1	0.00^{A}	0.13^{B}	0.00^{A}	0.23^{C}	0.00^{A}	0.00^{A}
Oleic acid (omega 9)	C18:1	8.72^{A}	9.56^{B}	32.75^{C}	35.14^{D}	49.34^{E}	50.61^{F}
Eicosenoic acid	C20:1	0.10^{B}	0.16^{C}	0.00^{A}	0.00^{A}	0.90^{D}	0.91^{D}
Nervonic acid	C24:1	0.00^{A}	0.00^{A}	0.14^{B}	0.00^{A}	0.01^{A}	0.00^{A}
Total Saturated Fatty Acids		8.82^{A}	9.85^{B}	32.89^{C}	35.37^{D}	50.25^{E}	51.52^{F}

Different letters represent statistically significant differences (Tukey $p < 0.05$).

Diferentes letras representan diferencias estadísticamente significativas (Tukey $p < 0,05$).

Polyunsaturated Fatty Acids

Oils derived from various oilseeds constitute a significant source of polyunsaturated fatty acids, particularly linoleic acid (C18:2, omega-6) and alpha-linolenic acid (C18:3, omega-3). Our results showed that sacha inchi oil, cold-pressed or hot-pressed, presented the highest concentrations of polyunsaturated fatty acids, with 84.36 g/100 g and 82.55 g/100 g, respectively. In contrast, hot-pressed peanut oil showed a significantly lower concentration, reaching 30.83 g/100 g (table 4). These findings underline the critical influence of extraction methods on preserving polyunsaturated fatty acids in oilseeds. Comparatively, these results exceeded values reported for avocado oil (*Persea americana)* in Ecuador (27), with total polyunsaturated fatty acid content of 62.33 g/100 g, even considering genotype and extraction conditions. The consumption of polyunsaturated fatty acids prevents various chronic diseases, like diabetes mellitus, obesity and cardiovascular diseases. These fatty acids activate the PPARα receptor (peroxisome proliferator-activated receptor alpha), which stimulates lipid oxidation, reduces insulin resistance and prevents hepatic steatosis (33).

Table 4. Polyunsaturated fatty acids in oils (sacha inchi, sesame, and peanut) obtained by cold and hot pressing.

Tabla 4. Ácidos grasos poliinsaturados presentes en aceites (sacha inchi, sésamo y maní) obtenidos por diferentes métodos de extracción (prensado en frío y en caliente).

		Oilseed + Extraction method					
		S.I + C.P	**S.I + H.P**	**S.M + C.P**	**S.M + H.P**	**P.N + C.P**	**P.N + H.P**
Linoleic acid (omega 6)	C18:2	27.38^{B}	25.57^{A}	51.81^{F}	47.58^{E}	31.95^{D}	30.47^{C}
Alpha-linolenic acid (omega 3)	C18:3	56.98^{E}	56.98^{E}	0.55^{D}	0.43^{C}	0.23^{A}	0.36^{B}
Total Saturated Fatty Acids		84.36^{F}	82.55^{E}	52.36^{D}	48.01^{C}	32.18^{B}	30.83^{A}

Different letters represent statistically significant differences (Tukey $p < 0.05$).

Diferentes letras representan diferencias estadísticamente significativas (Tukey $p < 0,05$).

Conclusions

This study demonstrated that oilseed type and extraction method significantly influenced bromatological characteristics (pH, acidity, peroxide index, relative density, and ash), except moisture content. Regarding fatty acid profile, sesame and peanut oils (both cold-pressed and hot-pressed) are excellent sources of monounsaturated fatty acids, with higher concentrations of omega-9 than sacha inchi oil. On the other hand, sacha inchi oil constitutes a source of polyunsaturated fatty acids, particularly omega-3 and omega-6. Consequently, these oilseeds may enrich the human diet, while offering industrial and food applications.

References

1. Abubakar, M.; Mohammed-Adewumi, A.; Amina-Ladidi, M.; Jibril -Hassan, L.; Agatha, N. 2024. Physicochemical properties of oil extracted from pumpkin (*Cucurbita pepo*) Seeds. Lafia Journal of Scientific & Industrial Research. 5-9. https://doi.org/10.62050/ljsir2024.v2n1.276
2. Akhtar, S.; Khalid, N.; Ahmed, I.; Shahzad, A.; Ansar, H.; Suleria. 2014. Physicochemical characteristics, functional properties, and nutritional benefits of peanut oil: A review. Critical Reviews in Food Science and Nutrition. 4. https://doi.org/10.1080/10408398.2011.644353
3. Alarcón-Rivera, R.; Pérez-Camino, M. C.; Chasquibol-Silva, N. 2019. Evaluation of the shelf life of microencapsulated sacha inchi oils (*Plukenetia huayllabambana* and *Plukenetia volubilis*). Journal of the Peruvian Chemical Society. 85(3). http://www.scielo.org.pe/scielo.php?script=sci_arttext&pid=S1810-634X2019000300005
4. Arab, R.; Casal, S.; Pinho, T.; Cruz, R.; Lamine Freidja, M.; Lorenzo, J.; Hano, C.; Mafani, K.; Makhlouf, L. 2022. Effects of seed roasting temperature on sesame oil fatty acid composition, lignan, sterol and tocopherol contents, oxidative stability and antioxidant potential for food applications. Moleculas. 27(4). https://doi.org/https://doi.org/10.3390/molecules27144508
5. Beshaw, T.; Demssie, K.; Tefera, M.; Guadie, A. 2022. Determination of proximate composition, selected essential and heavy metals in sesame seeds (*Sesamum indicum* L.) from Ethiopian markets and assessment of the associated health risks. *Toxicology Reports*, 1806-1812. https://doi.org/10.1016/j.toxrep.2022.09.009
6. Bocanegra-Morales, N.; Galeano-Garcia, P. 2023. Chemical composition, fatty acid profile, and optimization of the sacha inchi (*Plukenetia volubilis* L.) seed-roasting process using response surface methodology: Assessment of oxidative stability and antioxidant activity. Foods. 12(18). https://doi.org/https://doi.org/10.3390%2Ffoods12183405
7. Bonku, R.; Yu, J. 2020. Health aspects of peanuts as an outcome of its chemical composition. Food Science and Human Wellness. 9(1): 21-30. https://doi.org/10.1016/j.fshw.2019.12.005
8. Bravo, A.; Navarro, E.; Rincón, C.; Soriano, M. 2018. Physicochemical characteristics and fatty acid profile of two cultivars. Revista de Ciencias Naturales y Agropecuarias. 5(15): 9-18. https://www.ecorfan.org/bolivia/researchjournals/Ciencias_Naturales_y_Agropecuarias/vol5num15/Revista_de_Ciencias_Naturales_y_Agropecuarias_V5_N15_3.pdf
9. Edmund, H.; Sam, P. 2017. Anti-inflammatory and antioxidant effects of sesame oil on atherosclerosis: A descriptive literature review. Cureus. 9(7). https://doi.org/10.7759%2Fcureus.1438
10. FEN (Spanish Nutrition Foundation). 2013. White paper on nutrition in spain madrid: Spanish Foundation. Spanish Food Safety and Nutrition Agency. https://www.sennutricion.org/media/Docs_Consenso/Libro_Blanco_Nutricion_Esp-2013.pdf
11. Haile, M.; Duguma, H. T.; Chameno, G.; Kuyu, C. G. 2019. Effects of location and extraction solvent on physico chemical properties of Moringa stenopetala seed oil. Heliyon. 5(11). https://doi.org/10.1016/j.heliyon.2019.e02781
12. Hu, T.; Zhou, L.; Kong, F.; Wang, S.; Hong, K.; Lei, F.; He, D. 2023. Influence of oilseed type and extraction method on free fatty acid content in vegetable oils. Foods. 12(18): 3351. https://doi.org/https://doi.org/10.3390/foods12183351
13. ICONTEC (Instituto Colombiano de Normas Técnicas). 2018. NTC 287:2018 - Animal and vegetable fats and oils. Determination of moisture and volatile matter content. Animal and vegetable fats and oils. Determination of moisture and volatile matter content. https://tienda.icontec.org/gp-grasas-y-aceites-animales-y-vegetales-determinacion-del-contenido-dehumedad-y-materia-volatil-ntc287-2018.html
14. INEN (Ecuadorian Institute for Standardization). 1973. Ecuadorian Technical Standard 0038. Edible fats and oils. Determination of acidity. Ecuadorian standardization service. https://www.academia.edu/8969698/NTE_INEN_0038_Grasas_y_aceites_comestibles_Determinaci%C3%B3n_de_la_acidez
15. INEN (Ecuadorian Institute for Standardization). 1978. Ecuadorian Technical Standard 277. Fats and oils. Determination of the Peroxide Index. Ecuadorian standardization service. https://es.scribd.com/document/405847035/Inen-277-Indice-de-Peroxido

16. INEN (Ecuadorian Institute for Standardization). 2012. Ecuadorian Technical Standard 0035. Animal and vegetable oils and fats determination of relative density. Ecuadorian standardization service. https://es.scribd.com/document/339261140/NTE-INEN-35-1#:~:text=informaci%C3%B3n%20del%20documento-,Esta%20norma%20describe%20el%20m%C3%A9todo%20del%20picn%C3%B3metro%20para%20determinar%20la,relativa%20utilizando%20una%20f%C3%B3rmula%20dada.
17. INEN (Ecuadorian Institute for Standardization). 2012. Ecuadorian Technical Standard 34. Blend of edible vegetable oils. Requirements. Ecuadorian standardization service. https://es.scribd.com/document/339261140/NTE-INEN-35-https://es.scribd.com/document/534182662/nte-inen-34-2-Mezcla-de-aceites
18. Kittibunchakul, S.; Hudthagosol, C.; Sanporkha, P.; Sapwarobol, S.; Temviriyanukul, P.; Suttisansanee, U. 2022. Evaluation of sacha inchi (*Plukenetia volubilis* L.) by-products as valuable and sustainable sources of health benefits. Horticulturae. 344: 8. https://doi.org/https://doi.org/10.3390/horticulturae8040344
19. León-Sánchez, G.; Monteagudo-Borges, R.; Rodríguez-Jiménez, E. 2022. Characterization of the oil extraction process of *Moringa oleifera* in relation to seed type. Tecnología Química. 42(1). http://scielo.sld.cu/scielo.php?script=sci_arttext&pid=S2224-61852022000100024
20. Misganaw- Gedlu, A.; Amare -Aregahegn, D.; Atlabachew, M.; Abebe, W. 2021. Fatty acid composition, total phenolic contents and antioxidant activity of white and black sesame seed varieties from different localities of Ethiopia. Chemical and Biological Technologies in Agriculture. 8(1). https://doi.org/https://doi.org/10.1186/s40538-021-00215-w
21. Mohamed, A.; Ferhat, B.; Meklati, F. C. 2007. Comparison of different extraction methods: cold pressing, hydrodistillation, and solvent free microwave extraction, used for the isolation of essential oil from Citrus fruits. Journal of Chromatography A. 1210(2): 139-147. https://doi.org/10.1016/j.chroma.2008.09.085.
22. Montero-Torres, J. 2020. Nutritional and economic importance of peanut (*Arachis hypogaea* L.). Journal of Agricultural Research and Innovation. 7(2). http://www.scielo.org.bo/scielo.php?pid=S2409161820200002000 14&script=sci_abstract
23. Nagendra-Prasad, M.; Sanjay, K.; Deepika, S.; Vijay, N.; Kothari, R.; Nanjunda-Swamy, S. 2012. A review on nutritional and nutraceutical properties of sesame. Nutrition & Foods Sciences. 2(127). https://doi.org/http://dx.doi.org/10.4172/2155-9600.1000127
24. Neira Mosquera, J. A.; Coello Culluzpuma, A.; Sanche LLaguno, S. N.; Plua Montiel, J.; Viteri García, I. P. 2021. Study on the effect of variety and extraction conditions of avocado (*Persea americana*) oil for food purposes in Ecuador. Clinical Nutrition and Hospital Dietetics. 94-98. https://www.revistanutricion.org/articles/study-of-the-effects-ofvariety-and-conditions-of-the-avocado-oil-persea-americana-extraction-process-forfood-purposes-.pdf
25. Neira-Mosquera, J. A.; Menéndez-Viteri, O. F.; Ullón-Arcia, J. A.; Sánchez-Llaguno, S. N. 2022. Study of the vegetable oils of sacha inchi *(Plukenetia huayllabambana),* sesamum indicum and peanuts *(Arachis hypogaea)* and their influence on the preparation of "Frankfurt" type vegetable sausages, considering bromatological and organoleptic characteristic. Journal of Pharmaceutical Negative Results. 13(3): 623-627.
26. Oubannin, S.; Bijla, L.; Ahmed, M.; Ibourki, M.; El Kharrassi, Y.; Devkota, K.; Bouyahya, A.; Maggi, F.; Caprioli, G.; Sakar, E.; Gharby, S. 2024. Recent advances in the extraction of bioactive compounds from plant matrices and their use as potential antioxidants for vegetable oils enrichment. Journal of Food Composition and Analysis. 128. https://doi.org/https://doi.org/10.1016/j.jfca.2024.105995
27. Panpan Wei, F. W.; Xiaoyun, C.; Guige, H.; Qingguo, M. 2022. Sesame (*Sesamum indicum* L.): A comprehensive review of nutritional value, phytochemical composition, health benefits, development of food, and industrial applications. Nutrients. 14(19): 4079. https://doi.org/10.3390/nu14194079
28. Peroné, J.; Ruiz-Gutiérrez, V.; Barrón, L. 1999. High performance liquid chromatography for the separation of triglycerides from complex animal fats. Fats and Oils. 50(4): 298-311.
29. Rivera, M.; Ramos, M.; Silva, M.; Briceño, J.; Álvarez, M. 2022. Effect of pre-extraction temperature on the yield and fatty acid profile of *morete* (*Mauritia flexuosa* L. F.) oil. La Granja. 35(1): 98-111. https://doi.org/10.17163/lgr.n35.2022.08
30. Rodríguez, G.; Villanueva, E.; Glorio, P.; Baquerizo, M. 2015. Oxidative stability and shelf life estimation of sacha inchi (*Plukenetia volubilis* L.) oil. Scientia Agropecuaria. 6(3): 155-163. http://dx.doi.org/10.17268/sci.agropecu.2015.03.02
31. Rodriguez Cruz, M.; Tovar Armando, R.; Del Prado, M.; Torres, N. 2005. Molecular mechanisms of action of polyunsaturated fatty acids and their health benefits. Journal of Clinical Research. 57(3): 457-472. https://www.scielo.org.mx/pdf/ric/v57n3/v57n3a10.pdf
32. Romero- Hidalgo, L. E.; Valdiviezo- Rogel, C. J.; Bonilla -Bermeo, S. M. 2019. Characterization of *sacha inchi* (*Plukenetia volubilis*) seed oil from San Vicente, Manabí, Ecuador, obtained using non-thermal extrusion processes. La Granja. 30(2): 77-78. https://doi.org/https://doi.org/10.17163/lgr.n30.2019.07

33. Ruiz, S.; Sánchez, E.; Tabares Villareal, E.; Prieto, A.; Arias, J.; Gómez, R.; Castellanos, D.; García, P.; Chaparro, S. 2007. Biological and cultural diversity of the southern colombian amazon-diagnosis. Bogotá, Colombia: Coporamazonia, Humboldt Institute, Sinchi Institute. https://doi.org/https://repository.humboldt.org.co/entities/publication/a8f09059-7552-4fa8-968f-cd7a553af361
34. Schwingshackl, L.; Bogensberger, B.; Benčič, A.; Knüppel, S.; Boeing, H.; Hoffmann, G. 2018 . Effects of oils and solid fats on blood lipids: a systematic review and network meta-analysis. J Lipid Res. 59(9): 1771-1782. https://doi.org/10.1194/jlr.p085522
35. Seid, F.; Mehari, B. 2022. Elemental and proximate compositions of sesame seeds and the underlying soil from Tsegede, Ethiopia. Int J Anal Chem. https://doi.org/10.1155%2F2022%2F1083196
36. Suri, K.; Singh, B.; Kaur, A.; Singh, N. 2019. Impact of roasting and extraction methods on chemical properties, oxidative stability and maillard reaction products of peanut oils. J. Food Sci. Technol. 56: 2436-2445.
37. Torrejón, C.; Uauy, R. 2011. Fat quality, atherosclerosis and coronary heart disease: effects of saturated fatty acids and trans fatty acids. Journal of Medicine of Chile. 139(7): 924-931.
38. Xu, B.; Chang, K. 2008. Total phenolics, phenolic acids, isoflavones, and anthocyanins and antioxidant properties of yellow and black soybeans as affected by thermal processing. J. Agric. Food Chem. 56: 7165-7175. https://doi.org/10.1021/jf8012234
39. TIBCO Software. (2023). Software version 15.0 [Software]. TIBCO Software Inc.
40. StatPoint Technologies. (2024). STATGRAPHICS Centurion XVII [Software]. StatPoint Technologies Inc.

Green Synthesis and Foliar Application of Copper Nanoparticles in Sunflower (*Helianthus annuus* L.) to Improve Physiological Parameters and Yield

Síntesis verde y aplicación foliar de nanopartículas de cobre en híbridos de girasol (*Helianthus annuus* L.) para mejorar parámetros fisiológicos y el rendimiento

Sergio Andrés Granados Ortiz [1, 2, 3], Flavia Fátima Visentini [1], Elisa Soledad Panigo [3, 4], Fernando Felipe Muñoz [5], Juan Pablo Malano [2], Marcos Gabriel Derita [3], Lucas Damián Daurelio [2, 3], Carlos Alberto Bouzo [2, 3], Adrián Alejandro Pérez Rubin [1], Gabriel Céccoli [2, 3 *]

Originales: *Recepción:* 22/08/2024 - *Aceptación:* 04/08/2025

Abstract

Nanotechnology holds significant interest across various domains, including agriculture. The green synthesis of nanoparticles offers environmentally friendly solutions. This study aimed to synthesize copper nanoparticles (NPs) using *Aloe vera* extracts and evaluate their foliar application on two sunflower hybrids, Chané (Ch) and Calchaquí (Ca). The two types of *Aloe Vera* extracts used to produce nanoparticles were characterized by UV-vis spectral analysis and dynamic light scattering (DLS). The Np particles synthesized with *Aloe vera* Home (Np1) measured 242.8 nm (62.6%) and 74.87 nm (37.4%), while *Aloe vera* Commercial (Np2) resulted in sizes of 339.6 nm (90.7%) and 66.07 nm (9.3%). Two different doses of Np (150 ppm and 300 ppm) were applied to sunflower plants. We measured germination power (GP), plant height (PH), leaf number (LN), leaf area (LA), dry weight accumulation and achene yield. Chané's parameters improved at both nanoparticle doses, while Calchaquí only improved with the 300 ppm treatment. This research highlights the potential use of green nanotechnology to improve growth and yield in sunflower.

Keywords
plant physiology • oilcrops • agrotechnology • reducing agent • crop science

1 Área de Biocoloides y Nanotecnología. Instituto de Tecnología de Alimentos. Facultad de Ingeniería Química. Universidad Nacional del Litoral. 1° de Mayo 3250 (CP 3000). Santa Fe. República Argentina.
2 Universidad Nacional del Litoral. Facultad de Ciencias Agrarias. Cátedra de Fisiología Vegetal. Kreder 2805. C. P. 3080. Esperanza. Argentina.
3 Instituto de Ciencias Agropecuarias del Litoral (ICiAgro Litoral). Universidad Nacional del Litoral (UNL). Consejo Nacional de Investigaciones Científicas y Técnicas (CONICET). Facultad de Ciencias Agrarias (FCA). Laboratorio de Investigaciones en Fisiología y Biología Molecular Vegetal (LIFiBVe). Kreder 2805. S3080HOF. Esperanza, provincia de Santa Fe. República Argentina.
* gabrielcnbj@yahoo.com.ar
4 Universidad Nacional del Litoral. Facultad de Ciencias Agrarias. Cátedra de Morfología Vegetal. Kreder 2805. C. P. 3080. Esperanza. Argentina.
5 Universidad Nacional de Mar del Plata. CONICET. Instituto de Investigaciones.

Resumen

La nanotecnología es un área de gran interés en diferentes campos de la ciencia, entre ellos la agricultura. La síntesis verde de nanopartículas ofrece soluciones sostenibles para el medioambiente. El objetivo del presente trabajo fue sintetizar nanopartículas de cobre (NPs) utilizando como agente reductor el *Aloe Vera* y evaluar el impacto de su aplicación foliar en dos híbridos de girasol, Chané (Ch) y Calchaquí (Ca). Se utilizaron dos tipos de extractos de *Aloe Vera* como agente reductor, las cuales se caracterizaron mediante análisis espectral UV-vis y dispersión dinámica de luz (DLS). Las Nps sintetizadas con *Aloe Vera* Home (Np1) presentaron tamaños de partícula de 242,8 nm (62,6%) y 74,87 nm (37,4%), mientras que las obtenidas con *Aloe Vera* comercial (Np2) dieron como resultados tamaños de partícula de 339,6 nm (90,7%) y 66,07 nm (9,3%). Se midieron parámetros fisiológicos de la planta como fue el poder germinativo (PG), la altura de la planta (PH), el número de hojas (NL) y el área foliar (LA). Se aplicaron dos dosis diferentes de Nps (150 ppm y 300 ppm) a las plantas y se cuantifico la acumulación de materia seca en tallo, peciolo, hoja y capitulo. El híbrido Chané presentó una mejora respuesta con ambas dosis de nanopartículas, mientras que Calchaquí mostró una mejora en sus parámetros solo con el tratamiento de 300 ppm. Esta investigación destaca el uso potencial de la nanotecnología verde en girasol para mejorar el crecimiento y el rendimiento.

Palabras claves

fisiología vegetal • cultivos oleaginosos • tecnología agraria • agente reductor • ciencias de los cultivos

Introduction

Recently, nanotechnology has emerged as a novel field with far-reaching applications across diverse sectors, including agriculture. Nanoparticles, with unique physicochemical properties, have garnered significant attention in crop management strategies (35, 36). Among these nanoparticles, copper nanoparticles stand out for their multifaceted properties, such as high surface-area-to-volume ratio, excellent conductivity, and intrinsic antimicrobial attributes (8, 28, 33). Their application in agriculture, particularly increasing plant growth and defense mechanisms, has sparked immense interest (17).

The exploration of natural sources for nanoparticle green synthesis constitutes a focal point in this expanding field (3, 15). *Aloe vera*, popular for its medicinal and bioactive properties, is a compelling candidate for synthesizing copper nanoparticles, aligning with sustainable practices and offering biocompatible and eco-friendly nanomaterials for agriculture (31).

The green synthesis of copper nanoparticles using *Aloe Vera* provides various phytochemicals with significant electrochemical reducing power. *Aloe vera* contains active components like polysaccharides, flavonoids, phenolic compounds, and anthraquinones (21, 25, 31) with functional groups like hydroxyl (-OH) and carbonyl (-C=O), that possess reducing and stabilizing power. Polysaccharides, particularly mannose-rich polymers and acetylated mannans, reduce copper ions to copper nanoparticles (9, 23, 29). Hydroxyl groups also lead to the reduction of copper ions and subsequent formation of copper nanoparticles (4, 27). Additionally, synergistic effects among various bioactive compounds in these extracts help stabilization and control the synthesis of copper nanoparticles.

Aloe Vera as green reducing agent may influence the synthesis of copper nanoparticles (31). Homemade extracts (self-grown plants) may exhibit composition variations due to cultivar differences, growth conditions, extraction methods, and storage, potentially affecting concentrations of bioactive compounds. Alternatively, commercial products are subjected to standardized processing methods, potentially containing stabilizers or additives (21) that influence concentration and quality compared to homemade extracts (18). These variations in chemical composition and concentrations of bioactive compounds in *Aloe Vera* extracts might lead to differences in their reducing potential and, consequently, affect the synthesis of copper nanoparticles. Such differences can result in varied nanoparticle sizes, shapes, and stability, impacting their potential applications (34).

Parallely, the study of nanoparticle-induced responses in crop plants represents a promising alternative in agricultural research (17). Sunflower (*Helianthus annuus* L.) is an emblematic oilseed crop known for its adaptability to various environments and the capacity to provide oil, seeds, and biomass (1, 7, 39). Beyond their economic significance, sunflowers play a key role in phytoremediation and agricultural ecosystems (9, 20). Understanding the influence of *Aloe Vera*-based copper nanoparticles on growth, development, and nutrient dynamics of sunflower hybrids may optimize crop management strategies and contribute to sustainable agricultural practices.

This research aims to describe the mechanisms underlying nanoparticle-plant interactions, and how *Aloe Vera*-based copper nanoparticles affect growth, biomass accumulation and partitioning in two sunflower hybrids. This will expand our understanding of nanoparticle-mediated plant responses, for potential tailored nanoparticle-based strategies to optimize sunflower productivity and sustainability.

Materials and Methods

Synthesis and Characterization of *Aloe Vera*-based Copper Nanoparticles

Synthesis

Copper nanoparticles (Np) were synthesized using two *Aloe Vera* extracts as reducing agents. The first *Aloe Vera* extract (AVH) was obtained and characterized at the Biocolloids and Nanotechnology Laboratory of the Facultad de Ingeniería Química (FIQ), Instituto de Tecnología de Alimentos (ITA), Universidad Nacional del Litoral (UNL) in Santa Fe (Argentina). The second extract (AVC) was commercial (Jual Aloe Calchaquí SRL.). Np synthesis used two solutions containing copper sulfate pentahydrate ($CuSO_4.5H_2O$) (Anedra-Research AG) at [0.1 M]. The AVH and AVC were added to this solutions in a 8:2 ratio of copper salt and reducing agent. The obtained solutions were shaken (Fisatom-Model 753A) for 15 minutes at moderate and constant speed. Then, both solutions were placed in a thermal bath (Dalvo-Model BTMP) for 4 h at 85°C. Subsequently, they were left for 2 h at room temperature (25°C). The resulting solutions were oven-dried (Dalvo-Model FHR/I) at 90°C for 24 h, obtaining a green powder. This powder was weighed with a high-precision digital balance (Ohaus-Model PA 214), reconstituted with the same amount of evaporated water and stirred until a homogeneous solution was obtained. Then, solutions were centrifuged (Neofuge 18R Heal Force) at 3000 rpm or 1.016 g for 20 min at 20°C. Finally, supernatants were collected and stored, obtaining liquid Np1 ($CuSO_4.5H_2O$ with *Aloe Vera* Home) and Np2 ($CuSO_4.5H_2O$ with *Aloe Vera* commercial) (13).

Characterization

The Np were spectrally characterized using UV-vis spectroscopy (Perkin Elmer Lambda 20) to determine surface plasmon resonance (SPR) characteristic of metallic nanoparticles (35). Additionally, the percentage conversion was calculated using the normalized spectrum equation (12), and particle size was determined using the dynamic light scattering (DLS) technique (ZetaNano ZS Malvern UK) (37).

Plant Culture and Growth Conditions

Plant Material and Growth Conditions

This study was conducted under field conditions with summer rainfall and controlled irrigation at Donnet field, Facultad de Ciencias Agrarias (FCA-UNL) in Esperanza (31°26'34.4" S 60°56'26.3" W, Santa Fe, Argentina). Soil was a Mollisol subgroup typical Argiudol of the Esperanza Series, with 29% sand, 66% silt, and 5% clay in the Ap horizon (0 to 0.27 m deep) (7). A total of 440 sunflower (*Helianthus annuus* L.) seeds were sown, comprising 25 plants of the Chané (Ch) hybrid and 25 plants of Calchaquí (Ca) hybrid. The seeds underwent pre-germination treatment with dynasty-metalaxil-imida (DMI) to prevent fungal growth. Seeds were supplied by Dr. Daniel Álvarez (Estación Experimental Agropecuaria, Instituto Nacional de Tecnología Agropecuaria, EEA-INTA-Manfredi).

Experimental Design

Two plots were prepared, each undergoing two mechanical weed control sessions. Plot "A" was 6.26 m long and 4.30 m wide, with Ch hybrid sown in the western part and Ca hybrid in the eastern part. Similarly, plot "B" measured 6.47 m in length and 4.50 m in width. Ch was planted in the eastern section while Ca was planted in the western section of this plot. A total of 16 rows were created, 8 rows per plot, with 4 rows for each hybrid in both plots. Externally, plots were surrounded by three rows of plants with the same density to reduce edge effect. Sowing density was 3-4 seeds per linear meter, plus 15% for potential seed loss.

Soil Preparation, Germination, and Transplanting

Germination was carried out as previously described (5, 6, 7, 19). Briefly, seeds were washed with a 30% commercial bleach solution for 20 min, followed by three washes with distilled water and drying with inert paper. Subsequently, *in vitro* germination was conducted using 20 sterilized Petri dishes conditioned with inert paper and saturated with distilled water. Each Petri dish contained 22 seeds of each hybrid germinated under controlled conditions of saturated humidity and 27.2°C in a germination oven (Bioelec-Model RE-41.1). Temperature was monitored using a Data Logger (Cavadevices SATM), recording measurements every 15 minutes. After 72 h in the germination oven, seeds were transplanted, considering visible radicle without necrotic tissue.

Morphological and Physiological Parameters

We measured germination energy (GE), germination power (PG), plant height (PH), leaf number (LN), and leaf area (LA) of the 15^{th} and 18^{th} leaves. Parameters a, b, and X_0 were obtained by fitting Leaf expansion curves to a sigmoidal equation.

Harvest was carried out when plants reached physiological maturity, corresponding to stage R9 on the Scheiter and Miller scale (32). Dry weight accumulation was measured for the two copper nanoparticles (Np) at three doses (control, C; 0ppm; D1, 150 ppm of Np AVC and AVH; and D2, 300 ppm of AVC and AVH, respectively). Dry weight was partitioned into Heads, Stems, Petioles, and Leaves, then stored and oven-dried (DALVO-Model XHRF 6189) at 60°C until constant weight. Hybrids were harvested at 2141.7°C d^{-1} (5, 12).

Leaf Growth Analysis

Leaf Area (*LA*) was estimated as described in Eq.1 (6, 24) from length and width measurements as follows (2):

$$LA = L \times W \times 0.65 \quad (1)$$

Relative rate of leaf expansion was calculated as described in Eq.2 (6, 24) as the slope of the regression curve between LA natural logarithm and thermal time.

Leaf expansion dynamics were analyzed by sigmoid curves with three parameters (*a, b,* and x_0):

$$y = a / (1 + \exp\{- [(x - x_0) / b]\}) \quad (2)$$

Final LA was determined as the upper asymptote (a).

Maximum expansion velocity value (V_{max}) was calculated as follows (6, 24):

$$V_{max} = [a * (1/b)] / 4 \quad (3)$$

Absolute leaf expansion rates (AER) were calculated as the slopes of the linear regression between leaf area and thermal time between two consecutive measurements for the entire experimental time (6, 24).

Leaf relative expansion rates (RER) were calculated as the ratios between the differences in leaf area logarithms and thermal time interval between two successive measurements (hn-1 and hn), (Eq.4) (5, 24):

$$RER = (\ln LAhn - \ln LAhn\text{-}1)/(°Cdhn - °Cdhn\text{-}1) \quad (4)$$

Nanoparticle Foliar Application

The Np were applied to leaves 15 and 18 in each hybrid (Ch and Ca) using a trigger spray applicator, at two different thermal moments (1507.4°C d^{-1} and 1645.9°C d^{-1}), with temperatures of 25.6 and 24.1°C, respectively. Both applications were carried out in the morning, ensuring open stomata and no wind. A volume of 12.5 mL of Np solution was applied to each leaf at each thermal time, totaling 25 mL per plant. Np were applied at two different doses in both hybrids: D1, 150 ppm of Np per plant and D2, 300 ppm of Np per plant (14).

Statistical Analysis

Data were analyzed by ANOVA and Fisher's least significant difference (LSD) test for 5 % significance level. ANOVA assumptions were verified by Shapiro-Wilks and Levene tests (7). Statistical analyses were run using InfoStat Professional software (Universidad Nacional de Córdoba) (7).

Results and Discussion

Characterization of Copper Nanoparticles (Np)

Spectral Characterization and Particle Size

Other studies report that the green synthesis method also enabled the observation of the SPR phenomenon at a wavelength of 398 nm for copper nanoparticles (35). Additionally, other peaks were observed at wavelengths ranging from 277 to 305 nm, similar to those observed in the present work (26). Figure 1A (page 192), shows comparable peaks in copper nanoparticles synthesized using different reducing agents (*Aloe Vera* Home and *Aloe Vera* Commercial), potentially attributed to the small nanoparticles. Understanding particle size is crucial as it directly influences physical and chemical properties of nanoparticles (37). Employing the DLS technique (figure 1B and figure1C, page 192), Yugandhar *et. al.* (2018) observed synthesized copper nanoparticles of 61.1 nm. Furthermore, Sánchez Gómez *et al.* (2018) documented a size distribution of 50 nm for their synthesized copper nanoparticles. These findings can be compared to the second population observed in Np2. Notably, both nanoparticle sets synthesized using *Aloe Vera* exhibited sizes as those reported in the previously mentioned studies.

The different compositions of *Aloe Vera* extracts, whether Home or Commercial, might affect the reduction mechanisms or stabilize the nanoparticles differently during synthesis, potentially influencing particle size, as detected with DLS technique.

Plant Analysis

Physiological Parameters Before Nanoparticles Applicacion

Germinative Energy (GE) and Germinative Power (GP)

Germination energy in Ch was 94.0%, similar to that in *Pisum sativum* L. seeds with Treatment 1 (control) at 3 days (16). This implies that the Ca sunflower hybrid possesses a lower GE at 67.3% (figure 2A, page 192), while the Ch hybrid shows an even lower GE at 30.4%. Sánchez Gómez *et al.* (2018) analyzed GE at 7 days for Huaxyacac seeds *cv.* Cunningham (*Leucaena leucocephala* (Lam.) de Wit. treated with IA24 (water immersion at 24°C for 12 h), finding GE of 31.7%. In comparison, Ch sunflower hybrid seeds display a higher value (45.9%), while Ca seeds achieve 80.0% (figure 2b, page 192).

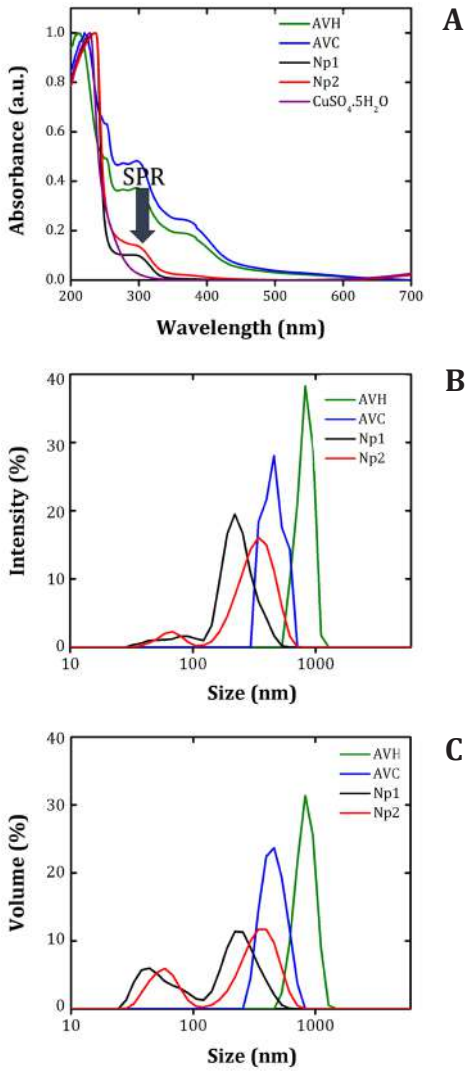

(Green line) *Aloe Vera* Home (AVH); (Blue line) Commercial *Aloe Vera* (AVC); (Black line) UV-Visible spectra of copper nanoparticles (Np1); (Red line) UV-Visible spectra of copper nanoparticles (Np2); and (Purple line) pentahydrated copper sulfate ($CuSO_4.5H_2O$).

(Línea verde) *Aloe Vera* Home (AVH); (Línea azul) *Aloe Vera* Comercial (AVC); (Línea negra) espectros de UV-Visible de nanopartículas de cobre (Np1); (Línea roja) espectros de UV-Visible de nanopartículas de cobre (Np2); y (Línea púrpura) sulfato de cobre pentahidratado ($CuSO_4.5H_2O$).

Figure 1. UV-visible spectra (A), Particle size distribution (PSD) based on Intensity (B) and Volume percentage (C) of the systems.

Figura 1. Espectros de UV-Visible (A)**,** Distribución del tamaño de las partículas (PSD) en función de la intensidad (B) y del porcentaje de volumen (C) de los sistemas.

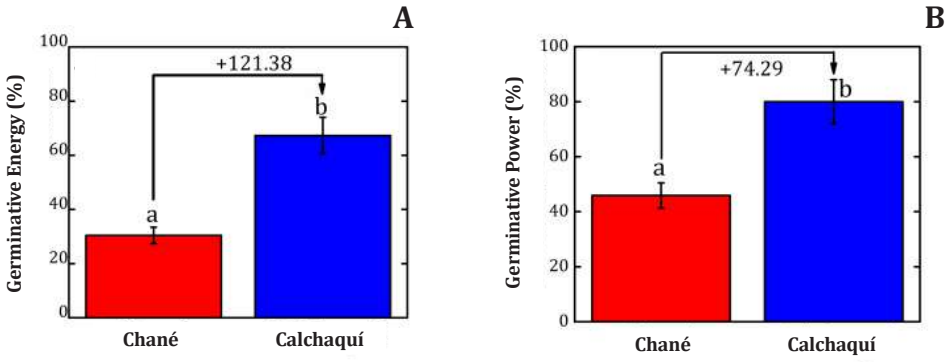

(A). Germination Energy at 72 h (EG) and (B) Germination Power (PG) at 168 h evaluated in two sunflower hybrids (*Helianthus annuus* L.) Chané (Ch) and Calchaquí (Ca).

(A) Energía Germinativa a las 72 h (EG) y (B) Poder Germinativo (PG) a las 168 h en dos híbridos de girasol (*Helianthus annuus* L.) Chané (Ch) y Calchaquí (Ca).

Figure 2. Germinative energy (%) and Germinative power (%) in two sunflower hybrids.

Figura 2. Energía germinativa (%) y Poder Germinativo (%) en dos híbridos de girasol.

Plant Height (PH) and Leaf Number (LN)

Figure 3A shows statistically significant differences in PH, except at 996.7 and 1283.7°C d^{-1}, probably since PH under controlled growth conditions is genotype dependent (24).

A research conducted by Ortis *et al.* (2005) involving 20 sunflower inbred lines found the KLM 295 hybrid exhibited similar behavior in PH as Ch and Ca hybrids, measuring 170 cm. Similarly, two sunflower hybrids PARSUN-1 and SMH-9707 (10), were shorter than Ch and Ca hybrids (136.61 cm and 137.63 cm, respectively). As previously described, this could be genotype-dependent. However, differences in PH can also be explained by internode elongation as a response to sowing density (1).

Figure 3B shows LN of Ch and Ca at eight different thermal times, starting from 528.3°C d^{-1}. At this moment, both hybrids had 18 visible leaves. Similarly, at 571.3°C d^{-1}, Ch exhibited 21 leaves while Ca had 22 leaves. Furthermore, at 611.7, 676.6, 731.5, and 884.1°C d^{-1}, Ch showed 23, 25, 27, and 29 true leaves, respectively. In contrast, during these days, Ca had 25, 27, 29, and 31 leaves, indicating an average difference of 2 extra leaves for Ca. Lastly, both hybrids had equal number of leaves (30 and 31) at 996.7 and 1283.7°C d^{-1} of plant development. As with PH, this difference in LN may be genetic (24).

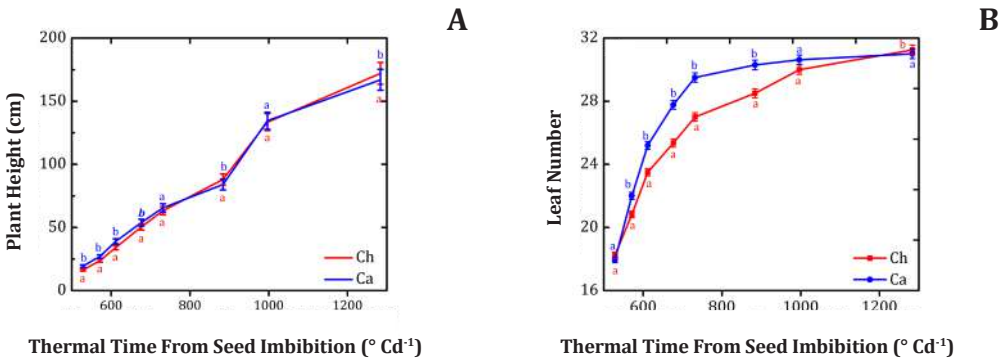

Figure 3. (A) Average plant height (cm) and (B) Leaf Number of two sunflower hybrids (*Helianthus annuus* L.), Chané (Ch), and Calchaquí (Ca).

Figura 3. (A) Altura media de planta (cm) y (B) número de hojas de dos híbridos de girasol (*Helianthus annuus* L.), Chané (Ch) y Calchaquí (Ca).

Leaf Expansion Dynamics of Leaves 15 and 18

Figure 4A (page 194), describes leaf expansion dynamics of the 15th and 18th leaves of Ch and Ca hybrids. Leaf 15 in Ch grew faster than Ca. Comparing these results with figure 3B, we concluded that Ch had fewer leaves but a bigger 15th leaf at all recorded thermal times. Figure 4A (page 194), shows that at 758.20°C d^{-1}, the Ch hybrid reached 50% of its final leaf area, while the Ca hybrid reached this value at 762.89°C d^{-1}.

Figure 4B (page 194), describes leaf expansion dynamics of the 18th leaf in both hybrids. When compared, both genotypes showed similar results in parameters "a" and "x_{0}", 34,307.21 and 808.31 for Ch, and 33,410.21 and 809.19 for Ca. Additionally, leaf expansion ceased at 979.08°C d^{-1} and 963.88°C d^{-1} in Ch and Ca, respectively. In conclusion, leaf growth dynamics of the 18th leaf were the same between hybrids and comparable to Céccoli *et al.* (2012).

Leaf area calculated by Eq. 2 (page 190).

El área foliar, para cada hoja y tiempo termal, fue calculado como lo indica la Eq. 2 (pág. 190).

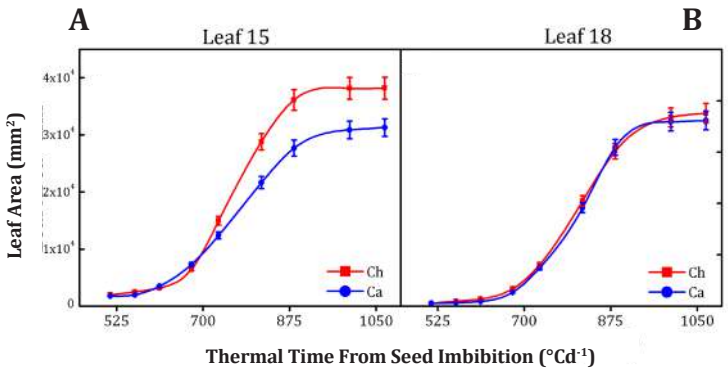

Figure 4. (A) Leaf area (LA) of the 15th leaf in Chané (Ch) and Calchaquí (Ca) hybrids; (B) Leaf area (LA) of the 18th leaf in Chané (Ch) and Calchaquí (Ca) hybrids.

Figura 4. (A) Área foliar (LA) de la hoja 15 en Ch y Ca; (B) Área (LA) de la hoja 18 en los híbridos Ch y Ca.

Leaf Growth Analyses

Figure 5 (page 195), compares different lea physiological parameters between leaves 15th and 18th, in Ch and Ca. Parameter "a" had statically lower area in leaf 15 of Ca (-12.97%; figure 5A, page 195), but no differences were seen for leaves 18 (figure 5A, page 195). Regarding parameter "b" in the 15th leaf, Ca had a significantly higher curvature in the sigmoid curve compared to Ch (figure 5B, page 195) while, the18th leaf showed no significant differences (figure 5B, page 195).

No significant differences were found for "x0" in the 15th leaf of any hybrid. Ca showed -0.42% (figure 5C, page 195), and Ch reached 50% leaf expansion in less thermal time compared to Ca (figure 5C, page 195). No statistically significant differences were found for leaf expansion cessation (figure 5D, page 195).

Leaf growth duration and Vmax increase were not statistically significant (figure 5F, page 195). Absolute leaf expansion rate (AER) was -33.82% in the 15th leaf of Ca with respect to Ch, with significant differences (figure 5G, page 195). The 18th leaf showed no significant differences (figure 5G, page 195). Finally, Leaf Relative Expansion Rate (RER) was -50.0% lower in Ca with respect to Ch in the15th leaf (figure 5H, page 195), and -33.33% considering the 18th leaf (figure 5H, page 195).

Physiological and Productive Parameters After Foliar Application of Copper Nanoparticles

Finally, Plant DW accumulation in Ch hybrid with Np1D1 and Np2D1 increased by 48.74% and 38.26%, respectively, compared to control plants. These Nps resulted in more benefits for this hybrid than for Ca, which decreased by 8.95% and 11.36% with Np1D1 and Np2D1, respectively (figure 6, page 196).

We conclude that dry weight accumulation using Np1 and Np2 at two doses suggests an interaction between the treatments and genotypes used (1, 7, 10, 11).

Foliar application of copper nanoparticles at 300 ppm is beneficial for plant development under saline stress, preventing biomass loss, while enhancing the levels of various bioactive compounds (17). These reported results can be compared with the present research, indicating positive effects of copper nanoparticles on leaf growth dynamics and dry weight accumulation in sunflower.

Significant increases in dry weight accumulation of head, stem, petiole, and leaf in Ch hybrid with Np1D1, Np2D1, Np1D2, and Np2D2 may indicate a better response to those specific doses or *Aloe Vera* genotypes. Conversely, the Ca hybrid showed varied responses, indicating diverse sensitivity upon *Aloe Vera* extracts (36, 38).

Differences in extract composition may lead to variations in synthesis or delivery of nanoparticles, altering their efficacy. The applied doses might have triggered diverse metabolic pathways, resulting in distinct responses between hybrids (1, 7, 10, 11).

Understanding these intricate relationships between nanoparticles, *Aloe Vera* extracts, and plant physiology requires further investigation to optimize nanoparticle application for enhanced agricultural production.

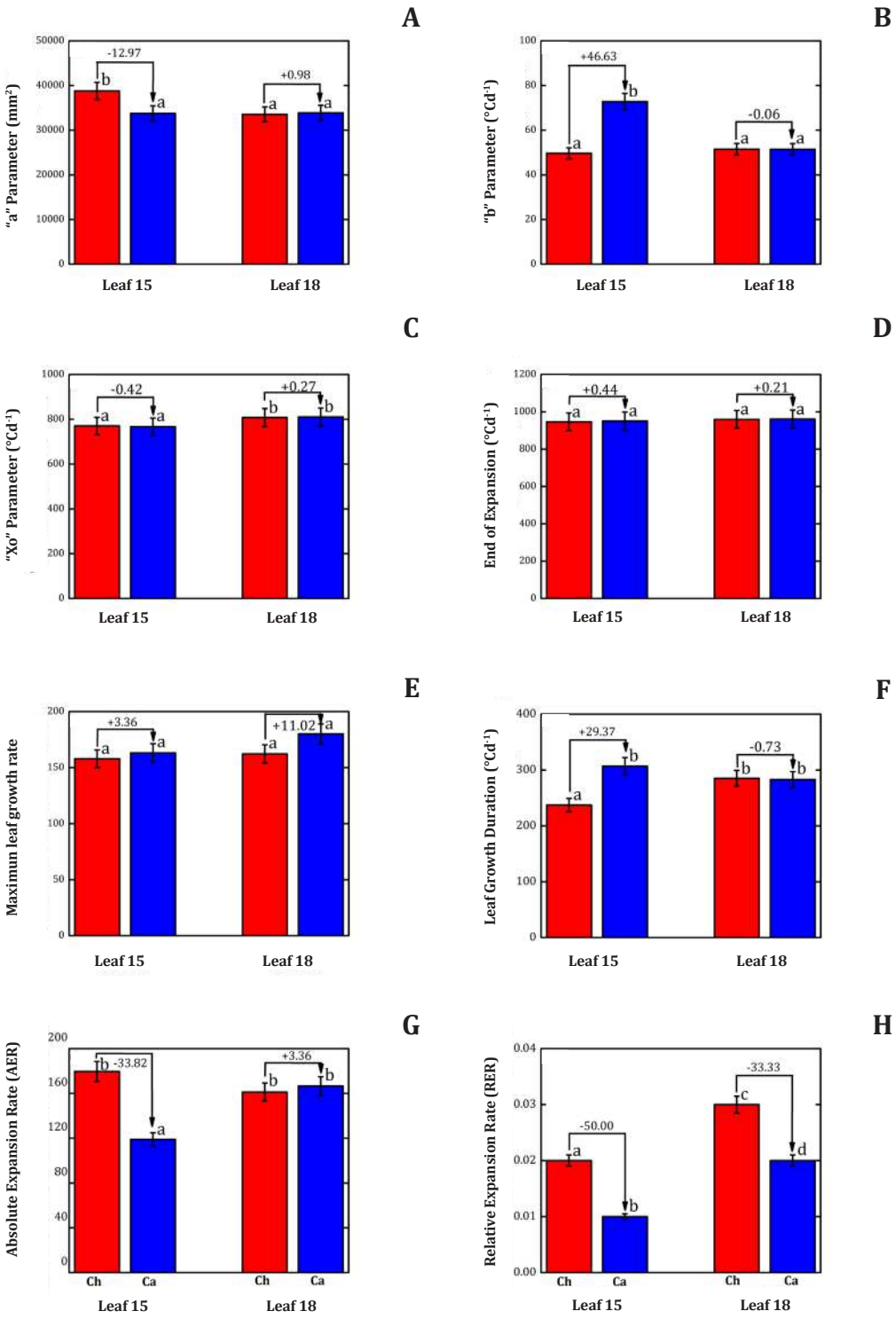

(A) Parameter "a" (mm^2), (B) parameter "b", (C) parameter "x0", (D) End of leaf expansion (°C d^{-1}), (E) parameter Vmax, (F) Duration of leaf expansion (°C d^{-1}), (G) Absolute rate of leaf expansion (AER, mm^2. $°Cd^{-1}$), and (H) Relative rate of leaf expansion (RER $°Cd^{-1}$) in two sunflower hybrids (*Helianthus annuus* L.), Chané (Ch) and Calchaquí (Ca) for leaf 15 and 18.

(A) Parámetro "a" (mm^2), (B) parámetro "b", (C) parámetro "x0", (D) Fin de la expansión foliar (°C d^{-1}), (E) parámetro Vmax, (F) Duración de la expansión foliar (°C d^{-1}), (G) Tasa absoluta de expansión foliar (AER mm^2.$°Cd^{-1}$), y (H) Tasa relativa de expansión foliar (RER $°Cd^{-1}$) en dos híbridos de girasol (*Helianthus annuus* L.), Chané (Ch) y Calchaquí (Ca) para la hoja 15 y la hoja 18, respectivamente.

Figure 5. Leaf Growth Analyses.

Figura 5. Análisis del crecimiento de las hojas.

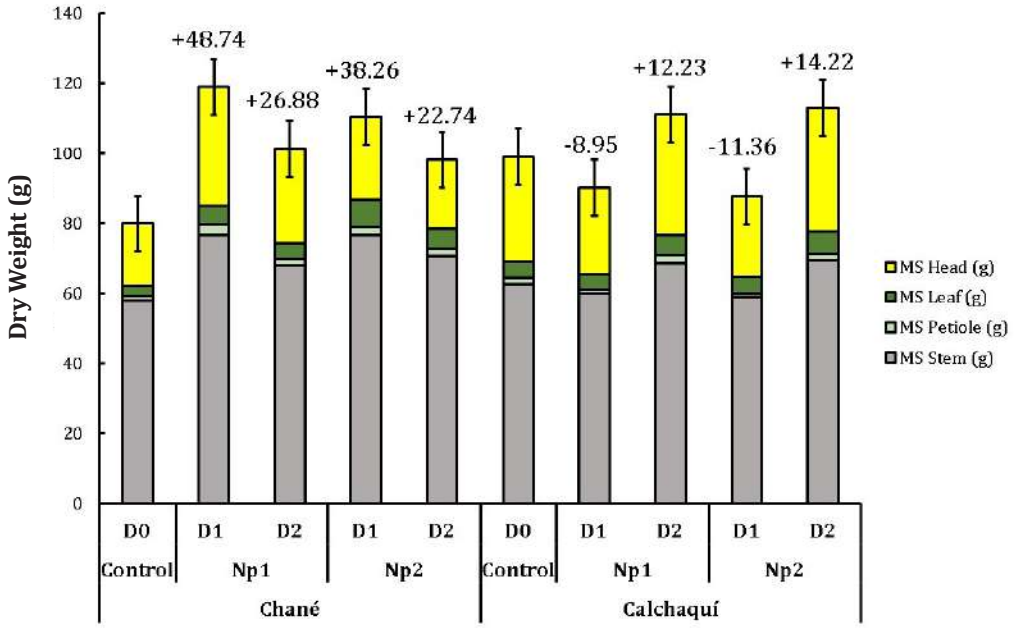

Figure 6. Dry weight accumulation of two sunflower hybrids (*Helianthus annuus* L.), Chané (Ch), and Calchaquí (Cal), partitioned into head, stem, petiole and leaf blade, after application of copper nanoparticles at harvest.

Figura 6. Peso de materia seca de los dos híbridos de girasol (*Helianthus annuus* L.), Chané (Ch) y Calchaquí (Cal), particionados en capitulo, tallo, pecíolo y lámina, luego de la aplicación de nanopartículas de cobre. La cosecha se realizó en madurez fisiológica.

Conclusions

This study assessed physiological responses in two sunflower (*Helianthus annuus* L.) hybrids, Chané (Ch) and Calchaquí (Ca), after foliar application of two types and doses of copper nanoparticles.

Different particle sizes of copper nanoparticles were observed employing *Aloe Vera* homemade extracts (Np1). The DLS technique allowed detecting two peaks at 242.8 nm and 74.87 nm, constituting 62.6% and 37.4% of the particles, respectively.

A comparison between sunflower hybrids showed that Calchaquí (Ca) had a higher Germinative Energy (GE) and Germinative Power (GP) by +121.38% and +74.29% respectively, than Chané. Leaf number was higher in the Calchaquí hybrid at all thermal times, except for the last measurement (1283.7°C d^{-1}). The Chane hybrid had higher expansion and relative expansion rates on leaf 15. Leaf 18 had similar parameter values in both hybrids.

Finally, Np1 ($CuSO_4.5H_2O$ with *Aloe Vera* Home), at 150 ppm (D1) for Chané (Ch), increased "Plant DW" accumulation by 48.74%. The study lays groundwork for further optimization of nanoparticle application to different sunflower hybrids.

References

1. Aguilar, L.; Escalante, J.; Fucikovsky, L.; Tijerina, L.; Engelman, E. 2005. Leaf Area, Net Assimilation Rate, Yield and Plant Density in Sunflower. Terra Latinoam. 23: 303-310.
2. Aguirrezábal, L. A. N.; Lavaud, Y.; Dosio, G. A. A.; Izquierdo, N. G.; Andrade, F. H.; González, L. M. 2003. Intercepted Solar Radiation during Seed Filling Determines Sunflower Weight per Seed and Oil Concentration. Crop Sci. 43: 152-161. https://doi.org/10.2135/cropsci2003.1520
3. Alishah, H.; Pourseyedi, S.; Ebrahimipour, S. Y.; Mahani, S. E.; Rafiei, N. 2017. Green synthesis of starch-mediated CuO nanoparticles: preparation, characterization, antimicrobial activities and in vitro MTT assay against MCF-7 cell line. Rend. Lincei. 28: 65-71. https://doi.org/10.1007/s12210-016-0574-y

4. Aminuzzaman, M.; Kei, L. M.; Liang, W. H. 2017. Green synthesis of copper oxide (CuO) nanoparticles using banana peel extract and their photocatalytic activities. AIP Conf. Proc. 1828. https://doi.org/10.1063/1.4979387
5. Céccoli, G.; Eugenia Senn, M.; Bustos, D.; Ismael Ortega, L.; Córdoba, A.; Vegetti, A.; Taleisnik, E. 2012. Genetic variability for responses to short- and long-term salt stress in vegetative sunflower plants. J. Plant Nutr. Soil Sci. 175: 882-890. https://doi.org/10.1002/jpln.201200303
6. Céccoli, G.; Bustos, D.; Ortega, L. I.; Senn, M. E.; Vegetti, A.; Taleisnik, E. 2015. Plasticity in sunflower leaf and cell growth under high salinity. Plant Biol. 17: 41-51. https://doi.org/10.1111/plb.12205
7. Céccoli, G.; Granados Ortiz, S. A.; Buttarelli, M. S.; Pisarello, M. L.; Muñoz, F. F.; Daurelio, L. D.; Bouzo, C. A.; Panigo, E. S.; Perez, A. A. 2022. Salinity tolerance determination in four sunflower (*Helianthus annuus* L.) hybrids using yield parameters and principal components analysis model. Ann. Agric. Sci. 67: 211-219. https://doi.org/10.1016/j. aoas.2022.12.005
8. Chowdhury, R.; Khan, A.; Rashid, M. H. 2020. Green synthesis of CuO nanoparticles using: Lantana camara flower extract and their potential catalytic activity towards the aza-Michael reaction. RSC Adv. 10: 14374-14385. https://doi.org/10.1039/d0ra01479f
9. Darroudi, M.; Ahmad, M. B.; Abdullah, A. H.; Ibrahim, N. A.; Shameli, K. 2010. Effect of accelerator in green synthesis of silver nanoparticles. Int. J. Mol. Sci. 11: 3898-3905. https://doi.org/10.3390/ijms11103898
10. Fayyaz-Ul-Hassan; Qadir, G.; Cheema, M. A. 2005. Growth and development of sunflower in response to seasonal variations. Pakistan J. Bot. 37: 859-864. https://doi.org/10.2298/hel0542159f
11. Flagella, Z.; Giuliani, M. M.; Rotunno, T.; Di Caterina, R.; De Caro, A. 2004. Effect of saline water on oil yield and quality of a high oleic sunflower (*Helianthus annuus* L.) hybrid. Eur. J. Agron. 21: 267-272. https://doi.org/10.1016/j.eja.2003.09.001
12. Gonzalez, M. A.; Bernardo, V.; Garita, S.; Plaza Cazón, J.; Arango, C.; Hernández, M. P.; Ruscitti, M. 2024. Morphophysiological and biochemical responses of *Schedonorus arundinaceus* to Zinc (II) excess: insights from biomarkers and elemental accumulation. Revista de la Facultad de Ciencias Agrarias. Universidad Nacional de Cuyo. Mendoza. Argentina. 56(2): 34-47. DOI: https://doi.org/10.48162/rev.39.135
13. Gunalan, S.; Sivaraj, R.; Venckatesh, R. 2012. *Aloe barbadensis* Miller mediated green synthesis of mono-disperse copper oxide nanoparticles: Optical properties. Spectrochim. Acta - Part A Mol. Biomol. Spectrosc. 97: 1140-1144. https://doi.org/10.1016/j.saa.2012.07.096
14. Hernández-Fuentes, A. D.; López-Vargas, E. R.; Pinedo-Espinoza, J. M.; Campos-Montiel, R. G.; Valdés-Reyna, J.; Juárez-Maldonado, A. 2017. Postharvest behavior of bioactive compounds in tomato fruits treated with Cu nanoparticles and NaCl stress. Appl. Sci. 7: 1-14. https://doi.org/10.3390/app7100980
15. Jayarambabu, N.; Akshaykranth, A.; Venkatappa Rao, T.; Venkateswara Rao, K.; Rakesh Kumar, R. 2020. Green synthesis of Cu nanoparticles using Curcuma longa extract and their application in antimicrobial activity. Mater. Lett. 259: 126813. https://doi.org/10.1016/j.matlet.2019.126813
16. Lastochkina, O. V.; Garipova, S. R.; Pusenkova, L. I.; Garshina, D. Y. 2023. Effect of Endophytic Bacteria Bacillus subtilis on Seedling Growth and Root Lignification of *Pisum sativum* L. under Normal and Sodium Chloride Salt Conditions. 70: 1-11. https://doi.org/10.1134/S102144372360085X
17. Lira Saldivar, R. H.; Méndez Argüello, B.; Vera Reyes, I.; de los Santos Villarreal, G. 2018. Agronanotechnology: A new tool for modern agriculture. Revista de la Facultad de Ciencias Agrarias. Universidad Nacional de Cuyo. Mendoza. Argentina. 50(2): 395-411. https://revistas.uncu.edu.ar/ojs3/index.php/RFCA/article/view/3067
18. Liu, C.; Cui, Y.; Pi, F.; Cheng, Y.; Guo, Y.; Qian, H. 2019. Extraction, purification, structural characteristics, biological activities and pharmacological applications of acemannan, a polysaccharide from *Aloe Vera*: A review. Molecules 24. https://doi.org/10.3390/ molecules24081554
19. Maya-Meraz, I, O.; Díaz-Calzadillas, M. F.; Ruiz-Cisneros, M. F.; Ornelas-Paz, J. de. J.; Rios-Velasco, C.; Berlanga-Reyes, D. I.; Pérez-Corral, D. A.; Alonso-Villegas, R. 2024. Effects of postharvest treatments based on calcium and silicon in hydro-cooling on the basic quality attributes of 'Bing' sweet cherries (*Prunus avium* L.) during storage. Revista de la Facultad de Ciencias Agrarias. Universidad Nacional de Cuyo. Mendoza. Argentina. 56(2): 114-125. DOI: https://doi.org/10.48162/rev.39.142
20. Mesquita, A. C.; Lima Simões, W.; Alcantara Campos, L. D.; Braga, M. B.; Alves Sobral, Y. R. 2024. Gas exchange in yellow melon (*Cucumis melo*) crop under controlled water deficit (RDI) and application of a biostimulant. Revista de la Facultad de Ciencias Agrarias. Universidad Nacional de Cuyo. Mendoza. Argentina. 56(2): 14-25. DOI: https://doi.org/10.48162/rev.39.133
21. Midatharahalli, M.; Shivayogeeswar, C.; Kotresh, E. N. 2019. Green synthesis of Zinc oxide nanoparticles (ZnO NPs) and their biological activity. SN Appl. Sci. 1: 1-10. https://doi.org/10.1007/s42452-018-0095-7
22. Ortis, L.; Nestares, G.; Frutos, E.; Machado, N. 2005. Combining Ability Analysis in Sunflower (*Helianthus annuus* L.). Pakistan J. Biol. Sci. 8: 710-713. https://doi.org/10.3923/pjbs.2005.710.713

23. Padil, V. V. T.; Černík, M. 2013. Green synthesis of copper oxide nanoparticles using gum karaya as a biotemplate and their antibacterial application. Int. J. Nanomedicine. 8: 889-898. https://doi.org/10.2147/IJN.S40599
24. Pereyra-Irujo, G. A.; Velázquez, L.; Lechner, L.; Aguirrezábal, L. A. N. 2008. Genetic variability for leaf growth rate and duration under water deficit in sunflower: Analysis of responses at cell, organ, and plant level. J. Exp. Bot. 59: 2221-2232. https://doi.org/10.1093/jxb/ern087
25. Prakash, S.; Elavarasan, N.; Venkatesan, A.; Subashini, K.; Sowndharya, M.; Sujatha, V. 2018. Green synthesis of copper oxide nanoparticles and its effective applications in Biginelli reaction, BTB photodegradation and antibacterial activity. Adv. Powder Technol. 29: 3315-3326. https://doi.org/10.1016/j.apt.2018.09.009
26. Rafique, M.; Tahir, R.; Gillani, S. S. A.; Tahir, M. B.; Shakil, M.; Abdellahi, M. O.; Rafique, M.; Tahir, R.; Gillani, S. S. A.; Tahir, M. B.; Shakil, M. 2020. Plant-mediated green synthesis of zinc oxide nanoparticles from *Syzygium Cumini* for seed germination and wastewater purification. Int. J. Environ. Anal. Chem. 00: 1-16. https://doi.org/10.1080/03067319.2020.1715379
27. Reddy, S. B.; Mandal, B. K. 2017. Facile green synthesis of zinc oxide nanoparticles by *Eucalyptus globulus* and their photocatalytic and antioxidant activity. Adv. Powder Technol. https://doi.org/10.1016/j.apt.2016.11.026
28. Ren, G.; Hu, D.; Cheng, E. W. C.; Vargas-Reus, M. A.; Reip, P.; Allaker, R. P. 2009. Characterisation of copper oxide nanoparticles for antimicrobial applications. Int. J. Antimicrob. Agents. 33: 587-590. https://doi.org/10.1016/j.ijantimicag.2008.12.004
29. Roy, A.; Bulut, O.; Some, S.; Mandal, A. K.; Yilmaz, M. D. 2019. Green synthesis of silver nanoparticles: Biomolecule-nanoparticle organizations targeting antimicrobial activity. RSC Adv. 9: 2673-2702. https://doi.org/10.1039/c8ra08982e
30. Sánchez Gómez, A.; Rosendo Ponce, A.; Vargas Romero, J. M.; Rosales Martínez, F.; Platas Rosado, D. E.; Becerril Pérez, C. M. 2018. Energía germinativa en guaje (*Leucaena leucocephala* cv. Cunningham) con diferentes métodos de escarificación de la semilla. Agrociencia. 52: 863-874.
31. Sangeetha, G.; Rajeshwari, S.; Venckatesh, R. 2011. Green synthesis of zinc oxide nanoparticles by *Aloe barbadensis* Miller leaf extract: Structure and optical properties. Mater. Res. Bull. 46: 2560-2566. https://doi.org/10.1016/j.materresbull.2011.07.046
32. Schneiter, A. A.; Miller, J. F. 1981. Description of Sunflower Growth Stages 1. Crop Sci. 21: 901-903. https://doi.org/10.2135/cropsci1981.0011183x002100060024x
33. Siddiqui, V. U.; Ansari, A.; Chauhan, R.; Siddiqi, W. A. 2019. Green synthesis of copper oxide (CuO) nanoparticles by *Punica granatum* peel extract. Mater. Today Proc. 36: 751-755. https://doi.org/10.1016/j.matpr.2020.05.504
34. Veisi, H.; Karmakar, B.; Tamoradi, T.; Hemmati, S.; Hekmati, M.; Hamelian, M. 2021. Biosynthesis of CuO nanoparticles using aqueous extract of herbal tea (*Stachys lavandulifolia*) flowers and evaluation of its catalytic activity. Sci. Rep. 11: 1-13. https://doi.org/10.1038/s41598-021-81320-6
35. Velsankar, K.; Aswin Kumara, R. M.; Preethi, R.; Muthulakshmi, V.; Sudhahar, S. 2020. Green synthesis of CuO nanoparticles via *Allium sativum* extract and its characterizations on antimicrobial, antioxidant, antilarvicidal activities. J. Environ. Chem. Eng. 8: 104123. https://doi.org/10.1016/j.jece.2020.104123
36. Vidovix, T. B.; Quesada, H. B.; Januário, E. F. D.; Bergamasco, R.; Vieira, A. M. S. 2019. Green synthesis of copper oxide nanoparticles using *Punica granatum* leaf extract applied to the removal of methylene blue. Mater. Lett. 257: 126685. https://doi.org/10.1016/j.matlet.2019.126685
37. Visentini, F. F.; Sponton, O. E.; Perez, A. A.; Santiago, L. G., 2017. Formation and colloidal stability of ovalbumin-retinol nanocomplexes. Food Hydrocoll. 67: 130-138. https://doi.org/10.1016/j.foodhyd.2016.12.027
38. Yugandhar, P.; Vasavi, T.; Jayavardhana Rao, Y.; Uma Maheswari Devi, P.; Narasimha, G.; Savithramma, N. 2018. Cost Effective, Green Synthesis of Copper Oxide Nanoparticles Using Fruit Extract of *Syzygium alternifolium* (Wt.) Walp., Characterization and Evaluation of Antiviral Activity. J. Clust. Sci. 29: 743-755. https://doi.org/10.1007/s10876-018-1395-1
39. Zhao, Y.; Li, Yuyi; Wang, J.; Pang, H.; Li, Yan. 2016. Buried straw layer plus plastic mulching reduces soil salinity and increases sunflower yield in saline soils. Soil Tillage Res. 155: 363-370. https://doi.org/10.1016/j.still.2015.08.019

Funding

This study was funded by Agencia Nacional de Promoción de la Investigación, el Desarrollo Tecnológico y la Innovación (Agencia I+D+i) PICT-2021-CAT-II-00097; Consejo Nacional de Investigaciones Científicas y Tecnológicas (CONICET) PIP 11220200100488CO; and the Universidad Nacional del Litoral (UNL) CAI + D 85520240100144LI.

Impact of Ozone-Based Postharvest Treatment on the Quality and Shelf Life of Radish (*Raphanus sativus* L.) Microgreens

Efectos del tratamiento poscosecha con ozono en la calidad y la vida útil de microgreens de rabanito (*Raphanus sativus* L.)

Florencia Pía Alloggia [1, 3], Roberto Felipe Bafumo [1], Daniela Andrea Ramírez [1, 2], Marcos Andrés Maza [1, 3], Alejandra Beatriz Camargo [1, 2*]

Originales: *Recepción:* 07/02/2025 - *Aceptación:* 20/10/2025

Abstract

Microgreens are young vegetable seedlings that have garnered significant attention due to their high concentrations of health-promoting phytochemicals. However, their highly perishable nature presents a significant challenge for postharvest storage. Among the various preservation technologies available, ozone treatment applied to microgreens-an innovative and environmentally sustainable method-has not been extensively studied. This study evaluated the effect of ozone-based sanitization on the shelf life and quality of radish microgreens. Conventional washing treatments using chlorinated water and tap water were compared to ozonated water. During refrigerated storage, key quality parameters were systematically monitored, including fresh weight loss, electrolyte leakage, color changes, and microbial counts. Ozonated water effectively reduced the initial aerobic mesophilic bacterial populations, with no statistically significant differences compared to conventional chlorine treatment. Furthermore, ozone treatment had minimal impact on color, and the weight loss remained below 1%. Although tissue wilting was observed, it was significantly less severe than that associated with chlorine treatment. These findings suggest that ozonated water is a promising alternative to conventional postharvest treatments for enhancing the shelf life and microbiological safety of ready-to-eat microgreens.

Keywords
micro-scale vegetables • *Raphanus sativus* • ozonated water • sanitization • storage

1 Universidad Nacional de Cuyo. Facultad de Ciencias Agrarias. Laboratorio de Cromatografía para Agroalimentos. Instituto de Biología Agrícola de Mendoza. CONICET Mendoza. Almirante Brown 500. Chacras de Coria. M5528AHB. Mendoza. Argentina.
* acamargo@fca.uncu.edu.ar
2 Universidad Nacional de Cuyo. Facultad de Ciencias Agrarias. Cátedra de Química Analítica.
3 Universidad Nacional de Cuyo. Facultad de Ciencias Agrarias. Cátedra de Enología I.

Resumen

Los microgreens son plántulas jóvenes de hortalizas reconocidas por sus altas concentraciones de fitoquímicos beneficiosos para la salud. Sin embargo, su naturaleza altamente perecedera representa un desafío significativo para su almacenamiento poscosecha. Entre las diversas tecnologías de conservación disponibles, el tratamiento con ozono aplicado a microgreens-un método innovador y ambientalmente sostenible- continúa escasamente investigado. Este estudio evaluó el efecto de la sanitización con ozono sobre la vida útil y la calidad de los microgreens de rabanito. Se compararon tratamientos convencionales de lavado con agua clorada y agua de red frente al uso de agua ozonizada. Durante el almacenamiento refrigerado, se monitorearon sistemáticamente parámetros de calidad como pérdida de peso fresco, pérdida de electrolitos, cambios de color y recuentos microbiológicos. El agua ozonizada redujo eficazmente las poblaciones iniciales de bacterias mesófilas aerobias, sin diferencias estadísticamente significativas respecto del tratamiento convencional con cloro. Además, el tratamiento con ozono tuvo un impacto mínimo sobre el color, y la pérdida de peso se mantuvo debajo del 1%. Aunque se observó marchitamiento tisular, su severidad fue significativamente menor que la asociada al tratamiento con cloro. Estos resultados sugieren que el agua ozonizada es una alternativa prometedora a los tratamientos poscosecha convencionales para mejorar la vida útil y la seguridad microbiológica de los microgreens listos para consumir.

Palabras clave
micro-hortalizas • *Raphanus sativus* • agua ozonizada • sanitización • almacenamiento

Introduction

Microgreens, the edible seedlings of various vegetable and herb species, exhibit a short growth cycle, typically lasting between 10 to 15 days. After this period, the stem, cotyledons, and the first pair of true leaves are consumed. Microgreens popularity has increased in recent years, driven by growing consumer interest in healthy eating (15). Numerous studies have underlined the high concentrations of bioactive compounds in microgreens, with several health benefits-such as anticancer and antioxidant properties-linked to their consumption (23). However, due to their young and tender nature, microgreens are highly perishable and have a limited postharvest shelf life.

Several factors influence postharvest preservation of vegetables, including temperature, humidity, gas composition during storage, packaging materials, and washing and sanitizing methods. Chlorine is commonly used as a sanitizer in the food industry. However, its use raises concerns regarding environmental contamination and the potential carcinogenic effects of its gaseous byproducts and degradation products (8, 25). In this context, various alternative physical and chemical technologies have been developed for postharvest applications (1). Among these, ozone is notable for its potent antimicrobial properties and its ability to decompose spontaneously into non-toxic byproducts (4, 30).

Numerous studies have reported the use of ozonated water for preserving minimally processed vegetables, including celery (30), asparagus (11), broccoli (7), spinach (18), as well as carrots and lettuce (21). For ready-to-eat products, microgreens undergo washing and sanitizing processes. Current research on washing and disinfection technologies for postharvest microgreens preservation has evaluated chlorine at various concentrations (13, 27) and its combination with citric (28) or ascorbic acid (6, 20). However, sanitizers based on novel, environmentally friendly technologies have not been widely explored for microgreens preservation. The use of ozonated water to extend the postharvest shelf life of microgreens is a promising approach that, to our knowledge, remains unexplored.

The objective of this study was to compare ozonated water with conventional treatments and assess their effects on quality of radish microgreens during postharvest storage. We measured quality parameters like weight loss (%), electrolyte leakage (%), color change, aerobic mesophilic bacterial counts, and mold and yeast counts.

Materials and Methods

Plant Material and Harvest

Radish (*Raphanus sativus* L.) microgreens were cultivated in a growth chamber under controlled temperature conditions (24 ± 2°C) with artificial LED lighting. The seeds were sown in trays filled with a commercial substrate composed of peat, coconut fiber, and perlite (Cocomix, Ing. Carluccio). Germination occurred in the dark, after which the trays were exposed to light and irrigated daily with tap water. The microgreens were harvested 12 days after sowing using disinfected scissors.

Washing Treatments, Storage, and Experimental Setup

Following harvest, the microgreens were divided into four groups and subjected to the following washing treatments: chlorinated water (100 mg L^{-1} NaClO) (19, 27), ozonated water (0.16 mg L^{-1} O_3) (30), tap water, and an unwashed control. Chlorinated water was prepared by dissolving commercial bleach (58 g L^{-1} Cl) in tap water. Ozonated water was generated by introducing gaseous ozone through a gas diffuser submerged in a container of tap water. Ozone was produced using an ozone generator (Pura® HMB2), and its concentration was monitored with a pH/ORP controller (Walfront Model PH-803W). Each group of microgreens was immersed in its respective sanitizing solution for 5 minutes. For the chlorinated water treatment, a subsequent 1-minute rinse with tap water was performed. After washing, the microgreens were centrifuged for 3 minutes using a manual centrifuge. Three replicates of 30 grams per treatment were stored in PET plastic containers with lids. All treatments were kept refrigerated in the dark at 8 ± 1°C for 12 days. Samples were collected on days 0, 6, and 12 of storage to evaluate postharvest quality parameters.

Quality Parameters

Weight Loss

The weight of each container was recorded using an analytical balance (Denver APX-200) at the beginning of storage (day 0) and during storage on days 2, 6, 8, and 12. Weight loss was expressed as a percentage (%) of the initial weight, calculated by determining the weight difference between the initial and final weights for each evaluation day (21).

Electrolyte Leakage

Electrolyte leakage, an indicator of tissue deterioration, was assessed following the procedure outlined by Xiao *et al.* (2014a), with modifications. Three-gram samples were periodically collected from each container and shaken with 90 mL of distilled water for 15 minutes. The electrical conductivity of the solution (µS cm^{-1}) was measured using a conductivity meter (Hanna HI 8733). Electrolyte leakage values were expressed as a percentage of the total electrolyte content, which was determined using the same procedure on a sample that had been previously frozen at -20°C for 24 hours and thawed at the time of measurement.

Color Determination

Color changes were measured using an 8 mm-aperture colorimeter (Konica Minolta Chroma Meter CR-400), which was calibrated to a standard white tile (Y 93.5, x 0.3114, y 0.3190). The CIELAB color space coordinates were recorded in quintuplicate for each sample on the transparent surface of the container. Measurements were taken at random locations on each sample to obtain color data from all parts of the microgreens, including both cotyledons and stems. The parameters a* (redness/greenness), b* (yellowness/blueness), and L* (lightness, ranging from 0 = black to 100 = white) were recorded (9). Hue Angle and Chromaticity were calculated from the a* and b* values using the following formulas:

$$\text{Hue Angle } (h°) = \tan^{-1}(b*/a*) + 180° \quad (5)$$

$$\text{Chromaticity } (C)* = \sqrt{(a^2 + b^2)} \quad (15)$$

The Hue Angle (h°) denotes the color tone and is expressed on a circular scale, where 0°/360° corresponds to red, 90° to yellow, 180° to green, and 270° to blue (29). Chromaticity reflects the overall color intensity or saturation, with brighter colors (*i.e.*, less white or black) exhibiting higher C* values.

Total Aerobic Mesophilic Bacterial Count (AMB)

To assess microbial quality, five-gram pooled samples per treatment were periodically taken in sterile stomacher bags (BPS-750, Microclar) and homogenized for 5 minutes with 50 mL of sterile peptone water (3, 12). Serial dilutions of these suspensions were plated in duplicate on Plate Count Agar. The plates were incubated for 24 hours at 30°C, after which the colony-forming units (CFUs) were counted. Results were expressed as log CFU g^{-1} (19).

Total Yeast and Mold Count (Y&M)

Using the same suspensions described for the total aerobic mesophilic bacterial count, serial dilutions were plated in duplicate on Potato Dextrose Agar. The plates were incubated for 48 hours at 22°C, and the CFU count was subsequently performed. Results were expressed as log CFU g^{-1} (19, 27).

Statistical Analysis

For each parameter evaluated, three replicates were analyzed per treatment on each sampling day during storage. Results were expressed as means ± standard deviation. Statistical analyses were performed using Infostat V.2020 software. Data were subjected to analysis of variance (ANOVA) with general and mixed linear models. Mean values for treatments, as well as their interactions, were compared using Duncan's Multiple Range Test (DGC) ($p \leq 0.05$).

Results

Weight Loss

The weight of radish microgreens was influenced by storage time in interaction with the washing treatments (table 1). Weight loss reached approximately 0.97% by the end of the experiment (day 12).

Table 1. ANOVA for weight loss, electrolyte leakage, lightness, chroma, hue angle, aerobic mesophilic bacterial counts, and yeast and mold counts of radish microgreens stored at 8°C for 12 days.

Tabla 1. ANOVA de la pérdida de peso, pérdida de electrolitos, luminosidad, croma, ángulo de tono, recuento de bacterias aerobias mesófilas y recuento de mohos y levaduras de micro-hortalizas de rabanito almacenadas a 8°C durante 12 días.

Source of Variance	WL (%)	EL (%)	L*	C*	h°	AMB	Y&M
Wash treatment (W)	NS	**	*	NS	NS	NS	**
Storage time (T)	**	**	**	**	**	**	**
T x W	*	**	NS	NS	*	*	NS

NS, *, and ** denote non-significant or significant effects at $p \leq 0.05$, and $p \leq 0.01$, respectively.

WL: weight loss, EL: electrolyte leakage, L*: lightness, C*: chroma, h°: hue angle, AMB: aerobic mesophilic bacteria, Y&M: yeast and mold.

NS, *, y ** indican efectos no significativos o significativos para $p \leq 0,05$, y $p \leq 0,01$, respectivamente.

WL: pérdida de peso, EL: pérdida de electrolitos, L*: luminosidad, C*: croma, h°: ángulo de tono, AMB: bacterias aerobias mesófilas, Y&M: mohos y levaduras.

Significant differences in weight loss were observed among the washing treatments only during the later stages of storage, starting from day 8 onwards (figure 1, page 203). On days 8 and 12, weight loss in the ozone-treated and unwashed control was significantly greater than in the chlorine and tap water treatments. The differences between the unwashed/ozone treatments and the chlorine/tap water treatments were 0.10% on day 8 and 0.17% on day 12.

Electrolyte Leakage

Figure 2 and table 1 (page 202), show the effect of washing treatments * storage time on electrolyte leakage in radish microgreens. All treatments exhibited a significant increase in electrolyte leakage over time, which was visualized as an increased tissue wilting. Moreover, electrolyte loss increased differentially depending on the treatment, which is confirmed by the significant treatment × storage time (T × W) interaction. Tap water resulted in higher leakage compared to chlorine, and chlorine showed more leakage than ozone.

Vertical bars represent ± standard error. Significant differences between wash treatments (within the same time point) according to DGC Test ($p \leq 0.05$) are indicated with different lowercase letters above the plots.

Las barras verticales representan ± error estándar. Las diferencias significativas entre los tratamientos de lavado (dentro del mismo día de muestreo) según la Prueba DGC ($p \leq 0,05$) se indican con letras minúsculas diferentes sobre los gráficos.

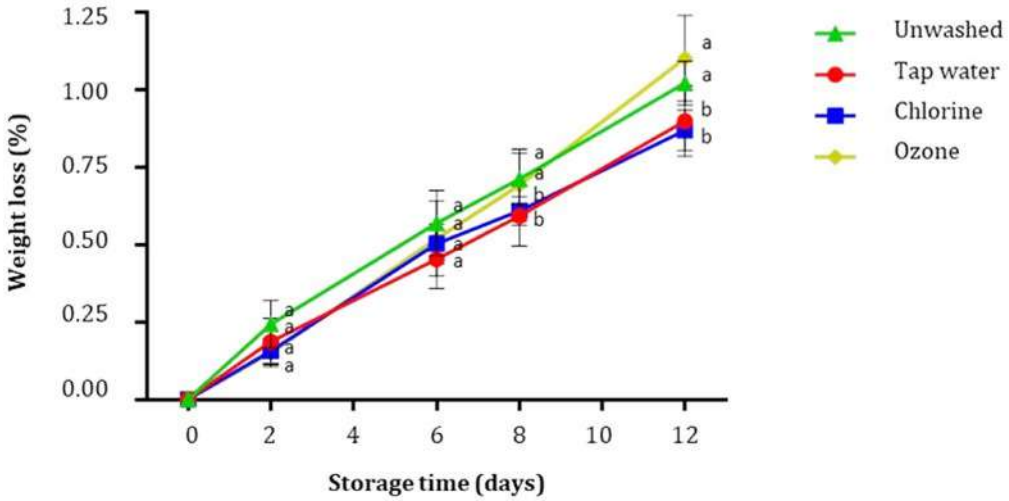

Figure 1. Effect of the washing treatments on weight loss (%) of radish microgreen during 8°C storage (n=3).

Figura 1. Efecto de los tratamientos de lavado sobre la pérdida de peso (%) en micro-hortalizas de rabanito durante el almacenamiento a 8°C (n=3).

Vertical bars represent ± standard error. Significant differences between wash treatments (within the same time point) according to DGC Test ($p \leq 0.05$) are indicated with different lowercase letters above the plots.

Las barras verticales representan ± error estándar. Las diferencias significativas entre los tratamientos de lavado (dentro del mismo día de muestreo) según la Prueba DGC ($p \leq 0,05$) se indican con letras minúsculas diferentes sobre los gráficos.

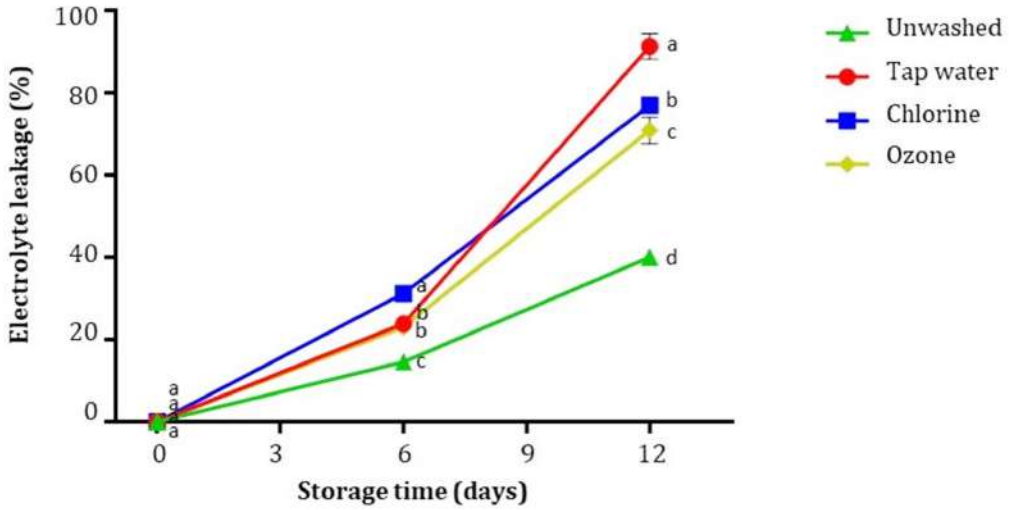

Figure 2. Effect of the washing treatments on electrolyte leakage (%) of radish microgreen during 8°C storage (n=3).

Figura 2. Efecto de los tratamientos de lavado sobre la pérdida de electrolitos (%) en micro-hortalizas de rabanito durante el almacenamiento a 8°C (n=3).

The unwashed control exhibited the lowest electrolyte loss compared to all washing treatments, this difference becoming more pronounced as storage time progressed.

Among the treatments involving wetting, by the end of the storage period, ozone treatment significantly reduced electrolyte leakage compared to chlorine and tap water. Tap water treatment, which involved wetting without disinfection, resulted in the greatest electrolyte loss compared to the other treatments.

Color

Washing effects on color were evaluated by considering the coordinates of lightness (L*), chroma (C*), and hue angle (h°) (table 1, page 202). No significant effects of the washing treatments were observed for C* or h°. Storage time had a significant effect on all three color parameters, with a significant treatment × time interaction for h° (figure 3).

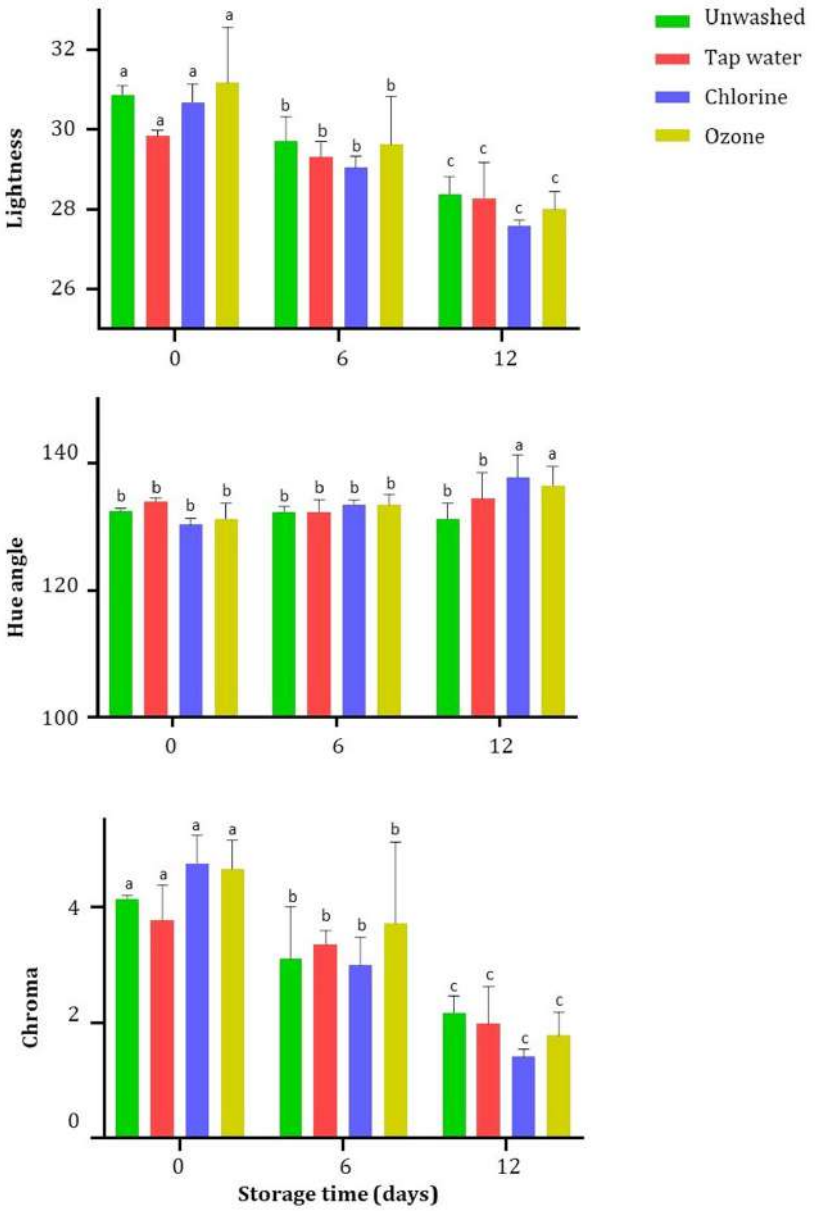

Vertical bars represent ± standard error. Significant differences between wash treatments (within the same time point) according to DGC Test ($p \leq 0.05$) are indicated with different lowercase letters above the plots.

Las barras verticales representan ± error estándar. Las diferencias significativas entre los tratamientos de lavado (dentro del mismo día de muestreo) según la Prueba DGC ($p \leq 0,05$) se indican con letras minúsculas diferentes sobre los gráficos.

Figure 3. Effect of the washing treatments on color coordinates of radish microgreen during 8°C storage (n=3).

Figura 3. Efecto de los tratamientos de lavado sobre las coordenadas de color en micro-hortalizas de rabanito durante el almacenamiento a 8°C (n=3).

Lightness values, regardless of the treatment, decreased approximately 8% by the end of storage, from around 30 to 28.

Hue angles exhibited minimal variation under the tested conditions. Significant increases in h° were only observed on day 12 in microgreens washed with chlorine and ozone. However, this variation was less than 3% and visually imperceptible (figure 4).

Figure 4. Image of radish microgreens subjected to different washing treatments during 12 days of storage at 8±1°C.

Figura 4. Imagen de micro-hortalizas de rabanito sometidas a diferentes tratamientos de lavados almacenadas a 8°C durante 12 días.

Chroma values decreased significantly in all samples as storage time progressed, from an average of 4.3 to 1.8. Chroma was the most affected color parameter by time, with a reduction of over 50%.

Total Aerobic Mesophilic Bacterial Count (AMB)

Aerobic mesophilic bacterial populations increased significantly over time for all sanitization treatments (table 1, page 202). However, a significant interaction between treatment and storage time was observed (figure 5).

The unwashed control showed an initial bacterial load of 8.49 log CFU g^{-1}. All washing treatments equally reduced aerobic mesophilic bacterial counts by approximately 0.6 log CFU g^{-1}. After 6 days of storage, all samples showed an increase in aerobic mesophilic bacteria counts, with the unwashed control exhibiting the slowest growth rate (0.64 log CFU g^{-1}). By day 12, bacterial counts increased significantly across all treatments. Treatments no longer differed significantly from the unwashed control, however, the unwashed and chlorine treatments showed higher growth rates.

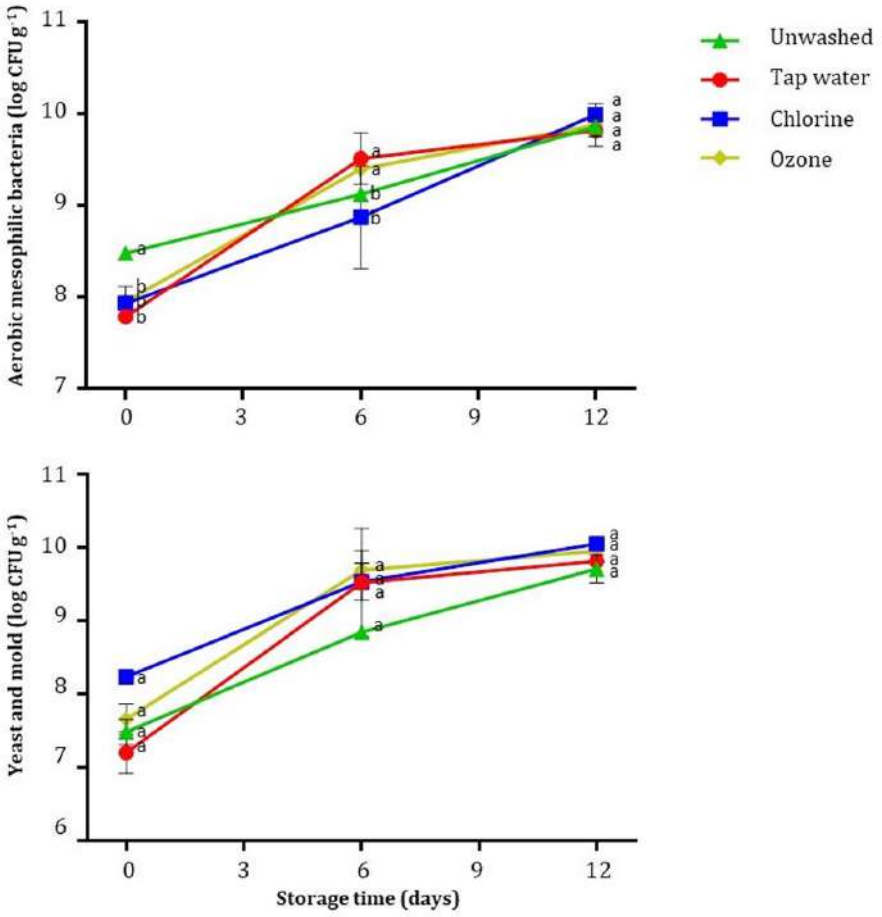

Vertical bars represent ± standard error. Significant differences between wash treatments (within the same time point) according to DGC Test ($p \leq 0.05$) are indicated with different lowercase letters above the plots.

Las barras verticales representan ± error estándar. Las diferencias significativas entre los tratamientos de lavado (dentro del mismo día de muestreo) según la Prueba DGC ($p \leq 0,05$) se indican con letras minúsculas diferentes sobre los gráficos.

Figure 5. Effect of the washing treatments on aerobic mesophilic bacteria and yeast & mold populations of radish microgreen during 8°C storage (n=3).

Figura 5. Efecto de los tratamientos de lavado sobre los recuentos de bacterias aerobias mesófilas y los mohos y levaduras en micro-hortalizas de rabanito durante el almacenamiento a 8°C (n=3).

Total Yeast and Mold Count (Y&M)

Yeast and mold counts were significantly affected by both storage time and washing treatment, although no significant interaction between treatment and time was observed (table 1, page 202).

Regardless of the washing treatment, yeast and mold counts increased significantly during storage. Initial counts were approximately 7.65 log CFU g^{-1}, rising to 9.89 log CFU g^{-1} by the end of storage (figure 5, page 206).

Regarding the effect of washing treatment, tap water and unwashed control samples exhibited lower counts (8.76 log CFU g^{-1}) than chlorine and ozonated water treatments (9.19 log CFU g^{-1}).

Discussion

This study evaluated the effects of different washing treatments on quality and shelf life of radish microgreens during refrigerated storage.

Regarding weight loss, washing treatments showed no significant differences in weight loss until later stages of storage, consistent with findings from other microgreens storage studies (28). After day 8, ozone and unwashed control treatments differed significantly from chlorine and tap water in weight loss. However, the recorded values were low and practically negligible for this parameter. Maximum mean weight loss observed at the end of storage on day 12 was 0.97%. Although these values are lower than those reported in other studies (10), similar results were found in daikon radish microgreens stored in the dark (26). Our experiment was conducted in a domestic refrigerator that remains dark when closed; thus, the results suggest that dark storage may contribute to reducing weight loss. By keeping the stomata closed, transpiration-induced weight loss may be reduced. Therefore, it can be concluded that the postharvest treatments evaluated in our study performed acceptably with respect to weight loss.

Electrolyte leakage is a key indicator of cell membrane damage and subsequent tissue deterioration, which can result from physiological stress or mechanical injury. It is closely associated with postharvest shelf life, as it reflects the extent of senescence in fresh-cut vegetables (10, 13, 15). In radish microgreens, washing treatments significantly increased electrolyte leakage over time. Furthermore, our results are consistent with several studies reporting a sharp increase in electrolyte loss after approximately 6 to 8 days of storage (10, 13, 17). The lower electrolyte leakage observed in the unwashed control compared to the washing treatments aligns with findings in the literature for microgreens (13). The high moisture content in the packages due to washing likely promoted microbial growth, which in turn contributed to tissue damage and increased electrolyte leakage. Among the washing treatments, ozonated water resulted in the lowest electrolyte leakage compared to chlorine and tap water, which agrees with similar studies in lettuce (25). Electrolyte leakage occurs when the integrity of the cell membrane is compromised, often due to oxidation of the phospholipids and unsaturated fatty acids that constitute the membrane. Both chlorine and ozone are oxidizing agents, with ozone being the stronger oxidizer of the two (24). Despite its higher oxidizing potential, ozone at 0.16 ppm caused less tissue damage than chlorine at 100 ppm. The lower ozone concentration may explain the reduced wilting compared to standard chlorine disinfection..

Sample visual appearance was analyzed by measuring surface color during storage, serving as an indicator of senescence progression. The washing treatments showed no effect on hue angle or chromaticity, aligning with previous studies indicating that disinfectants typically do not alter color (6, 7, 25). In this regard, it is crucial that treatments applied to extend the shelf life of vegetables do not negatively affect their visual quality.

The lightness (L*) values observed were consistent with those reported in other studies on radish microgreens (16). The decrease in L* over time, reflected by tissue darkening, was likely caused by browning (6).

Hue angle values were observed within the 90° to 180° quadrant, indicating yellow to green colors. The h° increases on day 12 in chlorine- and ozone-washed microgreens

indicate a shift toward a green-blue hue with reduced yellow. Yellowing due to chlorophyll degradation is a common phenomenon during storage (6, 26). The observed shift from green to blue in our study may be attributed to an incipient browning process. Browning is generally caused by the oxidation of phenolic compounds, leading to the formation of brown pigments such as melanin (10). Given that both chlorine and ozone are oxidizing agents (25), the color change observed may signal the onset of oxidation.

Chroma (C*), which reflects the saturation or intensity of color (16, 26), decreased significantly over time, suggesting a loss of color intensity during postharvest storage. Similar effects have been reported in microgreens of other species, where a general reduction in chromaticity during storage is associated with browning (10).

Regarding the populations of aerobic mesophilic bacteria, differences in the effect of washing treatments were observed depending on storage time. The initial population in the unwashed control was high, typical of leafy vegetables, and slightly above levels reported for other microgreen species (6, 13). Nonetheless, all washing treatments were effective in reducing the bacterial load. Notably, ozonated water at 0.16 ppm was as effective in reducing bacterial counts as chlorine. This result is consistent with studies demonstrating the efficacy of ozonated water on other vegetables, such as fresh-cut celery, cilantro, and broccoli (7, 24, 30). The bacterial rebound after 6 days in washed samples, matching or exceeding unwashed control, aligns with findings from other microgreen studies (27). Washing treatments may promote microbial growth due to residual moisture and tissue damage from postharvest handling (2, 13, 14, 23, 27). Therefore, if any washing treatment were to be applied for ready-to-eat microgreens, it would be advisable to consume them before 6 days of storage. This recommendation aligns with current safety standards for fresh-cut salads, which suggest a shelf life of 5 to 7 days (22).

The initial yeast and mold counts were comparable to those reported in other microgreen species (14, 27, 28). In contrast to the findings for aerobic mesophilic bacteria (AMB), none of the washing treatments reduced the initial Y&M populations compared to the unwashed control. Specifically, chlorine disinfection has been reported to exhibit intermediate sensitivity to yeasts and strong resistance to mold spores. Additionally, bacteria are generally more sensitive to ozone than yeasts and fungi (8). Lower counts in the unwashed control suggest that soaking microgreens, even with sanitizers, may be ineffective against fungal growth. These results are consistent with several studies indicating that washing treatments for microgreens can hinder effective decontamination. Such treatments can compromise product quality and potentially lead to microbial growth rebounds, that exceed those observed in unwashed samples (2, 13, 14, 23, 27).

Conclusions

This study evaluated the effect of aqueous ozone disinfection on the postharvest quality and shelf life of radish microgreens. The results demonstrate that ozonated water at 0.16 ppm was effective in preserving the microgreens during storage at 8°C. The initial load of aerobic mesophilic microorganisms was reduced without altering weight, color, or causing substantial wilting compared to other treatments. Based on these findings, ozone treatment is proposed as a viable alternative for the postharvest preservation of ready-to-eat radish microgreens. In this sense, it would be interesting to further evaluate the effects of different ozone concentrations to determine the optimal dose.

However, given that microgreens have low tolerance to washing processes, it is essential to develop dry disinfection technologies to extend their shelf life. In light of this, further research is needed to explore the potential of gaseous ozone as an alternative disinfection method for microgreens.

References

1. Ali, A.; Yeoh, W. K.; Forney, C. & Siddiqui, M. W. 2017. Advances in postharvest technologies to extend the storage life of minimally processed fruits and vegetables. Critical Reviews in Food Science and Nutrition. 58(15): 2632-2649. https://doi.org/10.1080/10408398.2017.13 39180

2. Ali, S.; Nawaz, A.; Naz, S.; Ejaz, S.; Hussain, S.; Anwar, R. 2022. Decontamination of Microgreens. In: Shah, M.A., Mir, S.A. (eds) Microbial Decontamination of Food. https://doi.org/10.1007/978-981-19-5114-5_6
3. Baenas, N.; Gómez-Jodar, I.; Moreno, D. A.; García-Viguera, C. & Periago, P. M. 2017. Broccoli and radish sprouts are safe and rich in bioactive phytochemicals. Postharvest Biology and Technology. 127: 60-67. http://dx.doi.org/10.1016/j.postharvbio.2017.01.010
4. Botondi, R.; Barone, M. & Grasso, C. 2021. A review into the effectiveness of ozone technology for improving the safety and preserving the quality of fresh-cut fruits and vegetables. Foods. 10(4): 748. https://doi.org/10.3390/foods10040748
5. Casajús, V.; Perini, M.; Ramos, R.; Lourenco, A. B.; Salinas, C.; Sánchez, E.; Fanello, D.; Civello, P.; Frezza, D. & Martínez, G. 2021. Harvesting at the end of the day extends postharvest life of kale (*Brassica oleracea* var. sabellica). Scientia Horticulturae. 276: 109757. https://doi.org/10.1016/j.scienta.2020.109757
6. Chandra, D.; Kim, J. G.; Kim, Y. P. 2012. Changes in microbial population and quality of microgreens treated with different sanitizers and packaging films. Horticulture, Environment, and Biotechnology. 53(1): 32-40. https://doi.org/10.1007/s13580-012-0075-6
7. Das, B. K.; Kim, J. G. 2010. Microbial quality and safety of fresh-cut broccoli with different sanitizers and contact times. Journal of Microbiology and Biotechnology. 20(2): 363-369. https://doi.org/10.4014/jmb.0907.07009
8. Deng, L. Z.; Mujumdar, A. S.; Pan, Z.; Vidyarthi, S. K.; Xu, J.; Zielinska, M. & Xiao, H. W. 2019. Emerging chemical and physical disinfection technologies of fruits and vegetables: a comprehensive review. Critical Reviews in Food Science and Nutrition. 60(15): 2481-2508. https://doi.org/10.1080/10408398.2019.1649633
9. Di Rienzo J. A.; Casanoves F.; Balzarini M. G.; Gonzalez, L.; Tablada, M.; Robledo, C. W. InfoStat versión 2020. Centro de Transferencia InfoStat. FCA. Universidad Nacional de Córdoba. Argentina. URL http://www.infostat.com.ar
10. Ghoora, M. D.; Srividya, N. 2020. Effect of packaging and coating technique on postharvest quality and shelf life of *Raphanus sativus* L. and *Hibiscus sabdariffa* L. microgreens. Foods. 9(5): 653. https://doi.org/10.3390/foods9050653
11. Huyskens-Keil, S.; Hassenberg, K.; Herppich, W. B. 2012. Impact of postharvest UV-C and ozone treatment on textural properties of white asparagus (*Asparagus officinalis* L.). Journal of Applied Botany and Food Quality. 84(2): 229.
12. Işık, H.; Topalcengiz, Z.; Güner, S. & Aksoy, A. 2020. Generic and Shiga toxin-producing *Escherichia coli* (O157:H7) contamination of lettuce and radish microgreens grown in peat moss and perlite. Food Control. 111: 107079. https://doi.org/10.1016/j.foodcont.2019.107079
13. Kou, L.; Luo, Y.; Yang, T.; Xiao, Z.; Turner, E. R.; Lester, G. E.; Wang, Q. 2013. Postharvest biology, quality and shelf-life of buckwheat microgreens. LWT-Food Science and Technology. 51(1): 73-78. https://doi.org/10.1016/j.lwt.2012.11.017
14. Kou, L.; Yang, T.; Liu, X.; Luo, Y. 2015. Effects of Pre-and Postharvest Calcium Treatments on Shelf Life and Postharvest Quality of Broccoli Microgreens. HortScience horts. 50(12): 1801-1808. https://doi.org/10.21273/HORTSCI.50.12.1801
15. Kyriacou, M. C.; Rouphael, Y.; Di Gioia, F.; Kyratzis, A.; Serio, F.; Renna, M.; De Pascale, S.; Santamaria, P. 2016. Micro-scale vegetable production and the rise of microgreens. Trends in Food Science & Technology. 57(Part A): 103-115. https://doi.org/10.1016/j.tifs.2016.09.005
16. Kyriacou, M.; El-Nakhel, C.; Graziani, G.; Pannico, A.; Soteriou, G. A.; Giordano, M.; Ritieni, A.; De Pascale, S.; Rouphael, Y. 2019. Functional quality in novel food sources: Genotypic variation in the nutritive and phytochemical composition of thirteen microgreens species. Food Chemistry. 227: 107-118. https://doi.org/10.1016/j.foodchem.2018.10.098.
17. Lu, Y.; Dong, W.; Yang, T.; Luo, Y.; Chen, P. 2021. Preharvest UVB application increases glucosinolate contents and enhances postharvest quality of broccoli microgreens. Molecules. 26(11): 3247. https://doi.org/10.3390/molecules26113247
18. Mersinli, E.; Koyuncu, M. A.; Erbaş, D. 2021. Quality retention of minimally processed spinach using low-dose ozonated water during storage. Turkish Journal of Agriculture and Forestry. 45(2): 133-143. https://doi.org/10.3906/tar-2004-75
19. Paradiso, V. M.; Castellino, M.; Renna, M.; Gattullo, C. E.; Calasso, M.; Terzano, R.; Allegretta, I.; Leoni, B.; Caponio, F.; Santamaria, P. 2018. Nutritional characterization and shelf-life of packaged microgreens. Food & function. 9(11): 5629-5640. https://doi.org/10.1039/ C8FO01182F
20. Patil, M.; Sharma, S.; Sridhar, K.; Anurag, R. K.; Grover, K.; Dharni, K.; Mahajan, S.; Sharma, M. 2024. Effect of postharvest treatments and storage temperature on the physiological, nutritional, and shelf-life of broccoli (*Brassica oleracea*) microgreens. Scientia Horticulturae. 327: 112805. https://doi.org/10.1016/j.scienta.2023.112805
21. Paulsen, E.; Barrios, S.; Baenas, N.; Moreno, D. A.; Heinzen, H.; Lema, P. 2018. Effect of temperature on glucosinolate content and shelf life of ready-to-eat broccoli florets packaged in passive modified atmosphere. Postharvest Biology and Technology. 138: 125-133. https://doi.org/10.1016/j.postharvbio.2018.01.006
22. Sarron, E.; Gadonna-Widehem, P.; Aussenac, T. 2021. Ozone treatments for preserving fresh vegetables quality: A critical review. Foods. 10(3): 605. https://doi.org/10.3390/foods10030605

23. Turner, E. R.; Luo, Y.; Buchanan, R. L. 2020. Microgreen nutrition, food safety, and shelf life: A review. Journal of food science. 85(4): 870-882. https://doi.org/10.1111/1750- 3841.15049
24. Wang, H.; Feng, H.; Luo, Y. 2004. Microbial reduction and storage quality of fresh-cut cilantro washed with acidic electrolyzed water and aqueous ozone. Food Research International. 37(10): 949-956. https://doi.org/10.1016/j.foodres.2004.06.004
25. Wang, J.; Wang, S.; Sun, Y.; Li, C.; Li, Y.; Zhang, Q. & Wu, Z. 2019. Reduction of *Escherichia coli* O157: H7 and naturally present microbes on fresh-cut lettuce using lactic acid and aqueous ozone. RSC advances. 9(39): 22636-22643. https://doi.org/10.1039/C9RA03544C
26. Xiao, Z.; Lester, G. E.; Luo, Y.; Xie, Z. K.; Yu, L. L. & Wang, Q. 2014a. Effect of light exposure on sensorial quality, concentrations of bioactive compounds and antioxidant capacity of radish microgreens during low temperature storage. Food chemistry. 151: 472-479. https://doi. org/10.1016/j.foodchem.2013.11.086
27. Xiao, Z.; Luo, Y.; Lester, G. E.; Kou, L.; Yang, T.; Wang, Q. 2014b. Postharvest quality and shelf life of radish microgreens as impacted by storage temperature, packaging film, and chlorine wash treatment. LWT - Food Science and Technology. 55(2): 551-558. http://doi.org/10.1016/j.lwt.2013.09.009
28. Yan, H.; Li, W.; Chen, H.; Liao, Q.; Xia, M.; Wu, D.; Liu, C.; Chen, J.; Zou, L.; Peng, L.; Zhao, G.; Zhao, J. 2022. Effects of storage temperature, packaging material and wash treatment on quality and shelf life of Tartary buckwheat microgreens. Foods. 11(22): 3630. https://doi.org/10.3390/foods11223630
29. Zappia, A.; De Bruno, A.; Torino, R.; Piscopo, A.; Poiana, M. 2018. Influence of light exposure during cold storage of minimally processed vegetables (Valeriana sp.). Journal of Food Quality. 2018(1): 4694793. https://doi.org/10.1155/2018/4694793
30. Zhang, L.; Lu, Z.; Yu, Z. & Gao, X. 2005. Preservation of fresh-cut celery by treatment of ozonated water. Food control. 16(3): 279-283. https://doi.org/10.1016/j.foodcont.2004.03.007

Acknowledgements

This research was supported by Proyecto SIIP 2022 06/A007T1 UNCuyo, Proyecto PIP 2021 736 CONICET, and Proyecto PICT 2019 03278 Préstamo BID.

REVIEW

Nursery Production of *Neltuma* Genus in Arid and Semiarid Regions of Argentine: a Review

Producción en vivero del género *Neltuma* en regiones áridas y semiáridas de Argentina: una revisión

Anabella Mirtha Massa Decon, Silvina Pérez *

Originales: *Recepción:* 26/05/2025 - *Aceptación:* 17/10/2025

INDEX

Universidad Nacional de Cuyo. Facultad de Ciencias Agrarias. Almirante Brown 500. M5528AHB. Chacras de Coria. Mendoza. Argentina. * sperez@fca.uncu.edu.ar

Abstract

Neltuma spp. (previously known as *Prosopis spp*.) are vital for ecological restoration and sustainable forestry in arid and semiarid environments. Although extensively studied, nursery techniques are still inconsistently applied, and poorly integrated. This review synthesizes recent scientific advances in seedling cultivation under controlled conditions, focusing on seed source selection, dormancy-breaking treatments, and substrate-container interactions. This review incorporates developments concerning seed source selection, plant physiology, and nursery trials to identify knowledge gaps and propose strategies for reforestation improvement. We offer actionable guidance for nursery operators, restoration professionals, and policymakers. Future research should focus on long-term field studies, genomic tools, standardization of nursery techniques, biological interactions that improve stress tolerance, and economic feasibility, especially for under-researched species.

Keywords
seed provenance • nursery propagation techniques • substrate-container interaction • algarrobo

Resumen

Neltuma spp. (anteriormente, *Prosopis spp*.) es una especie vital para la restauración ecológica y la silvicultura sostenible en ambientes áridos y semiáridos. A pesar de décadas de investigación, las técnicas de producción en vivero para estas especies siguen siendo inconsistentes y mal integradas. El objetivo de esta revisión es sintetizar los avances científicos recientes en el cultivo de plántulas en condiciones controladas, centrándose en la selección de la fuente de semillas, los tratamientos pre-germinativos y las interacciones sustrato-contenedor. Para ello, este trabajo incorpora avances en selección del origen de semillas, fisiología vegetal y ensayos de viveros para identificar lagunas de conocimiento, y proponer un marco estratégico para mejorar la reforestación. Para ello, se ofrece orientación práctica para los operadores de viveros, los profesionales de la restauración, y los responsables de la formulación de políticas públicas. Futuras investigaciones deberían focalizarse en estudios de campo a largo plazo, herramientas genómicas, estandarización de técnicas de vivero, e interacciones biológicas que mejoren la tolerancia al estrés y la viabilidad económica, especialmente para especies subestudiadas.

Palabras clave
procedencia de semillas • técnicas de propagación en viveros • interacción sustrato-contenedor • algarrobo

Introduction

Neltuma, previously known as Prosopis spp. (Hughes *et al.*, 2022), is a dominant genus in Argentina's arid and semi-arid ecosystems (Scaglia *et al.*, 2024). Neltuma spp. play a critical role in ecological functioning and service provision (Joseau *et al.*, 2023; Oliva *et al.*, 2010; Vilela & Ravetta, 2005; Villagra *et al.*, 2005). Their particular resilience to extreme environmental conditions makes them key species for restoration initiatives (Passera, 2000; Salto *et al.*, 2019). In addition, their presence in arid woodlands significantly influences understory plant communities and supports biodiversity and pastoral systems (Cesca *et al.*, 2012; Venier *et al.*, 2023), while providing important food and pharmacological resources (Mazzuca *et al.*, 2003; Pastorino & Marchelli, 2021; Vilela & Ravetta, 2005).

Landscape natural regeneration with *Neltuma spp.* is often limited by seed predation and habitat degradation (Braun Wilke *et al.,* 2000; Lerner & Peinetti, 1996; Marone *et al.*, 2000; Milesi & Lopez de Casenave, 2004; Villagra *et al.*, 2002), making active restoration efforts essential. State incentives have promoted native species cultivation, while shortage of robust seedlings hinders reforestation efforts (Salto *et al.*, 2013).

Researchers have extensively explored the ecological, physiological, and genetic characteristics of *Neltuma spp.*. Studies have typically focused on isolated components like genetic variability (Bessega *et al.*, 2019; Darquier *et al.*, 2013), germination protocols (Bravo *et al.*, 2011; Vilela & Ravetta, 2001), or substrate and container effects (Salto *et al.*, 2013, 2016; Senilliani *et al.*, 2021). However, these approaches do not offer integrated frameworks for nursery practices, leading to high failure rates in the field (Guzmán *et al.*, 2011).

Ecological data like germination and seedling establishment rates are essential for cost-effective and evidence-based restoration planning (Perez *et al.*, 2022). Addressing these challenges requires improved propagation protocols, nursery management, and scalable, successful restoration strategies (Pastorino & Marchelli, 2021).

This review integrates recent advances in genomics, plant physiology, and nursery trials, approaches not synthesized in previous literature. This review focuses on population genetic variation, dormancy-breaking treatments, and substrate-container interactions. We also provide practical recommendations for nurseries, restoration planners, and decision-makers. Producing high-quality seedlings for sustainable forestry and ecological restoration gains particular importance when considering climate change and land degradation.

Bibliographic Search Methodology

This review covers focused literature using Google Scholar as primary engine, complemented by Scopus and SciELO for regional coverage. Although this is not a systematic review, a structured and reproducible search strategy was applied. English and Spanish keywords included "*Prosopis*", "*Neltuma*", "seedling production", "forest nursery", "seed germination", "pre-germinative treatments", "containers", "substrate", and "soil". The inclusion criteria considered peer-reviewed research conducted in arid and semi-arid regions of Argentina between 1993 and 2025 addressing nursery production, seed germination, genetic variation, substrate composition, and container design. We excluded grey literature like non-peer-reviewed reports, theses or non-relevant studies. The selection process included (I) an initial screening based on titles, (II) an abstract review for relevance, (III) a full-text reading for studies meeting inclusion criteria, (IV) data extraction and synthesis related to species, treatments, morphological traits, and genetic data. A total of 79 peer-reviewed studies were selected and analyzed. We integrate ecological, physiological, and operational insights to guide nursery practices and restoration strategies for *Neltuma spp.*.

Seed Source Selection and Genetic Variation

Selecting the right seed source is crucial for successful reforestation with *Neltuma spp.* Genetic variation among populations is largely shaped by geographic and environmental gradients influencing the development of adaptive traits (Pastorino & Marchelli, 2021). As a result, seed origin directly affects morphological and physiological adaptations like seedling vigor, stress tolerance, and adaptability to local conditions (Mantován, 2002; Vega *et al.*, 2020). Intraspecific variation in traits like height, basal diameter, and salinity or drought tolerance has been widely documented, particularly in *N. alba* and *N. flexuosa* (Cony, 1996; Felker *et al.,* 2008, Fontana *et al.*, 2018; Kong *et al.*, 2023; Salazar *et al.*, 2019).

Provenance trials across Argentina consistently demonstrate that geographic origin significantly influences seedling performance in *Neltuma spp.* Notably, populations from Catamarca (*N. flexuosa*; Bessega *et al.*, 2019; Cony, 1996; Mantovan, 2002; Massa *et al.*, 2023), Formosa, Salta and Chaco (*N. alba*; López *et al.*, 2001; Venier *et al.*, 2021), have shown superior growth and stress tolerance under both nursery and field conditions. These findings are further supported by provenance trial data on superior performance of specific *Neltuma* populations across multiple species and traits relevant to restoration success (table 1, page 214).

Table 1. Seed sources for restoration: evidence from *Neltuma spp.* trials.
Tabla 1. Orígenes de semillas para la restauración: evidencia de los ensayos de *Neltuma spp.*

Specie	Origin	Observed Performance	Reference
N. alba	Ibarreta (Formosa), Castelli (Chaco), Gato Colorado (Santa Fe), Zona de Riego Río Dulce, Sumampa, Quimilí, Añatuya, and Pinto (Santiago del Estero) (Argentina)	Families from Ibarreta (Formosa) and Castelli (Chaco) showed superior diameter and height.	López *et al.*, 2001
N. alba	Santiago del Estero, Northern Salta, Western Formosa, Chaco (Argentina)	Salta excels in growth traits, while Chaco exhibits saline tolerance.	Venier *et al.*, 2021
N. chilensis	San Juan, La Rioja (Chamical, Lamadrid, Chilecito), Catamarca (Argentina)	No significant difference in germination capacity	Cony & Trione, 1998
N. chilensis	Fiambalá, Guandacol, Talampaya, Andalgalá, Astica, Belén, Villa Unión, Los Talas, Conlara, Tinogasta, Chilecito, Las Tucumanesas, Chancani, Soto, Catamarca, Patquia, Villa Dolores (Argentina) and Pama, Río Pama, Pama Alto-Bajo, ca. Mt. Patria, Mt. Patria, Agua Chica (Chile)	The spring budding pattern is associated with geographic and climatic gradients. No significant difference in shoot length, due to high intra-population variability.	Carranza *et al.*, 2000
N. chilensis	Fiambalá, Chilecito, Mogna, Villa Unión (Argentina)	Significant genetic differentiation. Most differentiated: Villa Union.	Chequer Chara *et al.*, 2021
N. ferox	Cerro Negro, Encrucijada, Yavi in the Puna region (Jujuy, Argentina)	Differences in seed protein electrophoretic patterns	Burghardt *et al.*, 2004
N. flexuosa	Bolsón de Fiambalá, B. de Pipanaco, Llanos de Catamarca, B. de Villa Unión, Chamical-Los Llanos, B. de Chilecito, L. de Angaco-Lavalle, Alvear, Nacuñán, Algarrobo del Águila-Limay Mahuida, B. de Rodeo, Río Colorado-General Conesa (Argentina)	B. de Fiambalá excels in height and basal diameter.	Cony, 1996
N. flexuosa	La Pampa, San Juan, La Rioja (Chamical, Lamadrid, Chilecito), Catamarca (Argentina)	Lamadrid displayed the highest germination capacity.	Cony & Trione, 1998
N. flexuosa	Mendoza, Catamarca, San Juan (Argentina)	Catamarca and San Juan differ in spine, total leaf, petiole, primary pinna, leaflet, fruit, and apex length.	Brizueela *et al.*, 2000
N. alba	Río Dulce Irrigation zone (Santiago del Estero), Pinto (Santiago del Estero), Castelli (Chaco), Ibarreta (Formosa) (Argentina)	Castelli and Ibarreta showed higher pod yield. Río Dulce Irrigation zone exhibited greater diameter, height and canopy diameter. Castelli was the most erect and showed resistance to *Psyllid* insects and fungal diseases.	Ewens & Felker, 2010
N. flexuosa	Bolsón de Fiambala, B. de Pipanaco, Chamical-llanos, B. de Mogna, Telteca, Ñacuñan, Río Colorado, General Conesa (Argentina)	B. de Fiambalá and Pipanaco were taller.	Maltovan, 2002
N. flexuosa	Fiambalá, Pipanaco, Mogna, Chilecito, Águila Limay (Argentina)	Fiambalá showed superior growth performance.	Bessega *et al.*, 2019
N. flexuosa	Fiambalá, Monte Comán (Argentina)	Fiambalá excelled in height.	Massa *et al.*, 2023

Recent studies highlight substantial adaptive variation across *Neltuma spp.* Genome-wide analyses in *N. alba* have revealed the molecular basis of key adaptive traits for selecting resilient genotypes (Kong *et al.*, 2023). *N. alba* shows high genetic diversity within populations and moderate differentiation among them, with local adaptation across morphotypes (Bessega *et al.*, 2015; Pastorino & Marchelli, 2021). The species also exhibits strong drought and salinity (Kong *et al.*, 2023; Velarde *et al.*, 2003; Venier *et al.*, 2021). Heritability for traits such as height and pod production suggests good potential for genetic improvement (Carreras *et al.*, 2017; Felker *et al.*, 2001). Hybridization with *N. nigra* and *N. ruscifolia* in contact zones contributes to increased variability and adaptive potential (Vega *et al.*, 2020).

N. flexuosa displays strong clinal variation in morphology and phenology along a north-south gradient, with northern populations being taller and single-stemmed, and southern ones shorter and multi-stemmed (Cony, 1996; Mantován, 2002; Massa *et al.,* 2023; Villagra *et al.*, 2005). Further, *N. flexuosa* shows high intraspecific variation in salt tolerance during germination (Cony & Trione, 1998), and traits like leaflet size exhibit high heritability (Darquier *et al.*, 2013). Genetic differentiation and local adaptation have been confirmed through SSR markers and QST-FST analyses (Bessega *et al.*, 2019; Darquier *et al.*, 2013). Hybridization with *N. chilensis* in sympatric zones further increases natural variability (Bessega *et al.*, 2022; Vega *et al.*, 2020).

N. ferox shows early signs of genetic divergence among populations, with polymorphism in polypeptide fractions and the presence of ecotypes likely driven by environmental pressure and geographic isolation (Burghardt *et al.*, 2004).

In contrast, *N. chilensis* exhibits low genetic variation in foliar traits among provenances (Bessega *et al.*, 2022) and weak adaptive responses to macro-environmental factors. For instance, plants originating in greater longitudes were related to greater frost sensitivity and lower initial growth rates, while higher altitude and precipitation inversely correlated with frost sensitivity (Verzino *et al.*, 2003). The data suggest a general pattern where high intrapopulation variation allows acclimatation, without major genetic alterations. (Verzino *et al.*, 2003). Microsatellite analyses show low but significant genetic differentiation (Chequer Charan *et al.*, 2021), while chemical variability among populations suggests potential for differentiation in secondary metabolites (Lamarque & Guzmán, 1997). Additional studies have linked bud break phenology and germination performance to geographic and environmental stress factors (Carranza *et al.*, 2000; Cony & Trione, 1998), supporting the potential for genetic improvement through selection and breeding (Lamarque & Guzmán, 1997).

A recent study successfully designed and validated 12 provisional Seed Transfer Zones (STZs) for *N. alba* in Argentina, aimed at supporting reforestation and afforestation efforts while minimizing maladaptation risks (Orquera *et al.,* 2025). Researchers developed an Ecogeographic Land Characterization (ELC) map based on bioclimatic, edaphic, and geophysical variables (Orquera *et al.,* 2025). The STZs were validated by showing strong concordance with morphological groups derived from adaptive traits, indicating that environmental factors significantly influence species' adaptive characteristics (Orquera *et al.,* 2025). This approach provides a robust and easy-to-apply tool for germplasm collection and transfer, addressing the endangered genetic diversity of *N. alba* due to deforestation (Orquera *et al.,* 2025). Additionally, the study identified gaps in existing germplasm collections, guidance for future conservation efforts (Orquera *et al.,* 2025).

Integrating morphological and physiological knowledge about variation among provenances (Brizuela *et al.*, 2000; Mantovan, 2002) allows selection and breeding programs (Carreras *et al.*, 2017; Vega *et al.*, 2020). However, many studies are short-term and focus solely on nursery traits, without tracking long-term field performance. Methodological inconsistencies in trial conditions or the use of outdated genetic markers limit cross-study comparability, in addition to the taxonomic and geographic bias, with research concentrated on a few species and regions. Operational feasibility is also underexplored; few studies address logistical or economic challenges of sourcing seeds from high-performing provenances. These gaps challenge current recommendations and complicate the development of scalable restoration strategies.

Early selection and breeding programs should prioritize traits linked to survival under arid conditions, while also considering pod quality and yield (Felker *et al.*, 2001; Lopez Maldonado *et al.*, 2001). Thus, to ensure field survival, seed source selection must consider ecological and operational criteria like (I) expanding genomic resources to underrepresented species such as *N. ferox* and *N. ruscifolia*; (II) standardizing protocols for seed collection, storage, and evaluation; (III) integrating socioeconomic considerations, including seed availability and cost-effectiveness; (IV) linking nursery performance to field success through long-term monitoring.

Seed Pre-treatment Methods for Enhanced Germination

Neltuma spp. are primarily propagated through seeds, often exhibiting physical dormancy. In natural ecosystems, frugivorous animals consume and disperse *Neltuma spp.* seeds. However, they do not inherently promote scarification (Passera, 2000; Peinetti *et al.*, 1993) and even decrease seed germination percentage (Pratolongo *et al.,* 2003). In fact, they may even reduce seed viability, particularly for seeds that remain encapsulated within the pod or are only partially digested (Peinetti *et al.*, 1993; Ortega Baes *et al.*, 2002). As a result, natural dispersal does not reliably enhance germination, and in nursery settings, dormancy must be actively broken through mechanical or chemical scarification to ensure uniform germination (Renzi *et al.*, 2024; Vilela & Rovetta, 2001).

Dormancy levels vary significantly according to species, seed origin, harvest year, and within seed lots, highlighting the need for species- and context-specific studies (Renzi *et al.*, 2024). For instance, in *N. ferox,* germination varies with scarification method, each affecting seed coat permeability and seedling emergence differently (Ortega Baes *et al.*, 2002).

At nursery scale, scarification treatments may be chemical or physical. Chemical methods, like immersion in concentrated sulfuric acid, erode the hard seed coat and facilitate water uptake. These methods are particularly effective for species with strong dormancy, such as *N. ruscifolia* and *N. alpataco* (Abdala *et al.*, 2020; Boeri *et al.*, 2019). Meanwhile, physical methods, including nicking with a blade, abrasion with sandpaper, or soaking in hot water, are effective for species like *N. chilensis* (Killian, 2012), *N. flexuosa, N. sericantha* (Funes *et al.,* 2009), *N. alba,* and *N. kuntzei* (Bravo *et al.*, 2011; Vilela & Ravetta, 2001), being safer and more practical for nursery-scale operations (Mathers *et al.*, 2007).

Table 2 summarizes species-specific responses to various scarification techniques. These data underscore treatment effectiveness across species and seed lots, reinforcing the need for tailored protocols. For example, germination of *N. alba* significantly increased after seed immersion in 100°C water for 24 hours (Salto *et al.*, 2016). Besides, mechanical scarification followed by soaking significantly increased germination rates in *N. flexuosa* (Brizuela *et al.*, 2000), *N. ruscifolia* shows optimal germination after 3 minutes in concentrated sulfuric acid (Abdala *et al.*, 2020), and *N. alpataco* achieves high germination rates with a 30-minute acid treatment and complete cutting of the seed coat edge (Boeri *et al.*, 2019). By selecting the appropriate pre-treatment method, nursery managers can significantly improve germination efficiency, uniformity, and overall seedling quality.

Table 2. Effective scarification techniques for *Neltuma spp*. seedling production.
Tabla 2. Técnicas efectivas de escarificación para *Neltuma spp*. en la producción de plántulas.

Specie	Chemical treatment	Physical treatment	Reference
N. alba, N. chilensis, N. flexuosa	Sulfuric acid 1N for 15 min, followed by washing and soaking in water	**Nicking seeds with a razor blade. Thermal treatment (with boiling water)**	Vilela & Ravetta, 2001
N. alpataco	**Sulfuric acid at** different durations (2, 5, 10, 20, 30, 40, 50, and 60 min)	Mechanical scarification by partial and **total cutting of the seminal cover edge**	Boeri *et al.*, 2019
N. kuntzei	Not Applicable	Nicking of the seed coat, **mechanical scarification, soaking in room temperature water, and soaking in boiling water**	Bravo *et al.*, 2011
N. ruscifolia	**Concentrated sulfuric acid for 3 min**	Cutting the seed coat, mechanical scarification, immersion in water at room temperature, and immersion in hot water	Abdala *et al.*, 2020

Bold font indicates treatments significantly increasing germination.

Los tratamientos en negrita han aumentado significativamente la germinación.

This review identifies several methodological limitations and inconsistencies in *Neltuma spp.* seedlings propagation techniques. For instance, germination trials often vary in experimental conditions like temperature, light exposure, water quality, and seed storage duration, hindering cross-study comparisons. While chemical scarification (especially with sulfuric acid) is frequently cited as effective, few studies address its operational risks, environmental impact, or feasibility in low-tech nursery settings. Physical methods, though safer, often show variable effectiveness depending on species and seed lots.

Moreover, the response of *Neltuma spp.* to microbial or enzymatic pre-germinative treatments has been poorly explored. These eco-friendly approaches could offer sustainable solutions for large-scale propagation (Zare *et al.*, 2011). Literature focuses on a few well-studied species, with insufficient data on taxa like *N. ruscifolia* and *N. alpataco,* which may have distinct dormancy mechanisms. Recent studies on endophytes in legumes suggest that microbial interactions can enhance germination and seedling vigor by enzymatically softening seed coats or hormonal signaling (Greeshma *et al.*, 2025). These approaches could offer sustainable, low-risk alternatives to chemical scarification, particularly in low-tech nursery settings.

In conclusion, seed pre-treatment is a critical step in overcoming dormancy and ensuring uniform germination in *Neltuma spp*. However, current practices remain poorly integrated and highly species-specific. Future research should (I) develop standardized and scalable protocols for species-specific seed sources, (II) conduct comparative trials assessing both germination success and downstream seedling performance, (III) explore and evaluate eco-friendly alternatives for cost-effectiveness and operational feasibility. A more holistic and evidence-based approach to seed pre-treatment will enhance efficiency, safety, and sustainability of *Neltuma* seedling production for ecological restoration in arid and semi-arid ecosystems.

Integrated Effects of Container and Substrate on Seedling Development in *Neltuma spp.*

The interaction between container and substrate often exceeds the sum of their contributions, significantly influencing seedling growth and development in *Neltuma spp.* (Salto *et al.*, 2013, 2016). A high-quality substrate may underperform in a poorly designed container, and vice versa (Salto *et al.*, 2016). Therefore, nursery design must consider both physico-chemical and biological requirements.

Container design should particularly consider volume, shape, and material (table 1, supplementary material). These characteristics affect root architecture, water dynamics, and operational efficiency (Mathers *et al.*, 2007; Senilliani *et al.*, 2021). Choosing between bare root and container stock types also affects seedling performance, with containerized systems often offering advantages in survival and establishment under challenging site conditions (Grossnickle & El-Kassaby, 2016). Moreover, morphological and physiological traits of *N. alba* seedlings are highly responsive to nursery management, reinforcing the importance of optimizing environmental and operational variables to enhance plant quality (Senilliani *et al.*, 2021).

Substrate selection is critical for root development and seedling vigour (table 2 in the supplementary material for comparative data). Physical and chemical properties like porosity, water retention, aeration and electrical conductivity directly influence root development and nutrient uptake (Vence *et al.*, 2013; Vilela & Ravetta, 2001). Soil texture plays a critical role in seedling growth rate of *N. flexuosa*, *N. argentina* and *N. alpataco* when comparing clay *versus* sandy soils (Villagra & Cavagnaro, 2000; Piraino & Roig, 2024). Flooding-prone soils, like those with shallow clayey horizon and high sodium content, can significantly decrease germination in *N. nigra* (Pratolongo *et al.*, 2003). Similarly, high electrical conductivity inhibits germination in *N. argentina* and *N. pallida* (Velardem *et al.*, 2003; Villagra, 1997), and reduce germination rates in *N. alpataco*, a species adapted to salinity (Villagra, 1997). Commonly used substrates include composted pine bark, perlite, peat, and vermiculite, as well as locally available organic materials like vermicompost, with strong potential to enhance seedling quality while reducing costs (Massa *et al.*, 2023; Mathers *et al.*, 2007).

Table 3 illustrates how container–substrate combinations shape the morphological quality of *Neltuma* seedlings (detailed container and substrate specifications are provided in Tables 1 and 2, supplementary material). Across trials, larger containers (*e.g.*, 250-270 cm^3) consistently supported greater height, root collar diameter, and biomass accumulation, particularly when paired with well-aerated substrates such as composted pine bark mixed with perlite or vermiculite (Salto *et al.*, 2016; Senilliani *et al.*, 2021). Soil-based substrates also performed well, especially in multi-cell trays, enhancing root collar diameter and overall seedling robustness (Salto *et al.*, 2013). These results show that container size and structure must align with substrate properties like porosity and water retention, to support optimal plant development (Salto *et al.*, 2016). Taller containers require substrates with higher water retention, while shorter ones benefit from more aerated mixes (Mathers *et al.*, 2007). *N. alba* seedlings grown in 250 cm^3 ribbed containers filled with a 1:1 mix of composted pine bark and perlite achieved superior height, root collar diameter, and biomass allocation (Senilliani *et al.*, 2021). Similarly, *N. nigra* performed best in seedling tubes and multi-cell trays filled with soil or a 2:1:1 mix of pine bark, perlite, and vermiculite. Soil consistently yielded the highest morphological quality (Salto *et al.*, 2013).

Table 3. Comparative effects of container-substrate combinations on morphological traits in *Neltuma spp.*

Tabla 3. Efectos comparativos de las combinaciones de contenedor-sustrato sobre los rasgos morfológicos en *Neltuma spp.*

Specie	Substrate Composition	Physical/ Chemical Characteristics	Type of Container	Volume (cm^3)	Height (mm)	Diameter (mm)	Observed Performance	Reference
N. alba	Composted pine bark and perlite (3:1)	TP (>85%), AP (55-70%), WR (20-30%)	TC	250	137	64	Seedlings grown in larger containers with a 1:1 mix were taller and had largest root collar diameter, and aerial/root biomass values.	Senilliani *et al.*, 2021
	Composted pine bark and perlite (1:1)	TP (32-51%), AP (20-21%), WR (11-30%)	TC	125	150	40		
N. alba and *N. nigra*	Soil	TP (46-52%), AP (43-48%), WR (3-4%)	IST	100	140	35	Soil consistently produced the largest root collar diameter and seedling height in both trays and seedling tubes, outperforming all other substrate combinations.	Salto *et al.*, 2013
			MCT	90	90	40		
	Composted pine bark	TP (51-69%), AP (32-45%), WR (19-25%)	IST	100	140	35		
			MCT	90	90	40		
	Composted pine bark and soil (1:1)	TP (41-66%), AP (36-61%), WR (5-8%)	IST	100	140	35		
			MCT	90	90	40		
	Composted pine bark, perlite and vermiculite (2:1:1)	TP (60-65%), AP (27-35%), WR (27-33%)	IST	100	140	35		
			MCT	90	90	40		
	Perlite and vermiculite (1:1)	TP (63-67%), AP (40-45%), WR (18-27%)	IST	100	140	35		
			MCT	90	90	40		

TC (Truncated cone with internal ribs), MCT (Multi-cell trays), IST (Individual seedling tubes), TP (Total Porosity), AP (Aeration Porosity), WR (Water retention).

TC (Cono truncado con nervaduras internas), MCT (Bandejas multiceldas), IST (Tubos de plántulas individuales), TP (Porosidad total), AP (Porosidad de aireación), WR (Retención de agua).

Table 3 (page 218), shows the best results for high-porosity substrates (*e.g.*, pine bark + perlite + vermiculite) paired with 100-140 cm^3 containers (Salto *et al.*, 2016; Senilliani *et al.*, 2021). Soil-based substrates consistently produced the largest root collar diameters, particularly in seedling tubes (Salto *et al.*, 2013). These interactions confirm that neither container nor substrate alone determines seedling quality; rather, their combination must be optimized based on species-specific responses. This reinforces the need for integrated nursery planning, considering physical infrastructure and biological requirements.

Beyond physical factors, the role of beneficial microbial interactions remains underexplored in *Neltuma spp.* nursery systems. Mycorrhizal associations can improve soil properties, like total biological activity, electrical conductivity, pH, and organic matter content (Sagadin *et al.*, 2023; Salto *et al.*, 2019, 2024). Multi-omic approaches can help select microbial inoculants with particular functional traits like growth promotion, abiotic stress tolerance, or improved nutrient uptake (Greeshma *et al.*, 2025). Considering *Neltuma spp.*, this technology could improve inoculation efficiency and overall seedling quality.

Despite these advances, several knowledge gaps remain. Few studies have tracked long-term field performance, and economic analyses of substrate and container choices are scarce (Oumahmoud *et al.*, 2023). Moreover, the role of microbial inoculants like mycorrhizal fungi is underexplored. Future research should prioritize (I) long-term, field-based evaluations to link nursery performance with restoration success, (II) cost-benefit analyses to assess scalability and economic feasibility of nursery practices, (III) integration of microbial inoculants to enhance seedling vigor and stress tolerance, and (IV) assessment of synergistic effects among bio-inoculants, substrates and container types.

Conclusion

Despite decades of research on *Neltuma* species, implementing effective nursery production techniques remains a challenge. Although breeding programs have identified superior traits and seed sources, their application in nursery practices remains limited due to poor standardised seed collection protocols, storage, pre-germinative treatments, and seedling management.

This review proposes several actionable insights ready to apply. For instance, nursery operators can (I) select seed sources based on provenances with superior performance under nursery and field conditions, (II) apply species-specific pre-germinative treatments validated for *N. alba*, *N. flexuosa*, and *N. ruscifolia,* and (III) optimize container-substrate combinations. Furthermore, restoration planners and policymakers are encouraged to (I) establish regional seed banks with documented provenance data, (II) promote training programs to disseminate evidence-based nursery practices, and (III) utilize ecogeographic tools such as Seed Transfer Zones (STZs) to guide germplasm collection and minimize maladaptation risks.

Enhanced propagation and restoration potential of *Neltuma spp.,* should prioritize (I) long-term field trials linking nursery performance with restoration success, (II) integration of genomic tools beyond *N. alba*, (III) standardization of nursery protocols across regions and species, (IV) exploration of biological interactions, including microbial inoculants and (V) evaluation of economic feasibility to guide scalable restoration strategies.

With coordinated action across science, practice, and policy, *Neltuma spp.* can become a cornerstone of climate-resilient restoration in arid and semi-arid ecosystems.

Supplemmentary material

https://docs.google.com/document/d/109syPEwVsHZFEAnRr_oR_X3qRIAHivVa/edit?usp=sharing&ouid=111310786017351827239&rtpof=true&sd=true

References

Abdala, N. R., Bravo, S., & Acosta, M. (2020). Germinación y efectos del almacenamiento de frutos de *Prosopis ruscifolia* (Fabaceae). *Bosque (Valdivia)*, *41*(2), 103-111. https://www.scielo.cl/pdf/bosque/v41n2/0717-9200-bosque-41-02-103.pdf

Bessega, C., Pometti, C., Ewens, M., Saidman, B. O., & Vilardi, J. C. (2015). Improving initial trials in tree breeding using kinship and breeding values estimated in the wild: the case of *Prosopis alba* in Argentina. *New Forests*, *46*, 427-448. https://doi.org/10.1007/s10342-016-0948-9

Bessega, C., Cony, M., Saidman, B. O., Aguiló, R., Villagra, P., Alvarez, J. A., & Vilardi, J. C. (2019). Genetic diversity and differentiation among provenances of *Prosopis flexuosa* DC (Leguminosae) in a progeny trial: Implications for arid land restoration. *Forest Ecology and Management*, *443*, 59-68. https://www.sciencedirect.com/science/article/pii/S0378112719302440

Bessega, C., Vilardi, J. C., Cony, M., Saidman, B., & Pometti, C. (2022). Low genetic variation of foliar traits among *Prosopis chilensis* (Leguminosae) provenances. *Journal of Plant Research*, *135*(2), 221-234. https://link.springer.com/article/10.1007/s10265-022-01378-9

Boeri P., Gazo M. C., Barrio D., Failla M., Dalzotto, D., Sharry, S. (2019). Optimum germinative conditions of a multipurpose shrub from Patagonia: *Prosopis alpataco* (Fabaceae). *Darwiniana, nueva serie*, *7*(2), 199-207. https://dx.doi.org/10.14522/darwiniana.2019.72.817

Braun Wilke, R. H., Picchetti, L. P., & Guzmán, G. F. (2000). *Prosopis ferox* gris: Estado actual de su conocimiento. *Multequina*, *9*(2), 19-34.

Bravo, S., Abdala, R., Abraham, F., & Pece, M. (2011). Treatments to improve germination of *Prosopis kuntzei*. *Seed Technology*, 55-62. https://www.jstor.org/stable/45133802

Brizuela, M. M., Burghardt, A. D., Tanoni, D., & Palacios, R. A. (2000). Estudio de la variación morfológica en tres procedencias de P*rosopis flexuosa* y su manifestación en cultivo bajo condiciones uniformes. *Multequina*, *9*(1), 7-15. https://www.scielo.org.ar/scielo.php?pid=S1852-73292000000100002&script=sci_abstract&tlng=en

Burghardt, A. D., Espert, S. M., & Braun Wilke, R. H. (2004). Variabilidad genética en *Prosopis ferox* (Mimosaceae). *Darwiniana, nueva serie*, *42*(1-4), 31-36. https://www.scielo.org.ar/scielo.php?pid=S0011-67932004000100003&script=sci_arttext&tlng=pt

Carranza, C., Verzino, G., Di Rienzo, J., Ledesma, M., & Joseau, J. (2000). Componentes de la variación adaptativa en *Prosopis chilensis*: el índice de brotación. *Multequina*, *9*(1), 55-64. https://www.scielo.org.ar/scielo.php?pid=S1852-73292000000100007&script=sci_arttext

Carreras, R., Bessega, C., López, C. R., Saidman, B. O., & Vilardi, J. C. (2017). Developing a breeding strategy for multiple trait selection in *Prosopis alba* Griseb., a native forest species of the Chaco Region in Argentina. *Forestry: An International Journal of Forest Research*, *90*(2), 199-210.

Cesca, E. M., Villagra, P. E., Passera, C., & Alvarez, J. A. (2012). Effect of *Prosopis flexuosa* on understory species and its importance to pastoral management in woodlands of the Central Monte Desert. *Revista de la Facultad de Ciencias Agrarias. Universidad Nacional de Cuyo*, *44*(2), 207-219. https://revistas.uncu.edu.ar/ojs3/index.php/RFCA/article/view/6305/5109

Chequer Charan, D., Pometti, C., Cony, M., Vilardi, J. C., Saidman, B. O., & Bessega, C. (2021). Genetic variance distribution of SSR markers and economically important quantitative traits in a progeny trial of *Prosopis chilensis* (Leguminosae): implications for the 'Algarrobo' management programme. *Forestry: An International Journal of Forest Research*, *94*(2), 204- 218.

Cony, M. A. (1996). Genetic variability in *Prosopis flexuosa* DC, a native tree of the Monte phytogeographic province, Argentina. *Forest Ecology and Management*, *87*(1-3), 41-49.

Cony, M. A., & Trione, S. O. (1998). Inter- and intraspecific variability in *Prosopis flexuosa* and *P. chilensis*: seed germination under salt and moisture stress. *Journal of Arid Environments*, *40*(3), 307-317.

Darquier, M. R., Bessega, C. F., Cony, M., Vilardi, J. C., & Saidman, B. O. (2013). Evidence of heterogeneous selection on quantitative traits of *Prosopis flexuosa* (Leguminosae) from multivariate QST-FST test. *Tree Genetics & Genomes*, *9*, 307-320. https://link.springer.com/article/10.1007/s11295-012-0556-x

Ewens, M., & Felker, P. (2010). A comparison of pod production and insect ratings of 12 elite *Prosopis alba* clones in a 5-year semi-arid Argentine field trial. *Forest Ecology and Management*, *260*(3), 378-383.

Felker, P., Ewens, M., Velarde, M., & Medina, D. (2008). Initial evaluation of *Prosopis alba* Griseb clones selected for growth at seawater salinities. *Arid Land Research and Management*, *22*(4), 334-345.

Felker, P., Lopez, C., Soulier, C., Ochoa, J., Abdala, R., & Ewens, M. (2001). Genetic evaluation of *Prosopis alba* (algarrobo) in Argentina for cloning elite trees. *Agroforestry Systems*, *53*, 65-76. https://link.springer.com/article/10.1023/A:1012016319629

Fontana, M., Pérez, V., & Luna, C. (2018). Efecto del origen geográfico en la calidad morfológica de plantas de *Prosopis alba* (Fabaceae). *Revista de Biología Tropical*, *66*(2), 593-604. https://www.scielo.sa.cr/scielo.php?pid=S0034-77442018000200593&script=sci_arttext

Funes, G., Díaz, S., & Venier, P. (2009). La temperatura como principal determinante de la germinación en especies del Chaco seco de Argentina. *Ecología austral*, *19*(2), 129-138.

Greeshma, K., Arutselvan, R., Teja, T. R., Baishnabi, D., & Chaudhary, S. (2025). Endophytes and Microbiome: Modern Techniques in Sustainable Crop. *Multi-omics Approach to Investigate Endophyte Diversity*, 103.

Grossnickle, S. C., & El-Kassaby, Y. A. (2016). Bareroot *versus* container stocktypes: a performance comparison. *New Forests*, *47*(1), 1-51.

Guzmán, A., Coronel de Renolfi, M., & Pece, M. G. (2011). Determinación de fallas en la siembra comercial de Algarrobo blanco (*Prosopis alba*) en un vivero de Santiago del Estero. *Quebracho (Santiago del Estero)*, *19*(1), 46-53. https://www.scielo.org.ar/scielo.php?pid=S1851-30262011000100006&script=sci_arttext

Hughes, C. E., Ringelberg, J. J., Lewis, G. P., & Catalano, S. A. (2022). Disintegration of the genus *Prosopis* L. (Leguminosae, Caesalpinioideae, mimosoid clade). *PhytoKeys*, *205*, 147. https://pmc.ncbi.nlm.nih.gov/articles/PMC9849005/

Joseau, M. J., Rodriguez Reartes, S., & Frassoni, E. J. (2023). Advances in the Use of *Neltuma* (ex *Prosopis*) Pods for Human and Animal Consumption. Pand their properties for human and animal food. In M. Hasanuzzaman (Ed.), *Production and utilization of legumes - Progress and prospects*. *IntechOpen*. https://www.intechopen.com/chapters/86609

Killian, S. (2012). Técnicas de germinación de *Prosopis chilensis* Moll Stuntz. *Biología en Agronomia*.

Kong, W.; Wang, Y.; Liu, Y.; Zhang, Y.; Zhang, Y.; Zhang, X. (2023). Genome and evolution of *Prosopis alba* Griseb., a drought and salinity tolerant tree legume crop for arid climates. *Plants, People, Planet*, *5*(6), 933-947. https://doi.org/10.1002/pei3.100

Lamarque, A. L., & Guzmán, C. A. (1997). Seed chemical variation in *Prosopis chilensis* from Argentina. *Genetic Resources and Crop Evolution*, *44*(6), 495-498.

Lerner, P., & Peinetti, R. (1996). Importance of predation and germination on losses from the seed bank of calden (*Prosopis caldenia*). *Rangeland Ecology & Management/Journal of Range Management Archives*, *49*(2), 147-150.

López, C., Maldonado, A., & Salim, V. (2001). Variación genética de progenies de *Prosopis alba. Investigación agraria. Sistemas y recursos forestales*, *10*(1), 59-68.

Mantovan, N. G. (2002). Early growth differentiation among *Prosopis flexuosa* DC provenances from the Monte phytogeographic province, Argentina. *New Forests*, *23*, 19-30. https://link.springer.com/article/10.1023/A:1015608430967

Marone, L., Horno, M. E., & Solar, R. G. D. (2000). Post-dispersal fate of seeds in the Monte desert of Argentina: patterns of germination in successive wet and dry years. *Journal of Ecology*, *88*(6), 940-949.

Massa, A.; Quagliariello, G.; Martinengo, N.; Calderón, A.; Pérez, S. 2023. Growth and slenderness index in sweet algarrobo, *Neltuma flexuosa*, according to the vermicompost percentage in the substrate and seed origin. *Revista de la Facultad de Ciencias Agrarias. Universidad Nacional de Cuyo, 55*(2): 12-19. DOI: https://doi.org/10.48162/rev.39.105

Mathers, H. M., Lowe, S. B., Scagel, C., Struve, D. K., & Case, L. T. (2007). Abiotic factors influencing root growth of woody nursery plants in containers. *HortTechnology*, *17*(2), 151-162.

Mazzuca, M., Kraus, W., & Balzaretti, V. (2003). Evaluation of the biological activities of crude extracts from Patagonian *Prosopis* seeds and some of their active principles. *Journal of herbal pharmacotherapy*, *3*(2), 31-37.

Milesi, F. A., & Lopez De Casenave, J. (2004). Unexpected relationships and valuable mistakes: non-myrmecochorous *Prosopis* dispersed by messy leafcutting ants in harvesting their seeds. *Austral Ecology*, *29*(5), 558-567.

Oliva, M., Alfaro, C., & Palape, I. (2010). Evaluación del potencial tecnológico de galactomananos del endospermo de semillas de *Prosopis sp.* para el uso en la industria de alimentos. *Agriscientia*, *27*(2), 107-113. https://www.scielo.org.ar/scielo.php?pid=S1668-298X2010000200006&script=sci_arttext

Orquera, R. M.; Marinoni, L.; Velazquez, M. A.; Pensiero, J. F.; Lauenstein, D. L.; Vega, C.; Zabala, J. M. (2025). Design of seed transfer zones and assessment of germplasm collections of Neltuma alba for reforestation and afforestation purposes in Argentina. *New Forests, 56*(1), 10. https://link.springer.com/article/10.1007/s11056-024-10072-8

Ortega Baes, P., de Viana, M. L., & Sühring, S. (2002). Germination in *Prosopis ferox* seeds: effects of mechanical, chemical and biological scarificators. *Journal of arid environments*, *50*(1), 185-189. https://www.sciencedirect.com/science/article/pii/S0140196301908596

Oumahmoud, M.; Alouani, M.; Elame, F.; Tahiri, A.; Bouharroud, R.; Qessaoui, R.; El Boukhari, A.; Mimouni, A.; Koufan, M. (2023). Effect of shading, substrate, and container size on Argania spinosa growth and cost–benefit analysis. *Agronomy*, *13*(10), 2451. https://doi.org/10.3390/agronomy13102451

Passera, C. B. (2000). Fisiología de *Prosopis spp. Multequina*, *9*(2), 53-80. https://www.scielo.org.ar/pdf/multeq/v9n2/v9n2a04.pdf

Pastorino, M. J., & Marchelli, P. (2021). *Low Intensity Breeding of Native Forest Trees in Argentina*. Springer: Berlin/Heidelberg, Germany. https://link.springer.com/content/pdf/10.1007/978-3-030-56462-9.pdf

Peinetti, R., Pereyra, M., Kin, A., & Sosa, A. (1993). Effects of cattle ingestion on viability and germination rate of calden (*Prosopis caldenia*) seeds. *Rangeland Ecology & Management/Journal of Range Management Archives*, *46*(6), 483-486.

Pérez, D. R., Ceballos, C., & Oneto, M. E. (2022). Costos de plantación y siembra directa de *Prosopis flexuosa* var. depressa (Fabaceae) para restauración ecológica. *Acta botánica mexicana*, (129). https://www.scielo.org.mx/scielo.php?pid=S0187-71512022000100500&script=sci_ arttext

Piraino, S.; Roig, F. A. 2024. Landform heterogeneity drives multi-stemmed *Neltuma flexuosa* growth dynamics. Implication for the Central Monte Desert forest management. *Revista de la Facultad de Ciencias Agrarias. Universidad Nacional de Cuyo. 56*(1): 26-34. DOI: https://doi.org/10.48162/rev.39.120

Pratolongo, P., Quintana, R., Malvárez, I., & Cagnoni, M. (2003). Comparative analysis of variables associated with germination and seedling establishment for *Prosopis nigra* (Griseb.) Hieron and *Acacia caven* (Mol.) Mol. *Forest ecology and management*, *179*(1-3), 15-25.

Renzi, J. P., Quintana, M., Bruna, M., & Reinoso, O. (2024). Environmental drivers of seed persistence and seedling trait variation in two *Neltuma* species (Fabaceae). *Seed Science Research*, 1-8. https://doi.org/10.1017/S0960258524000205

Sagadin, M. B., Salto, C. S., Cabello, M. N., & Luna, C. M. (2023). Respuesta micorrícica a la aplicación de inóculos de hongos micorrícicos arbusculares nativos en simbiosis con *Neltuma alba*. *Revista de Ciencias Forestales*, *31*, 1-2.

Salazar, P. C., Navarro-Cerrillo, R. M., Cruz, G., Grados, N., & Villar, R. (2019). Variability in growth and biomass allocation and the phenotypic plasticity of seven *Prosopis pallida* populations in response to water availability. *Trees*, *33*, 1409-1422. https://link.springer.com/article/10.1007/s00468-019-01868-9

Salto, C. S., García, M. A., & Harrand, L. (2013). Influencia de diferentes sustratos y contenedores sobre variables morfológicas de plantines de dos especies de *Prosopis*. *Quebracho (Santiago del Estero)*, *21*(2), 90-102.

Salto, C. S., Harrand, L., Javier Oberschelp, G. P., & Ewens, M. (2016). Crecimiento de plantines de *Prosopis alba* en diferentes sustratos, contenedores y condiciones de vivero. *Bosque (Valdivia)*, *37*(3), 527-537. https://www.scielo.cl/scielo.php?pid=S0717-92002016000300010&script=sci_arttext

Salto, C. S., Melchiorre, M., Oberschelp, G. P. J., Pozzi, E., & Harrand, L. (2019). Effect of fertilization and inoculation with native rhizobial strains on growth of *Prosopis alba* seedlings under nursery conditions. *Agroforestry Systems*, *93*, 621-629. https://link.springer.com/article/10.1007/s10457-017-0156-8

Salto, C. S., Sagadin, M. B., & Harrand, L. (2024). Inoculación de *Neltuma alba* con hongos micorrícicos arbusculares: efectos sobre el crecimiento y las variables edáficas en Entre Ríos, Argentina. *Bosque (Valdivia)*, *45*(2), 283-294.

Scaglia, J. A.; Flores, D. G.; Tapia, R.; Martinell, M. 2024. Effects of geomorphology and distribution of water sources for livestock on the floristic composition and livestock receptivity of the Arid Chaco. *Revista de la Facultad de Ciencias Agrarias. Universidad Nacional de Cuyo. 56*(1): 12-25. DOI: https://doi.org/10.48162/rev.39.119

Senilliani, M. G., Acosta, M., Oliet, J., & Brassiolo, M. (2021). Atributos morfológicos y fisiológicos de *Prosopis alba* Griseb en vivero con diferentes sustratos y contenedores. *Quebracho (Santiago del Estero)*, *29*(2), 92-101. https://www.scielo.org.ar/scielo.php?pid=S1851-30262021000200092

Vega, C., Teich, I., Acosta, M. C., Lopez Lauenstein, D., Verga, A., & Cosacov, A. (2020). Morphological and molecular characterization of a hybrid zone between *Prosopis alba* and *P. nigra* in the Chaco region of northwestern Argentina. *Silvae Genetica*, *69*, 44-54. https://sciendo.com/pdf/10.2478/sg-2020-0007

Velarde, M., Felker, P., & Degano, C. (2003). Evaluation of Argentine and Peruvian *Prosopis* germplasm for growth at seawater salinities. *Journal of Arid Environments*, *55*(3), 515-531.

Vence, L. B. (2008). Disponibilidad de agua-aire en sustratos para plantas. *Ciencia del suelo*, *26*(2), 105-114.

Vence, L. B., Valenzuela, O. R., Svartz, H. A., & Conti, M. E. (2013). Elección del sustrato y manejo del riego utilizando como herramienta las curvas de retención de agua. *Ciencia del suelo*, *31*(2), 153-164. https://www.scielo.org.ar/scielo.php?pid=S1850-20672013000200002&script=sci_arttext

Venier, P., Funes, G., Teich, I., López Lauenstein, D., & Lascano, R. (2021). Provenance matters: variability under saline stress in young plants of four populations of a *Prosopis* (mesquite) species from dry forests of Argentina. *Canadian Journal of Forest Research*, *51*(9), 1263-1270.

Venier, P., Ferreras, A. E., Lauenstein, D. L., & Funes, G. (2023). Nurse plants and seed provenance in the restoration of dry Chaco forests of central Argentina. *Forest Ecology and Management*, *529*, 120638. https://www.sciencedirect.com/science/article/pii/S0378112722006326

Verzino, G., Carranza, C., Ledesma, M., Joseau, J., & Di Rienzo, J. (2003). Adaptive genetic variation of Prosopis chilensis (Mol) Stuntz: Preliminary results from one test-site. *Forest ecology and Management*, *175*(1-3), 119-129.

Vilela, A. E., & Ravetta, D. A. (2001). The effect of seed scarification and soil-media on germination, growth, storage, and survival of seedlings of five species of *Prosopis* L. (Mimosaceae). *Journal of Arid Environments*, *48*(2), 171-184.

Vilela, A. E., & Ravetta, D. A. (2005). Gum exudation in South-American species of *Prosopis* L. (Mimosaceae). *Journal of arid environments*, *60*(3), 389-395. https://www.sciencedirect.com/science/article/pii/S0140196304001302

Villagra, P. E. (1997). Germination of *Prosopis argentina* and *P. alpataco* seeds under saline conditions. *Journal of Arid Environments*, *37*(2), 261-267.

Villagra, P. E., & Cavagnaro, J. B. (2000). Effects of clayish and sandy soils on the growth of *Prosopis argentina* and *P. alpataco* seedlings. *Ecología Austral*, *10*(2), 113-121.

Villagra, P. E., Marone, L., & Cony, M. A. (2002). Mechanisms affecting the fate of *Prosopis flexuosa* (Fabaceae, Mimosoideae) seeds during early secondary dispersal in the Monte Desert, Argentina. *Austral Ecology*, *27*(4), 416-421.

Villagra, P. E., Boninsegna, J. A., Alvarez, J. A., Cony, M., Cesca, E., & Villalba, R. (2005). Dendroecology of *Prosopis flexuosa* woodlands in the Monte desert: Implications for their management. *Dendrochronologia*, *22*(3), 209-213.

Zare, S., Tavili, A., & Darini, M. J. (2011). Effects of different treatments on seed germination and breaking seed dormancy of *Prosopis koelziana* and *Prosopis juliflora*. Journal of Forestry Research, 22, 35-38. https://link.springer.com/article/10.1007/s11676-011-0121-8

Acknowledgements

INTA EEA Junin, Mendoza, received funding in the first call for the National Forest Restoration Plan framed in the ForestAr 2030 platform of the National Ministry of Environment and Sustainable Development, Argentina.

Agricultural Land Valuation-Hedonic Pricing and Geostatistical Advances: A State-of-the-Art Review

Valoración de tierras agrícolas-Precios hedónicos y avances geoestadísticos: Una revisión del estado del arte

Vanina Fabiana Ciardullo *, Alejandro Juan Gennari

Originales: *Recepción:* 10/08/2025 - *Aceptación:* 14/11/2025

Index

Universidad Nacional de Cuyo. Facultad de Ciencias Agrarias. Cátedra de Economía y Política Agraria. Almirante Brown 500. M5528AHB. Chacras de Coria. Mendoza. Argentina. * vciardullo@fca.uncu.edu.ar

Abstract

This review examines international research on agricultural land valuation using hedonic pricing methods and geostatistical techniques. It brings together conceptual frameworks, functional forms, spatial econometric models, and empirical findings from key regions such as the United States, Europe, China, Australia, and Latin America. The main sections of the paper present comparative tables that summarise 23 studies applying log-linear or log-log models, R^2 values, and estimated marginal effects of irrigation water and other attributes. The review highlights methodological advances, identifies ongoing challenges in modelling spatial dependence and heterogeneous terrains, and outlines research gaps for developing robust valuation frameworks applicable to irrigated arid zones.

Keywords
hedonic pricing • land valuation • geostatistics • irrigation water • spatial econometrics • land characteristics

Resumen

Esta revisión examina investigaciones internacionales sobre la valoración de tierras agrícolas mediante métodos de precios hedónicos y técnicas geoestadísticas. Integra marcos conceptuales, formas funcionales, modelos econométricos espaciales y hallazgos empíricos de regiones clave como Estados Unidos, Europa, China, Australia y América Latina. Las secciones principales del trabajo presentan tablas comparativas que resumen 23 estudios que aplican modelos log-lineales o log-log, valores de R^2 y efectos marginales estimados del agua de riego y otros atributos. La revisión destaca los avances metodológicos, identifica los desafíos persistentes en la modelización de la dependencia espacial y la heterogeneidad territorial, y señala brechas de investigación orientadas al desarrollo de marcos de valoración robustos aplicables a zonas áridas bajo riego.

Palabras clave
precio hedónico • valoración de la tierra • geoestadística • agua de riego • econometría espacial • características del terreno

Introduction

The valuation of agricultural land is a fundamental issue in resource economics, rural development, and agricultural policy planning. In regions facing increasing water scarcity, such as the Mendoza River Basin in Argentina, accurately determining the economic value of farmland and its key attributes, particularly irrigation water, becomes increasingly relevant. Hedonic pricing models have long served as a robust methodology for decomposing the observed price of land into its constituent attributes, offering insight into the implicit values assigned to physical, economic, and environmental characteristics.

Recent advances in spatial econometrics and geostatistical modelling have enriched this analytical approach. These methods accommodate spatial dependence and geographical heterogeneity in data, both critical in explaining land price variations. This review provides a state-of-the-art synthesis of literature employing hedonic models-with a focus on the marginal contribution of irrigation water-and highlights geostatistical innovations designed to improve model robustness.

The article is structured as follows:

- Theoretical Framework: Hedonic Pricing and its Extensions, introduces the theoretical framework of hedonic pricing and its main extensions, establishing the analytical foundations for understanding land price formation based on the valuation of individual attributes.

- Irrigation Water as an Economic Attribute in Agricultural Land Markets: Hydrological Context, Use, and Value in the Mendoza River Basin, presents the hydrological, physical, and institutional context of irrigation water in the Mendoza River Basin, showcasing its importance as a production factor.

- Hedonic Models in the Estimation of Agricultural Land Prices: Foundations and Empirical Applications analyses, the conceptual foundations and international empirical applications of hedonic pricing in farmland markets.

- Methodological Advances: Spatial Hedonic and Geostatistical Models in Agricultural Land Valuation, outlines methodological innovations, including spatial and geostatistical extensions.

- Results: Review of Major Studies, compiles the main findings from comparative studies, and the conclusion summarises the lessons and gaps identified.

Theoretical Framework: Hedonic Pricing and its Extensions

The valuation of agricultural land is a cornerstone of rural economics and agricultural policy planning. Hedonic pricing models have proven to be a robust methodology for decomposing the price of land into its constituent attributes. This approach assumes that the price of a heterogeneous good (such as land) can be explained by the sum of the implicit values of its physical, economic, and environmental characteristics.

The hedonic pricing method (HPM) is rooted in the idea that a good can be valued based on its characteristics. In the case of land, the price is decomposed into the value of attributes such as soil quality, infrastructure, crop type, location, and access to irrigation water. Formally, a simple hedonic model is expressed as:

$$P=f(X1,X2,...,Xn)+\epsilon$$

where:

P = the land price

X1,...,Xn = its observable attributes

ϵ = the error term.

The conceptualization of this method is found in the seminal work by Rosen, S. (1974).

Functional Forms and Interpretation of Elasticities

In practice, the most widely used functional forms are the log-linear and log-log models. This choice not only helps stabilize variance but also facilitates the interpretation of coefficients:

- Log-linear model: $\ln(P)=\beta0+\sum j=1n\beta jXj+\epsilon$. Here, the coefficient βj is interpreted as the approximate percentage change in price for a one-unit change in attribute Xj. For example, if the coefficient for the dummy variable 'access to irrigation' is 0.19, this means that the price of the land increases by approximately 19% in properties with irrigation.

- Log-log model: $\ln(P)=\beta0+\sum j=1n\beta j\ln(Xj)+\epsilon$. In this case, the coefficient βj is interpreted as the elasticity of price with respect to attribute Xj. A coefficient of 0.45 for lnDist (distance) indicates that a 1% increase in distance is associated with a 0.45% decrease in price, which is very useful for comparing the relative importance of attributes across different scales.

Limitations and Methodological Advances

Although traditional hedonic models are highly useful, they present several limitations. Ignoring spatial dependence-the tendency for geographically close observations to be more similar-can bias coefficient estimates. To address this issue, several key methodological advances have been developed:

1. Spatial Hedonic Models

These models explicitly incorporate spatial autocorrelation. The most common approaches are:

- Spatial Lag Model (SLM)

Includes a spatially lagged dependent variable (Wln(P)) to capture the influence of neighbouring property prices.

- Spatial Error Model (SEM)

Assumes that spatial correlation lies in the error term, indicating omitted variables with a spatial structure.

2. Mixed Models (Hierarchical): These models nest administrative or ecological units (*e.g.*, district within a department) to capture variability at different levels and address the problem of non-independent observations.

3. Heteroskedasticity: Unequal price variance across different regions or districts (heteroskedasticity) is addressed through methods such as weighted least squares or variance structures like *varIdent*.

4. Geostatistics: Geostatistical methods, such as kriging, interpolate values in unsampled areas, providing a basis for mapping prices or attributes like soil quality from limited data.

Together, these methodological advances strengthen the ability of hedonic models to provide more robust and accurate estimates, particularly in rural land markets characterised by high environmental and institutional complexity, such as that of Mendoza.

Irrigation Water as an Economic Attribute in Agricultural Land Markets: Hydrological Context, Use, and Value in the Mendoza River Basin

Hydrological and Territorial Framework

The Province of Mendoza, Argentina, has an extremely arid hydrological regime, with average annual rainfall of around 220 mm. Agricultural production is concentrated in irrigated oases that occupy only 4 per cent of the provincial territory yet sustain 99 per cent of the population and most socioeconomic activity. Mendoza contains the largest collective irrigated area in the country (approximately 267,889 ha), accounting for about 20 per cent of the national total. The province's water supply system extends across five major rivers: Mendoza, Tunuyán, Diamante, Atuel, and Malargüe.

Water managers must balance competing domestic, agricultural, industrial, and environmental uses. Agriculture accounts for 93.75% of total water demand, compared with 5.45% for domestic use and 1% for industry. Given its strategic role, irrigation water directly affects land value, production efficiency, and territorial sustainability. The Department of Irrigation (Departamento General de Irrigación, DGI) oversees water management using tools such as the Hydrological Balance, Annual Runoff Forecast, and Automatic Measurement Networks. Economic instruments such as Virtual Water and Water Footprint indicators are also promoted.

Hydrological Crisis and Territorial Pressures

Between 2009 and 2022, Mendoza underwent the longest dry cycle in its recorded history, with 12 of 13 years classified as drought years. Reduced snowfall, pronounced climate variability, and sediment accumulation in reservoirs (for example, a 20 per cent loss of storage capacity in the Potrerillos Dam) have severely constrained water availability. Recent runoff forecasts (2019-2022) reported flows below 70 per cent of historical averages, prompting the implementation of extraordinary management measures.

Recent evidence from irrigated areas in eastern Mendoza shows a marked increase in abandoned cropland - 92 per cent between 2002 and 2020 - driven by water scarcity, accessibility constraints, crop type, and socio-economic vulnerability (Guida-Johnson *et al.*, 2024).

Against this backdrop of growing hydrological stress, limited irrigation availability raises production costs, reduces yields, and ultimately undermines the economic viability of farms. When adaptive capacity is constrained, these pressures frequently result in land abandonment, urban encroachment, or declining land values. In the Mendoza River Basin -the focal area of this review - Bacaro *et al.* (2017) documented over 28,000 hectares of abandoned irrigated land, illustrating how prolonged water shortages and structural pressures contribute to land-use decline within the basin itself. The increasing urbanisation of peri-urban irrigated zones further intensifies land-use conflicts and adds complexity to farmland valuation dynamics.

Water Rights System and Institutional Framework

Mendoza's irrigation system operates under a legally defined and hierarchically organised framework administered by the Department of Irrigation (DGI). The 1884 Water Law defines several categories of rights: definitive concessions (granted to users prior to 1884, with absolute priority), eventual concessions (granted after 1884, receiving between 50 and 80 per cent of the volume allocated to definitive users), and precarious permits-temporary and revocable authorisations for the use of surplus or drainage water that do not confer full ownership rights and therefore imply lower legal security (Pinto *et al.*, 2019). From a distributive perspective, because these permits were introduced after the 1884 Water Law, they are classified as *eventual* rather than *definitive* rights and thus occupy the lowest tier within the allocation hierarchy established by the Administrative Tribunal's 1929 ruling, receiving proportionally smaller water entitlements (Pinto, 2001). The DGI also manages drainage or summer reinforcement water, which it reallocates to stabilise irrigation supplies, a function described in the Hydrological Balance Report (DGI, 2016). In addition, the use of groundwater follows a specific regulatory regime that requires the authorisation of drilling, technical inspection of works, and systematic monitoring of aquifers. The DGI issues new extraction permits or replacement permits, applying technical and legal criteria that depend on hydrogeological conditions -such as recharge areas, confined or semi-confined aquifers, and natural spring zones- described in a recent diagnostic report prepared in collaboration with Mekorot (DGI, 2023).

Under Mendoza's legal framework, the right to use water is accessory to the land (*derecho de agua accesorio al inmueble*), meaning it cannot be sold or transferred independently from the property to which it belongs (Gobierno de Mendoza, Ley de Aguas, 1884). Unlike in other countries where water rights may be traded separately from land ownership, this principle in Mendoza legally binds water to the land, integrating their economic values within agricultural markets. Consequently, the economic value of irrigation water is capitalised in the value of irrigated land, reinforcing its dual role as both a productive input and a territorial asset in agricultural markets.

Relevance for Land Valuation

Understanding irrigation water as a marginal value attribute is crucial for land markets in arid basins like Mendoza. This review frames irrigation access as a key explanatory variable in hedonic models and connects it with productivity, soil quality and locational advantages.

Hedonic Models in the Estimation of Agricultural Land Prices: Foundations and Empirical Applications

Theoretical Background and Key Determinants

Hedonic pricing decomposes land value into its observable characteristics. Classical determinants include productivity, land use, and crop prices, while recent studies emphasise physical attributes (*e.g.*, slope, soil quality), irrigation infrastructure, secure water rights, urban proximity, land-use regulations, and macroeconomic expectations. The literature reports diverse model specifications and outcomes depending on geographical context.

In the United States, Faux and Perry (1999) estimated marginal irrigation water values ranging from USD 9 to 44 per acre-foot, whereas Roka and Palmquist (1997) and Miranowski and Hammes (1984) developed broader theoretical frameworks. In Spain, Gracia *et al.* (2004) linked rural population growth with land demand, and Decimavilla and Sperlich (2008) highlighted the effects of urban pressure and irrigation expansion, while in Chile, Troncoso (2005) and Schönhaut (1990) applied hedonic models based on classified advertisements, reflecting data constraints. In Argentina, research remains less developed, with persistent challenges related to spatial adaptation, data consistency, and regional heterogeneity.

Valuing Irrigation Water as a Scarce Environmental Resource

Indirect valuation approaches use land prices to infer the economic value of irrigation water. Bos (1999) reported a gross productivity of USD 0.22 per m^3 for viticultural and fruit systems, whereas Valencia (2012) estimated a marginal value of USD 3.2 per m^3 in northern Mendoza. Garrido (2004) identified marginal productivities of USD 0.586 per m^3 for flows of 1,100 hm^3, and Cano (1967)-as cited by Pinto (2005)-documented up to thousandfold increases in land value following the allocation of irrigation rights.

In Spain, Gracia *et al.* (2004) observed that irrigated land values were twice those of rainfed parcels, and Berbel (2007) calculated capitalised irrigation water values at €3.46 per m^3, with rental values ranging between €0.14 and €0.35 per m^3. Microeconomic models integrate soil fertility, on-farm improvements, infrastructure, and crop suitability, with irrigation rights consistently emerging as a key determinant of land value.

As Bencure (2019) and Sardaro (2020a) argue, sustainable land use requires incorporating water valuation into territorial policy. This study therefore emphasises the combined modelling of land and water to capture their economic interdependence, drawing on both traditional hedonic estimation and spatial analytical methods.

Methodological Advances: Spatial Hedonic and Geostatistical Models in Agricultural Land Valuation

Spatial Dependence and Econometric Tools

Geostatistics and spatial econometrics have strengthened the explanatory power of hedonic models by explicitly addressing spatial autocorrelation and heterogeneity. Spatial Lag Models (SLM), Spatial Error Models (SEM), and General Spatial Models (GSM) capture inter-parcel interactions and correct for spatial bias. Geostatistical techniques such as kriging enable interpolation in unobserved areas, producing predictive maps that support taxation, zoning, and policy design.

Journel and Huijbregts (1978) and Matheron (1963) formalised these principles through regionalised variable theory, introducing analytical tools such as variograms and spatial weights matrices. Applications in Illinois (Huang *et al.*, 2006), Spain (Dray *et al.*, 2006), and Argentina (Balzarini, 2014) validate these approaches. Huang *et al*. (2006) applied spatial lag models with AR(1) errors to 64,000 transactions, achieving better model fit and correcting for serial correlation.

Wang (2018) advocated the use of structural spatial panel models based on farm-level data, although limited data availability remains a constraint. Córdoba *et al.* (2021a) implemented a machine-learning approach-Spatial Quantile Regression Forest (S-QRF)-to estimate land values using big data and geospatial information, outperforming traditional regression and kriging methods.

Empirical Evidence and Comparative Findings

Yoo *et al.* (2013) introduced interaction terms and robust errors into hedonic models for urbanising areas of Arizona, identifying water rights as capitalizable urban assets. Mukherjee and Schwabe (2014) estimated interactions between salinity and water depth in California using GSM, revealing non-linear effects on irrigated land value. Lehn and Bahrs (2018) in Germany and Guadalajara *et al.* (2019) in Spain employed SEM and SLM frameworks with robust variance estimators to capture demographic, urban, and livestock-related spillover effects.

Kostov (2009) applied Bayesian semi-parametric additive models in Northern Ireland, highlighting soil and drainage as key determinants of land value. Across these studies, spatial models consistently outperform OLS specifications in diverse contexts, confirming the centrality of geographic information in hedonic land price analysis.

Results: Review of Major Studies

Two comparative tables summarise the reviewed studies. Table 1 (page 230-231) compiles classical works alongside more recent studies on the hedonic pricing method and the economic valuation of irrigation water, whereas table 2 (page 232-233) presents contemporary literature that integrates spatial and geostatistical approaches applied to agricultural land valuation.

Table 1 (page 230-231) summarises key studies applying the hedonic pricing method to the valuation of agricultural land and irrigation water. The results consistently confirm the positive and significant contribution of irrigation access or water rights to land values across diverse regions and crop systems. In addition to water-related attributes, other important determinants include soil quality, parcel size, distance to markets and urban centres, infrastructure, crop type, and physical improvements such as drainage systems or vineyard facilities. Early contributions established the theoretical and empirical foundations of the method, while more recent studies, such as Tauro *et al.* (2024), demonstrate its continued relevance for analysing how irrigation service type, reliability, and a wide range of physical, locational, and institutional attributes are capitalised into farmland prices.

Table 1. Comparative analysis of studies on hedonic valuation of agricultural land and the marginal contribution of irrigation water.

Tabla 1. Análisis comparativo de estudios sobre valoración hedónica de tierras agrícolas y la contribución marginal del agua de riego.

Author(s) / Year / Journal	City / Study Area	Model Functional Form	R^2	Key Significant Variables	Marginal Contribution of Irrigation Water	Main Conclusions
Faux, J. & Perry, G. (1999). *Land Economics*	Malheur County, Oregon, USA	Linear (heteroskedasticity-weighted adjustment)	0.92	Soil quality with irrigation water, estimated value of buildings, proximity to urban centres	Estimated implicit value of irrigation water ranges from $9 per acre-foot in less productive land to $44 per acre-foot in more productive land.	Irrigation is a significant determinant of agricultural land value. Water value is more capitalized in productive soils.
Chicoine, D. (1981). *American Journal of Agricultural Economics*	Illinois, USA	Log-linear	0.70	Soil quality, distance to markets, property size, infrastructure	Positive coefficient for irrigation access	Irrigation access increased land price, soil quality was the most influential variable.
Palmquist, R. & Danielson, L. (1989). *Land Economics*	North Carolina, USA	Linear	0.65	Soil type, topography, lot size, distance to cities	Positive and significant coefficient for irrigated plots	Land with irrigation capacity was significantly more valuable.
Fraser, I. & Hilder, C. (2007). *Australian Journal of Agricultural and Resource Economics*	Australia (Wine Region)	Log-log	0.82	Age of vines, grape variety, cultivated area, winery infrastructure	Positive coefficient for water availability (rights or wells)	Irrigation water is a key factor in vineyard price; vine age and grape variety also influence value.
Donoso, G. *et al.* (2013a). *Economía Agraria y Recursos Naturales*	Chile (from Coquimbo to Los Lagos)	Log-linear interaction effects and urban pressure, correcting for heteroscedasticity	0.60	Buildings, drip irrigation, fruit trees, distance to urban centres, agricultural exports relative to agricultural GDP	% of drip irrigation positively affects price (29%)	Land price increases with high-value crops, irrigation infrastructure, and urban development pressure.
Gracia, A. *et al.* (2004). *Estudios Agrosociales y Pesqueros*	Zaragoza, Spain	Log-linear	0.70-0.85	Crop type, area, soil quality, slope, altitude, urban proximity	No €/m^3 value estimated, but irrigation regime is significant	Legal water access, electrical availability, and urban potential influence agricultural land valuation.

Source/Fuente: our elaboration/elaboración propia.

Author(s) / Year / Journal	City / Study Area	Model Functional Form	R^2	Key Significant Variables	Marginal Contribution of Irrigation Water	Main Conclusions
Sardaro, R. *et al.* (2020b). *Land Use Policy*	Southern Italy, Provinces of Foggia and Bari	Linear	0.72	Access to irrigation water, rural infrastructure, proximity to urban centres, crop type, active territorial development policies	Access to irrigation increases land value by approximately 15% to 20%, depending on crop type and geographic area	Rural land markets reflect territorial, environmental, and productive dimensions, while pricing is strongly influenced by development policies and irrigation access
Caballer, V. & Guadalajara, N. (2005). *Estudios Agrosociales*	Spain	Log-linear	0.74	Area, yield, land quality, frost risk, location, tourism, climate	"Irrigation water" increases price by ~63%	Area, yield, location, and climate explain land value and profitability; models applicable to farmland valuation.
Díaz Visquerra, M. *et al.* (2014). *CEPAL Review*	Guatemala (14 departments)	Reduced log-linear	0.79	Area, distance to municipal centre, road infrastructure, natural region	Water value not estimated	Price per hectare depends on physiographic location, size, and road accessibility; useful for rural financing.
Decimavilla, E. & Sperlich, S. (2008). *Agricultural Economics Review*	Spain	Log-linear	0.68	Soil quality, property size, land slope, irrigation water, distance to regional capital	Irrigation water (dummy), acting as a speculative factor that increases land value in urbanized areas	Identifies speculative pressure. The methodology is useful for land-use planning and agricultural land management policies
Berbel, J. & Mesa, P. (2007). *Economía Agraria y Recursos Naturales*	Guadalquivir Basin, Spain	Quasi-hedonic method	R^2 not reported	Price differentials by crop and region	Water capital ~€3.46/m^3; water rental value €0.14-0.35/m^3 depending on rate	Water is a key determinant; capital and rental water values estimated based on capitalization rates.
Tauro, E. *et al.* (2024). Italian *Review of Agricultural Economics*	Apulia region, Italy (olive groves)	Log-linear (Hedonic model using FADN data)	0.78 (Model 1)	Type of irrigation service, irrigated surface area, irrigation volume, plant density, slope, altitude	Self-supply service premium ≈ 41% higher land value compared to collective service ($e^{\beta} - 1 \approx 0.4125$)	The type and reliability of irrigation service (self-supply vs collective) is capitalised into land value; self-supply lands achieve higher values.

Source/Fuente: own elaboration/elaboración propia.

Table 2. Spatial and geostatistical model applications with irrigation and environmental variables.
Tabla 2. Aplicaciones de modelos espaciales y geoestadísticos con variables de riego y ambientales.

Author (Year)	Study Area	Crop Analysed	Model Applied	R^2	Significant Variables	Main Conclusions
Yoo, J. *et al.* (2013)	Phoenix, Arizona, USA (semi-arid urbanizing area)	Farmland (151 transactions between 2001-2005)	Semi-log hedonic (OLS with robust errors)	0.3734 (M1) - 0.4819 (M3)	Water rights (+), land size (–), slope (-), distance to highways (–), % developed land (DEV3000), interactions water×DEV3000 (+) and water×city (+ Phoenix/Mesa; - Buckeye)	Water rights increase prices by 28% to 87%. Higher willingness to pay in urbanized and developed land areas.
Mukherjee, M. & Schwabe, K. (2014)	Central Valley, California, USA (629 plots, 2004-2010)	Irrigated agriculture	Log-log (General Spatial Model - GSM)	0.949 (M1) - 0.951 (M2)	Groundwater depth (+ with salinity), salinity (–), depth×salinity, orchards/ vineyards (+), distance to cities (–), population density (+), Storie index (+), precipitation, CVP water supply (mean +, variability -)	Salinity is critical and omission leads to bias. Proximity to saline water tables reduces value. Projected salinity increases imply significant damages.
Lehn, F. & Bahrs, E. (2018)	North Rhine-Westphalia, Germany (municipal data 2013)	Arable land	Linear (General Spatial Model – GSM)	0.4819 (Adj. R^2)	Spatial lags (+), change in used agricultural area (-), population density (+), population change (+), distance to major cities (+), livestock density (+), agri-environmental payments (-), farm size (U-shaped)	Urbanization and livestock drive prices. Fiscal regulation can reinforce increases. Spatial spillover effects amplify local impacts.
Huang, H. *et al.* (2006)	Illinois, USA (data 1979-1999)	Farmland	Log-log with spatial lag and AR(1) errors	0.798 (OLS) - 0.854 (ML)	Soil productivity (+), parcel size (-), quality (improvement +), distance to Chicago (-, highly influential), other cities (-), rural-urban code (-), lagged CPI (-), population density (+), per capita income (+), hog farm density (-)	Values show spatial and temporal correlation. Non-productive factors also matter. Hog farms negatively impact value; larger scale mitigates diseconomies.
Córdoba, M. *et al.* (2021b)	Córdoba Province (Argentina)	Mixed cropping (soybean, maize, wheat)	sQRF (Spatial Quantile Regression Forest)	0.73	Soil productivity index, appraisal zones, crop types, lease, distance to port	sQRF achieves high precision, captures complex spatial relationships, and outperforms linear regression and kriging. Generates digital valuation maps with uncertainty.
Kostov, P. (2009)	Northern Ireland	General agriculture (grazing, dairy)	Semiparametric additive hedonic (Bayesian via MCMC)	Not reported	Soil quality, drainage capacity, cattle density, distance to urban area, road access	Semiparametric models avoid functional form bias. No significant spatial dependence detected, nonlinear effects prevail.

Source/Fuente: our elaboration/elaboración propia.

Author (Year)	Study Area	Crop Analysed	Model Applied	R^2	Significant Variables	Main Conclusions
Mallios, Z. *et al.* (2009)	Municipality of Moudania, Chalkidiki region, Greece	Olive trees (70% of the irrigated area), fruit trees and vegetables	Log-Linear, three variants: OLS, SLM, SEM	OLS: 0.7141 SLM: 0.7389 SEM: 0.7774	Irrigation (dummy), elevation, plot area, distance to key features (sea, settlements, urban center, local and national roads), presence of olive trees	Irrigated land significantly increases value (105.07%), with SEM and GIS enhancing spatial valuation accuracy over OLS.
Zhang, J., & Brown, C. (2018)	Inner Mongolia Autonomous Region, China	Pastures (circulation of grazing rights)	OLS, Pseudo R^2 in quantile regressions, Moran I	OLS: 0.3929, Pseudo R^2: 0.2570 and 0.2650	Type of pasture, Land area, Irrigation condition, Distance to national highway, Contract type, Local per capita income, Contract term	Irrigation raises land prices by up to 30%, with locally driven, segment-specific effects and no spatial autocorrelation.
Demetriou, D. (2015)	Land consolidation area in Choirokoitia, Larnaca District, Cyprus, Greece	Citrus, olives, various fruit trees, and cereals	Linear, GIS environment for automated valuation	0.799	Negative: parcel size, slope, proximity to a stream, and distance from residential zones. Positive: access via registered roads, irrigation rights, and parcel orientation	The AVM approach reduced valuation time and cost (80%). High levels of accuracy and reliability (only a 15% sample of land parcels).
Guadalajara, N. *et al.* (2019)	Aragón, Spain (municipal data 2017)	Agricultural land (almonds, vineyards, fruits, grasslands, etc.)	Log-linear (SLM and SEM)	0.9510 (OLS) - 0.9610 (SEM)	Irrigation availability (+, 2.2×), parcel size (+, 5.7% per ha), income (+), population (+), density (+), average age (- for vineyards), cadastral value (+), natural reserves (+, 11-12.9%), altitude (mixed effects)	Spatial models outperform OLS. Both agricultural and non-agricultural factors matter. Larger parcels increase value (mechanization effect). Heteroskedasticity suggests omitted variables.
Giuffrida, L. *et al.* (2023).	Upper Treviso plain, Veneto region, Northern Italy	Arable crops (84.4%) and vineyards (11.8%)	Spatial Lag of X (SLX) Model – Generalised Spatial Two-Stage Least Squares (GS2SLS); comparison with OLS	0.483 (OLS) – 0.508 (SLX)	Soil permeability (+), distance to urban centres (–), low flood risk (+), airport and power line restrictions (–), corporate buyers (+ 25–43 %), professional farmers (+ 14.9 %), sales between relatives (– 19 %)	Spatial regression identifies direct and spillover effects: farmland prices increase near urban centres and low risk areas and decrease with easements. Buyer type and corporate ownership strongly influence price formation, with the SLX model outperforming OLS in capturing local spatial effects.

Source/Fuente: own elaboration/elaboración propia.

Table 2 (page 232-233) summarises recent studies that incorporate spatial econometric and geostatistical techniques into the hedonic valuation of agricultural land. These approaches enable a more accurate representation of spatial dependence, neighbourhood interactions, and environmental heterogeneity.

The findings highlight that land values are influenced not only by irrigation availability but also by spatially structured factors such as soil productivity, proximity to markets and urban centres, accessibility, and exposure to environmental risks. Spatial models-including SLM, SEM, GSM, and SLX-consistently outperform traditional OLS specifications, providing improved model fit and capturing both direct and spillover effects in farmland price formation.

Overall, most studies employ log-linear or log-log functional forms, with R^2 values typically ranging from 0.60 to 0.79, and only a few models reaching higher explanatory levels between 0.89 and 0.95. Classical hedonic models estimated through OLS or mixed-effects approaches (table 1, page 230-231) generally achieve higher R^2 values, reflecting well-defined relationships under relatively homogeneous conditions. In contrast, spatial and geostatistical models (table 2, page 232-233) tend to report lower or more moderate R^2 values, as they correct for spatial autocorrelation, account for heterogeneous terrains, and include additional sources of variability that reduce overall fit but enhance model realism and predictive accuracy.

Key predictors include soil quality, farm size, infrastructure, urban proximity, and crop type. Irrigation water-whether expressed as legal rights, technological access, or proximity to canals-consistently shows positive and significant effects on land value. The economic valuation of irrigation water varies across contexts, from US dollars per acre-foot in the United States to euros per cubic metre in Europe, with some studies estimating rental or capitalised values. Collectively, these findings highlight the dual role of water as both a productive input and a territorial asset.

Conclusion

The hedonic pricing method remains a foundational approach in agricultural land valuation, capable of isolating the marginal effects of key attributes such as irrigation water, infrastructure, and crop type. In arid and semi-arid regions such as Mendoza, where water scarcity and land-use pressures converge, understanding these marginal values is critical for sustainable resource management.

Incorporating spatial econometric and geostatistical methods significantly enhances model performance and improves the representation of geographic patterns and contextual complexities. Researchers still face challenges related to data availability, model specification, and the integration of socio-political variables, but the reviewed literature provides a rich basis for further exploration.

Future research should refine these approaches, particularly for developing countries experiencing climatic and demographic transitions. Enhanced data integration, remote sensing, and open-source GIS tools may offer promising avenues for more dynamic and granular valuations.

References

Bacaro, A., Satlari, G., & Martín, T. (2017). Demanda de agua en el área de interfaz en la cuenca del río Mendoza. En *XXVI Congreso Nacional del Agua–CONAGUA 2017* (p. 1-8).

Balzarini, M. (Comp.). (2014). *Buenas prácticas para el análisis de la variabilidad espacial del rendimiento y propiedades de suelo en lotes de producción agrícola*. Eudecor. https://www.cba.gov.ar/wp-content/4p96humuzp/2016/05/Libro-Buenas-Pr%C3%A1cticas_BALZARINI.pdf

Bencure, J. C., Tripathi, N. K., Miyazaki, H., Ninsawat, S., & Kim, S. M. (2019). Development of an innovative land valuation model (iLVM) for mass appraisal application in sub-urban areas using AHP: An integration of theoretical and practical approaches. *Sustainability*, *11*(13), 3731. https://doi.org/10.3390/su11133731

Berbel, J., & Mesa, P. (2007). Valoración del agua de riego por el método de precios quasi-hedónicos: aplicación al Guadalquivir. *Economía Agraria y Recursos Naturales*, *7*(14), 127-144.

Bos, M. G., & Chambouleyron, J. L. (Eds.). (1999). Parámetros de desempeño de la agricultura de riego de Mendoza, Argentina *(Serie Latinoamericana N° 5). International Water Management Institute (IWMI)*.

Caballer Mellado, V., & Guadalajara Olmeda, N. (2005). Modelos econométricos de valoración de la tierra de uso agrícola: Una aplicación al Estado español. *Estudios Agrosociales y Pesqueros*, *(205)*, 13-38.

Cano, G. J. (1967). *El recurso hídrico y la valorización territorial en Mendoza*. Universidad Nacional de Cuyo.

Chicoine, D. L. (1981). Farmland values at the urban fringe: An analysis of sale prices. *American Journal of Agricultural Economics*, *63*(3), 530-537.

Córdoba, J., Ledesma, L., & Peralta, R. (2021a). Aplicaciones de aprendizaje automático en la estimación de valores unitarios del suelo rural. En *Jornadas de Investigación y Extensión del INTA* (p. 1-10).

Córdoba, M., Carranza, J. P., Piumetto, M., Monzani, F., & Balzarini, M. (2021b). A spatially based quantile regression forest model for mapping rural land values. *Journal of Environmental Management*, *289*, 112509.

Decimavilla, E., & Sperlich, S. (2008). Urban pressure and land value in Spain: A hedonic pricing approach. *Agricultural Economics Review, 9*(1), 22-33.

Demetriou, D. (2015). A GIS-based hedonic price model for agricultural land. En D. G. Hadjimitsis, K. Themistocleous, S. Michaelides, & G. Papadavid (Eds.). *Proceedings of SPIE - The International Society for Optical Engineering,* (Vol. 9535, Paper 95350B). https://doi.org/10.1117/12.2192498

Departamento General de Irrigación. (2016). *Balance Hídrico Río Mendoza*. DGI.

Departamento General de Irrigación, Mekorot Israel National Water Co., & Consejo Federal de Inversiones. (2023). *Plan Maestro para el sector hídrico de la provincia de Mendoza: Informe 1. Estudio de la situación actual del sector hídrico*. Provincia de Mendoza, Argentina. https://www.irrigacion.gov.ar/web/wp-content/uploads/2025/03/1-PLAN-MAESTRO-PARA-EL-SECTOR-H%C3%8DDRICO-Informe-1-MENDOZA.pdf

Díaz Visquerra, M. E., Vanegas, E. A., & Camacho Sandoval, J. (2014). Determinación de modelos econométricos para la valoración de tierras rurales en Guatemala. *Revista Ciencias Técnicas Agropecuarias*, *23*(1), 47-52.

Donoso, G., Cancino, J., & Foster, W. (2013a). Farmland values and agricultural growth: The case of Chile. *Economía Agraria y Recursos Naturales*, *13*(2), 33-52. https://doi.org/10.7201/earn.2013.02.02

Donoso, G., Cancino, J., Olguín, R., & Schönhaut, D. (2013b). A comparison of farmland value determinants in Chile between 1978-1998 and 1999-2008. *Ciencia e Investigación Agraria*, *40*(1), 85-96.

Dray, S., Legendre, P. & Peres-Neto, P. R. (2006). Spatial modelling: A comprehensive framework for principal coordinate analysis of neighbour matrices (PCNM). *Ecological Modelling*, *196*(3-4), 483-493. https://doi.org/10.1016/j.ecolmodel.2006.02.015

Faux, J., & Perry, G. M. (1999). Estimating irrigation water value using hedonic price analysis: A case study in Malheur County, Oregon. *Land Economics*, *75*(3), 440-452.

Fraser, I., & Hilder, C. (2007). Vineyard capitalisation: A hedonic analysis of wine grape growing properties. *Australian Journal of Agricultural and Resource Economics*, *51*(1), 1-17.

Garrido, A., Palacios, E., & Calatrava, J., Chávez, J. & Exebio, A. (2004). *La importancia del valor, costo y precio de los recursos hídricos en su gestión*. Proyecto Regional FODEPAL, Gestión Integral de los Recursos Naturales.

Giuffrida, L., De Salvo, M., Manarin, A., Vettoretto, D., & Tempesta, T. (2023). Exploring farmland price determinants in Northern Italy using a spatial regression analysis. *Aestimum, 83*, 3-20. https://doi.org/10.36253/aestim-14986

Gobierno de Mendoza. (1884). *Ley de Aguas de la Provincia de Mendoza (Ley N° 4035).* Boletín Oficial de la Provincia de Mendoza.

Gracia, A., Pérez y Pérez, L., Sanjuán, A., & Barreiro Hurle, J. (2004). Análisis hedónico de los precios de la tierra en la provincia de Zaragoza. *Estudios Agrosociales y Pesqueros*, *(202)*, 51-69.

Guadalajara, H., García, L., & Rodríguez, J. (2019). Assessing the localization impact on land values: A spatial hedonic study. *Spanish Journal of Agricultural Research*, *17*(3), e0110. https://doi.org/10.5424/sjar/2019173-14961.

Guida-Johnson, B.; Vignoni, A. P.; Migale, G. M.; Aranda, M. A.; Magnano, A. (2024). Rural abandonment and its drivers in an irrigated area of Mendoza (Argentina). *Revista de la Facultad de Ciencias Agrarias. Universidad Nacional de Cuyo. 56*(1): 35-47. DOI: https://doi.org/10.48162/rev.39.121

Huang, H., Miller, G., Sherrick, B., Gómez, M. (2006). Factors influencing Illinois farmland values. *American Journal of Agricultural Economics*, *88*(2), 458-470.

Journel, A. G., & Huijbregts, C. J. (1978). *Mining Geostatistics*. Academic Press.

Kostov, P. (2009). A spatial Bayesian semiparametric approach to model housing preferences. *Computational Statistics & Data Analysis*, *53*(4), 1616-1628.

Lehn, F., & Bahrs, E. (2018). Analysis of factors influencing standard farmland values with regard to stronger interventions in the German farmland market. *Land Use Policy*, *73*, 138-146.

Mallios, Z., Papageorgiou, A., Latinopoulos, D., & Latinopoulos, P. (2009). Spatial hedonic pricing models for the valuation of irrigation water. *Global NEST Journal*, *11*(4), 575-582.

Matheron, G. (1963). Principles of geostatistics. *Economic Geology*, *58*(8), 1246-1266. https://doi.org/10.2113/gsecongeo.58.8.1246

Miranowski, J. A., & Hammes, B. D. (1984). Implicit prices of soil characteristics for farmland in Iowa. *American Journal of Agricultural Economics*, *66*(5), 745-749. https://www.jstor.org/stable/1240990

Mukherjee, M., & Schwabe, K. A. (2014). Where's the salt? A spatial hedonic analysis of the value of groundwater to irrigated agriculture. *Agricultural Water Management*, *145*, 110-122.

Palmquist, R. B., & Danielson, L. E. (1989). A hedonic study of the effects of erosion control and drainage on farmland values. *American Journal of Agricultural Economics*, *71*(1), 55-62.

Pinto, M. (2001), Transformación de derechos de uso de agua eventuales en definitivos en el régimen jurídico mendocino. *La Ley Gran Cuyo*, T°2001, p. 575.

Pinto, M. (2005). Reconocimiento jurídico del valor económico del agua. *La Ley Gran Cuyo*, Fallo comentado, 1-4.

Pinto, M. (Dir.), Andino, M., & Rogero, G. (2019). *Ley de Aguas de 1884: Comentada y concordada* (Tomo I). Mendoza, Argentina: INCA.

Roka, F. M., & Palmquist, R. B. (1997). Examining the use of national databases in a hedonic analysis of regional farmland values. *American Journal of Agricultural Economics, 79*(5), 1651-1656. https://doi.org/10.2307/1244397

Rosen, S. (1974). Hedonic prices and implicit markets: Product differentiation in pure competition. *Journal of Political Economy, 82*(1), 34-55. https://doi.org/10.1086/260169

Sardaro, R., La Sala, P., & Roselli, L. (2020a). How does the land market capitalize environmental, historical and cultural components in rural areas? Evidence from Italy. *Journal of Environmental Management, 269*, 110776.

Sardaro, R., La Sala, P., & Roselli, L. (2020b). Land pricing in rural development: The role of irrigation and territorial policies. *Land Use Policy, 94*, 104531.

Schönhaut, D. (1990). Valoración del precio de la tierra agrícola en Chile. *Revista de Estudios Agrarios, 50*, 31-55.

Tauro, E., Mirra, L., Russo, S., Valentino, G., Carone, D., & Giannoccaro, G. (2024). Economic analysis of irrigation services: An application of the hedonic price method on the FADN data. *Italian Review of Agricultural Economics (REA), 79*(2), 49-60. https://doi.org/10.36253/rea-14361

Troncoso, J. L. (2005). Determinants of agricultural land prices: The Chilean case. *Ciencia e Investigación Agraria*, 32(1), 51-60.

Valencia, M. J. (2012). *Economía verde y agua en Mendoza*. Universidad Nacional de Cuyo. https://www.uncuyo.edu.ar/relacionesinternacionales/upload/expoverde-mario-valencia.pdf

Wang, Y. (2018). A structural spatial panel model of land values: Application to agricultural land in the United States. *Land Economics, 94*(3), 343-363.

Yoo, J., Simonit, S., Connors, J. P., Maliszewski, P. J., Kinzig, A. P., & Perrings, C. (2013). The value of agricultural water rights in agricultural properties in the path of development. *Ecological Economics, 91*, 57-68.

Zhang, J., & Brown, C. (2018). Spatial variation and factors impacting grassland circulation price in Inner Mongolia, China. *Sustainability, 10*(4381).